



2nd International Conference of Thermal Equipment, Renewable Energy and Rural Development

TE-RE-RD 2013

**Băile Olănești
20-22 Iunie 2013**



2nd International Conference of Thermal Equipment, Renewable Energy and Rural Development TE-RE-RD 2013

ORGANIZERS:

University "POLITEHNICA" of Bucharest

Faculty of Mechanical Engineering and Mechatronics -

Faculty of Biotechnical Systems Engineering -

**National Institute of Research - Development for Machines and
Installations Designed to Agriculture and Food Industry
INMA, Bucharest**

**Hydraulics & Pneumatics Research Institute
(INOE 2000 - IHP), Bucharest**

Chamber of Commerce and Industry Valcea

PROCEEDINGS

Editors:

Prof.dr.ing. Lucian MIHĂESCU

Assoc. Prof.dr.ing. Gabriel-Paul NEGREANU

Băile Olănești – Romania
20-22 July 2013

ISSN 1843 - 3359

Editura

COVER: Assoc.Prof. dr.ing. Gabriel-Paul Negreanu

HONORARY COMMITTEE

Prof. Mihnea COSTOIU	ROMANIA
Prof.Ecaterina ANDRONESCU	ROMANIA
Prof. Tudor PRISECARU	ROMANIA
Prof. Gigel PARASCHIV	ROMANIA
Dr. Petrin DRUMEA	ROMANIA
Prof. Viorel BADESCU	ROMANIA
Dipl.Eng. Valentin CISMARU	ROMANIA

SCIENTIFIC COMMITTEE

Prof. George DARIE	ROMANIA
Prof. Alexandru DOBROVICESCU	ROMANIA
Prof. Ion DONA	ROMANIA
Dr. Jurgen KERN	GERMANY
Prof. Milan MARTINOV	SERBIA
Prof. Nicolay MIHAILOV	BULGARIA
Prof. Constantin PANA	ROMANIA
Dr. Ion PIRNA	ROMANIA
Prof. Mohand TAZEROUT	FRANCE
Prof. Marija TODOROVIC	SERBIA
Prof. Tanay Sidki UYAR	TURKEY
Prof. Gheorghe VOICU	ROMANIA
Prof. Viktorija ZAGORSKA	LATVIA
Dr. Mycola ZHOVMIR	UKRAINE
Dr. Corneliu CRISTESCU	ROMANIA
Prof. Lubomir SOOS	SLOVAKIA

ORGANIZING COMMITTEE

Chairman

Prof. Lucian MIHAESCU ROMANIA

Co-Chairmen

Dr. Sorin-Stefan BIRIS ROMANIA

Dr. Gabriel NEGREANU ROMANIA

Dr. Iulian DUTU ROMANIA

Members

Prof. Erol MURAD ROMANIA

Dr. Mihai NEDELCU ROMANIA

Dr. Ionel PISA ROMANIA

Dr. Elena POP ROMANIA

Dipl.Eng. Viorel BERBECE ROMANIA

Dipl.Eng. Gheorghe RIZOIU ROMANIA

Dr. Valentin VLADUT ROMANIA

Secretary

Dr. Mihaela DUTU ROMANIA

Lorena MATEESCU ROMANIA

Valentin MIROIU ROMANIA

CONFERENCE SPONSORS

CET GOVORA SA



**Str. Industriilor, nr.1
Ramnicu Valcea, Judetul Valcea
Cod postal: 240050
Telefon: +40-250-733601
Fax: +40-250-733603
Email: office@cetgovora.ro**

TURBOEXPERT SRL



Mobil 0722229638
e-mail: turboexpertromania@rdslink.ro



420035, Romania, Bistrita, str. Parcului, nr.7
Email: icpe@icpebn.ro
Tel-fax: +40 (0)263 210938

CONFERENCE PROGRAMME

Thursday, June 20	Friday, June 21	Saturday, June 22
	Breakfast	Breakfast
14.00-15.00 Registration of participants	08.30-09.30 Registration of participants	09.00-13.00 Visit to Ocnele Mari salt mine
15.00-15.30 Opening ceremony	09.30-11.00 Oral presentations "Thermal equipment and renewable energy"	13.00- Participants departure
15.30-18.00 Plenary session	11.00-11.30 Coffee break	
18.00-20.00 Welcome cocktail	11.30-13.00 Oral presentations "Biotechnical systems and rural development"	
	13.00-14.30 Lunch	
	14.30-16.00 Exhibition and Workshop "Clean Energy from Biomass: when and where is needed"	
	16.00-17.30 Workshop - Reduction of energy consumption in automated hydraulic systems using load sensing and digital hydraulics - Modern methods of education in hydraulics	
	19.30-22.00 Conference dinner	

CONTENTS

SECTION 1 THERMAL EQUIPMENT AND RENEWABLE ENERGY

Nr. crt	Paper	Authors	Page
TE1	FLUE GASES RECUPERATOR USING AN EJECTOR	D. Andreescu E. Cerchez	1
TE2	FUNCTIONAL AND CONSTRUCTIVE PARTICULARS OF STEAM TURBINES FROM BIOMASS POWER PLANTS	V. Berbece	5
TE3	GRAPH-ANALYTICAL METHOD FOR ESTIMATION OF FLOWS' DISTRIBUTION IN LOW-PRESSURE GAS TRANSPORT SYSTEMS	V. Bobilov, I. Iliev, P. Zlatev, Z. Kolev, G. Genchev, P. Mushakov	9
TE4	USE OF SATELLITE DATA TO COMPUTE AVAILABLE SOLAR RADIATION IN REMOTE AND RURAL AREA	M. Ceacaru Al. Dumitrescu, V. Badescu	15
TE5	SIMULATION OF AN ACTIVE SOLAR ENERGY SYSTEM INTEGRATED IN A 'BAUHAUS' BUILDING FROM GERMANY IN ORDER TO OBTAIN SYSTEM EFFICIENCY	M. Ceacaru, B. Platzer	19
TE6	ECVET IMPLEMENTATION IN THE NUCLEAR FIELD	M. Ceclan, R. E. Ceclan, C. C. Ramos	23
TE7	LPG USE FOR A CLEAN RUNNING DIESEL ENGINE	Al. Cernat, N. Negurescu, C. Pana	27
TE8	SYSTÈME MODERNE DE CALCULE COMPLET DE LA VIBRATION DE L'AUBE D'UNE TURBINE À VAPEUR OU À GAZ POUR LE RÉGIME NOMINAL	M. Delgeanu	33
TE9	SYSTÈME MODERNE DE CALCULE COMPLET DE LA VIBRATION DE L'AUBE D'UNE TURBINE À VAPEUR OU À GAZ POUR LE RÉGIME NON NOMINAL	M. Delgeanu	37
TE10	METHODS FOR DETERMINING RESIDUES AND CONTAMINANTS FUEL USED FOR POWER PLANTS IN THE RESIDENTIAL SECTOR	M. Dragomir	41
TE11	METHOD FOR DETERMINATION THE RATIO BETWEEN FLAME EMISSIVITIES OF LPG AND CH ₄ , AT COMBUSTION IN FURNACES	V. Ghiea	45
TE12	TURBULENT FORCED CONVECTION AIR FLOW IN A VENTURI CHANNEL	S. Igo, L. Mihăescu	51
TE13	THERMO-MECHANICAL ASPECTS OF MASS TRANSFER SELECTIV PHENOMENON THROUGH DIFFUSION IN THE FRICTION PROCESS OF COUPLE STEEL/COPPER ALLOY	F. Ilie	55
TE14	HEAT WASTE RECOVERY FROMCORROSIVE FLUE GAS STREAMSUSING AIR HEATERS THERMOSIPHON TYPE	I. Iliev	61
TE15	BENCHMARKING THE ENERGY PERFORMANCE OF SIX CAMPUSES OF RUSE UNIVERSITY	I. Iliev, V. Kamburova, A. Terziev	67
TE16	TESTING OF A 620 KW BURNER FOR SAWDUST IN SUSPENSION AND GAS ENRICHED IN HYDROGEN (HRG)	L. Mihăescu, E. Pop, M. E. Georgescu, Gh. Lăzăroiu, I. Pîșă, G. P. Negreanu, C. Ciobanu	73
TE17	RESEARCH ON THE PULVERIZATION QUALITY REFERRING TO THE ENERGETIC USE OF RAW VEGETABLE OILS OR VEGETABLE OILS MIXED WITH FOSSIL FUELS	B. Niculescu	79
TE18	GAS TURBINE BEHAVIOR AT THE AMBIENT CHANGE	I. Oprea	83
TE19	EXPERIMENTAL SETUP AND ENERGY BALANCE OF A HYBRID MICRO-COGENERATION GROUP BASED ON DIESEL ENGINE AND ORGANIC RANKINE CYCLE	T. Prisecaru, Al. Dobrovicescu, C. Petcu, V. Apostol, .M. Prisecaru, Gh. Popescu, H. Pop,	87

		C. Ciobanu, E. Pop, D. Stanciu V. Bădescu, A. Untea, M. H. Kadhum	
TE20	SOCIAL AND TECHNICAL MODEL FOR EMPLOYEE INDIVIDUAL RESPONSIBILITY ENHANCEMENT IN ORDER TO SHAPE AND DEVELOP A PERFORMANT LEVEL OF ENVIRONMENT AWARENESS	C. Sofronie, R. Zubcov	93
TE21	ANALYSIS OF THE EFFICIENCY OF STAGGERED COMBUSTION FOR A LIGNITE BURNER BY DEFINING A MIXTURE FUNCTION BETWEEN THE PRIMARY AND SECONDARY AIR FLOWS	D. Stanciu, L. Mihăescu, G. Negreanu, I. Pișă, I.Oprea	99
TE22	WOOD BIOMASS, ENERGY EXPLOITATION AND WOOD PROCESSING TECHNOLOGIES	G. Stefan	103
TE23	STUDIES ON BIOMASS SUPPLY BY THROWING OR PNEUMATIC INJECTION	G. Ștefan	107
TE24	ANALYSIS OF DEGRADATION FACTOR OF PHOTOVOLTAIC MODULES OPERATING UNDER FIELD CONDITIONS	A. Terziev, I. Iliev, V. Kamburova, D. Deltchev	113
TE25	RESEARCH ON CEREAL STRAW BRIQUETTING IN NORTHEASTERN MOLDAVIA	M. Toader	119
TE26	THE INFLUENCE CHANGES OF SELLING PRICE OF ELECTRIC POWER ON OPTIMAL SIZING OF CHP PLANTS BASED ON USING BIOMASS AND NATURAL GAS	P. Voicu	123
TE27	ANALYSIS OF ENERGY EFFICIENCY IMPROVMENT OF GREENHOUSES BY FUELL SWITCHING	P. Zlatev, Zh. Kolev, V. Kamburova, I. Iliev, V. Bobilov, G. Genchev, P. Mushakov	129

SECTION 2 THERMAL EQUIPMENT AND RENEWABLE ENERGY

Nr. crt	Paper	Authors	Page
RD1	RESEARCHES ON SEEDS MIXTURE MECHANICAL SEPARATION SYSTEMS ACCORDING TO THEIR SURFACE	V. Ciobanu, T. Căsandriou, R. Ciupercă, A. Păun	133
RD2	IRON-BASED MAGNETIC HYBRID NANOPARTICLES FOR HIGH EFFICIENT REMOVAL OF HEAVY METALS FROM WASTEWATER	C. Covaliu, S. Șt. Biriș, G. Paraschiv, Gh. Voicu	139
RD3	ENVIRONMENTAL POLLUTION REDUCTION THROUGH FIELD CROPS SPRAYING MACHINES VERIFICATION	D. Cujbescu, Gh. Bolintineanu, M. Nițu	141
RD4	BIOGAS, A MODERN RENEWABLE ENERGY IN THE EUROPEAN CONTEXT	M. Dilea, G. Paraschiv, N. Ungureanu, Gh. Voicu, S.Șt. Biris, M.Ionescu	147
RD5	RESEARCHES ON THE APPLICATION OF HIGH ACCURACY PHYTOSANITARY TREATMENTS WITH ORGANIC SUBSTANCES BY MEANS OF A HYDROPNEUMATIC MACHINE	A. Dumitrascu, M. Nițu, Al. Zaica, T. Căsandriou	153
RD6	STUDIES ON ENERGY OPTIMIZATION OF THE AGRICULTURAL PRODUCTS PROCESSING MACHINE BY PRESSING	M. Dutu, I. Dinu, O. Rusănescu, I. Dutu	159
RD7	SOME PROPERTIES OF MONASCUS PURPUREUS RED RICE – A NATURAL FOOD DYE	M. Ferdes	163
RD8	ACTUAL METHODS FOR OBTAINING VEGETABLE OIL FROM OILSEEDS	M. Ionescu, N. Ungureanu, S.Șt. Biriș, Gh.Voicu, M. Dilea	167
RD9	ANALYSIS AND DESIGN OF A BIOMASS GASIFIER SYSTEM USING COMPUTATIONAL FLUID DYNAMICS	G. Ipate, Gh. Voicu, E. M. Stefan, M. Ferdes	173
RD10	THE USE OF DIMENSIONAL ANALYSIS FOR THE MATHEMATICAL MODELATION OF SOME WORK PROCESSES IN AGRICULTURAL	C. Manole	179

	MECHANICS		
RD11	PROMOTION OF A TECHNICAL EQUIPMENT ENDOWED WITH ACTIVE WORKING PARTS DRIVEN FOR SOIL DEEP LOOSENING	E. Marin, Al. David, M. Matache, I. Pirnă	185
RD12	TECHNOLOGICAL EQUIPMENT FOR WEIGHING AND AUTOMATIC MANAGEMENT OF FINISHED PRODUCTS PACKED IN SACKS WITHIN MILLING UNITS OF SMALL AND MEDIUM CAPACITY	D. Milea, A. Păun, I. Pirnă, C. Brăcăcescu, M. Ludig	191
RD13	CURRENT STATUS OF SYSTEMS DEVELOPMENT FOR SEEDS SEPARATION WITH PLAN SIEVE AND IN AIRFLOW	M. Birsan (Mitu), T. Căsandriou, A. Păun	197
RD14	MISCANTHUS PLANT ENERGY CONSUMPTION DURING GRINDING WITH A LAB MILL GRINDOMIX GM 200	G. Moiceanu, P. Voicu, G. Paraschiv, Gh. Voicu, M. Chitoiu	203
RD15	EXTENDING THE USE OF HOTHOUSES THROUGH HEATING WITH RESIDUAL AGRICULTURAL BIOMASS	E. Murad, E. Maican, C. Dumitrescu, S. Șt. Biriș	209
RD16	MATHEMATICAL MODEL AND SOFTWARE FOR EVALUATION OF ENERGETIC POTENTIAL OF VEGETAL BIOMASS IN AN AREA	M. Nagy, C. Coța, N. Cioica	215
RD17	INNOVATIVE TECHNOLOGY IN MEDICINAL PLANT PROCESSING WITH IMPACT ON FINISHED PRODUCT QUALITY	A. Pruteanu, A. Muscalu, A. Danciu, L. David	221
RD18	MONTHLY AVERAGE TEMPERATURES DETERMINED ACCUMULATED WATER STORAGE TANK IN SUMMER AT SOLAR THERMAL PLANT	O. Rusanescu, G. Paraschiv, A. Gruia, M. Rusănescu, M. Duțu	-227
RD19	VEGETATION FILTERS FOR EXTENSIVE WASTEWATER TREATMENT PLANTS FROM THE RURAL AGGLOMERATION	V.V. Safta, M. Dilea, G.-Al. Constantin	233
RD20	ENVIRONMENTALLY DRYING VEGETABLES USING GREENHOUSES CROP RESIDUES	C. Sima , G. Haraga, E. Murad	239
RD21	SYSTEM FOR ENVIRONMENT MONITORING	G. Simion	245
RD22	MODELLING AND NUMERICAL ANALYSIS BY THE FINITE ELEMENT METHOD OF WHEAT MILLING PROCESS IN ROLLER MILLS	M. Stefan, Gh. Voicu, G. Ipate, A.G. Constantin	249
RD23	METHODS FOR WASTE NEUTRALIZATION IN CONTEMPORARY ROMANIA	N. Ungureanu G. Paraschiv, M. Dilea, M. Ionescu , Gh. Voicu, S.Șt. Biriș	255
RD24	INTEGRATED SYSTEM FOR DYNAMIC MONITORING AND WARNING IN CASE OF TECHNOLOGICAL RISKS IN THE CROSS-BORDER AREAS OF DANUBE RIVER. REACT PROJECT – ROMANIA-BULGARIA AREA	C. Vîlcu, Gh. Voicu, G. Alecu, G. Paraschiv, C. Lehr, S. Ionescu, A. Nedea	261
RD25	CURRENT STATUS OF EXPERIMENTAL RESEARCH ON BIOMASS COMPACTION	I Voicea, Gh. Voicu, .V. Vladut, M. Matache, M. Maria	267
RD26	ASPECTS REGARDING SOME CINEMATIC PARAMETERS OF MATERIAL PARTICLES MOTION ON SIFTING FRAMES OF REDUCTION ROLL 1 PLANSIFTER COMPARTMENT	Gh. Voicu, G.-Al. Constantin, M.E. Ștefan	273

SECTION 3 HYDRAULICS

Nr. crt	Paper	Authors	Page
FL1	RESEARCH ON IMPROVEMENT OF INJECTION DEVICES COMPONENTS OF FERTIGATION EQUIPMENT	G. Matache, Gh. Șovăiala, Șt. Alexandrescu, S. Anghel, I. Biolan	279
FL2	USING THE GAS GENERATOR TO SUPPLY THE IRRIGATION MOTOR PUMPS	A. Mirea, S. Anghel, .G. Matache, Adrian Pantiru	285
FL3	EXPERIMENTAL VERIFICATION IN STATIC REGIME OF PNEUMATIC ACTUATORS OF MEDIUM AND HIGH PRESSURE	I. Nita, G. Matache, Al. Marinescu, A. Pantiru, A.	289

		Popescu	
FL4	MODERN METHODS OF PERFORMANCE OPTIMIZING FOR CONVECTIVE DRYERS WITH BIOMASS	A. Pantiru, G. Matache, S. Anghel	293
FL5	TESTING OF DYNAMIC RESPONSE OF PROPORTIONAL ELECTROHYDRAULIC VALVES USING FFT SPECTRUM ANALYZER TECHNOLOGY	R.I. Radoi, I. C. Duțu	299
FL6	A NEW TECHNOLOGY TO OBTAIN BRIQUETTES FROM MAIZE STALKS	S. Anghel, C. Dumitrescu, Gh. Sovaiala, I. Dutu, G. Matache	303
FL7	DIGITAL HYDRAULICS REDUCES ENERGY CONSUMPTION IN FLUID POWER DRIVES	P. Drumea, , M.Al. Stoilă, Șt. Simionescu	307

FLUE GASES RECUPERATOR USING AN EJECTOR

Eng. Dan Andreescu¹ – TURBOEXPERT SRL Bucharest
Eng .Elisabeta Cerchez – ICPET TURBO SA Bucharest

ABSTRACT

Scope of paper is to develop a specific flue gases heat recovery system which preheats the combustion air by mixing fresh air with flue gases. This procedure is suitable when the initial combustion process has large excess air, more than 2.0. The mixture of the flue gases and fresh air, (half and half by weight), will double the quantity of flue gases flow but with half of the initial stack temperature. That allows to split the flow in two, half will be exhausted at stack and half will be used as combustion air having enough oxygen for combustion. The result will be the same flue gases quantity evacuated to atmosphere but with half of initial temperature. In the same time the fresh air used for combustion will have a higher temperature instead the ambient initial temperature, thus using less energy.

1. SCOPE OF WORK

Heat recovery from exhaust flue gases with a temperature higher than 150°C is very economical, taking into account actual fuel prices. The recovery processes, as well as the required equipments differ based on application, the fuel used and the sulphur content of the fuel.

SC TURBOEXPERT srl designed systems of heat recovery, heat recovery equipments, which not only recover heat, but are solving specific problems that are found in existing plants. The advantages are:

- „competitive price”, rapid installation, maximum fiability;
- Small footprint for the equipment;
- Minimum maintenance; the installations do not require personnel for operation.

On our company site [3] all these advantages are detailed. In previous papers, [1], the recuperator with <Pseudo heat pipes> was described; this application was operating at the desired parameters. These types of recuperators are compact surface heat exchangers, but are not covering the whole spectrum of heat recovery. There are cases when the composition of the flue gases permits the use of a mixing type of recuperator. This kind of heat recovery was installed in a (....) in fall of 2012.

2. TECHNICAL AND SCIENTIFIC CONSIDERATIONS

In numerous industrial processes the flue gases have the parameters that permit that some of the gases (about half) to be rerouted as combustion air, after mixing with the same quantity with the ambient air.

In the analysis of the heat recovery solution using mixing, the flue gases will be called primary gases, and the gases resulting after the mixing with the ambient air will be called secondary gases.

2.1. The thermodynamic mixing process.

By mixing the primary flue gases with ambient air (same quantity as in the initial combustion process), the flue gases quantity will be double. The excess air in the primary gases will diminish by a unit, than in the case without mixing.

¹ turboexpertromania@rdslink.ro

If the initial excess air (without recovery) is $\lambda_0=2,0$, there is a possibility of heat recovery through mixing of fresh ambient air (same quantity as in the process without mixing) with primary flue gases by splitting secondary flue gases 50% (gravimetric) for combustion and 50% to be exhausted at the stack.

During this process the temperature of the secondary gases will be half of the primary, and the combustion air will become preheated to the same temperature. This will produce saving in fuel consumption corresponding with the gradient of preheat.

Note: The mixing of flue gases with the fresh air increases the combustion products and decreases the oxygen component. The process is represented mathematically as a harmonic geometric series with the limit:

$$\lambda = \lambda_0 - 1$$

(1) relationship of recovery through mixing,
the lower limit is $\lambda_0 > 2, 0$.

An accurate stoichiometric calculation of the combustion process in the existing configuration will deviate from the above formula, but the approximation is in the acceptable limits for the design of the heat recovery system.

Schematic representation of the solution is shown in Fig. 1

The mixing process and the rerouting of the flue gases in the recovery solution presented will increase the pressure losses. Although efforts were made to minimize the pressure losses an additional fan was required. The mixing process between the primary gases and the ambient air is more complicated to be implemented in an existing installation.

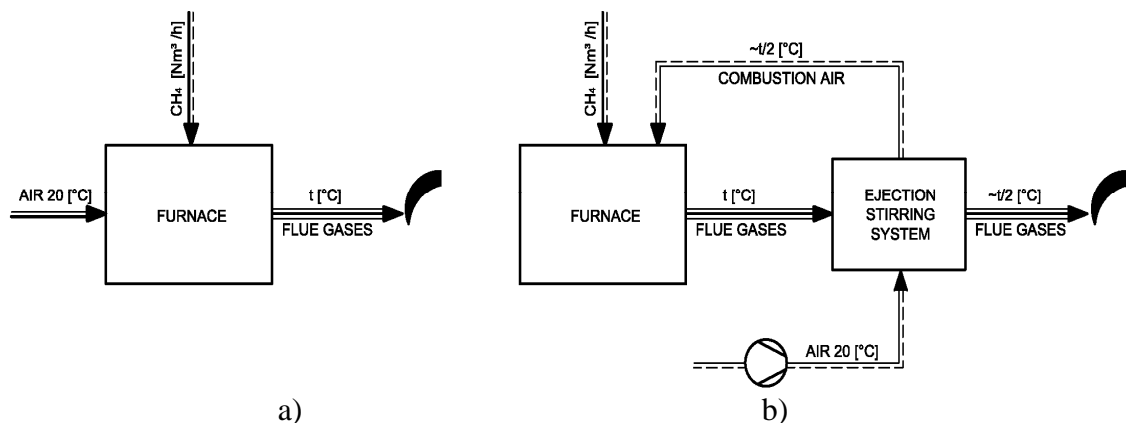


Fig.1 Recovery by mixing: a) initial; b) by mixing (with an ejector)

2.2. Description of technical solution

The simplified thermal considerations outlined above are not sufficient for using the mixing heat recovery; the existing installation must allow for this recovery.

The main thermal problems are:

a) Lowering of oxygen used in the burner as primary air;

The combustion air (the secondary flue gases) has a higher temperature than the ambient temperature. The existing system must accommodate this increase in temperature. By increasing the temperature of combustion air, for the same volumetric flow the mass flow decreases and proportionally the oxygen content decreases. Also due to mixing the oxygen content is lower than the initial conditions. The burners will operate with an oxygen quantity reduced to about half, so the combustion air must be introduced around the flame; the existing geometrical configuration must allow this modification.

b) The influence of increase temperature of combustion air on the burners;

Sometimes combustion air with significant higher temperature is incompatible for some type of burners, such as burners with embedded ventilation systems which contain bearings

c) The available space for installing the mixing chamber with a minimal pressure loss.

The mixing of the flue gases (primary gases) with the ambient air is done by injecting one into another, but without a properly designed aerodynamic solution the lengths of the mixing duct will be at least $15 \div 20$ times its transversal dimensions. Because the flows are in the order of tens or even thousands of m^3/h , the large cross sections will require extensive duct lengths; that may present a problem for the available space. If the mixing is done in a smaller volume the pressure losses become prohibitive. The separation/splitting of the secondary gases to combustion area and to the stack also require additional space and induce more pressure losses.

3.APPLICATION. RESULTS

Applying the above considerations TURBOEXPERT sol [3] has done a pilot installation of heat recovery using mixing with an ejector. The project beneficiary was in food processing industry, the project was used for a vegetable roasting oven as shown schematically in Fig.1b). Due to the seasonal character of the installation, the $4 \div 5$ roasting ovens work non stop a number of months of the year, using a high quantity of natural gas. The fuel contribution to the product cost is very high.

During the initial measurements it was found that the thermal efficiency of the process was around $7 \div 10\%$; this was a strong incentive for finding a recovery solution. The roasting oven shown in Fig. 2 is located in a very restrained location in all directions.

The excess air was high $\lambda_0=3,5$ so the method of heat recovery by mixing was feasible.

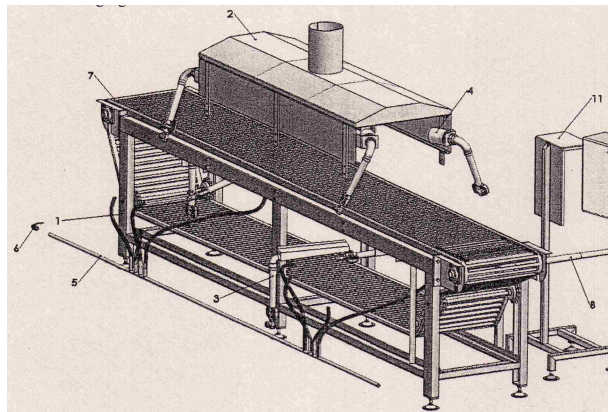


Fig 2. Roasting oven without recovery

Initial data:

- Fuel flow CH_4 : $42\text{Nm}^3/\text{h}$;
- Flue gases temperature <primary>: $620 \div 640^\circ\text{C}$;
- Efficiency: $7 \div 10\%$.

The mixing chamber design used a special system with an ejector; the primary fluid was ambient air and the induced one the flue gases <primary>.

The air is delivered by an additional fan (it uses a small amount of the recovered power $2 \div 3\%$).

In Fig. 3 shows the project and Fig. 4 shows a picture of the heat recovery installation.

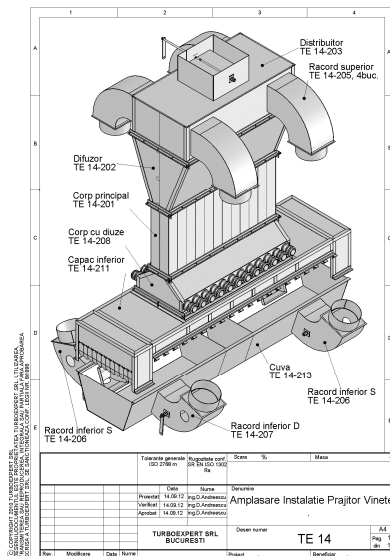


Fig. 3. Heat recovery system



Fig. 4. A picture of the heat recovery solution with the ejector

The operation of the system is as follows: the air brought in by the additional fan is delivered to the mixing chamber. The mixing chamber is on the top of the oven, in the location where the flue gases were delivered to the stack by natural draft.

In the mixing chamber, the primary flue gases are mixed with the combustion air by the ejector which mixes the jets coaxially. There natural compression in the diffuser after the ejector ensure the proper mixing as well as the increase in pressure in required for the flow. After the diffuser half of the secondary gases are exhausted to the stack and the remaining half in returned to the combustion area, some to the burners and some under the transporting grate.

In order to transport the gases to the lower transporting grate four descending ducts were installed, these also enclose the lower side of the transporter. Controlling dampers ensure a better control of air and gases.

The following results were obtained:

- Fuel consumption reduction by 30÷35%;
- Secondary gases temperature at the stack 310÷330°C, (about half of the initial temperature).
- Correct full combustion; visually the flame did not change the colour.
- The ejector operated as designed, producing the desired fluid circulation (a bit over designed).
- The pressure loss due to the additional fan uses about 2% from the recovered power.

4. Bibliography

- [1] Andreescu, D., Cerchez, E., Schema termica pentru recuperarea gazelor arse la cazanele industriale, UPB, TERERD 2012
- [2] Sokolov, E. Ia. Struinae apparata, GEI, Leningrad, 1960
- [3] www.turboexpert.ro

FUNCTIONAL AND CONSTRUCTIVE PARTICULARS OF STEAM TURBINES FROM BIOMASS POWER PLANTS

Viorel Berbece¹, Gheorghe Lăzăroiu, Gabriel-Paul Negreanu, Lucian Mihaescu,
Universitatea “Politehnica” din București,

ABSTRACT

On energy valorizing by burning renewable fuels, relative small thermal powers are achieved, so that the electrical power of such a plant will be limited to 2 MW, for agricultural waste and to 5 MW for wood waste. Manufacturing low power steam turbines involves solving a multitude of functional and constructive problems. The present paper analyzes solutions for steam turbines having no more than 2 MW of electrical power.

Keywords: biomass, steam turbine

Notations:

\dot{m} - mass flow rate [kg/s]
 ε - admission degree [-]
 c - absolute velocity of steam [m/s]
 u - peripheral velocity [m/s]
 d - mean diameter [m]
 l - height/length of nozzles/blades [m]
 v - specific volume [m³/kg]
 μ - mass flow coefficient [-]
 τ - section area factor [-]
 α - nozzle exit angle [rad]
 n - turbine speed [rpm]

Indexes:

1 - exit from nozzles
 2 - exit from blades
 a - nozzle
 p - blade
 ef - effective

1. INTRODUCTION

The steam turbines used in power plants that burn biomass from agricultural sources have some characteristics imposed to them by the low thermal potential of these sources. The main features of such turbines could be evaluated after a comprehensive study of the solutions available for this domain and of the parameters of the steam generators that have biomass as fuel.

Most of the functional and constructive features of the steam turbines derive from the enthalpy drop available from the live steam conditions and from the exit parameters, which in turn, depend on the cooling agent for the condenser or from the heat demand of the consumer in the case of back-pressure turbines and on the effective power at the coupling with the electrical generator, which is the product of enthalpy drop, mass flow rate and effective efficiency of the expansion process in the steam turbine.

2. FUNCTIONAL PARAMETERS OF THE STEAM TURBINES

The most important parameter is the specific volume of the live steam, which depends on the two nominal parameters: pressure and temperature.

¹ 313 Splaiul Independentei st., 060042 Bucharest, Romania; tel: +4.021.4029.158; e-mail: vberbece@caz.mecen.pub.ro;

The specific volume of the live steam or even better of the steam that leaves the first stage nozzles, coupled with the minimal height of the flow path, which is technologically feasible (usually 10 mm), impose the rotational speed of the turbine. That parameter can be determined from the flow rate equation:

$$\dot{m}_a \cdot v_1 = \pi \cdot d_1 \cdot l_{a1} \cdot \varepsilon \cdot c_{1a} \cdot \mu_a \cdot \tau_a \quad (1)$$

coupled with the optimal velocities ratio:

$$\left(\frac{u}{c_1} \right)_{opt} = k_x \cdot \frac{\cos(\alpha_{1ef})}{2 \cdot (1 - \rho)} \quad (2)$$

where: k_x is the velocity ratio factor (usually $k_x = 0.9$), while peripheral velocity u is given by

$$u = \pi \cdot \frac{n}{60} \cdot d \quad [\text{m/s}]. \quad (3)$$

The rotational speed of the steam turbine can be determined by the admissible value for the tension at the root of the last stage blades due to centrifugal forces, since they are proportional with the square of the speed:

$$\sigma_{cf} = K_f \cdot \omega^2 \cdot \pi \cdot l_p \cdot d \quad [\text{Pa}] \quad (4)$$

where K_f - is a form/shape factor that takes into account the variation in area of the section of the blade profile from root to tip. Noting the area of the exit section of the steam path by:

$$S_s = \pi \cdot l_p \cdot d \quad [\text{m}^2] \quad (5)$$

we get

$$\sigma_{cf} = K_f \cdot \omega^2 \cdot S_s \approx \omega^2 \cdot \frac{\dot{m} \cdot v_c}{c_{2a}} \quad (6)$$

where v_c is the specific volume of the steam at the exit from the last stage and c_{2a} is the exit axial velocity.

The enthalpy drop for a stage having a degree of reaction of ρ is [3]

$$H_{st} = k_h \cdot (1 - \rho) \cdot \left(\frac{d \cdot n}{k_{x \cdot \varphi \cdot \cos(\alpha_1)}} \right)^2 \quad [\text{J/kg}] \quad (7)$$

where k_h is a numerical coefficient that takes into account the energy recovery from the upstream stage and the units transformation, while φ is the velocity reduction factor in the nozzles.

From studying the above equations, which are available for the axial flow steam turbines, the main influencing functional factors upon the constructive solutions for the steam turbines can be easily observed:

- the degree of reaction is directly influencing the number of stages and the constructive solution (diaphragms and discs versus drum type rotor);

- the rotational speed influences the number of stages and the tension values due to centrifugal forces;
- the mean diameter and the length of the blades give the main dimensions of the turbine stages and the values of the tension at the root of the longest blades.

For other type of steam turbines used for energy valorization of biomass similar relations can be written, with the same influences on the constructive solutions to be chosen from.

3. CONSTRUCTIVE SOLUTIONS OF STEAM TURBINES FOR ENERGY FROM BIOMASS

The constructive solutions are greatly influenced, as stated before, by the magnitude of the thermal resource to be valorized, which is given by the following main parameters:

- the power of the driven electrical generator and the magnitude and the load type of the thermal power in the case of cogeneration;
- the parameters of live steam from the boiler (pressure, temperature and mass flow rate);
- the parameters of the steam at the exit from the steam generator;
- the rotational speed;
- the functional type derived from the degree of reaction (impulse type or reaction type).

For the smallest units having up to 200 kW, micro-turbines solutions are available:

Table 1. Single stage steam micro-turbines

Nominal Power [kW]/speed [rpm]	Live steam parameters [bar]/[°C]	Exit parameters [bar]/[°C]	Constructive solution	Observations
50..250/3000	4..12/140..250	2/sat.	Patented “bristles” solution; tangential inlet centripetal flow	[5] steam consumption 1.5..4[t/h]
15/26000	10..12/200..220	0.1/sat	Radial flow	[1] steam consumption/ rate 0.04[kg/s]/9.8[kg/kWh]
275/n.a.	13.8/n.a.	0.138/sat	Radial flow	steam consumption/heat rate 0.5[kg/s]/3.9[MJ/kWh]

For the larger power range, from 2 to 5 MW the functional and constructive solutions are those derived from the industrial steam turbines some examples are shown below:

Table 2. Multiple stage steam turbines

Nominal Power [kW]/speed [rpm]	Live steam parameters [bar]/[°C]	Exit parameters [bar]/[°C]	Constructive solution	Observations
3000/ 11543 / 1500	21/275	0.23/sat.	Axial flow reaction drum type with Rateau first stage	steam consumption/ rate 6.41[kg/s]/n.a.[4]
4.8/3000	42/425	0.8/sat	Axial flow impulse type; diaphragm and discs	steam consumption; efficiency elec./cogen. 8.33[kg/s];18.1%/93%
1000/10500/1500	35/435	0.1/sat	Axial flow reaction drum type with Rateau first stage and controlled extraction	steam consumption/heat production 2.78[kg/s]/4[MWt]

From the examples mentioned above the last is illustrative for the use of industrial type steam turbine for biomass valorization. In comparison to other type of turbines which have

smaller number of stages, as in the case of impulse type turbines, (or just one velocity compounded stage, for Curtis type turbines), which have lower thermodynamic efficiency, the turbine presented in figure 1 provides maximum efficiency, that is practically achievable, thus allowing faster investment return and better utilization of the biomass resources, in this particular case forest chips [2].

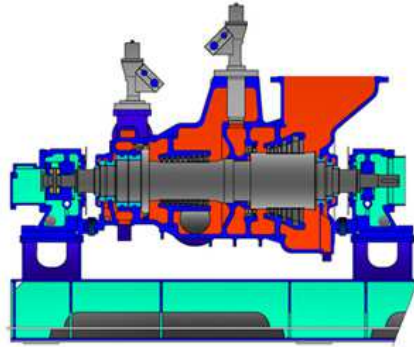


Figure 1. Reaction type steam turbine for biomass

For the intermediate power range 500 kW to 1000 kW, the functional and constructive solutions are mixed, combining elements from the high speed single constructions with lower speed multistage, “classical” design steam turbines.

4. CONCLUSIONS

The functional and constructive solutions of the steam turbines for biomass valorization are chosen according to the specific parameters of each case, in order to get optimal values for the technological and the economic performances of the power plants. For a better use of the biomass potential the cogeneration power plants are widely spread and in some instances encouraged by state founded incentives, such as the “green certificates”.

In the case of small power range novel types and solutions for the steam turbines are proposed, some of which have very promising efficiency values.

In the mid range cases other thermal energy solutions could be used, such as the Organic Rankine Cycle (ORC) turbine installations, which eliminate the main disadvantage of the water based cycles, the lower density values.

And last but not least, the economic analysis has the predominant role in the decision making process of choosing the right type of turbine installation and getting the funding from the potential investors, which are of different scale that in the case of large fossil fuel power stations.

References

- [1] <http://www.greenturbine.eu>
- [2] <http://www.ttk.hr/biomass-turbine.htm>.
- [3] Grecu T. s.a. – Turbine cu abur. Editura Tehnica. Buc. 1976
- [4] http://www.stromerzeuger-discount.de/Condensing_steam_turbine_3_MW_KKK_AFA_6_Da_20_bar
- [5] http://www.geeltd.org/images/stories/Step_Boilers/S2E_50_-_500GEE.pdf

GRAPH-ANALYTICAL METHOD FOR ESTIMATION OF FLOWS' DISTRIBUTION IN LOW-PRESSURE GAS TRANSPORT SYSTEMS

Valentin Bobilov¹, Ilia Iliev¹, Pencho Zlatev¹, Zhivko Kolev¹,
Georgi Genchev¹, Plamen Mushakov¹

¹Department of Thermotechnics, Hydraulics and Ecology,
University of Ruse, Ruse 7017, Bulgaria

ABSTRACT

The purpose of the work is to create a simplified physical model of a closed local gas system at low pressure (up to 500 mbar) for supply of consecutively connected single consumers or group consumers. Graph-analytical method for estimation the distribution of flows in ring and linear system for transport of technical fluids has been developed.

1. INTRODUCTION

In the transport process of isothermal incompressible fluids (water, liquefied petroleum gases, lubricants, diesel, oil, etc.) correction in the density of the fluid does not have to be done. In gaseous products (gas, acetylene, oxygen, compressed air, etc.) where are substantial pressure drops there should be introduced a correction for both the density and the compressibility factor.

The use of ring (closed) gas transport systems is determined by a variety of reasons - to ensure uniform and with a lower risk gas supply process, ensure quantity of fluid in duplicate gas distribution points with low let in ability, providing gas supply to customers in conditions of future infrastructure reconstructions, and so etc. [2, 3, 4].

The tasks that need to solve the developed graph-analytical method are:

- evaluation of the permeability capacity of the main contour and the deviations for the individual consumers in nominal work conditions;
- evaluation of the permeability capacity of the main contour and the deviations for the individual consumers in work conditions different than nominal (failures, introducing of new consumers, etc.);
- evaluation of the pressure drop in any contour section in nominal and different than nominal work conditions.

2. METHODOLOGY

In Figure 1 is shown a principal scheme of a gas supply ring system with one or more external gas sources (the second source is indicated by a dotted line) [1].

The input factors which are necessary for carrying out the specific calculations are:

- estimated consummated quantity of natural gas at nominal (or non-nominal) operation conditions for each of contour consumers $Q_n, \text{Nm}^3/\text{h}$;
- geometric and hydrodynamic characteristics of the gas pipe sections (lengths l_i, m ; specify diameters d_i, m ; type of local resistances ξ_i ; specify coefficients of friction λ_i ; average density of the natural gas $\rho, \text{kg/m}^3$);

¹ Department of Thermotechnics, Hydraulics and Ecology, University of Ruse, "Studentska" St., 7017 Ruse, Bulgaria,
+359 82 888 304, zkolev@uni-ruse.bg

- nominal working pressure of the circular gas transport system p , mbar;
- minimum working pressure at the point of supply to each consumer $p_{n,min}$, mbar.

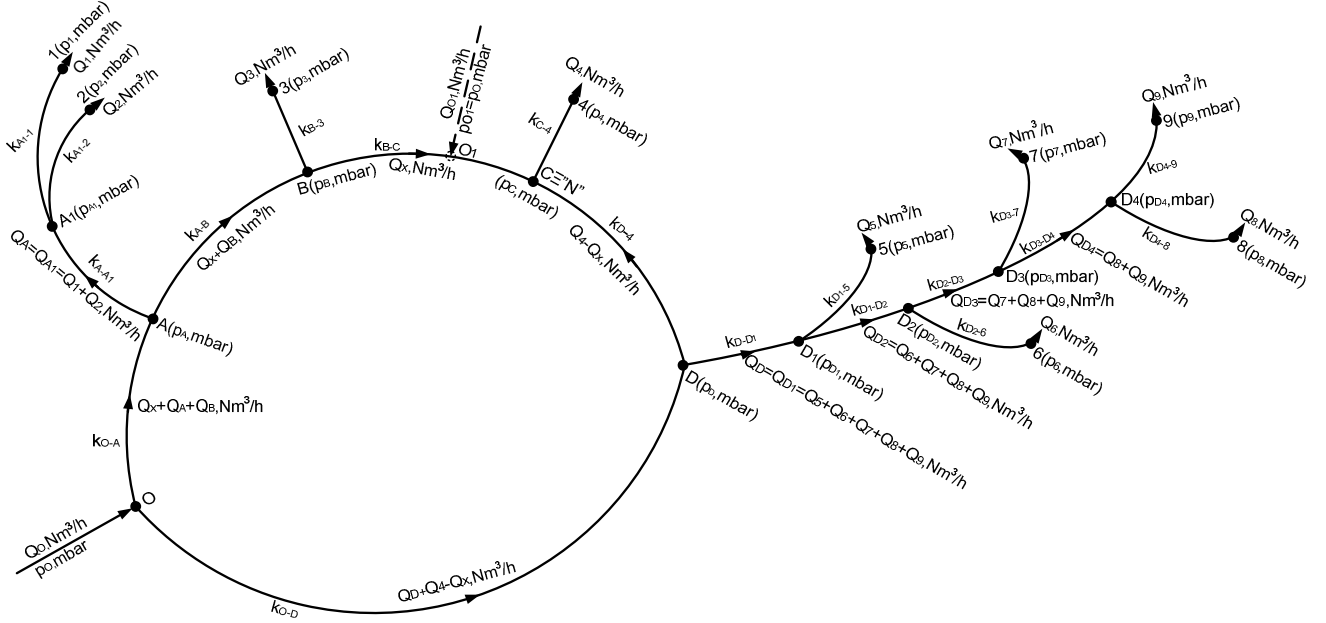


Figure 1: Principal scheme of the gas supply system

2.1. ANALYTICAL METHOD FOR IDENTIFICATION OF THE "NEUTRAL" POINT IN THE CIRCULAR CONTOUR

Evaluation of the permeability capacity of the main contour in nominal or non-nominal operation conditions has been done by specifying the location of the "neutral" point "N" and the balance sheet of the material flows. The "neutral" point in the main circular contour is the point where the gas enters from the two branches of the contour (left and right). Therefore, the sum of pressure drops in the left branch is equal to the sum of pressure drops in the right branch [1].

The points of the circular contour, leading to individual consumers or groups of consumers have been identified by letters, respectively, A, B, C, D and the point of the incoming gas flow in the circuit (the natural gas source) - with the "O". The gas consumers have been marked with numbers (from 1 to 9).

Drawing equation for pressure drops equality in the contours "left" and "right" to the "neutral" point "N", it has been reported that the only unknown parameter is the gas flow " Q_x ", entering the point "N", for example from the left.

The pressure drops in the pipeline contour have been determined by the classical equation [2, 3, 4]:

$$\Delta p_{ij} = k_{ij} \cdot Q_{ij}^2, \text{ Pa} \quad (1)$$

where: k_{ij} is the characteristic of the pipe section i-j, $\text{Pa}/(\text{Nm}^3/\text{h})^2$;

Q_{ij} – transported quantity of natural gas in the pipe section i-j, Nm^3/h .

The characteristic of the pipe section i-j has been determined by the equation:

$$k_{ij} = \left(\frac{\lambda_{ij} \cdot L_{ij}}{d_{ij}} + \sum \xi_{ij} \right) \cdot \frac{8 \cdot p}{\pi^2 \cdot d_{ij}^4}, \frac{\text{Pa}}{(\text{Nm}^3/\text{h})^2} \quad (2)$$

For specify the "neutral" point location in the circular contour the balance equation (3) has been used [1]:

$$\sum_{i,j}^L k_{ij} \left[\left(\sum_I^n Q_I + Q_x \right)^2 \right] = \sum_{i,j}^R k_{ij} \left[\left(\sum_I^n Q_I + Q_N - Q_x \right)^2 \right], \quad (3)$$

where: Q_I is the current quantity of gas flowing from left (L) or right (R) in the direction of the "neutral" point "N", Nm^3/h ;

Q_N - nominal quantity of natural gas in the "neutral" point "N", Nm^3/h .

The identification process is iterative, so it is logical the "neutral" point to be searched in the center of mass load as the first approach. If there is improper selection (incorrect identification), the roots of the algebraic equation describing the pressure drops on opposite points will be imaginary.

The analytical solution of equation (3) may lead to the following results:

► Receive at least one real root - it is assumed to be reliable and based on it the final distribution of natural gas within the contour is assumed as follows:

- from the left contour brunch: $Q_{N_L} = Q_x$, Nm^3/h ;

- from the right contour brunch: $Q_{N_R} = Q_N - Q_x$, Nm^3/h .

► Lack of real root - the procedure requires re-identification of the "neutral" point "N". It is advisable to make the choice of the next point along the contour (left L or right R) with less gas flow.

The next step is re-solving the equation (3), etc. to find a real root for Q_x .

After determination the exact distribution of the fluid to the consumers connected to the circular contour the next step is procedure of more precise determination of the fuel pressure drops. It can be assumed that the characteristics of the pipe sections k_{ij} are parameters, constant at a value and slightly dependent on pressure drops and the nature of the flow.

Comparing the received pressure p_n in the gas supply point of the specified consumer with the minimum operating pressure $p_{n,min}$ may result in an adjustment in the adopted diameter d .

In the example of a circular scheme shown in Figure 1 there is one source of natural gas (shown by a solid line), and it has been determined that the "neutral" point is point C. If there is a change of the operation conditions (include of new sources of natural gas, changes in the quantity of gas from the sources, include of new consumers, changing the quantity of gas consumed by any of the consumers, exclude of consumers, failures, etc.) there could be a change of the "neutral" point location.

2.2. GRAPH-ANALYTICAL METHOD FOR DETERMINATION OF PRESSURE DROPS IN GROUP OF CONSUMERS FROM CONTOUR SECTION AND THE PRESSURE OF SPECIFIED CONSUMER

When there is a group of consumers connected to ring gas supply contour it is essential to determine the distribution of pressure drops in the contour section. This is necessary for determination of the supply pressure p_n for each consumer, as it was described above (it is necessary $p_n \geq p_{n,min}$). For this purpose graph-analytical method has been developed. The method has been applied for the group of consumers supplied from point D (5, 6, 7, 8 and 9) and in particular, for determination of the supply pressure of consumer 7 (Figure 1).

Figure 2 shows the graphical model of the method applied to determination the pressure in point 7.

The method has been presented in „ $(-p, \Delta p) - Q$ ” diagram. Originally from point D (the point from which the contour section has been supplied) the graphically dependence “ $k_{D-D_1} = f(Q, \Delta p)$ ” has been built. When detecting k_{D-D_1} with the maximum flow of natural gas in the contour section ($Q_D = Q_{D_1} = Q_5 + Q_6 + Q_7 + Q_8 + Q_9$) the pressure drop Δp_{D-D_1} has been determined graphically. The next step is to build graphically the dependence

“ $k_{D_1-D_2} = f(Q, \Delta p)$ ” in the same „ $\Delta p - Q$ ” diagram from starting point D_1 . To better visualize the summation of pressure drops, each next diagram “ $k = f(Q, \Delta p)$ ” has been built over the previous one, considering the change of gas flow (in the case considering the deflected flow Q_5 to consumer 5).

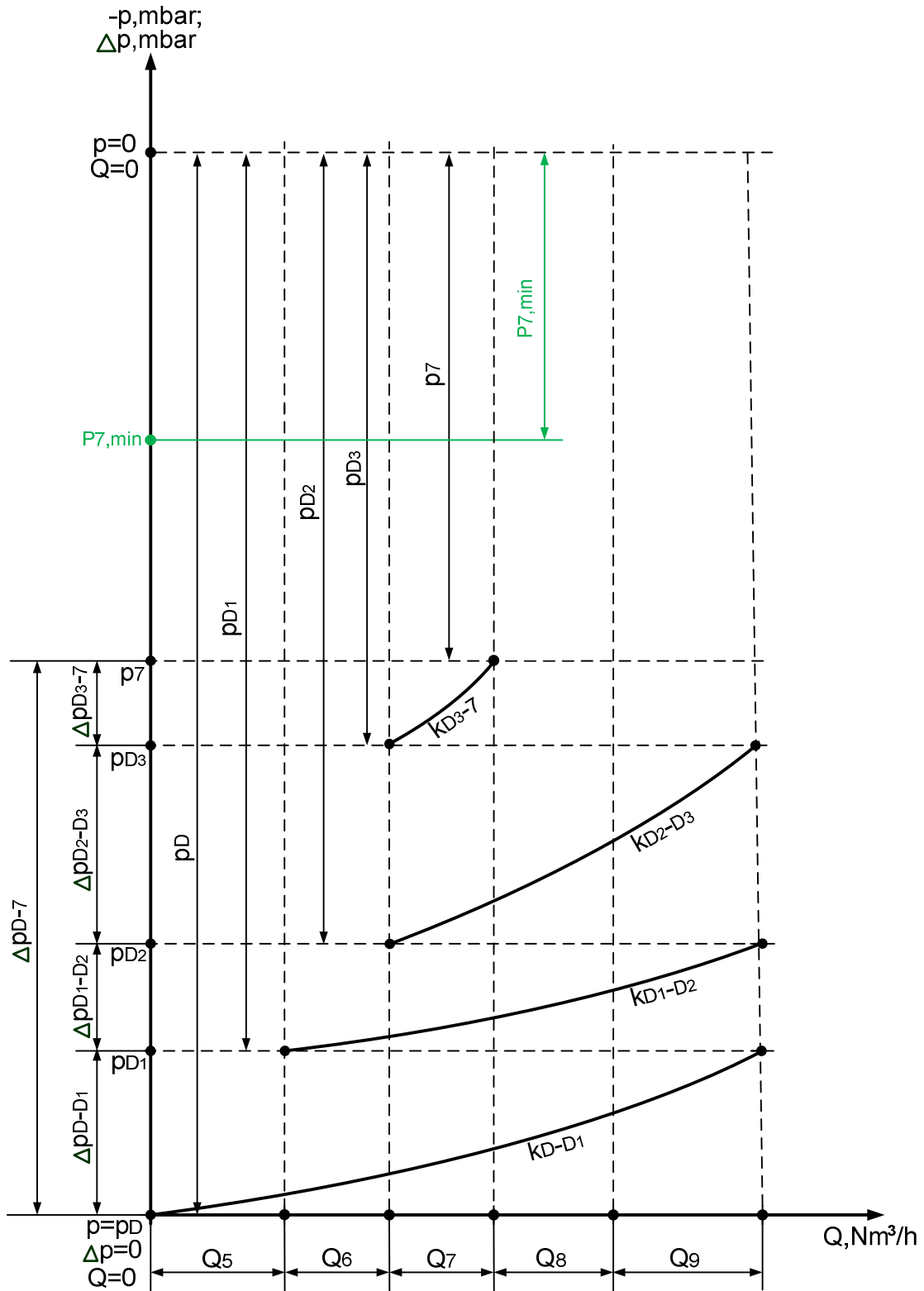


Figure 2: Graph-analytical method - determination of the supply pressure of consumer 7

When detecting $k_{D_1-D_2}$ with the flow $Q_{D_2} = Q_6 + Q_7 + Q_8 + Q_9$ the pressure drop $\Delta p_{D_1-D_2}$ has been determined. Similarly the pressure drop $\Delta p_{D_2-D_3}$ has been determined graphically. The next step is determination of the pressure drop in the line “D₃ – 7”. For this purpose the graphically dependence “ $k_{D_3-7} = f(Q, \Delta p)$ ” has been built from the starting point lying above the starting point for the diagram “ $k_{D_2-D_3} = f(Q, \Delta p)$ ”. When detecting k_{D_3-7} with the flow Q_7 the pressure drop Δp_{D_3-7} has been determined. The sum of the obtained pressure drops gives the total pressure drop Δp_{D-7} in the line „D – D₁ – D₂ – D₃ – 7”. On ordinate „(-p)” of „[(-p, Δp) - Q]” diagram the predefined minimum working pressure $p_{7,min}$ has been noted according to the requirements of consumer 7. The next step is determination of pressures in: point D (p_D), point D₁ (p_{D_1}), point D₂ (p_{D_2}), point D₃ (p_{D_3}) and the working pressure in point 7 ($p_7 = p_D - \Delta p_{D-7}$). It is seen that in the case shown in Figure 2 consumer 7 can work because $p_7 > p_{7,min}$.

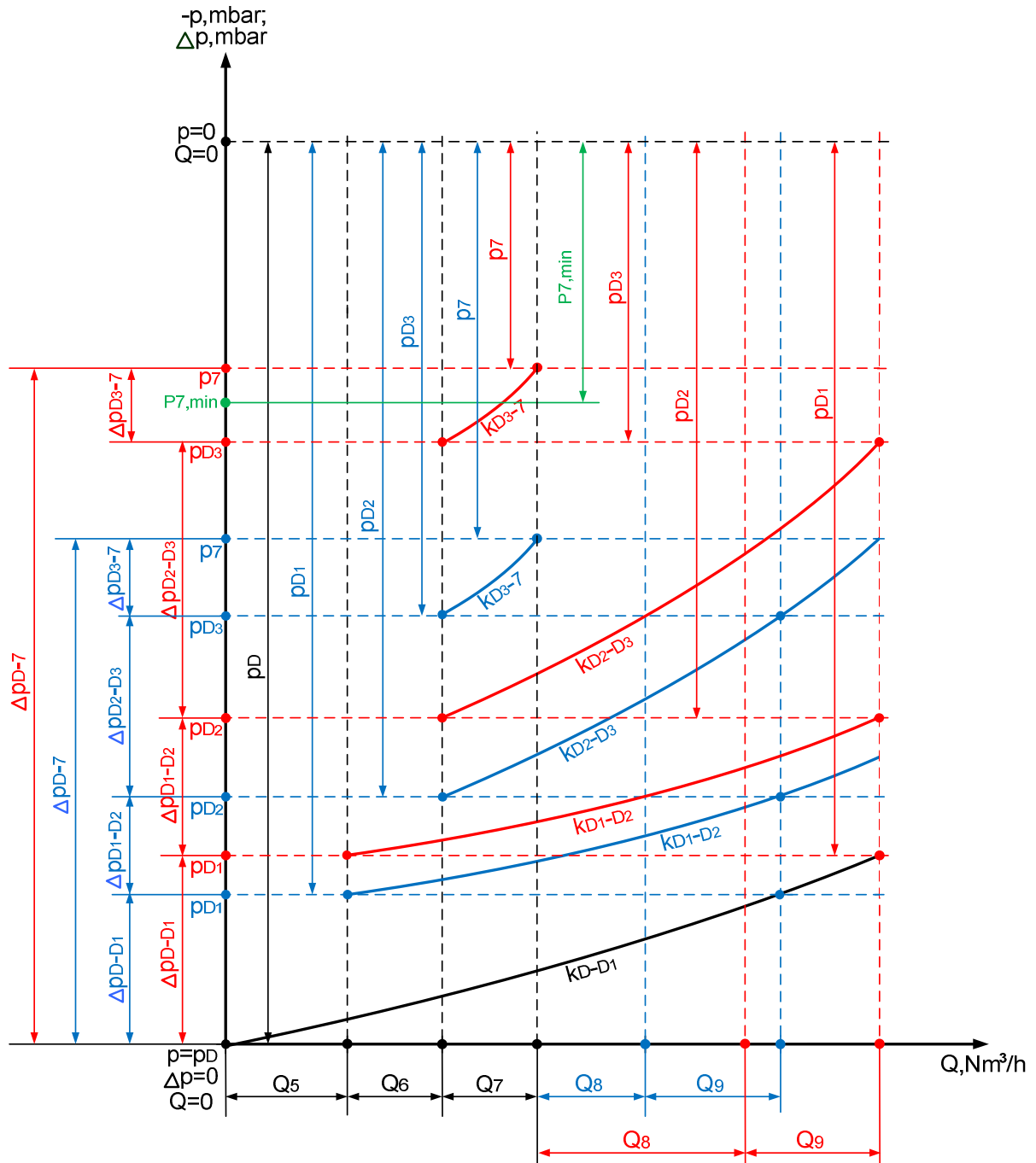


Figure 3: Graph-analytical method – varying of the working pressure of consumer 7 when there is a change of the gas flow to consumer 8

If there is a change of the working parameters of the system it is possible to change the supply pressure of any of the gas consumers.

In figure 3 is shown how by using of the developed graph-analytical model it can be visualized the reduction of working pressure of consumer 7 as a result of only the increased consumption of gas by consumer 8. The blue color shows the parameters in the initial moment (refer to Figure 2) and the red - the parameters after increased gas consumption Q_8 . It is seen that the increasing of Q_8 leads to increasing of the whole gas flow which supply point D ($Q_D = Q_{D1} = Q_5 + Q_6 + Q_7 + Q_8 + Q_9$). As a result bigger pressure drop Δp_{D-D1} has been reported. The starting point of diagram " $k_{D1-D2} = f(Q, \Delta p)$ " moves upwards. Since the gas flow Q_{D2} is bigger as a result of the increasing of Q_8 bigger pressure drop Δp_{D1-D2} has been reported. Similarly the pressure drop Δp_{D2-D3} has been increased. Because the consumed quantity of gas from consumer 7 does not change, it remains constant and the pressure drop Δp_{D3-7} in the line „D₃ – 7". As a result of increasing of Δp_{D-D1} , Δp_{D1-D2} and Δp_{D2-D3} the total pressure drop Δp_{D-7} have been increased. The latter leads to a reduction of the working pressure p_7 , and as is shown in the example illustrated in Figure 3, the pressure becomes less than the minimum working pressure for consumer 7 and the consumer can not work.

3. CONCLUSION

The developed analytical method for identification of the "neutral" point in the ring circular contour enables the dynamic redistribution of the gas flows. If in the system there are more than one sources of natural gas (the sources must supply gas with the same pressure) to determine the locations of the "neutral" points the scheme needs to be broken the required number of contours. The determination of the exact value of the static pressure p_i in any point of the circular contour allows display modes of unacceptably high pressure drops.

The developed graph-analytical method for group of consumers allows through appropriate software continuously monitoring of operating parameters and their influence on the final supply pressure for each consumer of natural gas. It is also possible that the method can be used in the design of the gas supply systems. The convenience of the proposed model consists of evaluating the visibility and simplified structure of utilities (software, graphics) and the ability to "clarify" the nature of the curves of hydraulic pressure drops as a function of flow rate.

References

- [1] Bobilov, V., D. Radev, Z. Kolev, P. Zlatev, G. Genchev, P. Mushakov. *Specifications for consumers' gas supply at ring circuit contour*. Scientific Conference of University of Ruse, volume 50, series 1.2, Ruse, Bulgaria, 2012, p.78-82. (in Bulgarian)
- [2] Zhila, V., S. Kalchevski. *Gas supply and effective use of natural gas*. Sofia, Bulgaria, 2013. ISBN 978-619-160-122-6. (in Bulgarian)
- [3] Komina, G., P., A. O. Proshutskii. *Hydraulic calculation and design of gas pipelines: a manual of discipline "Gas supply" for students from the speciality 270109 – Gas supply and Ventilation*. 2010. ISBN 978-5-9227-0179-2. (in Russian)
- [4] Nikolov, G. *Distribution and use of natural gas*. Sofia, Bulgaria, 2007. ISBN 978-954-92023-1-1. (in Bulgarian)

USE OF SATELLITE DATA TO COMPUTE AVAILABLE SOLAR RADIATION IN REMOTE AND RURAL AREA

Mihai-Cristi Ceacaru^{1(a)}, Alexandru Dumitrescu^{2(b)}, Viorel Badescu^{3(c)}

^aPolytechnic University of Bucharest, Bucharest, Romania, ^bNational Meteorological Administration (University of Bucharest), Romania, ^cPolytechnic University of Bucharest, Bucharest, Romania

ABSTRACT

This paper presents a method of calculating the global solar irradiance using satellite resources. The satellite database was taken from Meteosat, a geostationary satellite. In the first stage, a reference map on Romanian surface for cloudiness index from satellite data is deduced from sequential satellite images of time. In the next stage is calculated the global solar irradiance from the satellite in different days for three villages from Romania: Almaj (Dolj county), Baci (Cluj County), Limanu (Constanta county), considering the cloudiness index obtained from satellite and the global solar irradiance for clear sky days.

1. INTRODUCTION

Several papers refer to the calculation of solar radiation. One of the first papers that use satellite data to calculate solar radiation is [1]. In this paper, a statistical method is presented for the determination of the global solar radiation at ground level. It makes use of data from the meteorological satellites, which provide extensive coverage as well as adequate ground resolution. In the first step, a reference map of ground albedo is deduced from the time-sequence of satellite images. Then, by comparing the satellite data with the computed albedo map, a cloud coverage index is determined for each ground pixel of 5 km x 5 km. This index is linearly correlated to the atmospheric transmission factor. The regression parameters are estimated using a training set provided by ground pyranometers. Tests for two different time periods show a good agreement between the actual and model-derived hourly global radiation. Another work which also used satellite resources is [2]. In this reference, images taken by geostationary satellites may be used to estimate solar irradiance at the earth's surface. The Heliosat method is a widely applied procedure. It is based on the empirical correlation between a satellite derived cloud index and the irradiance at the ground. The modified method may open the way to use a generic relation between cloud index and global irradiance. Two other works that relate to the calculation of solar radiation are [3] and [4]. The present work aims to calculate the solar radiation in three different rural areas of Romania by using satellite data.

2. SATELLITE DATABASE

Satellite data was obtained from site [5] belonging to EUMETSAT. EUMETSAT is an intergovernmental organization formed by the meteorological services of countries in the European Union, with additional countries such as Norway, Turkey and Switzerland. After accessing the site, the next step is to register as user. After registration, one has access to the following data type: daily and monthly. To have access to the instantaneous satellite data used in this paper, a special request is needed, which is to be addressed to the site administrator. After request's approval, instantaneous satellite data can be downloaded. Three methods are available for satellite data downloading: by email, by CD and by using a ftp site. Satellite data download procedure used in this work is by using a ftp site. This procedure is recommended for two main reasons: (i) the ordered satellite data can be downloaded to any computer with internet access, having valid discharge for two weeks and (ii) the access to satellite data is very fast. The selected satellite data model is: 'CFC-

Fractional Cloud Cover'. In this paper satellite data were downloaded for the period between 01 October 2009 and 31 December 2009.

3. MAPS OF CLOUDINEES INDEX ON THE SURFACE OF ROMANIA

After downloading satellite data, they are processed using a script written in R language [6]. The output of this script is the cloudinees index n1, expressed in percentages. Using the R language, satellite images are extracted from the satellite data. They allow to see the spread of the cloudinees index on Romanian surface. Samples of these satellite images can be seen in Fig. 1, wich represents the spread of cloudinees index on the surface of Romania, on 03 August 2009 between 9.00 and 16.00 UTC. This is a clear days in the Southern parts of the country.

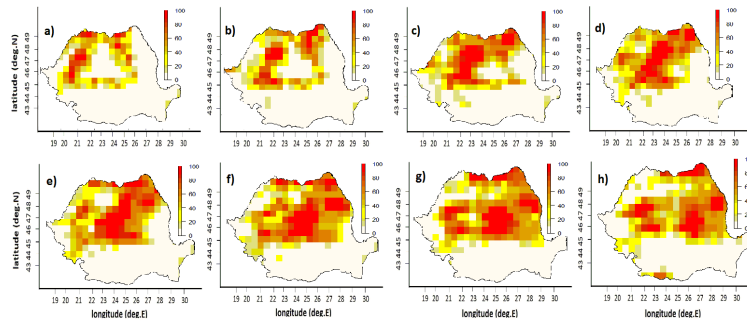


Fig.1 . Hourly maps of cloudinees index on the surface of Romania during 03 August 2009 between 9.00 and 16.00 UTC : a,b,c,d,e,f,g,g represents correspond to 9.00, 10.00, 11.00, 12.00, 13.00, 14.00, 15.00 and 16.00 UTC, respectively

4. CALCULATION OF GLOBAL SOLAR IRRADIANCE

While the performance or accuracy may be a major criterion in the selection of the most suitable calculation model for a specific application, it is by no means the only factor to be considered. Availability of input data would surely be another major factor. Others may include area of applicability and computational complexity.

4.1. Calculation of global solar irradiance in days with clear sky

Many very simple cloudless sky solar irradiance models have been proposed and tested in literature. Most of them evaluate just the global solar irradiance $I_{g,cs}$ on a horizontal surface. A few models predict the components of the global irradiance. The diffuse solar irradiance $I_{d,cs}$ may be computed by using the Daneshyar - Paltridge - Proctor (DPP) model [7]:

$$I_{d,cs} = 1429 + 2104 \left(\pi/2 - \theta_z \right) \quad (\text{Wm}^2) \quad (1)$$

Here θ_z is the zenith angle and enters in radians. The zenith angle is computed with the formula [7] :

$$\cos \theta_z = \sin \delta \sin \phi + \cos \delta \cos \phi \cos \omega \quad (2)$$

where δ is the astronomical declination, ϕ is the latitude of the place and ω is the orar angle. The astronomical declination is computed with the equation :

$$\delta = 23.45 \sin \left[360 \left(\frac{284 + n_{day}}{365} \right) \right] \quad (3)$$

where n_{day} is day number in the year. The global irradiance is:

$$I_{g,cs} = 951.39 \cos^{1.15} \theta_z \quad (\text{Wm}^{-2}) \quad (4)$$

After the diffuse solar irradiance and the global irradiance are computed, the beam irradiance on clear sky is obtained from:

$$I_{b,cs} = I_{g,cs} - I_{d,cs} \quad (5)$$

After the global irradiance for clear sky days was obtained, the formula below was used to calculate the global solar irradiance on cloudy days, depending on the cloudiness index n_1 obtained from satellite database and the global irradiance for clear sky days $I_{g,cs}$:

$$G_{sat} = n_1 I_{g,cs} + (1 - n_1) I_{g,cs} \quad (6)$$

4.2. Villages presentation

Three villages from Romania were selected: Almaj (Dolj county, latitude $45^\circ 47' 30''$ and longitude $20^\circ 43' 20''$); Baci (Cluj county; latitude $46^\circ 47' 34''$ and longitude $23^\circ 31' 30''$); Limanu (Constanta county; latitude $43^\circ 47'$ and longitude $28^\circ 31'$), as we can see in Fig. 2:

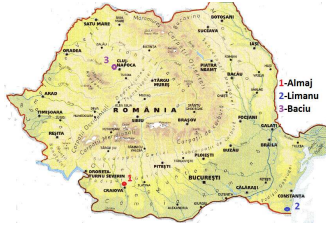


Fig.2. Romania map with the location of those three villages chosen for the calculation: 1-Almaj, 2-Limanu, 3-Baci

The three villages were chosen because they are in irrigated areas and areas with fertile land for agriculture developed. Following the steps in section 4.1, global solar irradiance can be calculated from satellite data for all the three villages presented above. The days chosen to calculate the cloudiness index n_1 are: 03.August.2009 and 12.august.2009.

4.3. Results for global irradiance

In Fig. 3 and in Fig. 4 can see a graphical comparison between cloudiness index values and respectively, a comparison between irradiance values for the three villages presented at point 4.2.

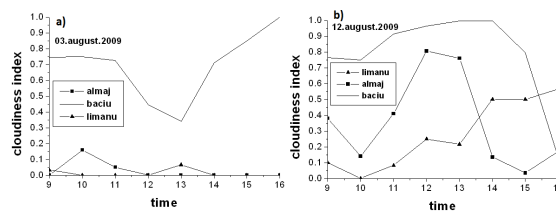


Fig.3 . Graphics comparison between n1, cloudinees index from satellite belonging to each villages, from time 9 :00 and 16 :00 UTC : a,b represents graphics comparison between cloudinees index belonging to each village for days : 03.august,12.august, year 2009, respectively

As you can see from the graphics, day 03.august.2009 for villages Almaj and Limanu is a clear sky day and for the village Baciú is a cloudy sky day and day 12.august.2009 is a cloudy sky day for all three villages.

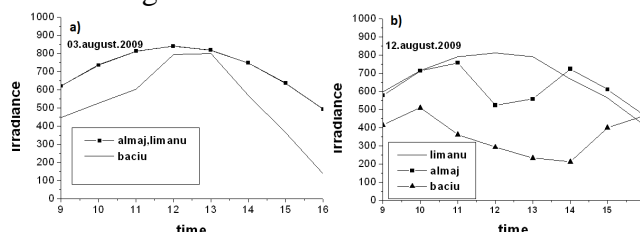


Fig.4 . Graphics comparison between global solar irradiance from satellite belonging to each villages, from time 9 :00 and 16 :00 UTC : a,b represents graphics comparison between global solar irradiance belonging to each village for days : 03.august,12.august, year 2009, respectively

From figure 4 can be seen as expected different results of global solar irradiance from satellite for each villages, except in day 03.august.2009 for villages Almaj and Limanu, global solar irradiance from satellite is almost the same because the results of cloudiness index is different only at the second decimal after comma.

5. CONCLUSIONS

This paper has presented a brief review of previous paper based on satellite data, satellite data base used for calculation of global solar irradiance, maps of cloudinees index on the surface of Romania results from R language, a method used for calculating global solar irradiance from satellite and results of global solar irradiance obtained for three villages placed in different regions of the country.

REFERENCES

- [1] D. Cano, J.M. Monget, M. Albuissou, H. Guillard, N. Regas and L. Wald - *A method for the determination of the global solar radiation from meteorological satellite data*, Solar Energy, vol.37, no.1, pp.31-39,
- [2] Georg Beyer H., Costanzo C. and Heinemann D. - *Modifications of the heliosat procedure for irradiance estimates from satellite images*, Solar Energy, no. 3, vol.56, pp. 207-212, 1996
- [3] Loutzenhiser M. - *Empirical validation of models to compute solar irradiance*, Solar Energy, no. 4, vol. 81, pp. 632-636, 2007
- [4] C Eftimie - *Computer program for climatological parameters calculation and radiation simulation*, Bulletin of the Transilvania, no. 51, vol. 2, pp273-278, 2009
- [5] The Satellite Application Facility on Climate Monitoring (CM SAF):
<http://wui.cmsaf.eu/safira/action/viewHome>
- [6] R Development Core Team (2011). R: A language and environment for statistical computing. R Foundation for Statistical Computing, Vienna, Austria. ISBN 3-900051-07-0, URL <http://www.R-project.org/>.
- [7] Badescu V. - *Verification of some very simple clear sky and cloudy sky models to evaluate global solar irradiance*, Solar Energy, 61, 251-264, 1997

SIMULATION OF AN ACTIVE SOLAR ENERGY SYSTEM INTEGRATED IN A 'BAUHAUS' BUILDING FROM GERMANY IN ORDER TO OBTAIN SYSTEM EFFICIENCY

Mihai-Cristi Ceacaru^{1(a)}, Bernd Platzer^{2(b)}

^aPolytechnic University of Bucharest, Bucharest, Romania, ^bChemnitz University of
Technology, Chemnitz, Germany

ABSTRACT

In this work we present a simulation of an active energy system. This system belongs to a building built in the style of 'Bauhaus' architecture. This style of architecture was founded in the Staatliches Bauhaus School from Germany. For this simulation, we use Solar Water Heating module, which belongs to the software RETSCREEN and this simulation is done for several cities in Romania.

1. INTRODUCTION

The 'Bauhaus' architecture was a landmark in the history of modern art and education and also is a reference to early modern times. The innovative architecture featured artist-teachers who individually and collectively influenced contemporary art education more than any educational institution in recent history. While many artist-teachers working within the school are significant, none of their accomplishments would have been possible without the leadership of its founder and longtime director, Walter Gropius. His experience and education as an architect greatly influenced and infused his educational approach and his vision integrated and recalled a philosophy with roots that extended back to medieval craft guilds; one that sought to bridge the gap that had developed between 'artist' and 'craftsman' [1].

2. ACTIVE SOLAR ENERGY SYSTEM

In the complex Hallenbades in the city Chemnitz, Germany there is a building during the period of 1930 [2]. The building is built in the style of the architecture called "Bauhaus". Staatliches Bauhaus commonly known simply as 'Bauhaus', was a school in Germany that combined crafts and the fine arts, and was famous for the approach to design that it publicized and taught. It operated from 1919 to 1933 [1]. At that time the German term 'Bauhaus', literally symbolize "house of construction", stood for "School of Building". The Bauhaus school was founded by Walter Gropius in the city Weimar, Germany [1]. In spite of its name, and the fact that its founder was an architect, the Bauhaus did not have an architecture department during the first years of its existence. Nonetheless it was founded with the idea of creating a "total" work of art in which all arts, including architecture, would eventually be brought together. The 'Bauhaus' style became one of the most influential currents in modernist architecture and modern design. The Bauhaus had a profound influence upon subsequent developments in art, architecture, graphic design, interior design, industrial design, and typography. The building from Chemnitz is composed of: a swimming pool of 50 meters, a entrance area of the building, swimming pool of 25 meters, a bath, a sauna, a tower, a residential complex and a commercial complex [2]. In fig.1 we can see a picture representing this building where we can observe the solar collectors.

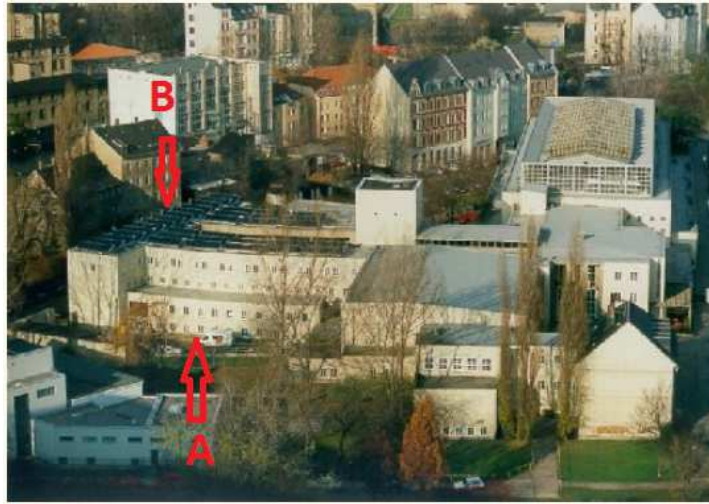


Fig1: General picture representing the 'Bauhaus' building: A- The 'Bauhaus' building, B- the solar collectors [2]

This active solar system is used to produce hot water for consumption, hot water used at heating the respective building and hot water required for the two swimming pool. The manufacturer of the solar collectors used is the company Wagner and CO and they are flat plate collectors, the type LB76. They were inclined at 30 degrees compared to roof and were used 38 solar collectors [2]. Their active total area is 288.8 square meters and the total flow rate through the collectors field is 3465,6 L/h [2], while their maximum operating temperature is 198 degrees Celsius [2]. In fig.2 we can see a scheme where we can observe the components of the active solar energy system.

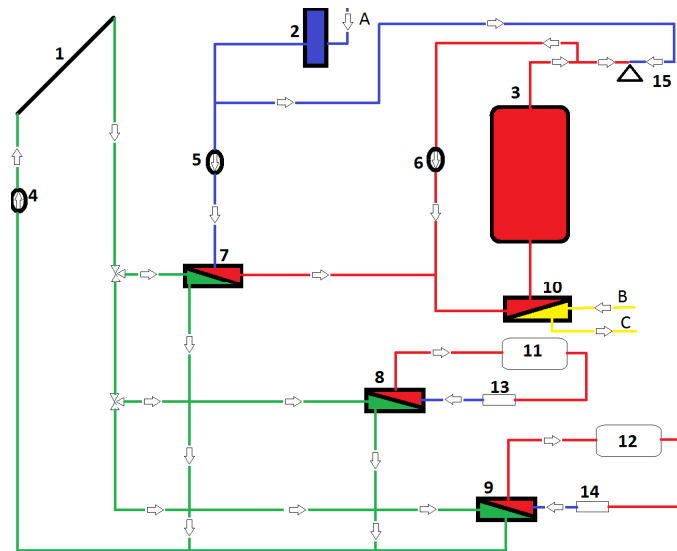


Fig.2: General scheme of the active energy system integrated in the 'Bauhaus' building: 1- solar collectors, 2- fountain, 3- storage tank 22000 L, 4,5,6- circulation pumps, 7,8,9,10- plate heat exchangers, 11- swimming pool 25 m, 12- swimming pool 50 m, 13,14- filters, 15- consumer, A- loading of the fountain with water, B,C- the heating circuit of the building

In the structure of the active solar system we can also find: a storage tank of 22000 L with the constant temperature of 60° [2], 4 plate heat exchangers and 3 circulation pumps.

3. SIMULATION OF THE ACTIVE SOLAR ENERGY SYSTEM

The simulation was made for 13 various cities from Germany. As input data in our software we have: some characteristics of the building and of the active energy system and the weather conditions specific to each city [3,4]. For the simulation, the specific characteristics of the building and of the active solar energy system were kept, only the weather conditions and geographical location varies depending on the city chosen for simulation. The city chosen for the simulation we can see them in table 1.

Table 1: The city chosen for the simulation

City from Germany	Geographical Coordinate (degrees)	
	latitude	longitude
Bremen	53,05	8,8
Dresden	51,12	13,68
Norderney	53,72	7,15
Nuernberg	49,5	11,08
Saarbruecken	49,22	7,12
Schleswig	54,53	9,55
Stuttgart	48,83	9,2
Trier-Petrieberg	49,75	6,67
Geisenheim	49,98	7,95
Hamburg	53,63	10
Hohenpeissenberg	47,8	11,02
Kassel	51,3	9,45
Werzburg	49,8	9,9

The weather conditions are taken automatically by the software from NASA (National Aeronautics and Space Administration) site [5]. As results of the simulation we have: solar radiation on tilted surface, renewable energy delivered and system efficiency of the active solar energy system, for various cities, we can see in fig.3.

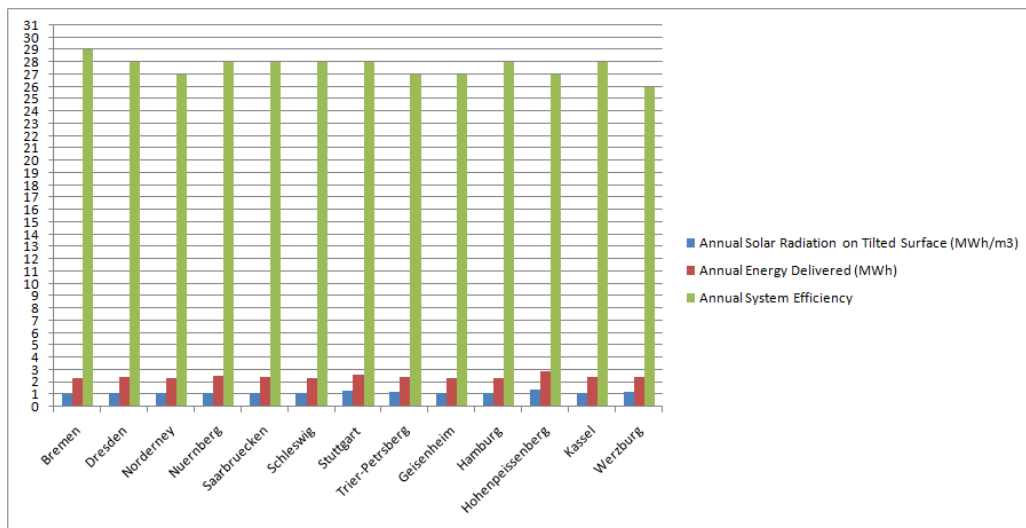


Fig.3: The results of the simulation representing: the annual radiation on tilted surface, the annual energy delivered and the annual system efficiency in various city of Germany

From fig.3, the system efficiency results are different, this aspect is normal because of the weather conditions which are specific to each city.

4. CONCLUSIONS

This work contains the following plan of composition: a brief introduction reminding the characteristics of a 'Bauhaus' building, description of the active solar energy system, also we present some specific information about this system. Finally, we presented the simulation of the active solar energy system for various cities from Germany and the simulation results. As a general conclusion, the annual system efficiency of the solar active system is between 25 - 30 %, varying due course of the different meteorological conditions.

REFERENCES

- [1] G. James Daichendt, *The Bauhaus Artist-Teacher: Walter Gropius's Philosophy of Art Education*, Teaching Artist Journal, 8: 3, 157 - 164, 2010
- [2] T. Freitag, U. Niersmann, M. Wutzler, U. Schirmer, *Wissenschaftlich-technische Programmbegleitung im Demonstrations- und Forschungsprogramm Solarthermie 2000 (Phase 2) und im Forderkonzept Solarthermie 2000plus*, Fakultät für Maschinenbau, Technische Universität Chemnitz, ISBN 978-3-9812586-0-8, 2000
- [3] M.C. Ceacaru, *Simulation of an Active Solar Energy System Integrated in a Passive Building in Order to Obtain System Efficiency*, American Institute of Physics Conference Proceedings, 1493, 223-229, 2012
- [4] RETScreen International, Empowering Cleaner Energy Decisions, <http://www.etscreen.net/ang/home.php>.
- [5] NASA (National Aeronautics and Space Administration), Surface meteorology and solar energy, <http://eosweb.larc.nasa.gov/sse/RETScreen/>.

ECVET IMPLEMENTATION IN THE NUCLEAR FIELD

Prof.dr.ing. Mihail Ceclan¹, Conf.dr.ing. Rodica Elena Ceclan¹,
and dr. César Chenel Ramos²,

¹University Politehnica of Bucharest, Romania, ² JRC-IET - Nuclear ECVET

ABSTRACT

The European Credit System for Vocational Education and Training (ECVET) is the new European instrument to answer to today's challenges for education and training in the nuclear field. In this context, the paper presents a summary of the results of UPB, nuclear engineering team from the Faculty of Mechanical Engineering and Mechatronics, in the implementation of ECVET at European level, in the nuclear field.

1. EUROPEAN CONTEXT IN NUCLEAR E&T

Today's challenge in the education and training in the nuclear field, within the EU-27 are:

- possible shortage of skilled professionals and ageing population; new approaches for human resource development in a multicultural environment;
- need for public understanding and acceptance; increasingly multidisciplinary and international character (especially in the energy sector);
- pan-European mobility in science and technology; towards a common language between the world of education and the world of work; impact of the new EU tools for E&T

The European Credit System for Vocational Education and Training (ECVET) is the new European instrument to answer to the above mentioned challenges for education and training system in the nuclear field.

The pan-European approach of work force development is based on the following instruments:

- **EQF**: European Qualification Framework for lifelong learning;
- **Europass**: portfolio of documents that describe the qualifications and competences (competences' description according to EQF)
- **a common language** between the world of education and the world of work (job taxonomy and European Competences)

Developed by the Member States, in cooperation with the European Commission, ECVET was adopted by the European Parliament and Council on 18 June 2009. ECVET ensure transformation of E&T system: from knowledge transfer to competence building.

The calendar for progressive adoption of ECVET by the EU member states has three stages: a) ECVET testing and development (2009-2011); b) countries create conditions for gradual implementation of ECVET (2012-2014); in 2014 is foreseen the first Report and Evaluation on ECVET implementation. c) ECVET implementation in all EU countries.

2. TOWARDS ECVET IMPLEMENTATION IN THE NUCLEAR SECTOR

EURATOM instruments for policy implementation in the E&T are: 7th EURATOM Framework Program and the Work Shop on Nuclear Jobs Taxonomy.

2.1 ECVET implementation in the nuclear sector

Following the calendar of progressive adoption of ECVET in EU, Euratom co-funded in the period 2009-2012 eight training schemes (“Euratom Fission Training Schemes” / EFTS) and qualification processes at EU level, in areas of nuclear fission and radiation protection as is mentioned in the table 1.

Table 1: Euratom co-funded eight training schemes

Project acronym	Area addressed
TRASNUSAFE	health physics sector (e.g., ALARA principle)
ENEN III	Training schemes: nuclear systems suppliers
ENETRAP II	nuclear safety authorities (e.g., Radiation Protection Expert)
PETRUS II	radwaste agencies (e.g., repository and engineered systems)
CINCH	nuclear and radio-chemistry (e.g., chemistry of nuclear fuel cycle)
CORONA	Regional Center of Competence for VVER Technology
EURECA!	Cooperation between EU and Canada on Super-Critical Water Reactors
GENTLE	Graduate and Executive Nuclear Training and Lifelong Education

Moreover, the ENSREG (“European Nuclear Safety Regulators Group”) meeting of 24 February 2012, Brussels underlined the importance of ECVET implementation in nuclear field:

- “new” description of jobs in terms of learning outcomes (KSC=knowledge, skills, competences)
- qualification process for higher level education and training schemes (depends of each MS)
- “Europass” whenever needed (= set of documents to describe qualifications of individuals) imply European harmonization process leading to the free circulation of nuclear experts in the EU

In order to accelerate the ECVET implementation in nuclear field, the JRC-Institute for Energy and Transport initiated a series of workshops for the definition of an ECVET-oriented Nuclear Job Taxonomy/NJT.

The general goal of the workshops on NJT encompasses the following ideas:

- to contribute to the implementation of ECVET in the nuclear area
- describing jobs and jobs requirements in terms of KSC (Knowledge, Skills and Competences)
- ECVET is intended to improve:
 - transnational mobility and mobility and portability between various sectors of the economy.
 - compatibility, comparability and complementarity of ECVET and ECTS
 - permeability between levels of education and training.

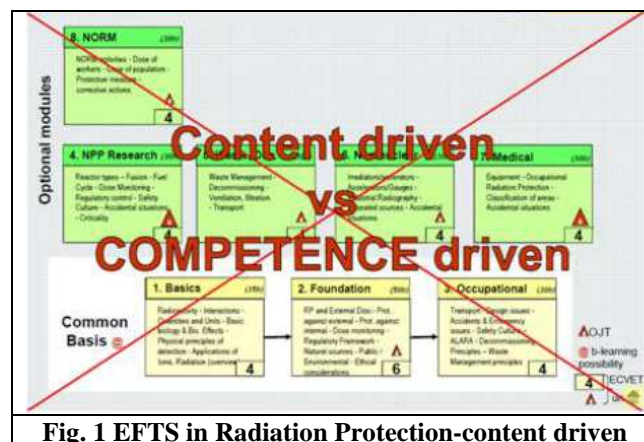
2.2 UPB contribution at ECVET implementation in the nuclear sector

UPB has a significant contribution at ECVET implementation in the nuclear sector, as a member within two “Euratom Fission Training Schemes”, ENETRAP II and ENEN III. Also UPB attended actively at all workshops on ECVET-oriented Nuclear Job Taxonomy/NJT.

The first approach within ENETRAP II project, in 2009, was to develop an modular EFTS in Radiation Protection for RPE, with the following characteristics, and represented in figure 1:

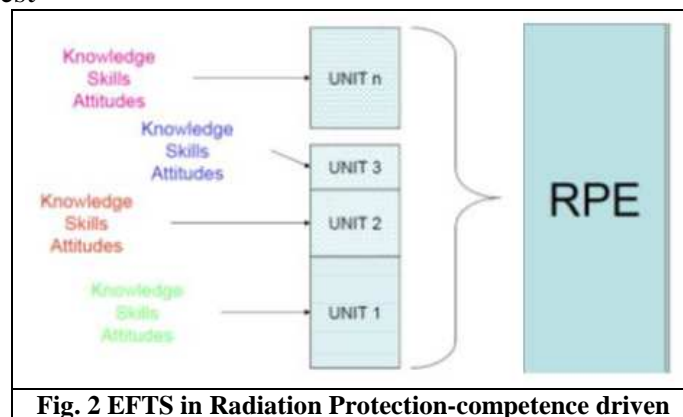
- content driven

- modular program (8 modules): common base (3 modules) and optional modules (5): NPP research; Waste&Decom; Non-nuclear applic; Medical; Norm
- this scheme allow a flexible professional itinerary



The ECVET approach, introduced in 2011, transformed EFTS in Radiation Protection into a competence driven scheme for RPE, with the new characteristics, and represented in figure 2:

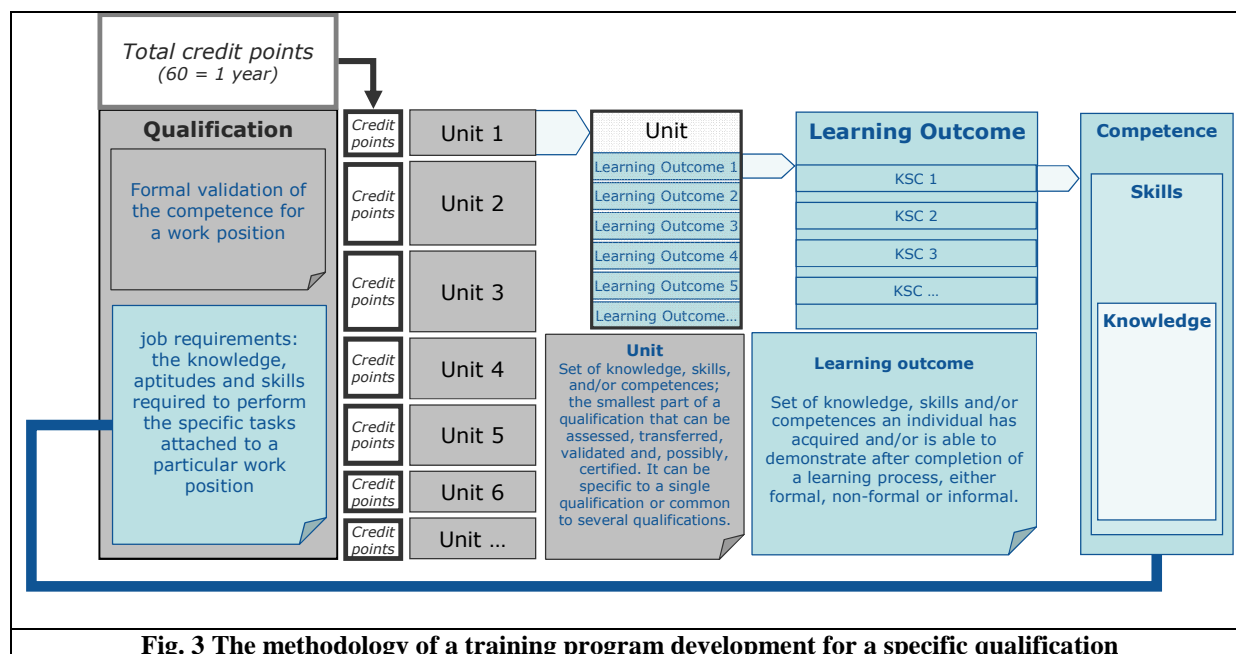
- the scheme is structured in LO Units; LO are defined in terms of KSC
- the competence driven scheme is more flexible that the content driven scheme
- a person will take only LO Units what's missing to get the RPE qualification in the area of interest



UPB contributed, within the workshops on NJT, at the methodology for training program development for a specific qualification (Fig. 3).

The specific steps to build the training program for a specific qualification are (Fig. 3):

- having the job description and the job requirements in terms of KSC or (LO), we can define a qualification;
- gathering together the families of jobs will obtain a qualification
- defining the Units of LO that correspond to a specific qualification will get the training program for a particular qualification



3. CONCLUSIONS

In the light of the ECVET approach and of results got by UPB in ECVET implementation, we can draw the following conclusions:

- The training scheme - competence driven together with other ECVET tools (job description in terms of LO (KSC), Europass) are able to improve:
 - transnational mobility and mobility and portability between various sectors of the economy.
 - compatibility, comparability and complementarity of ECVET and ECTS
 - permeability between levels of education and training.
- The training scheme- competence driven allow a very flexible professional itinerary
 - a person will take only LO Units what's missing to get the RPE qualification in the area of interest
 - allow the recognition of competences and qualifications got abroad

References

- [1] Livolsi, P.; Coeck, M.; Clarijs, T.; Massiot, Ph.; Stewart, J.; Schmitt-Hannig, A.; Vaz, P.; Fantuzzi, E.; Marco-Arboli, M.; Ceclan, M. Establish the RPE training standard: The ECVET approach as a tool, ETRAP 2013, 5th International Conference on Education and Training in Radiological Protection, **12 - 15 March in Vienna, Austria**
- [2] Livolsi, P.; Reaud, C.; Ceclan, M., International high-school student meetings: "Radiation protection workshops", ETRAP 2013, 5th International Conference on Education and Training in Radiological Protection, **12 - 15 March in Vienna, Austria**
- [3] Ceclan, M., Ceclan, R.E., Van-Goethem, G., 2010, Tendinte in constructia de reactoare nucleare de generatia a IV-a, A 9-a Conferinta Nationala de Echipament Termomecanic Clasic si Nuclear si Energetica Urbana si Rurala Proceedings, 25 Iunie 2010, Bucuresti, ISSN- 1843-3359, 51- 55;
- [4] Ceclan, M., Ceclan, R.E., Marco, M., Livolsi, P., Moebius, S., Schmitt-Hanig, A., Draaisma, F.S., Elsacker-Degenaar, H., Coeck, M., Stewart, J., de Regge, P.P., Vaz, J.P., Zagytai, P., Fantuzzi, A.E., 2010, ENETRAP II: a new approach to education and training in radiation protection, A 9-a Conferinta Nationala de Echipament Termomecanic Clasic si Nuclear si Energetica Urbana si Rurala Proceedings, 25 Iunie 2010, Bucuresti, ISSN- 1843-3359, 47 – 51;

LPG USE FOR A CLEAN RUNNING DIESEL ENGINE

Alexandru CERNAT¹, Niculae NEGURESCU², Constantin PANA²

University Politehnica of Bucharest

ABSTRACT

Liquid petroleum gas is a totally new alternative fuel for diesel engines that provides the possibility of diesel emissions level reduction. The engine performance and fuel efficiency can be maintained or improved with dual fuelling. The LPG is injected into the intake manifold into the inlet aspirated air, fuelling system using two electronic control units, for LPG and diesel fuel, connected back to back. The substitution of the diesel fuel by LPG will decrease with almost 45%....65% the smoke emission, with 30%.....77% the unburned hydrocarbons and 20%...40% the NO_x. The LPG cycle dose will affect the engine cycle maximum pressure which increases with ~ 10%...20% and maximum pressure rate, 68%...130% higher comparative to classic diesel engine, the values for COV in maximum pressure and IMEP. Following the simultaneous correlation between different parameters as soot emissions - break specific fuel consumption - cycle maximum pressure – IMEP-COV values, the optimal substitute ratio of diesel fuel by LPG can be establish.

Keywords – alternative fuel, diesel engine, smoke, LPG

1. INTRODUCTION

Replacing fossil fuel classical unconventional petroleum origin was initiated decades ago and is one of the major concerns of today and because it can thus provide a significant reduction in emission levels with saving oil reserves. Number of chemical species that are found in the exhaust gases is very high, about 1000, but only few of them are subject to the pollution laws: HC hydrocarbons, carbon monoxide CO, nitrogen oxides NO_x, particulate matter PM, and smoke (diesel engines), carbon dioxide is considered a greenhouse gas, [2], [3], [4], [5]. From gaseous alternative fuels, **Liquid Petroleum Gas** offers the most promising prospects of use. It can assure the operation of a diesel engine with low emissions of soot and NO_x, at the same level of efficiency. The low calorific value of LPG as 45892 kJ / kg (for a mixture of 50% propane and 50% butane), [7], is higher than that of diesel fuel, 42500 kJ / kg, direct influences the energy efficiency of the engine fueled with diesel fuel and liquefied petroleum gas, estimating a reduction or maintaining effective specific fuel consumption. Adiabatic flame temperature of 2054 °C for diesel fuel is higher than liquefied petroleum gas, allocated to 1990 °C. The smaller flame temperature in the case of LPG-air mixture combustion has direct implications on reducing combustion process temperature, on reduction of nitrogen oxides emissions from the exhaust gases, [7]. Is difficult to use LPG as single fuel in diesel engine due to its high resistance to autoignition, registering a very low cetane number value of CN = -2 ... -3, which involves the use of a diesel fuel pilot for LPG-air mixture ignition. [2], [3], [4], [5], [6], [7].

The mixture of air and LPG can be achieved outside the diesel engine cylinder by diesel-gas method. This involves the combustion inside of the engine cylinder of a mixture between diesel fuel and LPG, the diesel engine being equipped with an additional fuelling system for

¹Lecturer; ² Prof.; Prof.; Splaiul Independentei no.313, e-mail:cernatalex@yahoo.com, phone:0723470021

LPG, directly connected to the engine inlet (the gas injectors are directly connected to the intake manifold), ignition of the admitted mixture being made by the injection of diesel fuel pilot into the cylinder. The maximum amount of LPG sent it in the engine intake will be limited for reasons of maintaining the engine reliability, since it can be record it increased values of the in-cylinder maximum pressure and much higher values of pressure rate.

2. METHODOLOGY

The experimental researches were carried on an automotive diesel engine, type K9K –1.5 dci, power of 50 kW/4000 rpm and torque of 150 Nm/2000 rpm, equipped with a LPG injection electronic system, at the operating regime of maximum torque and for different substitution percents of the diesel fuel by LPG. The experimental engine was mounted on a test bench, figure 1, equipped with the next necessary instruments for measuring operations: Schenck E90 eddy current dynamometer, real time AVL data acquisition system for processing and storage of measured data's, AVL in-cylinder pressure transducer line, AVL DiCom gas analyzer and opacimeter for Diesel engines, Khrono Optimass mass flow meters, engine inlet air flow meter, thermo resistances for engine cooling liquid temperature, engine oil and air intake temperatures and thermocouples for exhaust gas temperature, manometer for air pressure from engine intake manifold, LPG gas detector for test bad cell, [7]. All instrumentation was calibrated prior to engine testing.

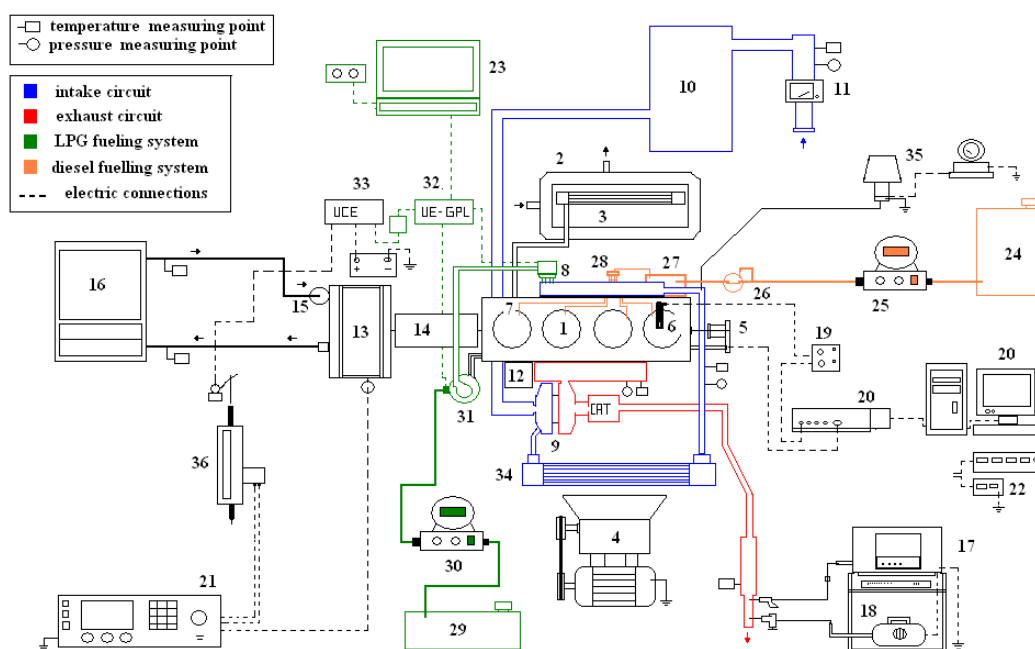


Figure1: Test bed schema

1 – 1.5 dci K9K diesel engine; 2 – engine cooling system; 3 – engine water cooler; 4 – intercooler fan; 5 – engine angular encoder; 6 –AVL piezoelectric pressure transducer; 7 – diesel fuel injector; 8 – LPG injector; 9 – Turbocharger; 10 – intake air drum; 11 – intake air flow meter; 12 – exhaust gas recirculation; 13 –Schenck E90 dyno; 14 – dyno-engine coupling; 15 –Schenck E 90 dyno cooling water pump; 16 –dyno cooling system; 17 –AVL Dicom 4000 gas analyser; 18 –AVL Dicom 4000 Opacimeter; 19 –AVL charge amplifier; 20 – PC + AVL data

acquisition system; 21 –Schenck E 90 dyno controller; 22 – temperatures displays: a) – exhaust gas; b) – intake air; c) – engine oil; d) – engine cooling liquid; e) – engine oil pressure; 23 – diesel fuel and LPG injection control Laptop; 24 – diesel fuel tank; 25 – diesel fuel mass flowmeter; 26 – fuel filters; 27 – high pressure pump for common Rail; 28 –Common Rail; 29 – LPG tank; 30 – LPG mass flowmeter; 31 – LPG vaporizer; 32 –LPG ECU; 33 –diesel engine ECU; 34 –intercooler; 35- supercharge pressure measuring system; 36- throttle actuator

The fuelling system for LPG uses an injectors unit connected to engine intake manifold and controlled by a LPG electronic control unit connected back to back with the main engine ECU in order to establish the LPG cycle dose for every operating regime, [2], [3], [4], [6], [7]. In order to control the fuels cycle doses, the LPG electronic control unit works in parallel with the main ECU of the engine and is connected to a computer which allows the modification of the injectors opening duration. In this way the diesel fuel cycle quantity is reduced at the increase of LPG dose in order to maintain the engine power for engine reliability keeping. Experimental research's carried out to obtain fuel consumption characteristics for different speeds and engine full load and to determinate the energetically and pollutant engine performance. Based on fuel consumption characteristics were obtained some graphic representations for different parameters such as: brake specific fuel consumption (BSFC), pollutants emissions level (HC, NO_x, smoke) versus to LPG substitute ratio, xc. Pressure diagrams of 50 consecutive cycles were registered in order to analyse the influence of LPG dose on the combustion process.

The experimental investigations were performed at different engine operating regimes for diesel fuel and LPG dual fuelling at various ratios of diesel fuel substitution, expressed by an energetic substitution ratio xc.

Figure 2 shows the pressure variation diagrams at 100% load and the speed of 2000 rpm, maximum torque regime, for different degrees of substitution of diesel by LPG.

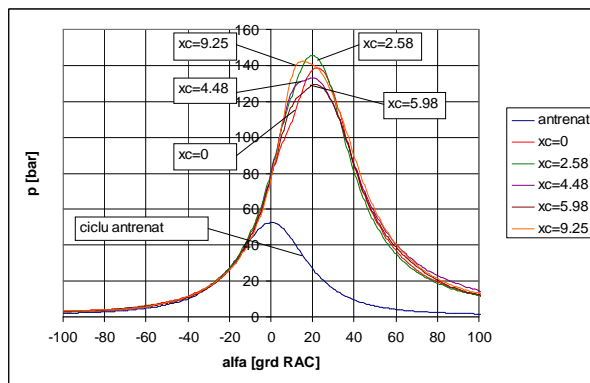


Figure 2: Pressure diagrams for 100% load, 2000 rpm

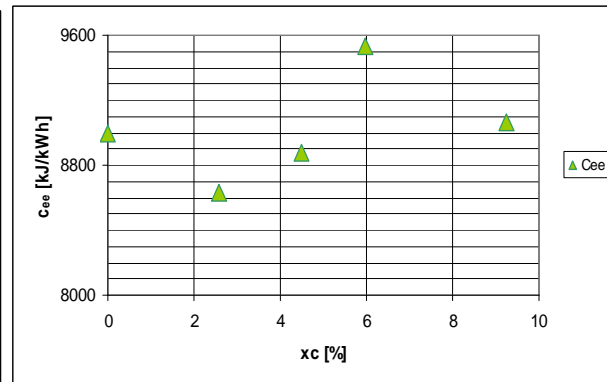


Figure 3: BSFC for 100 % load and 2000 rpm

The experimental investigations have revealed the influence of the substitution ratio of diesel with LPG on efficiency, on maximum pressure and maximum pressure rate and on pollutant emissions. Variations of these parameters depending on the xc substitution ratio of diesel fuel with LPG, at full load regime and 2000 rpm are shown in figures 3 ... 8.

For engine speed of 2000 rev / min it shows that the optimal value of the substitution ratio $xc = 2.58$ % for which the specific fuel consumption is reduced by about 4% comparative to standard regime when only the diesel fuel is used, figure 3. To the increase of substitute ratio, the specific fuel consumption increases with of 2.8% compared to maximum efficiency for $xc = 4.48$, the value still being lower by 1.27% compared to the amount allocated for diesel fuelling.

For higher percentages efficiency is reduced by 5.6% comparative to diesel fuelling, the substitution coefficient being $x_c = 5.98$. Considering a maximum variation of specific fuel consumption by 2%, compared to the reference value corresponding for diesel fuelling, is resulting a limit value of $x_c = 5\%$. The efficiency of engine fueled with diesel fuel and LPG, at maximum torque speed, tends to maintain or to improve for small LPG quantity admitted into the cylinder, $x_c = 2.58, 4.48$. For higher ratios of substitution, the specific fuel consumption increases comparative to classic fuelling solution, the limitation of LPG cycle quantity being in concordance with the limitation of engine efficiency reduction. In conclusion, at maximum torque speed, the specific fuel consumption values are relatively close to the reference, for all the values assigned to the ratio of substitution.

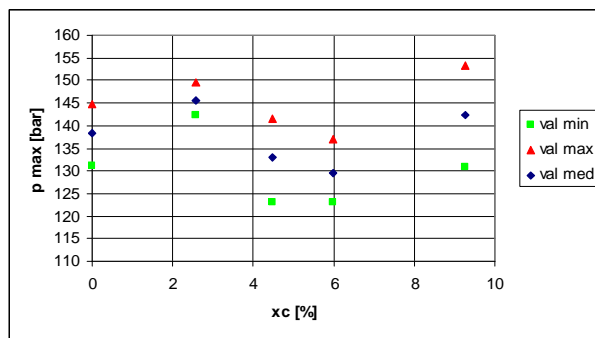


Figure 4: Maximum pressure for 100 % load, 2000 rpm

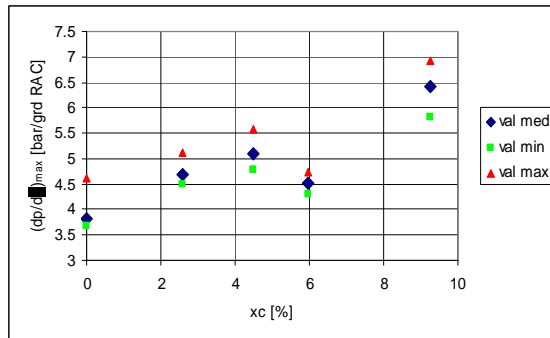


Figure 5: Maximum pressure rate for 100 % load, 2000 rpm

Increasing the amount of LPG leads to increasing of maximum pressure per cycle, and increasing of maximum pressure value dispersion and thus the degree of successive operational cycle's irregularity (figure 4). Also, the angle of maximum pressure α_{pmax} occurs, tends to approach the PMI, which corresponds in general to a more rapid combustion brutal [7]. Formation of high homogeneity mixtures between air and LPG leads to a faster combustion during the preformed mixtures combustion phase, by the reaction kinetics at low temperatures. This involves, besides the increasing of the in-cylinder maximum pressure up to 10% for maximum x_c (figure 4) also the increasing of the maximum pressure rate value. Thus, at 2000 rev / min and 100% load operating regime, the increasing of the in-cylinder LPG quantity leads to an increase of the maximum pressure rate, figure 5. Increasing of the maximum pressure derivative is maximum for $x_c = 9.25$ and represents a value higher with 68% comparative to the reference value. Increasing of the maximum derivative of pressure is limited to the substitute ratio value $x_c = 10$ for the maximum torque engine speed, resulting an obtain values that don't exceed 7 bar / CA deg. For other substitute ratios, the growth are lower, 23% for $x_c = 2.59$, respectively 33.8% for $x_c = 4.48$ [7].

In terms of specific fuel consumption maintaining to a value much closer to the standard diesel engine, it can provide it a significant reduction in the emission of unburned hydrocarbons by 68 ... 77%, figure 6. Also important HC emission reductions of 30....50% can be achieved while maintaining the engine operation efficiency. High-speed combustion of air-LPG homogeneous mixtures ensures the HC emissions reduction.

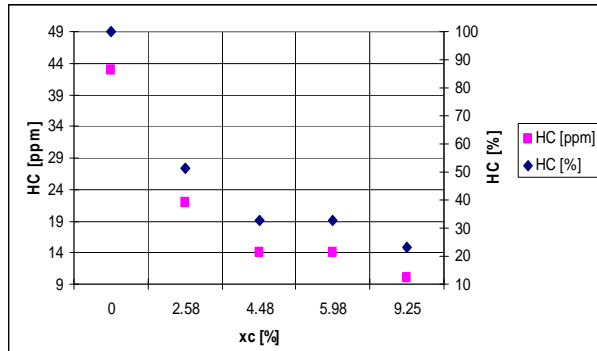


Figure 6: HC emission for 100 % load and 2000 rpm

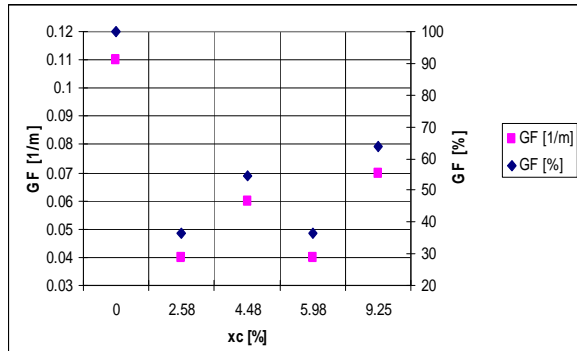


Figure 7: Smoke emission for 100 % load, 2000 rpm

The emission of smoke from the exhaust gases is appreciated by the degree of smoke GF, determined for each substitution ratio of diesel fuel by LPG. The emission of smoke was greatly diminished compared to values for only diesel operation. Reduce by 64% the level of smoke since the relatively low degree of substitution, $xc = 2.58, 4.48$, are achieved, figure 7. Over this xc values, the degree of smoke recorded an upward trend, with values below the reference value. For this reason, the trend of smoke increasing was one of the factors that limit during experiments, the substitution ratio xc .

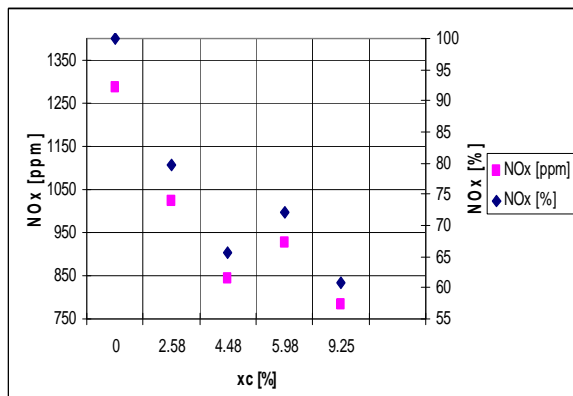


Figure 8: NO_x emission for 100 % load, 2000 rpm

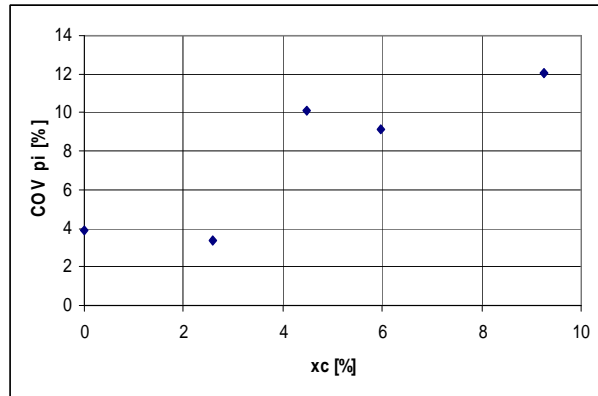


Figure 9: (COV)_{pi} coefficient for 100% load, 2000 rpm

The NO_x emission in case of diesel and LPG fuelling is reduced by up to 40% compared to the value recorded for only diesel fuelling, figure 8. A substitution ratio of 2.58% in diesel fuel ensuring a reduction in NO_x emissions with 21% compared to the value measured for diesel fuelling and with 35% at $xc = 4.48$. For $xc = 9.25$ is obtain the largest reduction of 40%, for which the engine efficiency is close to the classic engine or is slightly reduced. From this point of view It can be said that the maximum reached reduction of nitrogen oxide emissions is achieved while maintaining the engine efficiency. Under the aspect of maximum efficiency obtained criterion, for $xc = 2.58$, a significant reduction of emissions by 20% can provided, figure 8. For maximum torque speed, the cycle variability coefficient in IMEP (COV)_{pi} is about 3 times higher than the reference, at the maximum substitution ratio, figure 9. For this reason becomes clear the need of limitation of the used substitution ratio to $xc = 9.25\%$. If is admitted as limit value $[(COV)_{pi}]_{max} = 10\%$, a limit substitute ratio value of $xc = 8\%$ results.

3. CONCLUSIONS

The experimental study revealed the main characteristics of diesel engine fuelled with diesel fuel and LPG, the following main conclusions can be drawn:

1. Partial substitution of diesel fuel by LPG can be achieved, compared to only diesel fuelling, a significant reduction in hydrocarbons, smoke and NO_x , in terms of power performance maintaining and of a limited variation in specific fuel consumption.
2. Running on diesel fuel and LPG leads to a trend of increase in maximum pressure rate $(dp/d\alpha)_{\max}$ and in cycle to cycle variability for IMEP $(\text{COV})_{\text{pi}}$, versus classical diesel fuelling solution.
3. The substitute ratio of diesel fuel with LPG, x_c , is limited by the maximum values, or by the maximum range of variation admitted for some engine running characteristic parameters as it follows: if you admit for the cyclic variability a maximum level of $(\text{COV})_{\text{pi}} = 10\%$, the substitute ratio is limited to $x_c = 8\%$; if the maximum pressure rise is limited to $(dp/d\alpha)_{\max} = 8 \text{ bar/CA deg}$, the LPG substitution ratio is limited to $x_c = 10\%$; a reduction of smoke emission by 40% compared to diesel fuel operation can be achieved only with a substitution ratio of $x_c = 6\%$; at these limits of LPG substitution ratio, a reduction of 70% in hydrocarbon emissions and of 35% in NO_x emissions is obtained.
4. Brake specific fuel consumption (BSFC) variation is in the area of $\pm 2\%$ for the limit values of $x_c = 5\%$ to 2000 rev / min at full load regime.

References

- [1] S. Goto, L. Daeyup, "Development of an LPG DI Diesel Engine Using Cetane Number Enhancing Additives", Alternative Fuels 1999, SAE Inc., USA, ISBN 0-7680-0493-4, pp205-214
- [2] C. Pana, N. Negurescu, M. G. Popa, Al. Cernat, P. Despa, Fl. Bujgoi, "Aspects of the LPG Use in Diesel Engine by Diesel-Gas Method", FISITA World Congress, Munchen, 2008
- [3] C. Pana, N. Negurescu, M. G. Popa, G. Boboc, Al. Cernat, "Reduction of NO_x , Smoke and BSFC in a Diesel Engine Fueled with LPG", MECCA Journal of Middle European Construction and Design of Cars, vol III, No. 4, pp37- 43, December 2005, Praha, Czech Republic, ISSN 1214-0821
- [4] C. Pana, N. Negurescu, M. G. Popa, Al. Racovitza, G. Boboc, Al. Cernat, "Performance of a Diesel Engine Fueled by LPG", 5th International Colloquium Fuels 2005, pp 143-148, January 12-13, 2005, Technische Akademie Esslingen, Germany, ISBN 3-924813-59-0
- [5] C. Pana, N. Negurescu, M.G. Popa, Al. Racovitza, "Performance of LPG Fuelled Diesel Engine Using DMI method", 4th International Colloquium Fuels 2003, pp.451-460, January 15-16, 2003, Technische Akademie Esslingen, Germany, ISBN 3-924813-51-5
- [6] C. Pana, N. Negurescu, M. G. Popa, Al. Cernat, D. Soare, P. Despa, Fl. Bujgoi, "Dual Fuelling System with Alternative Fuels for Ecological Automotive Diesel Engine", Research contract no. X2C10/2006, University Politehnica Bucharest, Romania
- [7] Cernat Alexandru, "Contributii la studiul functionarii unui motor diesel la alimentarea cu motorina si gaz petrolier lichefiat", Teza de doctorat, U.P.B., 2010

SYSTÈME MODERNE DE CALCULE COMPLET DE LA VIBRATION DE L'AUBE D'UNE TURBINE À VAPEUR OU À GAZ POUR LE RÉGIME NOMINAL.

Dr. Ing. Mihai DELGEANU – L'Université Polytechnique de Bucarest.

ABSTRAIT.

L'ouvrage présent la réalisation d'une équation mathématique qui permet la construction d'un logiciel complexe pour obtenir la fréquence de vibration d'une aube de turbine.

1. CONSIDÉRATIONS GÉNÉRALES.

L'aube, due à sa forme de profil aérodynamique, s'approche de la plaque plane en mouvement vibratoire. D'ici l'idée d'utiliser thermes de la vibration de la plaque plane mais aussi des perfectionnements d'écoulement et de construction pour s'approcher de la valeur de la fréquence réelle mesurable.

2. LA TRAJECTOIRE MOYENNE DES PARTICULES DU FLUIDE CIRCULANT DANS LE CANAL BORDÉ PAR LES PAROIS DES DEUX AUBES VOISINES.

2.1. La particule de fluide sur la trajectoire.

Les forces supportées par la particule sont:

- la force d'impulsion de type action directe donnée de l'énergie cinétique du fluide circulant à la sortie de l'ajutage et à l'entrée du canal des palettes;
- la force d'impulsion de type réaction donnée par la sortie du fluide du canal des palettes avec une vitesse relative supérieure à la vitesse relative d'entrée;
- la force centrifuge donnée par la circulation sur la trajectoire courbe (associée à l'accélération correspondante);
- la force centripète qui maintient la particule sur la trajectoire (associée à l'accélération correspondante).

Les parois du canal sont l'intrados et l'extrados de la palette supérieure et inférieure.

2.2. L'équation différentielle de la trajectoire.

À l'aide des idées lancées en [4], nous voulons réaliser un abord rationnel du rapport entre le canal d'écoulement, comme élément déterminant, et le profil de la palette, comme paroi du canal, dans la détermination mathématique des profils des aubes.

I. La prémisses constructive qui représente l'utilisation uniforme de la largeur des palettes pour la production de la puissance, ce que mathématiquement [5] signifie (où B est la largeur axiale de l'étage mesurée dans la direction d'écoulement x):

$$[w/m] \quad \frac{dP}{dx} = \frac{P}{B} = \text{constant} \quad (2.1)$$

II. La prémisses fonctionnelle qui représente la réalisation des conditions de maximum énergétique (rendement maximal), ce que mathématiquement [5] signifie accélération constante dans la direction de la vitesse périphérique pour l'écoulement du fluide circulant en canal.

$$[J/kg] \quad w_a^2 + \left(w_u + \frac{h}{\Delta w_u} \right)^2 = w_{1a}^2 + \left(w_{1u} + \frac{h}{\Delta w_u} \right)^2 \quad (2.2)$$

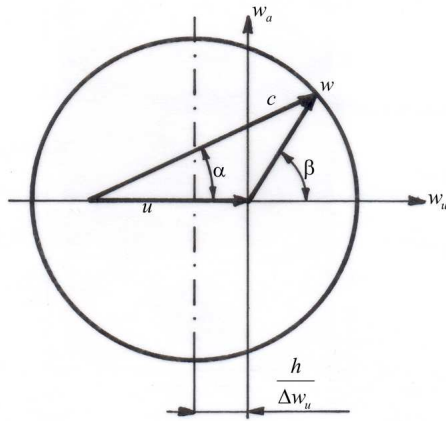


Fig.1. La représentation graphique de l'équation constructive de base.

Cette équation est représentée dans la (Fig.1.).

Sur les axes $w_a w_u$ elle est un cercle désaxé avec $h/(\Delta w_u)$ au long de l'axe w_u .

Sur ce cercle on peut marquer les vitesses:

- Absolue c
- Relative w
- Périphérique u

Et leur angles α et β .

On peut éliminer la vitesse w et on obtient l'équation différentielle de la trajectoire moyenne:

$$\frac{dy}{dx} = \frac{w_{1u} - \Delta w_u \frac{x}{B}}{\sqrt{w_1^2 + 2h \frac{x}{B} - \left(w_{1u} - \Delta w_u \frac{x}{B}\right)^2}} \quad (2.3)$$

2.3. L'équation intégrée de la trajectoire.

$$\frac{y}{B} = \sqrt{\frac{x}{B} \left(1 - \frac{x}{B}\right) + tg^2 \alpha_1} - tg \alpha_1 - \frac{\rho}{2(1-\rho)} \left[\arcsin \frac{\frac{x}{B} - \frac{1}{2}}{\sqrt{\frac{1}{4} + tg^2 \alpha_1}} + \arcsin \frac{\frac{1}{2}}{\sqrt{\frac{1}{4} + tg^2 \alpha_1}} \right]$$

2.4. Les éléments géométriques de la trajectoire.

L'équation de la trajectoire permet d'obtenir directement les angles d'entrée et de sortie dans le canal des palettes.

$$[\circ] \quad \beta_1 = \arctg \left[\frac{2(1-\rho)}{1-2\rho} tg \alpha_1 \right] \quad \beta_2 = \arctg [-2(1-\rho) tg \alpha_1] \quad (2.4)$$

3. LES PARAMÈTRES GÉOMÉTRIQUES DE CIRCULATIONS ET DE RÉSISTANCE DE L'AUBE.

3.1. L'éléments d'inertie pour la plaque plane en vibration.

Les liaisons tangentielles de la plaque plane augmentent le moment d'inertie équivalent face au moment d'inertie d'une barre classique pour l'ancien système de calcul.

$$[Nm^2] \quad D_i = \frac{E_0 I_{xi}}{\sqrt{1-\mu^2}} \quad (3.1)$$

3.2. La variation du débit de fluide circulant sur la longueur de l'aube d'impulsion.

Le débit d'un tronçon de canal pour le fluide circulant est: $\dot{M}_i = \frac{d_b + (2i-1)l}{100(d_b + 100l)} \dot{M}_p$

3.3. La force d'impulsion sur un tronçon de trajectoire.

$$[N] \quad f_{ui} = \dot{M}_i (w_{1i} \cos \beta_{1i} + w_{2i} \cos \beta_{2i}) \quad (3.2)$$

3.4. Le calcul du vrillage.

La forme finale utilisable est très simple mais très importante parce que elle donne le pas relatif, la trajectoire, l'équation de l'extrados et l'équation de l'intrados de l'aube pour le tronçon.

3.5. La longueur de l'aube.

$$[m] \quad l_p = \frac{\sqrt{2} - 1}{\sqrt{2}} d_b \approx 0,207106781 d_b \quad (3.3)$$

3.6. La largeur moyenne d'un tronçon.

$$[m] \quad B_i = B_b \sqrt{\frac{\pi - 2 \arctg(2tg \alpha_{1b})}{\pi - (\beta_{1i} + \beta_{2i})} \frac{\cos \beta_{1i} + \cos \beta_{2i}}{2 \cos[\arctg(2tg \alpha_{1b})]} \left[1 - (2i - 1) \frac{3l}{4d_b} \right]} \quad (3.4)$$

3.7. L'alignement des centres de poids sur l'axe longitudinal.

Pour empêcher la force centrifuge de donner moment de flexion sur la section de base, les centres de poids doit être alignées sur le même axe longitudinal de la palette. La construction par tronçons donne la nécessité d'obtenir la position du centre de poids avec ses coordonnées rapportées à un système d'axes commune au long de la palette.

$$[N] \quad f_{ui} = \dot{M}_i (w_{1i} \cos \beta_{1i} + w_{2i} \cos \beta_{2i}) \quad (3.5)$$

4. LA VARIATION DES CHARGEMENTS ENTRE LES POSITIONS LIMITES.

4.1. La flèche de l'aube de turbine assimilée à la plaque plane en vibration.

La variante I. L'aube avec charge uniforme distribuée sur tronçons sans préciser les liaisons en régime statique.

L'encastrement de base.

La variante II. L'aube avec charge uniforme distribuée sur tronçons en régime statique et avec bandage sur le but opposé à l'encastrement.

$$[rad], [m] \quad \varphi_k^{sB} = \varphi_k^s - \varphi_k^B \quad v_k^{sB} = v_k^s - v_k^B \quad (4.1)$$

La variante III. L'aube avec charge uniforme distribuée sur tronçons en régime dynamique.

$$\begin{aligned} [Ns^2] \quad \frac{F_i^c}{n^2} &= \rho_M S_i l (2\pi)^2 \left(\frac{d_b}{2} + il \right) & \frac{m_i}{n^2} &= \\ [Nms^2] \quad \frac{F_i^c}{n^2} v_i^s &= \rho_M S_i l (2\pi)^2 \left(\frac{d_b}{2} + il \right) v_i^s & & \end{aligned} \quad (4.2)$$

$$[rad], [m] \quad \varphi_k^d = \left(\frac{\varphi_k^d}{n^2} \right) n^2 \quad v_k^d = \left(\frac{v_k^d}{n^2} \right) n^2 \quad v_k^R = v_k^s - v_k^d \quad v_k^R = v_k^s - v_k^B - v_k^d \quad (4.3)$$

4.2. La fréquence propre de l'aube.

$$p^2 = \frac{g \sum_{i=1}^{i=i} F_i v_i}{\sum_{i=1}^{i=i} F_i v_i^2} \quad [s^{-2}]$$

$$f_p^a = f_p^c = \frac{1}{2\pi} \sqrt{\frac{g \left[\sum_{i=1}^{i=i} (q_i^a + q_i^L) v_i^a + 2 \sum_{i=1}^{i=i} \left(\frac{L_i^c}{l} \right) \right]}{\sum_{i=1}^{i=i} q_i^a (v_i^a)^2}} \quad (4.4)$$

5. LES PERTES QUI PEUVENT CHANGER LA FRÉQUENCE PROPRE

5.1. Les pertes d'énergie cinétique par frottement dans la couche limite.

$$q_i^L = 0,0371 \rho_{vap} w_{ui}^2 (2L_i) \left(\frac{w_{ui} L_i}{\nu} \right)^{-0,2} \quad (5.1)$$

L'influence des pertes sur la fréquence propre dépasse 10 %.

5.2. Les pertes d'énergie cinétique par friction centrifugeuse sur le profil de l'aube.

Pour le calcul de la fréquence propre on utilise le travail mécanique de déplacement perdu on utilise la valeur relative:

$$\left(\frac{L_i^c}{l} \right) = 0,15 \rho_{vap} L_i^2 l [d_b + (2i-1)l] \left(\frac{w_i L_i}{\nu} \right)^{-0,2} n^2 \quad (5.2)$$

L'influence de cette perte dépasse 5 % sur la fréquence propre.

6. CONCLUSION SUR LE PHÉNOMÈNE DE RÉSONANCE.

Si on utilise la (Fig.17.) et la relation (5.9) de l'ouvrage complète on peut discuter, mathématiquement, la résonance qui se réalise quand $f_p = f_i$.

Bibliographie selective.

1. Buzdugan, Gh.: **Calculul de rezistență la solicitări variabile**, București, Ed. Tehnică, 1963
2. Buzdugan, Gh.: **Măsurarea vibrațiilor mecanice**, Ed. Tehnică, București, 1964.
3. Delgeanu, M.: **Les vibrations des systèmes mécaniques. Applications.**, Edition U. S. T. O. (Université des Sciences et de la Technologie d'Oran), Génie mécanique, Post Graduation , 1984.
4. Delgeanu, M.: **CONTRIBUȚII LA STUDIUL VIBRAȚIILOR PALETELOR TURBINELOR CU ABUR ÎN REGIMURI NENOMINALE**, teză de doctorat, Universitatea Politehnica din București, 2007.
5. Delgeanu, M.: **MACHINES THERMIQUES. PROCESSUS THERMIQUES, CONSTRUCTION ET CALCUL DES TURBINES À VAPEUR ET DES CHAUDIERES DE VAPEUR**, Ed. MAN-DELY BUCUREȘTI, 2011, ISBN:973-7689-09-7.
6. Filipov, A.P.: **Vibrațiile corpurilor**, Moskva, Mașinostroenie 1970.

SYSTÈME MODERNE DE CALCULE COMPLET DE LA VIBRATION DE L'AUBE D'UNE TURBINE À VAPEUR OU À GAZ POUR LE RÉGIME NON NOMINAL

Dr. ING. Mihai DELGEANU – L'Université Polytechnique de Bucarest.

ABSTRAIT.

L'ouvrage présent la réalisation d'une équation mathématique qui permet la construction d'un logiciel complexe pour obtenir la fréquence de vibration d'une aube de turbine à vapeur pour le régime non nominal.

1. CONSIDÉRATIONS GÉNÉRALES.

L'aube, comme profil aérodynamique s'approche de la plaque plane en vibration.

2. L'AUBE EN RÉGIME DYNAMIQUE.

Le régime dynamique suppose mouvement de rotation avec une vitesse de rotation n qui produit force centrifuge. La force centrifuge, due à la flèche statique, produit moment face à l'encastrement. Ce moment produit une flèche dynamique qui diminue la flèche statique parce qu'elle s'oppose à celle-ci. Mathématiquement résulte une variable supplémentaire au temps des régimes non nominaux qui est la vitesse de rotation. Cela suggère l'idée de travailler toute jours relatif par rapport à n^2 de la force centrifuge.

3. LA FRÉQUENCE PROPRE DE L'AUBE.

3.1. Généralités.

L'aube est un système continu avec nombre infini de degrés de liberté. La difficulté ne consiste pas de résoudre mathématiquement du déterminant mais d'apprécier correctement des constantes élastiques du système élastique discrétisé.

3.2. La pulsation propre utilisant l'équation des énergies.

De l'égalité des deux énergies maximales résulte l'équation générale de la pulsation:

3.3. L'introduction des pertes d'énergie cinétique par frictions dans la couche limite.

3.4. L'introduction des pertes d'énergie cinétique par frictions de centrifuge sur le profil de l'aube.

Les calculs effectués à l'aide du program, développé montre que la valeur des pertes dues à l'effet de centrifuge peut influencer la fréquence avec 5%.

3.5. La fréquence propre de l'aube.

On peut calculer les fréquences:

$$[s^{-1}] \quad f_p^a = f_p^c = \frac{1}{2\pi} \sqrt{\frac{g \left[\sum_{i=1}^{i=100} (q_i^a + q_i^L) v_i^a + 2 \sum_{i=1}^{i=100} \left(\frac{L_i^C}{l} \right) \right]}{\sum_{i=1}^{i=100} q_i^a (v_i^a)^2}} \quad (3.1)$$

4. L'ALGORITHME FINAL DE CALCUL.

L'algorithme a été présenté dans l'ouvrage précédant.

4.1. Données d'entrée.

Les données d'entrée ont été présentées dans l'ouvrage précédant.

4.2. L'algorithme de calcul.

L'algorithme a été présenté dans l'ouvrage précédant.

5. LE RÉGIME NON NOMINAL ET SON INFLUENCE SUR LA VIBRATION DE L'AUBE.

5.1. Généralités.

Les régimes transitoires aux turbines à vapeur n'accomplissent pas les conditions mathématiques de variation en temps infini petit et ça ne nous permet l'utilisation des équations différentielles caractéristiques. Les organes de réglage sont très grands, avec réactions attardées, et le répons ne s'encadre pas dans les valeurs d'un régime transitoire mathématique. Correctement, un tel régime pourrait être défini comme non nominal, donc un régime en qui les paramètres varient face aux valeurs nominales normales de fonctionnement. Pour un tel régime le pente de variation des paramètres est petite et, mathématiquement, nous avons une variation de type rampe non de type échelon.

L'auteur découvrir personnellement dans sa thèse de doctorat que l'étude complexe du système enchainé rotor vibratoire (arbre en vibration, disque en vibration et aube en vibration) a le degré plus petit possible 16 en renonçant à 11 facteurs d'influence de petite importance (les facteurs impliqués et les corrélations qui doivent prises en considération sont déjà discutés). Les méthodes actuelles mathématiques de désenchaîner des systèmes enchainées jusqu'à 8 degré utilisent installations très puissantes mais avec accès très limité (Boeing Corporation, L'armée russe, L'armée américaine).

5.2. La modification des triangles de vitesses.

Illustrative pour la modification des triangles de vitesses est (Fig.1.). Les triangles de la (Fig.1.A.) sont celles initiales donc, de notre point de vue, celles du régime nominal donc avec paramètres non modifiés. On remarque que la turbine a été projeté pour ce régime et donc les paramètres géométriques des ajetages et des aubes sont construits et non modifiables. Donc ne sont pas modifiables, dans les régimes non nominaux, les paramètres:

Si on modifie la valeur de la vitesse c_1 (Fig.1.B.), comme les angles α_1 et β_1 et respective la vitesse périphérique u ne se modifie, la vitesse d'entrée d'aubes w_1 déviée se décompose dans une composante sur la direction géométrique d'entrée dans aubes β_1 et une composante normale à cette direction:

Cette dernière vitesse se décompose sur les directions prioritaires u et a comme on voit dans médaillon:

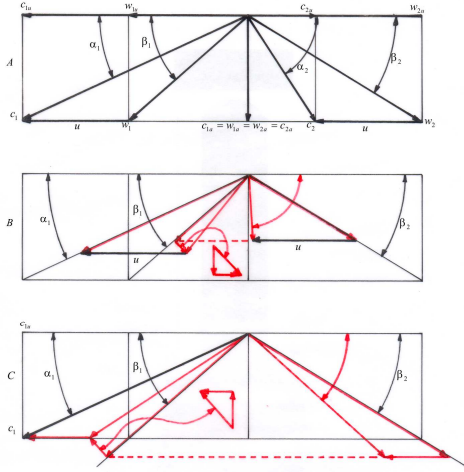


Fig.1. La modification des triangles de vitesses.

La composante sur axial augmente la vitesse axiale, donc l'énergie développée sur axial qui ne produit pas puissance et donc est nocive.

La composante périphérique est dans le sens contraire au mouvement de l'aube et donc diminue l'énergie utile produit par étage.

Ces résultats se voient aussi du triangle gauche où la vitesse w_2^m se diminuerait, diminuant l'énergie produite par réaction.

En même temps se diminuerait la composante périphérique de la vitesse c_2 approchant l'étage de la sortie idéale avec $\alpha_2 = 90^\circ$.

La modification de la vitesse périphérique u par la modification de la vitesse de rotation n (Fig.1.C.) quand la valeur de la vitesse c_1 et des angles $\alpha_1, \beta_1, \beta_2$ ne se modifient pas, change les triangles de vitesse de cette manière. Cette dernière vitesse se décompose sur les directions prioritaires u et a comme on voit en médaillon:

$$[m/s] \quad w_{1a}^{perpendiculaire} = w_1^{perpendiculaire} \cos \beta_1 \quad (5.1)$$

$$[m/s] \quad w_{1u}^{perpendiculaire} = w_1^{perpendiculaire} \sin \beta_1 \quad (5.2)$$

La section de sortie d'ajutage est construite et ne se modifie pas à la modification du débit. L'angle de sortie d'ajutage est déjà construit et ne se modifie pas à la modification du débit:

$$[m^3/s] \quad \dot{M}^m v_1^m = S_1 c_1^m \sin \alpha_1 \quad \dot{M}_0 v_1 = S_1 c_1 \sin \alpha_1 \quad (5.3)$$

$$\frac{\dot{M}^m v_1^m}{\dot{M}_0 v_1} = \frac{c_1^m}{c_1} \quad \frac{\dot{M}^m}{\dot{M}_0} = \frac{p_1^m}{p_1} = \frac{p_0^m}{p_0} \quad (5.4)$$

Le processus en ajutages reste adiabatique et, bien que n'est pas en totalité réel mathématiquement (mais les différences sont données des pertes relatives petites), on peut écrire d'après la (Fig.2.) et résulte:

$$[Nm/kg] \quad p_0 v_0^k = p_1 v_1^k = p_0^m (v_0^m)^k = p_1^m (v_1^m)^k \quad (5.5)$$

$$\frac{v_1^m}{v_1} = \left(\frac{p_1^m}{p_1} \right)^{-\frac{1}{k}} = \left(\frac{\dot{M}^m}{\dot{M}_0} \right)^{-\frac{1}{k}} \quad \frac{c_1^m}{c_1} = \frac{\dot{M}^m}{\dot{M}_0} \left(\frac{\dot{M}^m}{\dot{M}_0} \right)^{-\frac{1}{k}} = \left(\frac{\dot{M}^m}{\dot{M}_0} \right)^{\frac{k-1}{k}} \quad c_1^m = c_1 \gamma^{\frac{k-1}{k}} = c_1 \delta \quad (5.6)$$

5.3. Le logiciel de calcul pour la vibration de l'aube en régime non nominal.

L'aube, déjà construite, ne permet pas la variation des paramètres.

Pour l'aube encastrée à la base et libre au bout opposé ou avec bandage au bout opposé:

$$[m] \quad (v_i^R)^m = (v_i^s)^m - (v_i^d)^m \quad (v_i^R)^m = (v_i^s)^m - (v_i^B)^m - (v_i^d)^m \quad (5.7)$$

5.4. Le calcul de la fréquence modifiée et faire la résonance évitable.

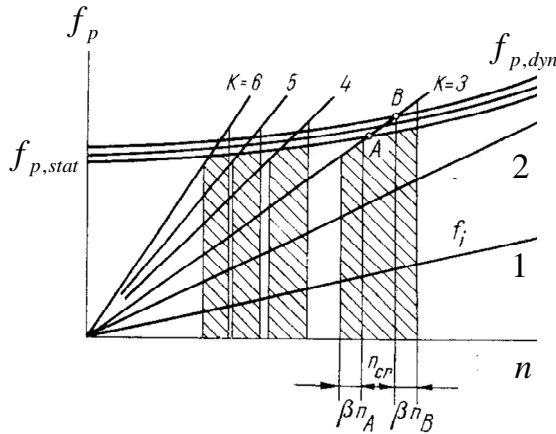


Fig.3. Le diagramme de la variation de la vitesse de rotation.

Les fréquences peuvent être calculées pour toutes variantes de chargement et, parce qu'elles sont fonctions de la vitesse de rotation, peuvent être représentées graphiquement. Un problème important est la détermination des vitesses de rotation de résonance comme valeurs où les fréquences propres devient égales aux fréquences imposées.

Les fréquences imposées aux aubes, considérées seulement du point de vue de l'étage, sont données des minimas de l'inégalité d'entre ajutages.

Les fréquences imposées deviennent:

$$f_{imp} = zn \quad (5.8)$$

Mathématiquement donc:

$$[s^{-1}] \quad \begin{aligned} f_{1,imp} &= n; \quad f_{2,imp} = 2n; \quad f_{3,imp} = 3n; \quad f_{4,imp} = 4n; \\ f_{5,imp} &= 5n; \quad f_{6,imp} = 6n \end{aligned} \quad (5.9)$$

La mise à l'égalité des ceux fréquences imposées avec les fréquences propres donne:

$$[s^{-1}] \quad (f_p^a)^m = (f_p^c)^m = \frac{1}{2\pi} \sqrt{\frac{g \left[\sum_{i=1}^{i=100} [(q_i^a)^m + (q_{i,u}^L)^m] (v_i^a)^m + 2 \sum_{i=1}^{i=100} \left(\frac{L_i^C}{l} \right)_u^m \right]}{\sum_{i=1}^{i=100} (q_i^a)^m [(v_i^a)^m]^2}} \quad (5.10)$$

Bibliographie sélective

1. Buzdugan, Gh.: **Măsurarea vibrațiilor mecanice**, Ed. Tehnică, București, 1964.
2. Delgeanu, M. : **Les vibrations des systèmes mécaniques. Applications.**, Edition U. S. T. O. (Université des Sciences et de la Technologie d'Oran), Génie mécanique, Post Graduation , 1984.
3. Delgeanu, M.; **CONTRIBUȚII LA STUDIUL VIBRAȚIILOR PALETELOR TURBINELOR CU ABUR ÎN REGIMURI NENOMINALE**, teză de doctorat, Universitatea Politehnica din București, 2007.
4. Delgeanu, M.: **MACHINES THERMIQUES. PROCESSUS THERMIQUES, CONSTRUCTION ET CALCUL DES TURBINES À VAPEUR ET DES CHAUDIERES DE VAPEUR**, Ed. MAN-DELY BUCUREȘTI, 2011, ISBN:973-7689-09-7.

METHODS FOR DETERMINING RESIDUES AND CONTAMINANTS FUEL USED FOR POWER PLANTS IN THE RESIDENTIAL SECTOR

Mirela Dragomir¹
Romanian Bureau of Legal Metrology

ABSTRACT

This paper focuses on developing methodologies extensive analysis and evaluation of their ability to provide complete and reliable measurement processes undertaken, identifying best practice evaluation methodologies with high accuracy and sensitivity of determination of residues and contaminants and assessment measures needed to align / further development of reference standards for traceability of measurement results and values of reference materials field concerned.

1. INTRODUCTION

As the science of measurement, metrology represents a horizontal scientific and technical field which stands at the foundation of all natural sciences and engineering. It is a multidisciplinary and technically vast domain of knowledge characterising in a consistent and systematic way the mathematical methods and tools used in data treatment of measurement uncertainty, comparability and traceability concepts.

The National Institute of Metrology (INM), a research and development oriented institute in the field of metrology, is directly involved in strengthen the capability of the metrology infrastructure, to provide traceability routes to the International System of measurement units (SI) for the measurement results and for the values attributed to the measurement standards in Romania. Within the frame of consolidating the position of Romania as a European state, the activity of the INM is particularly important, since it underpins the confidence in the measurement results both in the regulated and in the non-regulated area. By providing the traceability routes to the accredited or authorised calibration and verification laboratories, confidence is given in the tools needed to investigate the quality of goods and services offered by units of economy on region markets, and especially on the single European market.

To align the technical and metrological level of those national and reference measurement standards maintained/operated/developed to the facilities existing in homologues European metrology institutes, the National Institute of Metrology is also constantly preoccupied with the enlargement and integration of research activity performed in the institutional frame created at national and European level.

Main objectives were:

- disseminating measurement units to lower order measurement standards starting from the national and reference measurement standards;
- performing legal metrology control by means of metrological verifications, within the established competence limits;
- proposing and performing European and national research projects in metrology field;
- ensuring the trainers and themes to carry on the Training Program approved by the BRML;
- giving approval proposal to the Testing and Verifications Procedures developed by the units of economy applying for authorization;
- testing to pattern approve measuring instruments;

¹Galați, str. Științei, no.7, +40 745641314, mireladrago@gmail.com

- assuring technical assessors in the audit teams organized for authorization of the units of economy;
- periodically characterizing the national and reference measurement standards maintained in the INM, monitoring their stability and ensuring their maintenance;
- demonstrating the calibration and measurement capabilities by participating in key, regional or bilateral comparisons organized under the coordination of the Comité International des Poids et Mesures (CIPM);
- maintaining and improving a quality system appropriate for achieving the established quality objectives for each laboratory of the INM;
- drafting legal metrology norms;
- analyzing drafts of national regulations, international documents/recommendations (OIML) aiming at measuring instruments and measurements;
- representing the institute in EURAMET activities and in Consultative Committees of CIPM;
- disseminating the results obtained within the frame of national and international congresses, revues and other specialized publications.

Specific chemical analysis performed to control the quality often emphasis the need to approach at in more depth the issues of chemical measurements.

Beside the base principles of the environmental security, some of these European regulations document the methods to be applied in the common practice as well as the performance characteristics to be met by the methods used for control. To follow such documents it is important to have measures to assure the comparability and trace of the measurement results to accepted references of main SI units, implying:

- traceability routes of the agreed measurements;
- the use of valide methods of measurements;
- capability confirmation.

Since the base mission of a national metrology institute regarding the developing and maintaining national measurement standards internationally recognised, providing traceability to the SI, ensuring the suitability of these standard for national needs and providing metrological expertise, it is inherent the preoccupation of the National Institute of Metrology (INM) for this sensitive field.

The INM proposed in partnership with INCD ICECHIM (National Institute for Research and Development for chemistry and petrochemistry, INCD ICECHIM) and University “Politehnica” Bucharest (UPB) Research – Physics Department a research and development project in the Program Partnership in priority Domains (3125) aiming at “*Researches to establish the best practices to evaluate the methodologies having the highest accuracy and sensitivity to determine the residues and contaminants*”. The project, admitted for financial support (contract 51/084) led to obtaining several results – studies, new products and services developed [3].

2. COAL COMBUSTION RESIDUES (CCR) - SURFACE IMPOUNDMENTS WITH HIGH HAZARD POTENTIAL RATINGS

Over the past several years, it has undertaken a concerted effort to identify and to assess the structural integrity of impoundments, dams, or other management units, within the electric power generating industry, holding wet-handled coal combustion residuals or CCRs.

CCRs consist of fly ash, bottom ash, coal slag, and flue gas desulfurization (FGD) residue. CCRs contain a broad range of metals, for example, arsenic, selenium, cadmium, lead, and mercury, but the concentrations of these are generally low. However, if not properly

managed, (for example, in lined units), CCRs may cause a risk to human health and the environment.

Heavy metal contamination of soil may pose risks and hazards to humans and the ecosystem through: direct ingestion or contact with contaminated soil, the food chain (soil-plant-human or soil-plant-animalhuman), drinking of contaminated ground water, reduction in food quality (safety and marketability) via phytotoxicity, reduction in land usability for agricultural production causing food insecurity, and land tenure problems [5], [6], [7].

Information on the presence of these is important to local officials, including first responders, and the residents of local communities so that appropriate preparedness efforts can be undertaken, reviewed, or maintained. Many States have active dam safety programs and, in many cases, local government agencies, first responders, and the local community are involved in preparedness efforts.

3. THE ROLE OF NATIONAL METROLOGY INSTITUTES TO ASSURE TRACEABILITY AND COMPARABILITY OF MEASUREMENT RESULTS REPORTED IN ENVIRONMENT CONTROL

The confidence in the international measurement system is strengthened by the joint effort of the national metrology institutes all over the world to rely its performed measurements and reported measurement uncertainties on universally accepted units, meaning on measurement units of the International System of Units (SI).

It is extremely important for each country, by means of its own metrology organization, to compare national measurements and to establish the mutual equivalence not only in an effort to enlarge measurements capabilities but as a mean to reduce the trade technical barriers. How a national metrology institution can consolidate the mutual equivalence of national measurement standards and of measurement capabilities, having known measurement uncertainties, represents the measure that determines the capability of that country to participate in the international trade and in joint research-development-innovative programs.

The national measurement system is the technical infrastructure that makes possible the achievement of measurements accurate, trustable, fit for national purposes and internationally accepted regardless of the field they are performed. A national comprehensive measurement system includes several area of responsibility, among them may be given as examples:

- maintaining measurement references – measurement standards for units;
- ongoing development of measurement standards to meet the increasingly needs of society;
- elaboration of relevant document written standards [2].

For this purpose, a national metrology institute is involved in several activities regarding:

- maintaining and development of national measurement standards fit for the national needs;
- promoting the traceability to the International System of units (SI) concept;
- dissemination of SI units in accredited laboratories, other industrial and commercial laboratories and to other users from the country and clients from abroad;
- establishment of traceability arrangements with other NMIs and with the BIPM for those measurement units having no primary national measurement standards;
- ensuring the traceability of the values of the measurement standards used for verifications by the legal metrology authorities;
- maintaining an overview of the hierarchy of the national measurement standards / traceability (National System of Measurements) [1].

3. CONCLUSIONS

Taking into consideration the critical analysis of the ways to achieve the comparability of the results of chemical measurements reported in connection with the environment quality and their traceability to recognized references, several practical aspects have been concluded:

- technical and scientific support of measurement results reported in environment control is necessary to rely on national and international references recognized by traceable calibrations to the SI or by CMCs published in data bases;
- development of the national system of references ensuring the linking of all measurements to internationally recognized references bases on the participation with good results in relevant CIPM MRA comparisons;
- participation in relevant comparisons and the development of national references (physical measurement standards and certified reference materials) represents real small scientific research projects since the activities performed for this purpose, beside measurements, also implies development and validation of higher order measurement methods, estimation and reporting measurement uncertainty, evaluation of the degree of equivalence against the key comparison reference value etc.;
- calibration and measurement capabilities ensured at present in Romania partly cover the national needs and gave evidence for the vertical approach of the projects;
- assessment of the comparability of the reported results at testing laboratories level by means of interlaboratory comparisons is in line with the missions of the a national metrology institute and justifies the horizontal approach of the project.

References

- [1] Buzoianu, M., Boiciuc, D., Dută, A., Sandu, I., Cîrneanu, L., Simionescu, M., Cîrneanu I., *Achievements of the National Institute of Metrology in 2010*, www.inm.ro/pdf/2012-1-02-realizari-2011.pdf.
- [2] EURAMET Guide no. 10: EURAMET and the operation of NMIs, 2008.
- [3] Iacobescu, F., Popescu, I.M., Manolache, M., Buzoianu, M., Sălcianu, C., *Contributions to the development of traceable measurement methods of contaminants in foods*.
- [4] McLaughlin, M., J., Zarcinas, B.A., Stevens, D.P., and Cook, N., "Soil testing for heavy metals," Communications in Soil Science and Plant Analysis, vol. 31, no. 11–14, pp. 1661–1700, 2000, www.inm.ro/pdf/2010-4-05-contribuabili.pdf.
- [5] McLaughlin, M., J., Hamon, R. E., McLaren, R.G., Speir, T.W., and Rogers, S.L., "Review: a bioavailability-based rationale for controlling metal and metalloid contamination of agricultural land in Australia and New Zealand," Australian Journal of Soil Research, vol. 38, no. 6, pp. 1037–1086, 2000.
- [6] Ling, W., Shen, Q., Gao, Y., Gu, X., and Yang, Z., "Use of bentonite to control the release of copper from contaminated soil," Australian Journal of Soil Research, vol. 45, no. 8, pp. 618–623, 2007.
- [7] Wuana, R.A., Okieimen, F.E., *Heavy metals in contaminated soils: A Review of Sources, Chemistry, Risks and Best Available Strategies for Remediation*, International Scholarly Research Network ISRN Ecology Volume 2011.

METHOD FOR DETERMINATION THE RATIO BETWEEN FLAME EMISSIVITIES OF LPG AND CH₄, AT COMBUSTION IN FURNACES

by Victor V. Ghiea (Ghia) (Research Professor, Dr. Eng.)

Polytechnic University of Bucharest, Thermo-Mechanical Engineering Dep., Bucharest, 313 Splaiul Independentei, Sector 6, Romania, E-mail: ghiea_victor@yahoo.co.uk

ABSTRACT

An important effect due the natural gases replace by LPG gas fuels is the change of the useful heat transfer by radiation. For a systematic and advantageous solution, mainly was favorable to establish the ratios of non-luminous and total combustion flame emissivities of critic analyzed gas fuels. Thus it is developed a complex method for determination of combustion flame emissivity ratios, comparing LPG and CH₄, for non-luminous flame in the first stage and the total flame emissivities in the second stage, when the soot releases in flame. This last development, generated a complex calculation using results of measurements on combustion flame into the furnace. In addition, is obtained a general formula for calculation of flame total emissivity resulted by furnace operation especial with different gas and liquid fuels. By calculations, for non-luminous emissivities of propane, butane, methane..., are established $\varepsilon_{gb} \cong \varepsilon_{gp} \cong \varepsilon_{gy}$ and a small difference $\varepsilon_{gm} - \varepsilon_{gy}$ which represents a disadvantage for LPG comparative CH₄.

1.INTRODUCTION

There are huge consumptions of LPG gas fuels which especially are burned in place of natural gases. Usual, the natural gas consists of a high percentage of CH₄ (generally above 85 percent) with varying amounts of ethane, propane, butane and inert gases. For this reason in a first approximation for calculation, the natural gas will be assimilated with CH₄. The main characteristics which can determine positive and negative effects on furnaces efficiency and environment pollution, at combustion in furnaces of LPG and comparative CH₄, are: the total flame emissivity ε_g , the theoretic combustion temperature T_t and CO₂ emission output obtained by combustion. In this stage, the first characteristic, especially will be critic analyzed and developed especial for applications. Natural gases with majority content CH₄ (noted with index m) and LPG (mix of C₃H₈ with C₄H₁₀ noted with index y = bp, C₃H₈ with index y = p and C₄H₁₀ with index y = b) are used as domestic and industrial fuels with numerous useful applications consuming enormous quantities and heaving a very great economical importance [1]. For example, propane or butane are used as fuel in cooking stoves, different furnaces types (including livestock facilities), water heaters, grain dryers, but also at motor vehicles using internal combustion engines (for buses, locomotives, taxis...). Propane is the third most widely used motor fuel in the world and for example, over 15 billion gallons of propane being used annually only in U.S.A. It is especial important to increase the furnaces energetic efficiency by combustion flame emissivity increase. Usual by gas fuels with non - luminous combustion we understand a complete combustion process without soot release, as for example can be the complete combustion of CH₄. Propane can burn with visible flame and usually having a supplementary heat radiation emisivity [2]. Similar is the industrial .combustion of LPG gas fuels, but where the release of soot from flame is relative small due economic reasons and the soot can decrease with the increase of

combustion excess air ratio together with improving in homogeneity of mix between air and gas fuel. It is to underlined the release of nitrogen dioxide, which is favoured by circumstances of combustion for butane and (or) propane, and thus already represents a human health hazard. The increased combustion theoretic temperature of LPG in comparison with CH_4 ($T_{ty} > T_{tm}$) represent an important advantage. But the possible increase of CO_2 output by combustion of LPG comparative with CH_4 , determines the growth of thermal pollution. In essence, will be developed a method for determination of combustion flame emissivity ratio comparing LPG and CH_4 , for non-luminous flame in the first stage and the total flame emissivities in the second stage with soot release. Also this last development, will generate a complex calculation giving a general formula for calculation of flame total emissivity resulted by operation at furnaces for experiments with especial different gas and liquid fuels.

2.COMPARISON FOR RADIATION USEFUL HEAT TRANSFER AT FURNACES

The total flame emissivities for LPG can increase comparative with non-luminous emissivities due the release of soot in combustion process. By experiments resulted that especial propane can burn with visible flame, usually having a supplementary radiation emissivity and is much cleaner flame than for gasoline, though not as clean as for natural gas with majority content of CH_4 . However, at the propane sensible incomplete combustion give a decreased low heating value H_p with CO and C carbon fine particles in emissions, according to relation $2\text{C}_3\text{H}_8 + 7\text{O}_2 \rightarrow 2\text{CO}_2 + 2\text{CO} + 2\text{C} + 8\text{H}_2\text{O}$ [2]. Thus, the total emissivity ϵ_g of combustion gases, and useful heat transfer by radiation are determined by gas fuel kind and combustion conditions. Essential for ϵ_g values are the following characteristics: content of CO_2 and H_2O from gases resulted by fuels combustion, temperature of combustion gases T_g (especial determined by the of theoretic combustion temperature T_t), mean length of beam (layer thickness) l , possible soot content released in flame and combustion excess air ratio λ . With a small approximation can be considered valid values at $\lambda = 1.05$, for theoretic combustion temperature $T_{tm} \cong 2245$ K with $T_{ty} \cong 2308$ K, 2310 K, 2308 K and for $\lambda = 1.4$, $T_{tm} \cong 1865$ K with $T_{ty} \cong 1900$ K, 1902 K, 1901 K referring to methane, butane, propane and mix of the last two gas fuels (with $bp = 0.5b + 0.5p$). When miss soot in flame we obtain the non-luminous emissivity ϵ_g which is decreased comparative with the total emissivity $\epsilon_g > \epsilon_g$. Indeed, the content in CO_2 (V_{cp} , V_{cb} , V_{cm}) and H_2O (V_{vp} , V_{vb} , V_{vm}) and possible soot content of combustion gases, usual are function of the combustion excess ratio λ and gas fuel kind. Using specific equations, are obtained the H_2O , CO_2 contents in percentages, from gases resulted by complete combustion, of C_3H_8 , C_4H_{10} and CH_4 , gas fuel unity (for example 1m^3_N and V_{gp} ..., V_{cp} ..., V_{vp} ... V_{gb} ..., V_{cb} ..., V_{vb} ... are expressed in $\text{m}^3_N/\text{m}^3_N$):

$$V'_{vp} = 100V_{vp}/V_{gp} = 400/V_{gp}; V'_{cp} = 100V_{cp}/V_{gp} = 300/V_{gp} \text{ with } V_{gp} = 7 + 5(\lambda - 1) + 18.8\lambda \quad (1)$$

$$V'_{vb} = 100V_{vb}/V_{gb} = 500/V_{gb}; V'_{cb} = 100V_{cb}/V_{gb} = 400/V_{gb} \text{ with } V_{gb} = 9 + 6.5(\lambda - 1) + 24.44\lambda \quad (2)$$

$$V'_{vm} = 100V_{vm}/V_{gm} = 200/V_{gm}; V'_{cm} = 100V_{cm}/V_{gm} = 100/V_{gm} \text{ with } V_{gm} = 1 + 9.52\lambda \quad (3)$$

The resulted gases of complete combustion are: nitrogen, water vapour, carbon dioxide and oxygen in excess, but only the CO_2 and H_2O can radiate and receive thermal energy in selective bands of wave length. According (1), (2) and (3) resulted $V'_{vb} < V'_{vm}$, $V'_{vp} < V'_{vm}$, with $V'_{cb} > V'_{cm}$, $V'_{cp} > V'_{cm}$. Thus when $\lambda = 1.05$ result for $V'_{vp} = 14.82\%$, $V'_{vb} = 14.29\%$, $V'_{vm} = 18.18\%$ with $V'_{cb} = 11.43\%$, $V'_{cp} = 11.11\%$, $V'_{cm} = 9.09\%$. and when $\lambda = 2$ result for $V'_{vp} = 8.064\%$, $V'_{vb} = 7.766\%$, $V'_{vm} = 9.980\%$ with $V'_{cb} = 6.213\%$, $V'_{cp} = 6.048\%$, $V'_{cm} = 4.990\%$. The first case approximately corresponds at industrial furnaces working at high temperatures and the second case corresponds to domestic burners used to indoor kitchen with open

flames. Also the differences $V'_{vm} - V'_{vp}$ and $V'_{cp} - V'_{cm}$, decrease with the increase of λ and this variation is valid for LPG gas fuels in comparison with CH_4 . For furnaces having, the interior walls covered with cooled tubes as at numerous boilers unities and at oil distillery furnaces, the useful heat transfer especial being by radiation, using LPG (having index y) in comparison with CH_4 combustion, is:

$$\Delta Q_{uy} \cong \Delta Q_{um} (\epsilon_{gy} T_{gy}^4 - a_{gy} T_{py}^4) (\epsilon_{gm} T_{gm}^4 - a_{gm} T_{pm}^4)^{-1} \quad (4)$$

where T_p is the cooled wall temperature and a_g is the integral absorptivity of combustion gases. Since in general, $\epsilon_g T_g^4 \gg a_g T_p^4$ for a first approximation, the useful heat ΔQ_u is direct proportional with the combustion gases total emissivity ϵ_g and temperature T_g^4 . But, for the same T_g with constant value, changing CH_4 with LPG, is valid the relation $\Delta Q_{uy} / \Delta Q_{um} \cong \epsilon_{gy} / \epsilon_{gm}$. Really for the some value of λ , the T_g temperature become lager for LPG comparative with CH_4 combustion, because between combustion theoretical temperatures there is the inequality $T_{ty} > T_{tm}$. Thus at numerous furnaces, it is possible to have $T_{gy} > T_{gm}$ and for this reason, is possible to have the inequality $\Delta Q_{uy} > \Delta Q_{um}$. when $\epsilon_{gy} / \epsilon_{gm} (T_{gy} / T_{gm})^4 > 1$. The increase of $(T_{gy} / T_{gm})^4$ can compensate the eventual decrease of total emissivities ratio $\epsilon_{gy} / \epsilon_{gm}$. Indeed this change is possible, due the soot release at LPG combustion giving $\epsilon_{gy} / \epsilon_{gm} > 1$. Thus, in a first approximation for the mentioned cases, resulted :

$$\Delta Q_{uy} / \Delta Q_{um} \cong \epsilon_{gy} / \epsilon_{gm} (T_{gy} / T_{gm})^4. \quad (5)$$

Also (5), can be used, for estimations of ratio between the useful radiation heat transfer at combustion with open flames oat special furnaces, when the radiation of ambient medium is negligible in comparison with flame radiation. In fact, for industrial furnaces there are two main distinct cases: when the temperature in the working volume of furnace: has an imposed value which does not surpass the optimum value for development of technological process; and when this temperature can exceed the value obtained in the first case, even being a technological necessity, (similar as for some boilers). But also, there are industrial furnaces where for the efficient development of technological process is necessary to have an optimal constant temperature T_e for furnace exhausted combustion gases. For industrial furnaces which warm the technologic product at high temperatures, the useful radiated heat is transferred towards the technological product especial by the radiation of the furnace inner masonry and smaller by combustion gases. In consequence, the influence of total emissivity ϵ_g variation due the change of CH_4 by LPG have a decreased importance, on the useful heat transfer by radiation. Indeed, for this reason, a great amount of useful heat transfer is especially given by heat radiation of furnace arch (which have be favorable projected for increase of radiation heat transfer).

3. CALCULATION OF NON-LUMINOUS COMBUSTION FLAME EMISSIVITY RATIO

The calculation of selective non-luminous emissivity of flame ϵ_g can represent an important stage, which give an acceptable but useful approximation in projection especial when is negligible the soot released in flame. The use of empiric formulae with limited validity for obtaining ϵ_g , have to be avoided for relative new gas fuels. Indeed, the main purpose is to obtain the useful heat transfer by radiation which is especial necessary for projects and economic calculations. Thus, ϵ_g can be calculated by adding the afferent emissivity ϵ_{gc} of CO_2 component with the afferent emissivity ϵ_{gv} of H_2O component multiplied with a correction factor b [3]. Also this sum will be decreased for precision, with a non-significant amount $\Delta \epsilon_g$ (which can be neglected in a first approximation) due

superposition of some wave length bands for CO₂ and H₂O emissions. The values of ε_{gc} , ε_{gv} , b , usual are obtained from specific diagrams in function of temperature T_g and afferent p_l respective $p_v l$ (multiplying partial pressure of CO₂ or H₂O components with l) for determined emissivities, respective for b (in function of p_v and $p_v l$). It is to underlined the great importance of presented problems for projection of radiation heat recuperators of furnaces which can give a great increase of furnaces efficiency, by heating the combustion air till 1000 °C [4]. To give in evidence the resulted differences can express the ratio of non-luminous emissivities for LPG comparative CH₄, as follows:

$$R_{ym} = \varepsilon_{gy} \varepsilon_{gm}^{-1} \cong (\varepsilon_{gcy} + b_y \varepsilon_{gvy})(\varepsilon_{gcm} + b_m \varepsilon_{gvm})^{-1} \quad (6)$$

By calculation using (6), resulted in a first approximation, the values of non-luminous emissivities of methane, butane (in round brackets) and propane (in square brackets) that is ε_{gm} , ε_{gb} and ε_{gp} , when $\lambda = 1.05$, $T_g = 1273$ K, 1473 K, 1673 K, 1873 K and $l = 1$ m respective $l = 2$ m, as follows:

- 0.2585, (0.2465), [0.2472] ; 0.2237, (0.2161), [0.2168] ; 0.1909, (0.1781), [0.1783] ; 0.155, (0.1508), [0.1519] (for $l = 1$ m) and
- 0.3420, (0.3290), [0.3307] ; 0.2916, (0.2824), [0.2836] ; 0.2658, (0.2504), [0.2559] ; 0.2343, (0.2248), [0.2273] (for $l = 2$ m)

Taking into account of these and other numerous similar results, results a small increase of CH₄ non – luminous emissivity comparative with LPG gas fuels emissivities and can considered $\varepsilon_{gb} \cong \varepsilon_{gp} \cong \varepsilon_{gy}$ (valid also for bp mix LPG gas fuels). Thus for example when $\lambda = 1.05$, $l = 1$ m, $T_g = 1473$ K results $\varepsilon_{gm} = 0.2237$ with $\varepsilon_{gb} = 0.2161$ and $\varepsilon_{gp} = 0.2168$, giving a decrease in percents of maximum 4 %. Especial due the increased values of H₂O content from combustion gases of CH₄ in comparison with LPG gas fuels, result for CH₄ this advantage. Also using and other obtained results, was utile to trace the curves families $\varepsilon_{gm} = F_m(l, T_g)$, $\varepsilon_{gp} = F_p(l, T_g)$, $\varepsilon_{gb} = F_b(l, T_g)$, which are given the variation of non – luminous emissivities ε_{gm} , ε_{gp} , ε_{gb} in function of beam length l and temperature of combustion gases T_g , for $\lambda = 1.05$. Thus, especial results that mentioned non – luminous emissivities increase with l and decrease with the increase of temperature T_g , being negligible the difference between ε_{gp} , ε_{gb} and ε_{gbp} (mix of propane with butane) For LPG gas fuels emissivity ε_{gy} can be considered as equal with an arithmetic average value between ε_{gp} and ε_{gb} . Using (6), at a correct comparison, for example between ε_{gb} and ε_{gm} it is necessary to take an increased temperature $T_{gb} > T_{gm}$ for establish the value of ε_{gb} , because $T_{tb} > T_{tm}$.

3.DETERMINATION OF COMBUSTION FLAME TOTAL EMISSIVITIES RATIO, FOR LPG COMPARATIVE CH₄.

It was necessary to developed a method for determination of ratio between total flame emissivities ε_{gy} and ε_{gm} , but being independent of anterior presented method adjusted especial for projection This development is obtained in two stages, concerning : the establish of a complex calculation formula for total emissivities defining the afferent ratio, and which is follows by measurements using an special conceived a cooled mobile screen, mounted into the furnace. By writing the thermal balance equation for the unity surface belonging to the mince heated surface S (placed on refractory wall inner of an experimental furnace), results for i gas fuel in general, as follows:

$$f_{Ci} + f_{ri} = \varepsilon_{wi} \sigma T_{wi}^4 + (1 - \varepsilon_{wi}) f_{ri} + f_{ei} \quad (7)$$

where f_{ri} [W/cm²] is the total radiation incident flux to the receiving unit surface; f_{ci} - heat flux yielded to the receiving surface unit by convection; f_{ei} - heat flux transmitted to the environment by the unit receiving surface; ϵ_{wi} - total emissivity of the refractory wall; $\sigma = 10^{-8}$ C - the Stephan – Boltzman constant, with $C = 5.67 / 10^4$ [W/cm²K⁴].

The fluxes f_{ci} , f_{ri} , f_{ei} and E_{ti} , E_{gi} (notations which will follow, are orientated in direction (Δ) normal to the gas fuel flame symmetry axe. The reference mince surface S have the temperature T_{wi} . From (7) can obtain:

$$f_{ri} = \sigma T_{wi}^4 - (f_{ci} - f_{ei})/\epsilon_{wi} \quad (8)$$

and the total normal radiation from the refractory behind the flame is

$$f_{ti} = \sigma T_{wi}^4 + (1 - \epsilon_{wi}) f_{ri} = \sigma T_{wi}^4 - Z_i \quad (9) \quad \text{where } Z_i = (f_{ci} - f_{ei})(1 - \epsilon_{wi})/\epsilon_{wi} \quad (10)$$

The total energy flux E_{ti} results from the summation of the f_{ti} ($1 - \epsilon_{gi}$) and the total normal radiation from the gas fuel flame E_{gi} , that is:

$$E_{ti} = E_{gi} + f_{ti} (1 - \epsilon_{gi}) = E_{gi} + (\sigma T_{wi}^4 - Z_i) (1 - \epsilon_{gi}) \quad (11)$$

From (11) results taking into account of (10), the total emissivity of the i gas fuel flame:

$$\epsilon_{gi} = 1 - (E_{ti} - E_{gi})(\sigma T_{wi}^4 - Z_i)^{-1} \quad (12)$$

For a first variant, in the particular case when $Z_i = 0$, relation (12) become the Schmidt formula used for calculations also at “International Flame Research Foundation, IJmuiden” [5]. Thus, according (10) is admitted valid minimum one of the following conditions: $\epsilon_{gi} = 1$ and $f_{ci} = f_{ei}$. But values, T_{wi} relative near of these conditions, especial can be realized in an experimental furnace. Thus for comparison of LPG with CH₄, in a first approximation can use the expression of a specific ratio between ϵ_{gy} and ϵ_{gm} :

$$R_{ym} = \epsilon_{gy} / \epsilon_{gm} = [1 - (E_{ty} - E_{gy})(\sigma T_{wy}^4)^{-1}][1 - (E_{tm} - E_{gm})(\sigma T_{wm}^4)^{-1}]^{-1} \quad (13)$$

For special cases and increasing the range of applicability, especial for some experiments at industrial furnace, can be used the real value of Z_i calculated from (10). Indeed for modern furnaces the heat losses in environment are very decreased ($f_{ei} \cong 0$) but the useful heat transmitted by convection can be important (together with f_{ci}). When $\epsilon_{gy} > \epsilon_{gm}$, the difference between ϵ_{gy} and ϵ_{gm} in percent of ϵ_{gm} , results as follows:

$$\Pi = 100 (R_{ym} - 1) \quad (14)$$

The S surface temperature T_{wi} , currently is measured with a thermocouple Pt.- Pt. Rh adequate set up in the refractory wall. The fluxes E_{ty} , E_{tm} and E_{gy} , E_{gm} are measured with the twin-angle total radiation pyrometer sighting upon the direction (Δ). The conceived mobile cooled background screen can cover the surface S only when is measured the E_{gi} flux. Thus can obtain the characteristics necessary for calculation of compared total emissivities, at stable and practice

complete combustion regime and usual for the same furnace thermal power. Index m for afferent calculations, is valid for the natural gases with majority CH₄.

5. CONCLUSIONS

An important effect due the natural gases replace by LPG gas fuels is the change of the useful heat transfer by radiation. For a systematic solution, mainly was favorable to establish the ratios of non-luminous and total combustion flame emissivities. Thus it is developed a complex method for determination of combustion flame emissivity ratios, comparing LPG and CH₄. These ratios are obtained: for non-luminous flame in the first stage using the formula (6), important especial for projection and the total flame emissivities in the second stage, when releases the soot. In addition is obtained a general formula (12) for calculation of flame total emissivity resulted by furnace operation. It is used the real value of Z_i calculated from (10). But this formula can increase precision of results and have increased applications. Thus can be used for different materials with ϵ_{wi} great different of unity and when is an important heat transfer by convection ($f_{ci} \gg 0$). The ratio between afferent total emissivities ϵ_{gyz} : and ϵ_{gmz} is: $R_{ymz} = \epsilon_{gyz} / \epsilon_{gmz} = [1 - (E_{ty} - E_{gy})(\sigma T_{wy}^4 - Z_y)^{-1}][1 - (E_{tm} - E_{gm})(\sigma T_{wm}^4 - Z_m)^{-1}]^{-1}$. In the first variant when is considered $Z_i = 0$, for the afferent ratio resulted formula (13).. Also can be compared establishing emissivities for other two different gas fuels, or different liquid and even solid fuels burned as fine solid particles. From numerous calculations and the traced curves families $\epsilon_{gm} = F_m(l, T_g)$, $\epsilon_{gp} = F_p(l, T_g)$, $\epsilon_{gb} = F_b(l, T_g)$ resulted: $\epsilon_{gb} \cong \epsilon_{gp} \cong \epsilon_{gy}$ and a small difference $\epsilon_{gm} - \epsilon_{gp}$, but in favor of CH₄ representing a disadvantage for LPG. This inconvenience can be avoided when the inequality $T_{gy} > T_{gm}$ is sufficient important. This finding, results also from (5) because $\Delta Q_{uy} > \Delta Q_{um}$. when $\epsilon_{gy} / \epsilon_{gm} (T_{gy} / T_{gm})^4 > 1$ and the variation of the radiation useful. heat transfer is determined by the values of the ratios $\epsilon_{gy} / \epsilon_{gm}$ and $(T_{gy} / T_{gm})^4$. The huge consummations of LPG gas fuels especial in place of natural gases, required to establish the resulted main negative and positive effects, on furnace operation and environment pollution. By numerous calculations resulted $\epsilon_{gb} \cong \epsilon_{gp} \cong \epsilon_{gy}$ and a small difference $\epsilon_{gm} - \epsilon_{gp}$, but in favor of CH₄ representing a disadvantage for LPG. The main characteristics which can determine important effects are: the ratio of flame total emissivities above presented, the theoretic combustion temperature T_t and CO₂ emission output obtained by combustion. The increased combustion theoretic temperature of LPG in comparison with CH₄ ($T_{ty} > T_{tm}$) represent an important advantage. But the possible increase of CO₂ output by combustion of LPG comparative with CH₄, determines the growth of thermal pollution, which represents an important disadvantage, for present and future development of the humanity.

REFERENCES

- [1] ** <http://en.wikipedia.org/wiki/Propane> "Domestic and industry", 6 Dec. 2011 and <http://en.wikipedia.org/wiki/Butane>,
- [2] ** http://en.wikipedia.org/wiki/Nitrous_oxide, 26 Jun 2010
- [3] Mc. Adams, Transmission de la chaleur, Ed. Dunod, 1966.
- [4] V.Ghia., Recuperateurs et regenerateurs de chaleurs, Ed.Eyrolles, Paris, 1970, 424 p.
- [5] J.Cheddaille, Y.Brand, Mesure du transfert de chaleur. Fondation de Recherches Internationales sur les Flamme-Ijmuiden, Doc. No. 20/a/40, 1968.

TURBULENT FORCED CONVECTION AIR FLOW IN A VENTURI CHANNEL

Dr. IGO Wendsida Serge¹, Prof.Dr.Ing. Lucian MIHAESCU²

¹Research Institute of Applied Sciences and Technologies (IRSAT/CNRST). Department of Energy.

²Politehnica University of Bucharest (UPB), Department of Mechanical Engineering, Romania.

ABSTRACT

In this work, a turbulent forced convection air flow in a 2D rectangular venturi channel has been numerically simulated using the Fluent/Gambit software. The viscous model is the turbulent standard k- ϵ . The results are presented as velocity, streamlines, pressure and velocity vectors patterns. The turbulent parameters (turbulent viscosity, turbulent kinetic energy and his rate of dissipation) are also investigated in details.

1. INTRODUCTION

Venturi channels are widely used as scrubbers for particles and gaseous collection from industrial exhaust [1] or for gas flow rate measurements [2]. Due to their applications, they are suitable for turbulent flows. Despite this, turbulent studies about venturi channel are scarce. This situation is probably due to the complexity of the channel coupled with the very limited turbulent numerical procedures. Among the turbulence models, the k- ϵ model [3] is the most popular. However, it is well known that near the walls occurs important viscous forces, the standard k- ϵ turbulence model which is suitable for large Reynolds numbers is no longer applicable. To solve this problem, wall functions must be used to force the first node to be in the boundary layer [4]. The fluent software coupled with the mesh generator Gambit provides facilities to solve this problem.

2. PROBLEM FORMULATION

The venturi channel is composed of two iron plates of sections lengths (L1, L2, L3). The inlet radius is R_0 and the venturi diameter ratio is 1/2. The wall plates are subjected to a constant temperature T_w . A turbulent air flow with average velocity U_e enters at the venturi channel inlet with an uniform temperature T_e . It is assumed that the flow is incompressible and the transfers are two-dimensional, axisymmetric and steady state.

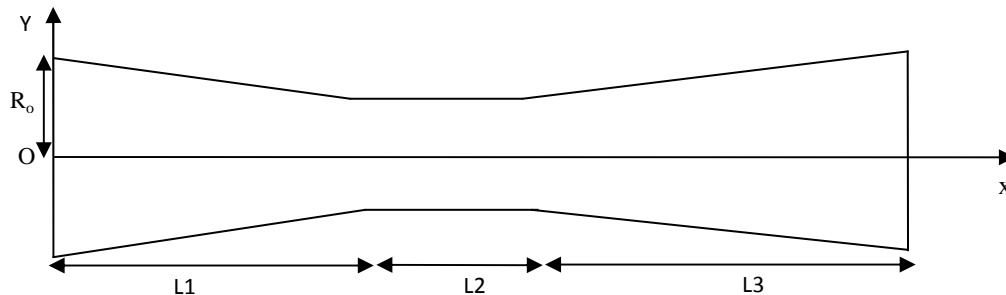


Figure 1. Schematic representation of the studied system in the (O,X,Y) referential

3. NUMERICAL SIMULATION

3.1 Mesh

¹ Corresponding author : 03 P.O. Box 7047 Ouagadougou 03, tel : +226 71258921, sergesigo@yahoo.fr

Due to symmetry, only the half domain needs to be considered. The mesh is generated using the Gambit software. The mesh size is very close near the walls to take account the turbulent boundary layer.

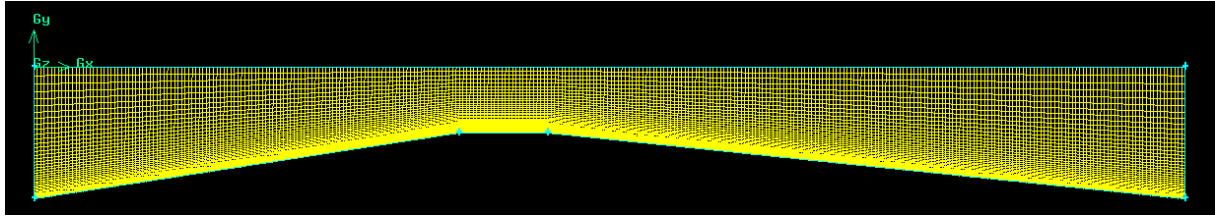


Figure 2. Channel mesh

3.2 Boundaries conditions

-At the inlet

A fully-developed power-law profile ($n=7$) is assumed for the streamwise velocity. As we consider the lower half channel, the inlet velocity profile is:

$$U = U_o \left(1 + \frac{y}{R_o} \right)^{1/n}$$

U_o is the centerline velocity.

$$U_o = U_e \frac{(2n+1)(n+1)}{2n^2}$$

U_e is the average inlet velocity which is correlated to the inlet Reynolds number Re .

$$Re = \frac{U_e Dh}{\nu_e}$$

Dh is the hydraulic diameter and ν_e the air inlet cinematic viscosity.

The inlet turbulent kinetic energy K_e and his rate of dissipation ϵ_e can be expressed as [5].

$$k_e = \frac{3}{2} (I_e U_e)^2$$

$$\epsilon_e = C_\mu^{3/4} (k_e)^{3/2} / l$$

C_μ is a constant of the k - ϵ model = 0.09

I_e is the inlet turbulence rate and l the turbulence scale:

$$I_e = 0.16 (Re)^{-1/8} \text{ for internal fully developed flows.}$$

$$l = 0.07 Dh$$

-At the walls : $U=0$, $V=0$, $K=0$, $\epsilon=0$, $T=T_w$

-At the outlet : Outflow boundary condition is imposed.

4. RESULTS AND DISCUSSIONS

In the present study, simulations were performed for $R_o=0.15m$, $L1=0.48m$, $L2=0.1m$, $L3=0.72m$, $U_e=13 \text{ ms}^{-1}$, $T_e = T_w = 300K$.

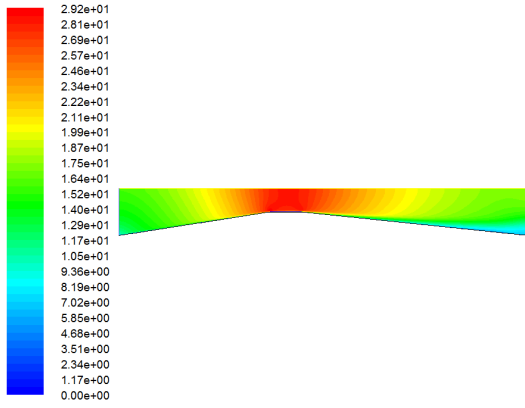


Figure 3. Contours of velocity magnitude

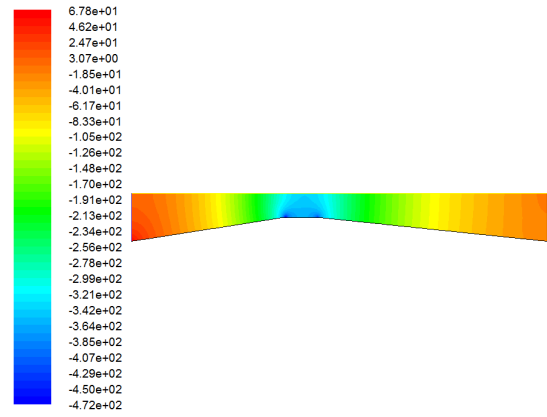
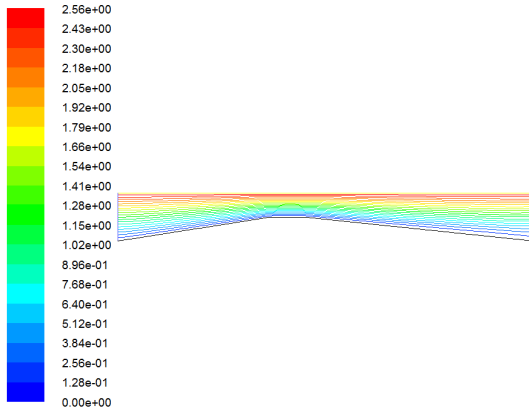


Figure 4. Contours of static pressure



5. Streamlines colored by velocity magnitude

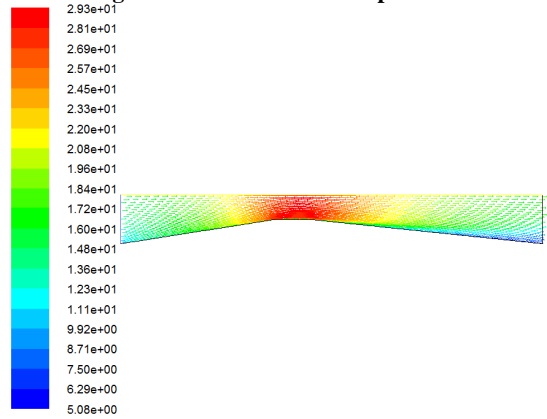


Figure 6. Vectors velocity colored by velocity magnitude

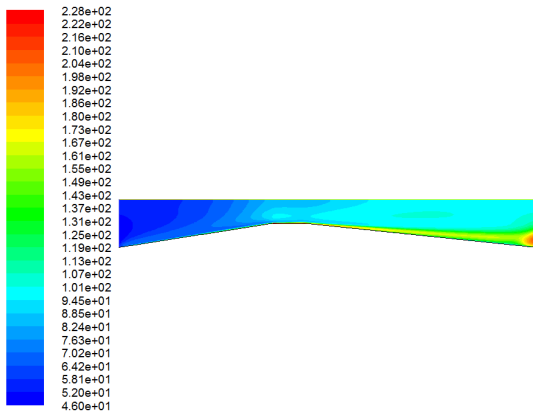


Figure 7. Contours of turbulence intensity

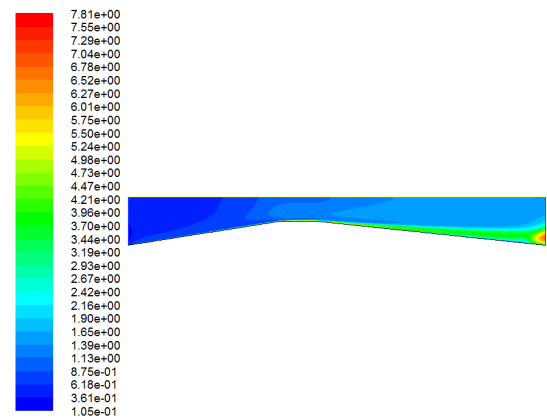
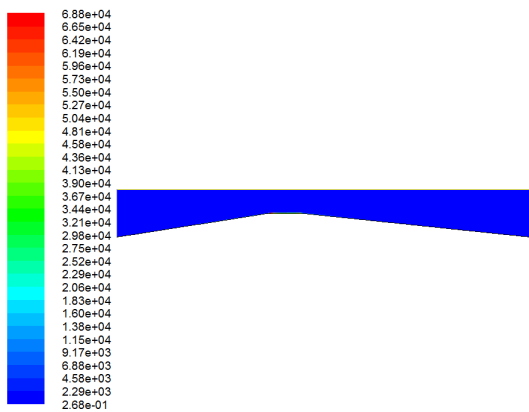


Figure 8. Contours of turbulent kinetic energy



9. Contours of turbulent dissipation rate

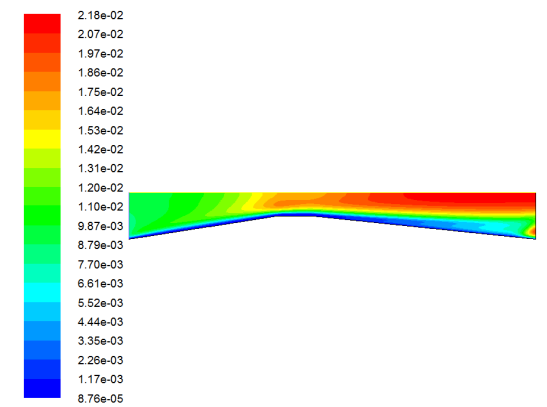


Figure 10. Contours of turbulent viscosity

Figures 3-4 show the contours of velocity magnitude and the static pressure. The flow velocity increases in the converging section and reached his maximum at the venturi throat. In fact, in the converging section, there is a continuous increase of the pressure drop due to the acceleration of the air velocity resulting of the conversion of the potential energy into kinetic one. According to the flow rate conservation law and considering the venturi diameter ratio equal to 1/2, we note effectively that the velocity has doubled in the throat. In the diverging section, the decrease of the velocity is observed due to the expansion of the channel diameter. The evolution of the static pressure is the opposite of the velocity and is an agreement with the Bernoulli law : this is venturi effect.

Figures 5-6 illustrate the flow structure. The flow is assumed turbulent fully-developed at the inlet and the inlet Reynolds number calculated with the inlet velocity is about 21.10^4 . Turbulent perturbations are naturally observed continuously in the flow notably at figure 5. However, The radical changes of streamlines is observed after the venturi throat near the wall consequently of the separation of the boundary layer. The part of the channel between the wall and the streamlines after the throat and toward the outlet appears more perturbed as seen in figure 6.

Figures 7-8 show the contours of the turbulence intensity and the turbulent kinetic energy respectively. According to the above, the turbulent kinetic energy and the turbulence intensity are more important after the throat, near the wall and toward the channel outlet. The rate of dissipation of the turbulent kinetic energy which is shown in figure 9 is very low in the channel.

Figure 10 show the contours of turbulent viscosity and confirm the fact that the turbulence is developing in the venturi channel from de inlet to the outlet. Maximum values are observed toward the outlet.

5. CONCLUSIONS

Turbulent air flow in a venturi channel was numerically investigated in the present study using the k- ϵ turbulent model. The model has been implemented by the Fluent/Gambit software. The major results are:

- The venturi effect is well predicted by the used model.
- The turbulence is developing gradually from the inlet to the venturi channel outlet.
- The turbulence intensity is more important after the throat, near the wall and toward the channel outlet.

Despite these results, this study must be improved by submitting the model and the computational procedures to different boundaries conditions and different geometries of the venturi channel.

AKNOWLEDMENTS

The authors thank the AUF (Agence Universitaire de la Francophonie) for his financial support.

References

- [1] Jonhstone, H.F., R.B. Fied and M.C. Tassler, Gas absorption and aerosol collection in venturi atomiser, Ind.Eng.Chem, 45, 1602-1608, 1954.
- [2] Jitschin, W., Ronzheimer, M., Khodabakhshi, S., Gas flow measurement by means of orifices and venturi tubes, Vacuum, 53, 181-185, 1999.
- [3] Launder B. E, Sharma B. I, application of the energy-dissipation model of turbulence to the calculation of flow near a spinning disc, letters in heat and mass transfer,1, 131-138, 1974.
- [4] Launder, B.E. and Spalding, D.B., mathematical models of turbulence, academic press, London, 1972.
- [5] Fluent inc. November 28, 2001.

THERMO-MECHANICAL ASPECTS OF MASS TRANSFER SELECTIV PHENOMENON THROUGH DIFFUSION IN THE FRICTION PROCESS OF COUPLE STEEL/COPPER ALLOY

Filip Ilie,

Department of Machine Elements and Tribology, Polytechnic University of Bucharest,
313 Spl. Independentei, 060042 Bucharest – ROMANIA, Phone: +40214029411, Fax: +40214029581,
E-mail: filip@meca.omtr.pub.ro.

ABSTRACT

In the process of friction of two materials and in the presence of own lubricants, wear phenomenon itself manifests as a transfer of material from an element of a friction couple on the other, this phenomenon being characteristic of selective mass transfer process by diffusion, forming a thin, superficial layer with superior properties, at minimum friction and wear. It's and the case of the friction couples, steel/copper alloy lubricated with glycerin or a special lubricant where certain that takes place a mass transfer by copper diffusion, on the friction surface of the steel. One of the phenomena accompanying material transfer by diffusion in the friction process, is and the thermal diffusion. The paper analyses the mass transfer phenomenon through diffusion, with the thermal aspects (thermal diffusion), which leading to the formation of soft, thin and superficial layer, tribological performance and the correlation between the thickness of this layer and the saturation degree of contact surfaces of the couple friction steel/copper alloy (bronze, brass).

1. INTRODUCTION

Diffusion in metallic materials has a fundamental role in the processes of extraction and purification of metals and alloys, and in processing technology [1, 2, 3].

Mass transport by diffusion is done by moving atoms and therefore, the diffusion in solid state allows information on thermal agitation of the atoms in the crystal lattice and of structural imperfections present in the network [4]. The knowledge of laws which rule the diffusion phenomena and mass transfer are important in the establishing kinetic relationships [5, 6], through technological parameters correlation (concentration, the temperature, the contact duration etc.), which allow a quantitative appreciation of transfer processes and making possible the intervention in their modification for intensifying the process and for establishing the optimum conditions for carrying it out [7].

It is known that in the solid materials the diffusion mechanism is a jump mechanism, the mass transfer is done through successive, activated thermal jumps of the atoms, from the old position in a position neighboring atomic, from a surface to another. [7, 8]. The way how occurs the diffusion process into solids is presented, schematized in figure 1, where is showing the distribution of atoms, in the moment start of diffusion $t = t_0$, when the atoms which diffuses are uniform distributed in the central part (Fig.1a), after the time $t = t_1$ relative small from the beginning of diffusion and after the time $t = t_2$ relative big from the beginning of this process, respectively how varying with the distance z , the concentration c , of the atoms alloying at the same moments (Fig.1b). The most probable, diffusion mechanism in solid solutions is diffusion through the vacancies. Mathematic, the diffusion in metals and the solid alloys is described with the Fick's laws help, quantitatively describing at microscopic level, the mass transport by diffusion [7, 8]. The first law describes the speed with which is produces the diffusion and is shown by the relationship:

$$J = -D \text{ grad } c, \text{ or the diffusion after a } z \text{ direction will be: } J = -D \left(\frac{\partial c}{\partial z} \right), \quad (1)$$

where: J – the material flow, which diffuses and passes through the surface unit in time unit, D – diffusion coefficient, c – constituents concentration.

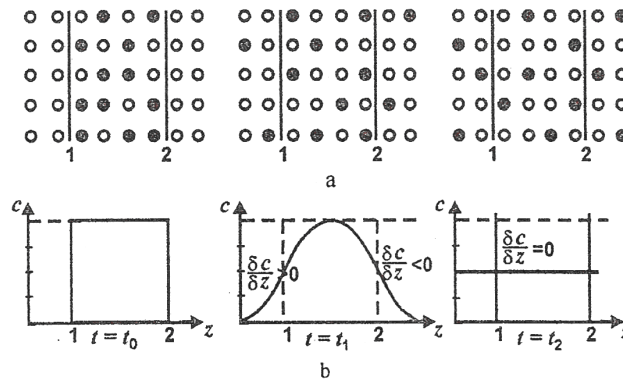


Figure 1 The diffusion process in solid solutions of **B** metal in **A** (a) and the variation with distance **z** of concentration **c** of the diffusing atoms (b): • - atoms of the base correspondent **A** (Fe); o - atoms of the diffusing correspondent **B** (Cu).

The modification of concentration in time is described by second Fick's law:

$$\frac{\partial c}{\partial t} = \text{div}(D \text{grad } c), \text{ and for diffusion after a direction becomes: } \frac{\partial c}{\partial t} = D \left(\frac{\partial^2 c}{\partial z^2} \right). \quad (2)$$

For execution, of a diffuse atomic jump is necessary the existence of a very big fluctuation of the atom's vibration energy, correlated with an adequate synchronization of the movement atoms neighbors and is realized through the average frequency notion of atomic jump, shown by the relation:

$$J = -1/z(v_0 a^2 e^{-E_a/RT}). \quad (3)$$

From the identification of (1) and (2) relations results:

$$D = 1/z(v_0 a^2 e^{-E_a/RT}) = D_0 e^{-E_a/RT}, \quad (4)$$

in which: z - the coordinative number of the network; v_0 - the atom's vibration frequency, $v_0 = 10^{13} \text{ s}^{-1}$; a - the distance between two atomic equilibrium positions which are adjacent in the network; E_a = actuation energy depending on how diffusion occurs [9, 10]; D_0 - the frequency factor, dependent of the coordinative number (interstitial available positions), frequency of vibration of particles diffused and of the distance between interstitial surfaces.

In relation (4) of the diffusion coefficient, the inter-atomic distance in the network **a**, varies very little with the temperature, having close values for all metals. As a result, the diffusion coefficient **D** varies rapid with the temperature and is different in alloys because of the jump average frequency variation, having values of $10^{-10} \text{ cm}^2/\text{s}$ type and D_0 is independent from temperature and for metals and solid alloys is included between the 0.1 – 10 cm^2/s limits [7, 8, 9].

2. THERMO DIFFUSION AND MASS TRANSFER THROUGH DIFFUSION

The diffusion mechanism in solids, being a jump mechanism, the mass transport is made through successive jumps from an equilibrium position into another. Both forms of diffusion are possible: self-diffusion and inter-diffusion. In real solids, the principal mechanisms depend of the defects and the solid solution type (alloys type): diffusion through interstice and diffusion through vacant nodes. The temperature gradient can lead to mass transfer from a surface on another when the energetic conditions from the contact area are ensured. Similarly to the concentration gradient **c** through thermal gradient (Dufour effect) it can transfer mass from a surface on another. The second Fick's differential equation is [9, 10]:

$$\frac{\partial c}{\partial t} = \frac{\partial}{\partial z} [D \left(\frac{\partial c}{\partial z} \right) + \left(\frac{\partial \alpha}{\partial z} \right) (c/\alpha_e)] \text{ for solids } \alpha_e = A e^{(-E_a/R\theta)}, \quad (5)$$

with **A** – constant; E_a - activation energy; **R** – gas universal constant; θ - temperature.

Differentiating the relation (5) after direction **z** and neglecting second order differentials, obtained:

$$\partial/\partial t = \partial/\partial z [D(\partial c/\partial z)] - (1/R) \partial/\partial z (DC/\theta) \partial E_a/\partial z + (1/R) \partial/\partial z (DcE_a/\theta^2) \partial/\partial z \quad (6)$$

The first part of relation (6) $\partial/\partial z (D \partial c/\partial z)$, represents Fick's second law in the classic way, and the other components are effects of temperature (Dufour effect). For solid materials, the diffusion coefficient **D** has a dependence of Arrhenius type (s. relation (4)), where $T = \theta$.

Defining flow concentration $J = -\partial/\partial z [D(z,t)c(z,t)]$ and according (4) results [11, 13, 14]:

$$J = (Dc/R\theta) (\partial E_a/\partial \theta - E_a/\theta) d\theta/dz - Ddc/dz \quad (7)$$

This relation shows that, if $\partial E_a/\partial \theta = \partial E_a/\partial \theta$, then thermo diffusion doesn't happen; if $\partial E_a/\partial \theta \leq \partial E_a/\partial \theta$, thermo diffusion occurs from the lowest temperature to the highest; if $\partial E_a/\partial \theta \geq \partial E_a/\partial \theta$, occurs from the highest temperature to the lowest, the flow **J** may be null, if the two terms are equal. Using Fick's second law is inferred differential equation of thermo diffusion [13, 15, 16]: $\partial c/\partial t = \partial^2 [D(z,t)c(z,t)]/\partial z^2$ (8)

If materials of friction couple have different concentrations of some of the component elements and in the friction area there are energetic formed conditions and a liquid with properties which avoids the oxidation and penetration of hydrogen, then thermo diffusion is possible and, as result, relation (8) can be applied. For the bronze/steel couple the lubricated with glycerin, copper can diffuse from bronze, on the steel surface forming through mass transfer of a layer „servowitte”. If we consider a bronze roughness 1 in contact with steel surface 2 (fig. 2) with Oz axe orientated in steel surface, then the differential equation of the diffusion process is obtained from (7).

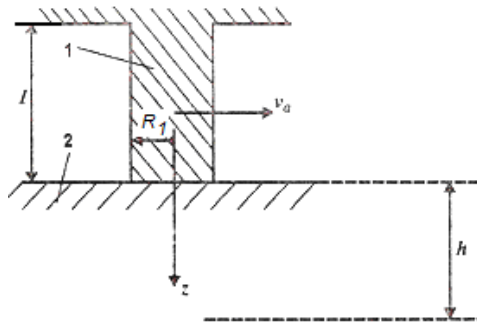


Fig. 2 Roughness from bronze in contact with a steel surface: 1-roughness; 2-surface

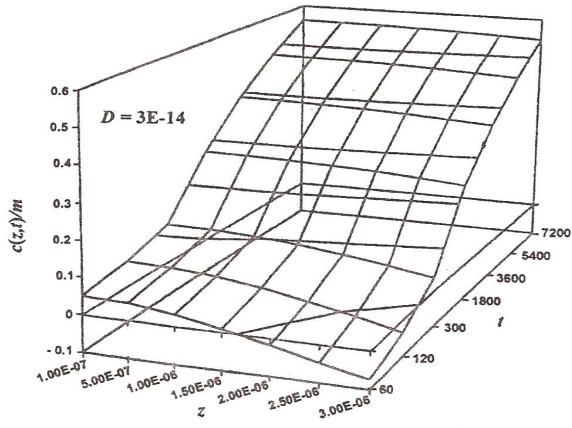


Fig. 3 Concentration's variation $c(z, t)$ with the depth from the surface z and time t in the conditions of mass transfer by diffusion

The equation's solution (9) is done for the next initial and on limit conditions:

1) $c = 0, t = 0, z > 0$; 2) $D \partial c/\partial z = \text{const} = m, t > 0, z = 0$; 3) $c = 0, t > 0, z \rightarrow \infty$, where **m** is the constant mass flux on the contact border and lead solution:

$$c(z,t) = m/\sqrt{D} [2\sqrt{t/\pi} e^{-z^2/4Dt} - z/\sqrt{D} \text{erf } c(z/2\sqrt{Dt})], \quad (9)$$

To see how the concentration **c** varies with the surface depth **z** and function time **t** in the conditions of mass transfer, has been resolved and represented in a graphic the relation (9) and then reproduced in Fig. 3, as $c/m = f(z, t)$ for a known diffusion coefficient $D = 3 \cdot 10^{-14} \text{ m}^2/\text{s}$, where it see that the concentration, increases in time and decreases with from the surface depth. To have a quantitative correlation with the experimental results has been represented graphic, also the concentration's variation with from the surface depth after an hour of friction couple functioning (Fig. 4); and with the functioning time in conditions of diffuse mass transfer, for depth $z = 3 \mu\text{m}$ (Fig. 5) and the same **D**, confirming the results in Fig. 3. A correlation example for the above dates using relation (9) and graphic

representations (Fig. 3, 4, 5) have allowed the establishing of copper concentration in steel, $c = 0,367 \text{ g/cm}^3$, with whose help was possible to obtain the mass flow, for bronze/steel couple, $m \approx 10^{-6} \text{ g/m}^2 \text{ s}$, which corresponds as size order with the specialty literature values.

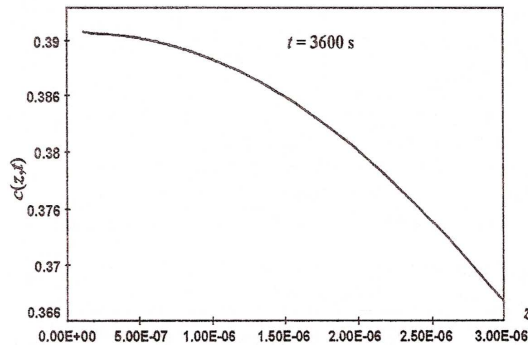


Fig. 4 Concentration's variation $c(z, t)$ with the depth from the surface z , after $t = 1$ hour

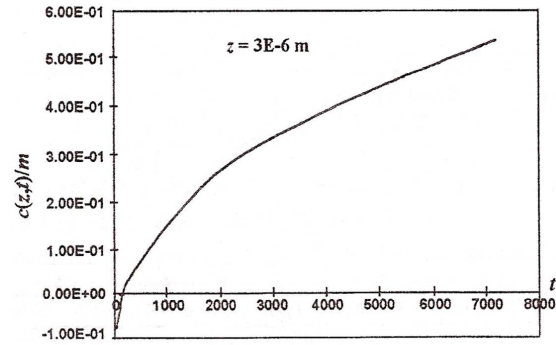


Fig. 5 Concentration's variation $c(z, t)$ with the functioning time t at depth $z = 3 \mu\text{m}$

Considering relation (9) it is possible to analyze the temperature's effect through parameter D (which depends of temperature) on variation of copper concentration with time t and with the depth from steel surface 2. It is observed the very important effect of parameter m , over diffusion. It is noted that this parameter's values possible to be determined experimental, are dependent of the used lubricant and the creation local conditions of the energetic transfer. The formed local area can be considered as a „membrane” of diffusion mass transfer [14]. This „membrane” can be completely opaque and the transfer doesn't appears or absolutely permeable and the transfer is maximum. The „membrane” must have such properties, so that the transfer by diffusion to be made in both directions.

3. CORRELATION BETWEEN TRANSFERRED LAYER'S THICKNESS AND THE SATURATION DEGREE

Defining the layer transferred by diffusion in mass transfer conditions as a layer of thickness $h = k\sqrt{Dt}$ in which was transferred a certain percentage copper quantity (k – constant, determined in function of the percentage of substance transferred). Considering the quantity of accumulation substance in the layer of thickness h (M_h) and the quantity of substance accumulated throughout the body height ℓ (M_ℓ) ($\ell > h$) (see Fig. 2), by the transfer determined on the contact area A_c , results:

$$M_h = A_c \int_0^h c(z, t) dz \text{ and } M_\ell = A_c \int_0^\ell c(z, t) dz. \quad (10)$$

Replacing in (9) $z = h = k\sqrt{Dt}$ and $u = z/2\sqrt{Dt}$, results M_h from (10) function $\Phi(k/2)$, respectively for $z = \ell$, results M_ℓ from (10) function $\Phi(k/2)$, where: $\phi(k/2) = (2/\sqrt{\pi}) \int_0^{k/2} e^{-u^2} du$, solvable numerically according with table 1.

Table 1
Solve numerical a function $\phi(k/2)$

k	1	2	3	4	5	6
$\phi(k/2)$	0.5205	0.8427	0.9661	0.9953	0.9996	1.0000

For $\ell \rightarrow \infty$, results $M_\infty = 2m A_c \cdot t$. Defining the saturation degree of concentration is

$$g_s = \frac{M_h}{M_\infty} = \phi(k/2) - \frac{1}{4} \frac{\phi(k/2)}{k^2} k^2 = \frac{1}{4} [(4 + k^2) \phi(k/2) - k^2] \quad (11)$$

whose variation is given in Fig. 6.

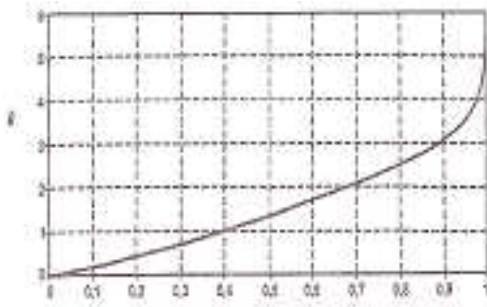


Fig. 6 The variation's saturation degree of at the copper concentration in bronze/steel surface

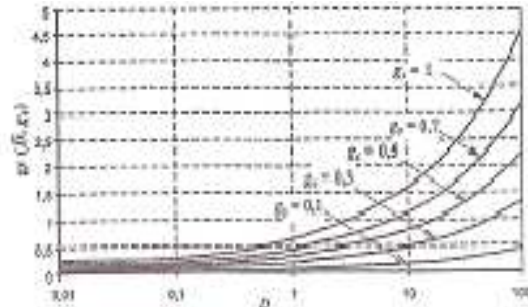


Fig. 7 Variation of relative saturation degree of at the copper concentration in bronze/steel surface

If a certain saturation degree (g_s) of the steel surface with copper from bronze is accepted then is possible to determine the constant k and the substance quantity in a layer $h = k\sqrt{Dt}$. Relative saturation (g_r) of the steel couple with the copper from bronze is:

$$g_r = \frac{M_h}{M_\ell} = \bar{D} \frac{(4 + k^2)\Phi(k/2) - k^2}{(4\bar{D} + 1)\Phi(1/2\sqrt{\bar{D}}) - 1}, \quad (12)$$

and the way how varies with \bar{D} is presented in Fig. 7.

The dimensionless parameter $\bar{D} = Dt/l^2$, similar to Fourier parameter (F_0) in thermal transfer, it can be explained depending on the elements geometry of the couple and the relative sliding, rolling and pivoting speed and the her combinations. So, for cylindrical roughness **1** (with ray R_1 and height ℓ) with contact on flat circular frontal surface and which moves with a relative sliding speed v_a (see Fig. 2), from the ideal flat surface (without roughness), the dimensionless parameter will be: $\bar{D}_1 = D_1(\theta) \cdot \ell_f / v_a \ell^2$, (13) in which: ℓ_f - friction length; $D_1(\theta)$ - diffusion parameter of the roughness material at the contact surface temperature.

For the ideal plane surface of h_1 thickness, the material having the diffusion parameter $D_2(\theta)$, the dimensionless parameter will be: $\bar{D}_2 = D_2(\theta) \cdot 2R_1 / v_a h_1^2$. (14)

For an unconformable roughness (spherical or cylindrical with a punctual or linear contact), the contact and transfer by diffusion time is dependent of the real contact area's size and the relative speed.

4. CONCLUSIONS

The mechanism of the mass transfer by diffusion is formed of:

- the diffusion and mass transfer of the reactants at the separation limit;
- the physical – chemical transformations at interface;
- the diffusion and the mass transfer of the reaction products from the interface.

At diffusion phenomenon's analysis and mass transfer is necessary to solve the next:

- the conditions for the realization of a certain number of phases and the laws which described the component's distribution, between they, determined by the laws of the phases and laws of the equilibrium;
- the conditions for phenomenon's development (operational conditions), determined by the initial and final conditions of the components and their quantities; the relations between the component's concentrations and quantities are obtained from the mass's conservation law (material balance's equation);
- the conditions which determine the diffusion speed and the mass transfer's speed from a surface on another and its dependence of the difference between the equilibrium

concentrations and operational, of the system's physical properties and of the thermal conditions from the contact area.

The phenomenological analysis of the main aspects from the friction area allows the explication of the diffusion mass transfer's characteristics.

It is estimated that the variation of the thermal conditions, both in time and in the proximity of the friction area is the principal cause of the diffusion mass transfer, if the lubricant pellicle avoids copper oxidation, and this was demonstrated through the analytical calculation of the thickness transferred layer's. Thermo diffusion in metals and alloys can have place only through the crystalline network, on the surface or at the grain limit.

Many investigations showed that thermo diffusion develops the fastest at the element's surface, a bit slower at the grain's limit and the slowest in the grain's volume.

So, thermo diffusion at selective mass transfer is a surface diffusion and this fact makes that the transfer of metallic particles, which is released in a relative short time, function the friction conditions (pressure, speed, and temperature).

The friction conditions influence direct the thermal flow and its evolution, so that the diffusion mass transfer is an example of positive self-adjustable of the tribological phenomenons.

References

- [1] Lebedev V.M., Polzer D., Garkunov D.N. – Issladovanie trenia pri izbiratelom pernose. Teoreticeskie i prikeadenie zadaci trenia, iznosa ismazka mašia – Izd. „Hanka” Moskva,.
- [2] Ilie F. - Studies and researches concerning the tribological behaviour of friction couple functioning with selective transfer, Tribology International, Vol.39, Issue 8, 2006, pp 774–780.
- [3] Padgurskas J., Rukuiža R., Jankauskas V., Andriušis A., Žunda A.- Tribological running-in investigation and surface analysis of copper coats made by electro-impulsive spraying, Vol.205, Issue 10, 2011, pp. 3328–3333.
- [4] Rybakova L.M., Kuksenova L.I. – Physical Criteria of wear Resistance of Metal Materials in Surface Active Lubricated Media – Proc. the Conference on Tribology „Friction Lubrification and Wear – 50 Years on”, London, IME, 1987, pp. 419-426.
- [5] Drozdov Yu.N., Rybakova L.M., Litvinov I.P., Pavlik B.B., Sidorov S.A. – Kinetic of Fracture of Constructions Steel Caused by Friction – Trenie i iznos, vol. 10, nr.5, 1982, pp. 773-778.
- [6] Gromakovski D.G., Bertayev B.M., Shkunova T.B. – Policular Features of kinetic Approach in Simulation Wear. This of Raports Submitted to the All Union Conference, Improvement of the Durability and Reability of Machines and Instruments, Kuybisen, KPt I, 1981, pp. 76-77.
- [7] Geru N. – Physical Metallurgy – E.D.P., Bucharest, 1981.
- [8] Gâdea S., Petrescu M. – Physical Metallurgy and Metal Study – vol. I, EDP Bucharest, 1979 și vol. III EDP, Bucharest, 1983.
- [9] Tudor A., Ilie F. – New Aspects Concerning the Selective Transfer Phenomenon in Friction Coupling – The Annual Symposium of the Institute of Solid Mechanics, Bucharest Romania Academy, 26-27 November, 1992, pp. 250-257.
- [10] Coeiger G.H., Poitier D.R. – Transport Phenomena in Metalurgy – Addison, Wesley Publ. Company, 1973.
- [11] Hebda M., Cicinadze A.V. – Spravocinik po tribotehnika – Tom I „Mašinostroenie”, 1989.
- [12] Iordache O., Smighelski O. – Equations of mass transfer phenomena and heat – Technical House, Bucharest, 1981.
- [13] Balakiu V.A. – Trenie i iznos pri vîsokih scorostiah scolojenia – Moskva, „Mašinostroenie”, 1980.
- [14] Tudor A., Ilie F. – Some Aspects Looking the Thermo diffusion and the Selective Transfer in Steel – Bronze Friction Couple – p. II, Conference „Selective Transfer, Coatings and Self-Organization: Practice & Development”, vol. 2, 7-11 October, 1994, Sofia, Bulgaria, pp. 104-111.
- [15] Nosonovsky M., Rohatgi P.K. - Thermodynamic Methods in Tribology and Friction-Induced Self-Organization, Biomimetics in Materials Science, 2012 – Springer New York, pp. 153-194.
- [16] Kotnarowski A. - Selective Transfer Phenomenon in Copper-Steel Tribological Systems, Materials Science and Engineering , Periodical Solid State Phenomena Vol. 147 – 149, 2009, pp. 558.

HEAT WASTE RECOVERY FROM CORROSIVE FLUE GAS STREAMS USING AIR HEATERS THERMOSIPHON TYPE

Iliya Iliev, Ruse University¹

ABSTRACT

One of the most important factors, determining the efficiency of the boilers operation is the temperature of the exhaust gases. In the energy steam generators that use lignite coals with high content of moisture and sulfur, the excessive lowering of the gas temperature leads to low temperature corrosion. Warmed air is supplied beforehand in the air heaters or regeneration of gases is used so this negative occurrence in the air heaters first level can be avoided. All of these methods partly solve the problem, but at the cost of lowering the energy conversion efficiency of the steam generator. The new technical solution for the construction of the air heater for industrial steam generator Viessmann Vitomax 200 burning heavy fuel oil is shown. The prospective results from different work modes in the air heater are presented. The possibilities are analyzed to avoid the low - temperature corrosion on the heating surfaces of the air heater. Cost-effectiveness analysis is made of the new air heater.

1. INTRODUCTION

The utilization of waste heat from the exhaust gases of the steam generators leads to increasing their energy conversion efficiency. Though, in most cases the “non-project” lowering of the temperature of the exhaust gases is constricted by the possible corrosion processes, which can greatly shorten the life cycle of the utilizers (air heaters, economizer etc.). From all of the methods for protection of the low temperature heated surfaces, the most effective are connected with the heightening of the metal work temperature over the sulfuric-acid dew point, operation of the air heater in the area with low corrosion of the corrosion curve [6] and burning of the fuel with minimal coefficient of excess air. From the cited three, the first method is the most reliable. The condensation of the water vapour is most possible in modes of start and in minimal boiler loads, i.e. in lower temperatures of the products of the burning. However these modes take up a very small part of the total boiler runtime and with lower loads the process of the corrosion is significantly weakened.

From formula (1) for determining of the local temperature of the work surface of the air heater:

$$(t_w)_i = (t'_{air})_i + \left(\frac{q}{\alpha_2} \right)_i \quad (1)$$

It follows that in the given conditions for heating, the temperature of the wall in the coldest part on the entrance of the air in the air heater depends on the temperature of the air on the entrance (t'_{air}) and the coefficient of heat transfer from the wall to the air (α_2) . Therefore to raise the temperature of the wall and to avoid the low temperature corrosion (t'_{air}) needs to be increased and (α_2) needs to be lowered. However the latter is contrary to the general trend for creating of package – model heating surfaces.

¹ Ruse, Bulgaria, e-mail: iiliev@enconservices.com; cell phone: +359 887306898

Universal method in accordance to prevention of gas corrosion is the approach with raising of the air temperature on the entrance in the air heaters, which actually takes place with the use of steam air heaters or by recirculation with hot flue gases. It should however be noted that with the use of the air heaters high enthalpy energy is spent so the low potential heat can be utilized, and the second approach is used to decrease the gross energy conversion efficient of the boiler. In all of the outlined methods connected with the raising temperature of the air at the entrance in the air heater as additional measure is recommended the separation of the “cold” part in separate section, in which the corrosion processes are the most intensive. In this way the reconstruction processes are forgiven and are cheaper, because only the separate section is changed. For example with the regenerative heat exchangers for their operational period to be expanded and for the comfort during repair the elements of the “cold package” is produced with width 1-1,5 mm instead 0,5 – 0,8 mm for the elements of the “hot package”.

2. METHODOLOGY

Promising direction for waste heat utilization of the exhaust gases of the steam generator of industrial and energy boilers is in the quality of the used additional air heater heat exchangers with intermediate heat carrier, i.e. with two-phase thermosiphon [2, 6]. This type of air heaters is installed in the “cool” part on air heater first level, where the wall temperatures of the pipes is between $80 \div 160^{\circ}\text{C}$. For lowering of the pollutions and corrosion on the pipes when burning heavy fuel oil with excess air in the combustion chamber $\alpha_{bc} > 1,04$, the minimal temperature of the wall must be maintained over 125°C , but with $\alpha_{bc} < 1,03$ the wall temperature can be $80-85^{\circ}\text{C}$.

According to the methodic for Heat calculations of boilers according to the Normative Method [5], complete exclusion of low temperature corrosion is provided when the temperature of the wall in the coldest area is higher than the dew point in all loads of the boiler is with $5 \div 10^{\circ}\text{C}$ higher (minimal values are for the minimal load).

According to the same methodic the minimal wall temperature of the pipe air heaters, for which are also the thermosiphons, is calculated according to the formula:

$$t_w^{\min} = \frac{\alpha_1 \cdot t_{gas}^{\min} \frac{d_2}{d_1} + \alpha_2 \cdot t'_{air}}{\alpha_1 \cdot \frac{d_2}{d_1} + \alpha_2}, ^{\circ}\text{C} \quad (2)$$

where t'_{air} is the medium temperature of the air in the air heater, $^{\circ}\text{C}$; t_{gas}^{\min} is the minimal temperature of the exhaust gases, described by:

$$t_{gas}^{\min} = t'_{air} + K_{out}^{\min} (t'_{gas} - t'_{air}), ^{\circ}\text{C} \quad (3)$$

K_{out}^{\min} iscoefficient, which is determined by [5, (fig. II-3)].

For heightening of t_w^{\min} it is appropriate an asymmetry of the inlet air temperatures to be created in height of the first stroke increasing from top to bottom.

Increase of the air temperature with 10°C leads to increase of $t_w^{\min} \approx 6^{\circ}\text{C}$.

In regenerative air heaters the heated surface of the changed part is chosen by the conditions of settlement to ensure there are no corrosive processes. Therefore the minimum accepted

temperature for the wall of the not changed “hot” part of the regenerative air heater (RAH) with nominal load of the boiler is estimated by the formula [5]:

$$t_w^{\min} = \frac{x_1 \cdot \alpha_1 \cdot t_{gas}'' + x_2 \cdot \alpha_2 \cdot t_{air}'}{x_1 \cdot \alpha_1 + x_2 \cdot \alpha_2} \quad (4)$$

where: α_1 and α_2 - coefficients of heat exchange in the “hot part”, W/(m².K);
 t_{gas}'' and t_{air}' are temperatures respectively of the gases on the exit of the “hot” part of the RAH and the air on its entrance, °C; x_1 and x_2 - share of the heating surface or section, circumfluent respectively by the gases and air.

During the burning of heavy fuel oil, the temperature of the exhaust gases in nominal mode is accepted in accordance to the content of sulfur in the heavy fuel oil [5].

3. DESCRIPTION OF THE BASELINE

3.1. Air heaters with heat pipes for energy boilers burning lignite coals

The used coals from the coal basin “Maritsa East” is characterized by low calories, high moisture and high content of sulfur. In table 1 the elementary content of coals is shown and its burning heat(LHV).

Table 1. Elementary content of burning lignite coals

C ^r , %	H ^r , %	S ^r , %	O ^r , %	N ^r , %	A ^r , %	W ^r , %	Q ^r _i , kJ/kg
19.02	1.60	1.92	5.70	0.33	16.28	53.50	6243

With enough accuracy for the practice, the theoretical temperature of sprinkling can be described by the equation [1,5]:

$$t_{op}^T = \Delta t_{op}^T + t_{H_2O}, \quad (5)$$

where: Δt_{op}^T [°C] – theoretical temperature difference between the acid temperature of the sprinkling of the gases and temperature of condensation of the water vapour;

t_{H_2O} [°C] – temperature of sprinkling of the clear water vapour;

$$\Delta t_{op}^T = \frac{200 \cdot \sqrt[3]{S_{np}^r}}{1.25 \cdot a_{OTH} \cdot A_{np}^r}, \text{ } ^\circ\text{C}, \quad (6)$$

where: a_{OTH} - the share of the blown away with the ash; S_{np}^r and A_{np}^r - adapted content of the sulfur and ash relative to 1000 kJ/kg from the heat of burning of the coals [5].

Following these formulas for the chosen base fuel according to Table 1 the theoretical point of sprinkling is reached: $\Delta t_{op}^T = 141.6 \text{ } ^\circ\text{C}$ The experimentally measured values with drill

confirm the theory. Until the installation of the new air heater with heat pipes (VP-TT), the temperature of the exhaust gases is maintained within $185 \div 190^{\circ}\text{C}$, with loads lower than the nominal, and energy conversion coefficient of the steam generator $-81 \div 82\%$.

Steam generators №5, 6, 7 and 8 were equipped with pipe air heaters of horizontal type. According [5] the temperature of the entering in the horizontal – pipe VP-I level air it should be higher than 80°C , and according to [6] respectively - 96°C . However in the practice the average temperature of the air at the entrance in the present VP -1 Level is maintained around 50°C , with methods lowering the efficiency of the burning process, i.e. by recirculation of the hot air in the furnace.

3.2. Air heaters with heat pipes for steam generators of heavy fuel oil:

Experts from the department of “Technology of the water and fuel” in Moscow Power Engineering Institute (The Technical University) offer choice of temperature of the exhaust gases after the boiler, where low temperature corrosion does not go over some accepted value. The presented below “on-line” calculations from the website of the Moscow Power Engineering Institute (The Technical University) [6] define the optimal temperature of the exhaust gases with accepted speed of corrosion, which is at 0.2 mm/year . During the calculations, the characteristics of the heavy fuel oil with different sulfur content are set, usually used as fuel for industrial steam generators.

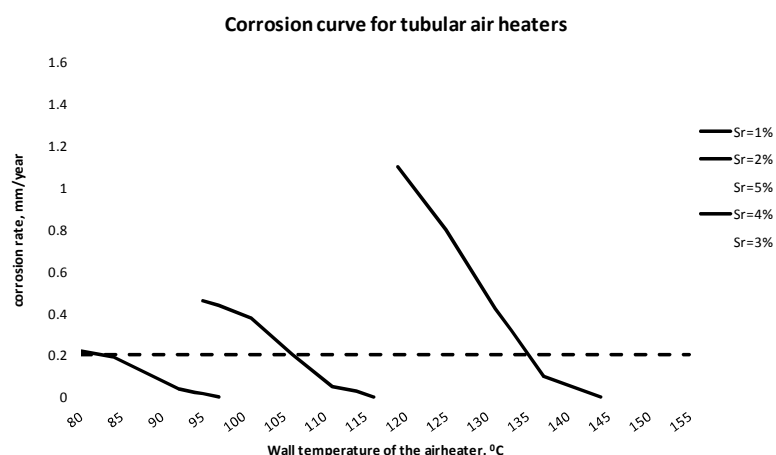


Fig. 1. Dependence of the level of corrosion on the temperature on the surface of the pipes of the air heater of the industrial steam generator Viessmann vitomax burning heavy fuel oil.

The graphic dependence shows the limit values for the temperature of the surface of the steam generators with chosen speed of corrosion. The chemical analysis of the heavy fuel oil showed that the content of the sulfur in the work mass in the fuel does not go over 2%. Therefore with the chosen method for utilization of the waste heat from the gases, with installation of pipe air heater can be achieved increase in the energy conversion efficiency of the steam generator in nominal mode with 2.9%, but on the condition that a speed of corrosion is accepted at 0.2 mm/year . Because the pipe air heaters are manufactured usually with pipes with wall width of $1.6 \div 2 \text{ mm}$, this should mean that the pipe air heater will be in operation for 2-3 years. Of course such investment is justified, but very risky.

Alternative method is offered for utilization of the heat from the exhaust gases for boiler *Viessmann vitomax 200* burning heavy fuel oil. The method includes use of air heater with heat pipes of thermosiphon type [3], where the experience is used from the realized in the period 2003÷2005 four air heaters in TPP “Maritsa – East-2” for steam generators type PK-38, burning high moisture sulphurous lignite coals [1,2].

Comparison is made between standard horizontal-pipe air heater and the offered for implementation in Tiger Corporation town Pirot (Serbia) air heater with heat pipes (AH-HP) regarding the corrosion safety of the pipe surfaces. The last lines on the way of the gases are studied, which are exposed to the most dangerous modes. The only criteria for prevention of the corrosion processes on the pipe surface is the surface temperature of the walls to be higher than the temperature of the dew point of the flue gases in all modes of work of the boilers [1, 4, 5].

In table 2 are presented the results from the calculated “thermodynamic dew points” using the empirical formulas, with different sulphur content in the elementary content of the heavy fuel oil, calculated according to the Normative Method (II-I) [5].

Table 2. Dew point temperature for different sulphur content of heavy fuel oil

LHV=41 GJ/t; asses air rate in chamber 1.15	Sulphur content in heavy fuel oil, S^r , %				
	$S^r=1\%$	$S^r=2\%$	$S^r=3\%$	$S^r=4\%$	$S^r=5\%$
Dew point temperature [5], °C	108.8	124.4	135.4	144.1	151.5

Following these formulas the chosen base fuel ($S^r=2\%$; LHV=41GJ/t) for steam generator *Viessmann vitomax 200* according to formulas (5,6) (look at Table 2) the theoretical dew point is $t_{dp}^T = 124.4$ °C.

Full calculations are done for the surface temperatures of the wall of the air heater with heat pipes (AH-HP). For the bunch heat pipes, the temperature values of the pipe surface are presented in Table 3.

Table 3. Temperatures of the surface of the pipes of VP–TT with different temperatures of the inlet air

Indicator	Temperature of the inlet air, $t^{\text{inlet air}}$, °C				
	0°C	20°C	30°C	40°C	50°C
Wall temperature of the top row, t_w^{top} , °C	170.3	173	175.3	179.4	182.8
Wall temperature of the middle row, t_w^{middle} , °C	141.9	144.5	146.8	150.8	154.1
Wall temperature of the bottom line, t_w^{bottom} , °C	113.5	116	118.3	122.2	125.4

The analysis of the analytical results (Table 3) shows that in mostly all of the presented modes, the pipe bunch of VP-TT will work in conditions without safety from corrosion processes, excluding the cases when the starting temperature of the heated air is under 200°C. However such cases are exceptions due to the air that is sucked into the room, in which the steam generator is placed. If, however for some reasons the sulphur content in the fuel is raised, a danger of corrosion exists, but only on the last lines of the heat exchanger. Therefore when constructing the air heater the last line is projected in the direction of the gases to be filled with thick walls $\phi 35/5$ mm.

4. BENEFITS OF THE IMPLEMENTAATION OF THE PROJECT

In the period 2003 – 2005 during the planned reconstruction in "Maritsa – East -2" are realized four additional air heaters with heat pipes with patented technology [2] for steam generators №5,6,7 and 8(PK-38 typewithsteamproductionof 250 t/h).

After the installation of the replacement air heaters type "heat pipes" after VP –I lvl, the flue gases are cooled to $170\div 165^{\circ}\text{C}$. The energy efficiency coefficient of the boiler is raised with $>1.7\div 2.3\%$ and the annual fuel economy only for one boiler is in the amount of 16000 tones. Another important advantage of the air heater with heat pipes is (unlike the previous horizontal – pipe VP – 1 lvl) that on the surface of the pipes in the gas part a temperature is maintained, higher than the dew point, which eliminates the possibility for corrosion processes. The resulted warm air after VP-TT is lead to the mixer unit without the need in this case to be used hot recirculation (exclusion make only some extreme modes of work of the boiler). From these some major economies are done from production costs, as well as keeping the normal technical state of the VP-1 for longer time without problems of embedding and corrosion in the starting area of the horizontal pipes.

5. CONCLUSIONS

1. The implementation of AH-HP minimizes the use of recirculation in the pre - heating of the cold air;
2. The tests show that the air heater with heat pipes (AH-HP) has a sufficiently high surface temperatures in the gas part ($> 150^{\circ}\text{C}$), which makes its operation safe in terms of corrosion activity. Surface temperatures are significantly higher than the dew point, and which conforms to the anticorrosion mode.
3. The heater with heat pipes (AH-HP) will provide heating of the outside air from $25\div 35^{\circ}\text{C}$ to $110\div 140^{\circ}\text{C}$, with guaranteed anticorrosion mode for AH-1st and AH-2st;
4. The implementation of AH-HP does not require reconstruction of existing air and smoke drawing fans;
5. The designed air heater with heating pipes gives high level of utilization, and for specific steam generator *Viessmann vitomax-200* the utilization power in nominal mode goes to 335 kW, and the air for burning is heated from 20 to 100°C , with cooling of the flue gases from 220 to 160°C ;
6. The exploitation period of the AH-HP exceeds 10 years.

References

- [1] Christov, Ch., Low temperature corrosion and contamination of the heating surfaces of steam generators, Habilitation work for obtaining academic rank Professor – 1st Level, Sofia, 1978
- [2] Christov, Ch., Iliev, I., Patent № 745/31.01.2002, Heat exchanger with heat pipes, 2002, Patent Office of Republic of Bulgaria
- [3] Iliev I., V. Kambourova, A. Terziev, M. Venev, Heat waste recovery from exhaust gases of heavy fuel oil boiler by using heat exchangers with heat tubes, International Scientific Conference 40yrs Dept. "Machinery and equipment for food industry", 9-11 May 2013y., Plovdiv
- [4] Thermal design of boilers (Normative methods), issue 3, revised and supplemented, St. Petersburg, 1998
- [5] http://twtmass.mpei.ac.ru/mas/worksheets/Opt_temp_uch_gazov.mcd
- [6] Pioro L.S., Pioro I.L., Двухфазные термосифоны и их применение в промышленности, Наукова думка, Киев, Монография, 1987.

BENCHMARKING THE ENERGY PERFORMANCE OF SIX CAMPUSES OF RUSE UNIVERSITY

Ilia Iliev¹, Ruse University ; Veselka Kamburova, Ruse University; Angel Terziev, Technical University of Sofia

ABSTRACT

The object of the study is benchmarking of energy performance of 8 campuses of University of Ruse on the base of performed energy audit. University campuses are heated by central heating and the costs for heating are significant. To reduce heating costs and identify energy efficiency measures, energy audits were prepared for 6 of the University campuses. The thermal characteristics of the buildings envelope were determined. The factors that make an impact on the specific heat consumption are determined. Regression analysis was conducted to establish there lationship between the studied parameters. A comparison between the thermal characteristics of the individual campuses is made, as well as conclusions on the state of the envelope of each building are presented.

1. INTRODUCTION

According to the analysis made, buildings are one of the largest energy consumers. The data for the European Union shows that 40% from the whole energy consumption comes from the 160 million existing buildings in Europe and 3/4 from the consumed energy is used for heating and cooling.

The households and business in Bulgaria consume considerably more energy for heating and cooling compared to Europe. According to the Agency for Sustainable Energy Development (ASED) the consumption of energy in the housing sector is more than 1/3 from the whole energy consumption in the country.

University of Ruse's costs for heating are also significant. In the last three years the University has spent for heating an average of 7000 MWh per year.

The only possibility to reduce energy used for heating of buildings with out causing deterioration of indoor thermal comfort is by introducing a number of energy efficiency measures in buildings - the main point being retrofitting and the replacement of window frames as well as update of the building heating system

2. RESULTS FROM THE ENERGY AUDIT OF SIX OF THE CAMPUSES OF RUSE UNIVERSITY

The subject of the energy audit was the buildings of the Rectorate and the campuses 3, 6, 7, 8 and 10. In Table 1 are shown the main building characteristics of the audited buildings, as well as the year of their commissioning [2, 3, 4, 5, and 6]. The views of campuses are presented in Figures 1 to 5.

¹ 7000 Ruse, Bulgaria, 8 Studentska str., Ruse, phone +359 887 306 898; e-mail: iliev@enconservices.com



Figure 1. View of the Rectorate



Figure 2. View of the Campus 3



Figure 3. Views of the Campus 6



Figure 3. Views of the Campus 7



Figure 4. View of the Campus 8



Figure 5. View of the Campus 10

In the survey conducted detailed analysis is made of the external envelope of buildings - exterior walls, windows, floors and roof. The values of the thermal transmittance U of different types of envelope are calculated taking into account the thermal conductivity of building materials and the heat transfer coefficients on the inside and outside of the building element. Controlled measurements of U were conducted for different types of walls. The results from these are close to the calculated ones. In Table 2 are provided the average values of heat transfer coefficients for different buildings and areas of the envelope [2, 3, 4, 5, 6].

Table 1: Main building characteristics of the audited buildings

Building	Year of commissioning	Built-up area, m^2	Total floor area, m^2	Heated area, m^2	Gross volume, m^3	Heated volume, m^3
Rectorate	1959	4,278	16,103	16,103	70,088	65,405
Campus 3	1971	2,141	3,038	3,038	16,958	14,493
Campuses 6 and 7	1959 и 1972	1,365	5,460	5,460	21,418	18,753
Campus 8	1959 и 1972	1,630	3,672	3,672	14,429	11,724
Campus 10	1972 и 1985	1,670	3,379	3,379	10,561	9,505

The campuses of the Ruse University are heated with central heating and thermal energy is purchased from Thermal Power Station "Ruse East". For the measurement of the consumed by the buildings heating energy only one meter is used. In practice the quantity of consumed energy by each of the campuses in question is not known.

Table 2: Average values of heat transfer coefficients for different buildings and areas

	Walls		Floor		Roof		Windows		Total	
	A, m ²	U, W/(m ² K)	A, m ²	U, W/(m ² K)	A, m ²	U, W/(m ² K)	A, m ²	U, W/(m ² K)	A, m ²	U, W/(m ² K)
Rectorate	5066	1.4	5494	0.42	4211	0.8	1934	2.37	16705	1.0387
Campus 3	2130	1.2	2142	0.42	2025	1.41	890	3.7	7187	1.3363
Campuses 6 and 7	2514	1.2	1347	0.28	1347	0.8	667	2.49	5875	1.0438
Campus 8	1186	1.32	1647	0.4	1633	0.72	694	3.33	5160	1.1068
Campus 10	1035	1.61	1170	0.64	1168	1.58	704	3.03	4077	1.5682

A model study is performed of the energy consumption in all buildings subject to the audit, based on the method from BDS EN 832 by using the software product ENSI.

For this purpose, each of the campuses is regarded as an integrated system in which the different factors and different systems affect the microclimate (occupants, external enclosures, climatic factors, energy sources, etc.). When creating the model it is accepted that each campus is to be seen as a thermal zone. The models are calibrated and normalized.

The results for the consumption of thermal energy for heating for all of the campuses are summarized in Table 3.

Table.3:Consumed thermal energy

Buildings	kWh/m ² yr.	MWh/yr.
Rectorate	71.8	1156
Campus 3	187.2	569
Campuses 6 and 7	85.7	468
Campus 8	99.5	365
Campus 10	109.7	317

Analysis of the results shows that Campus 3 has the highest value of Energy Use Intensity (EUI) for heating(kWh/m²yr). According to the data shown in Table 2, this campus has generalized heat transfer coefficient with 15% smaller than campus 10,and its specific energy consumption is 70% higher than that of campus10. That is also the reason why such analysis of the factors that affect the specific energy consumption is done.

3. REGRESSION ANALYSIS

Comparative analysis of the results for consumed heat can be done by using an appropriate regression model. The first step in preparation of this model must be the elaboration of the factors that affect the consumed heat for heating and cooling of the campuses. Generally, the biggest impacts make climatic factors, but in this case it will not be taken into account because the campuses are located a few dozen meters apart. This means they are in the same climatic conditions.

The main influencing factors that can be taken into account when developing the model are:

- Internal temperature;
- Form factor – the ratio of the total area of the envelope structures and elements to the heating volume;

- Relative size of windows;
- Average U-value;
- Thermal energy from residents;
- Thermal energy from internal sources of heat;
- Duration of operation of the campus (age).

At present, information was collected for the above factors, but it concerns only 5 of the viewed campuses. Thus the number of the influencing factors should be reduced in order to obtain adequate results from the regression analysis. In the overlooked campuses temperature is maintained at 19°C during working hours and it drops to 14°C. All of the buildings are considered learning campuses, so the values of heat from occupants and heat from internal heat sources are very similar. Overhaul and renovation of buildings are envisaged, and therefore at present this factor will not be included in the regression model.

In Table 4 the values of the impacting factors are provided, which are used in the model:

Table. 4: Values of the impacting factors

Campus	Thermal Energy, kWh/m ² /yr	Form Factor, m ² /m ³	Relative windows area [-]	Average U, W/(m ² K)	Heat from residents, W/m ²
	Y	X1	X2	X3	
Rectorate	71.8	0.26	0.13	1.0387	18.7
Campus 3	187.2	0.50	0.293	1.3363	8.1
Campuses 6 and 7	85.7	0.30	0.12	1.0438	9
Campus 8	99.5	0.45	0.189	1.1068	6.9
Campus 10	109.7	0.39	0.121	1.5682	7

A regression analysis is conducted, in which are examined the potential linear and nonlinear models. The analysis showed the following models as suitable:

$$Y = \exp(aX_1 + bX_2 + cX_3 + d) \quad (1)$$

$$Y = aX_1 + bX_2 + cX_3 + d \quad (2)$$

$$Y = aX_1 + bX_2 + cX_3 \quad (3)$$

The smallest sum of the average quadratic errors is observed in model (1), therefore for further considerations this model is selected.

$$Y = \exp(-0.164X_1 + 4.1595X_2 + 0.7442X_3 + 3.0535) \quad (4)$$

Residual Sum of Squares = 166.936; Adjusted coefficient of multiple determination (R_a^2) = 0.9177

The analysis of the resulting model (4) shows that factor 2 is with the highest weight (relative size windows), next in influence is the average heat transfer coefficient and the third-the form factor, where the dependence is inversely proportional. Table 5 presents a comparison of actual and model values of the specific heat rate for the 5 campuses that are under consideration. The largest deviations occur in buildings with the lowest value of the specific energy consumption.

Table 5. Comparison of actual and model values of the specific heat rate

Y	Calc Y	Residual	% Error	Abs. Residual	Min. Residual	Max. Residual
71.8	78.80613	-7.00613	-9.75784	7.006127301	-7.006127301	10.31039644
187.2	186.3145	0.885451	0.472997	0.885450946		
85.7	75.3896	10.3104	12.0308	10.31039644		
99.5	102.739	-3.23905	-3.25533	3.239048958		
109.7	110.2205	-0.52047	-0.47445	0.520470689		

The value of the relative area of windows (X_2) and that of the U-value for windows ($3.7 \text{ W} / (\text{m}^2\text{K})$) of Campus 3 is the biggest. This leads to a large value of the average U-value for the entire envelope of the building.

Small values of X_2 are observed in Campuses 6 and 7 (0.12), campus 10 (0.121) and Rectorate (0.13). For the Rectorate and Campuses 6 and 7 also the lowest values of the specific energy consumption for heating are identified. The exception is Campus 10, which shows the highest values of U-value for walls, roof and floor and therefore the biggest average U-value. Never the less this building has significantly lower specific energy consumption for heating compared to Campus 3 due to the relative small size of the windows.

4. CONCLUSIONS

In this paper a benchmarking process is developed using multiple regression. A benchmarking table is derived from removing the effect of significant factors using the regression model.

The comparative analysis can be used to determine the change of the specific energy consumption in case one of the influencing factors changes (e.g., an average U-value), as well as to predict the specific energy consumption for other university buildings.

This is the first step for these researches and the regression model can be improved in the presence of data from energy audits of other buildings of the University.

References

- [1] Ordinance № RD-16-1058 from 10th December 2009 about *Indicators for energy consumption and energy performance of buildings*, (Promulgated State Gazette 103 from 29.12.2009)
- [2] "EnCon Services" Ltd, *Energy Auditing of University of Ruse "Angel Kanchev" – Rectorate*, March 2012, Sofia;
- [3] "EnCon Services" Ltd, *Energy Auditing of University of Ruse "Angel Kanchev" – Campus III*, March 2012, Sofia;
- [4] "EnCon Services" Ltd, *Energy Auditing of University of Ruse "Angel Kanchev" – Campus VI and VII*, March 2012, Sofia;

TESTING OF A 620 KW BURNER FOR SAWDUST IN SUSPENSION AND GAS ENRICHED IN HYDROGEN (HRG)

L. Mihăescu, E. Pop¹, M. E. Georgescu, G. Lăzăroiu, I. Pișă, G.P. Negreanu, C. Ciobanu,
¹Politehnica University of Bucharest

ABSTRACT

For extending the use of biomass in electricity output, high thermal powers (over 1MW) are necessary. These thermal powers can be achieved by choosing the solution of suspension burning in equipments similar to pulverized coal burners and injection of gas enriched with hydrogen (HRG). In the present research we study the influence of HRG injection over the sawdust combustion process.

1. INTRODUCTION

The biomass has been used at the beginning especially in home burning equipment with low efficiency. In the last time it has been developed heat generators of low and medium power that burn various types of biomass (forests, agricultural waste) with high efficiency and low residues.

HRG injection before the burner has been proposed in order to support the ignition process. HRG is obtained through water electrolysis and it represents a mixture of atoms and radicals (H, OH, O, HO₂) having the low heat value of hydrogen (10760 kJ/ Nm³). The HRG is produced by a generator having a maximum volume flow rate of 4 Nm³/h [1].

For extending the use of biomass in electricity output there are necessary high thermal powers, over 1MW which can be achieved by choosing the solution of suspension burning, in equipment similar to pulverized coal burners.

An important part in the fuel cost is that connected to the storage and to the transportation of the fuel. These economical calculations are necessary in determining the costs of the heating of spaces using biomass. This operator cost shows the advantage of suspension burning of sawdust and wood slivers, where C_{ce} has much diminished.

2. THE BURNER CONSTRUCTION

In principle, an installation to burn sawdust in a pulverized state has the following components: a fuel bunker, for an autonomy range of 4 to 6 hours, a pneumatic system to feed the sawdust to the burner, a primary, secondary and tertiary air fan and also a flue gas fan. The burner ensures a flow of 0.5 kg/s of sawdust, having a 14115 kJ/kg calculation calorific heat value.

The elemental analysis of the sawdust was:

$$C^i = 42,7\%, \quad H^i = 4,7\%, \quad O^i = 36,3\%, \quad S_c^i = 0\%, \quad N^i = 1\%, \quad A^i = 5,5\%, \quad W_t^i = 9,8\%$$

A complete automatized boiler, with moving fire grate has the following auxiliary electrically acted: combustion feeder, acting moving grate, ash and slag discharge, air fan, gas fan.

¹ UPB-FIMM, Splaiul Independentei 313, email:elena.pop@upb.ro

For the suspension burning of sawdust, the feeding combustion is a pneumatic system from the air circuit, the auxiliary acting installations being:

- Air fan
- Gas fan
- Slag discharge

It remains as disadvantage the necessity of small dimension combustible particles, in the range of 1-3,0 mm. In nowadays technical stage there are few firms concerning with this problem, one of them being Saake [5]. As a result the members of Thermodynamics, engines, thermal and refrigeration equipments Department of University „Politehnica” of Bucharest proposed the construction of a burner for sawdust and wood slivers, in a modulating conception, starting from 600 kW thermal power. The burner is a multiple air swirling type. The HRG contribution is 20 kW resulting a 620 kW testing power.

3. CALCULUS

For the beginning, the project of the burner needs theoretic considerations about the combustible particles moving in the air flow and also the burning velocities.

The efficiency of suspension burning (in air flow) depends on the ratio between the combustible particles velocity W_p and the burning velocity K_{sc} and it also depends on the residence time in the furnace τ_s .

For a swirling flow, with upward air circulation, the velocity of the combustible particles in the air flow is written bellow:

$$W_p = k_p d \left(\frac{\rho_p - \rho_a}{\rho_a} \right)^{0,5} \text{ m/s} \quad (1)$$

where: $k_p = 254$, d [m]- the diameter of the particles, ρ_p and ρ_a , [kg/m³]- the density of particles and air.

For the wood slivers the imposed values were: $d = 0,002$ m, $\rho_p = 850$ kg/m³, $\rho_a = 0,85$ kg/m³ having as a result: $W_p = 254 \cdot 0,002 \left(\frac{850 - 0,85}{0,85} \right)^{0,5} = 16 \text{ m/s}$

The velocity of the consumption of biomass particle has two components parts: the emission and burning of volatile substances and coke burning. The wood biomass has 60-70% volatile matters from the total combustible matter.

The velocity of the carbon consumption is:

$$K_s^c = \tau \frac{C_o}{\frac{1}{\alpha} + \frac{1}{\beta}} \text{ m/s} \quad (2)$$

where: $\tau = \frac{12}{32}$ - the coefficient of stoichiometric transforming, C_o [kg/m³]- the oxygen concentration, α [m/s]- the volatile burning velocity, β [m/s]- the carbon burning velocity.

The burner has the next characteristics:

- Thermal power: max 600 kW;
- Reduced weight (under 50 kg);

- Self-supporting construction (all subassemblies are welded with the central channel of primary agent, which sustains the entire construction);
- Radial dimensions that permit to implement the burner in the furnace (furnace embrasure $\varnothing 168$).

The thermal normal operation of the fluids is in the next domain:

- The primary agent temperature ($60-90^{\circ}\text{C}$); this value is imposed by the humidity of the biomass at the entrance of the feeding system and the temperature of primary air.
- The primary air temperature is between $150-200^{\circ}\text{C}$ depending on thermal load. To avoid an accidental ignition of the biomass (of the emitted volatile matters of biomass in contact with the heated primary air) it can be used a dilution of the oxygen concentration by recirculating burnt gases.
- The secondary air temperature, $150-220^{\circ}\text{C}$.
- The tertiary air temperature, $150-220^{\circ}\text{C}$.

The primary air represents 30-40% of the total air necessary for burning. This air has the aim of pneumatic transportation of sawdust particles and also ensures the ignition and burning of volatile substances, which ensure the burning of fix carbon of the wood matter of sawdust. The excess air ratio at the end of the furnace is imposed at the level $\lambda_f = 1,25$.

In figures 1a and 1b is presented the constructed burner.

The burner has multiple swirling flows for the secondary and tertiary air. The wood biomass and the transportation air are introduced by the central channel un-swirled.



Figure 1 a The sawdust burner-front view



Figure 1b The sawdust burner-lateral view

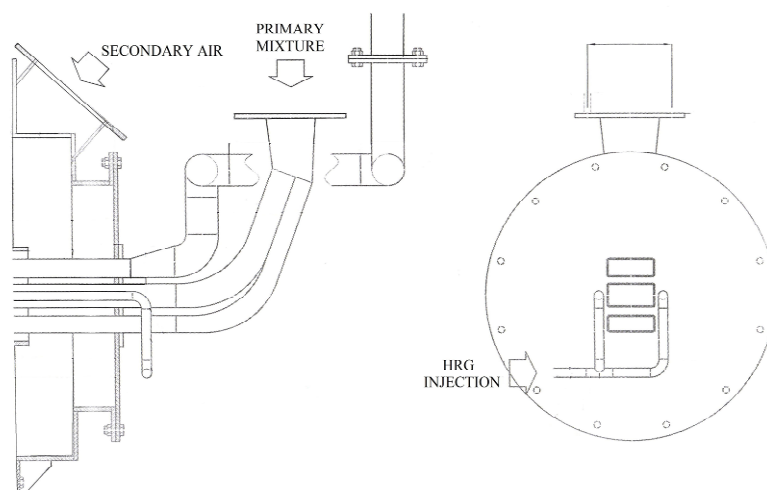


Figure 2. HRG Injection system

Figure 2 presents the HRG injection system placed before the biomass burner. Thus, the flame results also as a biomass-hydrogen co-combustion process.

The axial blades at the end of central channel swirl the secondary air.

A primary air to the secondary air ratio of $0.5 \div 0.8$ is proposed. The excess air ratio at the burner level is imposed in the limits: $\lambda = 1.2 \div 1.25$.

The burner has also a system of swirling blades for each of the air circuits.

The primary air velocity is recommended to be $W_1 = 25 - 35$ m/s, for the secondary air $W_2 = 30 - 35$ m/s, and for the tertiary air $W_3 = 20 - 30$ m/s.

An alternative for the axial blades system using one with radial blades is proposed. The swirl ratio used for different jet categories was of 1.2 for the secondary air and of 5.4 for the tertiary air.

The characteristics of burner working are:

1. The thermal support combustible quota:

- Gas volume/ sawdust mass:
-

$$q_B = B_g / B \quad (3)$$

where: B_g [Nm³/h]- the HRG gas flow capacity used as thermal support, B [kg/h]-the sawdust flow capacity. The calculus of sawdust flow capacity was $B = 80$ kg/h.

- Thermal quota:

$$q_B^* = \frac{B_g \cdot Q_g}{B \cdot Q_i^i} \quad (4)$$

where: Q_g – the calorific heat value of the thermal support gas ($Q_g = 10760$ kJ/ Nm³), Q_i^i - the calorific heat value of the sawdust.

2. The pneumatic transportation capacity of sawdust from the stoking bunker to the burner, defined by volumetric concentration of the sawdust in the air transport.

$$c = \frac{B}{\dot{V}_a} \quad (5)$$

where: \dot{V}_a -the air flow capacity for pneumatic transportation. As mass ratio, the sawdust concentration for transportation is:

$$c^* = \frac{B}{\dot{V}_a \cdot \rho_a} \quad (6)$$

where: ρ_a [kg/m³]-the density of the air for sawdust transportation (rectified for the real temperature).

3. The thermal load of the burner embrasure

$$q_a = \frac{B \cdot Q_i^i + B_g \cdot Q_g}{S_a}, \quad kW / m^2 \quad (7)$$

where: Q_i^i [kJ/kg]- the calorific heat value of sawdust, S_a [m²]- the aria of embrasure (for the embrasure diameter of 168 mm, the aria is 0.022 m²).

4. The thermal load of the furnace volume compared with the project one is:

$$q_v = \frac{B \cdot Q_i^{i_i} + B_g \cdot Q_g}{V_f}, \quad kW / m^2 \quad (8)$$

where: V_f – the active furnace volume.

The designed thermal load of the furnace volume has the value $q_v = 41 \text{ kW/m}^3$ ($V_f = 10\text{m}^3$)

4. EXPERIMENTAL RESULTS

The experimental tests aimed to find the ignition capacity and burning efficiency (in pulverized state) in an energetic medium power installation.

The tests were made in the pilot furnace of 2 MW_t of UPB, Thermodynamics, engines, thermal and refrigeration equipments Department, where it was implemented the new burner for wood slivers and multiple swirling jets of 620kW thermal power. Figures 3 and 4 presents the sawdust burner placed in the front of the pilot furnace.



Figure 3. Details of assembling the burner



Figure 4. Front view of the boiler

Figures 4 and 5 present the flame in the furnace, visualized from the back visiting door or the furnace, using a digital camera. It is noticed a strong intensity and radiation of the flame, similar to pit coal flame.



Figure 5. The general aspect of the flame evolution

The thermodynamics dimensions measured in the flame and also the general aspect of the flame show an intensive burning which recommends this burning technology.

The technology of suspension burning of sawdust with swirling burners makes possible the increase of power from medium to high energy production. So, if the tested burner has a thermal power of 620 kW_t , following the principles to realize it, the power can be increased to 3 MW_t for the next burners.

The coupling of more burners permits the achievement of steam generators or hot water boilers with power over 10 MW_t .

After processing the experimental data, resulted the characteristics already presented in „Calculus” method.

1. The thermal support combustible quota

Gas volume/ sawdust mass:

- the maximum value $q_B = 0,05 \text{ m}^3_{\text{N}}/\text{kg}$ sawdust

- the minimum value $q_B = 0 \text{ Nm}^3/\text{kg}$ sawdust

2. The pneumatic transportation capacity

The sawdust mass concentration in the transportation air was: $c = 0,24 \text{ kg/m}^3$ and $c^* = 0,19 \text{ kg/kg}$.

3. During the tests, the air excess value were:

$$O_2 = 1,2 - 6,6\%$$

$$\lambda = 1,06 - 1,45$$

4. The carbon monoxide emission was:

$$CO = 19,8 - 43 \text{ mg/m}^3$$

This value is incontestable lower to that of the layer burning technology. The NO_x emission was $\text{NO}_x = 375 - 387 \text{ mg/m}^3$.

3. CONCLUSIONS

The designed burner successfully achieved the rated thermal power 620 kW, for a sawdust flow capacity of 80 – 85 kg/h and 4 Nm^3 HRG.

In all these stages the flame had high temperatures, similar to pit coal flame working with. The flame had high brilliancy aspect and filled the entire furnace volume.

Under the influence of HRG the burning was stable and the emissions were low. The CO emission, which is high when using layer burning biomass, was extremely low, under 40ppm, when using suspension burning sawdust. This aspect offers an advantage to suspension burning of sawdust as also the possibility of higher power achievements.

References

- [1] T. Prisecaru, L. Mihaescu, C. Petcu, R. Popescu, M. Prisecaru, I.Pisa, E. Pop, C Ciobanu, „*Co-combustia c rbului cu gaz  mbog  t  n hidrogen (HRG)*” pp 145-149, a IX Conferinta Nationala de Echipament Termomecanic Clasic si Nuclear si Energetica Urbana si Rurala, Bucuresti, 25 iunie 2010, ISSN 1843-3359
- [2] L. Mihaescu, T. Prisecaru, M. Georgescu, G. Lazaroiu, I. Oprea, I.Pisa, G. Negreanu, E. Pop, V. Berbece, “*Construction and testing of a 600 kW burner for sawdust in suspension*”, COFRET’12, 11-13 Jun Sozopol, Bulgaria
- [3] Barta S., Pi   I, Mih  escu L, ao “*ERPEK company conception for boilers with wood biomass automatic feeding system*”, The 33-rd International Symposium of the Section IV of CIGR, Bucuresti, June 2011
- [4] Enache E, Mih  escu L, Pi   I, ao “*Achievements in the construction of boilers for agricultural biomass combustion*”, The 33-rd International Symposium of the Section IV of CIGR, Bucuresti, June 2011
- [5] SSB-D Dust Burner, http://www.saacke.de/en/products/special-plants/products/index.php?we_objectID=844

RESEARCH ON THE PULVERIZATION QUALITY REFERRING TO THE ENERGETIC USE OF RAW VEGETABLE OILS OR VEGETABLE OILS MIXED WITH FOSSIL FUELS

Drd. Ing. Niculescu Bogdan¹

In the category of alternative fuels we also have to take into account raw vegetable oils and those doped with liquid fossil fuels. Analyzing the energetic characteristics of vegetable oils, the result consists of their great resemblance to those of fossil liquid fuels.

The research conducted on the aspect of the pulverization characteristics aims to analyze the possibility of using conventional technologies for the burning of vegetable oils – the spray pump.

When using the spray pump, the viscosity is recommended to be between 1.5 and 2.5 (0.0676 to 0.1575 cm² / s). These values of viscosity for raw vegetable oils can be obtained at temperatures above 50 °C. Consequently, the viscosity of the sunflower oil varies from 0.125 cm²/s at 80C to 0.0874cm²/s at 180 °C.

Lower values of about 30-40% are obtained from raw corn oil and canola oil. In terms of raw oil viscosity, it does not mark very dissimilar values from the light fuel as, nowadays, the electrical preheating temperature can be easily achieved by heating in the burner before spraying.

The raw vegetable oils studied (sunflower, corn, canola and soya) enlist ignition points between 260 and 313 °C, values that are significantly higher than those of the liquid fossil fuels. Therefore, the ignition point of the light liquid fuels is 50-65 °C and the ignition point of black oil is 90-100 °C.

It appears from the above analysis that it is required a softer pulverization of raw vegetable oils. By mixing them with liquid fossil fuels, the ignition point noticeably decreases. We consider a mixing proportion in the 10-30% of light fuel oil.

On an experimental stand from UPB there have been performed pulverization tests using a mechanical injector at a pressure of 40 bar. We aimed to observe the average diameter of pulverization and to compare it with the one obtained when using light fuel type M.

1. MECHANICAL PULVERIZATION OF THE LIQUID FUEL

To characterize the smoothness of pulverization it is used the term ‘mean diameter of droplets’. Following the physical model, we can define the following mean diameters:

- The Sauter mean diameter, defined as the diameter of the droplets in a homogeneous cloud, which has the same area and the same number of cloud droplets as the research cloud:

$$d_s = \frac{\sum_{i=1}^k d_i^3 n_i}{\sum_{i=1}^k d_i^3 m_i} \quad (1)$$

¹ PhD student at Faculty of Power Engineering; email: bogdan.niculescu70@yahoo.com

- The Vitman mean diameter, which represents the diameter of the droplets of a homogeneous cloud and has the same weight and the same number of droplets as the research cloud:

$$d_v = \frac{\sum_{i=1}^k d_i^3 g_i}{\sum_{i=1}^k d_i} \quad (2)$$

Experimental research on the mechanical burners with a swirl pot revealed for the Vitman mean diameter the following relation:

$$d_v = d_0 C A \text{Re}^p \pi^k \quad (3)$$

where d_0 is the nozzle diameter, C - experimental constant and A is the geometric characteristics of the injector; p - coefficient with the value of -0.7, k - coefficient with the value of -0.1, $C = 47.8$.

$$A = \frac{(D_k - d_t) d_0}{n d_t^2}; \quad \pi = \frac{\eta_l^2}{\sigma \rho_l d_0} \quad (4)$$

Where: D_k is the swirl pot diameter, d_t - the diameter of the tangential channels, n - the number of the tangential channels, ρ_l - the density of the liquid, η_l - the dynamic viscosity.

The maximum diameter compared to the diameter of the nozzle depends on the Weber number. For injectors with a swirl pot, the following relation is proposed:

$$d_{\max} = \frac{3,72 \left(\frac{d_0}{2} \right)^{0.56} A^{0.11}}{\left(\frac{\sqrt{b} \Delta p}{\sigma} \right)^{0.33}} \quad (5)$$

where b is the height of the swirl pot and Δp is the pressure drop in the injector.

The angle of dispersion is particularly important for filling the furnace with flame, respectively for the combustion with a minimum excess of air. The size of the dispersion angle should be studied tightly connected to the way of bringing and guiding of air. If the injector is considered separately (stationary air injection), the relation will be:

- For less viscous fluids ($\pi < 4 \cdot 10^{-5}$)

$$\frac{\text{tg } \theta}{\text{tg } \theta_0} = 3,05 \cdot 10^{-2} \left(\frac{D_k}{d_0} \right)^{-0,4} \pi^{-0,33} \quad (6)$$

For more viscous fluids ($\pi > 3 \cdot 10^{-4}$)

$$\frac{\text{tg } \theta}{\text{tg } \theta_0} = k \pi^{-0,33} \cdot \text{Re} \quad (7)$$

where $tg \theta_0 = \frac{2,83(1-\tau)}{\tau^3(1+\sqrt{1-\tau})}$; $\tau = 1 - \frac{d_a^2}{d_0^2}$; d_a - the embrasure diameter

To determine the smoothness of pulverization there have been applied the relation (3) - for mixtures of raw sunflower oil and liquid fuel type M, for a burner with a swirl pulverization pot, flow of 170 kg / h, mounted on the experimental stand from UPB.

The swirl pot has the following dimensions: $D_k = 15$ mm, $d_i = 6$ mm, $n = 4$ channels, diameter of the pulverization nozzle $d_0 = 1$ mm.

It follows: $A = \frac{(15-1) \cdot 1}{4 \cdot 12} = 3,5$

Criteria, Re , π have the following values:

- Mixing with 20% light fuel type M, $Re = 3900$; $\pi = 2 \cdot 10^{-4}$
- Mixing with 30% light fuel type M, $Re = 4400$; $\pi = 2,7 \cdot 10^{-4}$

The mean diameter of the droplets using Vitman:

- for vegetable oil mixed with 20% light fuel type M

$$d_v = 1 \cdot 47,8 \cdot 3,5 \cdot (3900)^{-0,7} \cdot (2 \cdot 10^{-4})^{-0,1} = 530 \mu m$$

- for vegetable oil mixed with 30% light fuel type M

$$d_v = 1 \cdot 47,8 \cdot 3,5 \cdot (4400)^{-0,7} \cdot (2,7 \cdot 10^{-4})^{-0,1} = 380 \mu m$$

The pulverization smoothness is within acceptable limits. It is noted that pulverization improves along with the increase of light fuel mixing. It is recommended to use higher pulverization pressures for higher proportions of vegetable oil.

2. EXPERIMENTAL DETERMINATION

The theoretical conclusions were verified through pulverization experiments on the stall to the ETCN Department of the Polytechnic University of Bucharest. The research stall on pulverization is usable for liquid fuels that have to be preheated in order to pulverize. As a result, the light liquid fuels as well as the vegetable ones and their mixtures can be tested. The stand scheme is presented in Figure 1.

In Figure 1 it is presented the experimental stall equipped with a swirl pot injector and also with control of the flow return.



Fig. 1 The experimental stall for studying the



Fig.2. View of the experimental burner

pulverization of the liquid fuel



Fig 3. Jet 30% pulverized – oil and air swirl Fig 4. Jet 40% pulverized - oil and air swirl

3. CONCLUSIONS

Dosage within the limits of 20 - 40% of the vegetable oils in liquid fossil fuel does not create problems when using conventional combustion equipment.

The research on the use of the mixtures of liquid fuels with vegetable oils represents a direction of an easy recovery by combustion without any additional investments of renewable liquid fuels.

GAS TURBINE BEHAVIOR AT THE AMBIENT CHANGE

Prof. dr. ing. Oprea Ion
Politehnica University of Bucharest

ABSTRACT

It is known that the Romanian climate is a continental temperate one, with great difference in temperature not only with season but also diurnal. The paper presents the results of an analytical research focused on the gas turbine operation characteristics in different condition of inlet air temperature. An example could be the gas turbine power plants that operate in Bacau or Ploiesti cities. Based on this method may be easily estimated the behavior of any gas turbine for different ambient air temperature.

1. INTRODUCTION

Gas turbines power plants represent a promising technology for energy generation in Romania, especially for cogeneration. Some new gas turbines are now in operation, in a large range of power, until 275 MW, with advanced parameters and modern design. A characteristic of Romanian climate is the large variation of the ambient air temperature, with season and even diurnally. The inlet air temperature could vary in a day with about 20 °C and with about 50 °C in a year. In these conditions the gas turbine performances are strongly influenced by the air temperature, much more than other parameters. Generally is known that a decrease of inlet air temperature has good consequences on gas turbine characteristics, increasing power, efficiency and air flow rate, as shown on principle in figure 1.

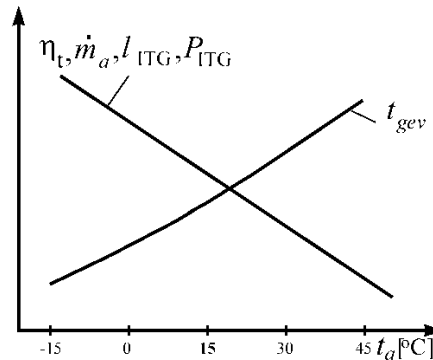


Figure 1: Inlet air influence

For each gas turbine this influence may have particular values, indicated by the designer. A thermodynamic analyzes of the gas turbine cycle offer the possibility to get a method to determine this influence according to the gas turbine characteristics and to plot the owner operation diagrams. Such a method is described in this paper.

2. THERMODYNAMIC ANALYSIS OF THE CYCLE

A simple analyze of the gas turbine Brayton cycle emphasizes the influences of the main parameters (ambient air temperature, extreme temperature ratio, pressure ratio) on the useful work and efficiency.

$$l_t = \theta h_1 \left(1 - \frac{1}{m} \right) (\theta - m) \quad [\text{J/kg}] \quad (1)$$

$$\eta_t = 1 - \frac{1}{m} \quad (2)$$

Where:

$\theta = T_3 / T_1$ – extreme temperature ratio;

$m = (k-1) / k$; k – adiabatic exponent;

h_1 – inlet air enthalpy.

The results of the ideal thermal cycle analyze give the effect or the atmospheric air temperature on the work, but are not appropriated for efficiency. Therefore the actual cycle, shown in figure 2 was considered.

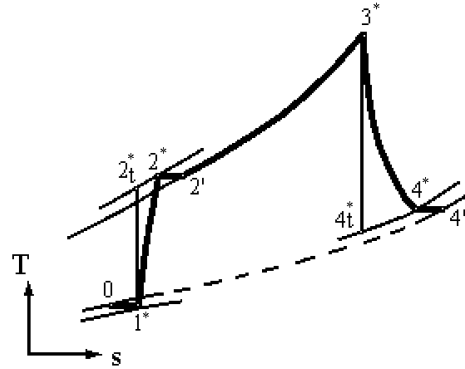


Figure 2: Actual Brayton cycle

The overall efficiency of the actual cycle is given by [3]:

$$\eta_e = \eta_c \frac{c_{pg34} \theta \eta_{eT} \frac{1 + \lambda L}{\lambda L} \left(1 - \frac{1}{\pi_t^{m_g}} \right) - c_{pa} (\pi_c^{m_a} - 1) \frac{1}{\eta_{ec}}}{\frac{1 + \lambda L}{\lambda L} c_{pgT3} (\theta - 1) - [\pi_c^{m_a} - 1] \frac{c_{pa}}{\eta_{adc}}} \quad (3)$$

Where:

- c_{pa} and c_{pg} – specific heat at constant pressure of air and flue gases for mentioned range of temperature; [kJ/kgK]
- $\pi_{t,c}$ – expansion, compression pressure ratio;
- λ – excess air coefficient;
- L – stoichiometric air quantity;
- η – effective, internal or adiabatic efficiency of gas turbine, air compressor and combustor;
- $m_{g,a} = (k_{g,a} - 1) / k_{ga}$; k – adiabatic exponent.

3. CASE STUDY

The objective of the case study is to get the influence of the inlet air temperature on the efficiency and power, for a particular gas turbine without internal heat recovery. In order to relieve this influence the thermodynamic analysis takes into consideration the actual turbine cycle.

The gas turbine system data are: electric output $P_e = 50$ MW, inlet turbine temperature $t_3 = 1200$ °C, compressor pressure ratio $\pi_c = 14$. The ambient air temperature varies from -15 °C to 35 °C, the inlet pressure and air relative humidity ISO standard condition and constant. The fuel is purely methane. The pressure losses at the compressor inlet, through the combustor and gas turbine exhaust are taken into consideration; due to these losses the compressor and turbine pressure ratio are different. In the same time the dependence of thermal and physical characteristics of air and flue gas on temperature and composition are considered. In any conditions of work the maximum temperature of the thermal cycle was maintained constant. This analytical model can be used for any type of gas turbine.

Results and discussion

The gas turbine efficiency, the excess air coefficient, air and fuel mass flows, the turbine power were calculated for various values of the inlet air temperature; the results are presented in table 1 and figures 2 and 3. It can be observed that a decrease of the inlet air temperature difference with 10 °C increase the efficiency with 0,3 percentage points (about 0.8 %) and the power with about 3 %. The others influences are: a decrease of the excess air coefficient with 2.2%, a decrease of air mass flow with about 3% and of the fuel mass flow with about 0.94%.

Table 1. Thermal cycle characteristics vs. inlet air temperature

			Inlet air temperature [°C]					
			-15	-5	5	15	25	35
Air excess coefficient.	λ	-	2.68	2.74	2.8	2.86	2.92	2.99
Compressed air temperature	t_2	°C	317.1	337.6	357.9	377.9	398.1	418.0
Air mass flow	\dot{m}_a	kg/s	117.94	121.61	125.51	129.64	134.06	138.75
Fuel mass flow	\dot{m}_f	kg/s	3.1643	3.1948	3.2274	3.2600	3.2972	3.3371
Efficiency	η	%	37.65	37.35	37.03	36.71	36.37	36.02
Power (total)	P	MW	58.77	56.01	53.09	50	46.69	43.17

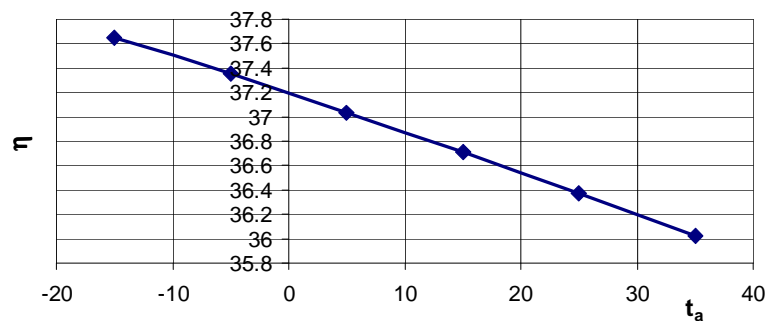


Figure 3: Efficiency vs. atmospheric temperature

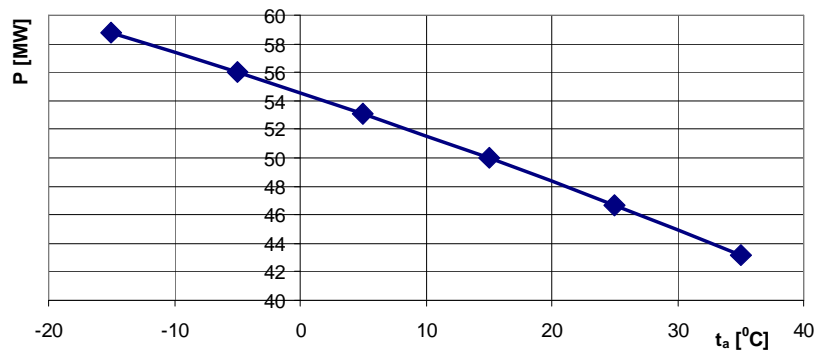


Figure 4: Power output vs. atmospheric temperature

The analytical model results show the positive influence of the ambient air decrease on the overall efficiency of the gas turbine system. An important gain in power or reduction the fuel mass flow is obtained. A better behavior in turbine service is therefore obtained during the night, cold days or in winter.

4. CONCLUSION

The operational today's gas turbine systems must be flexible in operation in order to ensure the heat demand and the grid balancing. The high variation of the ambient air temperature affects the turbine output and is very important to know in any moment the turbine behavior.

This analytical model gives the possibility to evaluate the main influence of the ambient air temperature on the gas turbine output and efficiency. In the same time many information on thermal cycle characteristics are obtained.

The presented case studied shown that a decrease in ambient temperature can improve the gas turbine output and efficiency. For any 10 °C again of about 3% increase in power is obtained. In the same time a reduction of the fuel mass flow takes place, so that the gas turbine becomes more efficient.

References

- [1] Horlock J.H., *Advanced Gas Turbine Cycles*, Elsevier Press 2003
- [2] Oprea, I., *Heat recovery in micro gas turbines for cogeneration*. 1st International Conference on Modern Power Systems MPS, November 8-11, 2006, Cluj-Napoca, Romania.
- [3] Oprea I., *Steam and Gas Turbines*, Ed. Printech, Bucharest 2004.
- [4] Bejan A., *Termodinamica tehnica avansata*, Ed. Tehnica, Bucuresti 1996.
- [5] Mihaescu L., Oprea I., Negreanu G., s.a. *Sisteme si echipamente termice pentru producerea de energie*, Ed. Printech 2012
- [6] Kehlhofer r.H., Plancherel A., Stirnimann F., Rukes. B., *Combined Cycle Gas & Steam Turbine Power Plants*, PennWell Corporation 2009

EXPERIMENTAL SETUP AND ENERGY BALANCE OF A HYBRID MICRO-COGENERATION GROUP BASED ON DIESEL ENGINE AND ORGANIC RANKINE CYCLE

Tudor Prisecaru, Alexandru Dobrovicescu, Cristian Petcu, Valentin Apostol, Mălina Prisecaru,
Gheorghe Popescu, Horațiu Pop¹, Cristina Ciobanu, Elena Pop, Dorin Stanciu
Viorel Bădescu, Adrian Untea, Mahdi Hatf Kadhum
Faculty of Mechanical and Mechatronics Engineering, University Politehnica of Bucharest
Rokura Company

ABSTRACT

The paper presents the experimental setup developed in the first stage of a Research Grant called "Hybrid micro-cogeneration group of high efficiency equipped with an electronically assisted ORC" (acronym GRUCOHYB). The Research Grant is in progress at the Thermal Research Centre, Faculty of Mechanical and Mechatronics Engineering from University Politehnica of Bucharest having as research partner the Rokura Company. The hybrid micro-cogeneration group involves the use of a 40 kW Diesel engine and an Organic Rankine Cycle (ORC). A brief description of the experimental setup according to the current stage of development has been delivered. The paper also presents the energy balance conducted in this research stage which aims to obtain the amount of waste heat available for the ORC. Preliminary experimental data and results have been presented. Results show that at full load the mechanical power that could be delivered by the ORC is in the range of 10.74 and 7.16 kW. Future improvement perspectives are also presented.

1. INTRODUCTION

The efficiency of thermal systems can be improved by waste heat recovery. One of the most promising solutions for waste heat recovery is the Organic Rankine Cycle (ORC) [1,2]. This technology can be successfully applied in case of electricity generators based on internal combustion engines (ICE) by recovering heat from exhaust and water cooling systems and converting it into work or electricity. In literature reports can be found regarding heat recovery systems based on ORC for heavy duty ICE [3,4]. Results point out fuel economy and enhanced thermal efficiency.

In this context, the present paper presents an experimental setup developed in the first stage of a National Research Grant called "Hybrid micro-cogeneration group of high efficiency equipped with an electronically assisted ORC" (acronym GRUCOHYB). The Research is in progress at the Thermal Research Centre, Faculty of Mechanical and Mechatronics Engineering from University Politehnica of Bucharest having as research partner the Rokura Company.

The hybrid micro-cogeneration group involves the use of an electricity generator based on a 40 kW overcharged Diesel engine and an ORC. At full load the electricity output is 36 kWe. The research objective is to recover heat from the exhaust and cooling systems of the Diesel engine and transfer it to the ORC in order to produce electricity as well as to heat a thermal agent and to improve the overall efficiency of the micro-cogeneration group.

Furthermore, the paper presents the energy balance conducted for the micro-cogeneration group in order to determine the amount of waste heat available for ORC. Preliminary results are delivered based on experimental data.

¹University Politehnica of Bucharest, Faculty of Mechanical and Mechatronics Engineering, Splaiul Independenței 313, Bucharest 060042, Romania, +0744903488, pophoratiu2001@yahoo.com.

2. EXPERIMENTAL SETUP DESCRIPTION

An overview of the experimental setup according to the current stage of development is presented in Figure 1.

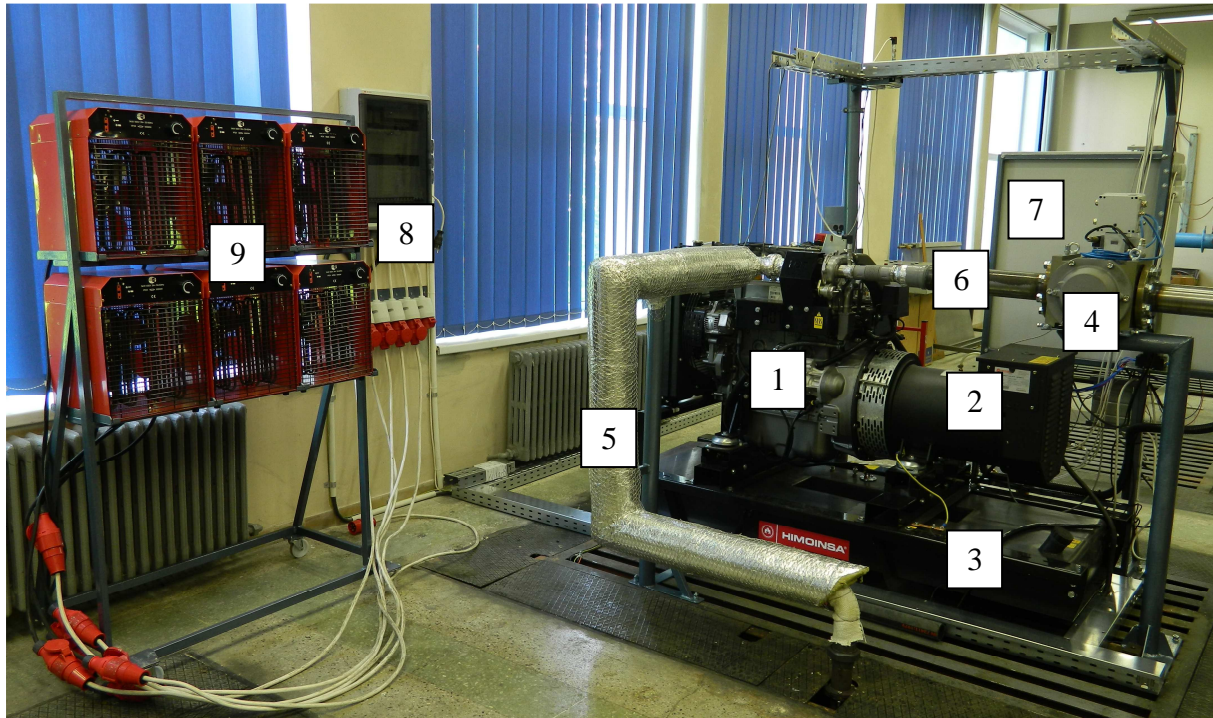


Figure 1: Overview of the experimental setup

The components visible and indexed in Figure 1 are: 1 – Diesel engine; 2 – electricity generator; 3 – fuel tank; 4 – air flow meter; 5 – exhaust pipe; 6 - air inlet pipe; 7 – automation and data acquisition panel; 8- electricity distribution system; 9 – electricity consumers. The experimental setup has many another components that will be presented in a much detailed work. The instrumentation available on the experimental setup and which allows conducting the energy balance is presented in Table 1.

Tabelul 1: Instrumentation of the experimental setup

Nr. crt.	Measured parameter
1.	Ambient pressure [bar]
2.	Ambient temperature [°C]
3.	Combustion air volume flow rate [m ³ /h]
4.	Overcharge air pressure [bar]
5.	Overcharge air temperature [°C]
6.	Engine intake air pressure [bar]
7.	Engine intake air temperature [°C]
8.	Cooling water inlet pressure [bar]
9.	Cooling water inlet temperature [°C]
10.	Cooling water volume flow rate [m ³ /h]
11.	Cooling water outlet pressure [bar]
12.	Cooling water outlet temperature [°C]
13.	Turbine inlet exhaust gas pressure [bar]

14.	Turbine inlet exhaust gas temperature [°C]
15.	Turbine outlet exhaust gas pressure [bar]
16.	Turbine outlet exhaust gas temperature [°C]
17.	Fuel engine intake pressure [bar]
18.	Exhaust gas temperature [°C]
19.	Hourly fuel consumption [l/h]
20.	Active Power [kW]

3. ENERGY BALANCE

According to the current stage of development the energy balance equation for the experimental setup can be written as follows:

$$\dot{Q}_{fuel} = P + \dot{Q}_{wcs} + \dot{Q}_{eg} + \dot{Q}_{rest} \quad (1)$$

Where: \dot{Q}_{fuel} is the heat flux received through fuel combustion; P is the amount of mechanical power produced; \dot{Q}_{wcs} is the heat flux rejected through the water cooling system; \dot{Q}_{eg} is the heat rejected through the exhaust gases and \dot{Q}_{rest} is the heat flux rejected through radiation and incomplete combustion that cannot be directly determined in this stage.

The heat flux received through fuel combustion can be computed as:

$$\dot{Q}_{fuel} = \dot{m}_{fuel} \cdot H_{ifuel} [kW] \quad (2)$$

Where $\dot{m}_{fuel} [kg / s]$ is the fuel mass flow rate and $H_{ifuel} [kJ / kg]$ is the inferior fuel heat value.

The fuel mass flow rate can be determined:

$$\dot{m}_{fuel} = [(C_h \cdot 10^{-3}) / 3600] \cdot \rho_{fuel} [kg / s] \quad (3)$$

In eq. (3), $C_h [l / h]$ is the hourly fuel consumption which is experimentally determined and $\rho_{fuel} [kg / m^3]$ is the fuel density and its value is considered from data available in literature for a temperature of 20 °C [5]. Thus $\rho_{fuel} = 822 \text{ kg} / m^3$. The inferior fuel heat value is also considered from data available in literature [5,6]: $H_{ifuel} = 42000 \text{ kJ} / \text{kg}$.

The power produced $P [kW]$ can be determined as follows:

$$P = P_{el} / \eta_{conv} [kW] \quad (4)$$

Where $P_{el} [kW]$ is the amount of electric power obtained and it is directly determined on the experimental setup; η_{conv} is a conversion factor of mechanical power into electrical power considered for the present calculation to be $\eta_{conv} = 0.98$ [7].

Next, the heat flux rejected through the water cooling system can be computed as follows:

$$\dot{Q}_{wcs} = \dot{m}_w \cdot c_w \cdot (t_e - t_i) [kW] \quad (5)$$

In eq. (5) $\dot{m}_w [kg / s]$ is the water mass flow rate; $c_w [kJ / (kgK)]$ the water heat capacity; $t_e [^{\circ}C]$ and $t_i [^{\circ}C]$ are water temperatures at engine outlet and inlet, respectively.

Water mass flow rate can be determined using experimental data as follows:

$$\dot{m}_w = [(\dot{V}_w \cdot 10^{-3}) / 3600] \cdot \rho_w [kg / s] \quad (6)$$

Where, $\dot{V}_w [l / h]$ is the water volume flow rate measured on the experimental setup and $\rho_w = 1000 kg / m^3$ is water density. For water heat capacity the following value has been considered $c_w = 4.186 kJ / (kgK)$ [7]. Water temperatures at the inlet (t_i) and outlet (t_e) of the engine are directly measured.

The heat flux $\dot{Q}_{eg} [kW]$ rejected through exhaust gases is computed as:

$$\dot{Q}_{eg} = \dot{Q}_{eg}^{total} - \dot{Q}_{air} [kW] \quad (7)$$

Where, $\dot{Q}_{eg}^{total} [kW]$ is the total heat flux available in exhaust gases and $\dot{Q}_{air} [kW]$ is the heat flux due to the fresh load.

The total heat flux available in exhaust gases can be determined as:

$$\dot{Q}_{eg}^{total} = \dot{m}_{ge} \cdot c_{pge} \cdot T_{ge} [kW] \quad (8)$$

In eq. (8) $\dot{m}_{ge} [kg / s]$ is the exhaust gasses mass flow rate; $c_{pge} [kJ / (kgK)]$ is the heat capacity at constant pressure of exhaust gases and $T_{ge} [K]$ is the temperature of exhaust gases. Heat capacity of exhaust gases is considered from available data in literature according to experimental data [5].

The exhaust mass flow rate is:

$$\dot{m}_{ge} = \dot{m}_{fuel} + \dot{m}_{air} [kg / s] \quad (9)$$

The fuel mass flow rate \dot{m}_{fuel} is computed according to eq. (3) and the air mass flow rate \dot{m}_{air} is determined as:

$$\dot{m}_{air} = (\dot{V}_{air} / 3600) \cdot \rho_{air} [kg / s] \quad (11)$$

Where, $\dot{V}_{air} [m^3 / h]$ is the air volume flow rate and it is experimentally determined; $\rho_{air} [kg / m^3]$ is air density computed for ambient parameters.

Thus, the heat flux due to the fresh load can be determined:

$$\dot{Q}_{air} = \dot{m}_{air} \cdot c_{pair} \cdot T_{air} [kW] \quad (12)$$

Where, $c_{pair} [kJ/(kgK)]$ is the heat capacity at constant pressure and its value is considered from data available in literature $c_{pair} = 1.013 kJ/(kgK)$ [7] and T_{air} is the measured ambient air temperature.

Based on eqns. (1)-(12) the heat flux that cannot be directly determined \dot{Q}_{rest} is:

$$\dot{Q}_{rest} = \dot{Q}_{fuel} - P_{el} - \dot{Q}_{wcs} - \dot{Q}_{eg} [kW] \quad (13)$$

As it can be noticed in eqns. (1)-(12) some data like H_{ifuel} , ρ_{fuel} and c_{ge} are adopted from literature because in the current stage of development the experimental setup does not allow their determination. In future research stages H_{ifuel} will be determined based on fuel elemental analysis and c_{ge} based on exhaust gases composition derived by using a gas analyzer.

4. EXPERIMENTAL RESULTS

According to the energy balance described in the previous paragraph preliminary experimental investigations have been carried out for loads ranging from 100 % to 24 %. The experimental results are presented in Table 2.

Tabelul 2: Preliminary experimental results

Functional regime	Load [%]	$\dot{Q}_{fuel} [kW]$	$P [kW]$	$\dot{Q}_{wcs} [kW]$	$\dot{Q}_{eg} [kW]$	$\dot{Q}_{rest} [kW]$	$\dot{Q}_{air} [kW]$
1.	100.00%	93.54	35.85	27.36	28.69	1.64	15.53
2.	92.47%	85.73	33.15	20.58	25.80	6.20	15.32
3.	81.73%	75.93	29.30	13.48	22.23	10.92	15.25
4.	72.37%	67.35	25.94	12.62	19.13	9.66	15.24
5.	58.54%	56.26	20.99	15.36	15.16	4.75	15.24
6.	48.29%	48.15	17.31	15.63	12.39	2.81	15.23
7.	24.22%	41.24	8.68	14.57	7.57	10.42	15.23

The total amount of waste heat available for the ORC can be computed as:

$$\dot{Q}_{available}^{ORC} = \dot{Q}_{wcs} + \dot{Q}_{eg} + \dot{Q}_{air} [kW] \quad (14)$$

Based on the experimental data presented in Table 2 the amount of waste heat available for ORC is presented in Table 3.

Former reports [3,8] of waste heat recovery in case of ICE using an ORC point out theoretical efficiencies between 15 and 20%, while realistic ones are between 7 and 10%. The amount of theoretical mechanical power $P_{output}^{ORC,t} [kW]$ and the realistic one $P_{output}^{ORC} [kW]$ provided by the ORC can be computed as:

$$P_{output}^{ORC,t} = \dot{Q}_{available}^{ORC} \cdot \eta_{ORC}^t; P_{output}^{ORC} = \dot{Q}_{available}^{ORC} \cdot \eta_{ORC} [kW] \quad (15)$$

Where, η_{ORC}^t and η_{ORC} are theoretical and realistic efficiencies of the ORC system respectively. If we assume for the present calculation a theoretical efficiency of $\eta_{ORC}^t = 0.15$

and a realistic one of $\eta_{ORC} = 0.1$ [3], than the corresponding mechanical power outputs are also presented in Table 3.

Tabelul 3: Waste heat available for ORC

Functional regime	Load [%]	$\dot{Q}_{available}^{ORC}$ [kW]	$P_{output}^{ORC,t}$ [kW]	P_{output}^{ORC} [kW]
1.	100.00%	71.58	10.74	7.16
2.	92.47%	61.7	9.26	6.17
3.	81.73%	50.96	7.64	5.10
4.	72.37%	46.99	7.05	4.70
5.	58.54%	45.76	6.86	4.58
6.	48.29%	43.25	6.49	4.33
7.	24.22%	37.37	5.61	3.74

5. CONCLUSIONS

The paper presents the first stage of an original research involving a hybrid micro-cogeneration group which is based on a Diesel engine and an Organic Rankine Cycle (ORC). A brief description of the experimental setup according to the current stage of development has been done. The energy balance conducted in this research stage has been presented aiming to determine the amount of waste heat available for the ORC. Preliminary experimental results show that the ORC could deliver at 100% load a mechanical power between 10.74 and 7.16 kW.

Future developments will include: elemental analysis of the fuel in order to obtain the inferior heat value, exhaust gas analysis which will lead to the heat capacity at constant pressure and also the amount of CO that gives the heat lost through incomplete combustion. Also future simulation will be conducted on the heat recovery system that will deliver data necessary for choosing the appropriate equipments for the ORC system.

References

- [1] Wang, H., Wang, H., Zhang Z., Optimization of Low-Temperature Exhaust Gas Waste Heat Fueled Organic Rankine Cycle, Journal of Iron and Steel Research, International, Vol. 19, Issue 6, p. 30-36, 2012.
- [2] Roy, J.P., Ashok, M., Parametric optimization and performance analysis of a regenerative Organic Rankine Cycle using R-123 for waste heat recovery, Energy, Vol. 39, p. 227-235, 2012.
- [3] Charles, S. III, Christopher, D., Review of organic Rankine cycles for internal combustion engine exhaust waste heat recovery, Applied Thermal Engineering, Vol. 51, p. 711-722, 2013.
- [4] Ho, T., Gerhard, R., Chris, C., AVL Powertrain Engineering Inc, Waste Heavy Recovery of Heavy-Duty Diesel Engines by Organic Rankine Cycle Part I: Hybrid Energy Systems of Diesel and Rankine Engines, 2007-01-0537, SAE Technical paper series, World congress, April 16-19, Detroit, 2007.
- [5] Kuzman, R., Tabela and Thermodynamic Diagrams, in romanian Publisher Editura Tehnică, Bucharest, 1978.
- [6] Chiriac, R., Internal combustion engines, basic operation principles, AGIR Publishing House, Bucharest 2012.
- [7] Marinescu, M., Baran, N., V., Radcenco, Dobrovicescu, Al., Technical Thermodynamics, in romanian Vol. I -III, Publisher Editura Matrix Rom, Bucharest, 1998.
- [8] New ecological method for electricity generation based on heat extracted from deep wells, in romanian, PN 4 Research Grant No. 21- 052/14.09.2007, beneficiary CNMP, 2007.

SOCIAL AND TECHNICAL MODEL FOR EMPLOYEE INDIVIDUAL RESPONSIBILITY ENHANCEMENT IN ORDER TO SHAPE AND DEVELOP A PERFORMANT LEVEL OF ENVIRONMENT AWARENESS

Corneliu Sofronie¹, Ruxana Zubcov
TRAINING AND ADVANCED TRAINING CENTRE BUCHAREST

ABSTRACT

The model we propose represents an instrument for organizational order layout, regarding the relationship human-equipment, in order to create and develop an increased level of environmental awareness.

This order doesn't suppose only to emphasize a hierarchy, but almost to set out the information about the general and specific behaviour of the employees within a matrix, able to warrant the efficiency and co-operation in an optimal environmental system conditions. Thus it is equally and instrument to learn about the human factor inside an organization. The model aims to increase the individual employee responsibility by means of an instrument named: THE OHSAS 18001 INDIVIDUAL PSYCHOLOGICAL FILE.

1. INTRODUCTION

This work was supported by a grant of the Romanian National Authority for Scientific Research, CNDI-UEFISCDI, project number 33/2012.

Developing an individual responsibility enhancement model for the employees of the national energy system according to the OHSAS 18001 standard appears as a necessity required by the overlapping three kinds of management: quality management, risk and uncertainty management and lean management, all three being jointly a reference framework for the management activity in ongoing situation in the energy system units.

We started this model having responsibility concept first as general understanding, and second regarding it from the management science point of view.

Notion definition. In largest sense, by *responsibility* is understood **the capacity to take a decision, without prior reference to a higher authority. Otherwise, mostly under juridical field, responsibility is perceived as an obligation to fulfil a task, a commitment, or to repair a mistake, that prejudiced a person or a collectivity (Larousse Dictionary).**

The Explanatory Dictionary of the Romanian Language (DEX) defines responsibility as: „**The obligation to perform an action, answer, to respond, to accept and bear the consequences; responsibility; job position, task for a respondent**” and the noun „**responsible**” equivalent to „**the bearer of the responsibility for an act, for a deed**” „**respondent**” and „**person appointed in a managing position, that bears responsibility tasks, to whom a responsibility was entrusted**”.

The civil procedure code – initiated as a draft in 2009, based on the Civil Code from 1865 uses mostly the terms “duties” and “obligations”. However the “civil responsibility” is deemed as the “obligation to repair the prejudice induced to another person through non fulfilment of a contract” or of any damaging act personally done by a person depending on the incriminated person, or by a cause under his tasks”. By “collective responsibility” is understood

¹ Bucharest, Dristor, 96; +40 731494606; cornelsofronie@yahoo.com

to consider all the members of a group as jointly responsible for any act committed by a member of the group.

In the Criminal procedure code – also a draft in 2009 – “criminal responsibility” is mentioned as the obligation to serve the punishment for the committed crime.

It is difficult to define in a sentence the expression management responsibility. Anyway it lays at the crossing of the management ethics and the business concept. Noting that on the bank notes of the most powerful state of the world, the USA, is written: “In god we trust”, a reputed analyst wrote that, in fact, not by this logo reached the Americans the economic, political and military the supremacy, the green bills serving sometimes ignoble purposes and arrangements. The analyst admitted anyway that Benjamin Franklin, co-author of the American Constitution – and the initial American presidents: George Washington, John Adams, Thomas Jefferson and Abraham Lincoln have always underlined the importance of the faith, deeming the Bible as a fundamental book.

In his famous work “Protestant ethics and the capitalism spirit” the German sociologist Max Weber warned about the risks that he capital world to irremediably divorce from the moral values, under the contradiction between the “convincement ethics” (moral) and “responsibility ethics” (business). One should not forget that the famous Machiavelli’s expression “the goal excuses the means” is typical for the business space.

“Management ethics” notion is almost recently introduced in the scientific language, it represents a “branch” applied to the ethics and aims mainly the behaviour type, and also the activity the managers develop in their organizations. The way the individuals or social groups (both from inside the organization and from the outside of it) react subsequent to the decisions taken by the manager is also analyzed. As management is itself a socio-human discipline (but also an economical one deeming the obtained results), acquiring the ethical norms is an obligation for managers and they should serve as models for employees. The management ethics, at national level, unfortunately is by far considered to be priority nor for the Romanian managers, and subsequently neither for employees. Moreover many of them see the ethical code observation as an impediment in achieving a profitable business. That is not far from truth, since the management ethics confronts the company’s economical opportunities with its social image.

A non ethical behaviour may be based mainly on the organization leader’s lack of management knowledge, on his wrong build strategic vision, lack of professional experience and knowledge with regard to working groups and teams, values and misconducts etc.

In the specific literature a series of guides has been proposed aiming to support managers and employees in adopting an ethical behaviour in any possible situation. A series of ethical codes was conceived to work as fundamentals for an adequate conduct. However one should keep in mind the fact that influences the management ethic accuracy (such as organizational internal codes and rules, in force legal regulations and ethic codes, individual features, company situation etc.).

An employee guiding his activity following the management ethic codes, should never forget that his actions are to be always based on fairness, law observation, trust, correctness, keeping the promises, responsibility for own acts etc., all these factors being supported by company organizational culture. A positive organizational culture where values, norms and ethical rules are promoted and equally supported by managers and employees, lays on the basis of the ethical manager conduct, these having a model effect on the company employees. One

need to add that an ethical code is required from the deep structures of the human conscience, that kind of consciousness that we could freely call an “eco – consciousness”.

2. METHODOLOGY

The methodology used for reaching the final goal, developing an instrument for increasing the individual responsibility of the employees of the national energy system, was a system of models following the concentric circles principle having as basis the model of professional responsibility ethics and on top the model of behaviour eco-consciousness.

Model of eco-professional ethics:

1. Think about the well being of the surrounding people. One should consider what means this “well being” for his team, for his mates, for his chiefs and also for the business partners. The non direct participants at one’s actions neither should nor be eluded neither directly affected by the results of his actions. Sooner or later things can turn on an unexpected way.
2. Think as a member of a group. To be ethic means actually a personal discipline, a permanent battle against oneself, but it doesn’t mean to think as an isolated individual. One belongs to group and that means to be connected to the values and behaviour of the surrounding people.
3. Observe and obey laws. According to these rules one has to observe working rules and procedures in force in a company; rules such as the ones regarding the conduct in the office, clothing, working hours, smoking regulations etc. as guidelines to be observed by all employees.
4. Consider yourself and your company as parts of the whole society. We mean here the business society. As aforementioned, one’s conduct and actions can influence the image of the company. It depends on you and on the example, good or bad, that the company presents to the business community.
5. Obey the moral rules, as being unconditioned. Observing the moral rules represents the fundamentals of ethical individual behaviour.
6. Think impartially, objective, neutrally (unbiased), uninterested. Any decision you take influences your behaviour related to the surrounding people. Be able to make a correct assessment both from your and from the others point of view.
7. Ask yourself what kind of human being are you. Compare your actions and conduct to similar persons. Do you agree with them? If not, why do you agree with yourself?
8. Respect others’ traditions, habits and conviction. You should not give up your beliefs/principles. You should only grant the due respect to principles of the surrounding people, even if they are different from yours.

Resuming the main ideas of this code, we can point out the most important attributes of successful employee in what concerns an ethical conduct:

- Responsibility towards oneself – personal evolution;
- Responsibility towards the company – respect for the acquired goods;
- Convince the others to adhere, but taking into considerations others’ opinions;
- Responsibility towards the environment and its preservation;
- Responsibility towards the clients and their necessities;
- To show confidence and to gain confidence;
- Social Responsibility, understanding of the economical and social environment where the company performs its activity;

- Responsibility towards all business partners.

Model of the behaviour eco-consciousness. Starting from these assumptions and with the purpose to develop an instrument for the increasing the individual employees' responsibility, we created a model for organizational eco-consciousness, build up on three behaviour levels: superior, middle, and inferior. Behaviour types are associated to the eight main personality types to be met inside the Romanian organizations, namely: 1) *The Competitor*; 2) *The Expert*; 3) *The Altruist*; 4) *The Perfectionist*; 5) *The Leader*; 6) *The Creator*; 7) *The Energetic one*; 8) *The Peace maker*.

Table 1

A. Superior consciousness

The Competitor	Genuine behaviour, focused on finding efficient solutions
The Expert	Knowledge aimed behaviour, visionary and innovative active in relations with the environment
The Altruist	Empathic behaviour, generous and careful towards the work environment
The Perfectionist	High responsibility behaviour, based on attachment to the job
The Leader	Heroic behaviour, with sacrifice spirit towards the organization, with deeds and actions granting him the feeling to be a strong person, the saver of humanity
The Creator	Sensitive and perceptive to everything around him, creative, original
The Energetic one	Enthusiast, capacity to anticipate the future actions concerning the organization, realistic and performing
The Peace maker	Self confident, peaceful and harmonious towards with the environment yet able to follow the successful models and examples in his activity inside the organization

B. Medium [average] consciousness

The Competitor	Pragmatic, versatile, wishing to be excellent, he conditions his involvement in organizational actions to the gain obtained for his own image
The Expert	Reasoning type: perceptive, innovator, discreet and isolated with the tendency to become apathetic or uninterested from the moment he has no longer the motivation to involve himself in the organization life
The Altruist	Generous, demonstrative, aiming to please to others, changing easily from the need to consider himself as indispensable in his environment to the feeling that he is inappropriate
The Perfectionist	Serious, principle based, disciplined behaviour but with the feeling that he is acting on obligation, fact that is reflected usually in his health
The Leader	Pragmatic and self confident, but with tendency towards being conceited, not accepting proposals or solutions from others
The Creator	Tendency to act as he were the centre of the world and to be too concessive to others, when noticing others aggressivity towards the environment
The Energetic one	Bohemian behaviour, mislaid and distracted, somehow excessive in his

	deeds but efficient
The Peace maker	Generally modest and agreeable, but resigned; hard to be convinced to attend actions related to his environment

C. Lower Consciousness

The Competitor	Unscrupulous behaviour, aggressive and based on appearances; not sincere in his attitude towards his organizational environment
The Expert	Detached from all around him and concerned only by his problems, separated from environment
The Altruist	Despotic and constraining with regard to the environment, on the background of negative feelings, or disappointments
The Perfectionist	Inflexible behaviour, contradictory and muddleheaded related to his environment
The Leader	Tendency to megalomania, aggressive and destructive to the organization life.
The Creator	Distant, tendencies to deny life, loathsome to people acting in his environment
The Energetic one	Recklessness in his relation with the environment, paralyzed in front of difficult satiations
The Peace maker	Neglecting, confused, prone to commit errors and wrongdoing frequently by happenstance and not purposely

Table 2
Individual psychological file OH-SAS 18001 (top confidential)

CRITERIA	COMMENTS
Name and surname	
Working place	
Job position	
Subject type of personality	
Personality strong points	
Personality weak points	
Professional behaviour features in normal work situations	
Professional behaviour features in critical work situations, under strain sources	
Professional behaviour features along a week	
Type of errors the subject is prone to	
Causes of such errors	
Conditions and motivations enabling error committing	
Recommendations/measures	

3. CONCLUSIONS

Our research resulted, as a general conclusion for the assertions made inside this work, in the elaboration of an instrument the increase the employee individual responsibility that we named: Individual psychological file OH-SAS 18001. The subject would sign when receiving the file (whose content is top confidential) and would commit himself/herself to acknowledge the information included in the file and would strictly follow the instructions. Applying the content of the psychological file is a part of the personal training mode, as a condition for an efficient solving the work tasks in fully safe conditions and psychological health. The psychological file would be updated once in three months.

The originality of the work consists in the fact that this model lays on original theory and a methodology entitled: Order Psychology – Quantum Psychology®. It is the first scientific methodology in the psychology domain proposing the measurement by means of forms as a complementary method to the calculus measurement.

References

- [1] Bonciu, C., *Instrumente manageriale psihosociologice*, Ed. All Beck, Bucuresti, 1998
- [2] Căndea, D., *Competentele emotionale si succesul în management*, Ed. Dacia, 2004
- [3] Cioroianu, A., *Epoca de aur a incertitudinii*, Ed. Curtea veche, Bucuresti 2012
- [4] Corzine, A., *Viata secretă a universului*, Ed. Corint, Bucuresti, 2010
- [5] Dâncu, S., *Comunicarea simbolică*, Ed. Dacia, Cluj Napoca 2004
- [6] Doumont, L., *Eseu asupra individualismului*, Ed. Humanitas, Bucuresti 2004
- [7] Enăchescu, C., *Tratat de psihologie diferentiață*, Ed. Polirom, 2008
- [8] Frankl, E. V., *Omul în căutarea sensului vietii*, Ed. Meteor Press, Bucuresti, 2008
- [9] Goleman, D., *Inteligența ecologică*, Ed. Curtea veche, Bucuresti, 2009
- [10] Goleman, D., *Inteligența socială*, Ed. Curtea veche, Bucuresti 2010
- [11] Larson, U. Ch., *Persuasiune, receptare si responsabilitate*, Ed. Polirom, Bucuresti 2007
- [12] Laszlo, E., *Transformarea cuantică*, Ed. Nemira, Bucuresti, 2002
- [13] Malita, M., *Cumintenia pământului*, Ed. Corint 2011
- [14] Orloff, J., *Libertatea emotională*, Ed. Paralela 45, Bucuresti, 2010
- [15] Penrose, R., *Mintea omenească între clasic si cuantic*, Ed. Stiintifică, Bucuresti, 2007
- [16] Sofronie, C., Zubcov, R., *Psihologia ordinii. Psihologia cuantică*, Ed. Perfect, 2005
- [17] Sofronie, C., Zubcov, R., *Testul de asociere numere cuvinte*, Ed. Perfect, 2011
- [18] Sofronie C, Zubcov R, *Măsură pentru diavol si bunul dumnezeu*, Ed. Fiat Lux, 2003
- [19] Wells, S., *Omul-o aventură genetică*, Ed. Stiintifică, Bucuresti, 2003
- [20] Weor, A. S., *Educatia fundamentală*, Ed. Ageac, Bucuresti, 2008

ANALYSIS OF THE EFFICIENCY OF STAGGERED COMBUSTION FOR A LIGNITE BURNER BY DEFINING A MIXTURE FUNCTION BETWEEN THE PRIMARY AND SECONDARY AIR FLOWS

Dorin Stanciu, Lucian Mihăescu, Gabriel Negreanu, Ionel Pișă, Ion Oprea
University Politehnica of Bucharest

ABSTRACT

The new designed burner allows the reduction of NO_x emission by staggered combustion. This technique is achieved by the aerodynamics of the primary air+coal dust and secondary air jets assembly. These jets have both variable admission lengths and different velocities.

1. INTRODUCTION

The staggered combustion supposes a slow admission of the secondary air into the primary air jets, following the different penetration of these jets in the combustion space. According to this combustion technique, the coal oxidation is under-stoichiometric until the jets homogenization in the combustion chamber center. For the primary air jets, that represents about 30 % of total necessary air. It follows that, until a total mixture with the secondary air, the combustion regime remains under-stoichiometric, and the NO_x emission is kept as low as possible.

The air mass increase in the jets assembly by secondary air penetration is characterized by a mixing function $R(x)$, x being the linear flow dimension. This function should have a slow increasing gradient, in order to maintain the required combustion conditions.

In order to find and verify the mixing function, we will further start a numerical modeling of the processes in the burner shown in figure 1.

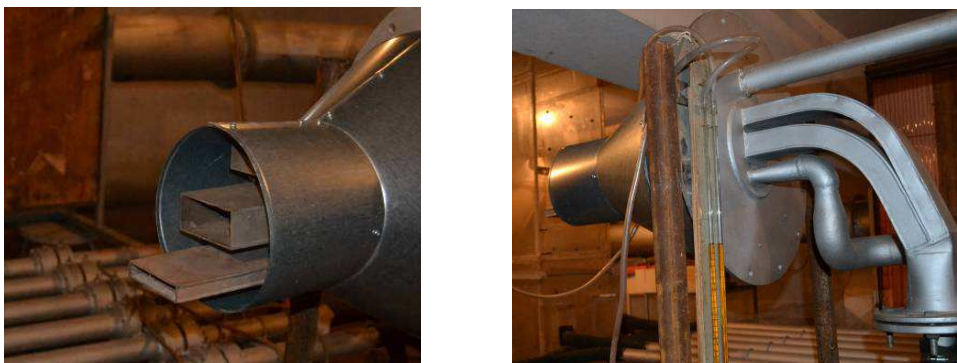


Figure 1. The new burner for lignite dust

2. MATHEMATICAL AND NUMERICAL MODEL

The mathematical model consists of full Reynolds Averaged Navier-Stokes equations (RANS). Due to its behavior in modeling the turbulent jets flows [2], the $k-\varepsilon$ RNG turbulence model with scalable wall function was used for closing the RANS equation system. The jets flow has a symmetry plane ($x=0$), so that only half of it is used in the computation. Thus, the

external boundary of the computing domain is half of a cylinder enclosing the injection jet devices, having a radius of 1 m and a length of 5 m. Figure 2 shows the computing domain and the boundary conditions used in the numerical simulation. Note that the *velocity inlet* boundaries consist of the three jets inflow areas as well as the area encompassed between the wall embrasure and all jet ports. Additional, the law of the wall boundary conditions was chosen for all wall boundaries appearing within the computing domain.

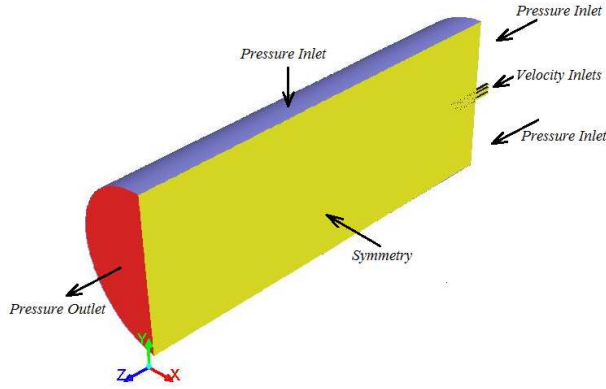


Fig. 2 Computing domain and boundary conditions

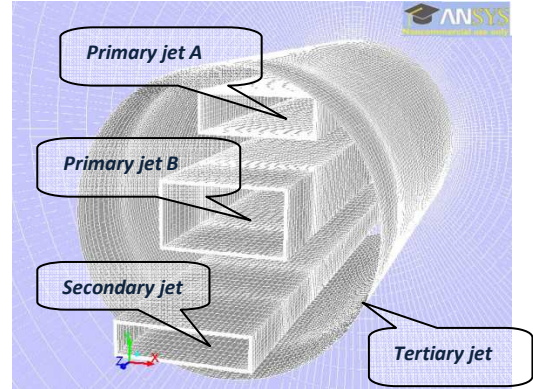


Fig. 3 Details of computing domain and jet air definition

A multi-bloc grid was used in the numerical simulation. Figure 3 shows a detail of the computational meshed domain consisting of all channel and embrasure jets and also the attracted inflow external air surrounding the embrasure. The primary air is divided in two jets A and B whose slots have different length. The secondary jet of air is injected through the third slot, having a greater length than those of primary air, while the tertiary air jet is introduced through the gap shaped between the embrasure and the primary and secondary jet slots. The computation was performed through the use of commercial software package Ansys FLUENT v14.01 on a Supermicro platform having 48GB of main memory and two Intel six core 2.4 GHz CPU. The pressure based solver in addition to least squares cell based gradient algorithm was used in the numerical simulation. The mean momentum and turbulence equations were solved by employing the Second Order Upwind and the QUICK discretization schemes, respectively. The pressure (Poisson) equation was resolved by the aid of STANDARD procedure, while the pressure-velocity coupling was assured by using the SIMPLE algorithm [3].

3. RESULTS AND DISCUSSIONS

The computations were performed for tow case studies whose boundary conditions are presented in *table 1*. There, w_{1A} și w_{1B} represent the inflow bulk velocities of primary air jets A and B, w_2 and w_3 are the inflow bulk velocities of secondary and tertiary air jets, while T' and T'' denote the temperature values set for primary air jets (A and B) and for all other jets respectively (including here the attracted jets that penetrate the computing domain through *pressure inlet boundary conditions*) respectively.

Table 1 Bulk velocities and temperatures of inflow boundary conditions used for air jets.

	w_{1A} [m/s]	w_{1B} [m/s]	T'_j [K]	w_2 [m/s]	w_3 [m/s]	T''_j [K]
Case 1	10.4	11.4	310	33.2	8.48	290
Case 2	10.4	11.4	310	33.2	33.2	290

The difference between the two case studies consists of the inflow bulk velocity value of tertiary air jet whose influence on the primary air jets penetration is studied. Neglecting the molecular heat diffusion, from the first law of thermodynamics one obtains that

$$\alpha = (T'_j - T) / (T'_j - T''_j) \quad (1)$$

where T is the temperature of any jet point and α represents the local mixing factor. Following the definition, at the inflow section of primary air jets, $\alpha=0$, while at any inflow section of all other air jets (including also all the *pressure inlet boundaries*), $\alpha=1$. The values of $\alpha>0$ occurring in the developing regions of primary air jets model the fraction of mixing between them and all the surrounding air jets.

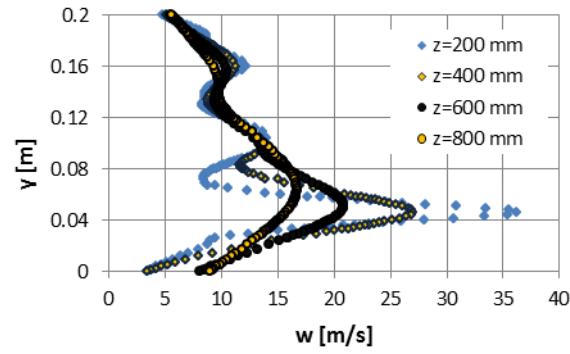
The main results of the numerical simulations are presented in figures 4 and 5. So, the figures 4a and 5a show the stream-wise velocity distributions on some cross-stream flow directions situated on the symmetry plan and measured from the end section of embrasure wall. One can observe that in the first study case, the exchange rate of momentum is lower in the regions surrounding the secondary and tertiary air jets and higher around the zone encompassing the primary and tertiary air jets. Beyond that, until $z=400-500$ mm, the interaction between the primary and tertiary jets and between the secondary and tertiary jets respectively are fully separately. As a results, at $z=600$ mm, the primary air jets are already encompassed in the tertiary jet, while the secondary one still keeps its individuality. In the second study case, due to the increment of tertiary jet momentum, a step by step mixing of primary air jets with other ones takes place. So, at $z=600$ mm the primary jet A is quite mixed with tertiary air jet, while the mixing between the primary jet B and the secondary and tertiary ones is ongoing. This last process still remains active at $z=800$ mm.

Figures 4b and 5b show the distributions of the mixing factor along some cross-stream flow locations, situated on the symmetry plan. For the first case study, one can observe a slow but separate mixing among the primary and tertiary air jets, until $z=600$ mm. Beyond this location a quick mixing occurs among the secondary jet and the primary ones, which are already encompassed by the tertiary air jet. Because of the momentum raise of tertiary air jet, in the second case, the momentum of tertiary air jet is considerable increased, so the mixing among the primary and tertiary jets is greatly enhanced. Further, the contribution of the secondary air jet at the mixing process becomes evident at locations greater than $z=600$ mm.

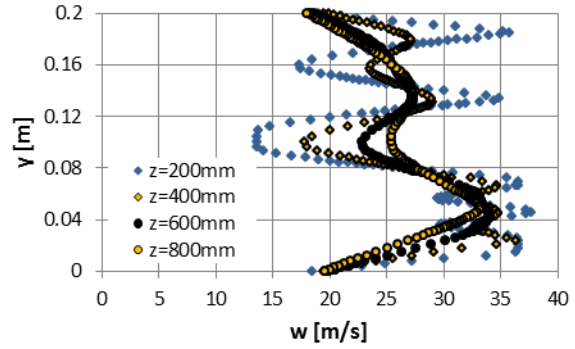
Figures 4c și 5d present the numerical profiles of the mixing factor along the symmetry lines of primary air jets (A and B). In the first case, their penetration with the air coming from the tertiary and secondary jets is lower and obviously does not assure the minimal conditions for a two stage combustion. In the second case, the mixing is greatly enhanced and a reasonable gap of the mixing factor between the primary air jets A and B is kept on the entire referenced length. This last distribution can assure the desired staggered combustion, needed for reducing the NO_x emissions.

4. CONCLUSIONS

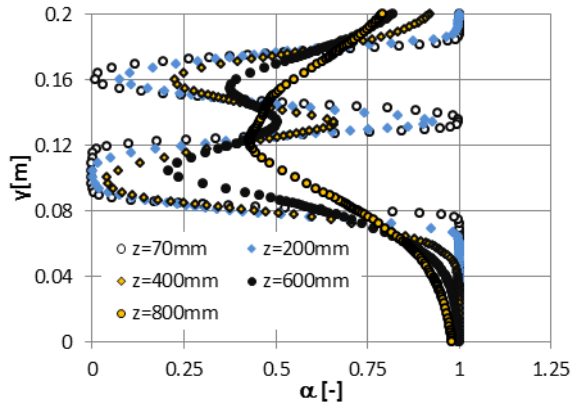
This paper presented a numerical investigation concerning the mixing of four air jets supplied by a burner designed for obtaining a staggered combustion of pulverized coal. The primary air jet (which could be mixed with the coal particles), is split in two streams A and B, the secondary jet closely follows the primary jet B and the tertiary one surrounds all the others. Two case studies were investigated, the difference between them consisting only of the inflow velocity value of the tertiary air jet (8.48 m/s and 33.2 m/s, respectively).



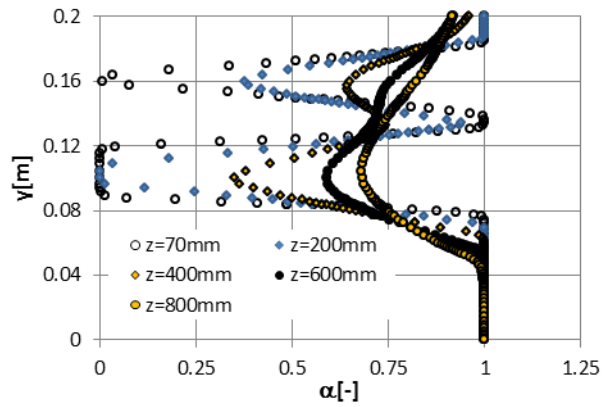
a) **Case1**: cross-stream distributions of stream-wise velocity



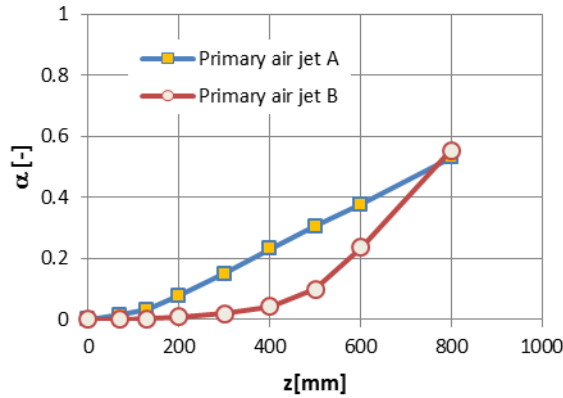
a) **Case2**: cross-stream distributions of stream-wise velocity



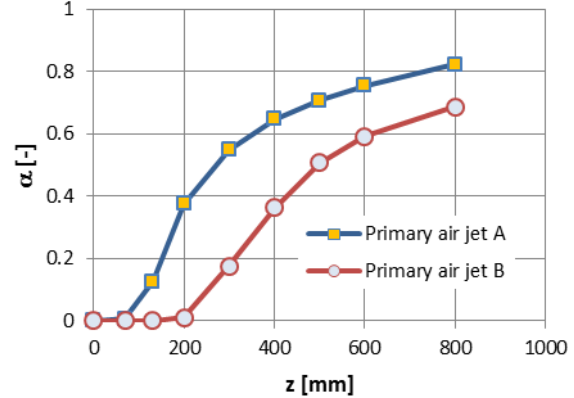
b) **Case1**: cross-stream distributions of mixing factor.



b) **Case2**: cross-stream distributions of mixing factor.



c) **Case1**: profiles of mixing factor along the symmetry line of primary air jets



c) **Case2**: profiles of mixing factor along the symmetry line of primary air jets

Fig.4. Velocity and mixing factor distributions for the first case study.

Fig. 5 Velocity and mixing factor distributions for the second case study

The results of the numerical simulations revealed that the second case study assures all the mixing conditions for obtaining a staggered combustion of the coal pulverized in both streams of primary air jet.

References

- [1] Negreanu G.P., Stanciu D., Mihăescu L., Pișă I., Oprea I., *Testing the operation of a new lignite low NO_x burner module by experiment and modeling*, ICAE 2013, 1-4 iulie 2013, Pretoria
- [2] Aziz TN, Raiford JP, Khan AA., Numerical simulation of turbulent jets. Engineering applications of computational fluid mechanics; vol. 2, No 2, 234-243: 2008.
- [3] ANSYS Inc. Ansys Fluent user manual V14., 2012.

WOOD BIOMASS, ENERGY EXPLOITATION AND WOOD PROCESSING TECHNOLOGIES

Ștefan Gabriel Adrian, Tudor Prisecaru, Nicolae Baran

University Politehnica of Bucharest

1. Introduction. Biomass in Romania and its role

Romania is a country that has a significant amount of biomass. Today this represents over 20% of the land area and is the easiest to spot on the map especially in the plateaus, the Carpathian foothills, valleys and depressions as well as the mountains. It is represented by the largest forests, especially the leafy beech hill or plateau area - and especially pine spruce forests and fir in the mountains and mountain valleys. In addition there are forests of oak, ash and birch but less numerous papers. Like in Fig.1 forests of Romania. Below, the green represents the forest area and the white area is the intended primary destinations for agricultural or other types of plants in red or red and pink borders are areas of intensive exploitation of wood and blue border areas illustrates risk areas illegal logging Abusive forest.

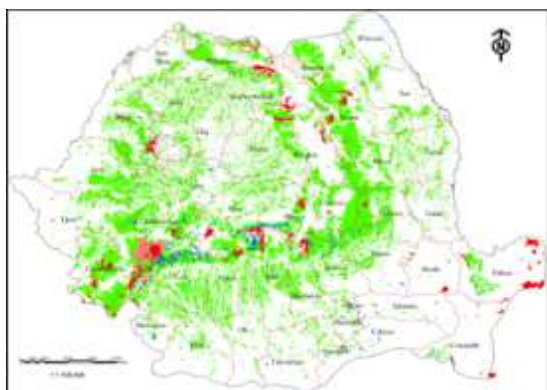


Fig.1.Romania's geographical map of forests and large wood harvesting red box.



Fig.2.Wood shavings called matchwoods

2. Biomass energy exploitation

Exploitation of biomass energy in Romania is very important, it represents about 63% of renewable energy used in the entire country in 2010. The most important sources of biomass they represent: logs and firewood, wood industry waste obtained as chips and sawdust. Medium and long term growth is assured quantity of biomass plantations of trees and shrubs with reduced period of growth and energy crops that are grown on land, disabled and other degraded lands set aside. Local energy potential of biomass in Romania is estimated at over 7,594 thousand toe / year, which represents 19% of total primary energy consumption in the year 2010. The heat resulting from the exploitation of biomass energy has different weights in the balance of primary resources by type and destination of final consumption. Thus 54% of biomass heat is obtained by burning forest residues, or 89% of the necessary heating homes and cooking in rural areas.

Biomass wood used in our country is of two types:

A) Natural biomass (generally it includes: chip wood and logs); Processed biomass (pellets and briquettes). Natural biomass is the simplest and most common fuel used for heating in the

domestic sector. Most convenient types of woody biomass used for heating homes are wood chips and logs. Wood chips are small pieces of wood that were low humidity with a much lower density than pellets, but with a higher moisture content than the latter. Chips requires a much larger storage room than pellets, but are cheaper per unit of energy than these.[5] For producing wood chips as in Fig.2. There are different types of wood cutting machines: with disc or propellers for matchwoods like in Fig.3.

Logs still use a lot of heating, the heating equipment using only manual feed. Not all mass burning logs or just, so each type of wood is unique to a species that belongs. Density and composition is unique in a quantity of wood burning, the most important indicator is the energy released from burning a fixed volume of logs.[2][3]



Fig.3. Equipment and woodworking machinery.



Fig.4. Sawdust in a pressure extruded to form pellets

B) Processed biomass

Wood pellets are bigger, harder and more dense than the matchwoods. They are produced by compacting sawdust (Fig.4) resulting from sawing of wood, using equipment similar to that used in the preparation of animal feed. As they cut to small size facilitates automatic power burner. Production costs and high processing level leads to a higher price per unit of energy. Wood briquettes or a general type of biomass is a fuel pellets prepared in a similar manner, but comparable in size with logs. They are being burned in combustion same equipment and facilities as logs.



Fig.6. Briquetting machine



Fig.7. Cylindrical lighter wood briquette.

Obviously biomass burning of classes resulting ash to be discharged and stored under its own special places. Emission levels are significantly reduced when burning pellets and briquetting. Sawdust is extruded into pellets resulting pressure that form of cylindrical bodies lengths of 2-3 cm, with a density of 1.12 kg/m^3 and a high calorific value of about 18 MJ/kg . Logs can generally use manual feed heaters, they burn with a dry humidity below 25%. Wood briquettes fuel represents a similarly prepared pellets and comparable in size with logs. Wood and agricultural biomass as a renewable source of energy is very important, its use ensures independence from imported oil and natural gas. The most common types of wood biomass for home heating, wood chips, pellets, logs and briquettes burn in specialized plants at temperatures from 600 to 700°C . [2][3]

3. Methodology. Calculating the moisture content

The direct way of calculation of wet biomass and moisture this also include the oxygen. Typically the moisture content must be less than 25% for logs and more than 35% for chips. There are two methods to calculate the moisture content used, "wet method" and "dry method." Most used is "wet" method, although rangers tend to use dry method. It is important to note that the two methods will give different results for the same piece of wood analyzed. Wet method of calculation is as follows: For a quantity of wood with a mass of 10kg is dried in an oven so that the entire quantity of water is removed and then the amount of wood is weighed. The new experimentally determined mass is 8 kg.[5]

1) The percentage of moisture content is calculated using the formula:

$$\text{Moisture content (CU)} = [(\text{mass of water}) / (\text{mass of wet wood})] \cdot 100\% \quad [1]$$

$$\text{CU} = 2\text{kg}/10\text{kg} \cdot 100\% \text{ results} = 0.2 \cdot 100\% \Rightarrow \text{with} = 20\%$$

2) Method Dry calculated for the same example above has the following formula:

$$\text{Moisture content (CU)} = [(\text{mass of water}) / (\text{mass of dry wood})] \cdot 100\% \quad [2]$$

$$\text{CU} = 2\text{kg}/8\text{kg} \cdot 100\% \text{ results} = 0.25 \cdot 100\% \Rightarrow \text{with} = 25\%$$

Making a simple calculation in an average between the two methods result in formula to calculate the average moisture content average mass loss resulting loss of biomass:

$$\Delta m = (0.20 + 0.25) / 2 \cdot 100\% \Rightarrow \Delta m = 22.5\% \quad [3]$$

Result a decrease in biomass weight at least 22.5% from the time when it was harvested and until is valued for energy.

The moisture content.

Freshly cut wood has a moisture content of 40-60% in wood.

Useful energy available depends on the amount of moisture found. The ideally wood fuel should be as dry as possible. Water does not contribute to the energy content of the fuel, it substantially reduces its useful energy value (Fig.8)



Fig.8. The dependence of moisture content and calorific value for softwood.

Seriously influences by the moisture content of wet biomass. Wood requires a long residence time in the drying oven that requires a higher grill in order to be burned. It also need high amount of energy to dry the fresh fuel. The dry the fuel is, the less energy is available as useful heat. The moisture of the biomass is also a major factor affecting transport costs. Transport costs per tone of wet wood is the same as the cost per ton of dry wood.

4. Conclusions. The characteristic proprieties of wood biomass.

The size characteristics of woody biomass are taken into account:

Table.2. The table below shows the characteristic sizes of commonly used fuels

Fuels	The energy fuel mass GJ / t	Energy per mass kWh / kg	The pile density Kg/m ³	Energy per volume MJ/m ³	Energy heure production per volume [kWh/m ³]
Wood chips (highly depend on moisture)	7 - 15	2 - 4	175 - 350	2000 – 3600	600-1000
Wood logs (stack dry air, humidity 20%)	15	4.2	300 - 550	4500- 8300	1300- 2300
Wood (solid - dry in the oven)	18 - 21	5 -5,8	450 - 800	8100- 16800	2300- 4600
Wood pellets	18	5	600 - 700	10800- 12600	3000- 3500
Coal (from lignite to anthracite)	20 - 30	5,6-8,3	800 - 1100	16000-33000	4500- 9100
Oil	42	11,7	870	3650	10200
Natural gas	54	15	0,7	39	10,8

Choosing the right fuel depends on many factors and overall customer priorities lead to choosing the right fuel. For example, pellets are suitable for a client with limited storage space and needs a fully automated heating system, while logs are ideal in a rural setting where the client uses its own resource timber.

The most important factors to consider when choosing fuel are:

- Availability - local sources on site and safety;
- Acquisition cost, including processing and delivery;
- Advantages and potential for automation;
- Availability of storage space;
- Cost of combustion equipment and the necessary fuel supply system

Tabel.1. The following table compares the different types of fuels that can be used[1][5]

Fuel	Advantages	Disadvantages
matchwoods	- They are easy to produce from local cosmetic cutting of forests; -Fuel costs are very low.	The combustion system has higher costs; -Suitable only for equipment greater than> 25 kW.
Wood pellets	-Lower capital costs due to drier and more homogeneous nature of the fuel; -Dense fuels means less storage and easy transport; -Suitable for very small installations.	-Higher fuel costs, pellets are made in presses that require additional costs; -It is unlikely that supply fuel to make it local; -It does not produce local economic impact.
Logs	-Easy-air circulation allows for better drying them; -Can be purchased easily on site.	-Requires large storage space to allow their preservation drying for 1-2 years.

5.References

- [1] Nicolae Pănoiu,Constantin Cazacu, Lucian Mihăescu,Cristian Totolo, Alexandru Epure - Instalații de ardere a combustibililor solizi , Editura Tehnică, Bucundrești – 1985;
- [2]N.Pănoiu, D.Grecov,C.Ungureanu,G.Singer, I. Carabogdan.-Instalații de ardere Editura Tehnică, Bucuresti, 1968;
- [3]Trif-Tordai Gavrilă-Cercetări privind arderea combinată a biomasei(2008),Editura Tehnica din Timișoara;
- [4] Gh. Băran, C.Mateescu, C.A.Băbuțanu ,N.Băran,L.Mândrea, C.Craiu, E.Pena Leonte, I.Ghiță,L.Dumitru, Realizări și perspective în industria biogazului,Editura PRINTECH, București 2007;
- [5]Tudor Prisecaru,Emil Enache,Lucian Mihaescu,Ionel Pisa,Gabriel Negreanu,Malina Prisecaru, Berbece Viorel,Popa Elena, - Achievements in the construction of boilers for agricultural biomass combustion,International Symposium of Section IV of CIGR -BRETS , 2011, Bucharest 23-25.
- [6] Lucian MIHĂESCU, Ion OPREA, Gabriel Paul NEGREANU, Tudor PRISECARU, Laurențiu Popper, Ionel PIȘA, Elena POP,Gabriel POPPER,Adrian ADAM, Adelina PANAIT -Valorificarea energetică a uleiurilor vegetale brute –, Editura PRINTECH, Bucuresti 2011;

STUDIES ON BIOMASS SUPPLY BY THROWING OR PNEUMATIC INJECTION

Ștefan Gabriel Adrian, Tudor Prisecaru, Ionel Pisa

University Politehnica of Bucharest

1. INTRODUCTION.THE IMPORTANT ROLE OF BIOMASS COMBUSTION AND HIS AVAILABILITY IN NATURE

This work study has the purpose to analysis the tested solutions to this days regarding the technology for energetic use of biomass for burners and installation .

The study also contain some contribution to the optimization to the vegetable biomass combustion solutions.[1]

One of the most important role in this paper work is the biomass type and the efficient use to burn it. The market is expanding and the use of biomass that is well needed as green energy supplement in transport and electricity.[2]

The study that I made illustrate the importance that biomass will represent especially in the next generation of solid biomass fuel burners for industrial and the same for single customers. Solid biomass covers a wide range of materials: woods, straws, agricultural residues, energetic fields especially made for energetic value supply, processing wastes, algae and seaweeds. Biomass is still widely used since dark ages and even now is widely spread in developing countries like Romania, because is chip and available. The technology is simple, that's way it is so popular in countries that have considerable reserve of biomass. This still is highly used despite the major efforts in this late decay to make more available other technologies like wind turbine and solar panels.[3]

My study is using as fuel only solid biomass like: woods, straws, agriculture residues and energetic fields for heat and electricity and sometimes transport.[1] This highly use of renewable biomass supply is so attractive and it is so geographically widely available that it can be used all over the world and more important this energy is storable. Current and future estimates of biomass utilization are subject to uncertainty and global values that can vary very much, but well-resourced information is available for major countries like US, Europe, Russia, China, India and Brazil.[9]

2. MATHEMATICAL MODELING OF PROCESSES OF OUTBREAKS

In this study there are presented the most important equations in which way that burner processes are design to ignite fuel and to maintain the constant burning of the biomass particles.

The most important constants used are: the particle diameter, the particle temperature, the gas temperature that surround the biomass particle, the speed on which the volatile particle are moving in the burner, the speed on which this particle are burning, and never the less the oxygen and the CO₂ gas concentration around the particle.[5][7]

Regarding the CO concentration that is made during the entire burning process this will result and could be determine from the general equation of burning gas.

$$C_{CO} = (CO'_2 - CO_2) \cdot \frac{1}{2} \cdot (0.605 + B_0) - C_{CO_2} \cdot \frac{(1+B_0)}{2} \cdot (0.605 + B_0) \quad (1)$$

where $C_{O_2}^i$ is the initial concentration, [kg/Nm³]. This analytical model has the disadvantage that shows the combustion process in the following way:

- Fuel particle is stationary in a stream of hot gas moving along it;
- Transfer of heat from the gas is mainly by convection but not evidenced dependent relative speed of particles and gases - which are considered constant;
- Relative speed is closely correlated with particle diameter ranging during the combustion process. [7][8]
- Is also observed as shown in kinematic equations and heat transfer by radiation under the influence of a factor φ of view it depends on the position that one has particle at a time.[6]

3.TEORETIC STUDIES ON BIOMASS SUPPLY BY THROWING OR PNEUMATIC INJECTION

We have a differential equation of motion of solid fuel particle injected into the combustion:

$$m\ddot{x} = C_f \cdot \frac{\pi d^2}{8} \cdot \rho_a (u_a^2 \cos^2 \alpha + u_p^2 \cos^2 \theta - 2u_a u_p \cos \alpha \cos \theta \cos \varphi) \quad (2)$$

$$m\ddot{x} = C_f \frac{\pi d^2}{8} \rho_a \{u_a^2 \cos^2 \alpha + u_p^2 \cos^2 \theta - 2u_a u_p \cos \alpha [\cos \alpha + \cos(\theta - \varphi)]\} \quad (3)$$

where: $\alpha - \varphi = \theta \Rightarrow \alpha - \theta = \varphi$

$$\cos(\theta + \varphi) = \cos \theta \cos \varphi - \sin \theta \sin \varphi$$

$$\cos(\theta - \varphi) = \cos \theta \cos \varphi + \sin \theta \sin \varphi$$

$$\cos \theta \cos \varphi = \frac{1}{2} [\cos(\theta + \varphi) + \cos(\theta - \varphi)]$$

$$\cos \alpha [\cos \alpha + \cos(\theta - \varphi)] = \cos^2 \alpha + \cos \alpha \cos(\theta - \varphi)$$

$$= \cos^2 \alpha + \frac{1}{2} [\cos(\alpha + \theta - \varphi) + \cos(\alpha - \theta + \varphi)]$$

$$\cos \theta \cos \varphi = \cos^2 \alpha + \frac{1}{2} (\cos 2\theta + \cos 2\varphi) = \cos^2 \alpha + \frac{1}{2} [\cos 2\theta + \cos 2(\alpha - \theta)] \quad (4)$$

$$\text{where: } \cos(\alpha + \beta) = \cos \alpha \cos \beta - \sin \alpha \sin \beta$$

$$\cos(\alpha + \beta) = \cos(\alpha - \beta) = 2 \cos \alpha \cos \beta$$

$$\alpha + \beta = a \Rightarrow 2\alpha = a + b \Rightarrow \alpha = \frac{a+b}{2}$$

$$\alpha - \beta = b \quad 2\beta = a - b \quad \beta = \frac{a-b}{2}$$

$$\cos 2\theta + \cos 2\varphi = 2 \cos \frac{2\theta+2\varphi}{2} \cdot \cos \frac{2\theta-2\varphi}{2} = 2 \cos \alpha \quad (5)$$

We know that: $k = C_f \cdot \frac{\pi d^2}{8} \cdot \rho_a$. After replacing all the terms in the original equation results:

$$\frac{m\ddot{x}}{k} = u_{ax}^2 + \dot{x}^2 - 2u_{ax} \cdot \dot{x} \cdot \cos(\alpha - \theta) \quad (6)$$

$$u_{ax} = u_a \cos \alpha = u_0 \sqrt{\frac{y_0}{0.316 C(x \cos \alpha + y \sin \alpha)}} \cdot \left[1 - \left(\frac{-x \sin \alpha + y \cos \alpha}{C(x \cos \alpha + y \sin \alpha)} \right)^{1.5} \right]^2 \cos \alpha \quad (7)$$

We know that:

$$W = C(x \cos \alpha + y \sin \alpha) ;$$

$$Z = -x \sin \alpha + y \cos \alpha ; \quad \text{and}$$

$$B = \sqrt{\frac{y_0}{0.316}}$$

Equation becomes after replacing terms:

$$u_{ax} = u_0 \cdot B \cdot \frac{1}{\sqrt{W}} \left[1 - \frac{\sqrt{Z^2}}{\sqrt{W^2}} \right]^2 \quad (8)$$

$$\frac{u_{ax}^2 \cdot W}{u_0^2 \cdot B^2} = 1 - 4 \sqrt{\left(\frac{Z}{W}\right)^3} + 6 \cdot \left(\frac{Z}{W}\right)^3 - 4 \cdot \sqrt{\left(\frac{Z}{W}\right)^9} + \left(\frac{Z}{W}\right)^6 \quad (9)$$

$$\text{We know that: } V = \left(\frac{Z}{W}\right)^3$$

Thus resulting final equation:

$$\frac{u_{ax}^2 \cdot W}{u_0^2 \cdot B^2} = 1 - 4\sqrt{V} + 6V - 4\sqrt{(V)^3} + V^2 \quad (10)$$

4.ELEMENTARY COMPOSITION ANALYSIS OF BIOMASS

Currently an important quantity from 25 to 40% of the total wheat straw, corn stalks and are not used although it may be an important source of renewable energy. Grain residues energy locally operated mainly in the plains are the most accessible and cheaper solid fuel [1][11]

Burning wood waste aims to harness the process is influenced by the amount of oxygen found in the air used for combustion.

Wood burning occurs to the total of body formed by oxidation of cellulose, lignin, hemicellulose, extracted, remaining only the inorganic (ash) composed of salts, soluble (sodium and potassium carbonates, sulfates, chlorides and silicates) and of insoluble salts (calcium oxide, phosphates, oxides of iron, manganese, etc).[12][13]



Fig.1. Biomass – crumble corn stalks

Emission levels are significantly reduced when processed and burned biomass; crumble corn stalks, cereal pellets and briquettes. Thus the ash content of a ton of biomass processed is 9 times lower than for a similar amount of coal, sulfur oxide content of at least 5 times lower nitrogen oxide, 2.6 times lower and the carbon dioxide 4 times. Obviously biomass burning of classes resulting ash to be discharged and stored under its own special places. [10][11][12][13]

Table 1. Elemental composition and calorific value of the six types of plant biomass and lignite.[10]

Biomass sample	C [%]	H [%]	O [%]	S [%]	N [%]	W [%]	A [%]	Other Metals[%] Cl,Ca,K,P	Q [kJ/kg] (Kcal/kg)
Wood	48-52	6.2-6.4	40-43.5	< 0.05	0.01-0.03	5- 60	0.4-0,5	0.8- 1.6	16500-17200
Wood pellets	51	6.3	41.8	0.01-0.002	0.02	7.7	0.7	0.8	17270-18500
Wheat straw	45.6	5.8	42.4	0.082	0.48	4.7	0.57	1.72	14800-16150
Corn cobs	45.7	5.3	41.7	0.12	0.65	8.9	0.9	0.65	13250-13750
Crumble corn stalks	45.7	5.3	41.7	0.12	0.63	6.4	0.9	0.65	14850-15750
Reed	46	5.9	42	0.25	0.75	5.9	0.98	3	14750
Lignite (lower coal)	53	4.77	23.5	3.43	1.65	8.7	1.85	6.8	21450

In my study, all data refers to the ideal of complete combustion and biomass fuel. So the volatile, all groups of large molecules and complex chemical substances contained in the biomass gradually decompose and burn almost complete.[10][11]

The corn cob – diagram chart and the table made by the analyser

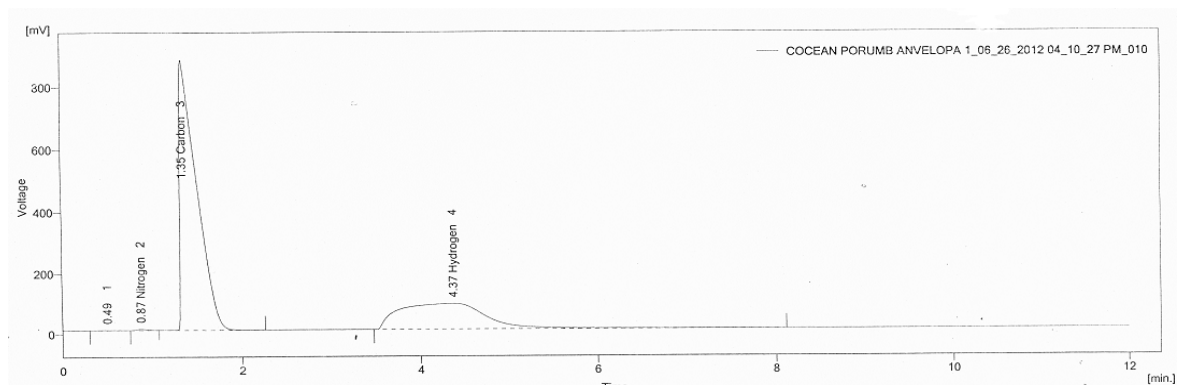


Fig.1. Corn cob diagram chart

Table.2. Results corn cobs diagram chart

	Reten. Time [min]	Response	Weight [mg]	Weight [%]	Peak Type	Element Name	Carbon Response Ratio
1	0.493	7.434	0.000	0.0			???
2	0.870	28.655	0.009	0.3	Refer	Nitrogen	0.003
3	1.347	11330.293	1.553	45.8	Refer	Carbon	1.000
4	4.370	5736.385	0.196	5.8	Refer	Hydrogen	0.506
	Total		3.390	51.9			

5. CONCLUSIONS.CURRENT TECHNOLOGY AND SOLUTIONS REGARDING THE BIOMASS COMBUSTION

There are many types of biomass combustion plants, but constructive solution can be chosen depends on the size biomass waste, the degree of humidity and many other criteria.

In terms of scale biomass burning may be: combustion of biomass in fixed bed (grilled), fluidized bed biomass-burning and combustion of biomass in pulverized state.

One solution is the biomass combustion technology on the grill of particles by throwing.

The solid biomass fuel combustion in these systems is placed on a rack or grill while combustion air is introduced at the bottom of the grill.

In practice, the biomass can be fed a grain size up to 200 mm, including very fine particles the dry biomass shook with recommended humidity below 20% .

Grate firing is a technology used to lower biomass or coal boilers, especially within industrial plants or local thermal with a capacity starting from 50 kW and up to 7 or 8 MW.[4]

Technology advantages of this are low operating and maintenance costs as biomass does not require high precision cutting or grinding fine, and construction is simple, the amount of volatile dust and other elements of the flue gases is small.

Disadvantages of this technology are given the difficulties encountered when reducing oxides of nitrogen, heterogeneous combustion because the air is not distributed evenly throughout the fuel layer. Also might be a blockage in the grate, where the primary air cannot enter the combustion chamber, the combustion will occur only with the amount of secondary air introduced.[4]

Biomass burning time τ depends mainly on the type of biomass and air flow is introduced into the furnace. Biomass type is known, the amount of corn cobs 5-10kg / h, which burns at an average temperature $T_m = 600^\circ\text{C}$ on a bottom air jet burner grill for intense and complete combustion.

Solid ash is discharged through a bottom nozzle equipped with waste collection gutter.

6.References

- [1]Combustion Technology,Some Modern Developments by Howard B.Palmer and J.M.Beer Editted by Academic Press(New York,San Francisco,London 1974);
- [2]Instalatii de ardere a combustibililor solizi de Nicolae Panoiu,Constantin Cazacu,Lucian Mihăescu,Cristian Totolo,Alexandru Epure, Editura Tehnica Bucuresti 1985;
- [3]Instalatii de ardere de N.Panoiu,D.Grecov,C.Ungureanu,G.Singer,I.Carabogdan, Editura Tehnica,Bucuresti 1968;
- [4]Cazane de abur si apa fierbinte.Manual pentru inginerii din exploatare si operatori cazane de Mihăescu Lucian, Prisecaru Tudor,Oroianu Ionica,Popa Elena,Lixandru Dumitra, Gramescu Stelian, Editura Perfect in colaborare cu Editura Printech 2007;
- [5]Valorificarea energetica a uleiurilor vegetale brute de Lucian Mihăescu,Ion Oprea,Gabriel Paul Negreanu,Tudor Prisecaru,Laurențiu Popper,Ionel Pîșă,Elena Pop,Lixandru Dumitra,Gramescu Stelian, Editura Printech,București 2011;
- [6] Modele numerice termice, de Constantin Brătianu,Tudor Prisecaru,Gabriel Paul Negreanu,Viorel Berbece,Editura Tehnica Universitatea Politehnica din București
- [7]Modelarea numerică a proceselor de ardere a combustibililor gazoși și solizi pulverizați, de Tudor Prisecaru, Editura Bren, București 2001;
- [8]Metode numerice în tehnică, de Mario G.Salvadori, Melvin.L.Baron, Editura Tehnică București 1972;
- [9]de Wit M. European biomass resource potential and costs. In: Faaji A, Londo M, editors. A road map for biofuels in Europe,biomass and bioenergy, vol 34;2010.p.157-250
- [10]Cercetări privind arderea combinată a biomasei cu cărbune, de Gavrilă Trif-Tordai, Editura Politehnica, 2008;
- [11]Thermal numerical models. Thermal modeling and simulation laboratory department of mechanical equipment and nuclear Classic. - By Constantin Bratianu, Tudor Prisecaru, Gabriel Paul Negreanu, Viorel Berbece, Technical Publishing House, Bucharest, 1994.
- [12]Valorificarea complexa a biomasei – de Măluțan Teodor, Editura Tehnica, Bucuresti 2008;
- [13]Cercetări privind arderea combinată a biomasei(2008) de Trif-Tordai Gavrilă, Editura Tehnica din Timișoara, 2008;

ANALYSIS OF DEGRADATION FACTOR OF PHOTOVOLTAIC MODULES OPERATING UNDER FIELD CONDITIONS

Angel Terziev¹, Technical University of Sofia, Ilia Iliev, Ruse University; Veselka Kamburova, Ruse University; Deyan Deltchev, Germany

ABSTRACT

The power output of photovoltaic modules operating under certain field conditions decreases over the time. The photovoltaic module degradation factor depends not only by the physical properties of the material but also by the change of parameters of the environment where the PV panel operate. The change of the PV modules degradation factor over the time reflects on the power output which is in a close relation with revenues from the purchased electricity produced by the modules.

The process of PV modules degradation is a normal process accompanying the operation of the panels. This process is a result of: increased losses in a linear connections; increased relative humidity of the ambient air, and the process of moisture evaporation; limitation of possibilities of the p-n junction; and destruction of protective coating.

The first abovementioned losses generally depends on the local atmospheric conditions where the panel operate. At higher local values of the average temperature and relative humidity of the air the rate of degradation increases. An analysis about the degradation rate of the PV modules operating under specific field conditions here is made.

1. INTRODUCTION

During the operation of the photovoltaic modules in field conditions over time their output power is reduced. This is a result from their degradation level, depending not only on the type of the material, from which they are made of, but also on the conditions in which they work. Every manufacturer of panels gives information for the degradation level, based solely on the properties of the material, from which they are made of. However, in field operation the rate of change of this factor will depend also on the conditions, in which the panel works, which will reflect on the change in their output power. Therefore, the determination of the influence rate of the major environmental factors on the degradation rate of the modules is very important. This way the production of electricity from a specific type of panel can be prognosed more clearly during the time, as well as a more precise analysis of the generated cash flow of the produced and sold with preferential price electrical power could be prepared.

2. METHODOLOGY

In order to establish the rate of impact of the atmospheric parameters on the factor of PV modul degradation a study on different photovoltaic modules, installed in various locations on the territory of Bulgaria is made. The location of the studied parks is shown in Figure 1. The photovoltaic parks are in the northeast, north central, middle central and southeast Bulgaria. For the presented locations a long-term information is collected and analyzed, regarding the local weather conditions. Detailed information for the solar radiation, average month temperature of the air and the earth surface, the relative humidity and wind velocity is presented in [1].

¹ 1000 Sofia, Bulgaria, 8 Kliment Ohridski blvd., Sofia, phone +359 889 23 53 61; e-mail: aterziev@tu-sofia.bg



Figure 1: Locations of the Photovoltaic Park

The climate in the indicated places is mixed, presented with not only different daily and yearly temperatures, but with relative humidity, especially for the locations near the seaside. For this reason, special attention is paid to the influence of these 2 parameters on the factor of degradation of the photovoltaic modules.

In Figure 2 (a and b) is presented information for the average monthly (long-term) relative humidity and temperature of the atmospheric air.

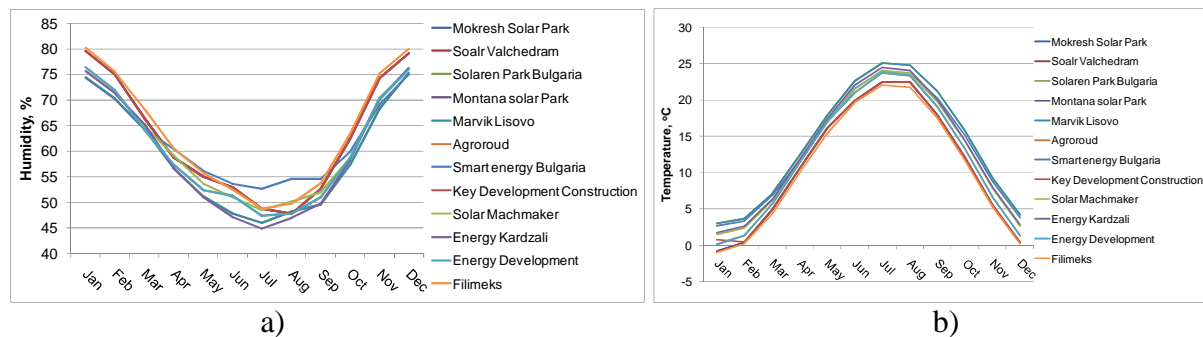


Figure 2: Long term data about: a) Monthly average humidity distribution, b) Monthly average temperature distribution

From Figure 2 follows that the site of the PV parks "Filimeks" and "Key Development construction" work in conditions of the highest relative humidity ϕ . Regarding the temperature changes, most affected will be photovoltaic modules "Mavrik Lisovo" and "Energy Kardzhali".

Here it must be pointed out that the determination of the output power of the photovoltaic panels in laboratory conditions is according the requirements of the standard: intensity of the solar radiation $I = 1000 \text{ W} / \text{m}^2$ and temperature $t = 25 \text{ }^{\circ}\text{C}$.

The output power of a certain cell depends mostly on the properties of the elements, from which it is made of: glass coverage, frame, protective material etc.

For each panel it can be calculated by the following relation:

$$P = I(a + b.I + c.W + d.T) \quad (1)$$

Where - I is intensity of the solar flux, W / m^2 ; W - monthly average wind speed, m / s ; T - monthly average temperature, $^{\circ}C$.

Each of the abovementioned parameters are function of the local weather (climate) conditions.

The value of the coefficients a , b , c , and d are presented in Table 1.

Table 1: Values of the parameters a , b , c and d

Parameters	Value, %
a	96.4
b	2.9
c	0.4
d	0.4

The efficiency of the photovoltaic modules on the other hand depends on each of the following parameters: Installed capacity (P); Radiation flux (I); Area of the selective coating (A).

The efficiency can be determined according the following relation [2]:

$$\eta(\%) = \frac{P}{I \cdot A}, \quad (2)$$

The minimal theoretical value of the power of the panel (P_{lim}) is determined according Eq. 3. It depends on the installed power, strictly defined in the technical documentation provided by the manufacturer, 5% deviation of the power of the panel, guarantee for the power output (P_{out} , %), and accuracy of reporting (T , %) [2, 3].

$$P_{lim} = P_0 \cdot 0,95 \cdot P_{out} \cdot T, \quad (3)$$

The warranty conditions, set by each manufacturer company are based mainly on the quality of the used material during the production of the panels. In general the warranty of the photovoltaic modules varies between 1 and 5 years. The factor of degradation of the panels and their reliability depends on: Adhesion losses; Connection status between silicon cells; Penetration of moisture inside the material; Degradation of semiconductor elements (not relevant to the polycrystalline solar panel).

The test results regarding the level (factor) of degradation for different photovoltaic modules, operating in certain climatic conditions are shown in Table 2. The tested panels are from polycrystal (p-Si) and respectively monocrystal (c-Si) type.

The results show that the factor of degradation for the polycrystal modules is approximately 0.3% (in conditions of tepid climate). The research is done in the town of Ispra, Italy for the period of 22 years. Analogical data is presented also for the researched types of photovoltaic modules [2, 3, 5].

Table 2. Test data for the level of degradation of the photovoltaic module, working in field conditions [2]

Location	Test duration	Module Tech.	Degradation rate (%/year)
Perth (Australia) (<i>Temperate climate</i>)	16-19 months	p-Si	1 - 2.9
Hamamatsu (Japan) (<i>Temperate climate</i>)	10 years	c-Si	0.62
Ispira (Italy) (<i>Temperate climate</i>)	22 years	p-Si	0.3
Lugano (Switzerland) (<i>Temperate climate</i>)	20 years	c-Si	0.53

The determination of the factor of degradation of the photovoltaic modules is a complex characteristic, which depends not only on the properties of the materials which is used for the manufacturing of the panels, but also on the conditions in which they operate. Therefore in the current analysis are taken in account not only the behavior of the panels when certain factors changes (temperature and relative humidity), but also exact nature conditions, during which the photovoltaic park operates.

The change of the coefficient efficiency for the studied types of panels depends on the change of the outside temperature. Because the nominal power of the panel, presented in the technical specification of the manufacturer company is at temperature $t = 25\text{ }^{\circ}\text{C}$, the change in energy conversion efficiency of the panels is considered in temperatures different from these. With certain average temperature of exploitation of the panels and intensity of the solar radiation 1000 W/m^2 the efficiency is accepted for 100%. At temperature $0\text{ }^{\circ}\text{C}$ the efficiency at the same intensity is raised with 15%, and when temperature raises with $25\text{ }^{\circ}\text{C}$, the efficiency decreases with 15%, meaning that it can be accepted for linear, the relation between the change of the output power of the panel when there is a temperature change [2,5].

According to the presented curves, the panels of type Chaori Solar and Solpro 44 will be characterized by a high degree of degradation, in comparison with the others. In terms of relative humidity (see Fig. 2a), the panels installed on PV park Filimeks (Qpro 230 and Qpro 240) and PV park Key Development construction (YL 200 P-26b) will be characterized by a higher degree of degradation compared to the others. [1]

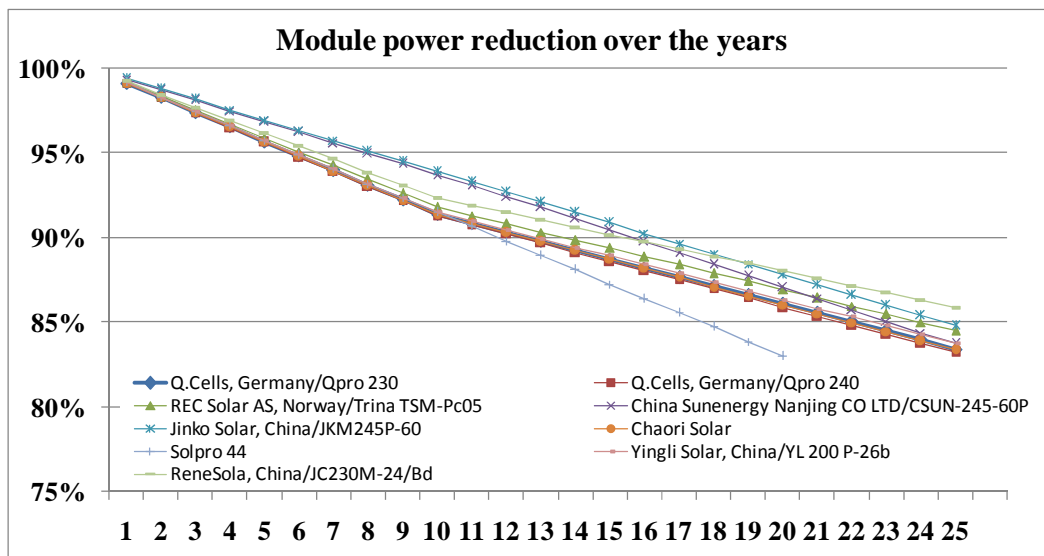


Figure 3: Modules output power reduction rate over the years

The reduction of the panel power (Wp) for the period is presented in [1]. Calculations are based on the coefficient of degradation of the modules.

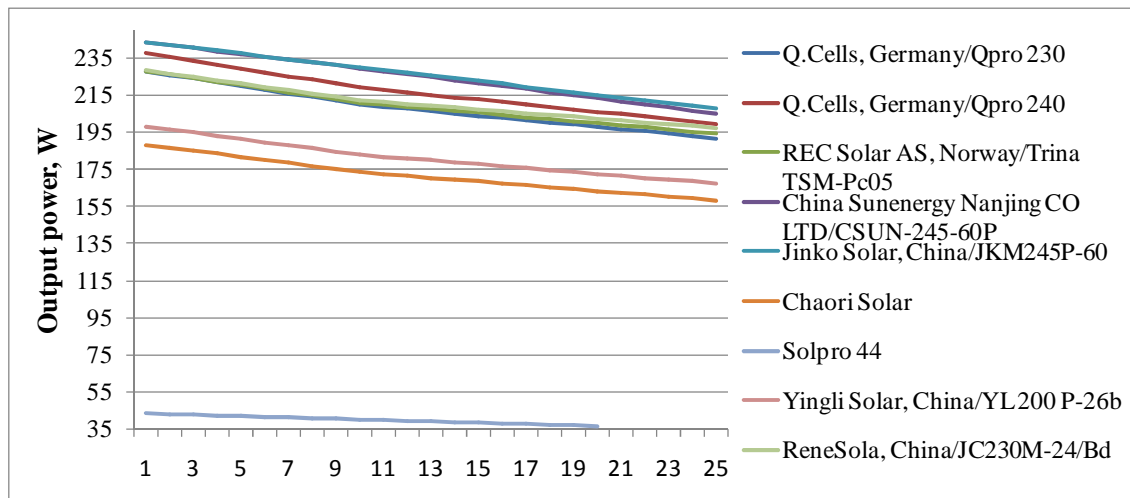


Figure 4. Reduction of the output power (Wp) of the panels over time

The reduction in efficiency of the photovoltaic modules over time during operation is shown in Fig. 4. With highest degree of degradation of the panels in field conditions are characterized the panels of type Qpro 240 and Chaori Solar.

The change in the equivalent coefficient of degradation of the presented photovoltaic panels for a period of 25 years is shown in [1]. The selected period meets the technical operational life of the equipment. For its determination are considered the specific properties (technical characteristics) of the panels, as well as the influence of external factors during operation of the panels in field conditions. The maximum coefficient of degradation of the panels indicated by the manufacturers is 10% for the first ten years of their operation, and another 10% for the next fifteen years. In [1] the factor of degradation for each year reflects the reduced value of the output power compared with the initial (starting at 100%).

3. CONCLUSIONS

This analysis is prepared on the basis of the presented technical documentation for the relevant panels in accordance with the climatic conditions in which they operate. During the analysis of climate data is used the long term database of NASA Datacenter and Joint Research Center [6,7]. The parameters of the ambient air, which affects most the performance of the photovoltaic modules, are analyzed in detail;

Evaluation of the influence of the temperature coefficient for each of the modules which affects the output power when temperature changes by one degree. In addition, the influence of the relative humidity of the ambient air on the performance of the panels is also studied. In terms of relative humidity by the panels of type Qpro 230, Qpro 240 and YL 200 P-26b will be influenced the most. In terms of temperature - the following panels will be affected: Chaori and Solpro 44.

The laboratory studies show in the most adverse operating conditions when the extent of degradation of the panels is the highest, the manufacturers ensure that the power output would be not less than 90% of the nominal in the first ten years of operation of the equipment, and linear reduction to a maximum of 80% by the end of its life.

The warranty of the basic element of a photovoltaic system – a photovoltaic cell, is an average of 20-25 years, and the amortization period may be even significantly higher. The normal operation of a PV park does not require any replacements of major components of the

plant as connecting cables and supporting structures. Due to high depreciation of the inverters, it is recommended that they should be replaced every 10 years of the system's operation.

In the course of work is presented the degradation factor modification over time in the field use of the panels as a function of the material from which they are made and the relevant parameters of the atmospheric conditions - ambient temperature and relative humidity. The probable range of variation of this parameter in real operating conditions is also shown.

References

- [1] Iliev I., A. Terziev, D. Deltchev, *Technical analysis of photovoltaic modules installed on the territory of Bulgaria*, Technical Report prepared for the Bulgarian Bank for Development by EnCon Services International Ltd, January 2013
- [2] Suleske, A. A., *Performance Degradation of Grid-Tied Photovoltaic Modules in a Desert Climatic Condition*, Arizona State University, December 2010.
- [3] <http://www.greentoronto.me/microfit-financials-pv-degradation-and-inflation/>
- [4] http://oa.upm.es/2724/1/INVE_MEM_2008_57620.pdf
- [5] http://ecogeneration.com.au/news/performance_degradation_in_solar_plants/055947/
- [6] <https://eosweb.larc.nasa.gov>
- [7] <http://re.jrc.ec.europa.eu/pvgis/apps4/pvest.php>

RESEARCH ON CEREAL STRAW BRIQUETTING IN NORTHEASTERN MOLDAVIA

Drd.ing. Mihai TOADER¹

Cereal straw provides a considerable potential for energetic use. The energetic exploitation of straw can be achieved by using discontinuous combustion installations (bales supplying) or continuous burning installations; briquettes are mostly used in these conditions.

Analyses on the briquetting installations show that the most appropriate one is the extraction press with hydraulic piston.

The piston pumps, when extruding the biomass (exhaust compression) will have to result into a resistant material with a safe form. The piston pumps' capacity is 40-1000kg / h.

The water content of straws is one of the most effective agents for binding and lubrication. Obviously, the strength and density of briquettes depend on an optimum humidity. Tests indicated that making straw briquettes when the humidity rises above 35% is totally defective. A moisture content of 12-17% is optimal for making briquettes of quality straws.

The particles' size represent another important criterion in briquetting. For briquettes with a diameter from 60 to 120 mm and length of 60-270 mm, tests have shown that an initial granulation of straws of 20-50mm size is optimal.

Presses use a mechanism with a piston that is actuated by a rod mechanical system or by a pneumatic one. Pressure may vary between 7-1300 bar. By pressing, a briquette of a certain form is obtained. This may be cylindrical or prismatic, usually with an inner hole. The inner hole serves to the evacuation of water vapor and volatiles from the compression process. Straw briquette quality is noticeably better at those that have an inner hole.

The relation for calculating piston pressure was obtained in the following form:

$$p = \frac{a\rho_0}{b} \left[\exp b \left(\frac{\rho}{\rho_0} \right) - 1 \right] \quad (1)$$

where a, b are constants that depend on the material. Density after compression was noted with p and p₀; density after compression was noted with kg/m³.

This relationship was developed in 1967 by Osobov as:

$$p = \frac{b}{a} [\exp a(\rho - \rho_0) - 1] \quad (2)$$

For low pressures, density was permitted under the pressure effect:

¹ PhD Student at the Faculty of Power Engineering; email: mihaimariustoader@yahoo.ca

$$\rho = \alpha + \beta \ln p \quad (3)$$

For the straw briquetting, the relation that matches mostly to the reality, is the one developed in 1986 by Faborde and O'Callaghan as:

$$p = \frac{a\rho_0}{b} f(r) \quad (3')$$

Where r is the densification rate

After theoretical and experimental research on establishing the straw briquetting pressure we have adopted the following relation:

$$\rho = \frac{a\rho_0}{b} [e^{b(r-1)} - 1] \quad (4)$$

p is the pressure of the piston

ρ_0 - initial density (kg/m³)

r -ratio of densification

a, b -constants

The constants' value was fixed as: $a = 0.035 - 0.045$ and $b = 0.47 - 0.52$

In figure 1, the briquetting station is presented, with its 5 lines arranged in a star, each of them making 60 kg briquettes per hour. Each line has a 3 kW electric motor and 5 kW electric resistors.

The briquettes could be cylindrical or polygonal in shape, both having a centerline hole.

The density of the briquettes is 900 – 1000 kg/m³. The briquettes have an 80 – 110 mm diameter and an 80 – 160 mm length.

These tests were conducted at a briquetting plant station with a production of 50-60kg / h for a single production line. During briquetting, the material was heated to 250 °C through an electrical system.



Figure 1. The Straw Briquetting Station

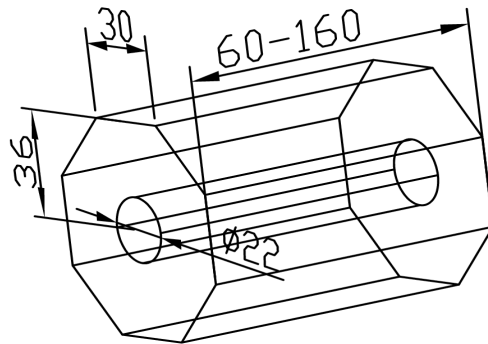


Figure 2. Briquette geometry



Figure 3. Images of briquettes

The briquette has a polygonal shape with the dimensions presented in Figure 2. The weight of a briquette is about $0.61 \div 0.63$ kg. Briquettes are obtained by compressing the straw and they have a very high density, about 1000 kg/m^3 .

The straw briquetting line in Figure 1 is functional in SC. E. MORARIT, in Vaslui County. There have been performed calculations for different rates of densification. In the calculations there have been considered the following values of the constants: . $a=0,04$; $b=0,5$. These values have been accepted after several experimental determinations on the briquetting line presented in Figure 1.

The initial density depends on humidity and on the straw size before briquetting. By chopping before briquetting, straw will have a size between 2.5 - 5mm.

For a densification from $p_0 = 200 \text{ kg/m}^3$ to $p = 900 \text{ kg/m}^3$, the densification rate will be $r = 900:200 = 4.5$. The piston pressure will be: $p = \frac{0,04 \cdot 200}{0,5} [e^{0,5(4,5-1)} - 1] = 76 \text{ bar}$

If p_0 is set to 150 kg/m^3 and the final density will be 900 kg/m^3 , then $r = 900:150 = 6$ and the piston pressure $p = 134 \text{ bar}$. For a higher densification, characterized by $p = 1000 \text{ kg/m}^3$, from $p_0 = 150 \text{ kg/m}^3$ the piston pressure increases to $p = 190 \text{ bar}$.

Long-term evidence showed that the optimum piston pressure is a value of $p = 160 - 180 \text{ bar}$.

During compression straw is heated using a system of electric resistors that have power for briquetting line of 3 kWh . Heating temperature is 2500°C .

Energy consumption for activating the plunger was 3 kWh / line . For a production of 60 kg , the specific energy consumption was 0.05 kWh / kg .

For heating, the average specific energy consumption was 0.05 kW / kg .

That results in an average energy consumption for briquetting of 0.1 kWh / kg . This consumption represents about $0.15\text{-}0.2$ of the selling price of the straw briquettes which is $270\text{-}350 \text{ RON / t}$ ($60 - 80 \text{ Eu / t}$).

REFERENCES

1. Willow Biomass: „An Assessment of the Ecological and Economic Feasibility of Growing Willow” Biomass for Colgate University -Jeremy Bennick, Andrew Holway, Elizabeth Juers, Rachel Surprenant, ENST 480, Spring 2008
2. “Renewable Energy from Willow Biomass Crops: Life Cycle, Energy, Environmental and Economic Performance”, Gregory A. Keoleian, Timothy A. Volk, Critical Reviews in Plant Sciences, 24:385–406, 2005; ISSN: 0735-2689 print / 1549-7836 online; DOI: 10.1080/07352680500316334;
3. “Life cycle energy and environmental benefits of generating electricity from willow biomass” Martin C. Heller, Gregory A. Keoleiana, Margaret K. Mannb, Timothy A. Volk; Renewable Energy 29 (2004) 1023–1042;
4. “Life cycle assessment of a willow bioenergy cropping system”, Martin C. Hellera, Gregory A. Keoleiana; Timothy A. Volk, Biomass and Bioenergy 25 (2003) 147 – 165;
5. “Life cycle assessment of a willow bioenergy cropping system”, Martin C. Hellera, Gregory A. Keoleiana; Timothy A. Volk; Biomass and Bioenergy. 2006, Vol. 30, pp. 16-27.

THE INFLUENCE CHANGES OF SELLING PRICE OF ELECTRIC POWER ON OPTIMAL SIZING OF CHP PLANTS BASED ON USING BIOMASS AND NATURAL GAS

Author: Paula Voicu¹
University Politehnica of Bucharest,
Faculty Entrepreneurship, Business Engineering and Management

ABSTRACT

In order to establish the technical-economic efficiency of cogeneration solution implementation is started from a mathematical model that is based on the discounted net value criterion. It aims to make the analyze of the effect the change of sales electric power price, the size which influencing optimal sizing and technical-economic efficiency of cogeneration solutions based on using biomass in combination with natural gas.

It will consider that in cogeneration systems using biomass and in heating peak systems, natural gas.

After applying the mathematical model for various values of selling price of electric power will determine the nominal optimal coefficient of cogeneration, for which discounted net revenue value is maximized. Optimal sizing of CHP plants based on using biomass and methane gas will be given by optimum coefficient of cogeneration determined following the application of the proposed mathematical model.

Key words: biomass, biomass cost, electricity sales price, cogeneration, coefficient of thermal cogeneration.

1. GENERAL ASPECTS

Biomass represents a diversity of vegetable origin elements that surround us from nature or those resulting from human activities, in order to capitalize their optimal. Refer to the diversity of nature and its miraculous power of regeneration in a quick and permanent.

One of the advantages of using plant on biomass is that biomass is a fuel almost free the only costs incurred are those that involve the collection and storage of biomass. By burning waste is resolved problem of their storage. Regarding the system as such, it is safer, more stable and less dangerous than one consuming fuel classic. By focusing on biomass, the consumer is protected from changes fossil fuel prices classics, such as coal, oil, gas.

As disadvantages, remember that systems based on such fuel are more expensive than which use fossil fuels. Handling and storage of biomass are relatively difficult and expensive process.

Thus, the systems which biomass burning are designed primarily communities, and not individual properties, in this way the original investment costs recovering rapidly but switching in profitable period of installation is made in a short period. [1]

Promotion of cogeneration production systems is a key way to respect the various legislative provisions concerning environmental protection, respectively reducing emissions of greenhouse gases. This is because high-efficiency cogeneration plants, against produce heat and power in separate sources, have important advantages, consisting in reduction of pollutant emissions (NO_x, Sox and particulates) and CO₂.

It'll treat mainly urban cogeneration solution in Romania, this sector showing a high interest due to the high degree of disconnection of consumers from some localities and

¹ Splaiul Independentei no. 313, sector 6, Bucharest, Romania, +40735941265, paulavoicu85@yahoo.com

accentuated physical and moral wear of installations, the centralized equipments systems heat supply available. In these cases cogeneration could be one way to revive the sector.

Energy performances of a cogeneration cycle are even better when electricity production (high quality) is higher or that production depends on the level heat which they are supplied to the heat and is even greater the more level its is the lowered.

The above is recommended use of biomass for urban consumers requiring low temperature levels.

In the case, CHP plants with steam turbine cogeneration, there are two variants namely: turbine with condensing and adjustable outlet and turbine with backpressure. They are used in area the average power through the use of a simple-cycle with low parameters of steam at the entrance.

Using hot water as the agent in primary circuit, the cycle with steam turbine backpressure can relax steam until to a low pressure with a good ratio between electricity and heat. The production of electricity is dependent on the heat consumer. When the heat demand is very low, it can use a further cooling in order to maintain the power generation and during summer.

Cycle of steam turbine with condenser and adjustable outlet is more complex, provides a lowered efficiency of electricity generation, but has the advantage that electricity production is ensured in periods when heat isn't required. Also, this cycle presents more flexibility on the proportion of heat and power products. The disadvantage is that it presents the higher expenditure of investment regarding the body of low pressure condenser and cooling system, but this expenditure is recovered by selling extra electricity. [2]

2. OPTIMUM SIZING OF THE COGENERATION PLANT USING BIOMASS IN COMBINATION WITH METHANE GAS

Urban heat demand is driven mainly by urban consumers, tertiary and those similar to them. It aims to heating and / or cooling and prepare hot water for sanitary purposes and domestic.

Heat demand for heating q_i is characterized by:

- size and changes over time caused by microclimatic parameters required for the enclosure (internal temperature, speed of displacement and relative humidity inside air) and outside macroclimatic characteristic parameters, in which there are that enclosure (outdoor temperature, solar radiation, air velocity external, solid and / or liquid precipitation);
- the required heat within the enclosure, which is constant during heating at a given temperature difference under the same outside. The value of the internal temperature is averaging 20 ... 24° C during heating (depending on the nature of the heated premises).

The demand of heat as hot water (q_{hw}) is characterized by a constant heat level ($t_{hw} = 50^{\circ}\text{C}$) and a variable flow (G_{hw}), depending on the type of consumer.

During the year ($\tau_u^{year} = 8760h / year$), urban heat demand structure depends on the type of its insurance.

We consider the following three climate zones with their specific values [3]:

	Hot areas	Cold areas	Average areas
1. annual duration of the heating period, h/year	4400	5760	5080
2. average demand during the heating $\left(\bar{q}_w^{md}\right)$, on the amount of calculation $\left(\bar{q}_w^c\right)$, %	0,45	0,50	0,48
3. the average demands of hot water by consumption during:			
▪ Heating $\left(\bar{q}_{hw}^{md}\right)$;	0,23	0,19	0,18
▪ Summer $\left(\bar{q}_{hw}^{md,s}\right)$, reported on a calculation $\left(\bar{q}_w^c\right)$, %	0,15	0,20	0,16
4. average total urban demand $\left(\bar{q}_u^{md}\right)$, reported at value of calculation $\left(\bar{q}_u^c\right)$, %	0,35	0,42	0,39

Achieving optimal sizing calculations cogeneration of solution is based on developing a mathematical model of calculation followed by a soft for the application respectively model.

It's made excel program where, for the three climatic zones of Romania, on the basis of economic criteria of decision (NPV) and determine the optimal nominal coefficient of thermal cogeneration of CHP plant. With help its, it can determine the mode of sizing of the CHP plant.

We analyze the situation when the equity investment is made.

The main calculation modules of logical scheme detailed of the calculation program considered for determination of the optimal nominal coefficient of thermal cogeneration were considered the paper [4], and for applying the calculation model were considered as inputs the following:

- maximum rated thermal power required by the consumer 10 MWth;
 - energy efficiency of CHP plant with steam turbine of condensing and outlet adjustable: the overall efficiency of CHP plant 80%, electrical efficiency for separate production of electricity 15%, thermal efficiency for separate production of heat - natural gas 90% ;
 - emission factor on CO₂ of biomass burned properly zero, respectively 0.22 tCO₂/MWh methane gas;
 - eco-tax on CO₂, 9 €/tCO₂;
 - the % of total costs, related to fuel consumption, maintenance and operation, they represent 65% of fuel costs;
 - biomass cost 6 € / MWh and 32 €/MWh, gas methane;
 - prices of recovery of electricity produced in CHP plant: 40 €/MWh;
 - specific investments for CHP plant (basic) and peak thermal installation:
- ➔ specific investment cogeneration plant biomass 1500 €/kWe;
- ➔ specific investment peak plant biomass 60 €/kWe.
- 10% discount rate;
 - number of green certificates awarded for each 1MWh electricity produced from biomass and high efficiency conditions:

→ 3 green certificates issued for electricity production based renewable energy resources;
 → plus the 4 - th green certificates granted for electricity based renewable energy resources in conditions of high efficiency.

– the value of green certificates for electricity based renewable energy resources:

→ $VCV = 28,157 \div 57,389 \text{ €/MWh}$ (choose the minimum 28€/MWh)

– number of hours per year the cogeneration plant 8400 h/year.

For analyze the effects due to changes in the selling price of electricity produced by CHP plant were considered average values estimated by OPCOM in years 2010 - 2011, 36 and 52 [€/MWh].

Following the application of the mathematical model, figures 1...3 are presented the effect of changes the sale price of electricity corresponding to the three climatic zones of Romania.

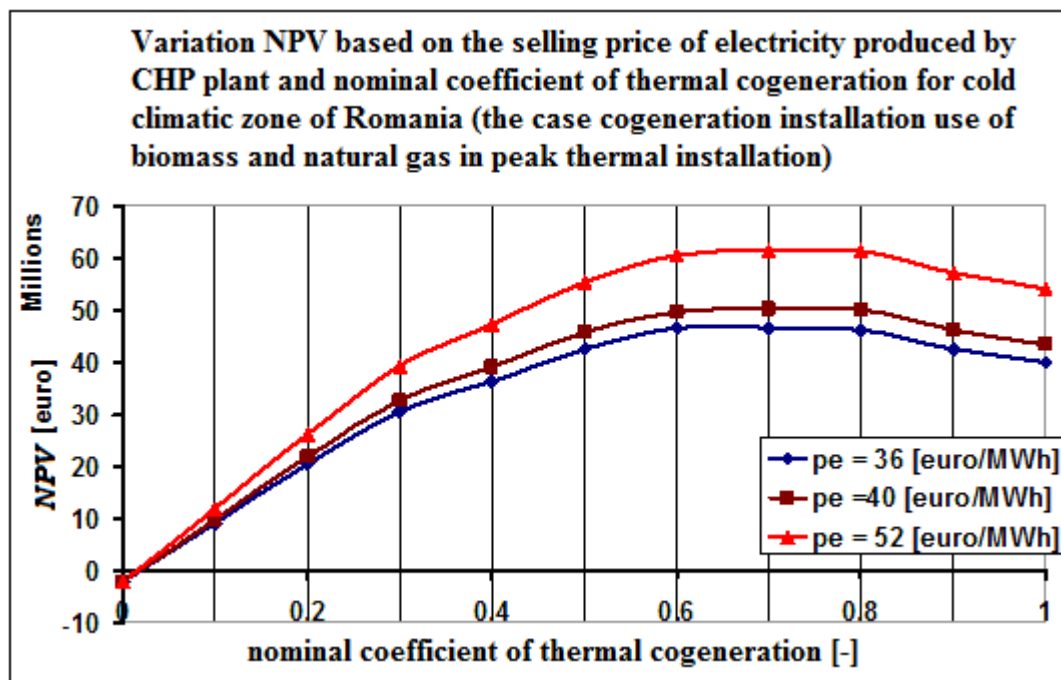


Figure 1. Variation NPV based on the selling price of electricity produced by CHP plant and nominal coefficient of thermal cogeneration for cold climatic zone of Romania
 (the case cogeneration installation use of biomass and natural gas in peak thermal installation)

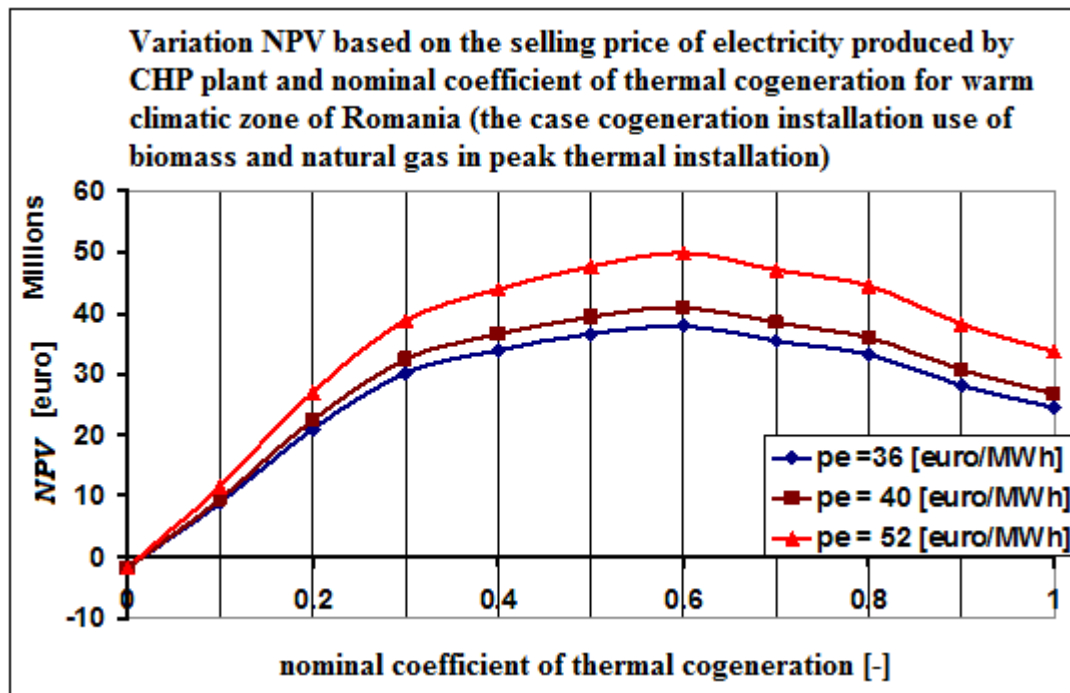


Figure 2. Variation NPV based on the selling price of electricity produced by CHP plant and nominal coefficient of thermal cogeneration for warm climatic zone of Romania (the case cogeneration installation use of biomass and natural gas in peak thermal installation)

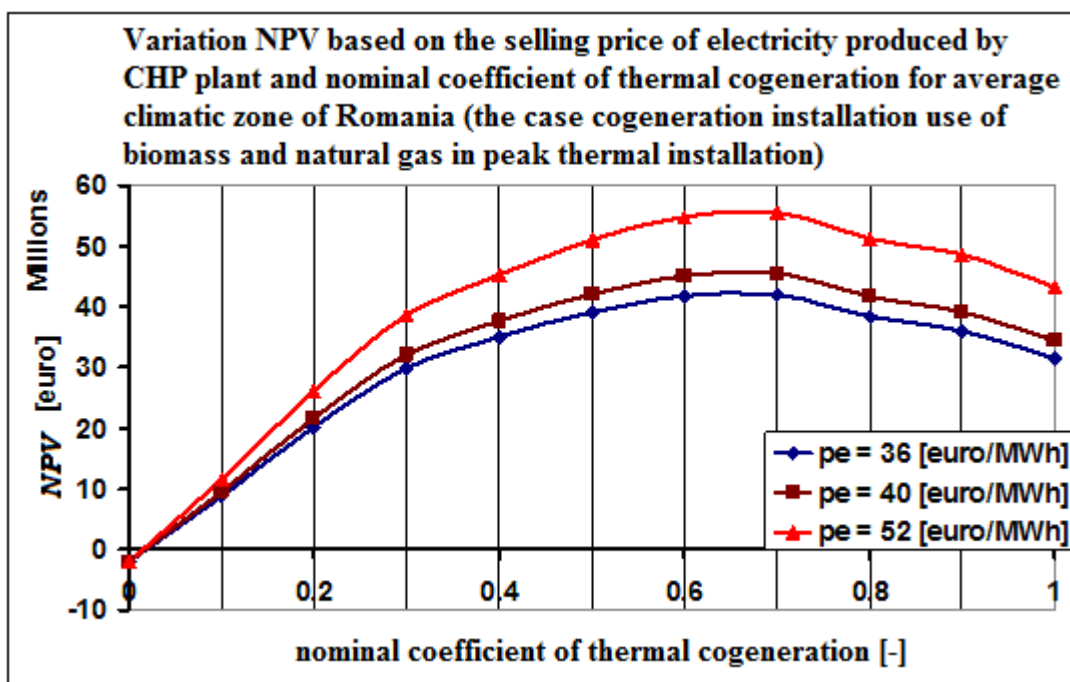


Figure 3. Variation NPV based on the selling price of electricity produced by CHP plant and nominal coefficient of thermal cogeneration for average climatic zone of Romania (the case cogeneration installation use of biomass and natural gas in peak thermal installation)

3. CONCLUSIONS

To the increase the sale price of electricity from 36 €/MWh to 52 €/MWh, corresponding to each climatic zone remains constant - see figures 1...3, except the cold

climate of Romania, which rises from 0.7 to 0.8 in the range considered. Effect of climate zone considered highlights the increasing shift from warm to cold areas of the country, the decrease in the transition from the warmer areas of the country average.

Also, the range considered the NPV increases by about 72-75%, for each climatic zone of Romania.

REFERENCES

- [1] <http://www.casamea.ro/casa/constructii/specialisti/centralele-de-incalzire-pe-biomasa-5785>
- [2] V. Athanasovici, I.S. Dumitrescu, R. Pătrașcu, I. Bitir, E. Minciuc, *Tratat de inginerie termică –Alimentări cu căldură, cogenerare*, Editura Agir, 2010, București
- [3] V. Athanasovici, C. Coman, *Cererea de căldură, factor determinant pentru soluția de alimentare cu căldură a orașelor*, Energetica, nr. 3, 2010, pag. 123 – 128
- [4] P. Voicu, V. Athanasovici, *Efectele modificării costului biomasei, respectiv a prețului de vânzare a energiei electrice asupra dimensionării optime a centralelor de cogenerare*, A XXXIXa Conferință anuală de termoeenergetică și termoficare din România, 28 -30 noiembrie 2012
- [5] Paula Voicu, Teză de doctorat, *Contribuții privind utilizarea resurselor de energie regenerabilă de tip biomasă în vederea alimentării cu căldură*, București, 2012

ANALYSIS OF ENERGY EFFICIENCY IMPROVEMENT OF GREENHOUSES BY FUELL SWITCHING

Pencho Zlatev¹, Zhivko Kolev¹, Veselka Kamburova², Ilia Iliev¹, Valentin Bobilov¹, Georgi Genchev¹, Plamen Mushakov¹
University of Ruse

ABSTRACT

This article provides an analysis of the increase in energy efficiency of a greenhouse through fuel switching. The peak heating load of the greenhouse and its change during the year has been evaluated. The consumption of energy in subsystems have been analysed and the measures needed to improve energy efficiency have been identified. It is proposed that the use of CHP provides the basic heat load and sufficiency of electricity. The capacity of the reduced harmful emissions as a result of the introduction of CHP and end benefits of changing fuel base has been estimated.

1. INTRODUCTION

The purpose of the work is analysis of realized option for improving the energy efficiency of greenhouses by switching the heavy and light fuel oils, which are used for the boilers, with natural gas, reconstruction of boiler rooms and implementation of combined heat/power production /CHP/.

For this purpose it is necessary to analyse the energy consumption and the possible measures that would increase energy efficiency. It is also necessary to know the nature of the load variation during the year, so that replacement of the fuel base and associated equipment can lead to increased energy efficiency. It was found that the basic cost of energy is for heating and electricity, making the appropriate introduction of CHP covers basic load and modernization of the boiler rooms to cover the remaining peak load. Furthermore, excess electricity can be sold at preferential prices, providing additional revenue.

2. METHODOLOGY

2.1. Analysis of heat losses from the greenhouses

The greenhouses consist of four blocks of 30dca each, made of glass with steel supporting construction. Calculation of the peak load of greenhouses can be estimated according to the following simplified equation [4]:

$$Q = K.F.(t_i - t_a)\eta_{inf}, kW \quad (1)$$

where: Q is peak heating load of greenhouses, kW;

F - total area of glass cover, dca;

t_i – average temperature inside the greenhouse, usually 16 °C;

t_a – outside temperature, °C (the design temperature for the region of Kresna, which is in 9 climatic zone of Bulgaria is -13°C[1]);

η_{inf} – infiltration losses.

The losses from infiltration have been calculated by the next equation [4]:

$$\eta_{inf} = (1 + \alpha(\rho_a - \rho_i)) \quad (2)$$

¹ Department of Thermotechnics, Hydraulics and Ecology, University of Ruse, “Studentska” St., 7017 Ruse, Bulgaria, +359 82 888 303, pzlatev@uni-ruse.bg

² University of Ruse - Branch Razgrad, “Aprilsko Vastanie” St, 7200 Razgrad, Bulgaria, +359 02 9880 052, veselkakamburova@dir.bg

where: α is factor taking into account the additional losses from infiltration of greenhouses covered with glass and its value is $\alpha=1$ [4];
 ρ_a – the density of outside air for design temperature, kg/m^3 ;
 ρ_i – the density of air inside the greenhouse, kg/m^3 .

Applying equations (1) and (2) the peak heat load of greenhouses has been defined, which amounts to 25.3MW. It has been assumed that the seasonal efficiency of boilers providing heat is 85% and the losses in transporting heat from boiler rooms to greenhouses will not exceed 3% of the total load. The final peak load for heating the greenhouses considering the efficiency of the combustion process and losses has been estimated at 30,68 MW.

Existing boilers consist of two cascades with a total output of 30 MW, which fully coincides with the designated peak heat load of greenhouses. The heat balance of the greenhouses has been done for the night mode of operation [4]. Processes of heat and mass transfer have been adopted for steady temperature regime because the temperature in distribution systems is changing very slowly. Using existing climate data for the nearest location "Sandanski" [1] an analysis of the heat losses from the greenhouses by months has been done. The obtained results are shown in Figure 1.

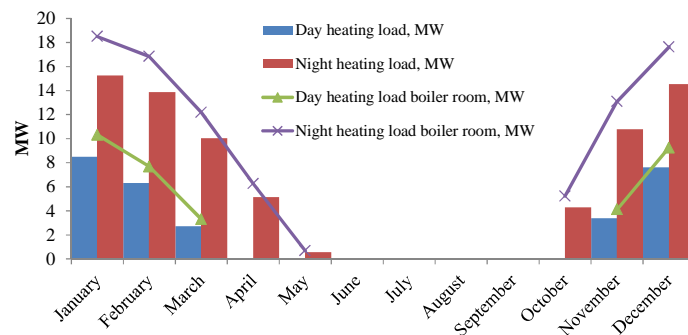


Figure 1: Average day and night heating load of greenhouses

The data in Figure 1 show that during the main season from January to April and from October to December the constant heat load does not exceed 2MW. The maximum heat load for the greenhouse can be expected only when outdoor temperatures are lower than -7°C , which typically occurs in 2 to 3 weeks of the entire heating period.

2.2. Analysis of energy consumption by subsystems

The greenhouses consume electricity, heavy and light fuel oil and water.

It uses electricity mainly for irrigation pumps, for technical equipment, for the boiler rooms and for lighting. The annual electricity consumption of the greenhouse is 438.4 MWh.

The heavy fuel oil has been consumed by the boilers situated in two boiler rooms. Four water heating boilers of type VM 3.5, with heating capacity 3.5MW each, have been installed in the first boiler room and four water heating boilers type VM4, with heating capacity 4MW each, have been installed in the second boiler room. The light fuel oil has been used for transport and as a supplementary fuel for the boilers.

The water has been used for technological needs, especially for irrigation, for the boiler rooms and for everyday needs and it has been supplied from own source.

The total yearly consumption of energy carriers and cost are presented in Table 1.

Table 1 Energy consumption and cost by subsystems

Type of Energy Carrier	Annual Consumption	Annual cost, EUR
Electricity	438.4 MWh	17 076
Heavy fuel oil	1,755 tons	517 752
Light fuel oil	93 tons	63 101
Water	36,800 m^3	141

2.1. Identification of energy efficiency measures in the greenhouses

The subsystem for distribution and consumption of thermal energy in the greenhouses includes the following elements and groups: heavy fuel oil storage facility, two hot water heating boiler rooms and greenhouses' heating systems. The heavy fuel oil storage consists of three fuel tanks with working volume of 1050m³ each. The light fuel storage consists of two tanks with working volume of 4.5m³ each. The total volume of heavy and light fuel tanks is 3159m³. For heating of heavy fuel two groups of electrical heaters with power capacity of 72kW each have been used. Also in the boiler rooms there are: three circulation water pumps with power capacity of 22 kW per unit and two circulation pumps with power capacity of 30 kW; four fans with installed power capacity of 4 kW per unit, a circulation heavy fuel oil pump with capacity of 2 kW and a recirculation heavy fuel oil pump with capacity of 1 kW.

The technical and operational conditions of the installed water boilers are not satisfactory. They operate with efficiency in the range of 80.0%÷81.0% and the temperature of the exhausted gases is very high in the range of 210÷220 °C. The working hours of the boilers in the first boiler room are 2,670 calculated per boiler and 1,503 working hours for the boilers in the second boiler room, calculated per boiler.

As it is seen from Table 1 the energy costs represent a major part of all production costs.

The existing hot water heating boilers and their heavy fuel oil burners are not effective and this leads to great greenhouse emissions and heat losses.

The usage of two types of liquid fuels requires two separate storage and fuel transporting systems.

To improve the energy consumption of greenhouses switching of fuel base and installation of co-generator have been implemented.

The switching of fuel base includes the following: external gas line construction and connection to the main gas transmission line of Bulgaria; building of internal gas network with automatic gas control station. The gas pipe lines have been installed underground. The automatic gas control station reduces the natural gas pressure from 5.5 MPa to 0.4 MPa. The internal gas network consists of: connection pipe lines between the automatic gas control station and the burning systems of the co-generator and the boilers. The internal gas network has working with pressure of 0.4 bars.

The implementation of combined heat/power /CHP/ production includes:

- Delivery and construction of co-generator type JMS 612 GS - N.LC Container;
- Delivery and construction of a transformer;
- Connection to the power system network;
- Reconstruction of two forecastles;
- Connection between the CHP and the first boiler room.

The gas co-generation module consists of an engine and a generator. The installed power capacity of the CHP is 1.850 MW. The AC voltage is 0.4 kV and the current frequency is 50 Hz. The connection to the power system network has been realized by means of a transformer.

The heating unit of the CHP includes waste-heating section. The appropriate heating capacity of the CHP including the waste-heating section is 1.99 MW which cover constant heating load during the whole season according to the recommendations in [2, 3]. The temperature of the outlet hot water is 90°C. In April the CHP covers only heating load during the night and for that reason one of the fuel tanks for heavy fuel is used as water heat storage during the day.

The reconstruction of two water heating boiler rooms includes:

- Delivery of two VIESSMANN boiler stations;
- Reconstruction of boiler rooms.

Each of VIESSMANN boiler stations consists of three water heating boilers. Two of the boilers have been equipped with combined gas – heavy oil burner type Weishaupt and the

third one has been equipped with gas burner of the same type. Each of the boilers has heating capacity of 4.89 MW and heating efficiency of 92 %. The power capacity of the burner motor is 13.5 kW. Each of the boiler rooms has been equipped with eight circulation pumps. The single power capacity is 11 kW. Two gas safety fans with power capacity of 2 kW have been installed in each boiler room.

2.2. Pre assessment of overall emissions of greenhouses gases

The assessment of the overall emissions of greenhouse gasses has been done according to the guidelines for the monitoring of greenhouse gas emissions pursuant to Directive 2003/87/EC of the European Parliament and of the Council Operational Guidelines for Design Documents of Joint Implementation Projects, Volume 1, and General Guidelines Version 2.3. The total annual CO₂ emissions before implementing fuel switching are presented in table 2.

Table 2 Pre assessment of CO₂ emissions

Fuel type	Units	Value	Emission factor, tCO ₂ /MWh or tCO ₂ /TJ	Total emissions, tCO ₂
Electricity	MWh	438	0.934	409
Heavy Fuel Oil	tons	1755	77.92	5415
	TJ	69.5		
Light Fuel Oil	tons	26	70.2	82
	TJ	1.16		

As a result of the project implementation the annual heavy fuel consumption has been decreased with 1,755 tons and light fuel oil consumption has been decreased with 26 tons per year with carbon emissions reduction of 5497 tCO₂/yr.

The natural gas consumption has been increased with 3 284 000 Nm³/year which leads to increase of carbon emissions with 6086 tCO₂/yr.

The total electricity savings including electricity sold to National Electrical Company /NEC/ is 11,695 MWh/yr. As result of the implementation of CHP the carbon emissions have been reduced with 10 409 tCO₂/yr.

The overall carbon reduction is 9819 tCO₂/yr.

3. CONCLUSIONS

As a result of the fuel switching and implementation of CHP cost savings of 30% has been achieved. Basically savings have been achieved by the commissioning of the CHP - approximately 20% and 10% as a result of the replacement of the heavy fuel oil with natural gas.

The gasification of the boiler rooms leads to significant reduction of the energy costs and the air pollution from liquid fuel oils. High efficient cogeneration unit type JMS 612 GS - N.LC Container, with 1,850 kW electrical output has been installed. The electricity produced by the CHP covers fully the expected future greenhouse consumption and the excess electricity generated has been sold to the National Electricity Company at preferential price. The CHP covers 14 % of the greenhouse hot water demand, while the rest of the hot water demand has been covered by two reconstructed boiler rooms capacity and where needed to cover the peak loads by the existing boilers.

References

- [1] American Society of Heating, Refrigerating, and Air Conditioning Engineers (ASHRAE), ASHRAE Handbook, Fundamentals Volume, 1997.
- [2] Robert Beith, Small and micro combined heat and power (CHP) systems advanced design, performance, materials and applications, Woodhead Publishing Limited, 2011
- [3] Milton Meckler, Lucas B. Hyman, Sustainable On-Site CHP Systems Design, Construction, and Operations, McGraw-Hill, 2011
- [4] Геннадий Шишко, Потапов В. А., Злобин Л. Л., Отопление и вентиляция теплиц, Киев, Будивельник, 1984

RESEARCHES ON SEEDS MIXTURE MECHANICAL SEPARATION SYSTEMS ACCORDING TO THEIR SURFACE

PhD. Stu Eng Ciobanu Valeria Gabriela^{1, 2}, Prof.PhD. Eng Tudor Căsandroi²., PhD.Eng Ciupercă Radu¹, PhD.Eng Păun Anișoara¹

¹National Institute of Research – Development for Machines and Installations Designed to Agriculture and Food Industry – INMA, Bucharest

². University Politehnica of Bucharest - Faculty of Biotechnical Systems Engineering

ABSTRACT

Optimal development of the livestock sector requires the fulfillment of appropriate conditions for livestock sector, which means a sufficient quantity and an high food quality animal. Therefore, it is necessary to achieve optimal conditions for crop establishment, which includes first quality seed material.

This paper aims to address a topic related to the mechanical separation of parasite seeds, especially of dodder seeds from the seed mass of fodder plants, by identifying the morphological features of seeds on the one anther hand and structural and functional characteristics of installation.

1. INTRODUCTION

In order to increase the production of fodder plants, it is necessary to use a high-quality seed material in the sowing process, which is primarily characterized by a high purity with contents of the stray seed.

The most dangerous parasites that infest agricultural crops seeds are the dodder seeds, if in the past they attacked fodder plants (alfalfa, clover, trefoil, etc.) or technical plants (hemp), today we found it in the vegetables crops: sorghum, maize, cotton, sugar beet, potatoes and in the case of leguminous plants, seeds, dodder seeds invades the seeds of the basic culture, risking their reproduction in the crops in the coming year, the harvest being compromised.

Getting a seed material is devoid of any stray seeds is being made by using a mechanical separation particularly those dodder seed mass by morphological identification of spurious seeds and their separation. The seeds contamination is directly influenced by structural and functional characteristics of the plant. [1]

2. CURRENT DEVELOPMENT OF SEEDS SEPARATION SYSTEM

There are several types of technical equipment used for the seed separation after their surface:

1. working equipment in continuous flow, working machines and machines with mixed cycle (continuous and in charge);
2. automatic machines with programmed cycles and cars without automation at witch the dosing powder and water, mixing time, etc. shall be fixed manually;
3. machines with electromagnets drums (coils in drums) powered by direct current from rectifier and machines with magnetic drums (away) where the reels power supply has been removed and the magnetic flux is achieved with permanent magnets.

¹1. PhD. Stu Eng Ciobanu Valeria Gabriela from National Institute of Research – Development for Machines and Installations Designed to Agriculture and Food Industry – INMA, Bucharest, ROMANIA, 6 Ion Ionescu de la Brad, Blv, sector 1, Bucharest 71592, OP 18, Phone: 004021-269.32.55, e-mail :dns.gabriela@yahoo.com

The technological process of separating the seed mixture with highest degree of separation is achieved according to the seed surface quality, technological process uses the principle of electro-magnetic and permanent magnet newest.

Seeds surface can be different: smooth seeds, seeds with roughness, seeds covered with fluff.

The element through which is the difference between the status of records of seed is the force of friction, which arise between the seed and the surface on which they are located.

The principle of elimination of parasitic of dodder seed is based on the separation of grown seed and dodder seeds depending on the physical and mechanical properties.

Literature shows that size and aerodynamic properties of weeds seeds and stray plants are almost identical with the seed plants we grown, he has used the differences in relation to the seed surface, grown seed plants have a smooth surface, but the weed including dodder seeds have small cavities on their surface, roughness that can be covered through dry or wet way with iron dust gaining ferromagnetic properties of which unlike those with smooth surface will be attracted to the equipped magnets.

Iron powder is applied on the seed mixture surface and is obtained by grinding a soft iron wire or electrolytic iron waste.

By grinding soft iron powder it has plates forms which adhere much better to seeds roughness than the splinters from electrolytic iron grinding.

Iron powder size should be able to separate the dodder seeds from of cultivated plants has to be between 1-50 microns.

Iron powder magnetic permeability depends on the presence in its composition of pure Fe element or Fe_3O_4 compound

Iron oxide negatively influences the process because this separation of seeds mixture according to their surface condition has been paramagnetic and diamagnetic properties and iron oxide (FeO) in isolation do not possess magnetic properties.

Seeds and impurities that have joined iron powder particles are retained in the magnetic field of magnetic, electromagnetic or that separate them from the seed.

Burning powder at the surface depends on the structure of the seed surface and the composition and smoothness of iron powder:

- the surface porosity and roughness are more pronounced it will stick more iron powder;
- powder high fineness helps to better coverage of the seeds. [3]

Data concerning roughness of cultural plants seeds and weeds outlined in table 1 shows that the weeds that are found in the cultures shown almost entirely were roughness, while cultural seeds are smooth, thus favoring the application of magnetic separation method, the method consists in the use of the technical properties of the seed to cover with different amounts of iron filings. Coverage depends on the condition of the seed surface, smooth seeds, which are characterized by a porous coating, cover with a layer of filings, thus gaining properties of ferromagnetic bodies.

Table 1 Roughness of cultural plant seed and weed

Crop seeds	Percentage of smooth seeds	Percentage rough seed	Weeds	Percentage of smooth seeds	Percentage rough seed
Clover	73-93	1-5	Dense buckwheat	-	96
Alfalfa	91	1	Corn	-	98
Sparceta	93	2	Tares	0,2	92
In	93	5	Pigeon crop	-	94
			Dodder	-	100
			Ryegrass	-	100

Magnetic separation method of the seeds mixture after their surface condition is applied to the dodder seed cleaning cultural plant, which cannot be completely separated by common methods [4]

The degree of iron powder adherence is the maximum of dodder and ryegrass seeds, flax does not cover at all, and clovers with her disabled under tab 2:

Table 2: Grip degrees of iron powder

Iron powder	Adherence				
	Clover	Dodder	Pigeon crop	In	Ryegrass
Trifolin extra	0,095	7,751	0	0,0	1,248
Trifolin 808	0,088	5,029	0,91	0,0	1,359
Trifolin A VISHOM	0,205	5,242	1,562	0,0	0,690
Trifolin VISHOM nr. 8	-	6,576	1,678	0,0	6,275

Determination of seed, water and iron powder in the mixture needed for magnetic separation is performed differently depending on the type and manufacturer of the machine.

Many types of mechanical systems for the separation of seed mixtures according to their surface condition are used, of which I enumerate the most representative name:

Petkus K 590 in Figure. 1 and Figure. 2 shows a continuous flow system, water and iron powder is permanent mixed using a mixer which is composed of two snails with alternating left-right turn to increase mixing time. A screw conveyor inclined leads the mixture on the vibrating table, eliminating the storage and dosage. Water dispenser and iron powder have a complicated construction. [7]

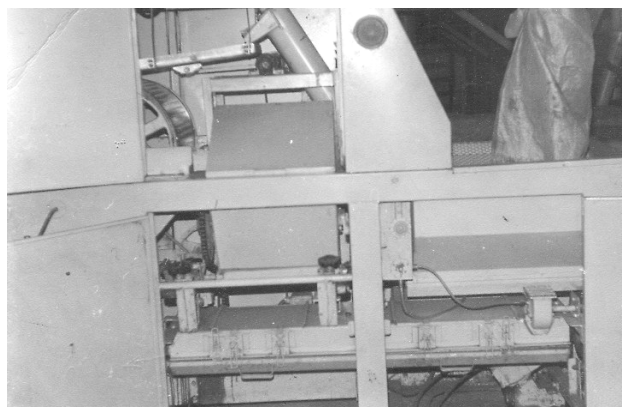


Figure 1: Petkus K 590 Machine

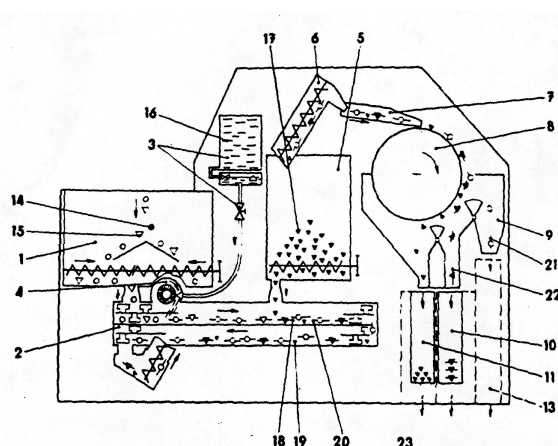


Figure 2: Technological scheme of Petkus K 590

1. Seed feeding tank with seeds
2. Mixer
3. Dampening unit

7. Vibrating table
8. magnetic drum
9. collecting tanks A

14. Vase with agitator worm gear
15. Inclined plane double
16. Water

- | | | |
|----------------------|------------------------|--------------------------------|
| 4. Humidifier | 10. collecting tanks B | 17. Powdered |
| 5. Iron powder dozer | 11. collecting tanks C | 18. Moistened seed with powder |
| 6. Helical conveyer | 13. Exhaust sort A | 19. Excess powdered |
| 20. Mixer | 21. Sort A | 22. Sort B |
| 23. Sort C. | | |

Machine for dodder seeds removing MDS represented in Figure 3 is a prototype designed and built by INMA Bucharest in 1994, addressed to small farmers. Operation in continuous flow and gravitational seeds and water dosage have greatly simplified kinematics. The mixer is also built on the principle of alternative worm turns left and right. Powder dispenser is operated mechanically and has a simple construction, which allowed calibration within the required limits of technology. Modest yield of 200 kg / h and the lack of rotating brushes were among the few shortcomings of the car. [7]



Figure 3: Machine MDS right side view

Machine for dodder seeds removing MD – 400 represented in Figure 5 and Figure 6 is equipped with magnetic ferrite drums, is designed to pick out the seeds of perennial fodder vegetables, flax, hemp, carrots, onion, chive, spinach, tomatoes, etc., for removing the dodder seeds, a parasite quarantine plant.

The machine is composed of a front frame that supports the selecting system endowed with magnetic drums and the electrical panel and a rear frame on which are fitted the mixer with the dampening unit and the powder dozer, the seed feeding tank and the helical conveyer.

The mixer has two parallel augers with adjustable paddles. On the mixer cover are mounted the seed dozer, the dampening unit and the iron powder dozer.

The selecting system with magnetic drums consists of a helical conveyer, two vibrating tables, two magnetic drums and the fractions collecting tanks. [2]



Figure 5: MD – 400 Machine

The machine for dodder seeds removing is designed to processing units and three - leaved seed selection.

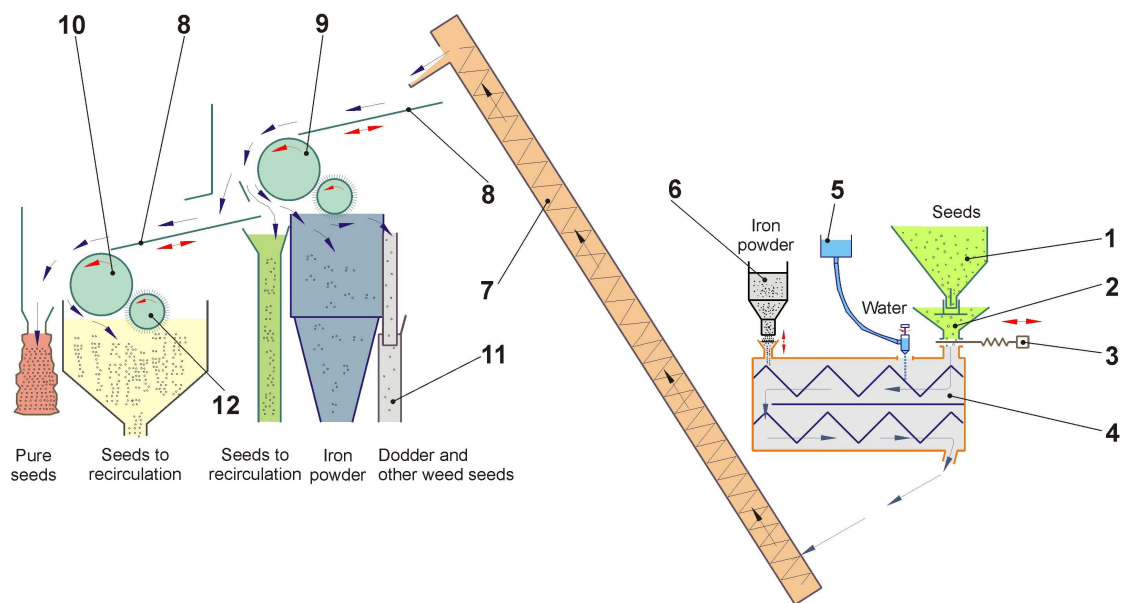


Figure 6: Technological scheme

- | | |
|----------------------|--------------------------------|
| 1. Seed feeding tank | 7. Helical conveyor |
| 2. Seed dozer | 8. Vibrating table |
| 3. Adjusting device | 9. Upper magnetic drum |
| 4. Mixer | 10. Lower magnetic drum |
| 5. Dampening unit | 11. Fractions collecting tanks |
| 6. Iron powder dozer | 12. Drum cleaning brushes |

3. CONCLUSIONS

After analyzing the constructive solutions of mechanical systems for the separation of the mixture of seeds after their area's status posed above could draw the following conclusions:

- The Petkus K 590 Machine has a certain magnetic drum with ferrite and select 3 varieties. The disadvantage of choosing a single drum, requiring multiple passes which means time and the advantage result from current economy.
- The MDS Machine is equipped with two magnetic drums with ferrite and 3 selected varieties and the operation results were better than those of Petkus K 590' machine.
- MD 400 machine is designed with 2 magnetic drums with ferrite and separate 5 varieties with 2 vibrating tables, the process is faster with iron powder and energy consumption less compared to other mechanical systems for the separation of the seeds mixture after their surface condition above.

By applying these technologies improving the technical and economic parameters of magnetic seed selection and their alignment to the performance requirements and compliance with the rules for protection of fodder crops existing at European level.

References

- [1] D. Hălălău, M., N., *Dodder of R.S. Romania and combat them*, Bucharest, 1980.
- [2] Ianati, N. *Tips on combating dodder*. Rev. Agricole Publishing House, Bucharest.
- [3] Fader Tudor . *Studies and researches concerning the separation of dodder of onion and carrot seed*, Bucharest, 1989.
- [4] M.N. Letosnev - *Agricultural Machines*, State Agro-silvică Publishing House, Bucharest, 1959.
- [5] Flora R.S.R. vol.XIII, Academy Publishing House R.S. Romania, Bucharest.
- [6] I.G. Voronov, I. E. Kojuhovsji (ș.a.). *Cleaning and sorting seeds*, State Agro-silvică Publishing House, Bucharest, 1955.
- [7] Brochures, catalogs, and web pages in the field.

IRON-BASED MAGNETIC HYBRID NANOPARTICLES FOR HIGH EFFICIENT REMOVAL OF HEAVY METALS FROM WASTEWATER

Cristina Ileana Covaliu^{*}, Sorin- Ștefan Biriș, Gigel Paraschiv, Gheorghe Voicu
Univeristy Politehica of Bucharest, Faculty of Biotechnical Systems Engineering, 313 Splaiul
Independentei Street, Bucuresti, 060042, Romania
cristina_covaliu@yahoo.com

ABSTRACT

Iron-based magnetic hybrid nanoparticles as novel adsorbent is expected to offer an attractive and inexpensive option for the removal of heavy metals by considering its simple obtaining method, high surface area value and special magnetic properties. Pb(II) and Cd(II) ions were chosen as the metal adsorbates because they commonly exist in the effluents of plating factories, electrolytic refining plants and acid mining industries. Thus, the purposes of this study are: to assess the performances of a magnetite nanoparticle and its polymeric nanohybrids for the selective removal of these heavy metals, to achieve the regeneration of all prepared magnetic adsorbents nanoparticles for reuse and to study the mechanisms of metal adsorption onto nanoscale prepared materials.

1. INTRODUCTION

Heavy metals from different types of waters have become a serious threaten for environment and health. Even if the high concentrations of dissolved metals have to be reduced according to legislative standards, the effluents discharged from different industrial processes must be removed by advanced treatment techniques in order to respect the legislation [1]. Adsorption represents one of the most efficient technologies for reducing concentration of heavy metals by using different types of adsorbent [2]. Recently, adsorption activities of nanoparticles for many heavy metal ions have been reported in the literature [3,4]. The iron oxides are most used nanoparticles for this purpose. For example, adsorption of Cr (VI) from mono-component solutions onto magnetite nanoparticles has been published [5,6]. Also, recent studies reported favorable responses of magnetite nanoparticles for the adsorption/reduction of several toxic metal ions (e.g. Ni^{2+} , Cu^{2+} , Cd^{2+} , Zn^{2+} and Cr^{6+}) and the catalytic degradation of some organic contaminants [7,8]. This is because magnetic iron oxide nanoparticles possess not only strong adsorption capacities, but also the property of being easily separated and collected by an external magnetic field [9,10].

Due the dissolved tendency of iron from nanoparticles, especially under acidic conditions, the preparation of some coated iron nano-oxides has gained attention recently. For example, cellulose acetate supported zero-valent iron nanoparticles for the dechlorination of trichloroethylene in water highlighted the successful preparation of reactive membranes by incorporation of Fe(0) nanoparticles into cellulose acetate films [11].

In this study, magnetite nanoparticles synthesized using a sol-gel method with cheap and environmentally friendly iron salts in the presence of a soft template, coated by PEG and PVP were developed for the selective removal and recovery of heavy metals such as toxic Pb(II) and Cd(II) ions from industrial wastewater (Fig.1)

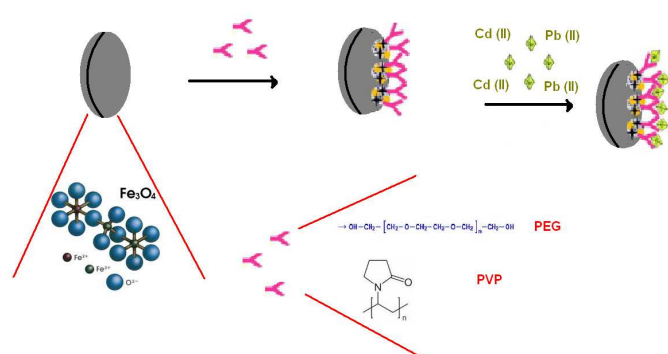


Fig.1 The scheme of nanostructured hybrids proposed for Pb(II) and Cd(II) heavy metals removal from wastewater

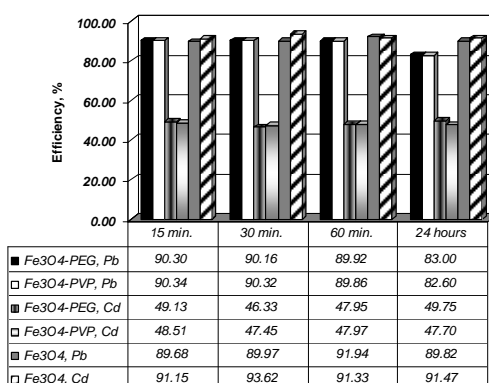


Fig. 2. The removal efficiency in time for Pb and Cd

2. METHODOLOGY

Adsorption studies were performed by mixing an amount of Fe_3O_4 , Fe_3O_4 -PEG and Fe_3O_4 -PVP respectively, with 100 mL mixed solution of Pb(II) and Cd(II), respectively at room temperature (21.5°C). All the adsorption studies were conducted at a shaking rate of 400 rpm. The adsorbent samples were recovered by magnetic separation and were analyzed by. All liquid samples containing metals were measured by AAS with a GBC 932 AB Plus spectrometer with spectral domain between 185 and 900 nm.

The effect of contact time for the adsorption of metals onto Fe_3O_4 , Fe_3O_4 -PEG and Fe_3O_4 -PVP was evaluated. The removal efficiency for Pb and Cd is shown in Fig. 1.

3. CONCLUSIONS

The removal efficiency of Pb (II) ions was higher in case of the two core-shell compounds, Fe_3O_4 -PEG and Fe_3O_4 -PVP then for magnetite nanoparticles. Regarding the Cd ions, the removal efficiency was higher for uncoated Fe_3O_4 (almost 90%) and almost 50% for the two core-shell compounds.

References

- [1] Banerjee S.S., Chen D.H. Fast removal of copper ions by gum arabic modified magnetic nano-adsorbent. *J. Hazard. Mater.* 147:792–799, 2007.
- [2] Booker N.A., Keir D., Priestley A.J., Ritchie C.B., Sudarmana D.L., Woods M.A. Sewage clarification with magnetite particles. *Water Sci. Technol.* 23: 1703–1712, 1991.
- [3] Diallo M.S., Savage N., Nanoparticles and water quality, *Journal of Nanoparticle Research*, 7:325–330, 2005.
- [4] Hu J., Chen G., Lo M.C.I., Removal and recovery of Cr (VI) from wastewater by maghemite nanoparticles. *Water Res.* 39:4528 – 4536, 2005.
- [5] Hu J., Lo I.M.C., Chen G. Removal of Cr(VI) by magnetite nanoparticle. *Water Sci. Technol.* 50:139–146, 2004.
- [6] Lo M.C.I., Hu J., Chen G., Iron-Based Magnetic Nanoparticles for Removal of Heavy Metals from Electroplating and Metal-Finishing Wastewater, In: *Nanotechnologies for Water Environment Applications*, Zhang C.T., Surampali Y.R., Lai K.C.K, Hu Z., Tyagi R.D., Lo M.C.I. (Eds.), American Society of Civil Engineers, Virginia, 213-264, (2009).
- [7] Manuel P.C., Jose M. M., Rosa T. M., Chromium removal with activated carbons, *Water Research*, 29, 2147 – 2180, 1995

ENVIRONMENTAL POLLUTION REDUCTION THROUGH FIELD CROPS SPRAYING MACHINES VERIFICATION

Cujbescu Dan¹, Bolintineanu Gheorghe¹, Nițu Mihaela¹

¹ INMA Bucharest

ABSTRACT

The periodical technical verification in UE countries members is mandatory for in exploitation plants protection machines, with the main purpose represented by environmental protection through consumption reduction of phyto-sanitary substances. The direct results of this check are represented by costs reduction for the used substances and by minimum negative influence on the environment.

The positive effects which result after plants protection machines verification are represented by an increase of personnel safety, reducing of environmental pollution with phyto-sanitary substances as well as the application of minimum quantity of substances for optimum plants protection.

The paper presents the checking method for field crop spraying machines described in SR EN 13790-1:2004, revealing the factors which could lead to a correct assessment of the wear state of the machine and the corrective measures which are imposed in case of unconformity.

1. INTRODUCTION

Basic economic branch through the social impact as well as the environment, extremely intensive agriculture practiced due to the high-technology level, has led to accentuated degradation of the environment and human life, by imposing to be introduced the concept of sustainable agriculture, in which conservation of resources is a fundamental condition, the rational use of resources ensures productivity, profitability and environmental protection.

The climatic conditions in Romania are particularly favorable for field crops, are also very favorable for the development of weeds that cause significant damage in terms of quantity and quality.

Herbicide (“herba=grass”, “cedo=to kill”) is a chemical method of weed control, plant protection from pests and diseases during all stages of cultivation of agricultural crops being a guarantee of obtaining a quality product. Applying herbicides complements other measures (agrotechnics, physics, biological) for destruction of weeds. Achieving technological operations for plant protection requires effective and performed use of technological operations.

With each year, the global market increases the diversity of spraying machines regarding the technological schemes and quality parameters, in the conditions in which is a continuous growth in requirements regarding the parameters and construction of the machine, the technological process quality, as well as reducing environmental pollution with toxic products.

2. METHODOLOGY

Herbicide machines are designed to perform a chemical treatment of field crops (dispersion of toxic liquid into fine droplets and specific quantities, transport and uniform distribution of droplets on treated surfaces) as well as plants with mineral liquid fertilizers and not only, having the following requirements:

- to require a small number of workers;
- possess a high mobility during work and to provide high security in operation;

- the apparatus and machines organs which come in contact with toxic substances must be constructed of anticorrosive materials or to have an anticorrosive protection;
- to dose the products exactly per unit treated area;
- maintaining during work the adjustments made on the installation parameters;
- to be equipped with automation and control devices during work;
- to achieve an uniformly as possible fragmentation, at a droplets density /cm² consistent with the agrotechnics requirements;
- to possess several adjustments possibilities, rigorous and can be able to perform treatments with a wide range of products in a wide variety of volumes;
- they must be lightweight, easy to handle and adjust, have a good labor protection;
- to be standardized and guaranteed for safety of use;
- to have a low manufacturing cost, in order to achieve as low depreciation;
- to allow the achievement of high productivity;
- to have a nice design, and assembly and disassembly facilities;
- to have a low energy consumption and high working efficiency.

With the EMERGENCY ORDINANCE from 29.11.2011 is established the institutional framework for achieving sustainable use of pesticides, by reducing the risks and their effects on human health the environment, including by promoting integrated pests management and of alternative approaches and techniques, such as non-chemical alternatives to pesticides.

The inspection of pesticide application equipment covers all important aspects to achieve a high level of safety and protection for human health and the environment.

The sprayer machine Servoplant P612 in basic crops is preliminary intended to perform herbicide works in field cropson medium and large surfaces, with hydraulic dispersion. Hydraulic dispersion consists in fluids passing through calibrated narrow (nozzles) holes under pressure. The dispersion is obtained due to the fact that the fluid under pressure, discharged by the pump, leaves with speed the calibrated orifice in the form of a diverge jet which rubes very strongly with air, fragmenting into droplets of increasingly smaller. One such jet is characterized by the flow, shape and angle of dispersion.

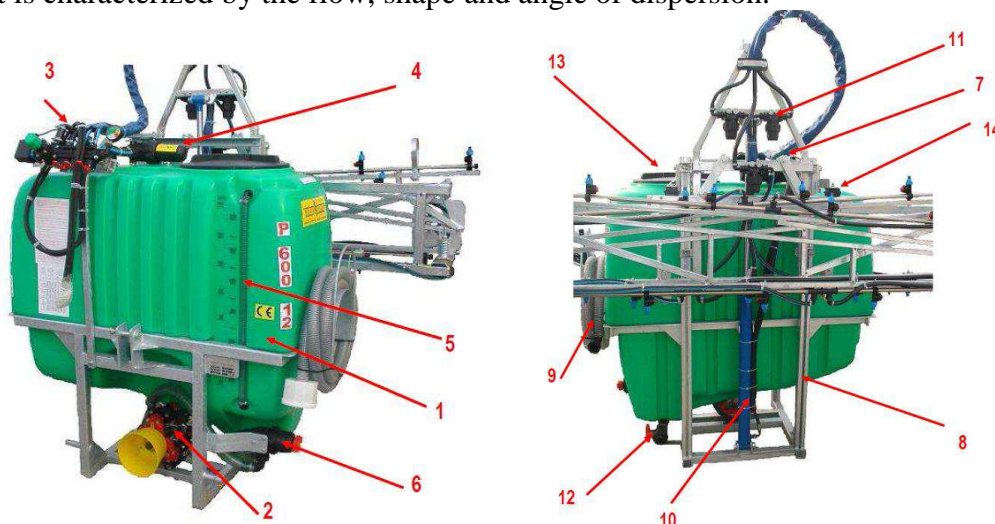


Figure 1: The sprayer machine SERVOPLANT P 612

1 - HDPE tank; 2 - pump; 3 - pressure control unit; 4 - pressure self cleaning filter; 5 - tank level indicator; 6 - suction filter with valve; 7 - boom with self leveling system; 8 - hot dip galvanized frame and boom; 9 - 5 m hose and filter for self loading; 10 - manual rising the boom with winch and rope or hydraulic; 11 - in line filter for boom ways; 12 - quick empty with ball valve; 13 - 420 mm x 254 mm lid and basket filter; 14 - automatic blocking in transport.

For the worn herbicide machine inspection Servoplant P612 in aggregate with the tractor U-650 was performed to determine the work quality indices (flow pump, pump volumetric efficiency, flow through the nozzle, transversal distribution, norm substance).

The attempts of the mechanical spray in staple crops were performed in accordance with specific testing procedure and standards in forced:

➤ SR EN 13790-1: 2004 - „Agricultural machinery. Mechanical spray. Examination of spraying machine in use. Part 1: Mechanical spray used in basic crops”.

In order to determine the quality work indices of the machine were executed the following necessary operations for preparing the product for testing:

- verifying the removable and non-removable joints to determine whether there is any cutting edges;
- verifying whether the adjusting operations are carried out easily, without blocking;
- verifying the overlapping of the telescopic rods of the cardanic transmission;
- verifying the correct installation of the nozzles;
- verifying the tightness of the hydraulic system;
- verifying the correct operation of the pressure regulator and manometer.

The environmental conditions for testing the sprayer machine in basic crops Servoplant P612 were: 50% humidity at a 15°C temperature.

In accordance with the specific testing procedure PSpl-04.01.00 in force within DI-LIMS, was utilized metrology checked equipments in the term of validity of verification: mechanical timer, roulette, centrifugal tachometer, manometer with elastic element, thermo-hygrometer, electronic hygrometer and graduated cylinder.

3. TEST RESULTS

3.1. Pump flow and volumetric efficiency of the pump

The pump flow was determined by the testing assistant using the volumetric method at an input speed of 540 rev/min. The liquid debited by the pump was captured through the hoses which leads it to the ramps for 1 minute in a bowl and measure with the capacity units from the laboratory endowment. Samples were carried out at pressures of 2, 2.5, 3, 3.5 and 4 bar.

The volumetric efficiency of the pump was determined by the testing responsible by calculating the relation:

$$\eta_v = \frac{Q_r}{Q_t} \times 100 [\%] \quad (1)$$

where:

Q_r = actual flow pump [l/min];

Q_t = theoretical flow [l/min];

$$Q_t = \frac{\pi \cdot \phi^2}{4 \cdot s \cdot n \cdot i} \quad (2)$$

where:

ϕ = pump cylinder diameter (inside) [dm];

s = piston stroke [dm];

n = pump speed [rot/min];

i = number of pump cylinder [$i = 3$].

Table 1: Pump flow and volumetric efficiency of the pump

Pressure [bar]	Pump flow [l/min]				Volumetric efficiency [%]
	R1	R2	R3	Media	
2,0	26,3	25,8	25,6	25,9	32,78
2,5	27,5	26,8	27,3	27,2	34,43
3,0	28,3	27,6	28,1	28,0	35,44
3,5	31,4	31,7	32,2	31,8	40,25
4,0	32,9	32,8	33,5	33,1	41,89

3.2. Nozzle flow

The nozzle flows ISO 11003 type were determined using the volumetric method collecting the leaked fluid within 1 minute from each nozzle, at pressure set of 2, 2.5, 3, 3.5, 4 bar.

Table 2: Flow through the nozzle 1 at pressures: 2, 2.5, 3, 3.5, 4 bar

Pressure [bar]	Number nozzle	Nozzle flow [l/min]			
		R1	R2	R3	Media
2	1	0,94	0,92	0,90	0,92
2,5	1	1,24	1,20	1,22	1,22
3	1	1,32	1,32	1,30	1,31
3,5	1	1,40	1,42	1,44	1,42
4	1	1,44	1,52	1,52	1,49

3.3. Determination of the transverse distribution uniformity of sprayer the machine in basic crops

Determination of uniform transverse distribution made on a sprayer machine in basic crops Servoplant P612 formed by a pad of 12 m (5 sections) equipped with 24 nozzles, and the metering equipment consisting of a scanner with 8 troughs , wide of 100 mm and depth of 80 mm (distance measured between the top and bottom of the gutter). The width of the scanner is 1.5 m, and the 8 cylinders are of the same type and size and have a capacity of 500 ml.

The scanner runs on rails under the sprayer ramp collecting and weighing liquid, thus covering the whole working width of the spraying machine.

The values of the measurements are sent by radio-link to a computer which processes and displays them graphically.



Figure 2: Test stand that verifies the transverse distribution
Measurements were made on the entire length of the working pressures of 2, 2.5, 3, 3.5, 4 bar, in three repetitions.

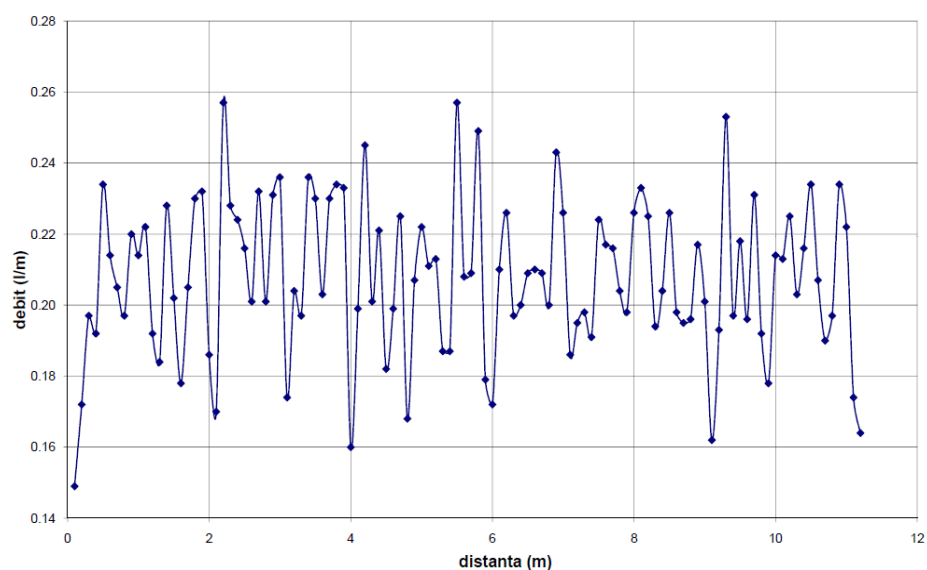


Figure 3: Transverse distribution of blue nozzle, code ISO 11003, pressure 2 bar, repetition 1

From the results, it is observed that the transverse distribution uniformity in crop sprayer base falls within $\pm 20\%$ required by EN 13790-1: 2004.

3.4. Substance rules

The substance rules was calculated by the testing assistant based on the flow testing substance, working width and the travel speed using the formula:

$$N = 60 \cdot \frac{q}{0,1 \cdot L \cdot V} \text{ [l/ha]} \quad (3)$$

where:

N = substance norm [l/ha];

q = substance flow [l/min];

L = working width of the machine [m];

V = working speed of the machine [km/h].

Table 3: Substance norms

Nozzle code	Pressure [bar]	Nozzle flow [l/min]	Speed [km/h]				
			6	8	10	12	16
			Norm [l/ha]				
103 Blue ISO 11003	2,0	1,04	208	156	124,8	104	78
	2,5	1,13	226	169,5	135,6	113	84,7
	3,0	1,20	240	180	144	120	90
	3,5	1,30	260	195	156	130	97,5

	4,0	1,38	276	207	165,6	138	103,5
--	-----	------	-----	-----	-------	-----	-------

4. Conclusions

The examination of the sprayer machine is made having regarded:

- the operator conducting the test safety;
- less potential risk of environmental contamination by crop protection products;
- good control of the pest with the minimum possible input of crop protection product.

References

- [1]. Bolintineanu Gh., Mihai M., Matache M., ș.a. - Reducerea poluării mediului / solului și creșterea indicilor calitativi de lucru ai echipamentelor tehnice pentru protecția plantelor, prin integrarea unui sistem centralizat de monitorizare și avertizare a acestora - Studiu tehnologic privind reglementările interne și internaționale referitoare la protecția mediului, Raport de cercetare, București, 2009.
- [2]. Bolintineanu Gh., Mihai M., Matache M., ș.a. - Reducerea poluării mediului / solului și creșterea indicilor calitativi de lucru ai echipamentelor tehnice pentru protecția plantelor, prin integrarea unui sistem centralizat de monitorizare și avertizare a acestora - Proiectarea modelului experimental și a sistemului centralizat de monitorizare și avertizare, Raport de cercetare, București, 2009;
- [3]. Bolintineanu Gh., Mihai M., Matache M., ș.a. - Reducerea poluării mediului / solului și creșterea indicilor calitativi de lucru ai echipamentelor tehnice pentru protecția plantelor, prin integrarea unui sistem centralizat de monitorizare și avertizare a acestora - Realizare model experimental, Raport de cercetare, București, 2009;
- [4]. http://cursuri-imapa.ucoz.ro/_ld/0/3_Curs_Agrotehnic.pdf
- [5]. <http://www.aitt.md/news/ma%C5%9Fini-de-stropit-cu-intensitate-energetic%C4%83-sporit%C4%83>
- [6]. <http://www.munax.ro/alte-articole/utilaje-de-erbicidat>
- [7]. <http://www.agricultor.ro/article/37762/Masini-de-erbicidat/0/4>
- [8]. <http://www.madr.ro/pages/152/oug-utilizare-pesticide-in-romania.pdf>

BIOGAS, A MODERN RENEWABLE ENERGY IN THE EUROPEAN CONTEXT

DILEA Mirela, PARASCHIV Gigel, UNGUREANU Nicoleta, VOICU Gheorghe,
BIRIS Sorin-Ştefan, IONESCU Mariana

University POLITEHNICA of Bucharest, Department of BIOTECHNICAL SYSTEMS

ABSTRACT

One of the main environmental problems of today's society is the continuously increasing production of organic waste. Biogas technology is widely used in Europe since several decades and is a highly developed technology. Biogas installations processing agricultural substrates are some of the most important applications of anaerobic digestion today.

In the present paper there are presented examples of biogas plants, anaerobic digesters and biogas storage tanks widely used in Europe.

1. INTRODUCTION

In Europe and worldwide production and use of biogas has increased considerably as a result of increasing demand for renewable energy as a substitute for fossil energy. Most agricultural and industrial biogas plants in Europe use biogas to produce electricity in cogeneration plants (CHP – Combined Heat and Power). Today there are over 8,500 biogas plants in Europe.

The interest in biogas has further increased today due to global efforts of displacing the fossil fuels used for energy production and the necessity of finding environmentally sustainable solutions for the treatment and recycling of animal manure and organic wastes.

To date, biogas is the only technologically fully established renewable energy source that is capable of producing heat, steam, electricity and vehicle fuel. It is, in the true sense of the word, a versatile energy source [1].

Production of biogas through anaerobic digestion of animal manure as well as of a wide range of digestible organic wastes, converts these substrates into renewable energy and offers a natural fertilizer for agriculture [2, 3].

Biomethane (biogas) is an alternative and renewable energy source produced through the anaerobic (oxygen free) digestion of organic matter whereby the organic matter is converted into a combustible biogas rich in methane (CH₄) and a liquid effluent. Anaerobic digesters have been used successfully in municipal and industrial wastewater treatment plants and on a number of livestock farms for many years [4].

The composition of the biogas is an important characteristic affecting the biogas combustion in the cogeneration unit and, therefore, the composition and temperature of the flue gas evacuated. This affects the quantity and quality of heat which can be used in a concept of thermal energy. Furthermore, the concept of the biogas plant is characterized by the temperature in digesters, which are usually heated to a part of the heat from the cogeneration unit in order to allow the bacteria a rapid decomposition of material [5].

In line with the other biofuels, biogas from anaerobic digestion is an important priority of the European transport and energy policy, as a cheap and CO₂-neutral source of renewable energy, which offers the possibility of treating and recycling a wide range of agricultural residues and byproducts, in a sustainable and environmentally friendly way.

A wide range of biomass types can be used as substrates (feedstock) for the production of biogas from anaerobic digestion. The most common biomass categories used in European biogas production are:

- Animal manure and slurry
- Agricultural residues and by-products
- Digestible organic wastes from food and agro industries (vegetable and animal origin)
- Organic fraction of municipal waste and from catering (vegetable and animal origin)
- Sewage sludge
- Dedicated energy crops (e.g. maize, miscanthus, sorghum, clover).

In the present paper there are presented the construction, operation and main components of biogas plants. Also, will be given representative examples of biogas plants used in European countries.

2. REPRESENTATIVE EXAMPLES OF BIOGAS PLANTS USED IN EUROPEAN STATES

Biogas installations processing agricultural substrates are some of the most important applications of anaerobic digestion today. Thousands of agricultural biogas plants are in operation in Europe and North America [1].

A biogas plant is a complex installation, consisting of a variety of elements. Depending on the type, size and operational conditions of each biogas plant, various technologies for conditioning, storage and utilisation of biogas are possible to implement [2].

The biogas plants have a common principle layout: manure is collected in a pre-storage tank, close to the digester and pumped into the digester, which is a gas-tight tank, made of steel or concrete, insulated to maintain a constant process temperature. Digesters can be or vertical, usually with stirring systems, responsible for mixing and homogenising the substrate, and minimising risks of swimming-layers and sediment formation or horizontal.

Apart from the digester, equipped with stirring system, the plant can include pre-storage for fresh biomass, storage for digested biomass and for biogas, and even a CHP unit [2].

Further, there is presented a representative examples of a farm biogas plant, with horizontal digester of steel [6].

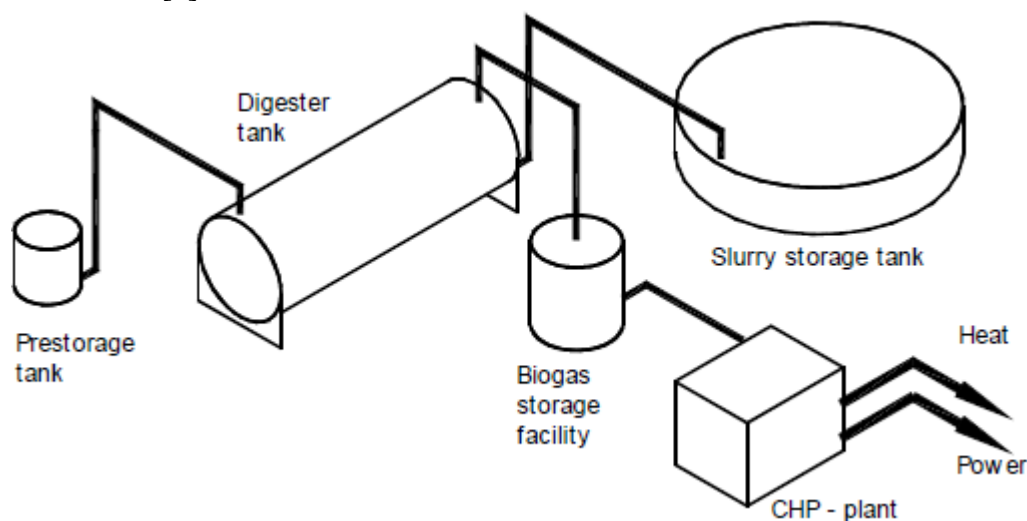


Figure 1: Schematic representation of a farm biogas plant, with horizontal digester [6]



Figure 2: Biogas plant for biomass and animal manure (Austria, 2004) [7]

Figure 3 shows the Denmark's largest biogas plant, located in Lemvig which started production in 1992. The plant processes yearly about 226,000 tons of biomass, consisting of 183,000 tons of annual manure and slurries and 43,000 tons suitable industrial waste (maximum 25 % of the total feedstock mixture).

The produced biogas is converted into electricity and heat by the CHP-unit of the biogas plant. In 2013, an additional new Caterpillar biogas-engine (1560 kW-el) was installed. More than 21 million kWh of electricity is generated every year and sold to the local grid. The surplus heat from the gas engine cooling system exceeds 18 million kWh per year and is sold for distributed to more than 1000 households in the area [8].



Figure 3: Example of co-digestion plant built in Denmark [8]

Many European countries have established favorable conditions for electricity production from biogas. Germany has a leading role in Europe with almost 4000 biogas plants, most of them on farms for cogeneration [9].

In Europe, other than market leader Germany, Sweden, Italy, Denmark and Poland have announced plans to increase their biogas markets substantially. Plans in Denmark include the construction of what will be the world's largest biogas facility [10].



Figure 4: Biogas plant south of Hanover, Germany [10]

In Romania the biogas sector is in an early stage of development. Romania is a country with many areas appropriate for biogas production. Bihor county is just an example, with 12 areas where people can get rid of harmful waste, and receive instead heat, electricity, bio fertilizer and a clean environment. The first bioethanol and biogas plant in Romania will be built and completed until 2013, in Remetea, Harghita. The plant will produce ethanol using agricultural products in the area, and the resulting pulp will produce biogas [11].

The core of a biogas plant is the digester - an air proof reactor tank, where the decomposition of feedstock takes place, in absence of oxygen, and where biogas is produced. Common characteristics of all digesters, apart from being air proof, are that they have a system of feedstock feed-in as well as systems of biogas and digestate output. In European climates anaerobic digesters have to be insulated and heated. There are a various types of biogas digesters, operating in Europe and around the world [2].



Figure 5: Vertical digesters built in Germany

Horizontal digesters have a horizontal axis and a cylindrical shape. This type of digesters are usually manufactured and transported to the biogas plant site in one piece, so they are limited in size and volume.



Figure 6: Horizontal digester, built in Denmark

The biogas is usually used soon after generation without storage, but there are situations in which the gas must be stored. Various types of biogas storage facilities are available today. The simplest solution is the biogas storage established on top of digesters, using a gas tight membrane, which has also the function of digester cover. For larger biogas plants, separate biogas storage facilities are established, either as stand-alone facility or included in storage buildings. The biogas storage facilities can be operated at low, medium or high pressure [2].

Figure 6 presents gas storage tanks with double membrane. Double membrane storage tanks are composed of an external membrane, which forms the outer shape of the tank, and an inner membrane, which is the actual space for biogas. Continuously, pressurized air is supplied in the space between the two membranes, in order to apply a constant pressure on the inner membrane (this ensures the pumping of biogas into the outlet pipe at constant pressure and volume) and to withstand external loads (given by snow and wind) [12].

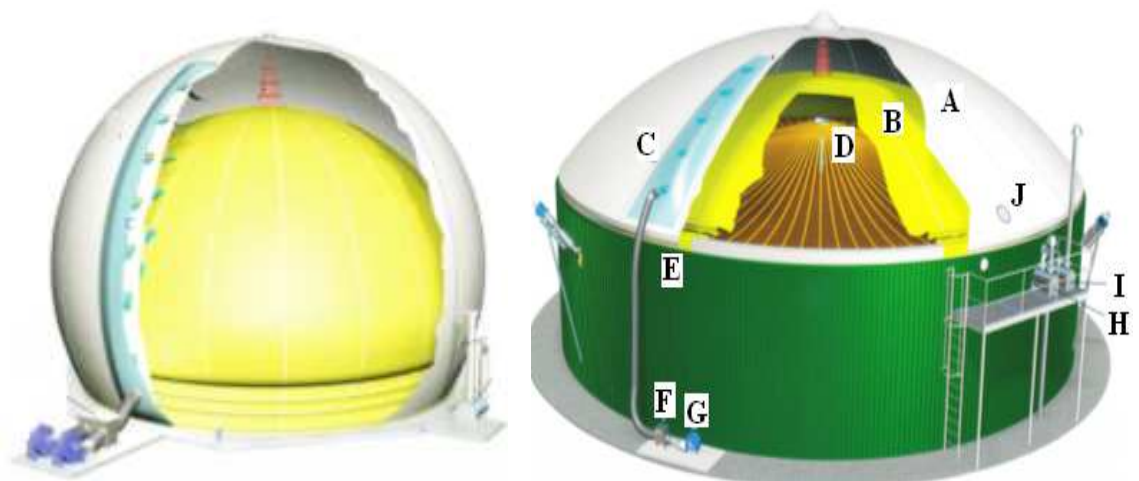


Figure 6: Gas storage tank with double membrane

A – external membrane; B – internal membrane; C – air flow system; D – rope system;
E – anchor ring; F – non return valve; G – blower; H – low pressure valve; I – excess pressure
valve; J – inspection window

3. CONCLUSIONS

Biogas technology is recognized as one of the most advanced possibilities for obtaining energy from renewable sources and valuable fertilisers. Biogas energy has an important role in the proper choice of scopes approved by European Directive for Energy from renewable sources (RED, 2009/28/CE), which states that 20% of final energy consumption must be ensured from renewable sources until 2020.

According to a study of the European Environmental Agency the potential from agricultural is still largely unexploited and this sector is expected to have the highest growth rates in the coming years.

Digestion of animal manure and organic waste has contributed to solve a substantial environmental problem in the majority states of European Union.

Biogas installations, processing agricultural substrates, are some of the most important applications of anaerobic digestion today. In our country the biogas sector is in an early stage of development.

References

- [1] EBA - European Biogas Association, *Biogas- simply the best*, Renewable Energy House, Brussels, Belgium.
- [2] Al Seadi, T., Rutz, D., Prassl, H., Köttner, M., Finsterwalder, T., Volk, S., Janssen, R., *BIOGAS – Handbook*, University of Southern Denmark, 2008, ISBN 978-87-992962-0-0.
- [3] Al Seadi, T., Lukehurst, C., *Quality management of digestate from biogas plants used as fertiliser*, IEA Bioenergy, May 2012.
- [4] Arogo Ogejo, J., Wen, Z., Ignosh, J., Bendfeldt, E., Collins, E.R., *Biomethane Technology*, Virginia Cooperative Extension, College of Agriculture and Life Sciences, Virginia Polytechnic Institute and State University, 2009.
- [5] Rutz, D., *Sustainable use of the thermal energy of biogas*, Renewable Energies, Munchen, Germany, 2012.
- [6] Hjort-Gregersen, K., *Danish Farm Scale Biogas Concepts- at the point of commercial break trough*, Danish Institute of Agricultural and Fisheries Economics, Proceedings of the International Conference Würzburg, Germany: Biomass for Energy and Industry, 8-11 June 1998, p 641-643.
- [7] Lipp, R., *Advanced Biogas Technology for the Food Processing Sector*, Lipp GmbH73497 Tannhausen Germany.
- [8] Lemvig Biogas, *An example of successful centralized co-digestion in Denmark*, IEA BIOENERGY TASK 37 *Energy from Biogas*, February 2013.
- [9] Edita Vagonyte, European biomass association, *Biogas & Biomethane in Europe*.
- [10] www.greentech-opportunities.com
- [11] NRG Energy News, *Biogas - Important Resource for Renewable Energy Development in Romania*.
- [12] Sattler Brochure, *Biogas storage tanks for each plant design*. Available online at http://www.sattler-ag.com/sattler-web/static/media/pdf/Broschuere_UT_EN.pdf.

RESEARCHES ON THE APPLICATION OF HIGH ACCURACY PHYTOSANITARY TREATMENTS WITH ORGANIC SUBSTANCES BY MEANS OF A HYDROPNEUMATIC MACHINE

PhD.Stud. Eng. Andrei Dumitraşcu ^{1) (*)}, PhD.Stud. Eng. Mihaela Niţu ¹⁾, PhD.Stud. Eng. Alexandru Zaica ¹⁾, PhD. Eng. Dragoş Manea ¹⁾, Prof. PhD. Eng. Tudor Căsandroiş ²⁾

1) National Institute of Research - Development for Machines and Installations designed to Agriculture and Food Industry - INMA, Bucharest

2) "Politehnica" University of Bucharest - Faculty of Biotechnical Systems Engineering

ABSTRACT

Some of the goals of "Horizon 2025" Sustainable Development Strategy of Romania are the natural environment protection and maintenance measures. In this context it is necessary to substantiate a new technology for applying phytosanitary treatments based on anti polluting substances (extracts, tea infusions, decoctions, emulsions and suspensions), allowed and recommended by the EU with a suitable machine. Within the mechanized technology of performing ecological spraying treatments to combat diseases and pests in orchards, INMA Bucharest has designed, developed and tested a towed hydropneumatic equipment, The Orchard Spraying Machine, MSL. This paper presents some experimental investigations on this machine.

1. INTRODUCTION

The phytosanitary treatments with chemical or biological means of pest control are currently applied by spraying, but it should be noted that these treatments were once performed by dusting, method that has been abandoned both worldwide and in our country due to the following drawbacks: reduced uniformity of the substance distribution on the treated surfaces, reduced control of the dosing strictness, lower biological effects, high pollution, low reliability of the installations, high costs of implementation and operation.

Installations for applying phytosanitary treatments have to dose exactly the products per unit area treated, to achieve an uniform fragmentation at a density of droplets conform to the management requirements, in the terms of low energy and high efficacy.

The homogeneous distribution of plant protection solutions on target surfaces, with strict abundance in dosing, while providing the anticipated biological effects, depends on the following factors:

- the flow of liquid jet sprayed, essential component of the working norm;
- the degree of fineness of the liquid spray flow;
- the uniformity of distribution of the fluid jet, related to the performance of the spray heads;
- the coverage and penetration of the vegetal mass;
- the spatial arrangement of target objects or areas to be covered;
- the atmospheric conditions. [1]

The main elements of a spraying machine are the nozzles. Their variety explains the wide range of these machines. The concerns of INMA, in the current context have been materialized in designing, constructing and testing an orchard spraying machine.

2. METHODOLOGY

2.1. Main parts of the Orchard Spraying Machine MSL, technological scheme and working process

The Orchard Spraying Machine MSL (fig. 1) works on the principle of hydraulic airborne jet spray.

(*) 6, Ion Ionescu de la Brad Blvd., Sector 1, Bucharest, Tel. 0761602569, email andreid753@gmail.com



Figure 1. The Orchard Spraying Machine MSL

1 - the chassis; 2 - the spraying device; 3 - the hydraulic installation; 4 - the angular gear; 5 - the system that detect the presence / absence of tree crown; 6 - the automated command system

The technological scheme of the equipment is shown in Fig. 2.

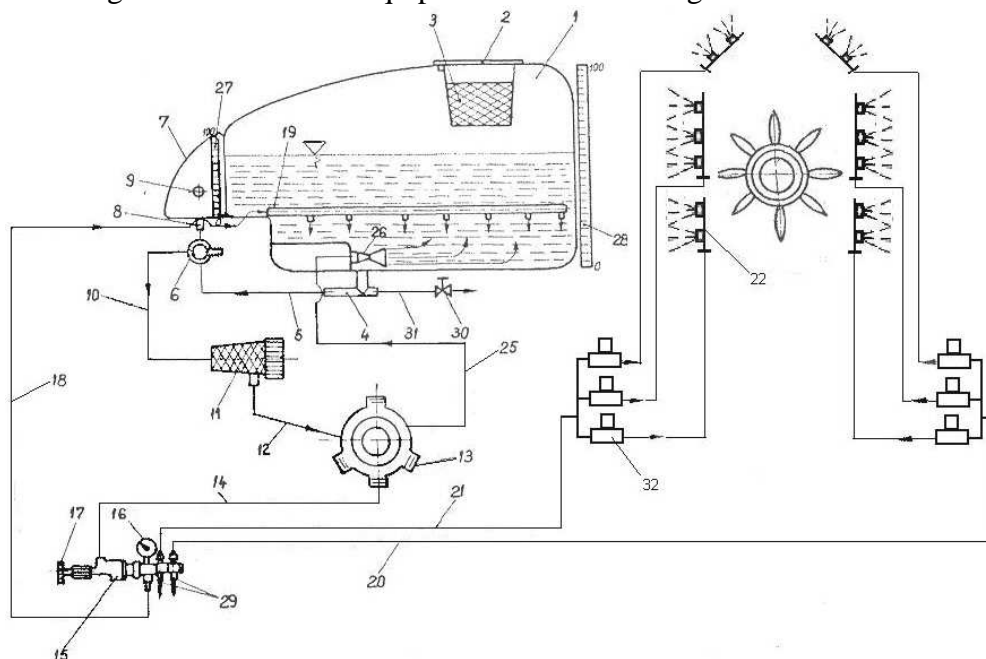


Figure 2. The technological scheme of the Orchard Spraying Machine MSL

1 – solution tank; 2 – tank cover; 3 – strainer; 4 – filling adapter; 5, 10, 12 – connecting pipes; 6 – three-way tap; 7 – clean water tank; 8 – adapter; 9 – tap; 10 – filter; 13 – three membrane pump; 14, 18, 20, 21 – manifold pipes; 15 – manifold; 16 – pressure gauge; 17 – pressure regulator; 19 – stirrer; 22 – spraying devices; 25 - ejector pipe; 26 – ejector; 27, 28 – level indicators; 29 – manifold taps; 30 – bleeder; 31 – emptying pipe; 32 - electrovalves

The working process is described below.

The liquid pump (13) driven by the tractor PTO takes the spraying solution from the solution tank (1) via the filling adapter (4), the connecting pipes (5, 10, 12), the three-way tap (6), the filter (11) and transmits part of the solution to the manifold (15) and the excess

solution is returned to the tank through the connecting element (18) and the stirrer (19) - a stainless steel pipe provided with holes along its whole length. A portion of the pump flow is directed through the ejector pipe (25) to the ejector (26). When passing, the solution produces a continuous stirring of the liquid. The manifold, fitted with pressure regulator (17), taps (29) and pressure gauge (16), provides both working pressure regulation and fluid passing to the electrovalves (32) and to the spraying devices (22) or stopping it. The pressure values are indicated by the pressure gauge. The spraying devices are equipped with anti-drip valves which limit fluid losses when closing the working circuits. The installation is also provided with a bleeder (30) for emptying the solution tank and transparent level indicators (28, 29) for viewing the level of liquid in the tanks.

Figure 3 details the automated command system.

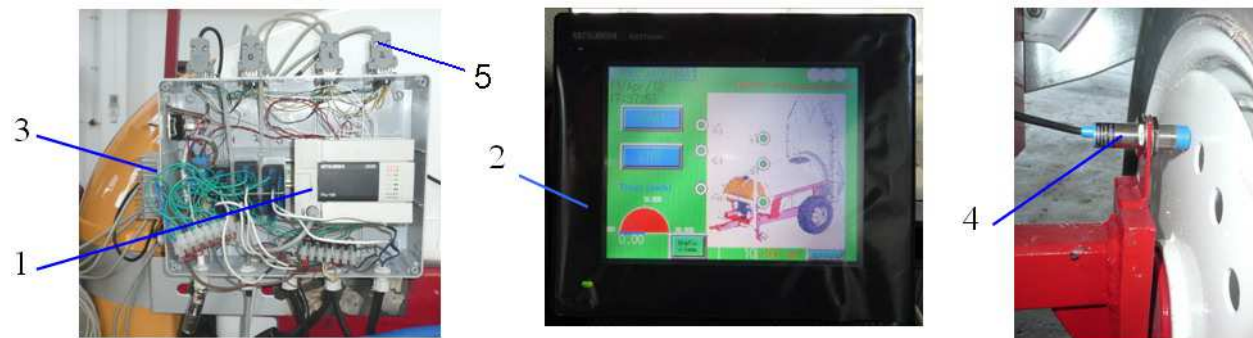


Figure 3. The the automated command system of the spraying device

1 - programmable logic controller (PLC); 2 - operating display; 3 - voltage converter 12 – 24 V AC; 4 - speed transducer; 5 - connectors and power cables

The ultrasound sensors detect the existence of vegetal mass. The information is transmitted to a PLC which controls starting and stopping the spraying devices supply by means of electrovalves. In the absence of vegetal mass the solution flow is stopped. Each sensor corresponds to two or three nozzles. Depending both on the distance that exists between the sensor and the spraying device and on the operation speed of the equipment, the PLC apply a time correction for opening the electrovalves, when the ramp passes the target to be sprayed. [2], [3]

2.2. Testing the Orchards Spraying Machine MSL

The testing of the Orchards Spraying Machine MSL was performed between 15.03.2012-15.04.2012 at the headquarters of INMA Bucharest.

The experiments were performed in accordance to the specified test procedure PSpI-04.01.01 „Testing plant protection machines – spraying machines in vineyards and orchards” issued by INMA Bucharest and the valid legislation. [4]

The preparations for tests of the Orchards Spraying Machine MSL consisted of the following operations technical expertise of the main components and all the removable and non-removable joints, verifying the way of mounting of the device on the spraying towed Orchards Spraying Machine MSL, verifying the operating mode of both spraying device and hydraulic system and final adjustment for actual working

At the same time, were carried out controls regarding the abidance by the security requirements according to the latest normatives.

At tests were determined the following qualitative work indicators :

- the flow through the nozzles;
- the substance norms;

- the pressure constancy during the discharge of the tank.

The flow through the nozzles was determined using the volumetric method. The liquid passed through the nozzles during 1 min was collected and then measured in 2 l graduated cylinders. For each pressure and type of nozzle were made three measurements.

On the spraying device were mounted nozzles manufactured by Lechler GmbH, with the hole diameter of 0.8 mm, 1 mm, 1,2 mm, 1,5 mm. The resulting liquid flow obtained for each type of nozzle are shown in tab. 1.



Figure 4 - Lechler nozzle

Table 1: The liquid flow through the nozzles

Pressure [bar]		5	10	15	20
Flow rate [l/min]	nozzle ϕ 0.8	0.49	0.67	0.87	0.98
	nozzle ϕ 1	1.14	1.76	2.09	2.4
	nozzle ϕ 1.2	2.10	2.61	3.10	3.60
	nozzle ϕ 1.5	3.48	4.64	5.37	5.85

With the nozzles mounting shown in fig. 4, the machine achieves liquid flows between 10.76...22.24 l/min in variant I and 37.68 - 63.90 l/min in variant II, at a working pressure range between 5 and 20 bar. The values mentioned in tab. 2 and graphically represented in the diagram of fig. 5 indicates the possibility of performing phytosanitary treatments in orchards with low solution norms.

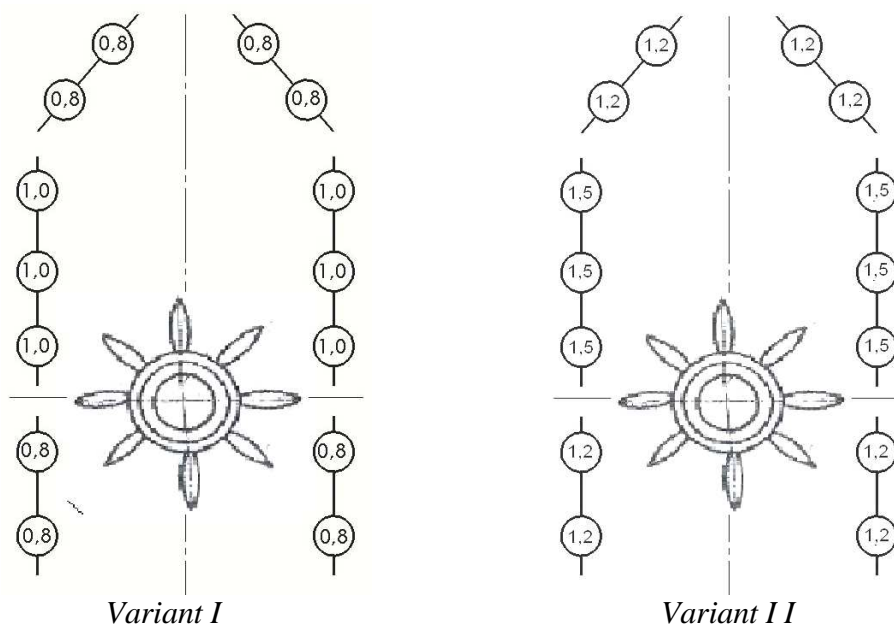


Figure 5. Nozzles mounting

Table 2: The liquid flow of the machine

Pressure [bar]	Liquid flow (l/min)	
	Variant I	Variant II
5	10.76	37.68
10	16.92	48.72
15	19.50	57.02
20	22.24	63.90

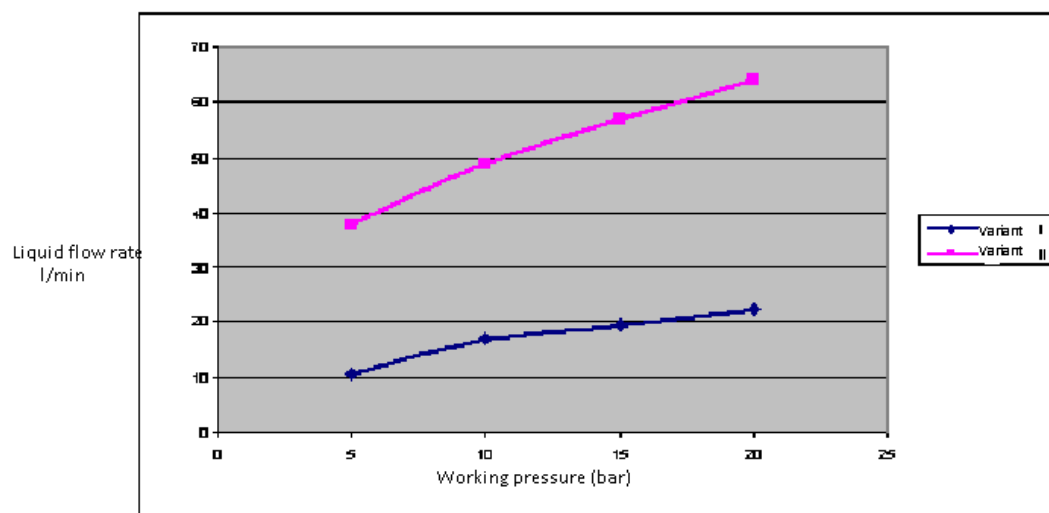


Figure 6. Variation of the liquid flow of the machine depending on the working pressure

The liquid norms were determined depending on the liquid flow of the machine, the nozzle types, the distance between rows and the speed of the tractor-machine unit. The working pressures ranged from 5 to 20 bar, the machine been equipped with 14 nozzles.

The liquid norms were between 70 and 210 l/ha in the area of interest -Ultra-Low Volume (ULV) solution treatments- and up to 1250 l/ha the Low Volume (LV) solution treatments area. The values obtained for liquid norms are given in tab. 3.

Table 3: Liquid norms [l/ha]

Pressure [bar]		Nozzle ϕ 0.8 mm				Nozzle ϕ 1 mm			
		5	10	15	20	5	10	15	20
Flow through nozzle [l/min]		0.49	0.67	0.87	0.98	1.14	1.76	2.09	2.40
Working speed [km/h]	Distance between rows [m]	Liquid norms (l/ha)							
4.14	4	255	340	400	500	580	840	1000	1250
	6	170	225	270	340	480	580	640	820
	8	112	170	200	250	390	435	500	610
5.69	4	185	250	290	370	425	620	670	910
	6	123	165	195	250	285	420	500	610
	8	92	125	145	175	210	315	370	460
7.54	4	140	180	220	275	320	550	560	680
	6	93	120	150	185	210	370	370	450
	8	70	90	110	140	160	240	280	340

The variation of working pressure during reservoir emptying was determined by repeated measurements of pressure at emptying the solution tank. The machine was set to operate at a pressure of 10 bar, keeping track of the pressure drop during the tank emptying. The pressure decreased to 9.2 bar when in the tank remained 30 l of solution. The machine meets the uniformity requirements of $\pm 10\%$, the resulting deviation being 8%.

To avoid unacceptable variations in the concentration of treatment suspension, the machine is equipped with an agitation system, the concentration values ranging between 0.950 and 1.025%, which means that the system meets the legislative normatives.

3. CONCLUSIONS

The research results constitute a useful database in order to design a new class of machines for phytosanitary treatments.

The application of this modern, innovative technology will have the effect of reducing environmental pollution due to the gradual replacement of chemicals with green products and the opening of new ways in achieving high precision equipments, that can accomplish phytosanitary treatments with small amounts of active substance, while increasing the treated area and reducing the working time.

Bibliography

- [1] Stahli W. (2003) - *Phytosanitary treatments and foliar crop fertilization machines*, AGROPRINT Publishing House, Timișoara;
- [2] Escolà A., Solanelles F., Planas S., Rosell J.R. - *Electronic control system for proportional spraying application to the canopy volume in tree crops*, Proceedings of the International Conference on Agricultural Engineering AgEng 2002, Budapest, Hungary, July 2002;
- [3] Bolintineanu Gh., Vlăduț V., Voicea I., Matache M., Savin L., Langenakens J. (2010) - *Integration of a centralized monitoring and warning system on the technical equipment for phytosanitary treatments within the concept of precision agriculture* INMATEH - Agricultural Engineering, vol. 31, no. 2, pag. 52-59, Bucharest.
- [4] *** - SR EN 13790-2:2004 – *Agricultural machines. Spraying machines. Examination of spraying machines during operation. Part 2: Jet spraying machines used in fruit growing shrubs*

STUDIES ON ENERGY OPTIMIZATION OF THE AGRICULTURAL PRODUCTS PROCESSING MACHINE BY PRESSING

Ph.D.Eng. Mihaela Florentina Duțu¹, Prof.Ph.D.Eng. Ion Dinu²,
Ph.D.Eng. Carmen Otilia Rusănescu³, Ph.D.Eng. Iulian Claudiu Duțu⁴
^{1,2,3} University Politehnica of Bucharest - Faculty of Biotechnical Systems Engineering
⁴ Hydraulics and Pneumatics Research Institute, Bucharest, Romania

ABSTRACT

The article is studying physical and mathematical models for agricultural material (organic) deformation process through pressing or briquetting, as well as the models used for optimizing the functional states of agricultural machinery. Organic material deformation is very interesting when studying pressing, briquetting and granulating processes of the agricultural products and can be represented through a physical model that consists of a series of elastic and viscous elements.

Energy and metal costs per productivity unit in vegetal material presses mainly depend on the value of the pressing pressure and they increase sharply when the pressure rises. One of the possible ways to decrease energy and metal consumption for presses is to use together a vibration and pressing method with which it will be achieved a decrease in compression resistance value.

Choosing the proper ratio between load applying time and load speed can lead to a significant enhancement of the technological pressing and briquetting processes simultaneously decreasing mechanical work. Obtained results can be used in other pressing processes for materials with both viscous and elastic properties.

1. INTRODUCTION

Organic material deformation it is an interesting process when studying the pressing, briquetting and granulation of agricultural products, this process can be represented by a physical model that consists of a series of elastic and viscous elements.

Theories regarding the behavior of hay and straw materials, proposed by many authors, show physical and mechanical properties that can be achieved in reality.

2. METHODOLOGY

When compressing a fibrous material it will appear elastic properties of its entire structure as well as of the material itself, characterized by different modules of elasticity.

The physical model of a fibrous material is given in Figure 1.

¹ No.313, Splaiul Independentei street, district 6, Bucharest, Romania, davidmihaela1978@yahoo.com

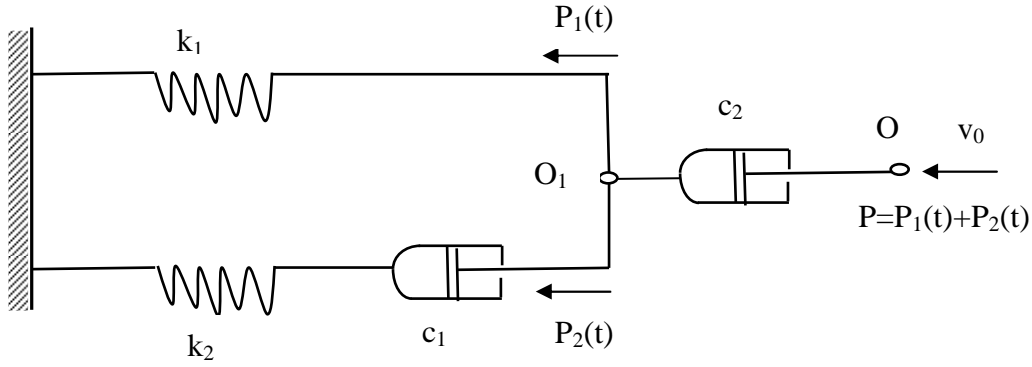


Figure 1: The physical model of a fibrous material

Movement of the point O on the model is given by the equation (1).

$$v_0 t = x = x_1 + x_2 \quad (1)$$

where: x – total displacement;

x_1 - branch displacement 1;

x_2 – branch displacement 2;

t – pressing time;

v_0 – speed of the press;

Displacement x_1 can be written in two forms:

$$x_1 = P_1(t)k_1 \text{ or } x_1 = P_2(t)k_2 + \int_0^t c_1 P_2(t) dt \quad (2)$$

where: $P_1(t), P_2(t)$ - force branch 1 or 2;

c_1 – viscous damping coefficient;

k_1, k_2 – elastic constants.

Displacement x_2 is given by the equation (3):

$$x_2 = \int_0^t c_2 P_1(t) dt + \int_0^t c_2 P_2(t) dt \quad (3)$$

where: c_2 – viscous damping coefficient.

Total displacement can be written as in equations (4) and (5).

$$\left\{ \begin{aligned} x = v_0 t = P_1(t)k_1 + \int_0^t c_2 P_1(t) dt + \int_0^t c_2 P_2(t) dt \end{aligned} \right. \quad (4)$$

$$\left\{ \begin{aligned} x = v_0 t = P_2(t)k_2 + \int_0^t c_1 P_2(t) dt + \int_0^t c_2 P_1(t) dt + \int_0^t c_2 P_2(t) dt \end{aligned} \right. \quad (5)$$

Solving the system of equations (4) and (5) we will obtain:

$$\left\{ \begin{aligned} P_1(t) &= \frac{v_0}{k_2(\lambda_2 - \lambda_1)} \left[\lambda_1 (e^{\lambda_2 t} - 1) - \lambda_2 (e^{\lambda_1 t} - 1) + \frac{c_2}{k_1} (e^{\lambda_2 t} - e^{\lambda_1 t}) \right] \\ P_2(t) &= \frac{v_0 (k_1 \lambda_2 + c_2) \cdot (k_1 \lambda_1 + c_2)}{c_2^2 k_1 (\lambda_2 - \lambda_1)} \cdot (e^{\lambda_2 t} - e^{\lambda_1 t}) \end{aligned} \right. \quad (6)$$

where: λ_1, λ_2 are given by (7):

$$\lambda_{1,2} = \frac{1}{2} \left(\frac{c_2}{k_1} + \frac{c_1 + c_2}{k_2} \right) \pm \sqrt{\left(\frac{c_2}{2k_1} \right)^2 - \frac{c_1 c_2 - c_2^2}{2k_1 k_2} + \left(\frac{c_1 + c_2}{2k_2} \right)^2} \quad (7)$$

Total force $P(t)$ is given by the equation (8):

$$P(t) = \frac{v_0}{c_2} - \frac{v_0}{c_2^2 (\lambda_2 - \lambda_1)} [\lambda_2 (k_1 \lambda_1 + c_2) e^{\lambda_2 t} - \lambda_1 (k_1 \lambda_2 + c_2) e^{\lambda_1 t}] \quad (8)$$

where: $P(t)$ is the total force.

As can be seen from equations (6), (7) and (8) the necessary force for the deformation of the physical model is directly proportional to the speed.

It appears that the pressing force increase if the speed increases. Energy consumption is low if the pressing speed is low and increases if the pressing speed increases.

If the pressing speed is not constant and changes its value over time, $v = f(t)$, then the solution for the system of equations is difficult to write, but the equations remain the same.

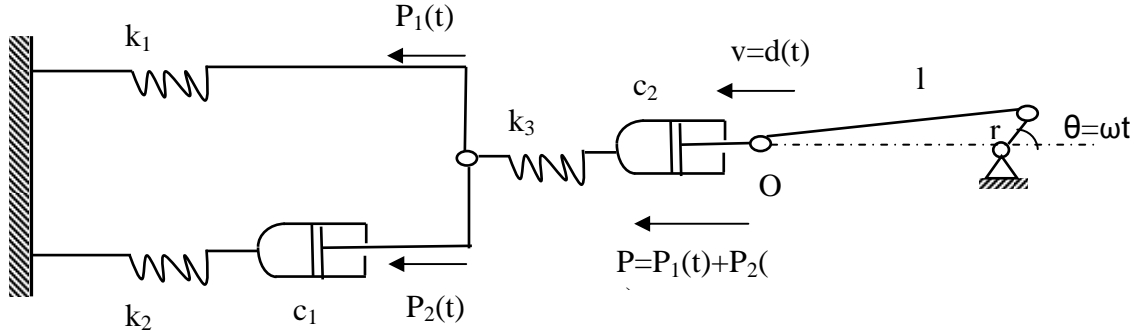


Figure 2: Model of a pressing process of a fibrous material in a press with a crank-rod mechanism

Figure 2 shows a model of a pressing process of a fibrous material in a press with a crank-rod mechanism, a case quite frequently encountered in practice.

In this case, the resulting system of equations (9) is:

$$\begin{cases} \omega \cdot r \cdot \sin \omega t = \dot{P}_1(t) k_1 + \dot{P}_1(t) k_3 + \dot{P}_2(t) k_3 + c_2 P_1(t) + c_2 P_2(t) \\ \omega \cdot r \cdot \sin \omega t = \dot{P}_2(t) k_2 + c_1 P_2(t) + \dot{P}_2(t) k_3 + c_1 P_1(t) + c_2 P_2(t) \end{cases} \quad (9)$$

The system (9) written in the canonical form appears as the (10):

$$\begin{cases} \dot{P}_1(t) = A \cdot [k_2 \cdot \omega \cdot r \cdot \sin \omega t + (c_1 k_3 - c_2 k_2) P_2(t) - c_2 k_2 P_1(t)] \\ \dot{P}_2(t) = A \cdot [k_1 \cdot \omega \cdot r \cdot \sin \omega t + (c_1 k_1 + c_1 k_3 + c_2 k_1) P_2(t) - c_2 k_1 P_1(t)] \end{cases} \quad (10)$$

Integrating system (10) it will be obtained the solutions given in (11):

$$P_1(t) = \frac{\lambda_2 b - a \omega}{\lambda_1 - \lambda_2} e^{\lambda_1 t} - \frac{\lambda_1 b - a \omega}{\lambda_1 - \lambda_2} e^{\lambda_2 t} + a \cdot \sin \omega t + b \cdot \cos \omega t \quad (11)$$

$$P_2(t) = \frac{1}{c_1 k_3 - c_2 k_2} \left[\frac{\lambda_2 \cdot b - a \cdot \omega}{\lambda_1 - \lambda_2} \left(\frac{\lambda_1}{A} + c_2 k_2 \right) e^{\lambda_1 t} - \frac{\lambda_1 \cdot b - a \cdot \omega}{\lambda_1 - \lambda_2} \left(\frac{\lambda_2}{A} + c_1 k_3 \right) e^{\lambda_2 t} + \left(\frac{a \omega}{A} + c_1 k_2 b \right) \cos \omega \cdot t - \left(\frac{b \omega}{A} - c_2 k_2 a + \omega \cdot r \cdot k_2 \right) \sin \omega \cdot t \right]$$

The necessary force for physical model deformation is given as (12):

$$P(t) = P_1(t) + P_2(t) = \frac{1}{c_1 k_3 - c_2 k_2} \left[\frac{\lambda_2 b - a \omega}{\lambda_1 - \lambda_2} \left(\frac{\lambda_1}{A} + c_1 k_3 \right) e^{\lambda_1 t} - \frac{\lambda_1 b - a \omega}{\lambda_1 - \lambda_2} \left(\frac{\lambda_2}{A} + c_1 k_3 \right) e^{\lambda_2 t} + \left(\frac{a \cdot \omega}{A} + c_1 k_3 b \right) \cos \omega \cdot t - \left(\frac{b \cdot \omega}{A} + c_1 k_3 a + \omega \cdot r \cdot k_3 \right) \sin \omega \cdot t \right] \quad (12)$$

where: $a = r$;

$$A = \frac{1}{k_1 k_2 + k_2 k_3 + k_1 k_3}.$$

$$b = c_1 k_1 + c_1 k_3 + c_2 k_1 + c_2 k_2$$

3. CONCLUSIONS

Energy and metal costs per unit of productivity in vegetal material presses primarily dependent on the pressing pressure value and rapidly increases when it raises.

One of the possible ways to decrease energy and metal consumption in presses is using the vibrant-pressing method, which reduces the resistance against compression of the vegetal material.

Choosing the right value for the load time application ratio, speed and its repeatability can lead to significant intensification of technological processes of pressing and briquetting simultaneously decreasing the specific mechanical work.

References

- [1] Dinu, I., „*Considerații teoretice asupra modelării matematice a presării materialelor vâscoelastice*”, Consfătuirea de mecanica solidelor, Cluj-Napoca, 1982.
- [2] Dinu, I., „*Modelarea produsului de presare a produselor vâscoelastice*”, Teza de doctorat, 1986
- [3] Vaicum, A., „*Studiul reologic al corpurilor solide*”, Editura Academiei RSR, 1978
- [4] Voinea, R., „*Elasticitatea și plasticitatea*”, I.P.B., 1976

SOME PROPERTIES OF *MONASCUS PURPUREUS* RED RICE – A NATURAL FOOD DYE

Mariana Ferdes *

University Politehnica of Bucharest,
Faculty of Biotechnical Systems Engineering, Department of Biotechnical Systems

Abstract

The aim of the present study was to determine the representative properties of red rice, a well-known product in asian countries. The red rice is obtained from *Monascus* genus that produces a mixture of red, orange and yellow pigments when is cultivated on starchy substrates.

The use of natural *Monascus purpureus* pigment improves the quality, durability, nutrition value and visual attraction of food products and promotes the positive health aspects.

The solid state fermentation of rice by *Monascus* has a long tradition in East Asian countries as food dye and for dietary staples. The fermented rice is called ang khak or Hong Zhu in China and beni koji in Japan. *Monascus* fungi produce at least six major pigments: 2 red colorants named rubropunctamine and monascorubramine, 2 orange colorants, rubropunctatin and monascorubrin and 2 yellowish colorants, monascin and ankaflavin.

The preservative effect of *Monascus* fermentate has also been confirmed; monascidin A inhibits bacteria of genera *Bacillus*, *Staphylococcus*, *Streptococcus* and *Pseudomonas*.

Monascus strain was cultivated onto glucose-yeast extract agar slants for maintenance, in tubes, at 30° C, for 7 days. Pigments biosynthesis was carried out on sterile ground rice, in Erlenmeyer flasks. 50 g of rice was inoculated with 10 mL of suspension of spores and incubated for 7 days at 30° C. Pigments were extracted in ethanol and hexane from the red rice to measure the absorbancy values at 400 nm (yellow pigments) and at 510 nm (red pigments).

Monascus dye was tested in terms of temperature and light stability and color variation at different pH values. These treatments proved a good stability at temperature up to 100° C, a red color between 4-9 pH units but a high sensitivity to light, after 3 weeks of exposure to daylight.

The antibacterial activity was tested against *E.coli*, *S.aureus* and *B.subtilis* and the hexan extract of red rice inhibits the growth of these bacterial strains. The red rice shows an antifungal activity against some *Aspergillus*, *Fusarium*, *Mucor*, *Penicillium* and *Alternaria* species.

1. INTRODUCTION

The production of synthetic colouring agents and other chemicals used as food additives is under increasing pressure due to a renewed interest in the use of natural products in food formulations and the strong interest in minimizing the use of chemical processes to produce food ingredients. In accordance with these requirements, there is a group of consumers who prefer so called all natural foods, i.e. without any synthetic additives. An approach to keep with this world trend will be applying the biotechnological process of natural *Monascus* pigment.

Monascus purpureus is a homothallic fungus found on red rice (Anka or Ang-kak). It has been used as a natural food colorant and traditional medicine in Asia for centuries (Ferdes et al, 2011) and has been used as a substitute for nitrite in meat preservation (Fink-Gremmels et al. 1991).

Easily found in several ecosystems, these fungi were used originally in Chine and Thailand, for the preparation of angkak, a fermented rice of strong red color which finds several uses, from conferring color to other products such as wine, cheese and meat, to medicinal uses and as meat preservative (Wong, 1981). At this moment, several industries commercialize the red,

grinded rice as a natural food supplement capable of lowering blood cholesterol, while others sell the dry product or purified extracts as food colorants.

Monascus species have been proven to produce many functional secondary metabolites. These pigments (yellow pigment: ankaflavin and monascin; orange pigment: monascorubrin and rubropunctanin; red pigment: monascorubramine and rubropuctamine) were investigated and applied to the food colorant in early study (Erdogrul et al. 2004; Wong and Koehler 1981).

2. MATERIALS AND METHODS

Fungal strain

The experiments were carried out using a mutant strain of *Monascus purpureus*, M5, from the culture collection of Microbiology Laboratory of Faculty of Biotechnical Systems Engineering. The fungal strain is cultivated on potato-dextrose-agar medium, is characterized by a high productivity potential and is used to produce the red rice.

Pigment biosynthesis

The cultivation of *Monascus purpureus* strain was carried out in solid state fermentation on sterilized moist rice, in 1500 mL Erlenmeyer flasks, at 30 °C, for 14 days, in darkness. The culture medium was dried, ground and treated to reduce microbial load. The final product was a dark-red powder with tinctorial properties.

Stability of pigments

The *Monascus* pigments were extracted in Et-OH and water and the absorbance at 400 nm and 510 nm were determined. The pigments solution was maintained 2 hours at 60 °C, 75 °C and 90 °C and the spectra were recorded. The stability against light was tested keeping the pigments in Et-OH extract in darkness and at light for 7 days. To test the stability of pigments at different pH values, aqueous extract was kept in citric acid and NaOH solutions at pH 2, 3,4, 5,6,7,8,9 and 10 and the absorbance values were compared.

Antimicrobial activity

Antibacterial activity was analysed against 2 strains of *Bacillus subtilis*, 2 strains of *Staphylococcus aureus* and 1 strain of *E. coli* using the the diffusion method. Antifungal properties of red rice were estimated against several mold strains of *Aspergillus*, *Penicillium*, *Mucor*, *Fusarium* by measuring the colony diameters of indicator mold in the presence of 0.5% powder of red rice added in the culture medium.

3. RESULTS AND DISCUSSIONS

In order to asses the sensibility of this food dye to different temperatures, the alcoholic extract maintained 1 and 2 hours at 60⁰C, 70⁰C or 90⁰C have been analyzed in terms of absorbance, at UV-VIS spectrofotometer. The values of specific absorbances for red and yellow pigments are presented in the following table and figures.

Table 1. The values of absorbance for the red and yellow pigments at different temperatures.

Temperature wavelength/Time	60 ⁰ C		75 ⁰ C		90 ⁰ C	
	400nm	510nm	400nm	510nm	400nm	510nm
0 h	1,54	0,87	1,54	0,87	1,54	0,87
1h	1,52	0,86	1,52	0,88	1,45	0,69
2h	1,49	0,83	1,48	0,84	1,39	0,72

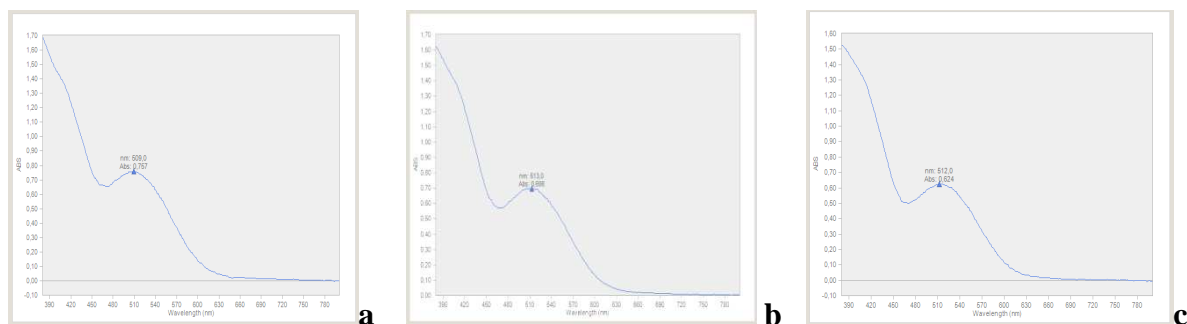


Fig.1 The absorption spectra of Monascus pigments in alcoholic extract after 2 hours a) at 60°C; b) 75°C c) 90°C

According to the data from the literature, the pigments produced in the culture of *Monascus purpureus* are more stable than the pigments from beetroot and anthocyanins from fruits and vegetables. The decrease of absorbance value after 2 hours at 90°C was of only 10% for yellow pigments and 20% for the red ones.

To demonstrate the sensitivity of *Monascus* pigments to light, the absorbances values were measured and the absorbance spectra (380-800nm) were recorded. The data are presented in the table 2 and figure 2.

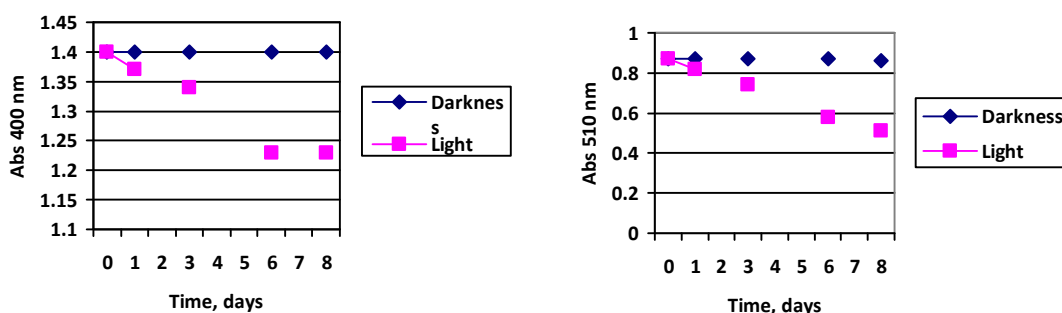


Fig.2 The values of absorbances for a) yellow and b) red pigments after 8 days of exposure to light and darkness

The sensitivity of Monascus pigments at different pH values is shown in figure 3.

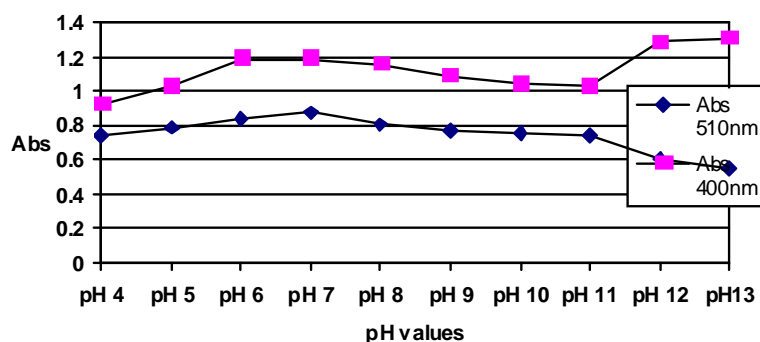


Fig. 3 The values of absorbances of yellow (400 nm) and red (510 nm) pigments at different pH values

The antimicrobial activity of red rice measured by the diffusion method demonstrated that the alcoholic extract inhibits the *B. subtilis*, *S. aureus* and *E. coli* growth on a diameter of about 1,2 cm. The inhibition growth of fungal strains, as shown in figure 4, was between 40% (for *F.oxysporum*) and 0% (for *A. niger*).

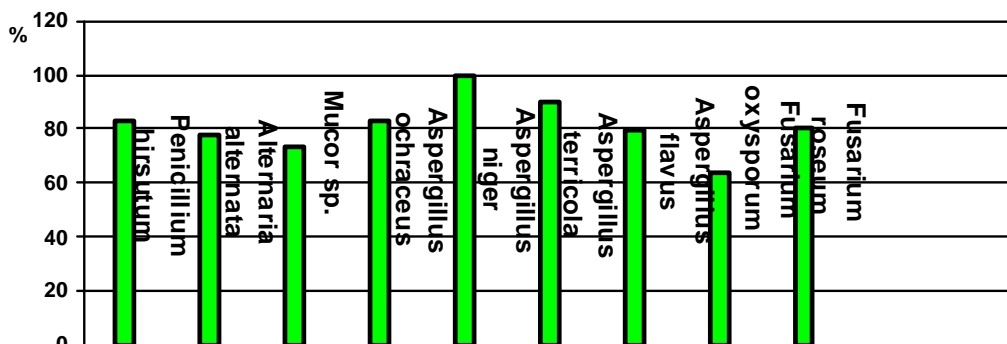


Fig. 4 The inhibition growth of fungal strains in the presence of 0,5% red rice

4. CONCLUSIONS

The *Monascus* red and yellow pigments are characterized by a good stability at high temperatures and at pH values between 4 and 9 units. The red pigments are however more sensitive to light radiation; after an 8-day exposure to light, absorbance dropped to 60% compared to initial value.

The antimicrobial activity was estimated against *B.subtilis*, *S.aureus*, *E.coli* and several fungi belonging to the genera of *Aspergillus*, *Penicillium*, *Fusarium* and others and it has been demonstrated by the growth inhibition effect in presence of red rice.

5. REFERENCES

1. Erdogrul O.et al, 2004, Turkish Electronic Journal of Biotechnology, vol2, 37-39
2. Ferdes, M. and Ungureanu, C., 2011. *Revista de Chimie*, **62**(1), pp. 75-81.
3. Fink-Gremmels, J.Dresel, Leistner L., *Fleischwirtschaft*, 1991,71:329-331
4. Júlio Cesar de Carvalho, Bruno Oliva Oishi, Ashok Pandey and Carlos Ricardo Soccol, 2005, *Brazilian Archives of Biology and Technology*, Vol.48, n. 6 : pp. 885-894
5. Wong, H. C., P.E. Koehler, 1981, *J. Food Sci.*, 46, 589-592
6. Wang C.W., Mousa S.A., *Complement Ther Med.* 2012 Dec;20(6):466-74

ACTUAL METHODS FOR OBTAINING VEGETABLE OIL FROM OILSEEDS

Ionescu Mariana*, Ungureanu Nicoleta, Biriş Sorin-Ştefan,
Voicu Gheorghe, Dilea Mirela

POLITEHNICA University of Bucharest, Department of Biotechnical Systems

ABSTRACT

Vegetable oils are an important component for both food (for feeding, margarine and canned food industry, bakery, confectionery) and for non-food industry (production of detergents, paints, special varnishes, fatty acids, pharmaceuticals and cosmetics products, and painting). Vegetable oils and fats are found in nature in plant tissue, being concentrated in seeds, pulp, stone fruits, and in the tubers or sprouts. In our country, the main raw material is represented by the oleaginous plants which produce seed. The oil can be obtained from different categories of plants: plants with oil concentrated in seeds (sunflower, soybean, rapeseed etc.), plants producing oleaginous fruits (olive, coconut and palm), plants producing oleaginous tubers (peanuts) and plants producing oleaginous germ (corn). Fatty materials processing is somehow different, varying with its nature and oil content. Thus, for centuries, various methods were adopted for oil extraction from oilseeds. The purpose of those extraction methods was to optimize the process by collecting the maximum quantity of the existing oil in oilseeds with the minimum costs.

1. INTRODUCTION

Oilseeds represent one of the most important components of modern agriculture. This is due to the fact that they provide easily highly nutritious human and animal food. Nutritionally, oils obtained from oilseeds provide the calories, vitamins and essential fatty acids in the human diet, while the de-oiled cake is a valuable source of protein for animal feeds,[4].

In plants, fatty matter is concentrated only in some parts such as seeds, fruits and tubers, stone fruits, sprouts, representing a reserve substance that the plant uses during its development as a source of energy. Although the oilseeds field is very wide, plants that can be used as raw material in vegetable oils industry are slightly because many of them have low oil content - being unprofitable, others with higher oil content present difficulties in oil extraction because of the special structure of the plant, [3].

Oleaginous products industry manufactures edible oils and oils non edible. Edible oils (which is about 2/3 of the total volume of the oil products) are used directly in food or used in the industry of margarine, mayonnaise, cooking fats, bakery products, confectionery, canned food, confectionery and others, and the non edible oils (representing one third of the total volume of oil produced) are used in production of detergents, paint, varnish, fatty acids, pharmaceuticals and cosmetics, [6]. The request for the vegetable oil industry increases with increasing population through the discovery of new uses. Thus, to satisfy the vegetable oil demand, it is necessary that the oil extraction methods to be faster and more efficient, [1]. The oil extraction methods from oleaginous materials are designed to obtain high quality oil with minimal undesirable components, achieve high extraction yields and produce high value meal, [10].

2. DESCRIPTION OF EXTRACTION METHODS

Fatty materials processing is somehow different, varying with its nature and oil content. Thus, for centuries, various methods were adopted for oil extraction from oilseeds. The purpose of those extraction methods was to optimize the process by collecting the maximum quantity of the existing oil in oilseeds with the minimum costs. Currently, worldwide there are four basic methods for obtaining vegetable oil: chemical extraction, supercritical fluid extraction, steam distillation and mechanical extraction.

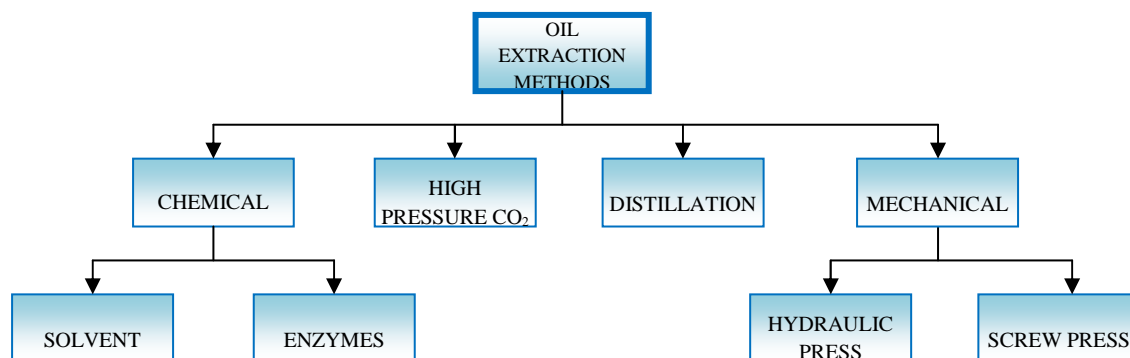


Figure 1: Basic methods for oil extraction, [12]

The most common method of extracting edible oil from oleaginous material, which has been practiced for thousands of years, is **mechanical pressing** of oilseeds. Mechanical oil extraction (also known as **pressing**) is based on mechanical compression of oleaginous materials. Through pressing, oil is separated from the oleaginous material (solid-liquid mixture) under the action of compressive external forces that arise in special machines called presses. This method ensures extraction of a non-contaminated, protein-rich low fat cake at relatively low-cost. The disadvantage of this method is that the mechanical presses do not have high extraction efficiencies, about 8-14% of the available oil remain in the press cake, [2].

During the Roman and Byzantine periods, the number of oil presses was in the thousands; in the area of the Golan Heights alone, 109 oil presses were found in 58 ancient sites, most of them operated during this period. The olive oil production process was based on two major steps: first step requires crushing the olives using a crushing stone, and collecting them into a basket; second step is done on another installation: the basket is pressed with force, extracting the oil out of the crushed olives and collecting the juice into a storing vat, [8]. Currently, pressing operation may be conducted in hydraulic presses, which are driven by fluid pressure, or in screw presses, where the pressing force is created by a helical body (worm) which rotates in a closed space (press chamber). Hydraulic oil press, so named because it works on the principle of the hydraulic ram, are originary from England and was first patented in 1795 by Joseph Bramah,[4].

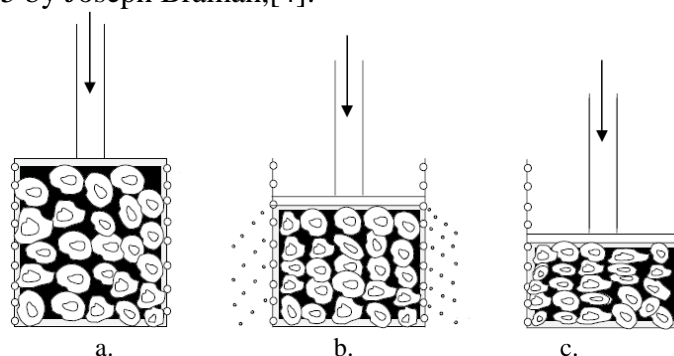


Figure 2: Stages of hydraulic expressions, [11]

a – initial stage; b – dynamic stage; c – consolidation stage (final stage).

Hydraulic expression of oil involves application of pressure through a ram to digested oleaginous material mash in a cylindrical cage. The cylindrical cage is usually perforated laterally. This results in axial compaction and radial oil flow. In a typical hydraulic pressing of vegetable oil seeds three distinct stages can be identified (fig. 2), [11]. The first cottonseed oil mill constructed in the United States (1920) utilized a hydraulic press. Seeds in filter bags were manually loaded into perforated, horizontal boxes between the head block and the ram

of the press. Boxes were pressed together by applying hydraulic pressure on the ram. Oil was pressed out through the filter bag. Then the filter bag containing spent cake was manually removed from the hydraulic press. Later versions of the hydraulic presses used cages instead of filter bags, [10].

In figure 3(a) is schematic represented a hydraulic press. Seeds are placed on a sieve plate covered with fine wire mesh in a temperature controlled ($30\text{--}100 \pm 1^\circ\text{C}$) pressing chamber with a diameter of 30 mm. Pressures up to 100 MPa are exerted by a hydraulic plunger. The press is fitted with a thermocouple ($\pm 1^\circ\text{C}$), pressure sensor and a position transducer (± 0.01 mm), which measures the distance the plunger traveled. Measured values are automatically recorded every second, [13]. Hydraulic presses were in use until the 1950s. They are replaced with continuous screw presses and continuous solvent extraction plants, which are less labor intensive. The olive oil industry still utilizes hydraulic press today.

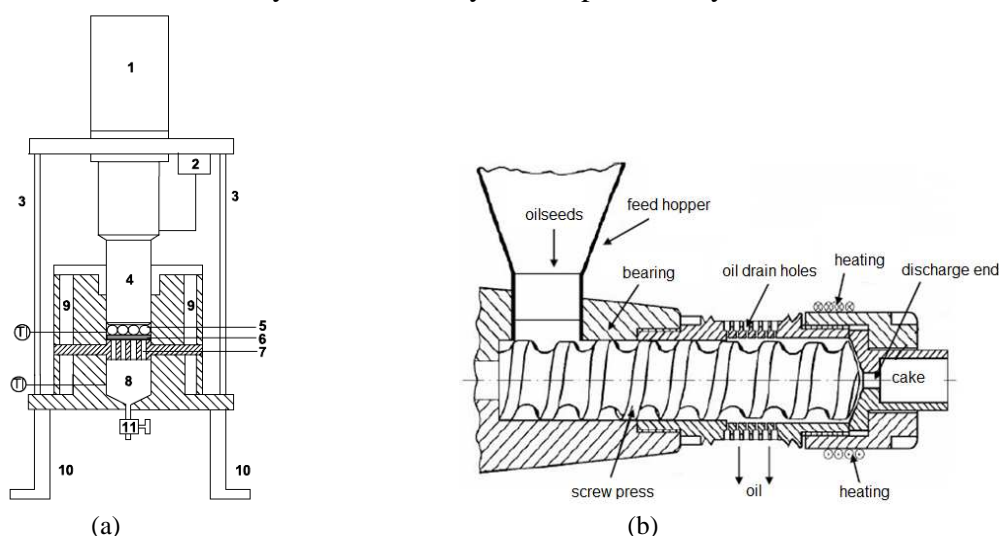


Figure 3: Equipments for oil expression: a. Hydraulic press, [13]; b. Screw press, [5]

1 – hydraulic unit; 2 – displacement sensor; 3 – support; 4 – plunger; 5 – seeds; 6 – filter medium; 7 – sieve plate; 8 – collection chamber; 9 – jacket; 10 – frame; 11 – needle valve; TI – thermocouple

The first screw oil press was developed in 1900 by V.D. Anderson in the United States. This press permitted continuous operation of hydraulic presses which resulted in greater capacities with smaller equipments and less labor, [4]. The mechanical screw press (fig. 3(b)) consists of a vertical feeder and a horizontal screw with increasing body diameter to exert pressure on the oilseeds as it advances along the length of the press. The barrel surrounding the screw has slots along its length, allowing the increasing internal pressure to first expel air and then drain the oil through the barrel. Oil is collected in a trough under the screw and the de-oiled cake is discharged at the end of the screw. The main advantage of the screw press is that large quantities of oilseeds can be processed with minimal labor, and it allows continuous oil extraction. [10].

Considerable efforts have been made in the past to improve the oil extraction efficiency of screw presses. Most of them have focused on optimization of process variables such as applied pressure, pressing temperature and moisture conditioning of the fed samples, [2]. Others improvements on oil screw presses was made for the design of the presses and for the material of presses construction.

To improve the cooking techniques, oil recovery and quality of oil and cake, an **extruding-expelling (E-E) technology** (fig. 4) have been adopted. This technology was applied by Nelson et al (1987) for extraction of oil from soybean. Extruding-expelling technology couples a dry extruder in which heat is generated by friction with continuous screw press. The coarsely ground whole soybean with 10-14% moisture content was extrusion

cooked for less than 30 seconds at the temperature of 135°C and then was immediately pressed in a continuous screw press. The extrusion prior to expelling greatly increased the throughput of the expeller over the rated capacity, the expelled oil was remarkably stable and a press cake with 50% protein and 6% residual oil was obtained. To improve the cooking techniques, oil recovery and quality of oil and cake, some leading screw press manufacturers have developed more efficient extruders. Anderson Hivex, is a new screw press design which combines pre-pressing and extruded collets formation into a single processing unit. Thus, a drainage cage and a pressing screw are included into the barrel of an expander.

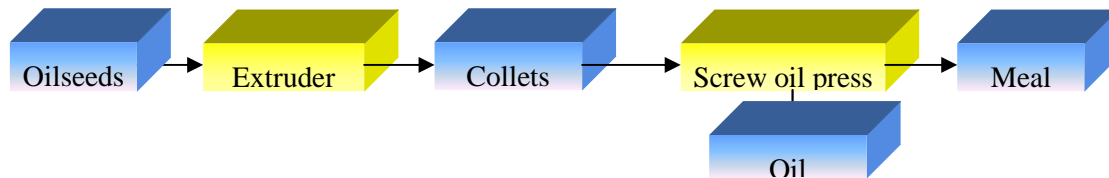


Figure 4: Flow diagram of an Extrusion-Expelling (E-E) technology, [10]

The chemical methods are another technology used for oil extraction from oilseeds. In the case of chemical methods, enzymes or solvents are used for the oil extraction, [12].

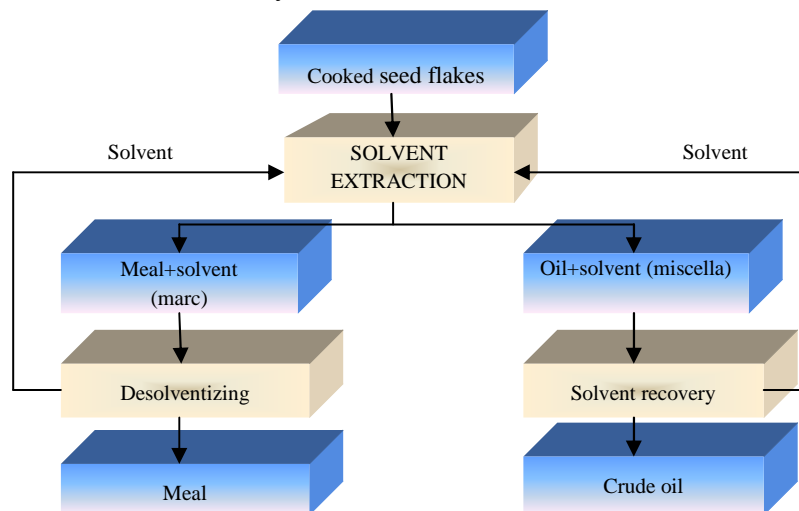


Figure 5: Flow diagram of solvent extraction method,[4]

Solvent extraction is the process of separating a liquid from a liquid-solid system with the use of a solvent. For oil extraction, the following light paraffinic petroleum fractions are used: pentane, hexane, heptanes and octanes. In solvent extraction, the seeds are first flaked (this operation is necessary in order to increase the contact area of the seed with the solvent, resulting in an increasing of the oil yield) and cooked (cooking denatures cell tissues so that solvent can penetrate the flakes more readily). After these operations, the cooked seed flakes are mixed with the solvent in order to extract the oil. It results a mixture of oil and solvent, called miscella, which is heated in evaporators at 80°C. Steam is injected on the shell side to vaporize and reduce hexane to about 5% of the oil, then the oil is directly steam-stripped in a vacuum tower at temperatures rising to a final 110°C, [4]. This is the most efficient technique to recover oil from oilseed. It is expected that the residual oil in the meal to be less than 1% after commercial solvent extraction. There are, however, some limitations and disadvantages related to the solvent oil extraction: the chemical solvents are harmful to human health, the chemicals used are highly flammable and the danger of fire and explosion always exists, the initial capital and operating costs are high, the energy requirements are high and the quality of recovered oil is lower than that of pressed oil. In order to improve the solvent extraction efficiency and to reduce the processing cost, the extrusion process was used as a pretreatment

of the oilseeds. The benefits obtained by using this pretreatment are the following: oil extraction rate increased, the amount of oilseed material present in the extractor increased, extractor capacity increased, steam requirement in the desolventizer reduced.

Another chemical method used for oil extraction from oilseeds is represented by **extraction using enzymes**. This method is implemented by big vegetable oil companies because the process produces many high value products. The first step necessary is the cooking of the seeds and after that, the cooked seeds are put into water. The following step is the enzymes adding which digest the solid material. At the end, the separation of the residual enzymes and oil are made using a liquid-liquid centrifuge, [12].

Taking into account the concerns about environmental and human health hazards produced by the organic solvents and residues in oil, it was necessary the replacement of the solvents for edible oil extraction. Thus, the replacement of solvents with supercritical fluids (SCF) have been studied for more than two decades. The **supercritical fluid extraction (SFE)** is a technique similar to conventional solvent extraction, but the solvent is not a liquid but rather a gas above its critical point. Supercritical fluid used in oil extraction is CO₂, this being the supercritical fluid most used in analytical applications because it does not extract molecular oxygen and is not a toxic fluid. In the supercritical carbon dioxide technique, the seeds are mixed with high pressure carbon dioxide in liquid form (at 31°C temperature and 7,3 MPa pressure). Then, oil dissolves in the carbon dioxide. When pressure is released from the system, the carbon dioxide returns to the gas phase and oil precipitates out from CO₂-oil mixture. The extraction efficiency depends on the temperature, pressure, contact time between the extracting fluid and the oilseed material and the solubility of the oil in the extracting fluid, [10].

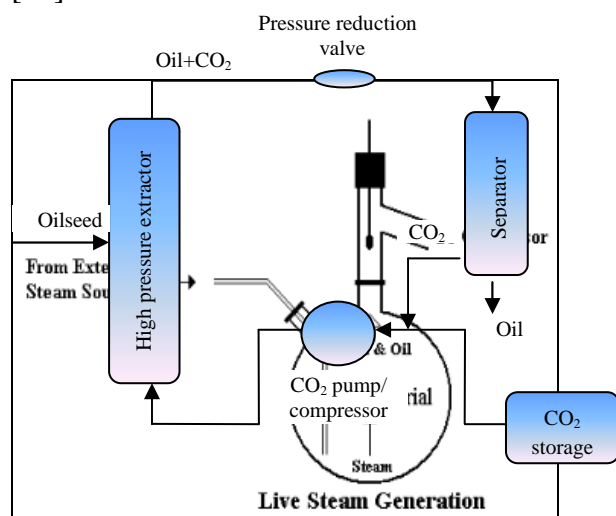


Figure 6: Flow diagram of a supercritical carbon dioxide extraction system, [10]

Figure 7: Distilling pot, [7]

SFE appears to be a cost-effective technique in laboratory scale, but an accurate economic evaluation for large-scale units requires supplementary experiments. The advantages of SFE-CO₂ extraction over the petrol ether extraction include: low operating temperature, hence no thermal degradation of most of the labile compounds; shorter extraction period; high selectivity in the extraction of compounds; no solvent residue with negative effects on the oils quality, [14].

The method of **steam distillation** is used for extraction of essential oils. Essential oils are the highly concentrated essences of aromatic plants used in healing of the body and the mind. When steam distillation is used in the manufacture and extraction of essential oils, the botanical material is placed in a still and steam is forced over the material.

The hot steam helps to release the aromatic molecules from the plant material since the steam forces open the pockets in which the oils are kept in the plant material. The molecules of these volatile oils then escape from the plant material and evaporate into the steam. The temperature of the steam needs to be carefully controlled - just enough to force the plant material to let go of the essential oil, yet not too hot as to burn the plant material or the essential oil. The steam which then contains the essential oil is passed through a cooling system to condense the steam, which form a liquid from which the essential oil and water is then separated. The steam is produced at greater pressure than the atmosphere and therefore boils at above 100°C which facilitates the removal of the essential oil from the plant material at a faster rate and in so doing prevents damage to the oil, [9].

3. CONCLUSIONS

This paper represents a review of actual methods used for obtaining vegetable oil from oilseeds. Studying the specialty literature, it was established that currently, worldwide there are four basic methods for obtaining vegetable oil: chemical extraction, supercritical fluid extraction, steam distillation and mechanical extraction. Taking into consideration the advantages and disadvantages presented by each method, the most used method for small scale production is mechanical pressing using screw presses, due to the simplicity of the process and equipments, the low investment cost and the high quality of the products. The main disadvantage presented by mechanical pressing is the higher residual oil quantity from the cake, comparing with the solvent extraction method.

References

- [1]. Alonge A.F. and all, "Effects of dilution ratio, water temperature and pressing time on oil yield from groundnut oil expression", Journal of Food Science and Technology, vol. 40, no.6, 652-655, 2003
- [2]. Bamgboye A. and Adejumo A., „Development of a sunflower oil expeller”, Agricultural Engineering International: the CIGR Ejournal. Manuscript EE 06 015, vol IX, September 2007
- [3]. Banu C., „Manualul inginerului din industria alimentară”, vol. I și II, Editura Tehnică, București, 1999
- [4]. Bargale P.C., „Mechanical oil expression from selected oilseeds under uniaxial compression”, Ph.D. Thesis, University of Saskatchewan, Canada, 1997
- [5]. Ferchau, E., „Equipment of Decentralized Cold Pressing of Oil Seeds”, Webpage of Folkecenter For Renewable Energy, www.folkecenter.dk, 2000
- [6]. <http://facultate.regielive.ro/cursuri/industria-alimentara/industria-produselor-oleaginoase-64663.html>
- [7]. <http://infohost.nmt.edu/~jaltig/SteamDistill.pdf>
- [8]. <http://www.biblewalks.com/info/OilPresses.html>
- [9]. <http://www.essentialoils.co.za/steam-distillation.htm>
- [10]. Nurhan D., „Oil and Oilseed Processing II”, Robert M. Kerr Food & Agricultural Products Center, FAPC-159
- [11]. Owolarafe O.K. and all, „Mathematical modeling and simulation of the hydraulic expression of oil from oil palm fruit”, Biosystems Engineering 101, 331-340, 2008
- [12]. Sari P., „Preliminary design and construction of a prototype canola seed oil extraction machine”, Ph.D. Thesis, Middle East Technical University, Ankara, Turkey, 2006
- [13]. Willems P. and all, „Hydraulic pressing of oilseeds: Experimental determination and modeling of yield and pressing rates”, Journal of Food Engineering 89, 8-16, 2008
- [14]. Xiao J.B. and all, „Supercritical fluid CO₂ extraction of essential oil from *Marchantia convoluta*: global yields and extract chemical composition”, Electronic Journal of Biotechnology ISSN: 0717-3458, vol. 10, no. 1, 2007

ANALYSIS AND DESIGN OF A BIOMASS GASIFIER SYSTEM USING COMPUTATIONAL FLUID DYNAMICS

George IPATE¹, Gheorghe VOICU, Elena Madalina STEFAN, Mariana FERDES
University POLITEHNICA of Bucharest

ABSTRACT

The gasification technology is now considered to be in an advanced stage of development. Hence there is huge expectation from the user industry for its application. This work has been carried out in order to perform computer simulation in a biomass gasification systems developed at Department of Biotechnical Systems, Faculty of Biotechnical Systems Engineering, UPB. Computational fluid dynamics (CFD) has become a well known aiding tool in these regards as to characterize the conversion process, optimize the design, and visualize the flow fields in the reacting flow environment. Combustion and reduction chamber of reactor gasifier system is modeled as three-dimensional (3-D) with finite control volumes (CVs), where conservation of mass, momentum and energy is represented by fluid flow, heat transfer analysis, oxidation and reduction reaction modules. With this background, the commercial code Ansys-CFX has been used to perform CFD simulations and analysis, temperature distribution across the chamber and mass concentration of gasification products.

1. INTRODUCTION

Biomass is a general term to describe all organic carbon-containing material produced by photosynthesis in plants. Biomass is available in many forms, comprising products as well as residues from agriculture, forestry, and the agro-industry. Gasifier is a device for heating biomass in order to cause it to evolve volatile and flammable gases, which are then combusted to provide energy, typically for cooking or space-heating. Our research has shown that gasifier chars consistently achieve high temperatures (750-950 °C) required for substantial development of surface area and micro-porosity in the char product. Therefore, gasifier biochars are a promising appropriate, low-cost and sustainable technology for affordable decentralized water treatment in rural and developing communities.

One of the main drawbacks of the small-scale biomass combustion applications is the limited possibility to regulate the combustion process. In commercial gasifier installations efficient combustion process control is applied to minimize emission levels and to optimize the thermal efficiency. The main project aim is to gather insight in the processes inside the test gasifier, and determine how it could be controlled. The understanding of the process is needed for:

- develop a reliable model for the prediction of (dynamic) behavior;
- predict process output in uncontrolled operations;
- predict when the operation becomes dangerous or harmful, for instance when temperatures in the gasifier get too high.

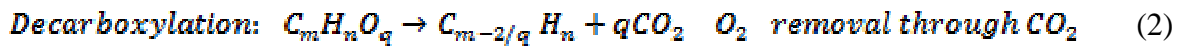
2. METHODOLOGY

Gasification is the complete thermal breakdown of biomass into a combustible gas, volatiles, char, and ash in an enclosed reactor or gasifier. Gasification is a two-step, endothermic (i.e. heat absorbing) process. In the first reaction, pyrolysis, the volatile components of the fuel is vaporized at temperatures below 600°C by a set of complex

¹ Corresponding author email : puiui pate@yahoo.com

reactions. Included in the volatile vapors are hydrocarbon gases, hydrogen, carbon monoxide, carbon dioxide, tar, and water vapor. Char (fixed carbon) and ash are the pyrolysis by-products, which are not vaporized. In the second step, the char is gasified through reactions with oxygen, steam, carbon monoxide and hydrogen. The heat needed for the endothermic gasification reactions is generated by combustion of part of the fuel, char, or gases, depending on the reactor technology.

Gasification of biomass also involves removal of oxygen from the fuel to increase its energy density. The oxygen is removed from the biomass by either dehydration or decarboxylation. The latter process, which rejects the oxygen through CO₂, increases the H/C ratio of the fuel so that it emits less greenhouse gas when combusted (Basu, 2010):



Product gas is generated by low-temperature (<1000°C) gasification. Gasification processes can be differentiated in direct (auto thermal) and indirect (or all thermal) processes. In most biomass applications the gasifiers are operated with air as gasification medium affording a product gas diluted with nitrogen. The choice for air or oxygen as gasification medium determines whether the product gas or biosyngas contains nitrogen. There is a large number of gasification processes in development. In downdraft gasifiers (co-current), the biomass feed and the gas stream moves in the same direction.

Gasification system design. Certain critical engineering design norms of the gasification system were first developed on a laboratory-scale model. These norms were then used to design a full-fledged commercial scale system with a thermal output of 288 MJ h⁻¹. This system (presently installed in the UPB campus) is seen in figure 1. It comprises of a reactor, a gas conditioning system, a heat exchanger and the burner. A schematic diagram of gasification processes is shown in figure 2 (adapted from Basu, 2010). The salient features of these components are given below.



Figure 1: Gasification system

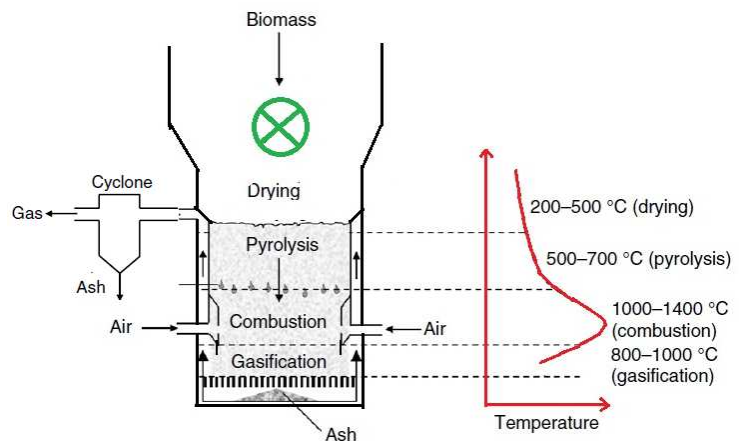


Figure 2: Product gas generation in a downdraft gasifier

a. **Reactor:** This was a downdraft, throatless and open-top reactor with an internal diameter of combustion chamber of 0.36 m and an active bed height of 0.79 m. It was designed for a heavy-duty cycle of 4200 hour per year operation.

b. **Gas conditioning system:** A completely dry dust collection system eliminated altogether the problem of wastewater. This consisted of a high efficiency cyclone separator and a

concentric tube heat exchanger (water coolant). This design is very environment-friendly. The char-ash from the cyclone was collected in barrels and emptied in an ash pit.

The gasification system was extremely simple to operate. A cold start took about ten-fifteen minutes whereas a hot start was effected in less than five minutes. Only one operator per shift of eight hours was required to operate the system, including the fuel and ash handling operations.

Fuel characteristics. The gasification system was successfully tested on wood pellets and corn cobs, etc. The physical properties of wood pellets under the actual operating conditions of the gasifier are given in table 1.

Table 1: Physical properties of biomass fuel

Particle size [mm]	10-20
Bulk density (dry) [kg/m ³]	580
Moisture content (wet) [%, w/w]	< 10 %

The size and density of the biomass fuel particles is also important. They affect the burning characteristics of the fuel by affecting the rate of heating and drying during the combustion process. Fuel size also dictates the type of handling equipment that is used (Ciolkosz, 2010). Table 2 gives the Proximate and Ultimate analysis of this fuel.

Table 2: Proximate and ultimate analysis of biomass (typical values)

A. Proximate analysis	
1. Fixed carbon, %	0.281
2. Volatile mater, %	0.652
3. Ash content, %	0.024
4. Higher heating value, MJ/kg	20.87
B. Ultimate analysis	
1. Carbon, %	0.32
2. Hydrogen, %	0.17
3. Oxygen, %	0.12
4. Nitrogen, %	0.39

Various designed parameters of the gasifiers are determined according to the recommendations given in the literature and based on the previous experience. Finally the following important parameters and dimensions are chosen for this analysis.

Table 3: Designed parameters of the gasifiers

1. Mass flow rate of wood =	3.5-7 kg/hr
2. Gas output =	8.5-17 Nm ³ /hr
3. Air requirement =	0.8- 1.6 kg/hr
4. Diameter of hearth =	0.33 m
5. Depth of reduction zone =	0.26 m
6. No. of nozzles =	6
7. Diameter of nozzle =	0.03 m

For simulation of the gasifier, an air inlet pipe has been taken into consideration where the exact combustion and reactions occurs in the biomass gasifier. The model for which

analysis has been considered is shown in the figure 3. The air passes through pipes to the nozzle area where air gets mixed with fuel (wood) which is coming from the top as shown in figure 5.

The geometry modeled as shown in figure 3 in Solid works, is exported to Ansys CFD software and meshing is generated. The unstructured triangular elements on surfaces and tetrahedral in flow domain are adopted in gasifier meshing as shown in figure 4. Number of nodes are 13710 and elements are 61091. The boundary conditions are applied, fuel inlet, air inlet and outlet of gas for heat transfer models. The figure 5 shows the air inlet and fuel inlet from top and product gas outlet to the cyclone. The air goes to the combustion area through the pipe with nozzles.

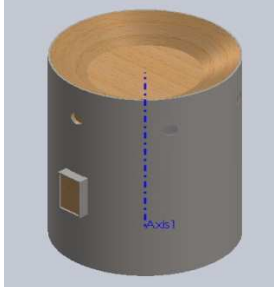


Figure 3: CAD model of reactor

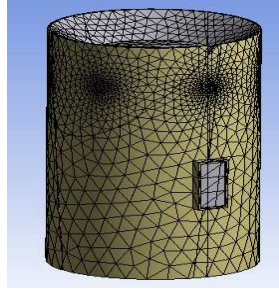


Figure 4: Meshed model

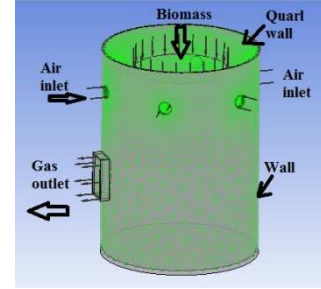


Figure 5: Boundary Conditions

3. RESULTS AND DISCUSSION

The initial moisture content fraction, air flow rate, temperature of the pyrolysis zone, and chemical composition of the biomass are required as an input data for the model to predict the composition of producer gas. The model is analyzed considering the wall of the combustion and reduction chamber. In this case an overall heat transfer coefficient ($U=20 \text{ W/m}^2 \text{ K}$, outside temperature $T=25 \text{ C}$) is used to represent the wall condition. The combustion starts only from the region where the air enters into chamber and the flow is downwards.

Airflow analysis is presented in figure 6 and shown the air velocity inside the reduction chamber varies from 1 to 4 m/s. The air flow is not reaching the wall efficiently and the gasification in this zone is poor.

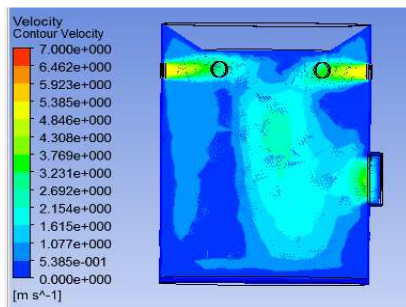


Figure 6: Air flow across the Reduction chamber

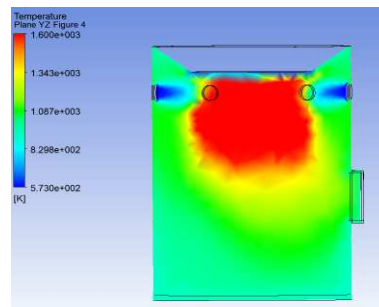


Figure 7: Temperature across the reactor

The temperature distribution across the gasification chamber is shown in the figure 7. The temperature is maximum at the combustion zone and in the wall region it varies from 1250 K to 1600° K. This maximum temperature of $\approx 1600^\circ \text{ K}$ is a little overestimated, but coincides

with the theoretical maximum of 1200° C (1473° K). The temperature at the outlet where the producer gas leaves the gasification chamber is about 800° C.

Figure 8 shows the mass fraction of oxygen, carbon dioxide, fuel gas (methane) and water vapor obtained in CFD at different levels, starting from the bottom of the reactor. However, validation of predicted results is essential to get confidence in the prediction procedure.

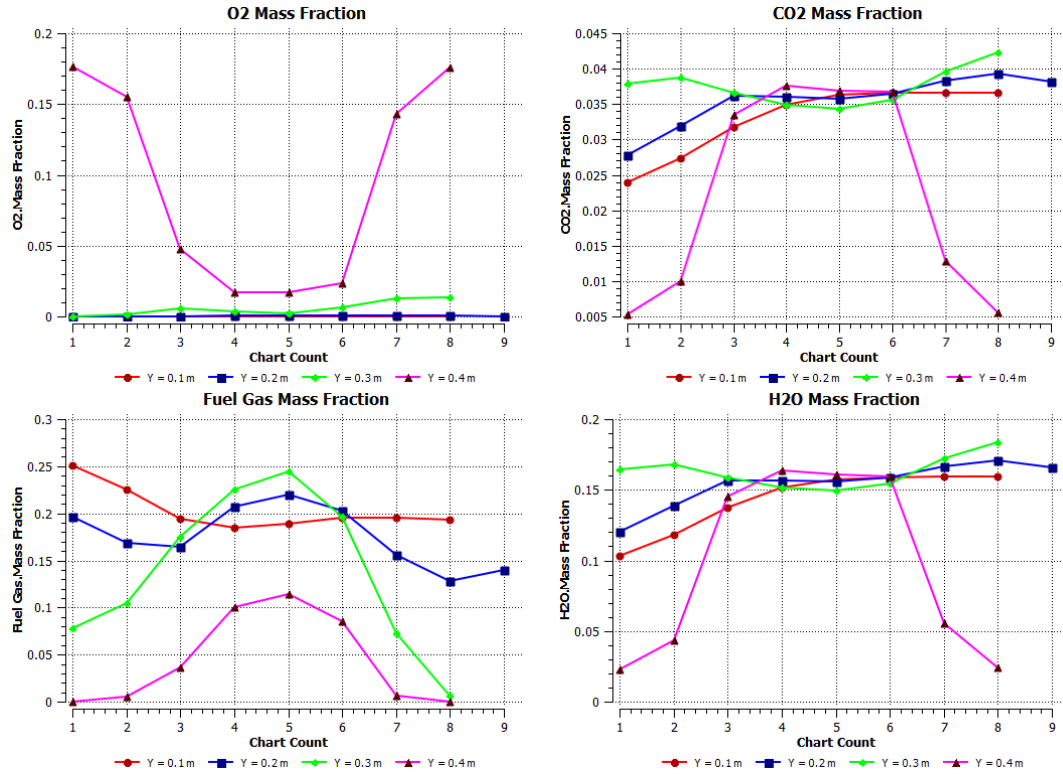


Figure 8: Predicted mass fraction of oxygen, carbon dioxide, fuel gas (methane) and water vapor

Gas concentration of CH₄, CO₂, N₂ and H₂O are shown in the figure 9. The approximate volumetric composition of producer gas at the outlet is H₂O - 16.1%, CH₄ - 1.08 %, CO₂ - 11.24 %, N₂ - 42.2 %.

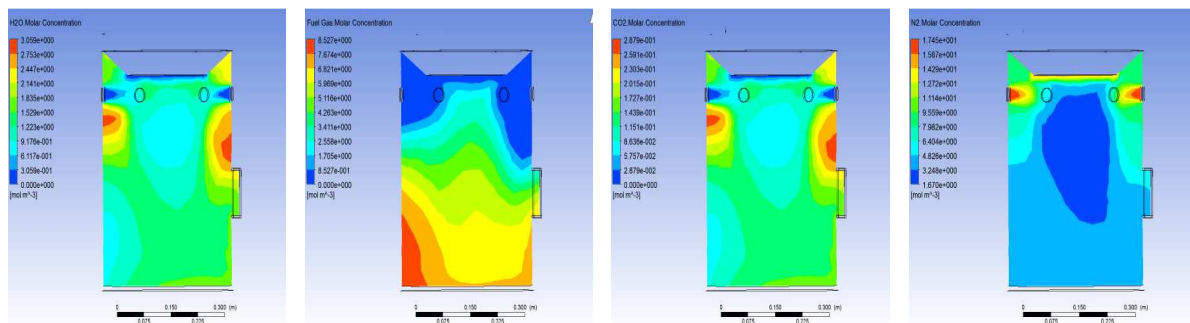


Figure 9: Predicted volumetric gas concentration of CH₄, CO₂, N₂ and H₂O

Air reaches all regions in the reduction zone efficiently when the average air velocity ranges from 3.5 m/s to 5 m/s. Gasification is almost complete and the gasification takes place throughout the reduction chamber when the maximum temperature produced is 1400° K. The percentage volumetric composition of CH₄ and CO₂ are well agree with the theoretical

prediction. The percentage volumetric composition of N_2 is higher than the theoretical prediction. This may be due to the poor gasification of biomass in the reduction chamber.

4. CONCLUSIONS

Biomass plays an important role in the actual global energy infrastructure for the generation of power and heat. The dominant biomass conversion technology will be gasification, as the gases from biomass gasification are intermediates in the high-efficient heat and power production. In the discussion on the utilization of gases from biomass gasification it is important to understand that the composition of the gasification gas is very dependent on the type of gasification process and especially the gasification temperature. The volume of gas obtained from gasification is much less compared to that obtained from a direct combustion system, but the lower volume of gas requires smaller equipment and hence results in lower overall costs.

Predictions for gas composition, temperature profile and gasification efficiency are found to be very sensitive within the encountered range of mass flow rate. Biomass gasification process is a very complex and difficult case for numerical investigation, as it entails multiphase flow, turbulent dynamics, heat transfer, species transport and chemical reactions. Also, due to data unavailability, certain modeling parameters were adopted by the corresponding literature.

References

- [1] Basu, P., *Biomass gasification and pyrolysis : practical design and theory*, Academic Press, Published by Elsevier Inc., 2010.
- [2] Boerrigter, H., Rauch, R., *Review of applications of gases from biomass gasification*, Published as Chapter 10, titled: "Syngas production and utilisation" in the Handbook Biomass Gasification, Biomass Technology Group (BTG), Netherlands, 2005.
- [3] Ciolkosz, D., *Characteristics of Biomass as a Heating Fuel*, The Pennsylvania State University, 2010.
- [4] Hansson, J., Leveau, A., Hultberg, C., *Biomass Gasifier for Computer Simulation*, Rapport SGC 234, August, 2011.
- [5] Jorapur, R., Rajvanshi, A.K., *Sugarcane leaf-bagasse gasifiers for Industrial heating applications*, Biomass and Bioenergy, Vol 13., No. 3, pp141-146, 1997.
- [6] Paes T., *Modeling for control of a biomass gasifier*, TU/e Eindhoven, 2005.
- [7] Sharma, A.Kr., *Modeling and simulation of a downdraft biomass gasifier 1. Model development and validation*, Energy Conversion and Management 52, pg 1386–1396, 2011.
- [8] Sivakumar, S., Pitchandi, K., Natarajan, E., *Design and Analysis Of Down Draft Biomass Gasifier using Computational Fluid Dynamics*, http://driveonwood.com/sites/default/files/pdf/b044_p12.pdf.
- [9] Sofialidis, D., Faltsi, O., *Design simulation of biomass gasification in Fluidized beds using computational Fluid dynamics approach*, Thermal Science: Vol. 5, No. 2, pp. 95–105, 2001.
- [10] Zachary, H., *Simulation and economic evaluation of coal gasification with sets reforming process for power production*, Louisiana State University, 2005.
- [11] *** *BTG Biomass Gasification*, BTG biomass technology group BV, www.btgworld.com, 2008.
- [12] *** *Handbook of Biomass Downdraft Gasifier Engine Systems*, Solar Energy Research Institute, U.S. Department of Energy, 1988.

THE USE OF DIMENSIONAL ANALYSIS FOR THE MATHEMATICAL MODELATION OF SOME WORK PROCESSES IN AGRICULTURAL MECHANICS

Prof.univ.dr.ing. Constantin MANOLE
Facultatea I.S.B., Universitatea Politehnica din București

Keywords: dimensional analysis, mathematical modeling, agricultural mechanic, work process, fundamental physical quantities, liquid medium, hole digging machine, threshing device.

Abstract

Dimensional analysis is a principal used in mechanical engineering in order to create pertinent hypotheses which are to be verified experimentally or through more advanced theories. Thus, between any physical phenomenon and its determinants, a set of equations will be established, which, after being solved, will lead to a more simple interpretation, but rigorous at the same time, of the respective phenomenon. In the present case the method will firstly be applied to verify some already known relationships, and in the second phase – in the study of some work processes in agricultural mechanics.

1. Introduction

Concerning the complex physics phenomenons – situation often met in agricultural mechanics – setting calculus relationships between the parameters which establish a work process is relatively difficult. Though, by imposing the condition for dimensional homogeneity of the measures which occur in the study of a physical phenomenon, a system of equations, whose solutions represent the exponents of the physical measures which characterise the considered phenomenon, will result.

The advantage of the method consists in the fact that the number of unknowns from the final expression reduces up to three, that is reduces with the number of the fundamental physical measures involved in the process, the latter being represented by three elements in mechanics: mass, length, time.

2. The application of dimensional analysis in the modelation of some work processes in the field of agricultural mechanics

2.1. The calculus of the theoretical output of liquid through a loop

The fact that the theoretical output of liquid through a loop is given by the section of the loop "S", the position "h" of the loop towards the reference level and the gravitational acceleration "g", at different powers, is well known.

Though, the formula of the debit can be written as: $Q = k \cdot S^{x_1} \cdot h^{x_2} \cdot g^{x_3}$ (1)

whose dimensional equation is: $\frac{m^3}{s} = (m^2)^{x_1} \cdot m^{x_2} \cdot (\frac{m}{s})^{x_3}$

By identifying the exponents, the following equation system will be obtained:

$$\begin{cases} 3 = 2x_1 + x_2 + x_3 \\ -1 = -2x_3 \end{cases} \quad \text{with the solutions} \quad \begin{cases} x_1 = \frac{5}{4} - \frac{1}{2}x_2 \\ x_2 = x_2 \\ x_3 = \frac{1}{2} \end{cases} \quad (2)$$

By introducing the solutions (2) into the debit formula (1), we obtain:

$$Q = k \cdot S^{\frac{5}{4} - \frac{1}{2}x_2} \cdot h^{x_2} \cdot g^{\frac{1}{2}}$$

which can be also written: $Q = k \cdot S^{\frac{5}{4}} \cdot (\frac{h}{\sqrt{S}})^{x_2} \cdot \sqrt{g}$ (3)

where the measures k and x_2 are expected to be experimentally determined.

Indeed, for $\sqrt{2}$ and $x_2 = 1/2$ the following well known relationship is obtained for the theoretical debit:

$$Q = S\sqrt{2gh} \quad (4)$$

As seen, the number of complex adimensional measures from the relationship (3) is equal to the unity, meaning equal to the number of measures which establish the phenomenon (three: S , h and g), except the number of fundamental measures used (two: length and time).

2.2. Establishing the expression of the necessary power for driving a centrifugal pump

The expression of the engine power for driving a centrifugal pump, which pumps a debit Q at a height h is given by the density of the fluid ρ , the rotation speed of the impeller of the pump n , the diameter of the pump d and the product gh , can be written as:

$$N = k \cdot \rho^{x_1} \cdot n^{x_2} \cdot d^{x_3} \cdot (Q)^{x_4} \cdot (gh)^{x_5} \quad (5)$$

whose dimensional equation is:

$$\frac{kg \cdot m^2}{s^3} = \left(\frac{kg}{m^3}\right)^{x_1} \cdot \left(\frac{1}{s}\right)^{x_2} \cdot (m)^{x_3} \cdot \left(\frac{m^3}{s}\right)^{x_4} \cdot \left(\frac{m^2}{s^2}\right)^{x_5}$$

Through identification, the following equation system is obtained:

$$\begin{cases} 1 = x_1 \\ 2 = -3x_1 + x_3 + 3x_4 + 2x_5 \\ -3 = -x_2 - x_4 - 2x_5 \end{cases} \quad (6)$$

with the solutions:

$$\begin{cases} x_1 = 1 \\ x_2 = 3 - x_4 - 2x_5 \\ x_3 = 5 - 3x_4 - 2x_5 \end{cases} \quad (7)$$

By substituting the measures (7) into the equations (6), we obtain:

$$N = k \cdot \rho \cdot n^3 \cdot d^5 \cdot \left(\frac{Q}{nd^3}\right)^{x_4} \cdot \left(\frac{gh}{n^2 d^2}\right)^{x_5} \quad (8)$$

where k , x_4 , x_5 will be experimentally determined.

Two adimensional complex functions are obtained (five measures which determine the phenomenon, minus three fundamental measures with which the five sizes which determine the phenomenon are represented).

2.3. Establishing the expression of the thrusting resistance of a body into a fluid environment

To find the expression of the resistance R at the thrusting of a body into a fluid environment, knowing that this is given by the density ρ of the fluid, the maximum cross section offered by the body S , the relative speed v of the body in the fluid environment and the dynamic viscosity η , the following functions relationships can be written:

The dragging resistance can be written as:

$$R = k \cdot \rho^{x_1} \cdot S^{x_2} \cdot v^{x_3} \cdot \eta^{x_4} \quad (9)$$

whose dimensional equation is: $\frac{kg \cdot m}{s^2} = \left(\frac{kg}{m^3}\right)^{x_1} \cdot (m^2)^{x_2} \cdot \left(\frac{m}{s}\right)^{x_3} \cdot \left(\frac{kg}{ms}\right)^{x_4}$.

We obtain the equation system: $\begin{cases} 1 = x_1 + x_4 \\ 1 = -3x_1 + 2x_2 + x_3 - x_4 \\ -2 = -x_3 - x_4 \end{cases}$ with the following solutions:

$$\begin{cases} x_1 = 1 - x_4 \\ x_2 = 1 - \frac{x_4}{2} \\ x_3 = 2 - x_4 \end{cases} \quad (10)$$

By substituting the solutions (10) in the equation (9), then:

$$R = k\rho S v^2 \left(\frac{\eta}{\rho \sqrt{S} v} \right)^{x_4} \quad (11)$$

By analysing the expression (11) for the values 0 and 1 of the exponent x_4 .

$$\text{a) } x_4 = 0 \rightarrow R = k \cdot \rho \cdot S \cdot v^2 \quad (12)$$

The relationship obtained for $x_4 = 0$ is the expression of the hydrodynamic resistance force at the thrusting of a body into a fluid environment, in the case of the neglect of the viscosity forces.

$$\text{b) } x_4 = 1 \rightarrow R = k \cdot \eta \cdot v \cdot \sqrt{S} \quad (13)$$

If we admit a circular pipe, we will have $S = \pi \cdot r^2$, and then $R = k\sqrt{\pi} \cdot \eta v r$ (14)

For $k = 6\sqrt{\pi}$, the *Stokes law* will result: $R = 6\pi\eta v r$.

2.4. Establishing a calculus relationship concerning the necessary power for the drill shaft digging machine

The scientific literature (relationship 7.22, page 191, [3]) indicates that for the necessary power for the drill shaft digging machine, the calculus formula is:

$$P = \frac{2nM_r}{450000\eta_m} \quad (15)$$

where n is the rotation of the drill [rev/min]; η_m – the mechanical efficiency of the transmission; M_r – the resistant moment at the drill shaft,

$$M_r = k_g \frac{\pi D^2}{4} s \quad (16)$$

where k_g is the specific resistance for digging holes [daN/cm²], D – diameter of the drill [cm], s – advance of the drill per rotation [cm/rev].

By substituting the expression (16) in (15), for the necessary power for the drill shaft, the following relationship is obtained (17):

$$P = \frac{0,736\pi}{9 \cdot 10^5 \eta_m} n \cdot D^2 \cdot s \cdot k_g \quad (17)$$

From a dimensional analysis of the relationship (17), it results that the power is given by the parameters k_g , n , D , s . In fact, the phenomenon is more complex than the one given in

the relationships (17); the necessary power for the drill shaft is used both for the splintering of the soil, as for raising the soil from the hole, for defeating soil friction and the drill of the hole wall and for throwing the soil around the hole.

This means that in addition to the listed parameters, for a closer realistic appreciation of the phenomenon, it is necessary to also consider other measures which characterise the energetic consumption per time unity at the hole digging, such as, the material flow rate, the gravitational acceleration, the depth of the hole, the height of the material layer thrown around the hole.

Analogously to this, the relationship (18) is obtained, which expresses the maximum power dependence (when the drill is in the terminal phase of digging the hole) on the parameters $Q_m, g, \omega, D, k_g, s, p$, which determine the phenomenon.

$$P = k \frac{Q_m \cdot g^2}{\omega^2} \cdot \left(\frac{D \cdot \omega^3}{g} \right)^{x_3} \cdot \left(\frac{g \cdot k_g}{Q_m \cdot \omega^3} \right)^{x_5} \cdot \left(\frac{\omega^2 \cdot s}{g} \right)^{x_6} \cdot \left(\frac{\omega^2 \cdot p}{g} \right)^{x_7}, \quad (18)$$

The terms x_3, x_5, x_6, x_7 are to be experimentally determined.

2.5. Establishing the expression of the power consume for the shaft nozzle of a threshing machine, for defeating the passive resistance related to air entrapping

The scientific literature [2, page 409, vol. II] shows that the power consume for the shaft nozzle of a threshing machine for defeating the passive resistance related to air entrapping is proportionate to the third speed of the angular velocity ω and at the same time depends on:

- γ_a – the specific air weight, N/m³;
- F – the frontal area of a bar with studs or of a rail, together with its stand, m²;
- r_f – the radius of the nozzle, measured from the center of the frontal surface, m;
- g – gravitational acceleration, m/s²;
- ω – the angular velocity of the nozzle, 1/s.

The power for the shaft nozzle will be:

$$P = k \cdot (\gamma_a)^{x_1} \cdot (F)^{x_2} \cdot (r_f)^{x_3} \cdot (g)^{x_4} \cdot (\omega)^{x_5} \quad (19)$$

whose dimensional equation has the following form:

$$\frac{kg \cdot m^2}{s^3} = \left(\frac{kg}{m^2 \cdot s^2} \right)^{x_1} \cdot (m^2)^{x_2} \cdot (m)^{x_3} \cdot \left(\frac{m}{s^2} \right)^{x_4} \cdot \left(\frac{1}{s} \right)^{x_5}$$

Through identification, the equation system is obtained:

$$\begin{cases} I = x_x \\ 2 = -2x_1 + 2x_2 + x_3 + x_4 \\ -3 = -2x_1 - 2x_4 - x_5 \end{cases}$$

with the solutions:
$$\begin{cases} x_1 = 1 \\ x_2 = 2 - \frac{x_3}{2} - \frac{x_4}{2} \\ x_5 = 1 - 2x_4 \end{cases} \quad (20)$$

By substituting the values of the main unknowns x_1, x_2, x_3 in the relationship (19), it results:

$$P = k \cdot \gamma_a \cdot (F)^{2 - \frac{x_3}{2} - \frac{x_4}{2}} \cdot (r_f)^{x_3} \cdot (g)^{x_4} \cdot (\omega)^{1 - 2x_4}$$

or

$$P = k \cdot \gamma_a \cdot F^2 \cdot \omega \cdot \left(\frac{r_f}{\sqrt{F}} \right)^{x_3} \cdot \left(\frac{g}{\sqrt{F} \cdot \omega^2} \right)^{x_4} \quad (21)$$

relationship which represents the necessary power for defeating the passive resistances related to air entrapping.

In the relationship (21), the coefficients k, x_3, x_4 are to be experimentally determined.

3. Conclusions

The dimensional analysis method can be easily applied when the physical studied phenomenon includes up to 5-6 physical measures, because thus, the composition of the complex adimensional measures does not show any difficulties. In the case where the number or the physical measures which influence the studied phenomenon passes 5 or 6, the composition of the complex adimensional measures becomes difficult. In such cases the *Teorema π* [1] is used.

4. References

- [1] – Vasilescu, Al.A., *Dimensional Analysis and the Theory of Similarity (Analiza dimensională și teoria similitudinii)*, Published by: Editura Academiei R.S.R., Bucharest, 1969.
- [2] – Krasnicenko, A.V., *The Book of the Manufacturer's Agricultural Machinery (Manualul constructorului de mașini agricole)*, vol. I and II, Published by: Editura Tehnică, Bucharest, 1963. (Translation from Russian).
- [3] – Scripnic, V., Babiciu, P., *Agricultural Machinery (Mașini agricole)*; Published by: Editura Agrosilvică; Bucharest, 1968.

PROMOTION OF A TECHNICAL EQUIPMENT ENDOWED WITH ACTIVE WORKING PARTS DRIVEN FOR SOIL DEEP LOOSENING

PhD. Eng. Eugen MARIN¹, PhD. Stud. Eng. Alexandru DAVID,
PhD. Stud. Eng. Mihai MATAACHE, Prof. PhD. Eng. Ion PIRNĂ

National Institute of Research - Development for Machines and Installation designed to
Agriculture and Food Industry - INMA Bucharest

ABSTRACT

This paper presents the results of experimental researches of a technical equipment endowed with active working parts driven for assuring the soil deep loosening, equipment designed and performed within INMA Bucharest. For determining the working indexes in field, the technical equipment worked in aggregate with New Holland wheeled tractor of T6070 type, of 103 kW (140 HP). The output obtained after the experimental researches in working conditions appropriate to agricultural fields of INMA Bucharest, allows to achieve a profound modification of soil features in the settled and impermeable horizon, thus increasing the water stock capacity, creating the conditions suitable to a normal soil aeration and heating and stirring up soil biological processes. At the same time, for enhancing the rural development, useful recommendations may be drawn up to farmers who will use the respective technical equipment, in order to restore the heavy and settled fields, alternatively affected by excess and lack of humidity.

1. INTRODUCTION

Currently at European level soils have a high susceptibility to the occurrence of negative processes of degradation by compaction.

Arable land that apply to conventional agricultural technologies, where the main component is the basic return furrow plowing, are most vulnerable to the appearance of surface and subsoil compaction (depth) [1].

Analyzing the two processes both economically and environmentally friendly, compacting the surface has a strong negative impact compared to the subsoil (depth). However in terms of sustainability, compaction of subsoil (depth) is more serious, as shown since 2004 reports the technical working groups established under the Thematic Strategy for Soil Protection [2].

In the definition of the subsoil the so-called "hardpan" is the top part of the subsoil and in many cases the most powerful compacted layer. By applying mechanical work or from natural processes by loosening soils affected by surface compaction can be remedied, they reach an optimal quality level in a relatively short time [3].

Subsoil compaction, is a cumulative process that intensifies over time, eventually leading to the formation of a homogeneous compacted layer. The resilience of the subsoil compaction is reduced, so compaction of the subsoil remains in time. There is a close relationship between compaction and erosion by water flooding since the compaction of surface and underground water infiltration capacity of the soil is diminished [4].

Seeking to meet these requirements, and given the extremely negative effects caused by subsoil compaction appearance in the paper were carried out experimental research into working conditions farmland on the site INMA Bucharest with a technical equipment with active parts driven for deeply loosening the soil

¹ 6, Ion Ionescu de la Brad Blvd., Division 1, Bucharest, Tel. 0749176922, Email: marin_43eu@yahoo.com

2. METHODOLOGY

Experiments were performed with an aggregate consisting of a machine with active organ involved for loosening the soil depth (Fig. 1) designed to INMA Bucharest and New Holland T6070 tractor with the following characteristics: overall dimensions (length \times width \times height), m: $5347 \times 2230 \times 3040$, mass, kg: 10000; wheelbase m: 2734; axle track width front / rear, m: 2030/2030, engine power: 103 kW (140HP) [5].

Main assemblies of machinery with active bodies for working towards raising the soil are provided at the front yoke with hydraulic cylinder for coupling the three-point linkage of the tractor; actively working body with a vertical oscillating knife and a vibrating chisel peak, transmission shaft and gear consists of conical left and right outputs, flexible couplings with bolts, right and left wheels to adjust the working depth; support leg to support when stationary, aggressive shredding roller, placing and additional leveling clods .

Technical equipment is connected to the tractor slow down and placed in the ground until the wheels touch the ground to support the set working depth. By moving the tractor and the cutting blades cause loosening soil from a maximum depth to the surface, due to the oscillating movement in the vertical plane of the blade tips, carried by the eccentric drive system.



Figure 1: Technical equipment with active parts driven for deeply loosening the soil

Main technical characteristics of the machinery used in experimental research are presented in Table 1.

Table 1: Main technical characteristics

Characteristic	Value
Equipment type	carried
Number of active parts [pcs]	2
Type of active parts	vibrating
Distance between working parts [m]	1.9
Diameter of supporting wheels and depth [m]	0.5
Maximum working depth [m]	0.8
Clearance [m]	0.35
Diameter of teeth roller [m]	0.46
Mass [kg]	1290

Experimental researches for the determining the technical equipment indicators in the field were made on agricultural land within the INMA Bucharest perimeter, under the following conditions:

- Soil type: red brown forest
- Soil category (in terms of specific resistance): medium to hard
- Previous crop: onions
- Previous work: harvesting with onion harvesting machine
- Technical equipment working depth: 60 cm
- Other considerations: the land was covered with crop residues remaining after harvest.

In accordance with the approved INMA-DI test procedures, during experimental research were used the following equipment for measuring and monitoring (EMM) and checked in metrological terms :

- Digital electronic cone penetrometer FIELDSCOUT SC 900;
- Capacitive soil moisture analyzers FIELDSCOUT TDR 300;
- The navigation Garmin GPSMAP 60 CSX;
- Frame with strain gauges;
- Transducer time-S2 + T4WA speed Hottinger;
- National Instruments data acquisition card USB 6343;
- Tachometer Extech Instruments 461 995.

The frame with strain gauges (Fig. 2) consists of three frames (central side 1 and two lateral ones 2, 3) and five adjustable supports four elastic rings that can be mounted by fasteners in three positions, making it possible coupling both suspending the three-point category 3, 3N, 4, 4N according to ISO 730:2009 [6] as tractors and agricultural machinery coupling devices of the the categories.



Figure 2: The frame with strain gauge marks, coupled to three-point linkages 3 category according to ISO 730:2009

Compactness of the soil was determined after measuring the resistance to penetration by digital electronic cone penetrometer FIELDSCOUT SC 900. For measuring was selected 0.01 m² cone with top angle of 60 °. Data storage was performed in the "data logger" and the location of sample points was connected navigation device Garmin GPSMAP 60 CSX. When performing penetration tests and relative humidity measured at ground level using capacitive soil moisture analyzers FIELDSCOUT TDR 300. Data on penetration resistance values and the depth of penetration of the cone penetrometer in soil and soil relative humidity were measured in the form of electrical signals whose levels were followed dials with digital display and recorded in memory devices as they were downloaded to a computer for processing.

One aspect during penetration resistance measurement is shown in Figure 3.



Figure 3: Aspect during penetration resistance measurement

For the determination of the energy indicators we used the strain gauge method [7] using a computer software package for measuring nSOFT speeds and torques, determining the amount of time the PTO and PTO speed idle and under load. To record measurements was used a laptop equipped with card purchase.

In these experimental studies measurements have been carried out [8] for the following parameters:

- Torque at the PTO;
- Thrust the bar coupling of technical equipment to the tractor;
- Tractor engine speed and PTO speed;
- The speed of the unit.

P_p is the power transmitted through PTO determined by the relation (1) ([8], [9]),

$$P_p = M_p \cdot \omega_p \quad [\text{W}] \quad (1)$$

where:

M_p is transmitted torque PTO shaft in Nm;

ω_p - angular velocity PTO shaft in rad / s

P_{tr} - power required to tow the technical equipment on a horizontal field in work conditions was calculated with equation (2):

$$P_{tr} = F_t \cdot v_l \quad [\text{W}] \quad (2)$$

where:

F_t is the pulling force measured in the coupling bar, N;

v_l - working speed (travel) in m/s

Analyzing the results of experimental research, of the tractor unit T6070 NEW HOLLAND with the technical equipment with active bodies involved to work towards loosening the soil, resulted as follows:

- active bodies and toothed roller by their structural and functional parameters, ensure the implementation of a quality, soil conditions in the experimental field INMA Bucharest for setting the working depth of 0.6 m;
- from the samples taken at a depth of 0.45 m of soil compactness, the experimental group showed that 53.2% of the area is easily compacted soil (penetration resistance values were between 2000 ... 2500 MPa), 30.5% ground poorly compacted (penetration resistance values were between 2500 ... 3000 MPa), and 16.3% occurring high resistance to penetration over

3000 MPa, so heavily compacted soil. Mean soil moisture was about 22.433%, a value that represents the optimal limit allowed for deep soil loosening work;

- from an average travel speed of 0.91 m / sa result a mean thrust 76530 W (104.08 hp).

Figure 3 presented an aspect during the determination of the thrust and in Figure 4 is shown a diagram of the resulting traction force for the first trial.



Figure 3: Image during determining the traction force

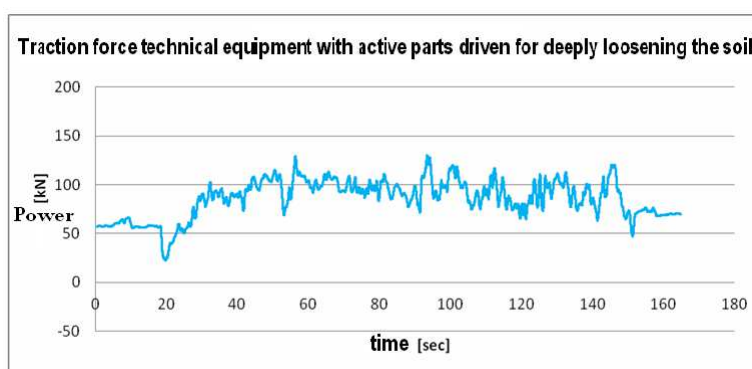


Figure 4: Traction diagram

Based on the data obtained and processed during experimental research in table. 2 shows the measured values determined in field of the technical equipment to perform the tests.

Table 2: Valorile măsurate și determinate ale indicilor în câmp

Proba	Working speed, v_1 m/s	Traction force, F_{tr} N	Average traction power, P_{tr}		Power transmitted through PTO, P_p	
			kW	CP	kW	CP
1	1.02	85480	87.850	119.48	1.903	2.59
2	1.02	87520	89.950	122.33	1.764	2.4
3	0.72	61850	61.810	84.06	2.116	2.88
4	0.86	80070	68.940	93.77	2.462	3.35
5	0.94	78480	74.120	100.80	2.829	3.85
Media	0.91	78680	76.530	104.08	2.214	3.01

3. CONCLUSIONS

- By performing experimental research was permitted partial validation of technical and technological solutions constructively approached in the design of main structure and strength of the working bodies of the technical equipment.
- In the final validation is necessary to carry out further experimental research the machinery tractor unit with a power greater than 103 kW (140 hp), working at depths of 0.6 m, but that not exceed 0.8 m (maximum operating depth).
- The experimental results allow the development of recommendations made useful for farmers who use agricultural machinery application of innovative technology amending soil horizon characteristics compact, compacted and impermeable.

References

- [1] Lobert M., Boken H. and Glante F., *Soil compaction – indicators for the assessment of harmfu; changes to the soil in the context of the German Federal Soil protection, Act.* Journal of Environmental Management 82, 388-397., ELSEVIER, 2007
- [2] Van-Camp. L., Bujarrabal, B., Gentile, A-R., Jones, R.J.A., Montanarella, L., Olazabal, C. And Selvaradjou, S-K. (). *Reports of the Technical Working Groups Established under the Thematic Strategy for Soil Protection.* EUR 21319 EN/5, 872 pp. Office for Official Publications of the European Communities, 2004, Luxembourg.
- [3] Van den Akker, J.J.H. and Schjønning, P., *Subsoil compaction and ways to prevent it.* Chapter 10 in: Schjønning, P., Elmholt, S. and Christensen, B.T. (eds.). *Managing Soil Quality: Challenges in modern agriculture.* CAB International, Wallingford, pp 163-184, Oxon, UK 2004.
- [4] Christy van Beek and Gergely Tóth, *Risk Assessment Methodologies of Soil Threats in Europe*, EUR 24097 EN – Joint Research Centre – Institute for Environment and Sustainability, Luxembourg: Publications Office of the European Union, 2012
- [5] www.agriculture.newholland.com/uk/en/Products/Tractors, 2011
- [6] ***ISO 730:2009: Agricultural wheeled tractors -- Rear-mounted three-point linkage -- Categories 1N, 1, 2N, 2, 3N, 3, 4N and 4, International Organization for Standardization, 2009
- [7] Constantinescu I., *Measurement of mechanical quantities using tensometriei*, Technical Publishing Bucharest, Romania, 1989
- [8] Popescu S., Năstăsoiu S., Tane N., *Considerations on the power consumption of agricultural machinery operated by PTO tractor* CIT Bulletin, vol. I, pag. 221-226, Braşov, Romania, 1988
- [9] Tecuşan N., Ionescu E., *Tractors and automobiles*, Didactic and Pedagogic Publishing, Bucharest, Romania, 1982

TECHNOLOGICAL EQUIPMENT FOR WEIGHING AND AUTOMATIC MANAGEMENT OF FINISHED PRODUCTS PACKED IN SACKS WITHIN MILLING UNITS OF SMALL AND MEDIUM CAPACITY

Eng. Milea D., PhD.Eng. Păun A., PhD.Eng. Pirnă I., Dr. Eng. Brăcăcescu C., Eng. Ludig M.

INMA Bucharest

Abstract

In this paper is presented modern technical equipment realised by INMA, intended for the milling units of small and medium capacity, performing simultaneously the weighing and automated management of the finished products packaged in sacks (flour and bran).

In order to increase of productivity, the device is provided with two working places serviced by a single operator and by the same electronic system for control and automated management.

The dosage of the quantities of product loaded in sacks is performed of two screw conveyers, one for grossly dosing, and one for fine dosing. During the process of dosing and weighing the two snails will have two regimes of speed.

Weighing of the products in bags is carried out through some tensometric doses transmitting the mass information to a PLC integrated into the automation installation of the equipment. The alternative supply left - right of the two bagging holes is achieved by the automatic changing of the direction of rotation of the dosing snails.

1. INTRODUCTION

Weighing, dosing and automatic management are processes that remove totally or partly the human intervention in the actual operations. Modern devices for weighing, dosing and automatic bagging are ingenious technical solutions that include from both the mechanical and the electronics fields and have high responsiveness and precision.

The weighing and dosing operations and also the technical equipment that perform these operations have a constructive and functional diversity in relation to various application.

The systems field and the fields for weighing equipment, dosing and packaging of agricultural food products is one of the fields with great economic impact in Romania (especially in recent years), but also in industrial developed countries.

Weighing and dosing technological operations are not independent in the manufacturing of products, but integrated into diverse processes so that the operation result does not distinctively show, and is cumulated in the final product. As a result, the quality of dosing / weighing directly influences the quality of the final product.

To define the technological operations of weighing and dosing, the following are required:

- knowledge of the volume to be partitioned;
- establishing a control parameter;
- transporting the product.

Using the *methods and technologies of automatic weighing* and dosing brings increased efficiency and has an immediate impact on the records of delivered material, also leading to increased quantity of products packed in bags and precision weighing.

2. METHODOLOGY

The technological equipment for weighing and automated management ECGA (fig. 1) designed within the project can be applied for milling units of small and medium capacity, open bags packing processes of finished products (flour and bran) which accomplishes two very important operations:

- automatic programmed weighing of bags with product that is done with a precision within the prescribed limits;
- automatical management of finished product quantities, packaged in bags for unspecified periods of time.

The equipment can be successfully integrated in technological flows for obtaining nutrients from the units that are associated with concentrated fodder or other units performing specific granular or powder packaging in bags.

It is equipped with two workstations driven by the same electronic control and management system eliminating equipment downtimes when changing bags. The manual laying solution for the bags was chosen and fitted with adjustable straps that have a special lock, and no more attaching it with a pneumatic device that requires more time to change the bag and equipping the unit with compressed air, resulting more extra investment costs.

Each bag has a closing flap controlled by a linear electric actuator. Determination of the amount of product loaded in bags is done by 2 worms; one for rough dosing and one for fine dosing. Their operation is done through two gearmotors.

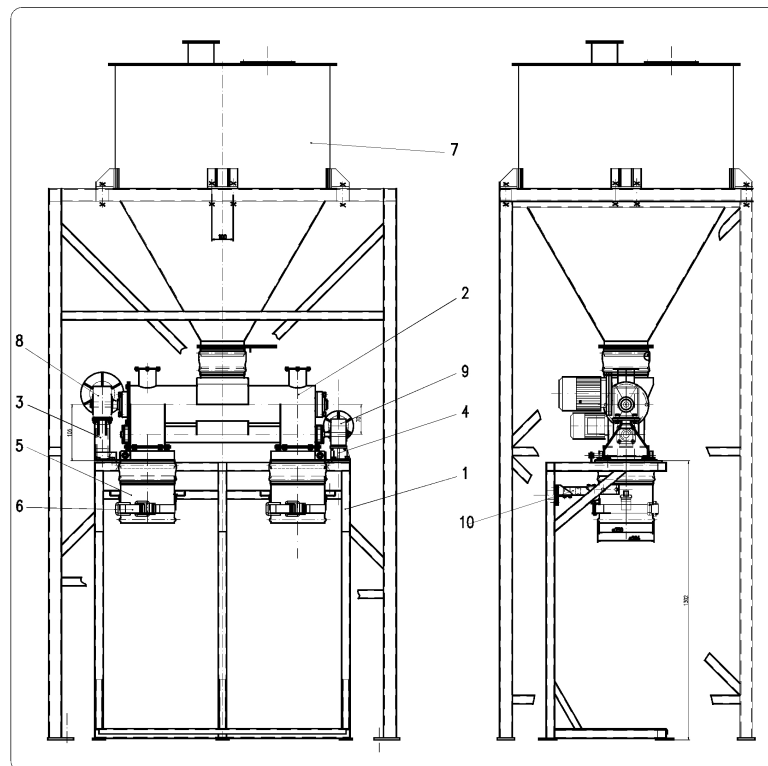


Fig. 1 - Automatic equipment weighing and management

- 1 Support frame; 2 - dosing group; 3 - gearmotor support 1; 4 - gearmotor Support 2;
5 - Bag opening; 6 - bag attachment strap; 7 - Bunker; 8 - gearmotor 1;
9 - gearmotor 2; 10 - strain gauge dose

ECGA technological equipment for weighing and automatic management, is shown in figure 1 and it is essentially composed of:

The support frame it is a rigid welded construction with has the role of supporting some component parts of the equipment for weighing and automatic management (dosing group, supports for gear motors, electric actuators, strain gauges, etc.)

Dosing group (Fig. 2). Is the subassembly that puts the doses into bags. It consists of a metal housing (position 1) with two drain cylinders within which worms rotate for dosage (poz.2 and poz.3). Worms are mounted inside the housing via spherical bearings that ensure a good seal against dust of any kind.

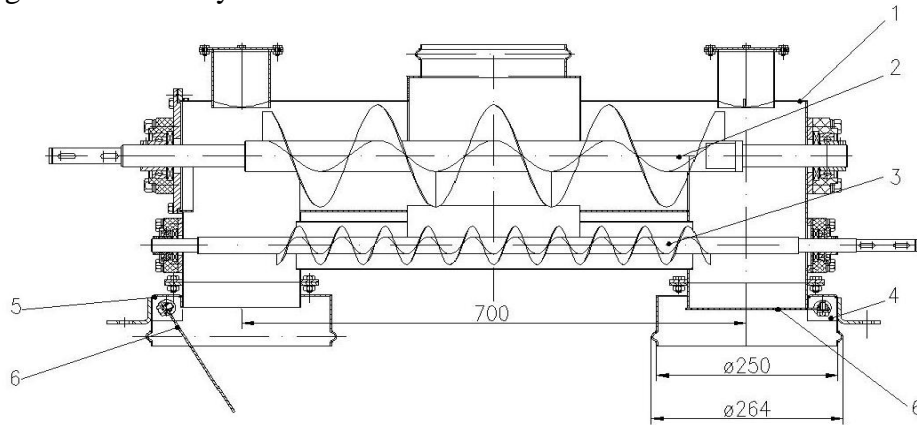


Figure 2: Dosing group

1-Housing; 2-Rough dosing worm; 3- Fine dosing worm;
4- Drainage opening 1 ;5- Drainage opening 2 ; 6- Flap

Bag opening, serves for sack supporting during filling and weighing.

It consists of a cylindrical tube of metal sheet on which mounting brackets are welded for mounting strap for bag setting, and a support that helps the opening to be mounted on the strain gauge.

Assembled strap serves for fastening by tightening the Bag on the bag's opening during filling and weighing process. Fastens on the bag opening and has a sealing and tightening system that ensures safe fixing of the bag and its rapid change after completion of filling and weighing processes.

The bunker stores a quantity of material to provide constant dosing to the group. It consists of a metal welded square pipe, on which the storage container is mounted which have above, removable cover on which the power connection stands. The connection between the bunker and the dosing group is elastical by means of a special fabric bellows.

Automation system is composed of a box in which the following main components are mounted; The PLC which has at least two analog inputs with a serial communication module for converters and signal amplifiers for strain gauge doses, an operating terminal with touchscreen, frequency inverters for gear motors, controllers for electric actuators.

In addition to the main components described above, beside sthe the automation equipment a number of auxiliary components can be found, such as a network manual, circuit breaker for motor protection, tripollar fuse, 24 VDC switching power source, start-stop buttons, emergency stop button, cables, etc.

Figure 3 shows the block diagram of the automation system.

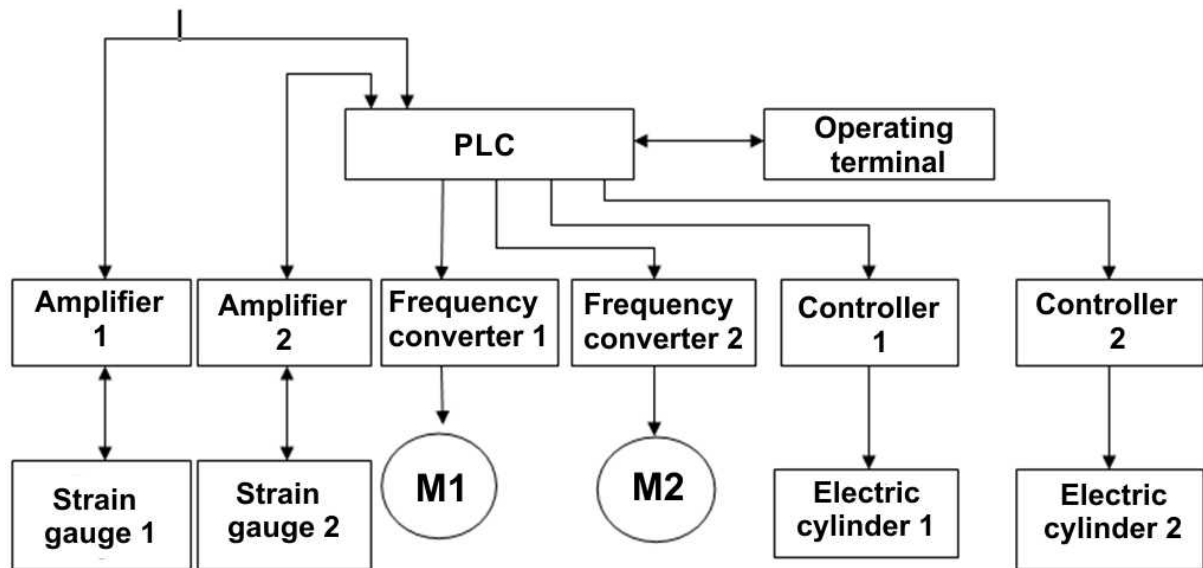


Fig. 3 Automation system block diagram

The weighing and management machine performs the following technological functions:

- programming the amount of dosed product within the limits 15-60 kg
- instantaneous display the amount of product that is inserted into the bag as it fills (kg);
- display time charging flow (t/h);
- automatic weighing the programmed quantity (kg);
- management by counting the total number of full loaded bags (units)
- managing the entire quantities that passes through the machine;

3. FUNCTIONING

Fasten the bag on one of the openings for bags. Press the corresponding start button for the workstation. At this point the system automatically does its taring to zero and after a short time („delay time when dosing starts "), the flap automatically opens simultaneously with the start dosing worms at the maximum prescribed speed. They operate at maximum speed until the quantity of product in the bag reaches a predetermined value, then it automatically switches to a originally scheduled lower speed. Now is the time when the amount of product required for completing the weighing phase has a weight of 100-150g. The big worm stops and the small one still operates at the lower prescribed speed, until the amount of product inside the bag reaches a setpoint, when the worm stops and the valve automatically closes. During rough dosage for one of the workstations, at the other workstation a bag is attached. After dosing and weighing completion on one of the bag openings, the process is initialized for the other by pressing the corresponding start button.

Equipment maintenance actions during work (setting emptying bags, removing the full bags, and so on) will be performed only during the rough dosing phase. During fine dosing, the equipment must not be touched because if so, it will have an influence on weighing. During precision dosing and weighing processes, the bag placed at the opening will stay from "suspended" position.

The automation equipment will operate alternately commanding workstation 1 or workstation 2. All system settings will be made from the touchscreen terminal: calibration, initial working parameters (nominal speeds, the amount of dosed product, etc.).

The PLC receives the mass information from strain gauges through, through amplifiers and therefore control the frequency converters which in turn drive the electric motors in and so,

achieving precise filling of bags. When the mass of the bag reached the predetermined value, the PLC commands the controllers that will drive the electric cylinders to close the dampers.

4. FUNCTIONAL AND TECHNICAL SPECIFICATIONS

The equipment for weighing and automatic management has the following dimensional and constructive specifications:

- Overall dimensions, mm	without bunker	with bunker
- length	1300	1640
- width	560	1200
- height	1739	3255
- bunker diameter, mm		1000
- coil diameter of the worm for rough dosing, mm		160
- coil diameter of the worm for fine dosing, mm		60
- bag opening diameter, mm		250
- dosing worms speed, rev/min		60...560
- motor power required to drive the rough dosing worm, kw		0,75
- motor power required to drive the fine dosing worm, kw		0,37
- productivity, no. bags/hour		2-4
- weighing expected accuracy, %		±0,1
- dosed quantity , kg		15 - 60

4. Conclusions

Through the adopted constructive and functional solutions, **The ECGA equipment for weighing and automated management** ensures:

- Increase labor productivity due to reduced maintenance time by overlapping some of the packaging activities, which is possible because the equipment has two workstations operated by a single person;
- Modernization and automation of production processes from within enterprises of small and medium milling capacity;
- Quick and easy management of the quantities of finished products (flour and bran) resulting from manufacturing;
- safe data storage in device memory for a certain period, regarding quantities of bagged products, data that can be made available to anyone interested;
- securing the packaging process by programming and modifying operating parameters and system configuration, which can be done only by authorized persons using access passwords known only by them;
- Increasing operator efficiency due to reducing extra movement.

References

- [1] Sîrbu S., Popescu S., Ola D., Lupşa R. - *Gravimetric Dosing of solid bulk products in agriculture and food industry*. Scientific papers *INMATEH* 2004, vol. I, pag. 81-88.
- [2] Popescu S. - *Influence of functional parameters of the gravimetric dosing process of granular agro-food material*. Buletin of The Transilvania University of Brasov, serie A, vol II (47), 2005, pag. 169-176.
- [3] Ola D., Popescu S., Sîrbu S., Lupşa R. - *The dosing of bulk solids from agriculture and food industry through volumetric methods*. Scientific papers collection *INMATEH* 2004, vol.II, pag.171-180.
- [4] Ola D., Popescu S. - *Functional peculiarities of gravimetric dosing systems used in agriculture and food industry*. Scientific papers *INMATEH* 2006,vol.III, pag.261-268, ISSN 1583 - 1019.
- [5] Ciauşu V. - *Research on packaging mechanisms in operation*. PhD thesis, Technical University of Iaşi, 1999.
- [6] Brochures and catalogs of specialized firms:
 - <http://metrisoft.hu/kolcsonzes>
 - <http://www.behnates.de/en/products.html>
 - <http://www.tehnostar.ro/16-masina-pentru-dozat-la-sac.html>
 - <http://www.balanta.net/ProduseE.htm>
 - <http://prut-construct.ro/produse.html>

CURRENT STATUS OF SYSTEMS DEVELOPMENT FOR SEEDS SEPARATION WITH PLAN SIEVE AND IN AIRFLOW

Phd. Eng. Birsan (Mitu) Mariana¹, Prof. Ph. Eng. Casandroiu, Ph. Eng. Paun Anisoara
National Institute of Research - Development of Machines and Installations Designed To
Agriculture and Food Industry – INMA

ABSTRACT

In the present paper will be presented and analyzed the most relevant technical equipment of cereals selection, in particular plane sieves and air currents separation systems, both in terms of construction, as well as the working process, in order to improve work parameters and upgrading such equipment to meet the requirements and standards of quality and safety imposed by the European Community.

The seeds separation equipments are used both in precleaning as well as in cleaning wards, to remove impurities from the cereal mass (grain, corn, rice, barley, etc.) in order to improve grain mill products (flour, cornmeal, barley, rice, semolina, bran, etc.), products that constitutes the raw material for the food industry. Also, the same operations performed before product storage in further processing, reduces substantially the risk of creating alteration outbreaks in the stored product mass and also allow better storage management.

In this regard, the paper aims to identify significant places within technical machinery where it can intervene to increase work performances and their modernization.

1. INTRODUCTION

Agricultural products resulted from harvest are used in important sectors of the economy and primarily in agriculture and food industry. In agriculture healthy cereal seeds are used for sowing and forage material consumption, for humans and animals. In the food industry more than 90% of the agricultural production is used as a raw material, which is processed by various methods [1,3,4].

In the conditioning process the precleaning and cleaning operations of the seed mass, obtained after harvesting with the combine, from the impurities it contains (plant debris, minerals, and/or weed seeds) are essential. These operations are necessary to ensure the imposed requirements by national standards and/or European depending on their destination (planting material, consumption, industrial processing, storage, etc.), The cleaning and sorting operations are performed using complex machinery for cleaning and sorting seeds [1,5].

The cleaning and/or sorting operations achieves seed mixture separation, in components that are differentiated by physical characteristics (size and geometric shape, aerodynamic properties, density, surface state, electrical properties, optical properties) which are underlying principles of separations and are the base of work process of the constituting technical equipments of complex systems, special for cleaning seeds.

Category of equipments that will be presented further analysis is the most widespread and common in production to achieve seed cleaning and consists of those technical systems that work on the principle of separation after differentiating between geometric dimensions and aerodynamic properties, separation carried out using sieves (usually provided with rectangular and circular holes) and air channels that forms the technical work system of the machine [1,3,4].

¹Address: Ion Ionescu de la Brad Blv. No. 6, Sector 1 Bucharest, Phone: 004021-269.32.55, Fax: 004021-269.32.73, E-mail: mitu@inma.ro

2. PRESENTATION OF REPRESENTATIVE TYPES OF EQUIPMENTS FOR CLEANING AND SORTING SEEDS

At national level, claims for improved cereal seeds quality used both for seeding, as well as consumption, designers and builders concerns to achieve machinery and cleaning installations and sorting seeds have advanced.

Therefore, we have new equipments whose performance must be improved continuously:

The SI 1520 intense separator, fig. 1, is designed to perform precleaning and cleaning operations of cereal seeds and technical plants in specific technological flows in mills, silos, breweries, oil factories etc. SI 1520 is made of solutions which give constructive simplicity, functionality and ease in operation.

Movement necessary to carry out the work process is performed by two unbalanced mass vibration generators, rigidly attached to the lateral sides of the sieves frame. The sieve frame is supported on the framework by means of elastic elements from rubber which allows the vibratory movement necessary for the work process.

This technical system, developed in the country, has a working capacity of 80 t/h when performing precleaning operations and 20 t/h when used for cleaning. The plane sieves block is composed of two levels, each having two sieves with a width of 1500 mm and length of 1000 mm [7]. The equipment working process can be pursued in the diagram below:

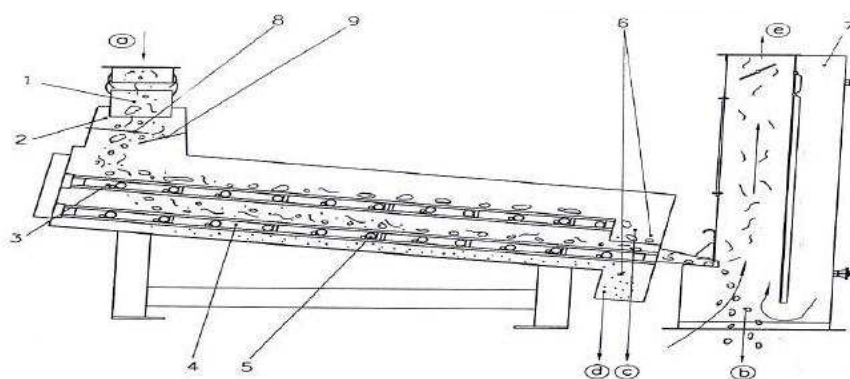


Figure 1: Technological scheme of the SI 1520 intensive separator [7]:

1 – supply connection; 2 – supply chamber; 3 – upper sieves system; 4 – lower sieves system; 5 – ball; 6 – evacuation opening for impurities; 7 – aspiration channel; 8 – flap supply; 9 – deflector; a – material for cleaning; b – cleaned product; c – big impurities; d – small impurities; e – light impurities.

The K 527 A sieve separator is a modern equipment, of high capacity, made in Germany. In fig.2 is represented the technological scheme of the separator with plane sieves type K 527 A, in which we can watch the separation technological flow and the main components. Some of the work details are mentioned below: [9]:

- seed precleaning flow = 20,8 kg/s = 75 t/h, of grain
- final cleaning flow = 11,1 kg/s = 40 t/h, of grain
- sieve size : length- 714 mm, width - 1530 mm
- sieves numbers = 3 (one superior, two inferior)

The light seeds are moved by the airflow that blows through the separation channel and are evacuated by the light seeds output. The separation process is continued in the prior cylinder. The system is powered by an electrical engine of 5.5 kW.

The MIAG Vibrocleaner (fig.4) is another model of high capacity separator used in cereal pre-cleaning. Within this technical system the cereal supply duct (1) is separated by the aspiration inlet and works based on high vibrations principle sent to sieves. The separated seeds are evacuated through the outlet (2), the small impurities evacuation is through the outlet (3) and the big ones through the outlet (4). Light impurities from the cereal mass are flowing through the channel (6) with the help of air currents aspirated by the channel (5) and moved into the separation system (cyclone or filter) through the outlet (8). With the lever 7 can be adjusted the speed and air flow from outside.

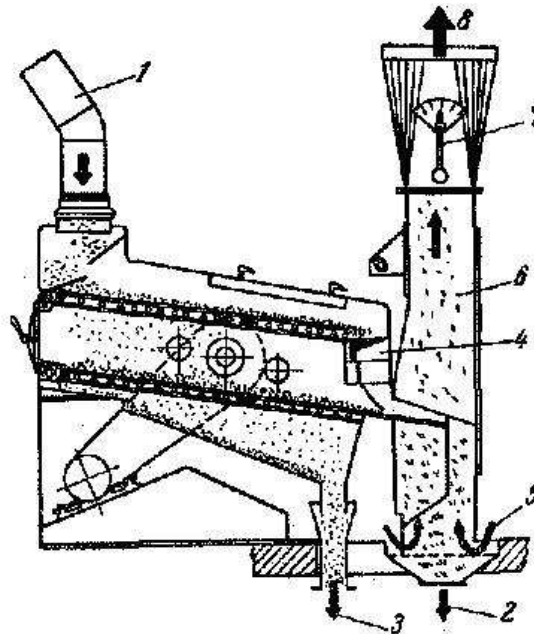


Figure 4: Technological scheme of MIAG vibrocleaner:

1 – hopper; 2 – cleaned product evacuation; 3 – small impurities evacuation; 4 – big impurities evacuation; 5 – air aspiration channel; 6 – aspiration channel for light impurities; 7 – lever for speed and air flow adjustment; 8 – connection to a suction system.

This type of separator is built with sieves having widths of 630, 800, 1000 and 1250 mm or in double construction 2 x 1 250 — 2 500 mm, in which case it provides a working capacity of 100 t/h with an air consumption of 300 mVmin and a force required of 4,8 CP. The double construction have sieves with widths of 2 X 816 mm and 2 x 1 016 mm, providing 64 and 80 t / h precleaning grains.

Analyzing the constructive solutions presented above, it was designed, projected and realized by INMA the experimental model of TC 600 Combined Separator, following to further research on optimizing the separation of cereal seeds to form the basis of new precleaning seeds technologies. This technical equipment makes the separation of impurities on the aerodynamic properties difference between seeds and impurities, being driven by electrovibrators and technical and functional parameters raised to global. The operating principle is shown in fig. 5.

The combined separator is composed of a suction case (1) and a vibrating sieve (4) mounted on four flexible rubber supports (11) and driven by two electrovibrators (10).

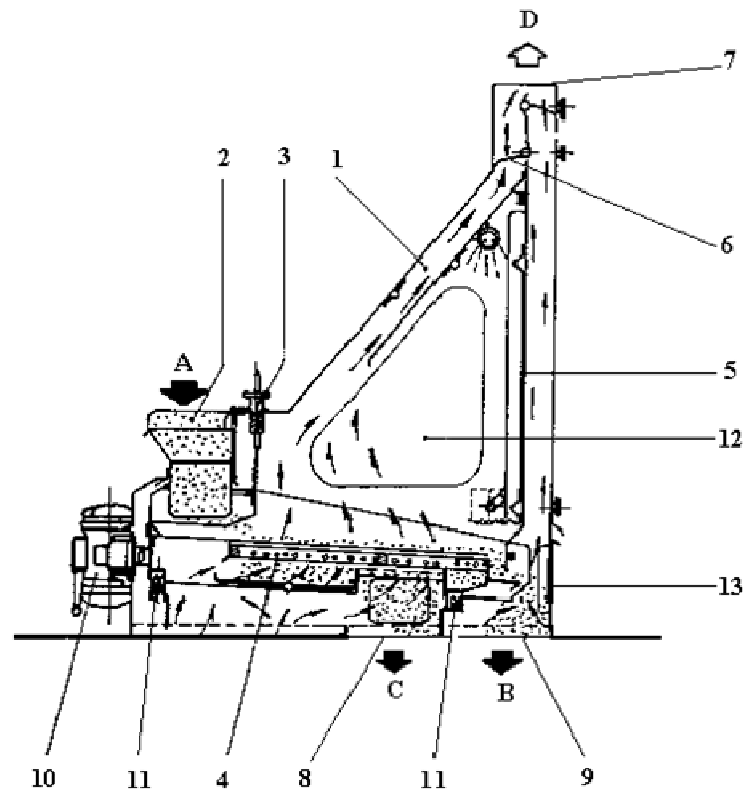


Figure 5: Flow sheet of the TC 600 combined separator:

1. - case; 2. - hopper; 3. - flow adjustment system; 4. – separation plan (vibrating sieve); 5. – air flow adjustment valve in the vertical channel; 6. - air flow adjustment aspiration valve off the sieve; 7. – the suction opening; 8. – small impurities evacuation funnel; 9. – clean product evacuation funnel; 10. – Electrovibrator; 11. – elastic elements; 12. – side viewfinder; 13. – visiting cap ; A – product supply; B – clean product evacuation; C – small impurities evacuation; D - evacuation of aspirated light impurities,[8].

The cleaning product is entering the equipment through the hopper (2) and flow adjustment device (3). Once arrived on the sieve that is actuated by those two electro-motors, it will be separated by size and airflow. The aspiration channel is double and is provided with independent air control devices (5,6); a suction channel is located above the vibrating sieve and controls the layered suction and the other is vertically mounted and controls the impurities suction from the light product fraction.

Controlling the rate of air flow from the suction channels is achieved by modifying the cross-section with the aid of control valves.

Removing impurities is progressive, with the product sliding on sieves (small impurity removal - C), under the action of ascending air current (light impurities located on sieve - D) and the second suction channel where the clean product suffers a new removal of light impurities.

Vibrating sieve cleansing is done with balls made out of a special rubber.

Working process visualization is possible due to inspection windows (12) with whom is provided combined separator. Dampening the vibrations of sieves is achieved with the aid of elastic elements (11) that allows the protection of the foundation against shock vibrations.

3. CONCLUSIONS

Conducting this study I came to the conclusion that national and private milling units have a number of general deficiencies at classic equipments and machinery, such as: low technological efficiency and economical use indices of raw materials and low electricity.

It was also found that the technological systems technical level in Romanian remained behind compared to those from abroad at several types of machinery (precleaning machines, interphase transport, milling and so on).

The parameters of current precleaning and cleaning technologies are: use of air currents produced by fans, mechanical outdated from the material consumption, in terms of energetic efficiency and technical performances; the comand and control systems are classic bases; conventional suspension systems which do not respond to the needs of vibration dampening in real-time.

Due to the very high prices of foreign equipments, not all milling units can afford a retrofit with foreign machinery and therefore is required retrofitting the milling industry by replacing the old equipments with new ones, which ensures quality and performance on world level, but at reasonable prices.

For this purpose, the machinery must meet certain requirements for smooth running of the work process, namely: to ensure getting a good quality product that meets the requirements of standards, not to cause harm to the seeds, to be more universal, simple and safe from the constructive point of view, allowing control in a wide range of key functional parameters related to the work specific process to each machine, to require an energy consumption as low as possible, to meet the requirements the Labour Protection norms[3, 4].

Therefore, the research results regarding the influence of constructive and functional parameters of active working systems used for cleaning and sorting seeds on quality and functioning indicators is the modern equipment designed by researchers at INMA Bucharest meeting thr requirements above, namely, Combined Separator TC 600 [8]. It is intended for precleaning both grains cereals (wheat, barley, rye) and maize, pulses and oilseeds, species with largest share in overall agricultural production carried out annually in small and medium farms.

Because the researches carried out both nationally as well as globally, concerning the equipments used to separate seeds have not exhausted all the issues to be taken into account, is necessary to continue these researches on the influence of structural and functional parameters of active working bodies of the machines used for cleaning and sorting seeds on work quality and operational indicators.

References

- [1] Căsândroiu Tudor - Utilaje pentru prelucrarea primară și păstrarea produselor agricole,Curs,Vol1,UPB, 1993
- [2] Căsândroiu T., David L. – Utilaje pentru prelucrarea primară și păstrarea produselor agricole, Îndrumar pentru lucrări de laborator, UPB, 1994
- [3] F. Stoica – Studii și cercetări privind îmbunătățirea, parametrii constructivi și a regimului cinematicla sitele plane folosite la mașinile de curățat și sortat semințe în vederea măririi capacității de lucru,T. Doc., UPB, 2004
- [4] Birsan (Mitu) Mariana – Constructive elements and working process of seeds separating systems with plan sieve and in airflow, Exam II, PhD, UPB,
- [5] I.G. Voronov, I.E. Kojuhovski, s.a. – Curatirea si sortarea semintelor, Ed. Agro-Silvica de Stat, Buc., 1955
- [6] MICM, CIT, IM BV – Carte tehnică, mașina de curățat semințe MCS 5/2,5
- [7] xxx – Si 1520 Intensive Separator , technical book, Tehnopam-CCD
- [8] xxx –INMA brochures, technological schemes of seed sorting machines
- [9] xxx –Petkus brochures, technological schemes of seed sorting machines

MISCANTHUS PLANT ENERGY CONSUMPTION DURING GRINDING WITH A LAB MILL GRINDOMIX GM 200

Georgiana Moiceanu , Paula Voicu, Gigel Paraschiv, Gheorghe Voicu, Mihai Chitoiu
University "Politehnica" from Bucharest

ABSTRACT

Taking into consideration the use of biomass as an energy resource, mechanical processing it's necessary starting with harvesting. In both harvesting versions it is necessary after an according drying process, a mechanical processing through grinding in many stages till it is brought to a specific graininess which allows biomass densification process and transformation into pellets. In this paper experimental research regarding miscanthus grinding with a lab mill Grindomix GM-200, with two bevel disks are presented, in order to estimate the specific energy consumption at grinding. It is presented the mills grinding equipment components, speed distribution of the grinding disks of the drums diameter and the work process of the mill, and also the specific energy consumption taking into consideration the angular speed, for leaves as well as for miscanthus stalks. Also, grinded material size distribution its presented taking into consideration the angular speed of the drum and the correlation with the energy consumption during grinding.

1. INTRODUCTION

Physical characteristics of a miscanthus harvest significantly influence the grinding process and the grinded material characteristics, but it mainly offers information for designers and equipment builders in order to make the proper machinery and its necessary tuning. Initial dimensions of grinded material, if this has been subjected earlier to a milling process, as well as mechanical characteristics of resistance and durity significantly influences energy consumption and the required power for grinding [2,3].

Hammer mills (fixed of articulated) are the most popular equipments for grinding/milling. Inside them, miscanthus stalk of the pre-grinded material fragments (cut or grinded) are subjected to complex mechanical strains resulting in the grinded material at the required dimensions, used for pellet production [6].

2. METHODOLOGY

Laboratory mill Grindomix fig.1 is a laboratory mill with a plate and two steel knives, inclined disposed towards a circle of 55mm radius under a 115 degrees angle. The knives are inclined backwards of the rotation sense, the interior cutting side diameter is of 55mm and the exterior diameter of 120mm. Activating the mill is done with an electric motor with 900 W power, its speed being of 2000-10000 rpm according to the hardness and grinding resistance of the subjected material. The plate volume is of 750mm, but cutting takes place at the base of the plate on a hight of 10.15mm, the two knives being at a distance from one another of 5mm.

As the grinding takes place, the material that has yet to be grinded falls in the two knives and it grinds, leading to very small dimensions. The knife support is made of plastic material, the lower part is with a helicoidally shaped support that leads the material towards the knives. The mill also has the possibility to regulate grinding time in order to realize the grinding in required limits.



Figure 1: Lab mill GRINDOMIX GM 200, Mills steel box [5]



Figure 2. a. GM 200 Mills knife; b. Clamp meter Extech [5]

Mill knife speeds distribution is schematically presented in fig.3.

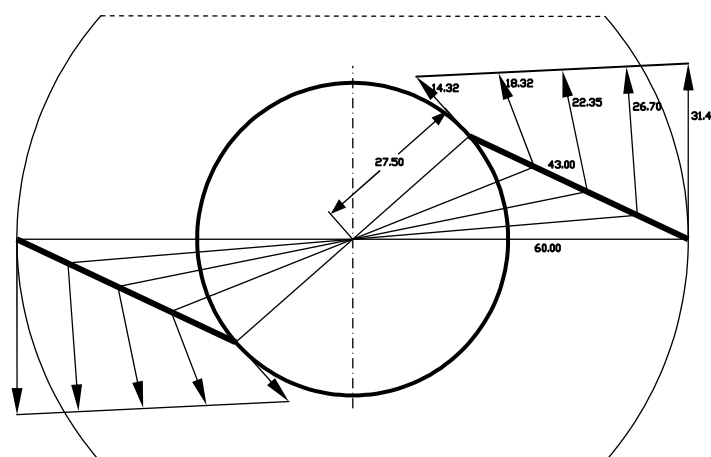


Figure 3. Mill knife speed distribution

The material used for experiments was of miscanthus plants pregrinded and separated into 3 length classes:

- Large material particles, with lengths of 15-20mm (45%);
- Medium material particles, with lengths of 8-15mm (27%);
- Small material particles, with lengths of 1-8mm (28%).

Each of these fractions was subjected to the grinding process with the help of the mill for one minute; the recording took place with the help of a counter for active electric energy for the energy consumption, which was later reported at the grinding table. On the basis of data obtained at experimentations for grinded material temperature and the specific energy consumption at grinding we drew the temperature variation graphs according to the average dimensions of the three material fractions used for grinding. (fig 4, a and b).

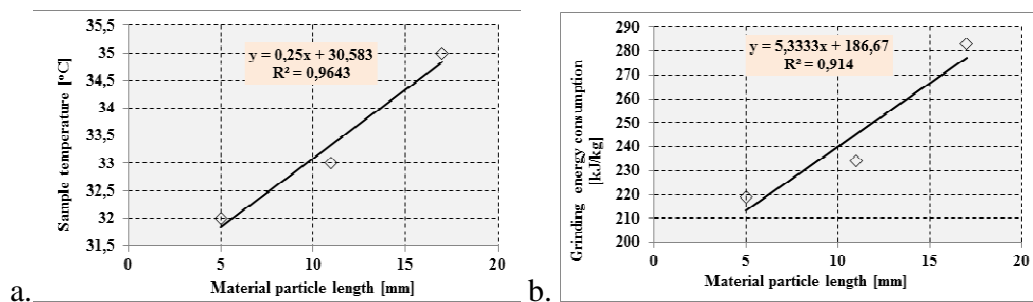


Figure 4.a. Particle temperature variation according to initial dimensions, b. energy consumption variation according to the material initial dimensions.

From the tests done on energy consumption at milling miscanthus stalks we could see that the required energy for grinding was greater when large particles were used. So, for the fraction of small dimensions, the energy consumption was of 219.8 kJ/kg, for the fraction of medium dimensions (8-15mm) was of 234,0 kJ/kg, and for the large particle fraction was of 283.5kJ/kg. The grinded material was manually sieved with a square orifice sieve with 1mm side, the percentage of material remaining in the sieve was 2-3.5% for each of the three cases.

We could see, also that grinded material temperature grew in all three cases, from a 20°C to 32°C for the fraction of small particles, 33°C for the medium fraction, and 35°C for the large particle fractions, which shows that the larger the particles the larger the energy consumption for grinding processes.

Obs: Initial material temperature was measured with a multimeter check rod with thermocouple.

For experimental determinations regarding energy consumption at grinding, probes of 10g were weighed, which were grinded at different speeds: 3000, 4000, 5000, 6000, and 7000rpm. Distribution of initial material after leaf length was random, these leaves were introduced in the machine in a random way (lengths of 10-190mm). For determining granulometric distribution of grinded material we used three sieves with orifices of 3.15, 5 and 6.3mm (1 minute manual sieving). The ponder of the four fractions was determined and the variation curves were drawn according to mill rotor speed (fig 5a)

During miscanthus grinding experiments, stalk probes were taken from different internodes, with lengths if 15mm. 10g material were weighed, which were grinded, at the same speeds as the mill rotor as the plant leaves.

Grinded material was sieved through the same set of sieves. On the basis of material and the four granulometric fractions obtained, the experimental points were drawn and afterwards, the fraction variation curves. (fig 5.b).

For power variation curve drawing, respectively grinding specific energy, according to mill rotor speed, the linear distribution function was used.

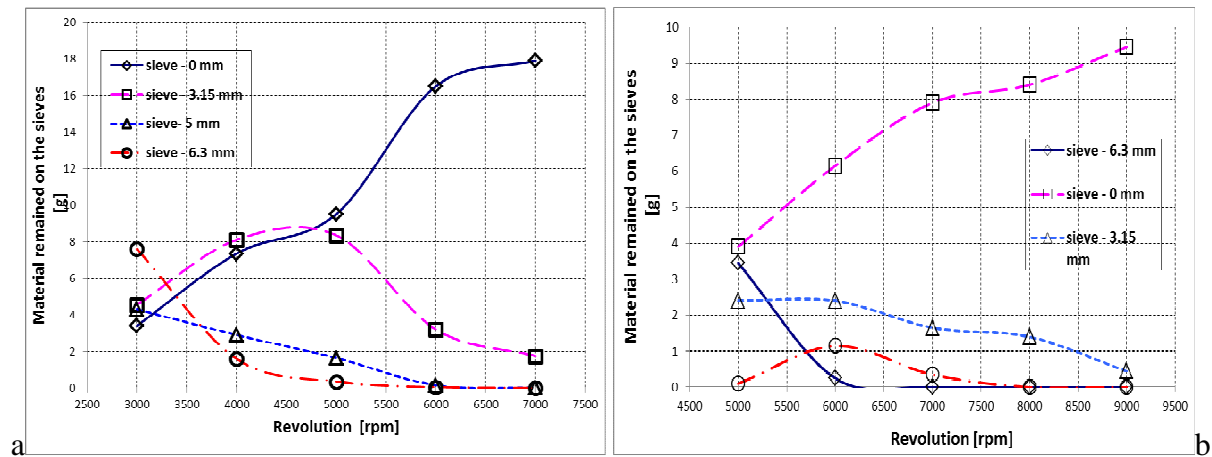


Figure 5. Grinded material distribution, on dimension classes, according to mill rotor speed (1000 rot/min=6.33 m/s, a. leaves, b. stalks)

Tabel 1. Grinding power and distribution after the grinded material dimensions (leaves) [4]

Nr. crt.	Turația rotorului (rpm)	Temperatura finală (°C)	Energia specifică (kJ/kg)	Puterea maximă (w)	Distribuția materialului pe site (%)			
					0 mm	3.15 mm	5 mm	6.3 mm
1	3000	38	1275	425	17	22.75	21.5	38
2	4000	38	1260	420	36.75	40.5	14.5	8
3	5000	38.5	1245	415	47.5	41.75	8.25	1.75
4	6000	39	1425	475	82.5	16	0.75	0.25
5	7000	39	1335	445	89.5	8.75	0	0

Tabel 2. Power and distribution after the grinded material dimensions (stalks) [4]

Nr. crt.	Turația rotorului (rpm)	Temperatura finală (°C)	Energia specifică (kJ/kg)	Puterea maximă (w)	Distribuția materialului pe site (%)			
					0 mm	3.15 mm	5 mm	6.3 mm
1	5000	38.5	0.594	435	39	24	1	34.5
2	6000	38	0.738	440	61.5	24	11.5	2.5
3	7000	39	0.918	460	79	16.5	3.5	0
4	8000	39	1.062	455	84	14	0	0
5	9000	40	1.08	480	94.5	4.5	0	0

In the case of leaf grinding, it has been concluded that the fraction with dimensions between 3.15-5mm, presents a growing variation of remaining material on the sieve ($\phi=3.15$ mm) with the rise of grinding machine speed, after it starts as in all cases of fractions to drop. The same decreasing variations of remaining material on the sieve and the grinded stalk fractions in can be seen, disregarding the fraction that remains of the sieve of 6.3mm.

We can appreciate that in the case of stalk grinding, the machine rotor speed must be larger than in the case of leaf milling, in order to reach a corresponding granulation, stalk hardness being a lot bigger than the leaves case.

Also, during almost whole leaves, calculated periphery speed was between 18.84 – 43.98 m/s. In the case of miscanthus stalks, peripheral speed was between 31.4 – 56.5 m/s for knife exterior diameter, and for the interior diameter it had values of 14.4 – 25.9m/s. For leaves, at speed of 5000 rpm we can see a percentage of 41.75% particles between 3.15 – 5mm while for the same speed, but in stalk case, a percentage of 16.5% was obtained for particles of 3.15-5mm in dimension.

Through these data we can appreciate the fact that the grinded miscanthus stalk fractions, with dimensions under 3.15mm always had values of over 40%, while for leaves we found values of over 17%. It is recommended that speeds of over 7000 rpm should be used for the two components of the plant if a high degree of grind is needed. Energy consumption measured with the active electric energy counter for stalks showed a value of 1062MJ/kg for 8000rpm speed.

Another experiment [4] had the objective to determine miscanthus plant stalk necessary power for grinding.

Both in the case of leaves as well as stalks, the specific energy consumption was calculated, its values being random, due to the difference between the measured energy consumption and the calculated one on the basis of grinding necessary power. For example, using the maximum power consumed and probe time, for miscanthus stalks the calculated energy consumption was of 2.610 MJ/kg while the measured electric consumption was of 0.584MJ/kg.

We can say that the biggest rotor speed (31.4m/s) is at the knife peaks, and the lowest value of cutting speed (14.4m/s) is in the connection point of the knife with toe knife support (on the inside diameter).

On the basis of results obtained at experimentations, maximum power necessary for grinding and the grinding specific energy for different steps of speed of the mill rotor through linear distribution law computer regression analysis were drawn. From graph analysis, we can see a good correlation of experimental data, for both characteristics (power and specific energy) appreciated through coefficient value of correlation R^2 ($R^2 > 0.9868$ for grinding power)

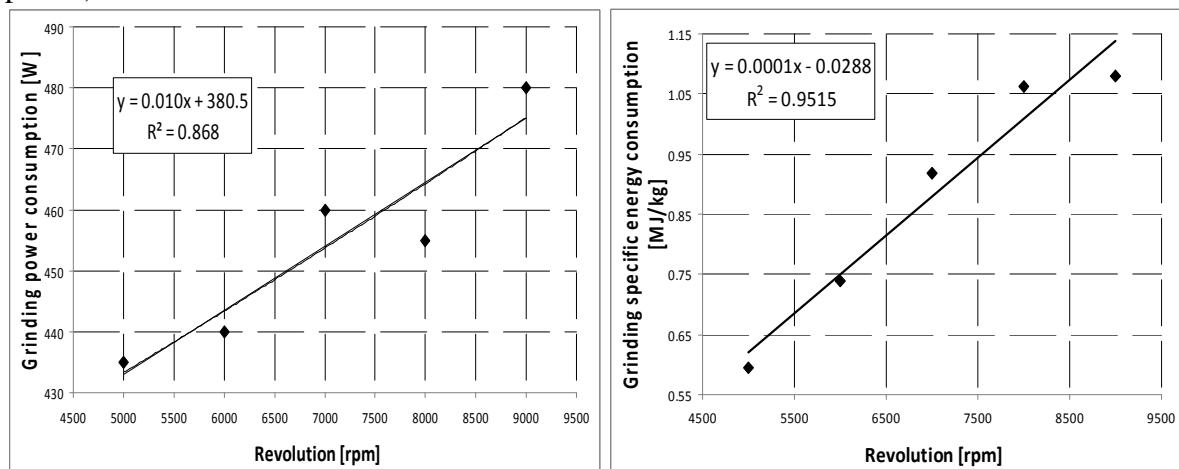


Figure 6 Power variation curves and grinding specific energy

Also, we could see a rise in mill speed, necessary for the grinding process, for miscanthus stalks, comparative to plant leaves. This was relevant from the experimental tests in the moment that the stalk grinding at 3000, respectively 4000rpm was wanted, speeds at which leaves could be grinded, but stalks couldn't. We draw the conclusion that knife centrifugal force necessary for grinding must be larger for stalks than for leaves.

3. CONCLUSIONS

Grinding miscanthus stalks takes relatively high energy consumption, in order to bring the material to dimensions needed for pelletization. For high values of mill rotor peripheral speed 18.84-43.98 m/s and 31.41 – 56.54 m/s for leaves respectively stalks, the degree of grinding was over 90%

Also we must mention that the miscanthus plant grinding process is a heat emission process due to the fact that through particle breaking into smaller dimensions, temperature of grinded material grew with 16-18°C from the initial room temperature of 20-22°C. Material mass distribution on dimension classes shows a drop in large fraction ponder, both for leaves as well as stalks, with a rise in grinding machine rotor speed. We appreciate that, for grinding stalks, the rotor speed of the grinding machine must be larger by 2000rpm than in the case of leaf grinding, which means a rise of peripheric speed with aprox. 10 m/s [1,4].

References

- [1] Q. Fang, I. Bolloni, E. Haque, and C.K. Spillman, "Comparison of energy efficiency between a roller mill and a hammer mill", Appl. Eng. In Agric. 13(35): 631-635, 1997;
- [2] C.W Hall, D.C. Davis, „Processing Equipment for Agricultural Products”, The AVI Publishing Company, Inc. Westport, Connecticut, 1979;
- [3] Y. Manlu, A. R. Womac, C. Igathinathame, S. Sokhansanj, S. Narayan, „Direct Energy Measurement Systems for Rotary Biomass Grinder – Hammermill”, ASABE Meeting Presentation no. 066217; 9 - 12 July 2006;
- [4] G. Moiceanu, Gh. Voicu, G. Paraschiv, Cr.I. Poenaru, E. Maican – „*Physical characteristics of miscanthus plants and power demand at grinding process*” , Proceedings of 11th International Scientific Conference „Engineering for Rural Development”, vol.11, , Jelgava, Letonia, pag.222-297 (ISSN 1691-3043) (indexed magazine AGRIS, CAB Abstracts, CABI full text, EBSCO Academic Search Complete, Thomson Reuters Web of Science, Elsevier SCOPUS, PROQUEST), 24-25 mai 2012;
- [5] Moiceanu G., 2012. Research Regarding Energetic Plant Behavior during Mechanical Operation of Cutting and Grinding”, PhD. Thesis, University “Politehnica” from Bucharest;
- [6] L. G. Tabil, S. Sokhansanj, “*Compression and compaction behavior of alfa grinds*”, Part 1: compression behavior, Power Handeling and Processing 8(1), 17-23, 1996;

EXTENDING THE USE OF HOTHOUSES THROUGH HEATING WITH RESIDUAL AGRICULTURAL BIOMASS

Authors: Murad Erol¹, Maican Edmond¹, Dumitrescu Cătălin², Biriş Sorin Ştefan¹

¹POLITEHNCA University of Bucharest, ²INOE-2000 IHP

ABSTRACT

The paper presents a study on increasing energy independence of a 200 m² horticultural hothouse, by means of heating it with thermal energy from a TLUD gasification procedure of local residual agricultural biomass, chopped at 10-50 mm and dried at 10-15% RH. Hot-air heating system and forced circulation is equipped with two GAZMER 40/150G energetic modules, which are rechargeable, simple, safe, efficient and environmentally friendly. They can gasify chopped or pelletised biomass. From biomass gasification results an average of 14% biochar, which is a valuable amendment and helps carbon sequestration in soil. Energy production can continue with complete gasification of biochar to ashes. To study the microclimate evolution, it was used a complex numerical model adapted for a 200 m² hothouse for growing tomatoes, completed with the model of a heating system with an automatic control algorithm adapted to the hothouse characteristics and BGM modules. Biomass from tree cuttings was used, with 15% RH and LHV of 15.3 MJ/kg, from which the totally gasified part is 86.5% with LHV=14 MJ/kg. Simulated experiments were carried out for frosty days and, estimated, for the whole warming period. Each year 13.44 t of biomass are consumed, resulting 1.78 t of biochar which, when introduced in soil, produces a -6.2 t/year negative balance of CO₂. The cost of heating by means of agricultural biomass is 4 times less than with pellets and 20 times less than with diesel fuel.

1. INTRODUCTION

Essential to increase food security of Romania and to increase the health of the local population, is production of current consumption of vegetables throughout the winter. Winter vegetable production comes up to about 2/3 out of unheated hothouses and the difference comes from industrial type greenhouses. Due to competition in the global floricultural products, much of protected crop surfaces are allocated to flowers production, at the expense of production of vegetables. By reducing expenses necessary for heating hothouses and greenhouses, there can be produced more vegetables, with high quality and making an adequate profit both for producers and consumers.

To increase the life of the vegetable hothouses in order to increase vegetable production during the cold season, heating is required with simple thermal systems, with low costs both in investment and operation.

To reduce dependence on fossil fuels, with high CO₂ emissions, currently the share of biomass for heating increases and, more rarely, biomass is used in cogeneration plants. Currently it is used the biomass compacted into pellets, easy to carry and use as fuel, which required an extension of the use of this form of compaction. Burning is done with high superficial speeds which produces a higher concentration of PM that clogs the heat exchanger and pollute the environment. EU environmental legislation heavily restricts the concentration of PM, which leads to use of smoke filters or towards reducing the intensity of the thermal process. These in turn have the effect of price increases and a decrease of overall performance. For the production and transportation of pellets, an average of 200 kWh/t is consumed, which for a thermal/electric conversion efficiency of 25% represents about 16-20% of the calorific energy of the compacted biomass. It is issued into the atmosphere a large amount of CO₂ from the production of electricity consumed and from the manufacturing of production equipment. The current price is 140...160 €/t, slightly higher during the cold season. [12]

¹ Erol Murad; Spl.Independentei 313, Bucharest, sect.6, Romania; Faculty ISB; erolmurad@yahoo.com

Alternatively, a more ecological and economic alternative for thermal energy production needed to extend the useful life of hothouse with three months, or working like a greenhouse during the entire cold season, it is proposed and analyzed the use of local agricultural biomass residues at the level of current technology, with minimal mechanical processing. [1, 4, 5]

Agricultural biomass, derived from fruit growing, viticulture and vegetable growing, is chopped at 10...50 mm and naturally or forced dried at 10...15% RH. Energy consumption from harvesting to use is 100 kWh/t less than in case of pelletization, and 50 kWh/t less for transport on distances under 30 km. On average is 50 kWh/t. This represents about 25% of the power consumption pelleting, or 4-5% of the calorific power of used biomass. It is estimated that this type of local fuel can be used at maximum 50 €/t. [1, 7, 8]

The most important reasons for using this type of biomass consists of ecological and economic advantages (lower consumption of fossil fuels), dependency reduction on unstable geopolitical entities. It also has the effect of encouraging the efficient use of local energy resources, innovation and employment growth in rural areas.

2. PRODUCTION OF HEAT WITH TLUD ENERGETIC MODULES

To convert the local chopped biomass at 10-50 mm, with 10-15% moisture, in thermal energy there can be used relatively low conversion efficiency combustion plants that produce a lot of PM (smoke), or thermo-chemical gasification can be applied, which means lack of smoke and good efficiency. Conventional gasification plants are still relatively complex equipment, are sensitive to moisture and size of biomass, require highly trained operators, thus slowing down their use in agriculture. In order to reduce both the initial investment and the running operation costs, it is proposed the TLUD (Top-Lit-Up-Draft) process of gasification, which is tolerant and functional auto-adaptive to the particle size and moisture of biomass. It is also characterized by PM and CO very low emissions. Energetic modules for producing thermal energy based on the TLUD process have a simple design, are durable and safe under operation, and benefit from a cheaper price. [5, 6, 7, 8]

The TLUD gasification process is a reverse downdraft process that works in batch mode with reduced thermal load. Kinematics and dynamics of the gasification process are similar. At 25 .. 30% excess of air for gasification, not all carbon in biomass is reduced. Thereby at the end of the charge results 10 to 15% charcoal, called biochar, with incorporated ash. Biochar has proven to be a valuable agricultural amendment to increase soil fertility. Considering biochar as a high usable value product, is obtained a thermal energy conversion efficiency of the completely gasified part of biomass of 92...96%, according to the operating conditions and characteristics of used biomass [2, 6, 7, 8]. From the tests it was found that the lower calorific value of produced syngas is $LHV_{gas} \in (3.5, 4.5) \text{ MJ/Nm}^3$ which, summed with hot gas enthalpy at 500 °C, leads to an available energy of 1.2-1.5 kWh_{th}/Nm³. [2, 8, 10, 13]

In the reactor, the produced gas has a very low superficial velocity $v_s = 0,03 - 0,06 \text{ m/s}$, providing a very low concentration of solid particles ($PM_{2.5} \leq 2.4 \text{ mg/MJ}$), practically smokeless operation, far below standards imposed on the field. To operate with a high energy conversion efficiency and with minimum emissions, the minimum load of energetic modules is limited to 40%. [2, 3, 8, 13]

3. HOT AIR HEATED HOTHOUSE

To determine the specific greenhouse heating with TLUD energetic modules, a Quonset-Metric type hothouse was chosen. It consists of 28 base modules having 6 m, height 3 m, pitch of 1.2 m, and has a surface area on the ground of 200 m² and a volume of 475 m³. It is covered with a double layer, inflatable, polyethylene, with high thermal resistance. [4, 5]

The hothouse is heated with hot air, distributed through a flexible duct which has openings for the jets in the greenhouse space. Part of the inside air is recirculated and mixed with the outside air necessary for venting the greenhouse. The mixture is heated with an internal-flue heat exchanger (HE). This design eliminates the need for regular ventilation, which are producing energy losses and decreases in temperature, which could prove harmful if not properly managed. Indoor crop consists of Vidra Romanian varietz of tomato, for which experimental data for breath and perspiration are available. In order to protect the plants from contact with too warm air currents, the maximum temperature of the jets is limited to 40 °C, which required a constant mass flow ($D_{am} = 2 \text{ kg/s}$) of the air heating the greenhouse.

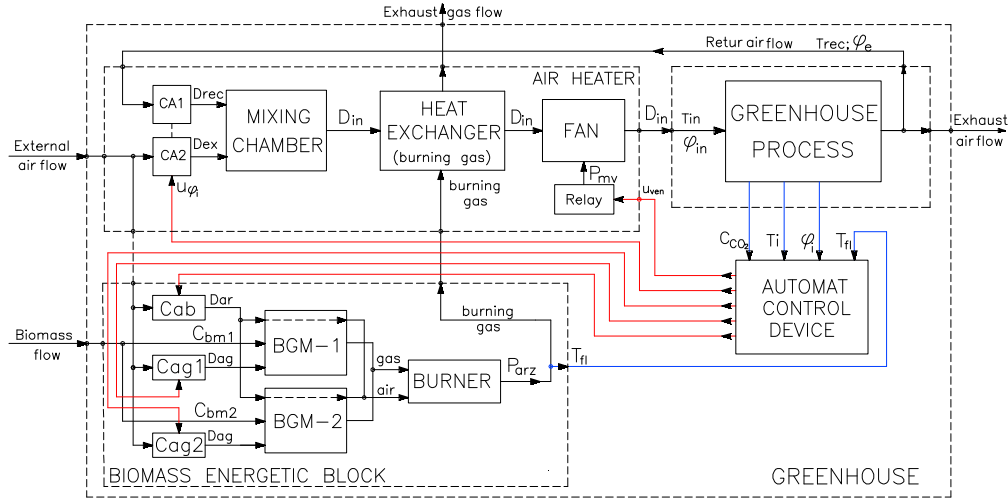


Figure 1: Block diagram of a hothouse heated by TLUD energetic modules

Figure 1 shows the block diagram of a hothouse heated by two BGM (Biomass-Gasification-Module) thermal modules. The two modules are connected to the burner mounted at the entrance of the internal-flue heat exchanger operating at a constant flow of heated air, and therefore, having a minimum efficiency of 85%.

The experiment was simulated for a winter day temperatures within $-25 \dots -5 \text{ }^{\circ}\text{C}$, and constant indoor temperature ($T_i = 10 \text{ }^{\circ}\text{C}$) and humidity ($U_i = 70\%$). It has been determined the maximum thermal power required to heat the greenhouse: $P_{inc \max} = 58 \text{ kW}$. It follows that the maximum thermal power (PBGM) produced by a BGM module must be at least:

$$P_{BGMn} \geq \frac{P_{inc \max}}{\eta_{SC} N_{BGM}} = \frac{58}{0.85 \cdot 2} = 34.12 \text{ kW} \quad (1)$$

where: η_{SC} is minimum return of the heat exchanger; N_{BGM} –number of modules.

There have been selected two GAZMER 40/150G energetic modules with a 400 mm reactor diameter and a height of 1500 mm. Reactor size was determined by the possibility of using agricultural biomass, whose layer density is between 200 and 300 kg/m^3 . Rated power of an energetic module is $40 \pm 5 \text{ kW}$, with an average specific biomass consumption of 100 $\text{kg.bm/m}^2\text{h}$.

4. SIMULATED EXPERIMENTS

The block diagram in Figure 1 shows the basic structure of the SERMGB27.DP simulation program, which is designed for hothouses microclimate. Simulated system consists of four subsystems: hothouse conditioning process, air heater, power unit with two BGM modules, subsystem for automatic control. To model the process of conditioning the hothouse in the block diagram have been highlighted the following specific parameters: input flow D_{in} having temperature T_{in} and relative humidity ϕ_{in} ; evacuated D_{ev} and recirculated D_{rec} air flows.

BGM energy subsystem has two modules loaded with biomass, out of which every hour are consumed C_{bm1} și C_{bm2} (kg.bm/h), depending on the air flow for gasification D_{ag} (kg.air/s), regulated by C_{ag1} și C_{ag2} flaps. The fuel gas produced is burnt with an air flow D_{ar} adjusted with the flap C_{ab} . Flue gas enters the HE and transfers heat to the air that warms the hothouse. [4, 5, 11]

Automatic control subsystem must be able to adjust key parameters that define the hothouse microclimate: indoor temperature (T_i) and humidity (U_i), CO_2 concentration (C_{CO2}), as well as burner flame temperature (T_{fl}). Setting the indoor temperature is done with a PID numerical algorithm, which develops a control parameter that changes the energy load of modules by varying gasification flow rates (D_{ag}). Simultaneously, a dynamic optimization algorithm changes the flow of combustion air, so that the flame temperature (T_{fl}) to be as close to the maximum possible value. Burner efficiency is thus maximized, like that of SC. [3, 4, 5, 9, 11]

5. RESULTS AND DISCUSSION

Figure 2 presents the result of an experiment with the model of studied hothouse, for an average winter day, used to calculate heating requirements in Ilfov County, with a reference for the indoor temperature $r_{Ti}=10^\circ C$ by night and $12^\circ C$ during the daytime, and for an indoor relative humidity $r_{Ui} = 70\%$.

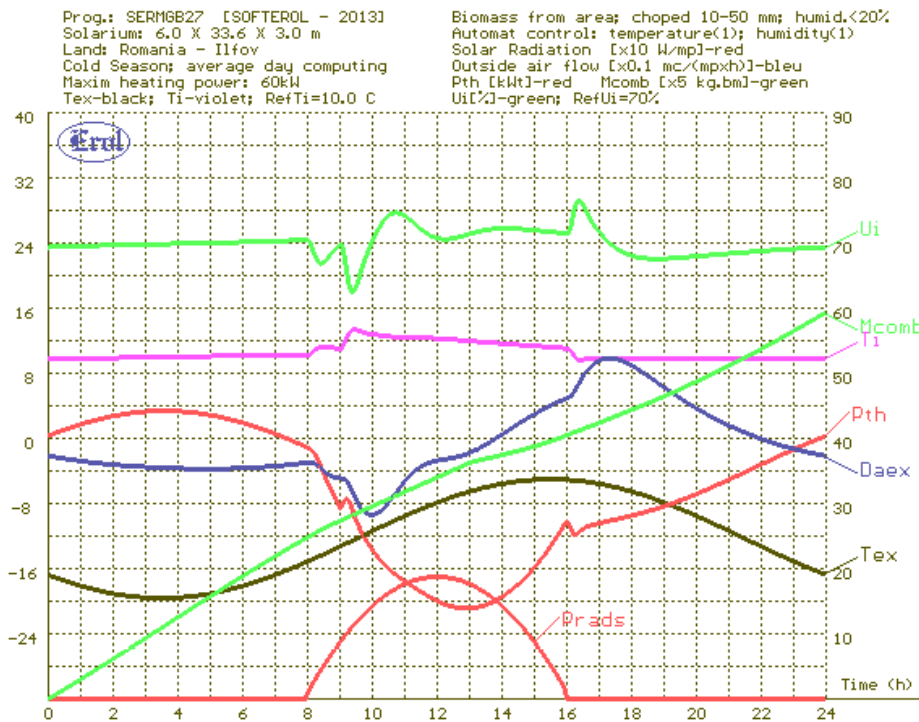


Figure 2: The evolution of a hothouse microclimate in a winter average day

Variations of the following parameters are displayed: T_{ex} - external temperature, R_{ads} - solar radiation, T_i , U_i , P_{th} – produced thermal power, M_{comb} – biomass consumption. It is found that T_i has little variation compared to the reference, but U_i varies somewhat more than the imposed reference. This shows that the automatic control algorithm does not achieve full performance requirements.

Table 1 summarizes the simulation results of the heating for the cold season months when using chopped agricultural biomass, compared to using diesel. The first important resulted value is the annual consumption of biomass which is of 13440 kg.bm/year, and which

occupies a volume of 54 m³ in warehouse in 108 containers of 0.5 m³. Another valuable characteristic is the average specific consumption of biomass for heating during winter $c_{bms}=13.2$ kg.bm/K·day. With this value can be quickly and accurately size heating systems for greenhouses and hothouses. From biomass gasification in BGM results 1780 kg of biochar each year, that can harness 200 €/t, or that can be incorporated as amendment for the soil in solarium with a negative annual CO₂ balance of -6.2 t./year.

Table 1: Simulated experimental results

Parameter	Month	Oct.	Nov.	Dec.	Jan.	Febr.	Mar.	Cold season
Heating period	day/month	15	30	31	31	28	15	150
Average outside temp.	grade C	7.00	5.20	-0.10	1.20	5.60	7.00	3.71
Indoor average temp.	grade C	10.50	10.50	10.50	10.50	10.50	10.50	10.50
Average required heating	K·day/month h	52.50	159.00	328.60	288.30	137.20	52.50	1018.10
Biomass specific consumption	kg.bm/K·day	13.20	13.20	13.20	13.20	13.20	13.20	13.20
Biomass consumption	t.bm/month	0.693	2.099	4.338	3.806	1.811	0.693	13.439
Biochar production	t.bc/month	0.092	0.278	0.575	0.504	0.240	0.092	1.781
Price - chopped agric. biomass	€/t	50.00	50.00	50.00	50.00	50.00	50.00	50.00
Price - biochar as amendment	€/t	200.00	200.00	200.00	200.00	200.00	200.00	200.00
Cost biomass for heating	€/month	34.65	104.94	216.88	190.28	90.55	34.65	671.95
Revenue capitalization biochar	€/month	18.36	55.62	114.94	100.85	47.99	18.36	356.13
Net cost heating fuel	€/month	16.29	49.32	101.93	89.43	42.56	16.29	315.81
Specific cost - biomass heating	€/m ² ·month	0.173	0.525	1.084	0.951	0.453	0.173	0.672
Net cost - biomass heating	€/m ² ·month	0.081	0.247	0.510	0.447	0.213	0.081	0.316
Diesel consumption for heating	L.mt/kg.bm	0.35	0.35	0.35	0.35	0.35	0.35	0.35
Diesel – monthly cost	€/month	327.03	990.44	2046.92	1795.88	854.65	327.03	6341.96
Specific cost – diesel heating	€/m ² ·month	1.64	4.95	10.23	8.98	4.27	1.64	6.34
CO ₂ balance with carbon sequestration	t.CO ₂ /month	-0.32	-0.97	-2.00	-1.76	-0.84	-0.32	-6.20

Average specific cost of biomass for hothouse heating during winter is 0.672 €/m²·month, which is about 20 times lower than with diesel and four times lower than with pellets. This clearly shows the economic efficiency of minimally processed local agricultural biomass into gas-producing TLUD.

6. CONCLUSIONS

By heating hothouses with thermal generators based on TLUD gasification process, local agricultural biomass residues, minimally processed, can be used economically and environmentally efficient at a price of 50 €/t. The specific costs for heating are four times lower than for pellets and 20-fold lower than for diesel fuel.

Analyzed hothouse can be used as greenhouse throughout the entire cold season with a consumption of 13.5 tons biomass, from which results 1.8 tonnes of biochar that can be sold as charcoal, or that can be incorporated as amendment for the soil in solarium with a negative annual CO₂ balance of -6.2 t./year.

Biomass hothouse heating in the analyzed version is done with virtually no emissions of toxic effluents, pollutants, and with negative balance of atmospheric carbon.

A comprehensive program was developed to simulate the hothouse microclimate, SERMGB27.DP, the model also including the TLUD process thermal generators model. Automatic control algorithm for hothouse climate has been verified, which ensures both maintaining optimal microclimate parameters and automatic control of heat generator. The model developed for simulation is a strong basis for research and development in the field, being open source.

Results require an experimental validation on a real hothouse, both for confirming the results of simulated experiments and to determine the real economic aspects derived from extending the useful life during cold season.

Intensive use of local agricultural biomass resources for the production of heat and biochar leads to an increase in the use of labor in rural areas, to a better use of local resources, and to a higher living standards and sustainable development in the area.

References

- [1] Daugherty E. Ch., *Biomass Energy Efficiency – Analyzed through a Life Cycle Assessment*, Thesis, LUND University, feb 2001.
- [2] Mukunda H.S., ș.a., *Gasifier stoves – science, technology and field outreach*, CURENT SCIENCE, Vol.98, nr.5, 10 martie 2010.
- [3] Murad E., *Optimisation of biomass gasification load regime*, International Conference ENERGIE - MEDIU CIEM 2005, UPB, București oct. 2005.
- [4] Murad E., Maican E., Haraga G., Biriș Ș S., *Greenhouse module heating with biomass*, International Symposium, HORTICULTURA știință, calitate, diversitate, armonie, USAMV- Iași, 26-28 mai 2011.
- [5] Murad E., Maican E., Biriș Ș.S., Vlăduț V., *Heating greenhouses with TLUD biomass energy modules*, 3rd International Conference „Research People and Actual Tasks on Multidisciplinary Sciences” 8 – 10 June 2011, Lozenec, Bulgaria.
- [6] Murad E., Culamet A., Zamfiroiu G., *Biochar- Economically and ecologically efficient technology for carbon fixing*, Simpozion HERVEX 2011, 9-11 noiembrie Călimănești , ISSN 1454-8003.
- [7] Murad E., Achim Ghe., Rusănescu C., *Valorificarea energetică și ecologică a biomasei tăierilor din livezi*, Sesiunea de comunicări științifice – ICEDIMPH-HORTING, 20 septembrie 2012.
- [8] Murad E., Dragomir F., *Heat Generators with TLUD Gasifier for generating energy from biomass a negative balance of CO₂*, International Conference – HERVEX-2012, 7-9 nov., Călimănești-Căciulata, Romania, 440-447.
- [9] Murad E., Dumitrescu C., Haraga G., Dumitrescu L., *Pneumatic measurement of the biomass consumption for TLUD generator*, International Conference HERVEX 2012, Călimănești, 7-9 noiembrie 2012.
- [10] Reed T.B., Das A., (1988) - *Handbook of Biomass Downdraft Gasifier Engine Systems*, U.S Department of Energy, Colorado, 1988.
- [11] Ramírez-Arias A., Rodríguez F., Guzmán J.L., Arahall M.R., Berenguel M., López J.C., *Improving efficiency of greenhouse heating systems using model predictive control*. Copyright © 2005 IFAC.
- [12] Risovic S., Dukic I., Vukovic K., *Energy analysis of pellets made of wood residues*, Croat Journal for engineering, nr.1, 2008.
- [13] Varunkumar S., *Packed bed gasification-combustion in biomass domestic stove and combustion systems*, Ph.D.Thesis, Department of Aerospace Engineering Indian Institute of Science, Bangalore, India, febr.2012.

MATHEMATICAL MODEL AND SOFTWARE FOR EVALUATION OF ENERGETIC POTENTIAL OF VEGETAL BIOMASS IN AN AREA

Nagy Elena Mihaela¹, Coța Constantin¹, Cioica Nicolae¹,
¹INMA Bucharest-Cluj Napoca Branch,

ABSTRACT

Vegetal biomass is one of the major sources of renewable energy. In this context knowing the real energy potential of biomass is important because it allows farmers to choose correctly the type of biomass grown to be energy harnessed. Based on systemic analysis and statistics data available we developed a mathematical model that allowed the development of a software to determine real energy potential of vegetal biomass in an area. Systemic analysis that underlies mathematical model consists of an evaluation and analysis of all factors involved in production, transport and processing of biomass followed by its conversion to energy

1. INTRODUCTION

Biomass is considered the renewable energy source with renewable nature and positive impact on the environment due to the cyclicity of production and conversion processes, and also with high availability due to its variety.

National technical potential of biomass consists of five main categories: forestry residues and firewood, wood waste, sawdust; agricultural waste resulting from grain, corn stalks; remnants of grape-vines, branches of trees, etc. .; biogas, municipal household waste.

Theoretical all agricultural waste can be used as fuel, but their range is practically limited due to the possibilities of production, compaction, transport and use. The analysis of statistical data on agricultural production that generates waste categories that can be used for energetic purposes, it can be done a quantitative evaluation of them. Thus the total production of biomass that can be used for energy purposes, at national level, is presented in Table 1 [3,4]:

Tabelul 1: Productia totala de biomasa pentru utilizare in scopuri energetice

-straw	3.357 thousands t/year
- corn stalks and corn cobs	17.286 thousands t/ year
-sunflower	7.530 thousands t/ year
- vine-ropes	255 thousands t/ year
-ton of flax and hemp	5,590 thousands t/ year

Lack of information on types of biomass that can be used as an energy source, as well as those about their energy potential, slow implementation of new technologies to generate energy from biomass.

In this context, the software presented in this paper, is a useful tool to assess the real potential biomass energy crop, allowing the evaluation of the energy stored in a given category of biomass or those from a particular area.

2. METHODOLOGY

The mathematical model is based on systematic analysis of the process of production and use of biomass for energy. This analysis involves quantifying all activities throughout the "life cycle of biomass" - ie production, transport, processing, conversion into energy, reevaluate or disposal of waste resulting from the conversion [1].

Energy potential of vegetal biomass can be expressed by equation 1, where

$$W_V = SW_{Vi} = S(W_{Viu} - W_{Vic}) \quad (1)$$

W_{Vi} - the total amount of energy from vegetal biomass, in category i , available in the selected area, [kJ];

$i = 1, \dots, n$ - types of vegetal biomass, eg 1-vegetal biomass resulting from the wheat crop; 2 - vegetal biomass resulting from maize, etc.

W_{Viu} - the total amount of energy stored in total amount of vegetal biomass, of category i , available in the selected area, as energy source, [kJ];

W_{Vic} - the total amount of energy consumed to obtain vegetal biomass, of category i , available in the selected area, as energy source, [kJ];

The total amount of energy stored in the total amount of vegetal biomass, in category i , available in the selected area, as energy source, can be calculated with relation 2, where:

$$W_{Viu} = H_{Vi} \times M_{Vi} \quad (2)$$

H_{Vi} - average calorific value of vegetal biomass, in category i , available in the selected area;

M_{Vi} - the total amount of vegetal biomass, in category i , available in the selected area [kg];

Activities performed in the process of energetic use of vegetal biomass are grouped into two main stages: the stage of vegetal biomass production and conversion stage. The first stage, includes all operations performed in order to obtain vegetal biomass, from category i (for eg. works related to biomass cultivation, primary processing, transportation, etc.)

To the production stage of vegetal biomass, of category i , is associated an independent system, generically called "BIOMASSV" (fig.1)[2]. The input (I) of the system represents the total energy consumption (W_i) associated to activities/processes in vegetal biomass cultivation process, of category i . The output of the system (O) are represented by the energy stored in the vegetal biomass (W_o), obtained in the production stage. On the considered system acting other specific features (S_f), whose action can not be eliminated, such as soil characteristics, weather conditions, etc.

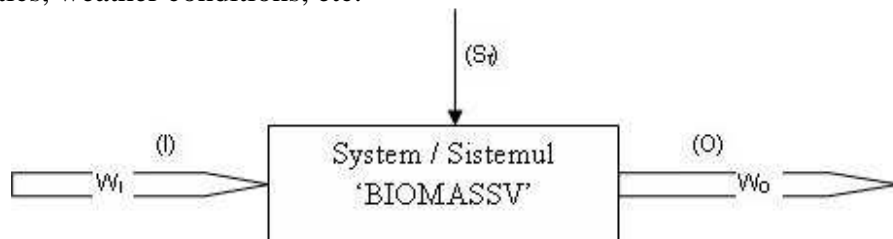


Figure 1. Block diagram of the independent system "BIOMASSV"

The behavioral equation of the "BIOMASSV" system, it is given by relation 3

$$E_{\text{prod}} = f(I, O, S_f) \quad (3)$$

where E_{prod} is total amount of energy available from the production process of vegetal biomass, and it is determined as a function of inputs I, outputs O, and specific features S_f , and the interdependencies between them.

The quantitative expression of the inputs(I), outputs (O), and the correlation between them, leads to the determination of an explicit mathematical expression, based on which is determined the total amount of energy available from the production process of vegetal biomass and, respectively, the energy consumption from process. To determine the mentioned mathematical expression, it is necessary to divide the "BIOMASSV" into subsystems associated with each operation of the composition of analyzed process.

The amount of total energy input, W_I , can be expressed as a sum of elemental (partial) energies, associated to working stages required to develop processes into the system of vegetal biomass production - relation (4)[2],

$$W_I = \sum_{i=1}^{n_1} W_{I,i}^j, i = 1, 2, 3, \dots, n_1 \quad (4)$$

where:

I - represent the inputs;

n_1 - the total number of different types of energy inputs in subdivision of order 1;

j - superscript, represent the category of the subdivision of energy input.

Else, the relation (4) can be expressed as relation (5) [2],

$$W_I = W_{I,1}^1 + W_{I,2}^1 + W_{I,3}^1 + \dots + W_{I,n_1}^1 \quad (5)$$

where:

$W_{I,1}^1, W_{I,2}^1, W_{I,3}^1, \dots, W_{I,n_1}^1$ – represent all the energies required for all the activities associated to different types of inputs defined into subdivision of category 1. So, eg. $W_{I,1}^1$ -represents energy input associated to agricultural machines used in vegetal biomass production; $W_{I,2}^1$ – represents energy input associated to fertilizers (chemical fertilizers-store the energy of the production, transport, distribution) etc.

Development of inputs system is continued until each elementary energy can be expressed quantitatively and can not be divided into further subcategories

The outputs (O), can be analyzed in the same way as the inputs, so, the total output energy (W_O), in our case, can be calculated using the relation (6) [2],

$$W_O = \sum_{i=1}^m W_{Opr,i} + \sum_{i=1}^m W_{Obpr,i} \quad (6)$$

where:

W_{Opr} –is the energy stored in the main products;

W_{Obpr} –is the energy stored in the by-products.

In the same way it is possible to analyse the specific features of the system S_f . These factors are abstract because they are not clearly defined quantitatively but they are distinct elements in the energies system. Thus, the functional relation (7) express S_f as a functional element of the system,

$$S_f = f(S_c, C_c, T_c, \dots O_c) \quad (7)$$

where:

S_c - is associated with soil characteristics;

C_c - is associated with climate characteristics;

T_c - is associated with characteristics of the technology used;

O_c -represents other characteristics.

3. RESULTS

Based on the mathematical model described above was performed a software program for assessing the energy potential of a farm. The program allows farmers to determine the energy potential of their farms depending of the type of farm: crop farm (which has as main activity

crop production), animal farm (profile only on livestock) or mixed farm (in which there are both crop and livestock).

Depending on the type of the farm, the program uses general data and specific data (depending on crop type or livestock type), entering these data is from the keyboard. The program uses also calculated values in the program (by formulas), which are displayed in the final energy balance.

Thus for a vegetal farm we have collected data from the keyboard, for example the data in Table 2, and we have calculated data, for example Table 3.

Tabel 2: Collected data from the keyboard

General data		Crop specific data	
Name	Simbol	Corn crop	
Total cultivated area (ha)	St	Total cultivated area (ha)	Sp
Energy consumed by irrigation pump (kwh)	Pi	Total amount of seeds used (kg)	spu
Number of hours (h)	Hp	Total amount resulting grains (kg)	Pbr
The total amount of oil used (L)	Mt	Total amount of vegetal material results (kg)	Pmv
The total amount of N used (kg)	FN	Total amount of vegetal waste (kg)	Pda
The total amount of P ₂ O ₅ used (kg)	FP ₂ O ₅	Cultura grâului	
The total amount of K ₂ O used (kg)	FK ₂ O	Total cultivated area (ha)	Sg
The total quantity of organic fertilizer (kg)	Fo	Total amount of seeds used (kg)	Sgu
The total amount of MCPA used (kg)	Mcpa	Total amount resulting grains (kg)	Sgr
The total amount of 2,4D used (kg)	D	Total amount of vegetal material results(straw) (kg)	Gpo
		Total amount of vegetal waste (kg)	Gda

Tabel 3.Calculated data (shown in the energy balance):

Name	Symbol and formula
Energy consumption with agricultural machines (with fuel) (kj)	CEma = 38,7Mt + 38,2Bt
Energy consumption with fertilizers (kj)	CEfe = 78,1FN + 17,4 FP ₂ O ₅ + 13,7FK ₂ O + 83,5Fo
Energy consumption with pesticides(kj)	CEpe = 130Mcpa + 85D + 61Fer + 397Ben
Energy consumption with irrigation (kj)	CEpi = Pi*Hp
Corn crop	
Seed energy consumption (kj)	CEps = 100spu
Energy stored in grains (kj)	EOPbr = 100 Pbr
Energy stored in vegetal material(straw)(kj)	EOPmv = 14,7Pmv
Wheat crop	
Seed energy consumption (kj)	CEgs = 13 Sgu
Energy stored in grains (kj)	EOgb = 13 Sgr
Energy stored in vegetal material(straw)(kj)	EOgp = 15,2Gpo
Total energy consumption = CEma + CEfe + CEpe + CEpi + CEps + CEgs	
Total energy stored = EOPbr + EOPmv + EOgb + EOgp	

The constants observed in the formulas are taken from the literature and have the following significance (Table 4):

Tabel 4. Constants taken from the literature

Vegetal farm	
Calorific value of diesel	38,7kj/L
Calorific value of petrol	38,2 kj/L
Energy contained in 1 kg fertilizer:	
N =	78,1 kj/kg
P2O5 =	17,4kj/kg
K2O =	13,7 kj/kg
Organic fertilizer =	83,5 kj/kg
Energy contained in 1kg pesticides:	
MCPA =	130 kj/kg
2,4D =	85 kj/kg
Calorific value of corn seed =	100 kj/kg
Calorific value of corn grain =	100 kj/kg
Calorific value of corn strains =	14,7 kj/kg
Calorific value of wheat seed =	13 kj/kg
Calorific value of wheat grain =	13 kj/kg
Calorific value of wheat straw =	15,2 kj/kg

The program may include more crops according to the needs of the farmer. Like the data for a vegetal farm, the program contains data for a livestock farm, too (raising cows, pigs or sheep).

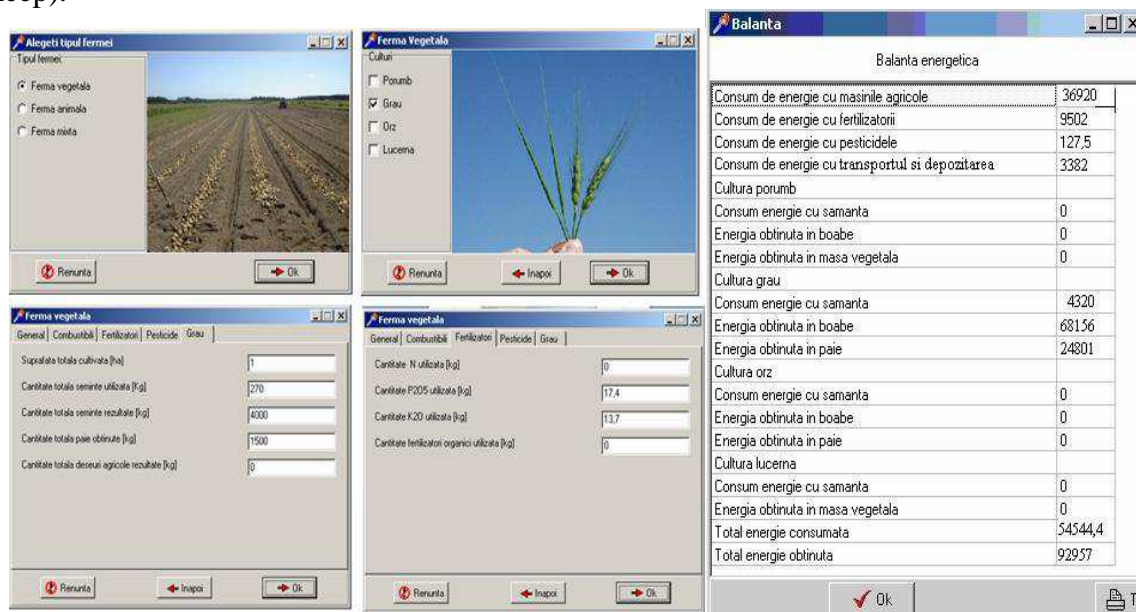


Figure 2. Software interface.

The software has a simple and friendly interface, it is easy to use and the results are displayed in tabular form easy to interpret.

After entering the required data by pressing OK the program will complete by opening a new window with generic name "energy balance" in which the energy balance of the farm is presented, on each crop type or livestock type, and an overview of energy consumption and energy obtained from the farm.

Using the program described above, a simulation was done for the case of wheat crop from an cultivated area of 10 hectares, brown-reddish soil, no irrigation, determining real energy potential of vegetal biomass obtained (Figure 3)

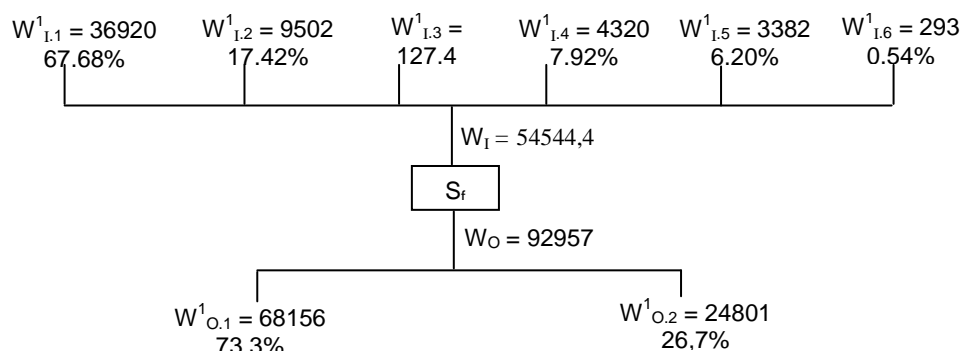


Figure 3 Energy balance for wheat crop, W is expressed in [MJ]

Where:

- $W_{I,1}^1$ – energy input associated to agricultural machinery;
- $W_{I,2}^1$ – energy input associated to chemical fertilizers;
- $W_{I,3}^1$ – energy input associated to herbicides;
- $W_{I,4}^1$ – energy input associated to seeds germination;
- $W_{I,5}^1$ - energy input associated to transportation and storage;
- $W_{I,6}^1$ – energy input associated to human labor.

4. CONCLUSIONS

Due to its modular structure the developed software is flexible and can be applied for energy assessment of different activities within a farm. Using this program you can make comparative studies in terms of energy, between different crops. Based on the results displayed in the energy balance it can be seen the activities with high energy consumption, thereby enabling to act to optimize the workflow from the point of view of energy consumption.

In the example shown is observed that the energy associated with agricultural machinery used is more than 50% of the total energy input into the system. The more it reduces the value of these kinds of energy, the higher the energy potential of the crop is, and thus, the profitability of biomass obtained.

References

- [1] Ros, V., “Systemic evaluation of energy production from biomass in a life cycle perspective” Buletin USAMV, nr 66 (1-2)ISSN 1843-5386, Cluj-Napoca, 2009.
- [2] Roș,V., Teodora Chira, G. Bâlc, L. Fechet, Metodă de evaluare a potențialului energetic dintr-o fermă agricolă, 2004, Balkan Agricultural Engineering Review Journal, vol.5, ISSN 1312 – 5443.
- [3] ***, ICEMENERG SA, INL, - Studiu privind evaluarea potențialului energetic actual al surselor regenerabile de energie in Romania (solar, vant, biomasa, microhidro, geotermie), identificarea celor mai bune locatii pentru dezvoltarea investitiilor in producerea de energie
- [4] ***, Strategia Nationala pentru dezvoltare Durabila a Romaniei – Orizonturi 2013-2020-2030, www.strategia.ncsd.ro , Bucuresti, 2008

INNOVATIVE TECHNOLOGY IN MEDICINAL PLANT PROCESSING WITH IMPACT ON FINISHED PRODUCT QUALITY

Pruteanu Mirabela Augustina ¹⁾, Muscalu Adriana ¹⁾, Danciu Aurel ¹⁾, David Ladislau ²⁾

1) National Institute of Research - Development of Machines and Installations for Agriculture and Food Industry - INMA Bucharest

2) Polytechnic University of Bucharest - Faculty of Biotechnical Systems Engineering

ABSTRACT :

In the world there is a spectacular comeback in natural medicine, forasmuch health is the most precious asset of man. Vegetable products obtained from medicinal herbs are preferred in treating various human diseases, because they are well tolerated by the organism.

In our country, medicinal plants have been known and used since ancient times. Therefore the requirements for useful vegetal raw materials are increasing, causing an increasing market value. Processing medicinal plants includes a entire assembly operations through which the operation is done, respectively the transition of the harvested vegetal material in a proper state for storage, packing or further processing.

This paper presents a medicinal plant processing technology in which are being used the following equipments : experimental technical system model type oven (heated with infraceramic radiators), grinder machine type Timatic, inclined band conveyor, chopped plant sorter and percalator type Timatic. Experiments whose results we present, revealed work performances which define the technologic process by the quality of finished products.

1. INTRODUCTION

An innovative technology means generating an idea and turning that idea into a useful application. The minimum requirements for an innovation is that the product, process, organizational method must be new or significantly improved. Without marketing of new innovative products, the innovative idea do not deliver benefits and has no economic value.[6]

Also a *innovative technology* refers to the choice of operations and phases, machines and devices, as well as improved production procedures of process. The result should be significant in terms of: the level of production, product quality or reducing production costs and distribution.[6]

In terms of structure, the technological process of primary processing of medicinal plants represents the part of the manufacturing that includes all operations and interrelated phases necessary for the preparation, namely the turning the harvested or purchased vegetal material, in a proper condition of storage, packing or further processing, within a production unit. The sequence of operations and phases in the primary process of medicinal and aromatic plants is determined by the primary material and the followed purpose.[4]

Thereby the fresh vegetal material, consisting of medicinal herbs, after screening, can potentially be chopped, then to be subjected to complicated operations of: extraction of volatile oils, obtaining natural extracts in different solvents, extraction of natural juices etc. Fresh vegetal material destined for drying, is dehydrated after conditioning, then, is chopped or crushed, depending on subsequent destination or the harvested active parts. [4]

Primary processing of medicinal plants involves operations: conditioning, chopping, drying, crushing, extraction of bioactive substances, made with specialized equipment, through which the raw material is transformed successively, quantitatively and qualitatively of the initial state in a finished product state.[4] These are forms under which medicinal plants are marketed. Thus, they may be: fhythosanitary products for internal or external use, nutritional and dietary

supplements, flavoring food additives, concentrated extracts, volatile oils, cosmetics, growth promoters for farm animals etc.

The phytotherapeutic action of medicinal plants is due to the presence of bioactive chemical components (active principles) with effects in the whole body metabolism. [2] Their valorization in quality products, involves their retrieval in various formulations, at the highest concentrations.

By cultivating medicinal herbs on scientific bases can be obtained a product rich in active principles and more homogeneous, can be avoid substitutions and counterfeits, and harvesting can be done in an optimal time (when the content of active principles is maximum)[3]

2. METHODS

At innovative technology experimenting for medicinal plant processing with impact on the finished product quality has been considered testing each of the equipment from the work technological flow, watching it work qualitative indices.

In view of the experiment technology for medicinal plants processing was carried out previously the experimentation, the following equipments (Figure 1) :

- Oven (poz.1);
- Medicinal plants cutting machine type Timatic (poz. 2);
- Inclined conveyor belt (poz.3);
- Chopped herbs sorter (poz. 4);
- percolator type Timatic (poz. 5).



Figure 1 Technological work flow of equipments for processing medicinal plants

Medicinal plants used for experimentation were : sage (*Salvia officinalis*), woolly finger (*Digitalis lanata*) and yarrow (*Achillea millefolium*).

The experimental model of Oven (*CE -0*) was used to dry medicinal plants. Due to the heating elements of infra-ceramic radiators type, the thermal process that takes place in the oven is a combination of thermal and radiation convection. Between the drying fluid (air) and solid (dry medicinal plants) it occurs the transmission of a complex thermal flow, under the conditions of warm air recirculation and refreshment.

Development of the process of drying medicinal plants is carried out, in three successive phases :

a) the preheating period, during which the heat is almost entirely consumed for heating the product until setting the temperature regime ;

b) the drying period with a constant speed, constitutes the actual drying period and lasts until reaching hygroscopic moisture in the peripheral layer;

c) The final drying period, with decreasing speed, in which the dehydration speed is reduced gradually. [1]

For drying medicinal plants in their preparation is proceeded according to species, is then manually distributed in drawers. Once completed the loading operation and closing the oven, it is set the maximum drying temperature (depending on the product) by using a temperature regulator, after an algorithm adjustment.[5]

The medicinal plant chopping machine type Timatic is used for grinding dry vegetal material or freshly harvested, at predetermined dimensions. It functions in the primary processing flow of medicinal and aromatic plants being fed manually onto the conveyor belt, so that the stems are oriented in the direction of its movement. The plants must be placed in the form of bundles to be easily handled. After pressing, they arrive at the cutting device which is equipped with a removable stainless steel knife with an adjustable cutting length. A self-sharpening blade ensures a longer and efficient cutting head. The cutting system is type guillotine.

Due to the automated command and control system, fitted to the equipment, can be adjusted and programmed: material supply, cutting length or the operating time. Cut plants at a predetermined size, depending on their subsequent use, fall on the inclined conveyor belt. [4]

The inclined conveyor belt has the role of retrieving the shredded product that falls from the plant cutting machine and to transfer it in the sorter, at the corresponding height of its supply.

The plant cutting sorter has the role of separate the shredded vegetal material, received from the inclined conveyor belt, in four sorts the dimensions of which depend on the sieve mesh size. Sorting is made by refusals method, using sets of sieves, with different mesh sizes, depending on the purpose for which we can obtain certain sizes.

When passing through the three sieves of the sorter, the chopped plants are separated on four varieties that are collected in bins, as follows:

- refusal of the upper sieve (sieve 1) can be used to extract bioactive substances;
- refusal of the sieves 2 and 3 may be packed in bags or sachets for medicinal teas;
- sifting the bottom sieve represents, in most cases, the waste.

The amplitude and frequency of the sieves vibration can be adjusted by modifying: inclination angle of the electric vibrating motors; vibrating motors counterweight; the rotation frequency of the vibrating motors.

The percolator type Timatic carries the extraction in a solvent, by percolating under pressure, of bioactive substances from dried vegetal material or freshly harvested. The extraction cycle is carried out in two phases, alternating a dynamic phase obtained from a programmed pressure, with a static phase, for the extract transfer in the solvent. The process is carried out automatically, the parameters are prescribed, controlled and displayed by a programmable automatic with display. Also the extraction takes place at a low temperature, resulting in a clean pre-filter extracts.

The types of raw materials for the percolator may be represented by: flowers, leaves, fruits, bark, roots, buds, seeds, stems of medicinal, aromatic, culinary or other plants.

3. RESULTS

The experimentation of each medicinal plant processing equipment were conducted at the INMA headquarters. Their objective was the technological process conducted by the five

equipments for processing three different species of medicinal plants: sage, woolly thumb and yarrow.

During the experiments performed with the experimental model oven could achieve and maintain any air temperatures $< 65^{\circ}\text{C}$. Due to the air temperature regulator, the steady state of the regime temperature varied maximum $\pm 1^{\circ}\text{C}$ toward the established limit. The furnace operated in a drying specific regime for each medicinal plant under study, as followed:

- **sage**, the regime temperature was $34,5^{\circ}\text{C}$, and the drying degree ranged from 64,22 to 11,8 %;
- **woolly finger**, the regime temperature was 40°C , iar and the drying degree ranged from 68,11 to 8,23 %
- **yarrow**, the regime temperature was $32,5^{\circ}\text{C}$, and the drying degree ranged from 62,12 to 9,89 %.

The experimentation of the medicinal plants cutting machine type Timatic, has been adjusted at 6 mm cutting length and the dry vegetal material mass from each plant subjected to shredding was 6 kg for each plant. In these conditions the following results were obtained:

- for **sage** in a range of 260 s, the chopping degree was 62,2 %,
- for **woolly finger** in a range of 182 s, the chopping degree was 61,3 %
- for **yarrow** in a range of 230 s, the chopping degree was 62,7 %.

During experiments the inclined conveyor belt functioned with a minimum speed of $0,007\text{ m s}^{-1}$ and the maximum speed was $0,57\text{ m s}^{-1}$.

For the experiments the medicinal plant sorter was adjusted for an optimal angle of inclination of sieves of 13° , the left electrovibrator sorter angle was $15^{\circ}40'$ and respective the right one was $17^{\circ}20'$. The following results were obtained for sorting at a cutting length of 6 mm:

- for **sage** the degree of sorting was 31,02 %,
- for **woolly finger** the degree of sorting was 20,05 %,
- for **yarrow** the degree of sorting was 29,4 %.

The experimentation conditions for the percolator type Timatic were the following:

- The bioactive substances extraction time was 60 min;
- The percolation pressure was $3 \cdot 10^5\text{ Pa}$;
- The dry vegetal material mass used in the extraction of each plant was 200 g;
- The solvent used was distilled water.

The degree of extract obtained was: 19,1% for **sage**, 25,1% for **woolly finger**, 24,2% for **yarrow**.

Were performed 3 repetitions for each experiment, in the same initial conditions, the values presented being an average of three determinations.

In figure 2 are presented the comparison of the degree of drying values, shredding, sorting and extraction for the three plant species, obtained from the use of innovative technology for processing medicinal herbs.

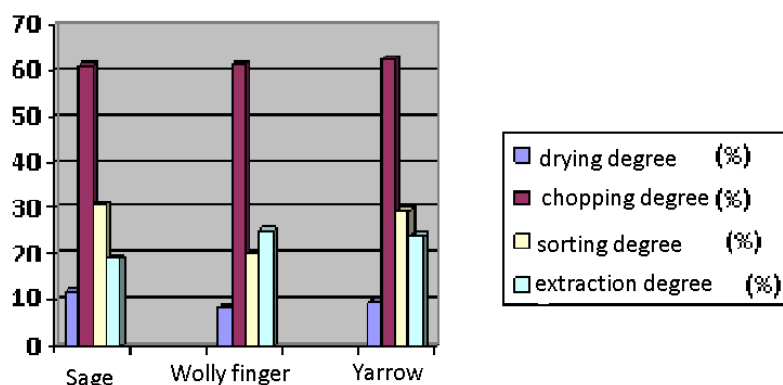


Fig. 2 Value of the degree of: drying, shredding, sorting and extractives, according to the medicinal plant

4. CONCLUSIONS

The drying degrees obtained after experiencing the drying oven with the three types of medicinal herbes are in accordance with the values required in practice for each type of product (sage 11,8%, wolly finger 8,23% and yarrow 9,8%) for avoiding the distruction of the bioactive substances content.

The chopping degree resulted for each of the three studied plants, with values between 61,2 and 62,7% respects the working conditions imposed by the extraction operation. A very advanced chopping degree may aggravate the extraction and can facilitate the extraction of substances without interest.

The sorting degree rendered by the sorting fractions uniformity on sives by the refusal method, with dimensions of approximately 6 mm, recorded values rening between 20,05% at wolly thumb and 31,02% at sage. These values are important for the future destination of medicinal plants.

The extraction degree recorded values of: 19,1% to sage, 25,1% to wolly thumb and 24,2% to yarrow. These values indicate an efficient extraction of medicinal plants rendered by the finished product quality.

The corresponding values of the drying degree of medicinal plants make possible subsequent chopping operations, transport, sorting and finally bioactive substances extraction according to specific technologies of the five equipments presented.

Through this innovative technology of precessing modicinal plants are opening new perspectives:

- Promotion of medicinal plants cultivation by diversifying processing equipments;
- Reduction of medicinal plants processing time;
- Increasing the quality of finished products obtained from medicinal plants due to the use of advanced processing equipments;
- Incresing the income of rural families due to the involvement in the cultivation and processing field of medicinal plants;
- Possibilities of production export by specialized operators.

The modern technologie presented is intended to process and efficiently use medicinal plants in order to improve the finished product and life in the rural areas quality.

REFERENCES:

1. Banu Constantin, 1998 – *Handbook of food industry engineer*, Technical Publishing House, Bucharest, Romania, ISBN 973-31-1188-0
2. Dihoru Al., Dihoru Gh., 2008 – *Plants used in human and animal digestion*, ARS DOCENTI Publishing House, Bucharest, Romania, pages 9, 11
3. Gabriela Păun, Oana Gheorghe, Mirela Diaconu, 2011 – *Medicinal plants advanced processing (cours)*, MedPlaNet project, Bucharest, Romania, pages 2-3, 8-11, 29
4. Muscalu Adriana, Vladut Valentin, Pruteanu Augustina, Nitu Mihaela, 2012 - *Harvesting and primary processing of medicinal and aromatic plants*, Terra Nostra Publishing House, Iasi, Romania, (ISBN 978-606-623-012-4); pages 28, 29, 51, 52.
5. Muscalu A., Mihai M., Chitoiu M., Dune A., Martinov M., 2010 – *Modern technical application for extending the domain of sericicultural exploitation and of medicinal plants cultivation in Romania*, INMATEH – Agricultural Engineering, vol. 32, nr. 3, Bucharest, Romania, ISSN 2068-2239, pages 65-71
6. *OSLO Manual*. 2005 - Guidelines for collecting and interpreting innovation data. 3rd ed. OECD / European Communities

MONTHLY AVERAGE TEMPERATURES DETERMINED ACCUMULATED WATER STORAGE TANK IN SUMMER AT SOLAR THERMAL PLANT

Rusănescu Carmen Otilia¹, Paraschiv Gigel¹, Gruia Adriana Irina¹, Rusănescu Marin²,
Duțu Mihaela Florentina¹

¹University Politehnica of Bucharest, Faculty of Biotechnical Systems Engineering, Romania

²Valplast Industry, Bucharest, Romania

ABSTRACT

In this paper, we present a solar thermal system for hot water supply of family housing to be functional and to exploit solar heat all year round: in summer for hot water and cold season contributes to heating the water in the storage tank. For this purpose we chose a storage tank with two coil type heat exchanger (exchanger for solar circuit and the other for connecting to a boiler) and a 2 kW electric resistance (to heat water in the boiler when any of the two sources is not available). We determined the average monthly temperatures accumulated water storage tank in summer.

Keywords: solar system, solar heat, solar collector field

1. INTRODUCTION

This paper is part of the new technological approach that takes account of capitalization “clean sources” which provide effective protection of the environment. Solar energy is available worldwide. Solar energy is the only form of clean energy that does not create harmful by products, as in classical and nuclear fuels, solar energy does not release heat in other forms of energy, but heat transport from the place of capture to the user. The traditional system for domestic hot water production, harnessing, always use a collector containing heat (liquid or gaseous working fluid) with or without accumulation system.

The principle of operation of these facilities is relatively simple and is based on the conversions of solar radiation into heat energy used to heat domestic water. Installation of solar energy conversion into heat is the main equipment solar collectors that convert solar radiant energy into thermal energy, solar heat storage devices, network transmission and distribution pipelines solar heat to consumers and automation elements whole process of production, storage, transport and distribution of solar heat. Typical, application systems for producing solar water heating provides hot water supply temperature of 45 °C in summer. In March-April and September-October the system can take only part of the thermal load required to produce hot water.

In practice it was found that the production of hot water at a temperature of 45 °C, considering the cold water temperature of 10 °C, 35 °C water temperature must be raised. Under these conditions the collector absorbing surface must reach a temperature of 50-70°C to transfer heat to the heat and domestic hot water then an acceptable efficiency.

Systems for domestic hot water still running and in winter, because they can provide even sunny winter days the amount of heat to be transferred to the domestic hot water.

All the practice has been established that a person consumes 50 liters per day hot water. This requires an area of 1,5 m² of collector covering domestic hot water needs a rate of 90-100%.

Average solar radiation is considered 1000 kW/m² per year.

Depending on the size of the solar hot water preparation and constructive solution adopted to obtain 300-500 kW/m² per year.

2. METHODOLOGY

When choosing a solar system for hot water, you first need to set the preferred temperature hot water usage and quantity and distribution needs throughout the day. Temperature of hot water use in most practical installations in operation temperature is 45°C. Hot water needs, depend on the attitudes and habits of consumers and the characteristics and specific features of each application.

The study concerns a family home consists of four that has a fuel consumption of 50 liters / person / day, so the solar system will need to produce 200 liters of hot water daily. Distribution of daily consumption of hot water, over 24 hours is considered statistically consistent with values determined by measurements.

On this basis we determined that the volume of storage tank which should cover domestic hot water scarcity at peak hours, you must be at least 120 liters. Therefore we chose a boiler with a capacity of 200 liters.

Cold water temperature used in hot water take into account the value of 10°C. Hot water will be prepared so that the user can reach a temperature of 45°C. To ensure that temperature is required at the point of storage temperature is higher, setting the value of 45°C Achieved by means of mixing valve placed on the grid, leaving the boiler. Typically, the point of storage is practiced temperature 60°C [1], which provides safe disinfection of hot water from Legionella bacteria.

In terms of health it is recommended that the hot water system to intervene household disinfectant at least once a year by raising water temperatures above 60 °C stored for a period of time.

The solar system object of this study will be operational throughout the year, in summer for hot water and cold season to contribute to preheat cold water in the boiler, following the rise in temperature of water use by at 45 °C is achieved by heating boiler (gas and condensation) or a 2-kW electric resistance heater mounted.

In terms of health it is recommended that the hot water system to intervene household disinfectant at least once a year by raising water temperatures above 60°C stored for a period of time.

The solar system object of this study will be operational throughout the year, in summer for hot water and cold season to contribute to preheat cold water in the boiler, following the rise in temperature of water use by at 45°C is achieved by heating boiler (gas and condensation) or a 2-kW electric resistance heater mounted.

For this purpose choose a bivalent boiler with two coils and electrical resistance of 2 kW.

Basic options for choosing solar thermal system for domestic hot water is to optimize the investment and operating costs. For this purpose we adopted the solution of solar thermal energy recovery throughout the year.

For this purpose we analyzed three offers of technically all three offerings using the same schematic structure of the solar system, all using vacuum tube panels, constructive solutions are relatively similar, which makes choosing the lowest bid price, respectively HELIS solar system. It provides heating to 200 liters of water at $t_0 = 10^\circ\text{C}$ (cold temperature) to $t_{\text{acm}} = 45^\circ\text{C}$ (temperature hot water consumption).

3. Results and discussion

- The amount of solar heat (Q_n) for heating water volume of 200 l is given by:

$$Q_n = m_a \cdot c_a \cdot \Delta t \quad (1)$$

- m_a - mass of water in kg corresponding to a volume of 200 l ($m_a = 200$ kg);
- c_a = specific heat of water ($c_a = 4,173 \cdot 10^3$ J/kg·°C);
- Δt = temperature difference in °C ($\Delta t = 35^\circ\text{C}$).

- The area calculated as required solar collector:

$$S_{col} = \frac{Q_n}{\eta_{col} \cdot G_{\beta med}} \quad (2)$$

- η_{col} - collector efficiency HELIS ($\eta_{col} = 0,83$ %);
- $G_{\beta med}$ - global radiation on collector plane averaged from March to October;
 $G_{\beta med} = 16,6$ MJ/m²·zi.

$$S_{col} = \frac{29,21}{0,83 \cdot 16,6} = 2,12 \text{ m}^2.$$

- Actually used a solar collector area of supply is 3.7 m² favorable situation because it has reserves to compensate for the heat losses along the primary circuit and the heat exchanger S_1 .

Theoretical explanations:

Solar circuit heat transfer in the boiler is achieved by S_1 which is heated in the heat exchanger fluid. Solar system with heat exchanger circuit S_1 form a closed system in which the movement is made by heating liquid.

The process can take place so that natural circulation and forced circulation as (solar circuit pump that increases the productivity of exchange). Heat load of the heat exchanger is determined from the heat balance equation [3]:

$$\dot{Q} = G_1 \cdot c_1 \cdot \Delta t_1 = \frac{1}{\eta_{sc}} \cdot G_2 \cdot c_2 \cdot \Delta t_2$$

where: \dot{Q} [W] is the flow of heat from the solar circuit;

G_1, G_2 [kg/h] is the mass flow of liquids;

c_1, c_2 [J/kg·°C] is the specific heat of liquids

The heat transfer due to a temperature difference occurs by conduction and radiation through the surface S_1 by the equation:

$$\dot{Q} = k \cdot S \cdot \Delta t_{med} \text{ [W]}$$

where k is the overall heat exchange coefficient [W/m²·°C]

To simplify assessment levels recorded in stored water temperature in the boiler use:

- The relationship of heat quantity:

$$Q_a = m_a \cdot c_a \cdot \Delta t$$

where: Q_a [J] is the amount of heat (thermal energy) received water from the boiler during the exchange, which is equal to the change in internal energy.

- expression exchanger efficiency:

$$Q_a = \eta_{sc} \cdot Q_d \text{ [2]}$$

where: Q_d [J] is the amount of heat absorbed by the solar collector heat solar heating cycle.

- Heat quantity Q_d :

$$Q_d = S_{col} \cdot \eta_{col} \cdot G_{\beta med} \quad (3)$$

- The amount of heat Q_a :

$$Q_a = \eta_{sc} \cdot Q_d \quad (4)$$

Q_n [MJ]	S_{col} [m ²]	Q_d [MJ]	Q_a [MJ]
29,21	2,12	$Q_d = 50,98$	$Q_a = 45,88$

- The relationship determine the amount of heat stored in the boiler water temperature t_{sb} :

$$Q_a = m_a \cdot c_a \cdot (t_{sb} - t_0) \quad (4)$$

$$t_{sb} = t_0 + \frac{Q_a}{m_a \cdot c_a} \text{ } ^\circ\text{C} \quad (5)$$

$$t_{sb} = 10 + \frac{45,88 \cdot 10^6}{200 \cdot 4,173 \cdot 10^3} = 64,97 \text{ } ^\circ\text{C}$$

This temperature is the average temperature of the water stored in the tank during the hot season.

- To determine the monthly average temperatures during each month of the hot season, from relations (3) and (4) calculate the amount of heat taken from the water heater:

$$Q_a = \eta_{sc} \cdot Q_d = G_{\beta_{med}} \cdot \eta_{sc} \cdot \eta_{col} \cdot S_{col}$$

$$Q_a = G_{\beta_{med}} \cdot 0,9 \cdot 0,83 \cdot 3,7 = 2,76 \cdot G_{\beta_{med}}$$

The value of q is introduced in relation (5) becomes:

$$t_{sb} = t_0 + \frac{2,76 \cdot G_{\beta_{med}}}{m_a \cdot c_a}$$

Table 1: Monthly average temperatures in the months of March to October















$t_{sbIII} \text{ } ^\circ\text{C}$	$t_{sbIV} \text{ } ^\circ\text{C}$	$t_{sbV} \text{ } ^\circ\text{C}$	$t_{sbVI} \text{ } ^\circ\text{C}$	$t_{sbVII} \text{ } ^\circ\text{C}$	$t_{sbVIII} \text{ } ^\circ\text{C}$	$t_{sbIX} \text{ } ^\circ\text{C}$	$t_{sbX} \text{ } ^\circ\text{C}$
47,91	60,82	68,31	75,44	73,92	72,50	66,40	42,97

Level during April-September temperatures of over 60°C will ensure sterilization of water stored in the tank against Legionella bacteria.

Hot water temperature of 45°C will ensure the automatic mixing valve is placed at the exit of the boiler. The calculated values for cylinder temperature which explains the company MEGASUN as typical boiler cold water temperature = 10°C, cylinder temperature = 60°C and hot water temperature prepared by mixing = 45°C. Heater coil is calculated so that the solar circuit is circulated heat with temperatures between 55°C and 80°C.

Schematic structure of the solar system HELIS

Solar system presented consists primarily of the following components:

	solar collector field		filling valve drain
	shut off valves		heating cooling equipment off the cycle primary
	retaining flap		expansion box
	temperature sensors		air vent
	pump		thermostatic mixing valve
	safety valve		coil heat exchanger
	flow sensors		panel

Scheme solar system consists of components and equipment HELIS package is shown in Figure 1:

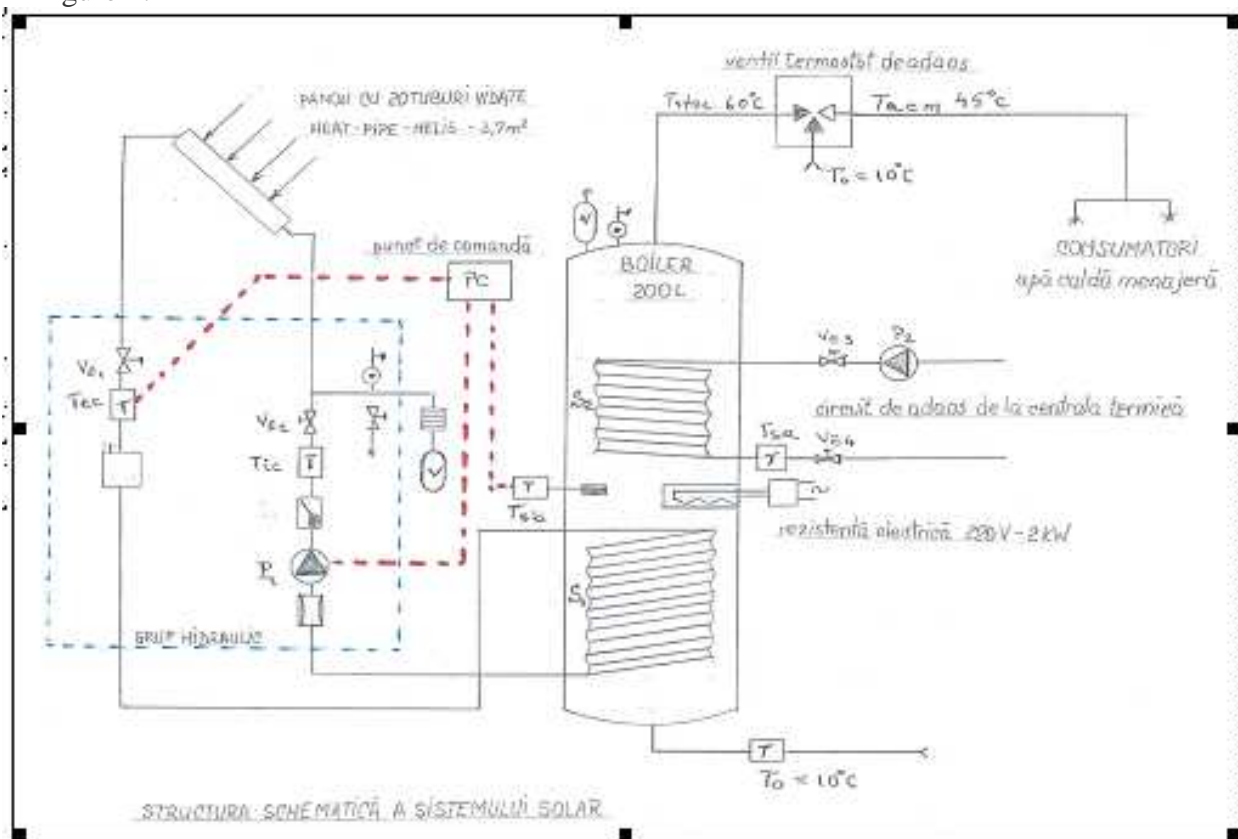


Figure 1: HELIS solar system diagram

4. CONCLUSIONS

In this paper, we chose a solar thermal system for hot water supply of family housing to be functional and to exploit solar heat all year round: in summer for hot water and cold season contribute to the heating of water in the storage tank.

For this purpose we chose a storage tank (tank) with two coil type heat exchanger (exchanger for solar circuit and the other for connecting to a boiler) and a 2 kW electric resistance (to heat water in the boiler when any of the two sources is not available).

To purchase equipment solar system components we considered that most companies that have manufacturing and marketing concern such facilities supplied equipment packages and electronic components integrated for different types of applications that use solar thermal. As a result, the three bids considered that the technically used the same schematic structure of the solar thermal system we chose the one with the lowest price.

We determined the average monthly temperatures accumulated water storage tank in summer. Especially solar panel scheme used HEAT-PIPE Helis presents a major advantage to be taken into account in that outside a maximum efficiency of 80% has the advantage that installs with simple installation procedures. It is worth noting that the entire solar installation can be installed and functionally tested prior to actually mount the solar collector vacuum tubes. They can be mounted at the end of trial operations of the solar system in a very short and very simple installation procedure.

References

- [1] www.megasun.com - Solar thermal
- [2] Răducanu P. *Technical Thermodynamics*, Bren Publishing House, Bucharest, 2010
- [3] Kicighin M.A., Kostenko G.N. - *Heat exchangers and vaporizing facilities*, Technical Publishing House, Bucharest, 1958

VEGETATION FILTERS FOR EXTENSIVE WASTEWATER TREATMENT PLANTS FROM THE RURAL AGGLOMERATION

Safta Victor-Viorel*, Dilea Mirela, Constantin Gabriel-Alexandru
University POLITEHNICA of Bucharest, Department of BIOTECHNICAL SYSTEMS

ABSTRACT

Taking into account that implementation in the rural area of sewage systems and wastewater treatment in classic form, involves considerable investments, there are presented as particularly attractive alternatives, viable and significantly cheaper, both in construction and in operation, the use of modern and efficient sewage solutions and the use of *extensive wastewater treatment plants*.

In the present paper there are presented the construction, operation, the characteristics and performances of some extensive wastewater treatment plants with *vegetation filters*.

1. INTRODUCTION

Extensive treatment processes are wastewater treatment processes which are very close to the natural processes of water purification (self-purification processes) where the main role is played by microorganisms (bacteria). Naturally, into the contaminated water there are microscopic algae which use solar energy to produce the required oxygen by photosynthesis necessary to the bacterial cultures which are found dispersed or fixed on different supports in the water subjected to the process, to achieve the purification of water by a biological process. Therefore, the extensive treatment processes present the great advantage that the vast majority of them, don't need external input of energy for carrying out wastewater treatment processes, making it very economical in use. Also, the extensive wastewater treatment plants have the advantage of very high efficiency to remove the organic loads and the nutrients from water that is subjected of treatment providing high quality effluent, that can be discharge without danger to natural watercourses. Another advantage of the the extensive wastewater treatment plants is that they have a very natural appearance (not like an industrial plant), fit perfectly into the natural landscape, without affecting this one at all.

It is to be noted that extensive wastewater treatment plants have been developed in different European countries (France, Germany, Spain, Netherlands, and so on) usually for serving small communities with a population of around 500 equivalent inhabitants [1,2].

In the present paper there are presented the construction, operation, the characteristics and performances of some extensive wastewater treatment plants with *vegetation filters*. For this purpose will be analyzed the most common types of vegetation filters, namely: *vertical flow vegetation filters* and *horizontal flow vegetation filters*.

Will be given representative examples of extensive wastewater treatment plants with vegetation filters from the country and the world, highlighting the constructive features and the performances obtained.

2. OPERATING PRINCIPLES, CONSTRUCTION AND PERFORMANCE OF VEGETATION FILTERS

Vertical flow vegetation filters (Figure 1) are extensive plants with aerobic bacterial biomass in the form of film fixed on the granular material of filled successive layers (gravel or sand, usually with different particle sizes, depending on the polluting load of the wastewater to be treated), placed in an uninsulated excavation, if it is built on impermeable land, or waterproofed with waterproof geomembrane, if it is built on permeable land. On the surface of granular layer of the filter is planted wetlands specific cultures (such as reed, rush, etc.).

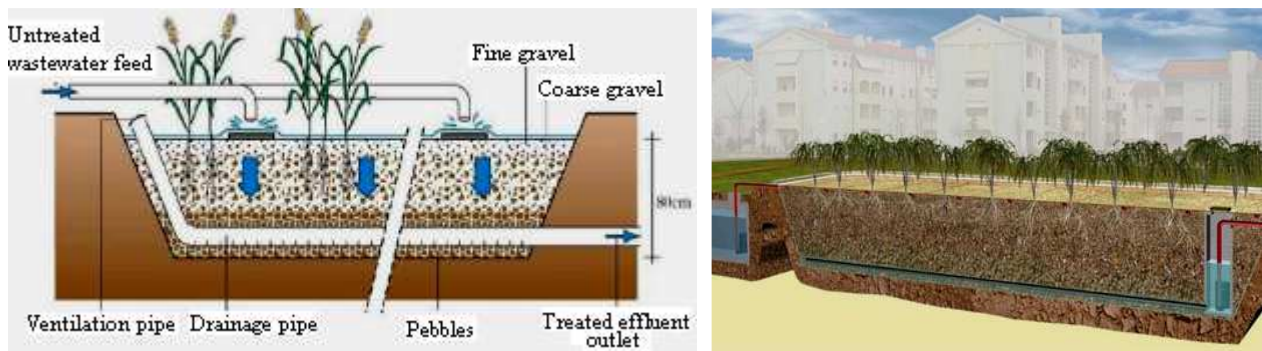


Figure 1: Principle and construction of vertical flow vegetation filter [2,3]

The performances obtained by wastewater treatment plants with vertical flow vegetation filters are the following:

- the reduction of biochemical oxygen demand (CBO₅) below 25 mg/l;
- the reduction of chemical oxygen demand (CCO) below 90 mg/l;
- the reduction of suspended solid below 30 mg/l;
- the reduction of organic nitrogen below 10 mg/l, on average, with the maximum not exceeding 20mg/l;
- the reduction of phosphorus is usually lower and depends on the absorption capacity of the granular layer and on the age of the plants;
- the reduction of the number of pathogenic (from 10 to 100 times).

Horizontal Flow Vegetation Filters (Figure 2), are extensive plants with aerobic bacterial biomass in the form of a film fixed on a granular filler material, placed also in the excavation somewhat similar to that of the vertical flow vegetation filters, but with some particularities, namely: during the operation the layer of granular material is constantly almost completely saturated with water to be treated; the wastewater influent is introduced into plant at one end, through a distribution system buried in the filler material, that makes a uniform administration of this throughout the cross-section of the filler bed. The water to be treated flows gravitationally to the other end of the plant, due to the bottom slope in a direction that is practically horizontal.

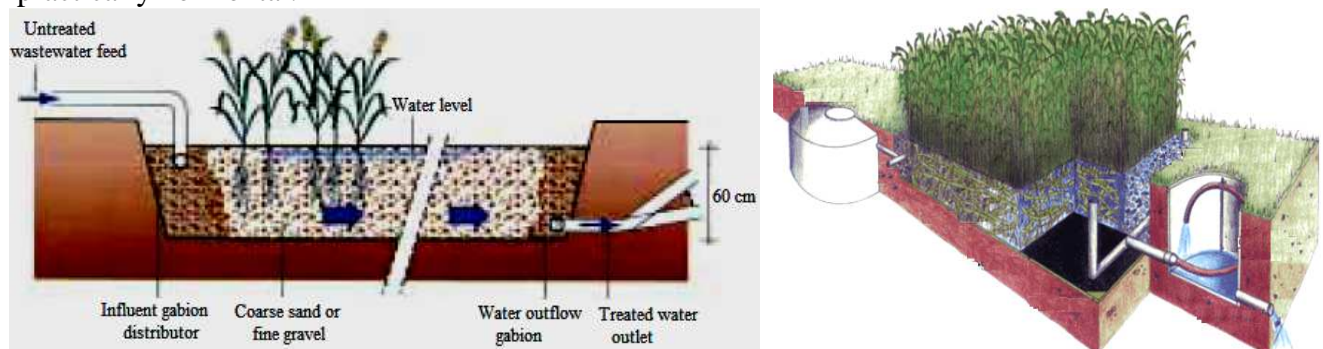


Figure 2: Principle and construction of horizontal flow vegetation filter [2,4]

The performances obtained by wastewater treatment plants with horizontal flow vegetation filters are the following:

- the reduction of effluent biochemical oxygen demand of about 70 – 90%, for different influent pollutant load varying from 50 to 200 mg/l CBO₅, and for a sizing of 3 to 5 m²/equivalent inhabitants of installation using gravel as a filler;
- nitrification is limited but denitrification is very good;
- the removal of phosphorus depends of the type of soil used, but remains relatively low.

3. REPRESENTATIVE EXAMPLES OF FILTERS VEGETATION

At the present, vegetation filters have become an attractive alternative solution, viable and significantly cheaper, both in construction and in operation to plants of sewage and wastewater involving considerable investments.

Because these systems present several advantages, such as: very economical in use (do not require any type of energy supply), a very natural appearance and very high efficiency to remove the organic loads and the nutrients from wastewater, they are widely used in the most countries of the Europe.

Further, there are presented representative examples of horizontal flow vegetation filters and vertical flow vegetation filters, used in Europe.

The vegetation filters are used in the United Kingdom of Great Britain and Ireland, which proved to be the most effective natural method to treat wastewater.

Water flowing through vegetation filter can be used for garden irrigation, for sports facilities (golf courses, hippodromes, lawn), for supermarkets, office buildings etc.

In figures 3 and 4 there are presented horizontal flow vegetation filters used in the Ireland [5].



Figure 3: The construction of a horizontal flow vegetation filter in Ireland [5]

In figure 4 is presented a horizontal flow vegetation filter used since 2005 for wastewater treatment from a small farm from Ireland, Fermanagh. The system has worked very effectively in reducing BOD (figures show 870 mg/litre at the inlet reducing to 26 mg/litre at the discharge) and suspended solids [5].



Figure 4: Horizontal flow vegetation filter in Ireland, Fermanagh [5]

Further, there are presented examples of vegetation filters used in different regions of Germany (figures 5 - 7) [6].



Figure 5: Vegetation filter in Lahstedt-Gadenstedt, Niedersachsen (1998)



Figure 6: Vegetation filter in Bad Emstal (Hessen), 2002



Figure 7: Vegetation filter in Naumburg (1999), height of the reeds up to 4 m



Since around 1990, a special vertical flow vegetation filter for treating wastewater has been used in France called the „French System”. In France all the filters are usually planted with reed [7].

Moelle et al. (2005) recommend dividing the first stage for wastewater treatment into three vertical flow vegetation filters, and the second stage for secondary treatment into two vertical flow vegetation filters. Molle et al. (2005) reported for the very highly loaded gravel bed a removal efficiency of 80% BOD, 86% total suspended solids and 50% the organic and ammonia nitrogen, which is more efficient than any conventional pre-treatment process.

In figures 8 and 9 can be seen the “French System” constructed to treat wastewater from Albondon, Spain [8].



Figure 8: “French System” constructed to treat wastewater from Albondon, Spain [8]



Figure 9: Distribution pipes for wastewater in French System in Albondon, Spain [8]

Furthermore, because of the advantages presented above, these extensive wastewater treatment plants with vegetation filters have been widely adopted by developing countries around the world.

In the figures below there are presented such extensive wastewater treatment plants with vegetation filters constructed in developing countries from America.

The figures 10 and 11 show the construction of a horizontal flow vegetation filter in Lima, Peru and in Bayawan City, Philippines [7].



Figure 10: Vertical flow vegetation filter under construction in Lima, Peru [7]



Figure 11: Vertical flow vegetation filter under construction in Bayawan City, Philippines [7]

A combination of a vertical and a horizontal vegetation filter is recommended to ensure suitable treatment efficiency for waste water to be treated.

Figure 12 shows a representative example of combined horizontal and vertical flow vegetation filter.

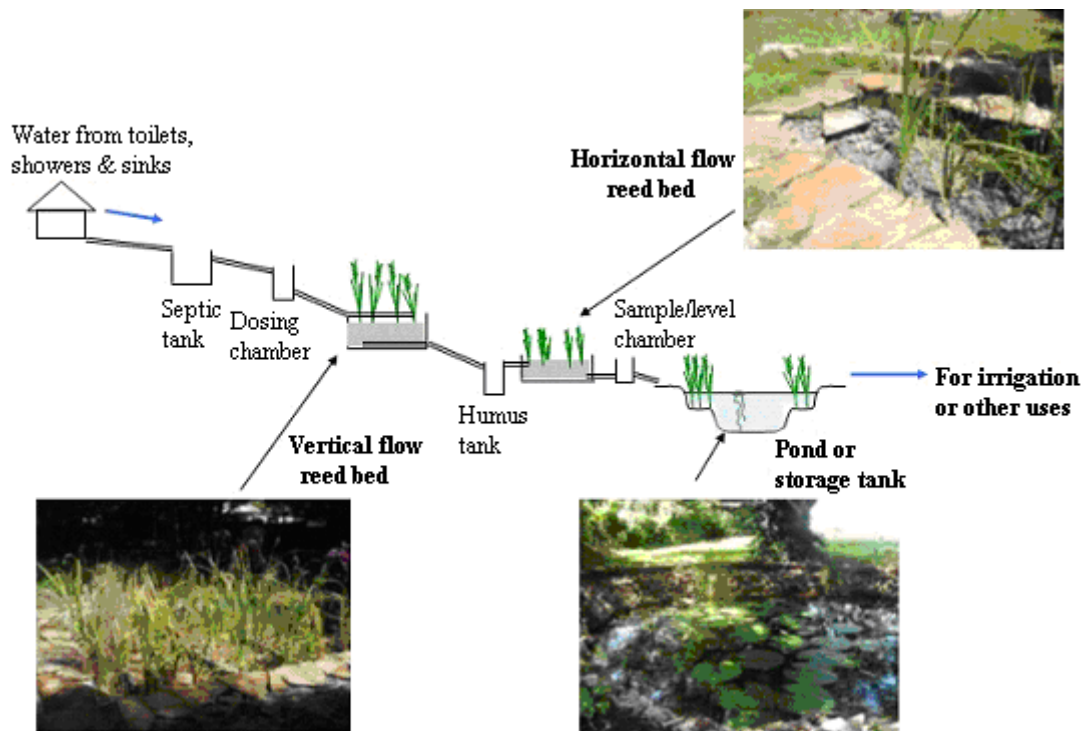


Figure 12: A combination of reed bed system [9]

4. CONCLUSIONS

In the present paper there was presented aspects regarding the construction, operation and the characteristics and performances of some extensive wastewater treatment plants with *vertical flow vegetation filters* and *horizontal flow vegetation filters*.

Using the vegetation filters systems in wastewater treatment represents one of the most practical and inexpensive method that is widely adopted in many countries around the world. This, has proved to be an effective method in the removal of suspended and dissolved organic substances and nutrients up to 80%.

The vegetation filter systems are effective in treating wastewater coming from different industrial, agricultural and domestic activities, being particularly suitable for small towns.

AKNOWLEDGEMENTS

The co-author Constantin G.A. wishes to thank the Sectoral Operational Programme Human Resources Development 2007-2013 of the Romanian Ministry of Labour, Family and Social Protection through the Financial Agreement POSDRU/107/1.5/S.76903.

References

- [1] Safta, V.V., *Procedee extensive de epurare a apelor uzate*, Note de curs la disciplina Dezvoltare rurală durabilă și protecția mediului (Facultatea Ingineria Sistemelor Biotehnice, licență anul IV, Specializarea Dezvoltare rurală durabilă) - anul universitar 2012-2013.
- [2] ***Guide, *Extensive Wastewater Treatment Processes - adapted to small and medium sized communities (500 to 5000 population equivalents)*, Office of official publications of the European Community, Luxembourg , 2001.
- [3] <http://www.carradepurazioni.com>.
- [4] <http://www.cee-environmental.com>.
- [5] ***NIRBC Ltd, *Treating water, naturally – Reed bed sewage system & wastewater treatments*, www.nireedbeds.co.uk.
- [6] *** *Natural Treatment of sewage sludge in Reed Planted Dewatering Beds*, Ingenieurburo Blumberg – Gansemarkt 10 – D-37120 Bovenden, Germany, www.blumberg-engineers.de.
- [7] Hoffmann, H., Platzer, C., Winker, M., Elisabeth von Muench, *Technology review of constructed wetlands, Subsurface flow constructed wetlands for greywater and domestic wastewater treatment*, Eschborn, Germany, 2011.
- [8] Molle, P., Liégnard, A., Boutin, C., Merlin, G., Ivema, A., *How to treat raw sewage with constructed wetlands, an overview of the French system*, Water Science and Technology **51**(9), 11-21, 2005.
- [9] Environmental Water and Sanitation Solutions – Green Water, <http://www.green-water.org/index.htm>.

ENVIRONMENTALLY DRYING VEGETABLES USING GREENHOUSES CROP RESIDUES

Sima Cristian*, Haraga Georgeta**, Murad Erol**

*Marvior Expert, ** University POLITEHNICA Bucharest

Abstract

The reduction possibilities of production costs for generating thermal energy for vegetables dryers were studied using local biomass derived from crop residues in greenhouses. Greenhouses crop residues used for thermal energy generation can get to an annual average of 5.7 t/ha dry biomass with an energy potential of 73 GJ/ha-year at a cost of up to 60 €/t. The 10-50 mm chopped biomass and with a humidity below 15% is gasified using TLUD gasification process characterized by very high energy conversion efficiency, stability and security; emissions of CO and PM are very low. TLUD gasification process produces on average 14% biochar that can be used as fuel, as filter material or as an amendment to increase the fertility of agricultural soil and sequestration of carbon from the atmosphere. For the biomass resulting from sorting and drying greenhouses crop residues were defined characteristics for gasification in a TLUD modules and the resulting biochar. Simulated experiments were performed with a model developed for USCMER 30/60MGB dryer equipped with two heating modules GAZMER type MGB 40/150 for convective drying tomato slices. For generating a thermal energy use biomass from tomato crop residues with a LHV=15.2 MJ/kg, with a LHV=14.6 MJ/kg for a integrally gasified biomass and an average 14% biochar product. A batch of 252 kg of tomato slices to 9 h dried to a moisture content of 93% to 8%, with a consumption of 106 kg biomass and resulting 14.6 kg biochar. The cost of biomass used is 6.34 €, ie 8 times cheaper than diesel. When drying it sliced tomato tonne obtain 57.86 kg biochar in soil which introduced leading to a negative balance -158.5 kg CO₂. Harvesting, processing, storage, distribution and use for energy a residual biomass from crop residues is coming from the effective realization of of both social and environmental local resources, contributing to local sustainable development.

Keyword: drying, greenhouse residues, gasification, biochar, simulation

1. Introduction

This paper makes an analysis of the utilization of agricultural biomass derived from crop residues, especially from the ones produced in greenhouses, for the vegetables convective drying, with the aims to reduce thermal energy consumption, to significantly decrease the CO₂ emissions and to enhance the energy independence degree of the drying facilities.

The cropped residual biomass is sorted in order to separate the leaves from the creeping stalks, the last ones being chopped to 10 - 50 mm, deposited in containers, transported and dried naturally or forced to attain a 15% humidity level. The stored biomass may be gasified using the TLUD process characterized by a very high energy conversion efficiency, stability and operation safety, and by CO and PM very low emissions.[10,11,13,14]

From the used biomass, the TLUD process generates also 10 to 15 percent biochar that may be used as fuel or agricultural amendment destined for the soil fertility growth and for the atmospheric carbon sequestration. For exemplifying the tomato slices drying, the team has chosen to use the biomass resulted from the tomato creeping stalks. The used biomass and the resulted biochar were chemically and energetically defined in conformity with the gasification process TLUD, data used in the simulated experiments with a model of the USCMER 30/60MGB drier equipped with two energy modules GAZMER type MGB 40/150. [10,13]

The experimental results demonstrate that the utilization of the biomass resulted from the vegetable growing is feasible, the cost of the thermal energy being in average eight times lower than in the case of diesel fuel burning.

From an environmental point of view, the biomass utilization is made with a CO₂ balance close to zero. The operation in a biochar production regime and its incorporation into the soil for fertility growth purposes, results in a sequestration in the soil for a long period of time of approximately 25% of the carbon generated by the gasified biomass. In this particular situation, from the 8.7 tones/hectare · year processed tomato crop biomass residues, may result

1.13 tones of biochar that contains 910 kg of carbon which, incorporated in soil, generates a CO₂ negative balance of -3.3 tones/hectare · year. The efficient utilization of the residual biomass from vegetables growing contributes to a better turning to account of the agricultural resources, to a decrease of the environmental impact of the thermal energy intensive agricultural facilities, and to an occupation growth in rural areas.

2. Greenhouses crop residues properties

The quantities and the humidity of the vegetables biomass residues varies by crop category and plantation density. Initially, the whole residual quantity is cropped and than the leaves are mechanically separated from the creeping stalks; on average only 20% remains from the initial quantity. The creeping stalks are chopped to 10-50 mm and dried naturally or by mechanical ventilation up to an average humidity of 10%, with a density of the bulk of approximately 200-250 kg/m³. [2,11,13,14]

Table 1 presents the characteristics of residues for the main eight species of vegetable crops from Romania, an estimation of the annual average mass of crop, the humidity and the energy potential. Because of the vegetable crop diversity, the biomass residues are characterized by different chemical and energy properties, therefore in order to make a global estimate, one can use the average characteristics presented in table 1. [2,14]

Table 1. Greenhouses crop residues proprieties

Crop species	Crop Wastes	Wastes sorted	Ash (dry bm)	Humidity	HHV BM sorted	HHV (dry)	LHV (dry)	BM (dry)	Energy content
	t/ha·year	t/ha·year	%	%	MJ/kg	MJ/kg	MJ/kg	t/ha·year	GJ/ha·an
Courgette	20.00	4.00	3.42	20	12.85	16.06	14.67	3.20	46.95
Cucumber	24.00	4.80	3.50	20	12.60	15.75	14.36	3.84	55.14
Aubergine	27.00	5.40	2.65	20	16.53	20.66	19.27	4.32	83.26
Tomato	49.00	9.80	3.04	20	14.82	18.53	17.14	7.84	134.34
Bean	23.00	4.60	2.88	20	17.00	21.25	19.86	3.68	73.08
Green pepper	28.00	5.60	3.56	20	15.26	19.08	17.69	4.48	79.23
Water melon	24.00	4.80	3.08	20	14.25	17.81	16.42	3.84	63.06
Melon	33.00	6.60	3.21	20	13.50	16.88	15.49	5.28	81.76
Mean	28.50	5.70	3.17		14.60	18.25	16.86	4.56	77.10

It is to be emphasized the important value of the average potential energy of the vegetable biomass that reaches 73 GJ/ha, the equivalent of 20.27 MWh or 2150 L diesel fuel.

Table 2. Processed biomass from greenhouses crop residues

Crop Species	BM sorted (dry)	LHV (dry)	Humidity	LHV (wet)	BM sorted (wet)	BCH (mean)	LHV BCH (mean)	LHV BM (gasif.)	Energy content (gasif.)
	t/ha·year	MJ/kg	%	MJ/kg	t/ha·year	%	MJ/kg	MJ/kg	GJ/ha·year
Courgette	3.20	14.67	10.00	13.20	3.56	14.00	18.50	12.34	37.74
Cucumber	3.84	14.36	10.00	12.92	4.27	14.00	18.50	12.02	44.09
Aubergine	4.32	19.27	10.00	17.34	4.80	14.00	18.50	17.15	70.81
Tomato	7.84	17.14	10.00	15.43	8.71	14.00	18.50	14.93	111.82
Bean	3.68	19.86	10.00	17.87	4.09	14.00	18.50	17.77	62.49
Green pepper	4.48	17.69	10.00	15.92	4.98	14.00	18.50	15.50	66.36
Water melon	3.84	16.42	10.00	14.78	4.27	14.00	18.50	14.17	52.00
Melon	5.28	15.49	10.00	13.94	5.87	14.00	18.50	13.20	66.59
Mean	4.56	16.86	10.00	15.18	5.07	14.00	18.50	14.64	63.99

Among analyzed crops it is to be highlighted the tomato crop with high density, that generates 9.8 tones/hectare of residual biomass that can be processed, with a 134 GJ/hectare potential energy, the equivalent of 3988 L diesel oil.

For the processed biomass for its use as fuel, gasification or pellet production, table 2 presents the main characteristics.

3. Greenhouses crop residues gasification

The free combustion of the chopped vegetables biomass generates huge quantities of pollutants and an enormous waste of energy. The combustion of gas fuels is more complete and cleaner than the combustion of solid fuels, due to a better mix between air and fuel. Therefore, it is more environmentally friendly and more economically to use the gasification processes as first phase of the biomass conversion.

As an ecological and economical alternative for the biomass gasification generated from the agriculture it can be used the micro-gasification process TLUD (Top-Lit-Up-Draft) conceived by Thomas Reed in 1985. In the case of classical gasification process in co-current, the biomass layer descends continuously and enters gradually in the pyrolysis and oxidation areas that have a fixed position in the gasifier's reactor. At the TLUD process, the biomass layer is fixed in the reactor, and the pyrolysis and oxidation front is continuously descending consuming biomass, characteristics that insure a safe and controllable operation. [5, 8, 10, 13]

The gasification process TLUD can be stopped when all the biomass from the reactor was pyrolyzed, and were it remains a quantity of unconverted carbon, named biochar current; or the gasification can be continued until the biochar becomes ash. The percentage of biochar is situated between 10 and 15 % from the biomass entered in the gasification process and depends on the lignin content, on the average temperature of the oxidation layer and on the heating speed. The biochar can be used as fuel, as a filter material or, more efficiently as an agricultural amendment incorporated in soil, contributing also to the sequestration for a long period of a part of the carbon from the utilized biomass. [4, 5, 10]

In order to be used in the TLUD gasification process, the vegetable biomass must be chopped to 10-50 mm and dried naturally or forced up to an average of 10 % humidity. From the TLUD gasification process results an average of 14% biochar and 86% from the biomass is gasified and completely converted in thermal energy. For the tomato slices drying it will be utilized the residual biomass generated by the tomato crop. The characteristics of the processed biomass for gasification with the TLUD process are presented in table 3.

Table 3. Processed tomato wastes from gasification

Features	UM	Input Biomass	Biochar	Gasified Biomass
<i>Relative mass</i>	%	100	14	86
Carbon	%	40.29	74.70	34.70
Oxygen	%	40.98	3.70	47.05
Hydrogen	%	5.98	2.10	6.62
Ash	%	2.74	19.50	0.00
Water	%	10.00	0.00	11.63
LHV	MJ/kg	15.20	18.60	14.64
Average bed density	kg/m3	225.00	180.00	-
Specific mass	t/ha	8.70	1.22	7.48
CO ₂ balance	t/ha	0.00	-3.34	0.00

4. Tomato slices drying

In order to dry the tomato slices it is used the drier category USMER 30/60MGB destined for the convective drying of the vegetal agricultural products, that has a 30 m² laying surface on caskets and needs a 60 kW thermal power. It is equipped with two energy modules GAZMER type MGB 40/150 where it is processed the biomass from tomato crop residues with the TLUD process. [3, 8, 13]

For the determination of the drying performances, simulated experiments were conducted with the numeric model of the drier USCMER 30/60MGB materialized in the simulation program US30GB04.PAS developed in the modelling environment – numerical simulation SIMUSCONV-V.1.3 for processes and facilities for convective drying developed at the Biotechnical Systems Department from the Bucharest Polytechnic University. [1, 6, 7, 9]

In the automatic management software were introduced energy optimization procedures of the drying process and of the quality of the dried products, and also for the optimization of the energy modules TLUD GAZMER type MGB 40/150 operation. [7, 8, 9, 10, 12, 13]

5. Results and discussions

Table 4 presents the experimental results simulated for the drying of the tomato slices with processed biomass from tomato crop residues.

Table 4 Convective tomato slices drying with USCMER 30/60MGB

Indicator	UM	Value
Slices' initial humidity	%	93.00
Slices' final humidity	%	8.00
Average drying efficiency	%	41.10
Mass of the humid tomato slices	kg.cum	252.00
Mass of the dried tomato slices	kg.cus	19.20
Biomass consumption	kg.bm	105.60
Biochar generation	kg.bch	14.58
Gasified biomass consumption	kg.bmg	91.02
Use of primary energy	MJ	1328.89
Energy consumption for 1 kg of humid slices	MJ/kg.cum	5.27
Energy consumption for 1 kg of dried slices	MJ/kg.cus	69.21
Biomass unit consumption	t.bm/t.cum	0.42
Humid slices mass dried with a tone of creeping stalks	kg.cum/t.bm	1233.06
Price of the biomass from tomatoes crop waste	€/t.	60.00
Cost of the thermal energy from biomass per charge	€/charge	6.34
Unit cost for the thermal energy from biomass	€/t.aim.	25.14
Diesel fuel consumption	L/charge	41.63
Diesel fuel price	€/L	1.35
Cost of the thermal energy from diesel fuel	€/charge	56.13
Ratio of the diesel fuel/biomass costs		8.86
Biochar generated by 1 tone of dried humid slices	kg	57.86
CO ₂ balance for 1 tone of humid slices	kg.CO ₂ /t.cum	-158.47

In a drying charge were introduced 252 kg of sliced tomatoes from which have been extracted 232.8 kg of water and resulted 19.20 kg of dried slices. For the generation of thermal energy there were consumed 106 kg of biomass with a humidity of 10% and it resulted 14.6 kg of biochar.

If it is considered in our calculations the estimated maximum cost for the harvested, chopped, dried and distributed biomass of 60 €/t it results a significant cost difference compared to the use of diesel fuel, when the expenditure for thermal energy is eight times higher. The cost of the used biomass for the generation of 1 kilo of tomato dried slices is 0.33 €/kg.cus. For an average sale price at the producer of a minimum 10 €/kg.cus and a 30% profit, the percentage of the biomass utilized for drying in production costs is 5.2 %.

From an environmental point of view, the utilization of the biomass is made with a CO₂ balance close to zero. The production of biochar and its incorporation into the soil for fertility growth purposes conducts to the sequestration in soil for a long period of time of approximately 25% from the carbon resulted from the gasified biomass. In the analyzed case, from the processed biomass tomato residues of 8.7 t/ha may result 1220 kg of biochar that contains 910 kg carbon which incorporated in soil produces a negative balance of -3330 kg CO₂/hectare·year.

The agro-technical effect of the soil fertility growth is experimentally proven but there is no certainty for this. The present accepted standard is 10 tones/hectare biochar, this fact showing that in approximately 3 years it can be attained the proposed standard.

4. Conclusions

An economical and environmental way of turning to account of the energy potential of the greenhouse crop wastes can be utilized for the thermal energy and biochar generation with a CO₂ negative balance consists of harvesting, sorting, chopping at 10 - 50 mm, drying to a humidity of 0 – 15% with a production cost situated between 40 – 60 €/t.

The thermal energy generation can be achieved environmentally friendly with the TLUD process for the biomass gasification characterized by a high energy conversion efficiency, generation of biochar and CO and PM very low emissions. The TLUD energy modules are easy to operate, safe, tolerant to the biomass properties' variations, all these insuring a good adaptability to the variety of the biomass local resources.

The USCMER 30/60MGB drier was conceived for the use of the biomass obtained from the agricultural biomass residues, with a drying efficiency of minimum 40% and with expenditures for thermal energy eight times lower than for the diesel fuel. From the yearly tomatoes crop residues can be dried, in biochar generation regime, approximately 20 tones of sliced tomatoes with an average cost of the thermal energy of 25.2 €/tone of sliced tomatoes.

It is recommended the turning to account of the generated biochar through its soil incorporation as an agricultural amendment that contributes to achieving of a negative CO₂ balance of -3.3 tones/ hectare·year.

5. Reference

1. Badileanu M., Murad E., Bulearca M., Sima C., *Avantajele economice ale deshidratarii legumelor si fructelor*, Conferinta de Nationala de Pomicultura, INCD Pomicultura Maracineni Argeş, 24 septembrie 2007
2. Callejon-Ferre A.J., and all, *Green crops residues: Energy potential and models for the prediction of their higher heating value*, Renewable and Sustainable Energy Reviews, vol.15, 948-955, 2011
3. Catana L., Murad E., Sima C., s.a., *Indrumar pentru realizarea unei unitati de deshidratare a legumelor si fructelor*, Ed PRINTECH, mai 2008
4. McLaughlin H., S. Anderson P., Shields F., Reed Th., *All Biochars are Not Created Equal, and How to Tell Them Apart*, North American Biochar Conference, Boulder, CO, august 2009
5. Mukunda H.S., and all. *Gasifier stoves – science, technology and field outreach*, CURRENT SCIENCE, vol. 98, no. 5, 10 march 2010
6. Murad E., Sima C., Bădileanu M., Bălăcianu G., *Modelarea – simularea proceselor de uscare convectivă*; Simpozion: Tehnologii moderne de uscare a legumelor si fructelor, IBA, 11 martie 2006
7. Murad E., Sima C., Balacianu G., Ipate G., *Modelarea si simularea proceselor si instalatiilor de uscare convectiva*, AMFI-2007, Bucuresti, 9-10 noiembrie 2007
8. Murad E., Haraga G., Bulearcă M., BădileanuM., *Convection dryers under cogeneration*, International Conference ENERGIE - MEDIU CIEM 2009, UPB, Bucureşti 12-14 noiembrie 2009
9. Murad E., Safta V.V., Haraga G., *The control of the convective drying processes of fruits and vegetables according to a model*, International Conference U.T Ghe. Asachi, Iaşi, 22-23 octomber 2009
10. Murad E., Haraga G., Biris S.S., Sima C., *Module energetice TLUD pentru biomasa*, Conference - Alternative Renewable Energy Business Opportunities, Camera de Comert şi Industrie Râmnicu Vâlcea, 1-2 iulie 2010
11. Murad E., Seiculescu M., Sima C., Haraga G., *Utilizarea potenţialului energetic al corzilor de viţă*, Annual Conference, INCVV Valea Călugărească, 10 iunie 2010
12. Murad E., Sima C., Haraga G., Safta V.V., *Reduction of final humidity dispersion of bodies in convective drying process*, The 4th International Conference on Advanced Concepts on Mechanical Engineering, Iaşi, 17-18 iunie 2010
13. Murad E., Haraga G., Culamet A., Radu M., *Reducing environmental impact and cost of production for drying fruits*, Proceedings, R.I.F.G. Pitesti, Vol. XXVIII, 2012, 23 septembrie 2012
14. * * * GcBiomass – Greenhouses Crop, MORGAN AQUA Environmental Technologies, Madrid, Spain

SYSTEM FOR ENVIRONMENT MONITORING

Gabriela SIMION¹,
University Politehnica of Bucharest
Departament Biotechnique Systems

ABSTRACT

Environment monitoring systems are designed for constant and organised control of the pollution substances registered values. Generally, these systems work with unstructured data collections. One of these methods is neuro-fuzzy classification. In an environment problem it is necessary to find pollution source and then distribution of pollutants in time and space for ecosystem. The paper deals with air pollution variables. So available data set are containing concentration of pollutants from air like: sulphur dioxide (SO₂), dust (sediment powders), lead (Pb) and cadmium (Cd). There are so many data sets as number of environment data acquisition points is. Data classification is made related to pollutants concentration values comparative to admissible concentration value (AV).

1. INTRODUCTION

There is a growing demand from the environment protection community to leverage upon and transform the vast quantities of environment data into a value-added for decision-quality and in fact useful knowledges. Data mining has a boom of interest from researchers and software producers. From the diversity of available data mining tools, the paper focuses on possibilities of neuro-fuzzy classification to predict outcomes for dangerous environment situations.

For the last years, a main problem of science is the estimation of the biosphere survivability in the condition of the increasing noxious factors. Environment monitoring systems are designed for constant and organised control of the pollution substances registered values. Generally, these systems work with unstructured data collections. Each concrete environment situation requires specific knowledge for case representation, indexation, similarity evaluation, adaptation and evaluation. Case based reasoning (CBR) needs some methods and soft tools to analyse the data and to transform it into information that supports decision. One of this methods is neuro-fuzzy classification. In an environment problem it is necessary to find pollution source and then distribution of pollutants in time and space for ecosystem is important to be determined. For realising this target, data from different environment state measurement points are processed.

If pollutant is dangerous for men and animals, toxicity level is estimated and the environment monitoring system must attention those regions which have these problems. The paper deals with air pollution variables. So available data set are containing concentration of pollutants from air like: sulphur dioxide (SO₂), dust (sediment powders), lead (Pb) and cadmium (Cd). There are so many data sets as number of environment data acquisition points is. Data classification is made related to pollutants concentration values comparative to average concentration value (AV). There are considered values from two environment registration points.

¹Splaiul Independentei 313, 0214029637, gacsimion@gmail.com

2. A NEURO-FUZZY CLASSIFICATION

A neuro-fuzzy classification (NEFCLASS) is used in order to realise interpretable classification of environment data. Adaptive clusters are generated in this case. The goal of a NEFCLASS model is to discover fuzzy rules from a given set of data and to find shape of membership functions to determine the correct class of an input pattern . There are some cases when fuzzy rules are given and NEFCLASS must determine only parameters of used neural network for optimum classification of data .

Usually, a cluster algorithm aims at minimizing the objective function :

$$J(X, u, v) = \sum_{i=1}^c \sum_{k=1}^s (u_{ik})^m d^2(v_i, p_k) \text{ where}$$

$X = \{p_1, \dots, p_s\}$ is data set , c is number of clusters, u_{ik} is the membership degree of datum p_k to cluster i , v_i is the prototype for cluster i and $d(v_i, p_k)$ is the distance between prototype v_i and datum p_k . Parameter m is fuzzyness index . So for $m \rightarrow 1$ the clusters tend to be crisp , for $m \rightarrow \infty$, $u_{ik} \rightarrow 1/c$. Usually $m=2$ is chosen.

A fuzzy rule has the following form :

"If i_1 is μ_1 and i_2 is μ_2 ...and i_n is μ_n , then the environment pattern (i_1, i_2, \dots, i_n) belongs to class c_i ".

$\mu_1, \mu_2, \dots, \mu_n$ are fuzzy sets and i_1, i_2, \dots, i_n elements of vector describing concentration of pollutants.

The Neuro-fuzzy Classification System , proposed by Nauck and Kruse [1] is implemented with a fuzzy perceptron . Perceptron structure is organised as a 3-layer feedforward neural network. First layer has a number of neurons equal with number of elements of input vector. Hidden layer is named rule layer and it is formed by a number of neurons corresponding to number of rules. Output layer(classes layer) contains as more neural units as the classes are.

Connections between first and second layer are values of membership functions having a label corresponding to linguistics terms. Neurons of rule layer are connected to neurons of classes layer by unitary or null weight.

When we use NEFCLASS system , we have to define number of initial fuzzy sets partitioning , the domains of the input features and the largest number of rule neurons.

According to Nauck and Kruse approach , the membership functions are triangular with three parameters:

$$\mu(x) = \begin{cases} \frac{x-a}{b-a} & \text{if } x \in [a, b) \\ \frac{c-x}{c-b} & \text{if } x \in (b, c] \\ 0 & \text{otherwise} \end{cases}$$

NEFCLASS-PC [2] is an interactive simulation software to develop, train and test a Neuro-Fuzzy System for Classification , based on NEFCLASS model. It is able to give the user graphical and textual displays for interpreting the results . This software tool does some statistics to get prior knowledge about the data. Maximal number of input units (variables)and output classes is 50 and maximal number of rules is 500. Each variable can have a maximum of seven fuzzy sets and it must have at least one. If it is specified only one fuzzy set for a variable, this means that is ignored for the classification of patterns.

Data with classification information is divided into two parts : one part for training the network (training pattern file) and one part for testing the performance of the trained network (test file).

Network is created by aiding pattern file and the performance of this trained network is first to be tested with learning data.

Number of rules is introduced by user , but rules can be created during learning algorithm or they are edited by user . Learning process can be stopped after a number of epochs, or when a specific error is reached. The maximal number of misclassifications is also defined. The best stop criterion is that minimal error isn't decremented for a given number of epochs.

3.STUDY OF AIR POLLUTANTS

If pollutant is dangerous for men and animals , toxicity level is estimated and the environment monitoring system must attention those regions which have these problems. Our paper deals with air pollution variables. So available data set are containing concentration of pollutants from air like sulphur dioxide (SO₂), dust (sediment powders), lead (Pb) and cadmium (Cd). There are so many data sets as number of environment data acquisition points is. Data classification is made related to pollutants concentration values comparative to maximum admissible concentration value (AV) . There are considered values from two environment registration points (Table 1 and Table 2).

Tabel 1.Pollutants values set from registration point 1(in µg/l)

Pollutant	SO ₂	Dust	Pb	Cd
Values Range	0÷267	0÷361	0÷45.5	0÷0.79
AV	17	104	3.662	0.036

Tabel 2 .Pollutants values set from registration point 2 (in µg/l)

Pollutant	SO ₂	Dust	Pb	Cd
Values Range	0÷400	0÷377	0÷25.2	0÷0.318
AV	28	116	2.448	0.026

Each type of pollutant has four fuzzy sets of concentration levels, with labels : very small, small, large, very large. Concentration values under $\frac{1}{2}$ AV are low concentrations (very small), values from $\frac{1}{2}$ AV to AV are normal values (small) , values from AV to $\frac{3}{2}$ AV are high values (large) and values greater $\frac{3}{2}$ AV are noxious (very large).

There are considered four classes for environment data : normal class (1000), attention class (0100), overclass (0010) and alarm class (0001).

Inference rules are :

R1:If SO₂ is very small and dust is very small and Pb is very small and Cd is very small then pattern is from normal class.

R2: If SO₂ is small and dust isn't large or very large and Pb isn't large and very large and Cd isn't large or very large then pattern is from attention class.

R3: If SO₂ isn't large or very large and dust is small and Pb isn't large and very large and Cd isn't large or very large then pattern is from attention class.

R4: If SO₂ isn't large or very large and dust isn't large or very large and Pb is small and Cd isn't large or very large then pattern is from attention class.

R5: If SO₂ isn't large or very large and dust isn't large or very large and Pb isn't large or very large and Cd is small then pattern is from attention class.

R6: If SO₂ is large and dust isn't very large and Pb isn't very large and Cd isn't very large then pattern is from over class.

R7: If SO₂ isn't very large and dust is large and Pb isn't very large and Cd isn't very large then pattern is from over class.

R8: If SO₂ isn't very large and dust isn't very large and Pb is large and Cd isn't very large then pattern is from over class.

R9: If SO₂ isn't very large and dust isn't very large and Pb isn't very large and Cd is large then pattern is from over class.

R10: If SO₂ is very large and dust is very large and Pb is very large and Cd is very large then pattern is from alarm class.

4. PRACTICAL ASPECTS

Generally, problem of environment classification data consist in :

1. There is enough and representative data to be classified.
2. A soft system for classification as NEFCLASS-PC.
3. It is important to determine classification precision, so the user wants to know the performance of the classification system.
4. The classification system is able to modify its structure and parameters, in order the user has the possibility to find out if the performance can be improved.
5. Prior knowledge about the data as classification rules can be used by the classification system.
6. The environment specialist can be able to interpret the results obtained .

NEFCLASS-PC should be able to solve most of these demands. Environment data to be classified are vectors with four elements:

$V = (V_1 \ V_2 \ V_3 \ V_4)$ where

$V_1 = [\text{SO}_2]$

$V_2 = [\text{dust}]$

$V_3 = [\text{Pb}]$

$V_4 = [\text{Cd}]$.

For two sets of training data composed each of 364 patterns , there is made performance analyse of classification related on number of used rules (see in Table 3 and Tabel 4).

If number of rules is reduced above 8 , number of missclassification is increasing. The same result for a number of rules greater than 11. The best performance is obtained using 9 rules. In order to reduce number of missclassification another try is to modify number of fuzzy sets for input variables. In case of the first set of data , a number of 4 fuzzy sets (very small, small, large, very large) is used for V_1 , V_2 , V_3 ad 3 fuzzy sets for V_4 (small, medium and large). A number of misclassification equal to 79 is obtained. For the second set of data a number of 4 fuzzy sets (very small, small, large, very large) is used for V_2 , V_3 , V_4 ad 3 fuzzy sets for V_1 . In both cases number of missclassified patterns is proportional to number of patterns from the class.

There are two modalities to improve performances of the NEFCLASS system for processing of environment data : increasing or decreasing number of rules and changing of fuzzy sets number for each element of input environment vector.

A future direction for classification optimization with NEFCLASS-PC is to use an algorithm for finding number of rules and optimum number of fuzzy sets for elements of environment pattern. . A genetic algorithm with objective function representing number of missclassified patterns in each class is recommended.

References

1. D. Nauck, R.Kruse "Nefclass-A Neuro-Fuzzy Approach for the Classification of Data" ,Proc.of the 1995 ACM Symposium on Applied Computing , Nashville, Feb.26-28., pp. 23-27, 1995
2. D. Nauck, F.Klawonn "Neuro-Fuzzy Classification Initialized by Fuzzy Clustering", Proc.Fourth European Congress on Intelligent Techniques and Soft Computing EUFIT96, Aachen , pp.1-6, 1996.

MODELLING AND NUMERICAL ANALYSIS BY THE FINITE ELEMENT METHOD OF WHEAT MILLING PROCESS IN ROLLER MILLS

Ștefan Elena-Mădălina¹, Gh. Voicu¹, G. Ipate¹, A.G. Constantin¹
P.U. Bucharest / Romania
E-mail: madalina.stefan@upb.ro

ABSTRACT

In the paper are presented the results of 3D finite element numerical simulation of the behaviour of wheat seed during the milling process with fluted rolls (deformation values, shear strain values, energy consumption).

The researches has been conducted considering the wheat seed caught between the fluted milling rolls in position: dull-to-dull (D/D) and sharp-to-sharp (S/S); the torsion moment of 750 N·mm for roll 1, roll 2 considering the role as the bearing (slowly roll).

3D modelling was performed using SolidWorks software. It was used as a tool for finite element analysis ANSYS Multiphysics software package.

1. INTRODUCTION

In the roller mills, wheat seeds are crushed (fragmented) using grinding machines equipped with pairs of fluted rolls. The fluted rolls are designed to catch the wheat seed and create the possibility of maintaining it so that shear stresses are applied on it, [1,2].

When a wheat seed is caught and pulled through two milling rolls, it is subjected to compressive and shears strain, simultaneously, (see figure 1).

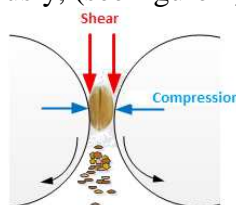


Figure1: Strains that a wheat seed caught between a pair of grinding rolls is subjected

The fluted rolls not act by friction force on the material particle, but by direct catching its. The fluted rolls ensures a optimum grip of seeds, increases the grinding process due to the increasing of shear effect, breaking de wheat seeds so that the shell tends to remain large, and the endosperm are broken into small particles. Thus, it is easier to separate these two components (bran and endosperm), [1,2,3].

The characteristics of rolls flutes are determined by their profile, flutes inclination with the roll generator, number of flutes on the roll circumference, flutes disposition, [2,3,4,5,6]. *Flutes profile* refers to their geometrical shape and dimensions (flutes depth, flutes pitch) and is determined by the nature of the seeds subjected to grinding, but especially the degree of fineness of milling products to be obtained, [4,5]. *Flutes inclination* ensures a continuous effect of compressive and shears stress on the seeds and material particles. *Flutes disposition* has an important role in the process of grinding. Flutes disposition refers to the possibility of intersection of the flutes dull or sharp from a roll with the flutes dull or sharp of the second roll. Asymmetry of flutes shape and differential speed allows the rolls to operate in four different dispositions of flutes: dull-to-dull (D/D), sharp-to-sharp (S/S), sharp-to-dull (S/D),

dull-to-sharp (D/S), [2,6].

An example of catching of a wheat seed between two rolls with flutes surface and S/S flutes disposition is shown in figure 2.

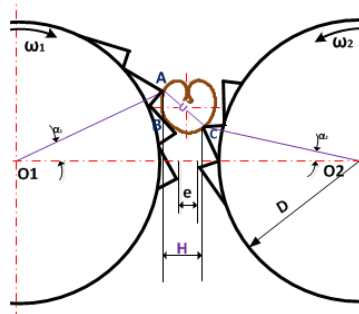


Figure 2: Catching of a wheat seed between two fluted rolls (S/S flutes disposition)

The Finite Element Method (FEM) solves mechanical processing problems by approximating each variation in time or in space of studied size of discrete variations. The purpose of this method is to obtain information about how to conduct the process by substantially reducing the number of experiments and thus time finding the answers.

In this paper was used the Finite Element Method to simulate the behavior of wheat seed during grinding process with fluted rolls.

The main objective of the study of wheat seeds grinding in roller mills is the knowledge and understanding of the factors influencing the grinding process, and also knowledge of the grinding equipment, so that the work parameters to be properly chosen and to obtain products of superior quality, high extraction efficiency, as well as significant economy is energy consumption.

2. METHODOLOGY

To achieving the modeling and simulation of wheat seed grinding process it was used as a tool for finite element analysis ANSYS Multiphysics software package.

The first step of this study was to design three-dimensional geometric model of wheat seed and two rolls flutes. 3D modeling was performed using SolidWorks software.

In the second stage of the simulation, the 3D model was imported into ANSYS 14.0 software and were introduced the material characteristics. To achieve the modeling is necessary to know the modulus of elasticity of the material (E) and Poisson's ratio (ν), which in the case of wheat seed with the density of $\rho = 1250 \text{ kg/m}^3$, and considered to be made up of several layers, the isotropic case, $E = 480 \text{ MPa}$ and $\nu = 0,3$, (see table 1). The geometry analysis performed using SolidWorks program is shown in figure 3.

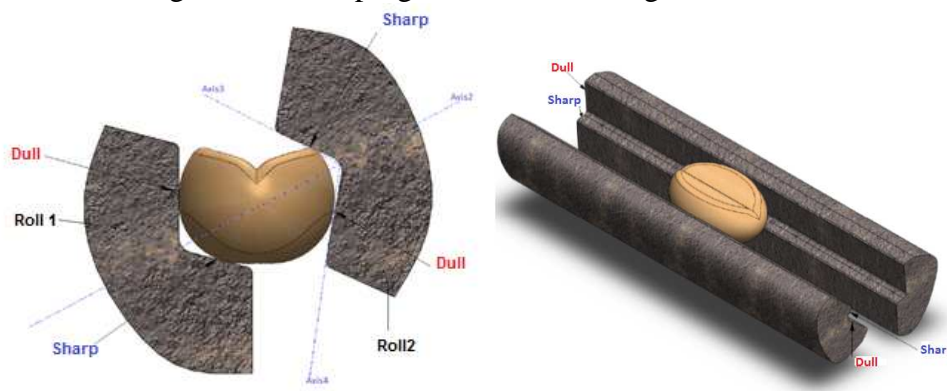


Figure 3: 3D geometry

Table 1: The characteristics of materials used in model

Object	Density (kg m ⁻³)	Young modulus (MPa)	Poisson's ratio
Wheat	1250	480	0,3
Roll	7850	2,e+005	0,3

The third stage of the simulation process is the finite elemnt mesh model, figure 4.

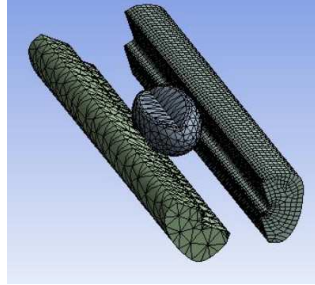


Figure 4: Finite element meshing of the geometrical model

In the stage of processing is chosen first the analysis procedure used. For this simulation we used a steady state analysis. The results are graphically shown in the form of areas covered by the contours of different colors and the parameter value referred to is displayed in a color legend.

The researches has been conducted considering the wheat seed caught between the fluted milling rolls in position: dull-to-dull (D/D - figure 5) and sharp-to-sharp (S/S – figure 10); the torsion moment of 750 N·mm for roll 1, roll 2 considering the role as the bearing (slowly roll).

- The case of D/D flutes disposition

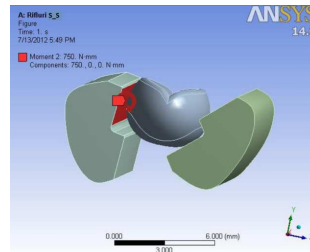


Figure 5: The application of loads on the model

In figure 6 are illustrated and presented values of relative deformations that occur at the shear strain on XY, YZ and XZ planes, and figure 7 shows the maximum shear strain that occurs to action of flutes on wheat seeds for 1 second, if the flutes disposition is D/D.

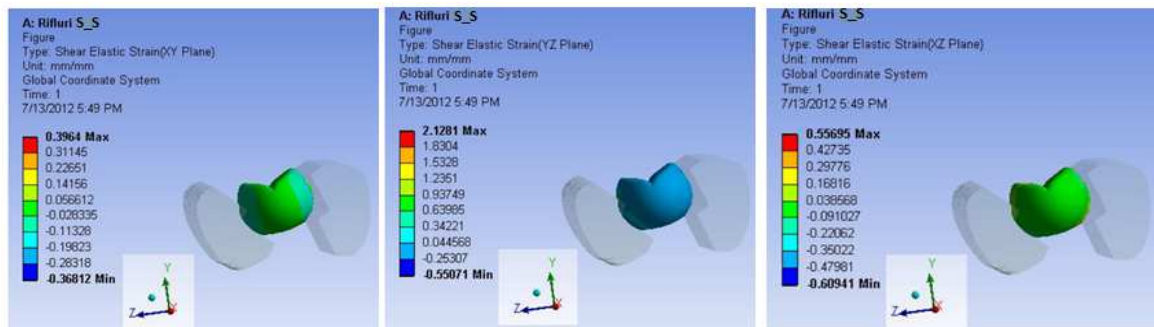


Figure 6: Values of relative shear deformations that occur in wheat seeds for D/D flutes disposition

It is noted that the relative shear deformation presents the highest value (2.349 mm/mm) in the YZ plane, namely in the direction of contact of the two rolls with the wheat seed. The lowest value is in XY plane (0.396 mm/mm), followed by a deformation in the XZ plane (0.556 mm/mm), to a small difference. For these values of relative shear deformation was a maximum stress of 406.76 MPa.

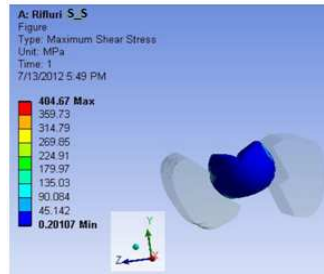


Figure 7: Maximum shear strain

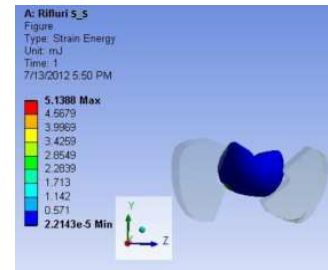


Figure 8: Values of consumed energy to deformation of wheat seed

In figure 9 are presented the deformations that occur in the three directions of deformation (X, Y, Z) and the total deformation (strain) of wheat seed.

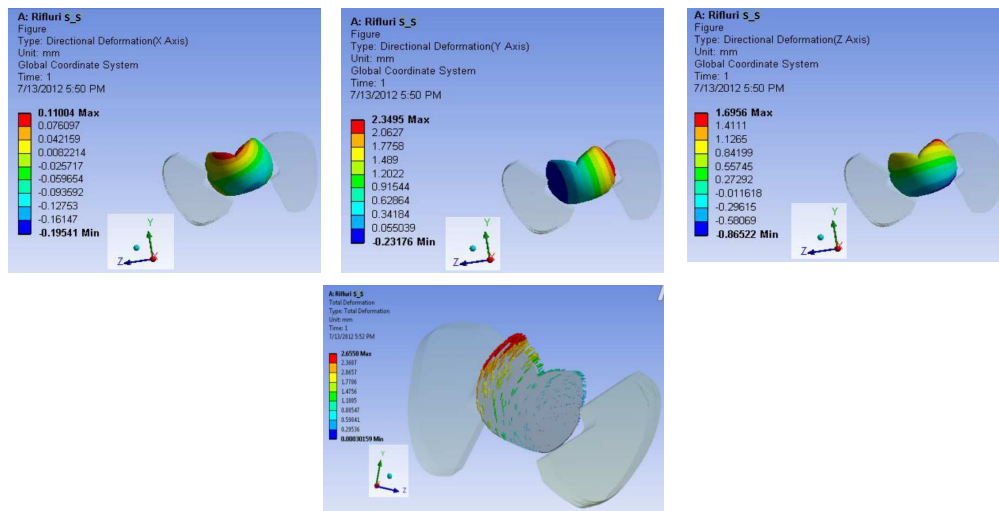


Figure 9: Values of absolute deformations for D/D flutes disposition

It is found that the maximum deformation on Y axis direction has the highest value (2.349 mm) and is held in contact with the flute of fast roll. On the X axis direction the deformation has the lowest value (0.110 mm) and observes that the seed is not deformed to contact with the rolls, the maximum deformation being at its crease, as found in the scientific literature, [7]. The maximum total deformation of the seed is of 2.655 mm and is held in contact with the fast grinding roll. The maximum value of consumed energy for wheat seed deformation is 5.138 mJ.

- The case of S/S flutes disposition

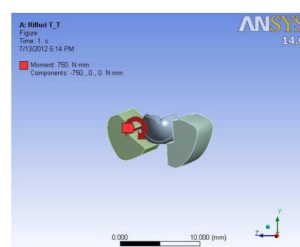


Figure 10: The application of loads on the model

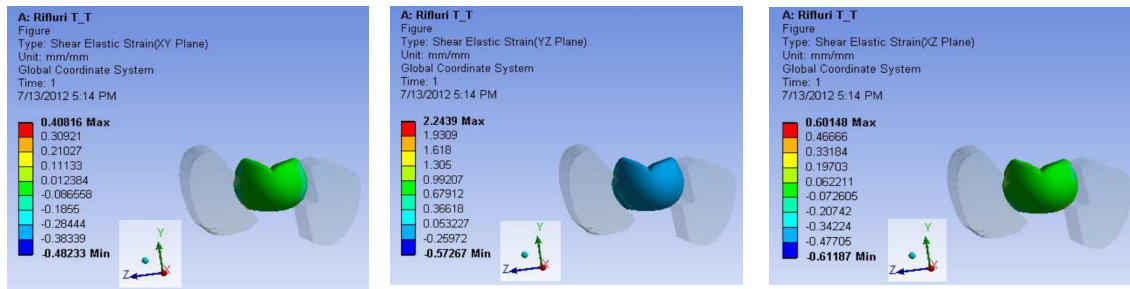


Figure 11: Values of relative shear deformations that occur in wheat seeds for S/S flutes disposition

Just as in the previous case, and in this case (S/S flutes disposition) the shear relative deformation has the highest value (2.243 mm/mm) on the YZ plane, followed by deformation in the XZ plane (0.601 mm/mm) and deformation in the XY plane (0,408 mm). The maximum shear strain has a value higher (443.57 MPa) than D/D flutes disposition case.

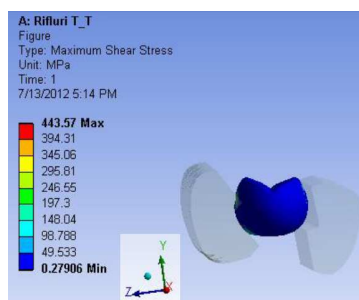


Figure 12: Maximum shear strain

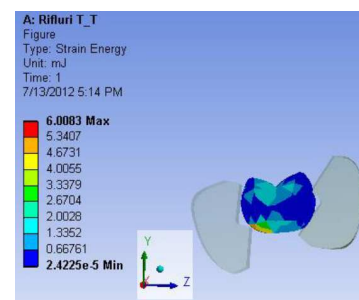


Figure 13: Values of consumed energy to deformation of wheat seed

The largest deformation of seed is obtained on the Y axis direction (1.869 mm), as in the D/D disposition case, but has a lower value. It is noted that, the maximum deformation occurs at the contact of seed with the edge of fast roll flute. The maximum total deformation has a value of 2.054 mm and is less than in the D/D disposition case, but at higher energy consumption (6.008 mJ).

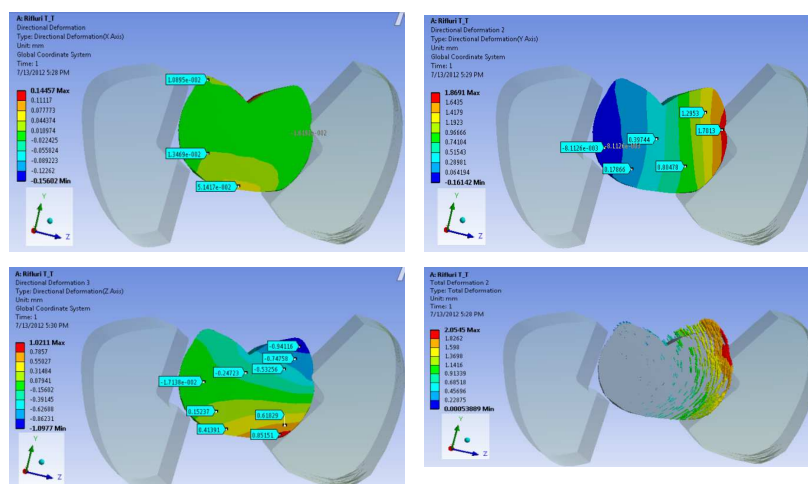


Figure 14: Values of absolute deformations for S/S flutes disposition

Table 2 presents the values of deformations, maximum shear strain and energy consumption resulting from the finite element analysis of grinding process of wheat seed with fluted rolls.

Table 2: Data obtained from finite element analysis

Relative shear deformation, (mm/mm)			Maximum shear strain, (MPa)	Absolute deformation of seed, (mm)			Total deformation, (mm)	Energy consumption, (mJ)
XY	YZ	XZ		x	y	z		
D/D flutes disposition								
0,396	2,128	0,556	406,67	0,110	2,349	1,695	2,655	5,138
S/S flutes disposition								
0,408	2,243	0,601	443,57	0,144	1,869	1,021	2,054	6,008

CONCLUSIONS

Grain breaking modeling by FEM requires knowledge of the mechanical characteristics of seeds, which is determined only by experimental research. However, the method does not take into account all real aspects of conducting the grinding process.

From the data obtained in the simulation it was found that in both cases the flutes disposition (D/D and S/S), the seed maximum deformation has the highest value on the Y axis direction (for D/D disposition – deformation is 2.349 mm, and for S/S disposition – deformation is 1.869 mm), and on the X axis direction the deformation value is lower (D/D – 0.110 mm, S/S – 0,144 mm). On the X axis direction the seed is not deformed to contact with the rolls, but in the crease of its. At the compression of a wheat seed, the first fissure in its internal structure, starting near the crease and continue on the direction of the contact with the highest load.

As in the case of D/D flutes disposition, as well as for the S/S disposition case, the maximum total deformation of wheat seed is held in contact with the fast grinding roll. Fast roll having a rotational speed higher than the slowly roll, determines penetrations of flutes edge in seed, which is sustained by the slowly roll.

Also, it has been found that wheat seed deformation for the S/S disposition case has a lower value (2.054 mm) than in D/D disposition case (2.655 mm), but at higher energy consumption (6.008 mJ for S/S disposition and 5.138 mJ for D/D disposition).

References

- [1] Fang C., Campbell G.M., *Stress-Strain Analysis and Visual Observation of Wheat Kernel Breakage During Roller Milling Using Fluted Rolls*, Cereal Chem. 79(4), p.511–517.
- [2] Campbell G.M., *Roller Milling of Wheat*, Handbook of Powder Technology, Volume 12, 383-421, ISSN 0167-3785.
- [3] Ene Gh., *Echipamente pentru mărunțirea materialelor solide. Bazele proiectării*, Editura Impuls, București, 2003.
- [4] Moraru C., *Disciplina: Tehnologii moderne în industria morăritului*, Universitatea Galați, 1985.
- [5] Panțuru D., Bârsan I.G., *Calculul și construcția utilajelor din industria morăritului*, Editura Tehnică, București, 1997.
- [6] Kuprit I.N., *Tehnologia morăritului*, Editura Tehnică, București, 1954.
- [7] Romański L., Stopa R., *Badania elastooptyczne ziarniakow pszenicy w zakresie odkształcen sprężystych* (Wheat kernel elastooptical investigation in the elasticity range of deformation, Inżynieria Rolnicza 7/2005, p.265-272.

METHODS FOR WASTE NEUTRALIZATION IN CONTEMPORARY ROMANIA

UNGUREANU Nicoleta*, PARASCHIV Gigel, DILEA Mirela, IONESCU Mariana, VOICU Gheorghe, BIRIȘ Sorin-Ștefan
Universitatea POLITEHNICA din București, Departamentul de SISTEME BIOTEHNICE

ABSTRACT

For our country, especially in the current phase of accelerated alignment with European Union requirements, environmental issues, as well as and human health issues, are very important and very topical. In terms of environmental protection, one of the most important problems Romania faces is waste management.

This paper approaches methods for waste neutralization currently used in Romania. Selection of the processing and neutralization method of waste is done according to their origin and composition. Thus, for waste having mainly organic content (animal waste, vegetable waste, domestic waste and food industry waste, etc.), methods of composting and anaerobic digestion are widely used. Residual wastes that cannot be recovered (hazardous waste) are treated by methods of incineration and co-incineration.

1. INTRODUCTION

In the 21st century, the sustainable management of municipal solid waste became necessary at all phases of impact, from planning to design, to operation, and to decommissioning. As a consequence, the spectrum of new and existing waste treatment technologies and managerial strategies has also spanned from maintaining environmental quality at present to meet sustainability goals in the future, [8].

For Romania, especially in the current phase of accelerated alignment with European Union requirements, environmental and human health issues are very important and topical. In terms of environmental protection, one of the most important problems Romania must face is waste management. This refers to the activities of collection, transport, treatment, recovery and waste disposal. Responsibility for waste management activities lies with their generators, according to the "polluter pays" principle or, if appropriate, with their producers, according to the "producer responsibility" principle, [6].

This paper presents the methods of waste neutralization currently used in Romania. Selection of the processing and neutralization method of waste is done according to their origin and composition. Waste with large content of organic matter (animal waste, vegetable waste, domestic waste and food industry waste, etc.) is neutralized by composting and anaerobic digestion.

The composting process produces a harmless product that can be used as organic fertilizer, while the anaerobic decomposition (fermentation) produces biogas (renewable energy) and digestate (which, enriched with compost, results in a high quality fertilizer).

Mechanical-biological treatment of the organic fraction of municipal solid waste is now the main strategy to reduce biodegradable municipal solid waste in waste in the UK and in Europe, [9]. It consists of mechanical pre-treatment followed by an aerobic (composting-like process) or anaerobic process, so that waste impacts are reduced. These processes have attracted attention because they produce stabilized waste that can be sold as fertilizer or disposed off in landfill, in which case it will have a low impact on the environment, [1]. As a

result, the biological stability of digestate after biological processing has become of particular interest recently. Digestate can be defined as the material resulting from the anaerobic digestion of separately collected bio-waste, [10]. Quality of digestate is related to the absence of phytotoxicity and weed seeds, and the presence of both organic and inorganic elements, [2]. Composting of organic waste is a bio-oxidative process involving the mineralization and partial humification of the organic matter, leading to a stable, sanitized and humus-like material rich in organic matter and free of offensive odours resulting from the composting process, [10].

Residual waste that cannot be recovered (hazardous waste) is treated by methods of incineration and co-incineration. Choosing incineration as a method of waste disposal ensures its fast and complete neutralization. One undisputed is the fact that incineration plants need relatively small surfaces and can be located near settlements, which leads to the reduction of transportation costs. In this case, environmental pollution can be reduced by using appropriate filters, [7]. The incineration sector has undergone rapid technological development over the last 10 to 15 years. Much of this change has been driven by legislation specific to the industry and this has, in particular, reduced emissions to air from individual installations. Continuous process development is ongoing, with the sector now developing techniques which limit costs, whilst maintaining or improving environmental performance, [11].

2. DESCRIPTION OF WASTE NEUTRALIZATION METHODS AND EQUIPMENTS USED IN ROMANIA METHODOLOGY

Anaerobic fermentation of waste. Biogas is an alternative and renewable energy source produced through the anaerobic digestion of organic matter whereby the organic matter is converted into a combustible gas, rich in methane and a liquid effluent. Usually, biogas consists of 55-80% CH₄ and 20-45% CO₂. However, depending on the source of the organic matter and the management of the anaerobic digestion process, small amounts of other gases such as ammonia (NH₃), hydrogen sulfide (H₂S), and water vapor (H₂O) may be present.

Agricultural biogas plant mainly processes substrates from agriculture, e.g. manure, residues and by-products of agricultural crops and energy crops. Cattle and pig manure is the main raw material for most biogas plants, although, in recent years, the number of factories that use energy crops (maize, rapeseed, soybean, sunflower, Miscanthus etc.) increased. Also, the fermented sludge from wastewater treatment plants produces biogas. Dairy manure biogas is used in combined heat and power applications (CHP) that combust the biogas to generate electricity and heat for on-farm use.

Design and technology for biogas plants vary from country to country, depending on the climate and national frameworks (laws and energy policies), the availability and affordability of energy. Depending on the relative size and their locations, agricultural plants with anaerobic digestion can be classified as, [5]: family biogas plants (very small scale); farm plants (small, medium large scale); centralizes systems / unified co-digestion (medium or large scale). Regarding biogas technology, although Romania is among the countries which previously had serious concerns for biogas production, currently is preferred the import of technology and equipment, knowing the expertise and results obtained by countries where this technology is enhanced and proven to be economically viable, [3].

The first attempt to exploit pig manure for biogas production was at Tomești-Iași in 1975, using a fermenter with the capacity of 30 m³. Another pilot plant for the production of biogas from pig manure was built at S.C.C.C.P Periș, with a capacity of 580 m³/biogas.day. Starting with 1982, the number of biogas plants using pig manure has increased (e.g., I.S.C.I.P Caracal in Olt county with a biogas production of about 8000 m³/day, Roman in Bacău, Codlea in Brașov, Pecineaga in Constanța), [6]. Biogas production has a good potential in the

field of wastewater treatment. There are many municipal wastewater treatment plants in Romania, producing their own biogas which they use to produce energy required for their domestic use, but they only represent less than 5% of all treatment plants. There are 732 wastewater treatment plants in our country, of which 416 are municipal, respectively 316 industrial treatment plants. It must be noted that basically, this is the main sector that generates biogas in Romania. In 2010 for example, the installed capacity of energy production from biogas was 4 MW and a gross energy production of 19 GWh, [14].

Usually, in the design of a biogas plant, the following elements are found:

- a. Actual production unit, which consists of anaerobic fermenter, a storage tank and/or a sanitation drive, as well as the removal system of the fermented manure;
- b. Biogas storage and purification systems;
- c. Equipment for the use of gas and fertilizer, [4].

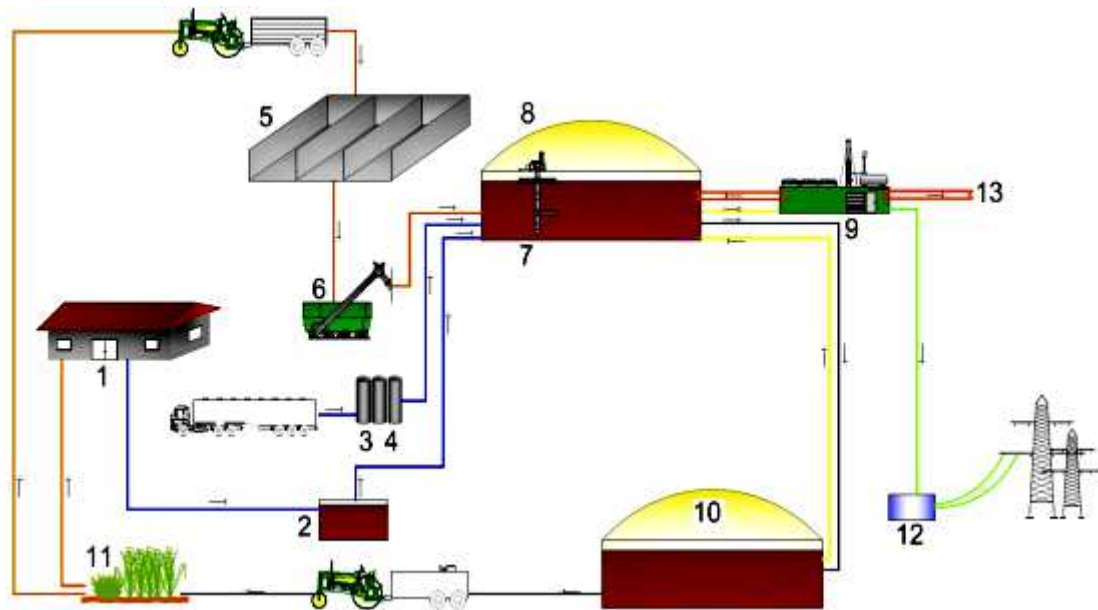


Figure 1: Agricultural co-digestion biogas plant using manure and maize silage, [17]

- 1 – stalls; 2 – liquid manure tanks; 3 – collection bins for biowaste (co-substrate);
 4 – sanitation tank; 5 – drive-in storage tanks; 6 – system for solid waste feed-in; 7 – biogas reactor (digester); 8 – biogas storage tank; 9 – CHP plant; 10 – digestate storage;
 11 – agricultural fields; 12 – transformer/ power to grid; 13 – heat utilisation

Romania has hundreds of small capacity biogas plants, fed with manure and vegetable waste. Installations for the production of fermentation gas for domestic use in rural areas are built as burries watertight tanks, without being equipped with heating systems. Optimal temperature for the use of these plants is 30°C.

Composting of biodegradable waste. Composting is a complex process of interaction between organic waste and the microorganisms found in the waste. Composting takes place if biodegradable waste is piled and its structure allows the diffusion of oxygen and if waste has a dry matter content which is proper for microbial growth.

Directive 99/31/EC on waste disposal stipulates that the content of organic matter must be minimized through the reduction of biodegradable waste with 50% until December 31, 2013 and with 65% until December 31, 2016. Given the international experience, Romania became aware that an effective use of the composting methods first requires the selective collection of biodegradable matter from waste. It must be avoided the composting of mixed

municipal waste, as they have a high content of heavy metals (Cd, Pb, Cu, Zn, Hg). Also, in dense urban environments, the selective collection of good quality biodegradable waste is not possible, [13].

Curently, composting can be done in open spaces, using non-polluted organic waste collected from parks and gardens, without with no need for air supply, or in enclosed spaces, in order to accelerate the process and to avoid disturbing odours. In the latter case, waste is previously grinded, sieved and homogenized. The following diagram presents the working phases for a composting plant that processes, in common, municipal solid waste and sludge from urban waste water treatment plants, [7].

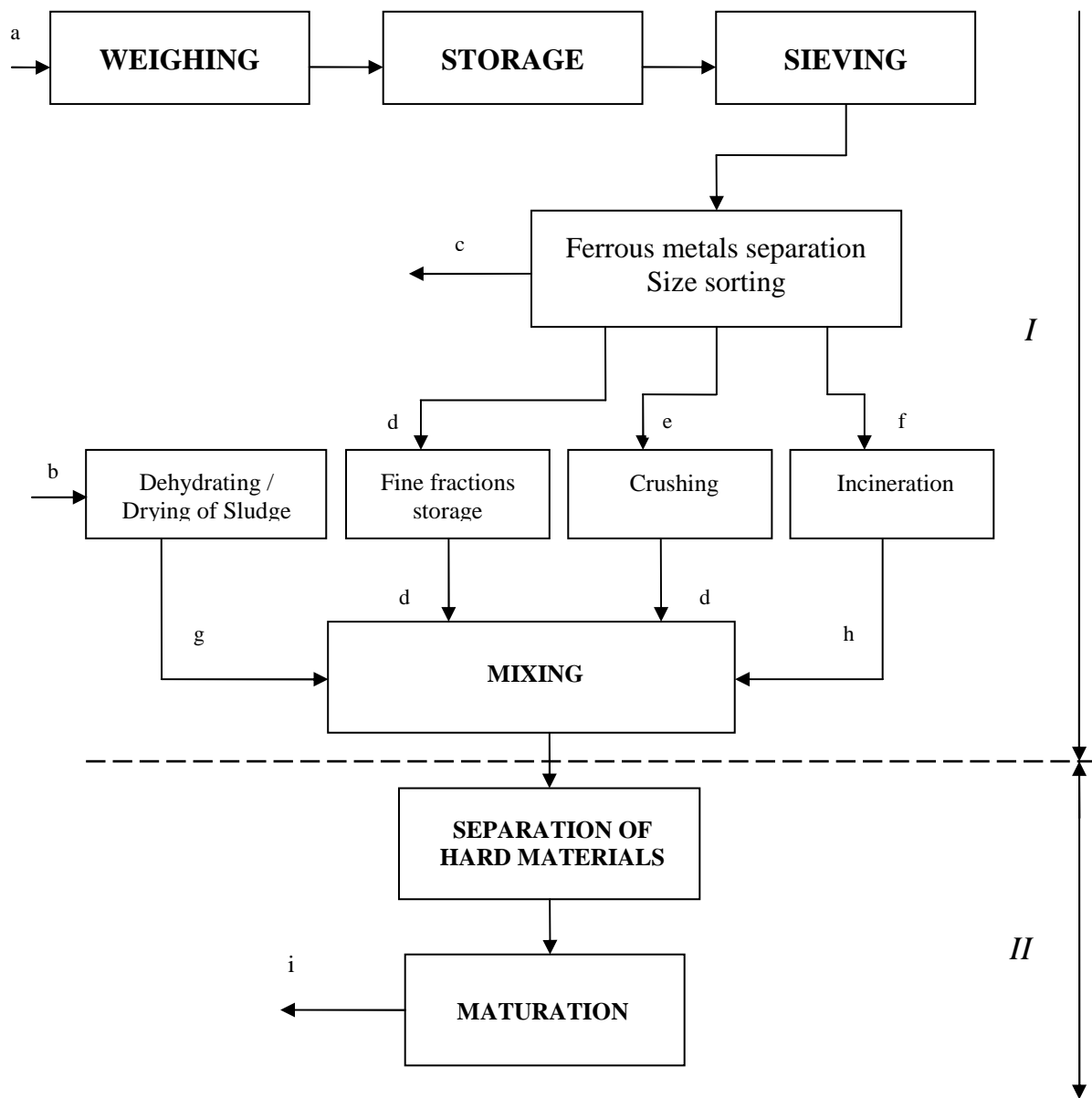


Figure 2: Working phases at a composting plant, [7]

I – Preparation of raw materials; II - Maturation (production of raw compost)

a – fresh solid waste; b – sludge and waste waters; c – ferrous pieces; d – fine fractions; e – medium size waste; f – coarse fractions; g – dehydrated sludge; h - ash; i – raw compost

Waste incineration. Incineration is a method of thermal destruction of waste, which, besides the recovery possibilities of the obtained heat, offers the advantage of transforming waste into less polluting and less bulky residue, [7]. The most appropriate method for burning waste is incineration without the addition of auxiliary fuel. Processes in which incineration is achieved by mixing waste with fuels are used only in extreme cases.

All waste incinerators, whether industrial, medical or municipal, must meet the objectives of European and national legislation. Also, these plants must meet the requirements about energy recovery, such as heat recovery and other forms of energy resulting from incineration. Municipal waste incinerators are effective only if the quantity of municipal waste is higher than 150.000 tones/year. Thus, considering that a single person produces 500 kg/pers.year, municipal waste incinerators should be constructed in areas with minimum 300.000 habitants, [13].

A usual waste incineration plant includes the following operations: reception of incoming waste; storage of waste and raw materials; pretreatment of waste (if required); waste loading; thermal treatment of waste; energy recovery and conversion; flue-gas cleaning; flue-gas cleaning residue management; flue-gas discharge; monitoring and control of emissions; wastewater control and treatment; ash/bottom ash management and treatment (ash from the combustion stage); discharge/disposal of solid residue. These stages, however, may vary due to plant design and type of waste, [16].

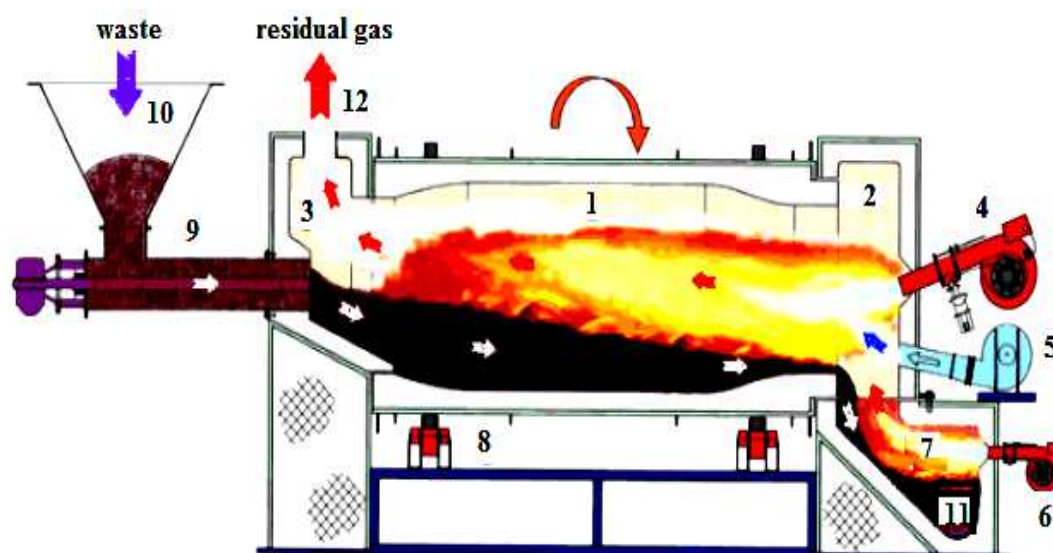


Figure 3: Diagram of rotary furnace for waste [12]

1 – rotary firing chamber; 2 – bottom part; 3 – upper part; 4 – igniter and device for flame maintenance; 5 – primary air feed; 6 – automatic ash burner; 7 – ash chamber; 8 – device for chamber rotation; 9 – waste inlet; 10 – liquid, paste, solid waste; 11 – ash removal device; 12 – residual gas circuit to post-combustion chamber

For example, in rotary furnaces, depending on the combustion temperature, the ash burner device is not always necessary. For temperature over 1150°C, ash is agglomerated, and if temperature exceeds 1300°C, ash is melted and vitrified. Residual ash mainly consists of: 3-5% non-incinerated waste; 7-10% ferrous and non-ferrous material; 5-7% coarse particles; 80-83% fine particles, [12]. Iridex incineration plant for dangerous waste (Bucharest) was designed for a working capacity of 12500 tones/year, [13].

3. CONCLUSIONS

In the current conditions of economic development and demographic explosion, the existence of large urban areas, proper management of waste is a priority due to the impressive increase of their volume and to the inability of on-site destruction.

The recovery and recycling solutions of biodegradable waste are represented by composting (aerobic digestion) and anaerobic digestion with biogas production and collection.

Processing technologies of dairy manure for the production of biogas are known and used in Romania, starting with 1975. However, biogas is widely obtained from the fermentation of sludge in waste water treatment plants.

Application of neutralizing composting process does not depend exclusively on agriculture needs, being primarily a service of health. In some cases the costs are covered by municipal or state funds.

The most appropriate method for burning waste is incineration without the addition of auxiliary fuel.

References

- [1] Adani, F., Tambone, F., Gotti, A., Biostabilization of municipal solid waste. *Waste Manag.* 24, 775–783, 2004.
- [2] Baffi, C., Dell’Abate, M.T., Nassisi, A., Silva, S., Benedetti, A., Genevini, P.L., Adani, F., Determination of biological stability in compost: a comparison of methodologies. *Soil Biol. Biochem.* 39, 1284–1293, 2007.
- [3] Henning H., Enrico R., Development of a sustainable biogas market in central and Eastern Europe. *Biogas, renewable energy.* Trinergi Grup, România.
- [4] Naghiu L., Feeding systems for biogas bioreactors, *Agriculture – Science and practice*, nr. 3-4 (71-72)/2009.
- [5] Ofițeru, A., Adamescu, M., Bodescu, F., Ionescu, D. *Biogas - A practical guide*, 2008.
- [6] Păunescu I., Paraschiv G., Environmental management and biogas production in pig farms. Faculty of Biotechnical Systems Engineering, Politehnica University of Bucharest. AGIR Publishing.
- [7] Păunescu, I., Paraschiv, G., Installations for waste recycling, AGIR Publishing, p. 60, Bucharest, 2006.
- [8] Pires A., Martinho G.C., Chang N.B., Solid waste management in European countries: A review of systems analysis techniques, *Journal of Environmental Management* 92 (2011), 1033 – 1050.
- [9] Scaglia, B., Adani, F., An index for quantifying the aerobic reactivity of municipal solid wastes and derived waste products. *Sci. Total Environ.* 394, 183–191, 2008.
- [10] European Commission, Working Document: Biological Treatment of Biowaste, 2nd draft (Online). Brussels, 12 February 2001, Available: www.compost.it/www/publicazioni_on_line/biod.pdf.
- [11] European Commission, Integrated Pollution Prevention and Control - Waste Incineration, 2006.
- [12] Ministry of Environment and Water Protection. Methods and technologies for waste management. Methods of thermal treatment. Available online at <http://www.deseuri-online.ro/new/download/Trataretermica.pdf>
- [13] Waste management plan in Bucharest. Municipality of Bucharest. March 2009. Available online at http://www.pmb.ro/servicii/gestionare_deseuri/docs/Plan%20Gestionare%20deseuri.pdf
- [14] Study on the potential of biogas production in transborder region Timiș-Csongrad. Timișoara, 2011. Available online at http://www.greenpower.store.ro/docs/studiu2_ro.pdf
- [15] Waste Management Guide, Press House and Tribuna Publishing Sibiu, ISBN 978-973-7749-42-0.
- [16] <http://www.epem.gr/waste-c-control/database/html/WtE-00.htm>.
- [17] <http://www.guascorpower.com/docs/Biometanizacoin.pdf>

INTEGRATED SYSTEM FOR DYNAMIC MONITORING AND WARNING IN CASE OF TECHNOLOGICAL RISKS IN THE CROSS-BORDER AREAS OF DANUBE RIVER. REACT PROJECT – ROMANIA-BULGARIA AREA

Constantin VÎLCU¹, Gheorghe VOICU², Georgeta ALECU³, Gigel PARASCHIV²,
Carol LEHR⁴, Silviu IONESCU¹, Adrian NEDEA⁵

¹INCD Gas Turbines – COMOTI, ²UPB – Biotechnical Systems Engineering, ³INCDIE – ICPE-CA, ⁴INCD – ECOIND, ⁵University of Southampton UK

ABSTRACT

The integrated system for monitoring and warning is realized at theoretical project level. REACT represents a hardware-software complete system of data regarding environment quality acquisition and of continuous evaluation of physicochemical parameters with the scope of registering, processing and modelling the processes that are the basis of ecosystems.[1, 2] The measurements effectuated through reliable methods are continuously realized in situ by a network of sensors for air/water placed in RO-BG cross-border area. The set of monitored parameters and quality indicators, with spatiotemporal cover, assure through the elaborated software the possibility of pollution control through real time warning of critical cases of environmental pollution in the cross-border area.

1. INTRODUCTION

The REACT monitoring and warning integrated system designed is situated as an Environment Informational Systems (EIS) unit. As part of EIS, it realizes locally and regionally the impact monitoring by the structural monitoring of air and water quality. The REACT integrated system executes the monitoring of the environment found under the direct impact of potential pollution sources, by measuring with a well defined scope of a group of parameters in their spatiotemporal dynamics. The main function of the monitoring system is to warn in real time the decision factors to technological risks in case of industrial accidental pollution in the Romania – Bulgaria cross-border area.

In Fig. 1 there is presented the general architecture of the integrated system of monitoring and warning. This one defines the quality data flow of the environment (air/water) which is established between the sensors placed in situ (CSP) and the final users of the information in the social environment (operating personnel, data validation personnel, decision factors and public).

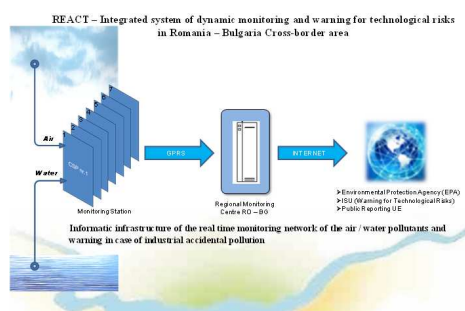


Fig. 1: The architecture of REACT integrated system of monitoring and warning

2. THE TOPOGRAPHY OF THE SENSORS NETWORK IN THE CROSS-BORDER AREA

The REACT monitoring & warning integrated system is a combined system which monitors simultaneously the air and water quality. A monitoring network of graph type under reticular form with the eyes of 1000 km² [1] and the continuous sampling stations or points in the graph's nodes solves theoretically but uneconomically the spatial density of the monitoring network. Such a uniformly distributed network will be particularised according to the requirements from the cross-border area, for obtaining the structural monitoring of the air and water quality, so that the number of the continuous sampling points (stations) to remain sufficiently representative for the monitored area (Fig. 2):

- the topography of the sensors network for the real time monitoring of the environment quality must cover minimum the “hot” points’ area, with major risk of industrial pollution, situated on the Danube left and right bank in the RO – BG cross-border area;
- for the water environment factor with the quality selected indicators, the solution of surface waters monitoring will be adopted, for the Danube and its affluents, in the upstream and downstream sections in the affluence points, through sensors or sensors batteries immersed on the whole Danube flow in the RO – BG border area;
- the REACT monitoring and warning network is a layer complementary to the network of monitoring of the environment quality, existent and functional in the RO – BG cross-border area.

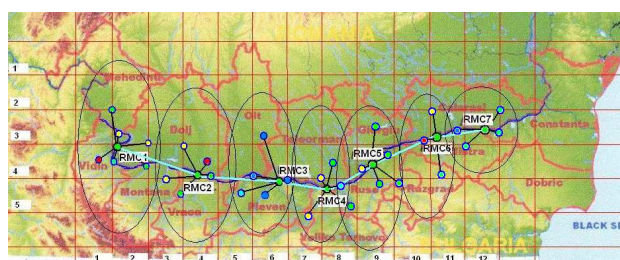


Fig. 2: Topography of the sensors network of REACT system

3. THE INFRASTRUCTURE OF THE MONITORING AND WARNING NETWORK

The infrastructure of the REACT monitoring and warning network is composed of the set of equipments (sensors and analyzers) of measuring the quality parameters of air and water environmental components, reunited with the set of IT equipments (Data Loggers, Station Desktop) and of the auxiliary systems equipments of the monitoring stations. They are included in special compartmented enclosures or tanks which are placed in situ in the impact areas.

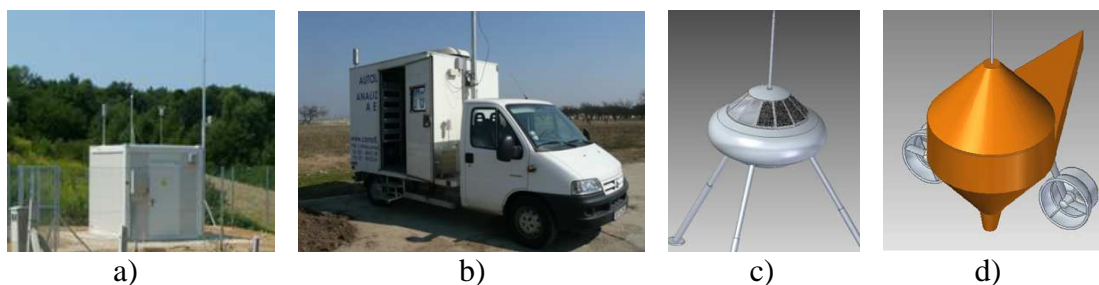


Fig. 3: Stations for the monitoring of the quality of environment components air and water

The CSPs and the RMCs are stations of continuous monitoring of environment samples with fixed positioning (Fig. 3,a) or with semi-mobile positioning (Fig. 3,b). Regardless of the case used, the equipments from the station (see Fig. 4) for air/water quality monitoring will be installed in an enclosure of air-conditioning tank type and with its own sources of electrical energy for assuring the long period functioning in the insulated variant as well.

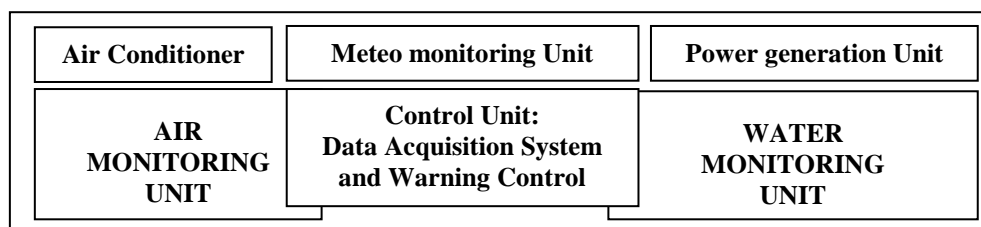


Fig. 4: Combined station for the monitoring of the quality of air and water environmental components

To obtain a *flexible* infrastructure regarding the realization of an optimum network of REACT monitoring and warning system, two structures have been designed, intended only for the CSP locations. The *capsule* type structure from Fig.3,c) is equipped with sensors and analyzers for the monitoring of the quality indicators of air environmental factor. The *buoy* type structure from Fig.3,d) is equipped with sensors and analyzers for the monitoring of the quality indicators of water environmental factor. The “capsule” and “buoy” type structures are installed in situ at distances between 300 ÷ 3000 m for being able to assure the wireless communication between them. They can operate together but also isolated depending on the investigated impact case from the cross-border area.

4. THE LIST OF THE ENVIRONMENT (AIR/WATER) PARAMETERS, CORRESPONDING TO THE SAMPLES OF THE POLLUTANTS MONITORED IN SITU

The indicators used in an environment monitoring program of air and water environmental components are selected according to the utility of the information provided. They are main elements on the base of which the evaluation of the environment real status is made. The most important parameters are frequently analysed when the general characteristics which describe the “*health status*” of an ecosystem. [1]

The monitoring equipments chosen for the instrumentation of the monitoring stations of the REACT integrated system include sensors and analyzers with unified signal output (4...20 mA sau 0...10 V). The analogical signals provided cover at least the general indicators of the environment air/water factors. The flexibility of the designed monitoring system allows extension also for the physico-chemical specific indicators of environment condition from impact area which describe the health condition of the ecosystem. [1]

The list of polluting substances is according to DIRECTIVE 2010/75/EU OF THE EUROPEAN PARLIAMENT AND OF THE COUNCIL of 24 November 2010 on industrial emissions (integrated pollution prevention and control). The samples monitored continuously for the air environmental factor refer to the following determinations by quality indicators: SO₂; NO, NO₂, Nox; PM_{2,5}; PM₁₀; CO; O₃; H₂S; NH₃; Organic pollutants. The samples monitored continuously for the water environment factor refer to the following determinations by the quality indicators: Turbidity; Spectral Absorptions Coefficient (SAC); Total Organic Carbon (TOC); Redoxpotential; pH Value; Dissolved oxygen – DO (O₂); Conductivity (χ); Nitrate (NO₃-N); Ammonia (NH₄-N); Phosphate (Pges); Ortho-P (PO₄-P); Chlorophyll.

5. REACT SYSTEM HARDWARE AND SOFTWARE

According to the common list of parameters, corresponding to the pollutants monitored for air and water quality, the number of samples in a situ that can be taken continuously in a CSP (measured in unified analogical signal) is generally of $40 \pm 10\%$, depending on the monitoring scope and program. For this fact, there is integrated as hardware a modular platform, scalable for the application flexibility, CompactRIO system model, which will represent the DAQS from the environment station CSP. The implemented corresponding software will be LabVIEW Real-Time application, which will allow through the elaborated program the automatic upload of DB-REACT.

In Fig. 5 there is presented the configuration of the modular platform of the environment data acquisition system for the REACT real time application, which will equip the CSP stations in situ.



Fig. 5: DAQS hardware configuration

At the installation of the monitoring station and this one's put into functioning in situ, the software parameterization of the data acquisition system DAQS from the CSP of REACT environmental integrated system according to the program presented in Fig. 6.

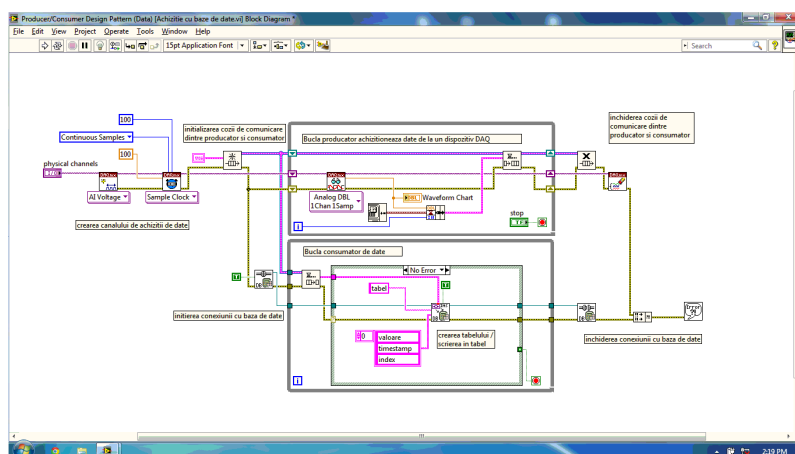


Fig. 6: DAQS software parameterization of CSP station equipping

6. DB-REACT INTERACTIVE DATABASE FOR REAL TIME MONITORING OF THE INVESTIGATED ABIOTIC ENVIRONMENT

DB-REACT is a distributed, relational, spatiotemporal and interactive database (with real time accessing) whose structure is designed so that each sample [Pi], physically determined by a measuring channel in the CSPs from the RO – BG cross-border investigated area, is unique by its registration due to the attributes described in the registers file. Therefore, DB-REACT is a sum of files of environment data organized relationally. Each file corresponds to a quality indicator of the continuously measured environmental component. The investigated situ is spatially localized by GPS. The data acquired from every situ is stored in a RMC data server.

A database structure has been optimised, at SQL code level, with the scope of establishing and organizing the optimum and professional method of acquisition, storage and

visualisation in real time of the parameters monitored by equipments of air, water, ground or meteorological conditions analysis from any location in the RO – BG cross-border area.

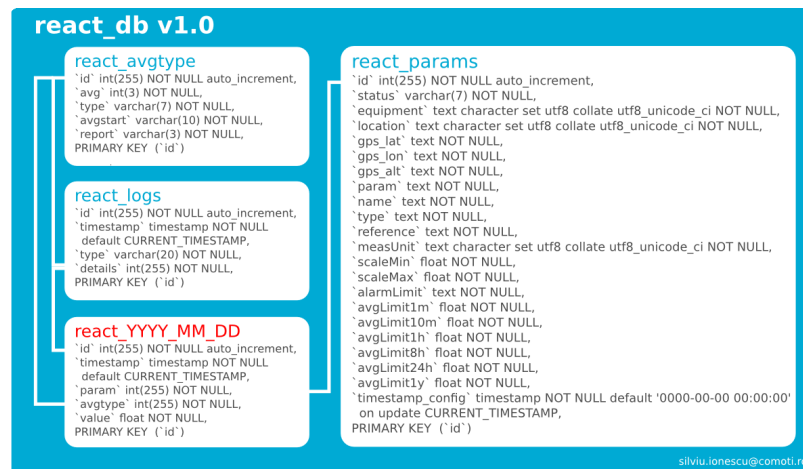


Fig. 8: The DB-REACT database of the REACT integrated system in *MySQL*

The optimum solution of acquisition, transfer and storage for such parameters with low frequencies of sampling is that every location to have a local database to allow synchronization through network to a central database. It is obvious that the decision / alarm factors can be applied both individually on the area, as well as central server level. This synchronization must allow not only the measured values transfer, but also the problems connected to the maintenance of the investigated areas.

7. DATA COMMUNICATION AND THE CONFIGURATION OF THE NETWORK OF REACT MONITORING AND WARNING SYSTEM

The data flux regarding the communication of the automatic monitoring and warning it can be detailed in the following way:

- The direct sensors or the complex analyzers for the quality parameters of air and water must offer analogical or digital output signals, compatible with each area's acquisition system;
- The analogical signals are registered by each area's acquisition system, where the operating system of the local station will initiate periodically an automatic procedure of archived data uploading towards the central area 0. In case the connection can not be initialised, the monitoring local station will have sufficient storage capacity for at least a week;
- The information securely transmitted through VPN will be processed by area 0 and will be offered automatically in the user's interface. Depending on the options chosen by the final user, this one can receive automatically an analysis report or can be alarmed when the pollutants admissible limits are exceeded;
- The decision factors regarding the warning of the monitoring system will be configured at area 0 level which will initiate automatically sound/light messages in the user interface and also e-mail messages to predefined lists, possibly SMS messages at mobile operators level;
- In case one of the parameters that needs to be registered does not present activity in the user interface or one of the stations presents connectivity problems, the maintenance users can be announced automatically with the help of the control processes developed at area 0 level;

- f) The maintenance users will access a separate network with a higher security level for being able to have the possibility of controlling the monitoring stations and of this ones' developing depending on the necessities that appear.

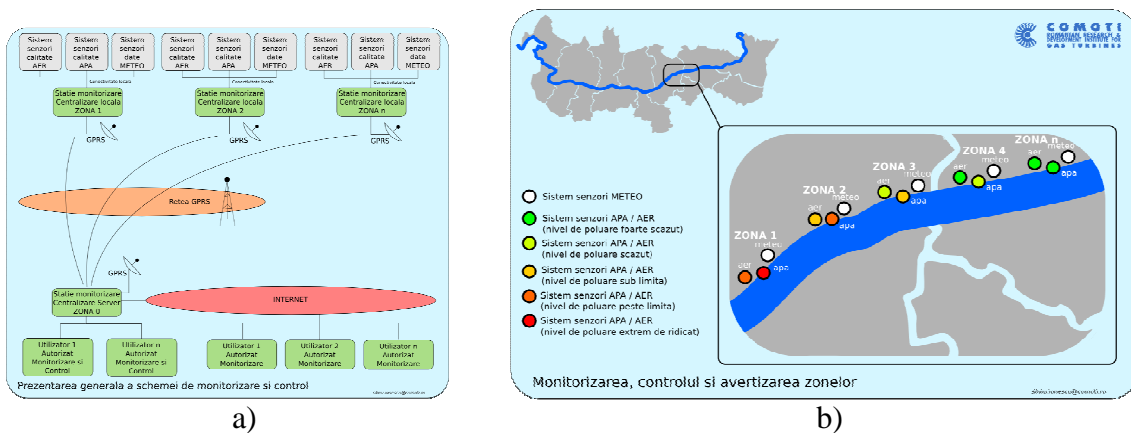


Fig. 9: a) The block diagram of REACT data communication; b) The main interface for control and warning of REACT integrated system

8. CONCLUSIONS

The REACT environment integrated system is a component of the reaction (warning) anthropological factor for abiotic environment protection. It is composed of an intelligent sensors network placed in situ with automatic processes of continuous sampling, data transmission, automatic reporting, control and decision. The main function of REACT system is of *warning for technological risks* in case of industrial accidental pollution in RO-BG cross-border area.

For transmitting a credible and faultless warning to the decisional factors for emergency situations, the REACT integrated system realises:

- The monitoring of the quality indicators of the environment (air/water) factors through the integration in the monitoring network of the measuring equipments (sensors and/or analyzers) through trustworthy methods of the environment pollutants, according to the European regulations from the environment domain;
- Data acquisition through DAQS allows the data automatic insertion in DB-REACT, realised as relational-distributed, spatiotemporal and interactive database;
- Data validation is made automatically through the development in the applications server of a knowledge base initiated by the values of the domains prescribed in EN and developed in time as historic;
- The accessing of the entire system is made securely with authentication levels;
- The traceability at warning/alerting will be established by the negotiation between the project leader with the ANPM decision factors. [3]

References

- [1] Cioplan, O., *Integrated monitoring of ecological systems*. University of Bucharest, Ars Docendi Publishing House, 2005;
- [2] Rojanschi, V., Bran, F., Diaconu, G., *Environment protection and engineering*. Bucharest, ECONOMICA Publishing House, 1997;
- [3] RP4 – Project REACT: „*Integrated system for dynamic monitoring and warning for technological risks in Romania-Bulgaria cross-border area*”, July 2012

CURRENT STATUS OF EXPERIMENTAL RESEARCH ON BIOMASS COMPACTION

PhD.Stud.Eng. Voicea I.¹⁾, Prof. PhD. Eng. Voicu Ghe.²⁾, PhD. Eng. Vladut V.¹⁾,
PhD.Stud.Eng. Matache M.¹⁾, Eng. Maria M.¹⁾
¹⁾ INMA Bucharest; ²⁾ P.U. Bucharest

ABSTRACT

Biomass in its original form is difficult to use successfully as a fuel in large applications because it is bulky, wet and dispersed. Pelleting and briquetting are the most common processes used for compacting biomass to meet the demands of solid fuel. These high-pressure compaction technologies are usually made using a screw press and piston. This paper presents the current state of experimental research on biomass compaction process.

Keywords: compaction, biomass, experimental research.

1. INTRODUCTION

Compaction of the biomass represents technologies for the conversion factory of fuel residues. These technologies are, also, known as granulation, briquetting, or agglomeration, which improves the handling characteristics of the material for transport, storage, etc. Pelleting and briquetting processes are used for many years in several countries.

William Smith was the first that issued a patent in the United States (1880) for biomass densification. Using a steam hammer (60°C), Smith compacted sawdust waste.

Conventional processes for biomass densification can be classified as: wrapping, molding, pelletisation – extrusion and briquetting, which are performed using a pelletizer, compacting using a piston, screw, roller, etc. Pelleting and briquetting are the most common processes used for biomass densification to meet the demands of solid fuel. These high-pressure compaction technologies, are usually accomplished either using a screw or piston press. In a screw press, the biomass is continuously extruded through a heated conical die. The briquettes produced by using a screw press are of a much better quality compared with the use of a press piston. However, by comparing the degree of wear of the parts in a press piston to the screw press, the wear of the piston press is much reduced. Many researchers have studied the densification of herbaceous and woody biomass for the production of pellets using mechanical presses with screw or piston, [2].

Tabil (1996) and Tabil & Sokhansanj (1996) suggest that the compaction process of biomass during pelletization can be attributed to the elastic and plastic deformation of the particles at higher pressures. According to their studies, two important aspects to be considered during pelletization are [5]:

1. capacity to form pellets, with a considerable mechanical resistance,
2. capacity to increase the density of the process.

In the capillary phase, the agglomeration is fully immersed in the liquid, and the primary particles are held only by the surface tension of the droplet. The attraction between the particles is due to electrostatic or magnetic forces of Van der Waal. The attraction is inversely proportional to the distance between the particles, where at long distances the attraction is smaller. The influences on bonding electrostatic forces between particles is negligible, being found usually in fine dry powder, where inter-particle friction can contribute to particle bonding, when magnetic forces exist. Centralization of particles can help provide mechanical power required to overcome the destructive forces caused by elasticity recovery after compression. Figure 1 presents the mechanism of deformation of the powder particles by compression, [2].

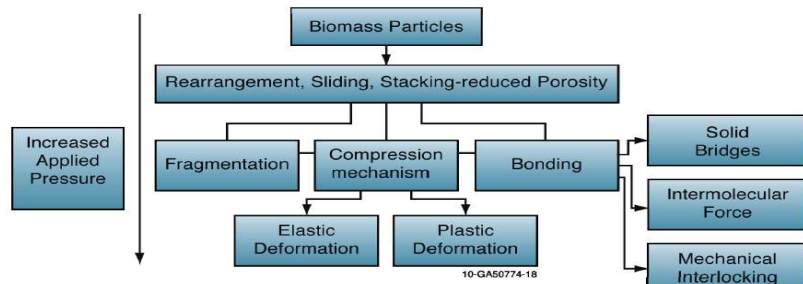


Fig.1. Deformation mechanisms of powder particles under compression

2. METHODOLOGY

Experimental Research on particles sizes

Particle size of chopped reeds were determined by a sieve analysis: <0,5; 1...2; 3...4; 5...6; 7...8;12...13; 22...33 mm. Fine particles immediately absorb moisture, then the large particles, and, therefore, subjected to a high of degree of conditioning, an important indicator of the size of the particles is the necessary cutting power. The specific cutting energy per unit mass increases considerably from 2000 J kg⁻¹ to 4000 J kg⁻¹ when the size of grindings is modified from 20 at 10 mm. Compacting biomass represents the conversion technologies of biomass in a solid biofuel in the form of briquettes or pellets. Studying the compacting behavior of reed particles through experiments should help us understand the mechanism of compaction that could produce high-quality products, compacted and to design such mechanisms with low power consumption. Compacting experiments were carried out using a hydraulic press, and the reed was inserted into a cylindrical shape with a diameter of 35 mm, as shown in figure 2, [4].



Fig.2. Stand experimentally compacted form of reed biomass in Latvia [4]

During compaction experiments the characteristics force-displacement were determined. The forms of the characteristics force-displacement of the compacting process, of different reed particles sizes were similar, obtaining linear curves presented in figure 3. The maximum displacement of the piston necessary to compact reed particles is 13 MPa. Pressing the final material appears in a more rapid increase in pressure, with a small piston movement, of approximately 1-2 cm. This force-displacement characteristic is necessary and important for the design of mechanism for compacting biomass.

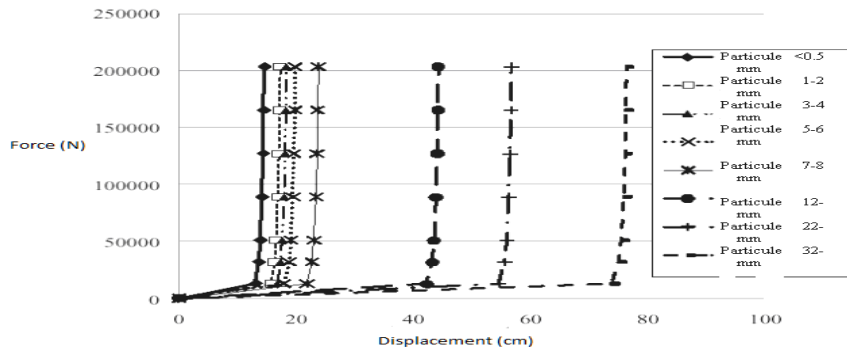


Fig. 3. Characteristics force-displacement of the compacting process, of different reed particles sizes

The density of reed briquettes obtained by compacting with the pressure of 212 Mpa is shown in tabel 1 (D1-D9- listing briquettes), [4].

Table 1. Obtained briquettes density, [4]

Dimensiuni	D1, g cm ⁻³	D2, g cm ⁻³	D3, g cm ⁻³	D4, g cm ⁻³	D5, g cm ⁻³	D6, g cm ⁻³	D7, g cm ⁻³	D8, g cm ⁻³	D9, g cm ⁻³	Densitate medie [g cm ⁻³].
< 0.5	1.014	1.025	1.026	1.034	1.046	1.052	1.058	1.022	1.032	1.034 ± 0.012
1 - 2	1.005	0.999	1.000	1.010	1.002	1.003	1.011	1.004	0.998	1.004 ± 0.011
3 - 4	0.964	0.960	0.985	0.982	0.974	0.982	0.990	0.985	0.994	0.980 ± 0.012
5 - 6	0.922	0.959	0.961	0.953	0.946	0.942	0.947	0.949	0.969	0.950 ± 0.009
7 - 8	0.894	0.879	0.886	0.921	0.893	0.903	0.920	0.923	0.933	0.906 ± 0.014
12 - 13	0.879	0.879	0.888	0.891	0.883	0.893	0.887	0.902	0.889	0.888 ± 0.008
22 - 23	1.013	0.980	0.970	0.954	0.957	0.958	0.977	0.971	0.964	0.972 ± 0.014
32 - 33	1.026	1.019	1.000	1.045	1.004	1.038	1.029	1.047	1.028	1.026 ± 0.016

Minimum density of 0.87 g cm⁻³ have the briquettes with particles size of 12÷13 mm, but the maximum density of 1.03-1.04 g cm⁻³ have the particles with sizes <0.5mm and 32-33mm, according to figure 4, [4].

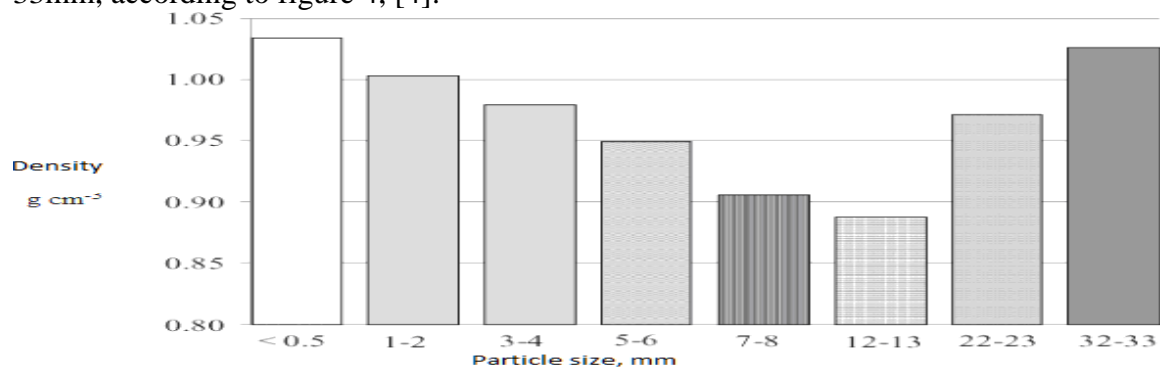


Fig.4. Obtained briquettes density, [4]

Figure 4 presents the energy consumed necessary for pressing the reed material in briquettes. The maximum value (aprox. 172 kJ kg⁻¹) was obtained for particles size of 32...33 mm, the maximum value (aprox. 53 kJ kg⁻¹) for particles smaller than 0.5 mm, [4].

Experimental research regarding pressing energy

Within the article of Repsa Edgars, Eriks Kronbergs, Mareks Smits, Latvia University of Agriculture - EVALUATION OF BIOMASS COMPACTING MECHANISMS is achieved a wedge between the mechanism of compaction achieved using hydraulic presses with screws and piston hydraulic presses. The specific energy consumption of the screw press and the piston hydraulic press for compacting biomass was calculated using the formula, [3].

$$E_{sc} = \frac{3600P}{Q} \quad (1)$$

Where:

- E_{sc} - The specific energy of the compression mechanism, [kJkg^{-1}];
- P - power of the compression mechanism, [kW];
- Q - capacity of the compaction mechanism [kg h^{-1}].

For determining the density, the sawdust briquettes were produced experimentally during compactation (Fig. 5) using a screw press and piston hydraulic press.



Fig.5. Equipment utilized in testing the compaction process, [3]

The technical parameters of the hydraulic piston press: permissible humidity of the raw material at the entrance 8-18%, density of the briquettes produced $600\ldots1100 \text{ kgm}^{-3}$, maximum hydraulic pressure 18 MPa, capacity 30-60 kg/h, power 4kW. Technical parameters of the screw press: permissible humidity of the raw material at the entrance 8-10%, density of the briquettes produced $900\text{-}1400 \text{ kgm}^{-3}$, capacity 250-300 kg/h, power 22kW, the electric heater power 6 kW. The produced briquettes from sawdust using a screw press have a cross section in the shape of a hexagon with an average size of 46 mm and internal orifice of 20. Sawdust briquettes made with the hydraulic piston press have an oval cross section with an average diameter of 64,5 mm and square shapes with the dimensions edges of 64x150 mm.

The laboratory experiments were conducted in a closed mold with a diameter of 35 mm, by means of a hydraulic press according to figure 6, [3].

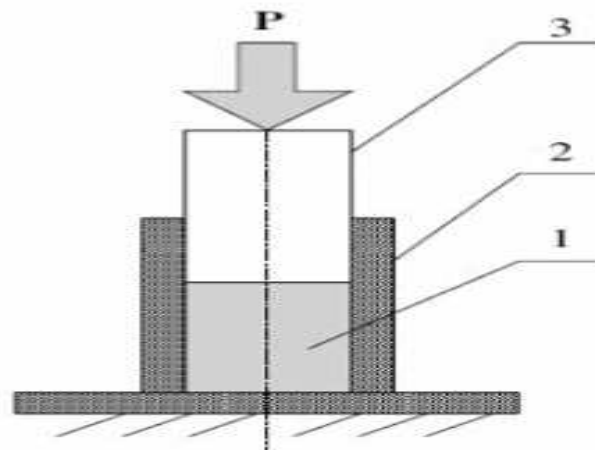


Fig.6. -Closed mold for compacting: 1-biomass, 2-cylinder, 3-piston, [3]

Figure 7, shows an increase of compaction pressure of $136\div276 \text{ MPa}$, the density of the reed briquettes are rising from $956\div1040 \text{ kg m}^{-3}$, [3].

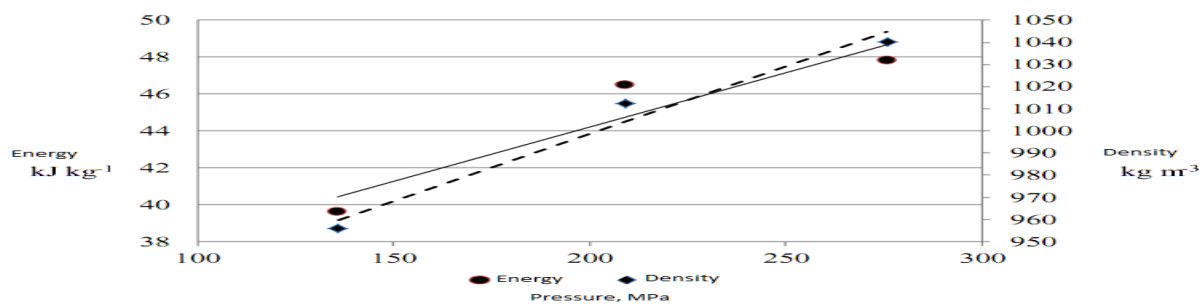


Fig. 7. Briquettes energy and density depending on the compaction pressure, [3]

For the compacting experiment were used three pressure levels: 136, 206 and 276 MPa. The specific energy of the press was increased from 39 to 47 kJ/kg, but the density of 1000 kg m⁻³ was achieved only at a compaction pressure greater than 200 MPa.

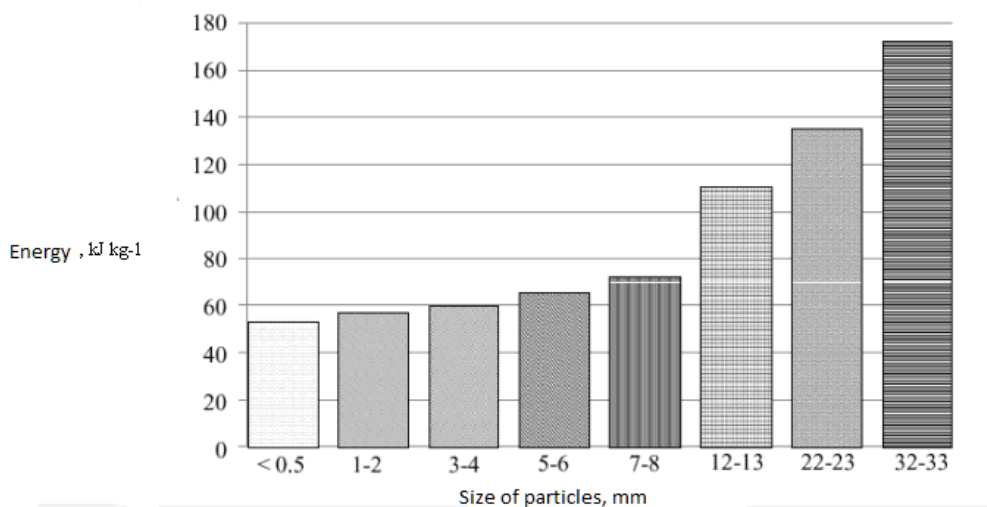


Fig.8. Compacting energy, [4]

3. CONCLUSIONS

Regarding the mechanism of the compacting process, following the conducted research can be inferred that there are three stages in the process of compaction of biomass:

- In the first step, the particles are re-arranged to form a tight mass in which the most part of the particles retain their properties and the energy is dissipated as a result of inter-particle friction.
- In the second step, the particles are forced into one another suffering a plastic and elastic deformation, which increases the contact area between particles significantly, becoming bonded due to the electrostatic forces of Van der Wall.
- In the third phase, a significant reduction in volum at grater pressure resulted from the reduction in density of the pellets reaching a real density. By the end of the third stage, broken and deformed particles can not change their positions because of the low number of goals and the presence of decreased inter-particles compliance with 30%. It is important to understand the process of densification (compaction), and the variables that govern the performances, such as combination, temperature, pressure and process equipments. In case that is not carefully optimized or at least carefully controlled, these variables, can influence the formation of inter-particle gaps of biomass ans result in a negative effect on the conversion process, such as enzymatic hydrolysis.

In terms of technologies used for compacting biomass, they are: extrusion, briquetting, compression (tablets).

Biomass processing with the help of extrusion compaction involves the following mechanisms:

- Before reaching the compression zone (usually represented by an area where the amount of material is reduced), the biomass is partially compressed to be ultimately packed. During this phase, a maximum energy is required to overcome the friction force between the particles.
- After the biomass reaches the compression zone, the material is relatively soft due to high temperatures (200-250 °C), and during this heating, the material loses its elastic nature, resulting in an inter-contact area between particles. At this stage, are forming the so-called material agglomerations when the particles are close to each other. During its passage through the compression zone, the biomass absorbs energy due to friction, so that it can be heated and mixed evenly.
- In the third step, the biomass enters the conical part, where a portion of moisture is further evaporated due to the prevailing temperature of 280°C, thus contributing to a better wetting of the biomass and growth of the compression phenomenon of the material.
- In the final stage, the removal of steam and compaction will take place at the same time, the pressure across the material is normalized, resulting in a uniform extruded piece.

As regards to the particles granulation of biomass, in the compacting process (pelletizing) of materials, we mentioned that the medium and fine materials are more desirable, because in the pelletizing process, at these sizes, the material provides a large surface area to add moisture during the steam conditioning. High starch content of the biomass may result in an increase of the starch gelatinisation during the pelletization and helps to provide a better jointion, while the grosser material will tend to create natural cracks in the pellets. According to the data presented in the literature the specific energy of compression compaction (briquetting) is less than the energy compaction by extrusion.

With regard to energy consumption during compaction using compression technology, only 37-40% of the energy input was required to compress the material; the remaining energy was required to overcome the friction force during the compression of the material.

References

- [1]. **Mani S.**, L.G. Tabil and S. Sokhansanj, - „*Evaluation Of Compaction Equations Applied To Four Biomass Species*”, Canadian Biosystems Engineering, Biomass and Bioenergy 30 (2006) 648–654. Received 14 January 2004; received in revised form 17 January 2005; accepted 17 January 2005, Available online 31 March 2006, www.elsevier.com/locate/biombioe.
- [2]. **Mani S.**, Tabil Lope G., Sokhansanj Shahab - „*Effects of Compressive Force, Particle Size and Moisture Content on Mechanical Properties of Biomass Pellets from Grasses*”, Biomass and Bioenergy 30 (2006) 648–654, www.elsevier.com/locate/biombioe.
- [3]. **Repsa Edgars**, Eriks Kronbergs, Mareks Smits, - „*Evaluation Of Biomass Compacting Mechanisms*” Renewable Energy and Energy Efficiency, 2012 Conditioning of the energy crop biomass compositions, Latvia University of Agriculture.
- [4]. **Repsa Edgars**, Eriks Kronbergs, Mareks Smits - „*Compacting Mechanisms Of Common Reed Particles*”, Proceedings of the 8th International Scientific and Practical Conference. Volume 1 © Rēzeknes Augstskola, Rēzekne, RA Izdevniecība, 2011, ISSN 1691-5402 ISBN 978-9984-44-070-5 Environment Technology Resources.
- [5]. **Tumuluru J. S.**, C. T. Wright, K. L. Kevin, and J. R. Hess. 2011 - “*A Review on Biomass Densification Technologies to Develop Uniform Feedstock Commodities for Bioenergy Application*,” BioFPR (Under review), The INL is a U.S. Department of Energy National Laboratory operated by Battelle Energy Allianc, INL/EXT-10-18420, 2011.

ASPECTS REGARDING SOME CINEMATIC PARAMETERS OF MATERIAL PARTICLES MOTION ON SIFTING FRAMES OF REDUCTION ROLL 1 PLANSIFTER COMPARTMENT

Gheorghe VOICU¹, Gabriel-Alexandru CONSTANTIN, Mădălina-Elena ȘTEFAN
University Politehnica of Bucharest, Faculty of Biotechnical Systems Engineering

ABSTRACT

Sifting and sorting of grist from the technological passages of wheat milling plants is performed in plansifter compartments. Each technological passage has a corresponding pair of grinding cylinder and an compartment with overlapping sieve for sifting. Plansifter motion is a plane circular motion which is transmitted to sifting frames and, hence, to the material from the sieves, so that each material particle describe circular trajectories with a radius different from the radius of plansifter motion, depending on thickness of material layer and of friction coefficient with sieve fabric. In the paper is analyzed the motion of material particles on sifting frames of plansifter compartment which is part of technological passage Break 1, for a wheat milling plant of 100 t/24 h. The analysis includes the determination of particles radius trajectory, travel speed of their on the sieves and the critical speed (possible) for each sifting frame, in conjunction with sieve fabric type and aperture dimensions. Are specified the sifting condition for each material fraction. Specifications from the paper can be of great use to technologists and specialists in the milling industry, particularly in the choice of sieve fabric from each plansifter compartment, given that the plansifter has a fixed speed.

Keywords: plansifter, sifting, grist, particle trajectory, speed limit.

1. MOVEMENT OF PARTICLES ON THE SIFTING SURFACE. CALCULATION OF TRAJECTORY OF A PARTICLE

In order to ensure the sifting is necessary to choose the movement speed of particles on the sieve, so as to permit sifting of their. And refusal not to remain stuck in apertures. When the revolution of main suspended shaft, exceeds the value calculated, the particles are no longer moves along with sieve surface, but on this surface there is a displacement after own trajectories.

To calculate the speed of movement is first necessary to determine the radius of the circle on which it is moving the particle. During operation, plansifter has a circular translation movement. Any point of its describe a circle with center in O_1 and radius r_1 (fig. 1). An isolated particle M on the surface of plansifter, in motion towards it, describe a circle with center in O and of radius r_p , constituting trajectory of relative motion. The trajectory of the particle movement to the plane of function of the plansifter (fixed) is trajectory of absolute motion. If the particle would be mounted on the surface of plansifter, she would describe trajectory of absolute motion, equal to the trajectory of a point of the sieve, of radius r_1 . When is friction, trajectory of relative motion is always smaller than the radius of absolute motion trajectory of the sieve [1, 2, 3, 4].

According to calculation assumptions of Jucovski, on a particle in motion acts centrifugal force due to plan circular motion of plansifter $F_{c1} = m \cdot \omega^2 \cdot r_1$ (1), centrifugal force due to relative motion of rotation of particle $F_{c2} = m \cdot \omega^2 \cdot r_p$ (2), friction force in the relative movement of the particle $F = \mu \cdot m \cdot g$ (3), where ω is the angular velocity of plansifter, including of the particle in relative motion, m – particle mass; and μ is the coefficient of sliding friction between the particles and sieve surface. At equilibrium, the vector sum of the three forces must be zero. Knowing that forces F and F_{c2} are perpendicular can be written $|F_{c2}| = \sqrt{|F_{c1}|^2 - |F|^2}$ (4), and, after replacement, results $m \cdot \omega^2 \cdot r_p = \sqrt{(m \cdot \omega^2 \cdot r_1)^2 - (\mu \cdot m \cdot g)^2}$ (5), from where [1, 2, 3, 4]:

¹Splaiul Independentei, 313, District 6, Bucharest, Romania, ghvoicu_2005@yahoo.com.

$$r_p = r_1 \cdot \sqrt{1 - \left(\frac{\mu \cdot g}{r_1 \cdot \omega^2} \right)^2} \quad (6)$$

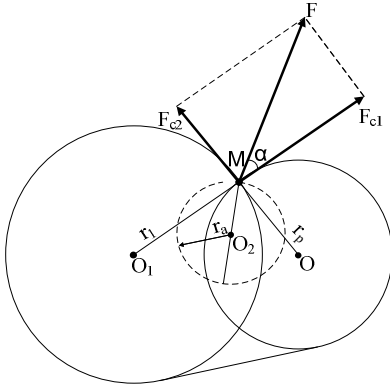


Fig. 1 The trajectory of the particle on sieve surface (adapted after [1,2,4])

where α is the angle formed by the forces F and F_{c1} .

By introducing the above relationship in the relationship of r_p results: $r_p = r_1 \sqrt{1 - \cos^2 \alpha}$ (11), relation that is valid in the case of an isolated particle. Actually, on sieve are particle of height h . The coefficient of friction between the particles is greater than the coefficient of friction between the particle and the sieve. In this case, range of motion of the particle is expressed by the relation:

$$r_p = r_1 \sqrt{1 - K_1^2 \cdot \cos^2 \alpha} \quad (12)$$

where K_1 is a coefficient that takes into account the influence of layer thickness h on the sieve and of friction between the particles. The above expression is known as the generalized relation of Jucovski. Hence, results that speed at which the particle is moving on circle of radius r_p will be [1, 2, 3, 4]:

$$v_p = \omega \cdot r_p \quad (13)$$

2. ESTIMATION OF SPEED LIMIT OF DISPLACEMENT OF THE PARTICLES ON SIFTING SURFACE

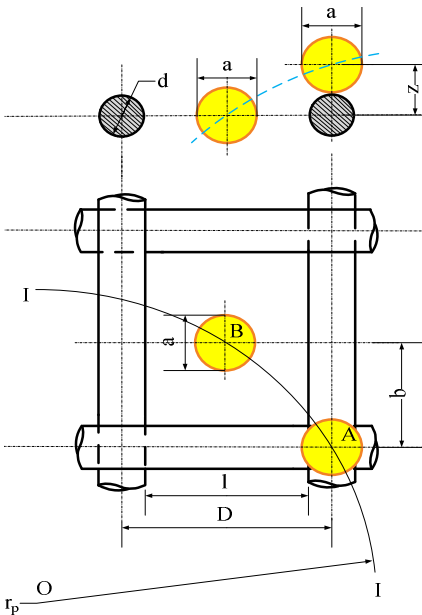


Fig. 2 Scheme for calculating the particle velocity; case $a \leq l$ (adapted after [1,2,4])

Speed limit of displacement of the particle on the sifting surface is determined for the case of sifted particles $a \leq l$.

In this case ($a \leq l$ – fig. 2), for the sifting can be carried out must be met the following conditions [1, 2, 3, 4]:

- Sifting particle to reach over the aperture of sieve;
- Upon reaching over the aperture the particle must have time to fall through it in the high $z = (d+a)/2$, otherwise it will not be engaged in passing through the aperture.

Particle is moving on the circle of radius r_p , from A to B, in point B it falling under its own weight.

$$z = \frac{d+a}{2}, \quad D = d+l \quad (14)$$

where d is the thickness of sieve wire, and a is the sifted particle diameter.

Due to the fact that the particle is in free fall, in point B, height of fall, will be [1, 2, 3, 4]:

$$z = \frac{1}{2} g \cdot t^2 \quad (15)$$

where g is the gravitational acceleration.

Space crossed by particle in a horizontal plane in a time equal to the fall time is:

$$S = v_p \cdot t \quad (16)$$

Following the figure 2, is observed that the space S is equal to the length of the arc AB, which can be approximated by chord AB corresponding to it [1, 2, 3, 4]:

$$S = \sqrt{\frac{D^2}{4} + b^2} \quad (17)$$

From the above relations is obtained, after calculations, particle speed limit expression $v_{p.lim.}$ on sieve surface, namely:

$$v_{p.lim.} = \sqrt{\frac{g \cdot \left(\frac{D^2}{4} + b^2 \right)}{d + a}} \quad (18)$$

Worst case is when the particle is moving to the surface of sieve parallel with wire, namely $b=0$. In this case particle limit speed will have the expression:

$$v_{p.lim.} = \sqrt{\frac{g \cdot \left(\frac{D^2}{4} \right)}{d + a}} = \sqrt{\frac{g \cdot \left(\frac{d + l}{2} \right)^2}{d + a}} \quad (19)$$

If the $l=a$, results [1, 2, 3, 4]:

$$v_{p.lim.} = \frac{1}{2} \cdot \sqrt{g \cdot (d + l)} \quad (20)$$

From the analysis of sifting of particles by a size smaller than sieve apertures results that the speed of the particle depends on the particle size and of apertures as well as of bulk density and the height h of the layer of material, because it hampers the movement of the material layer in contact with sieve.

Numerical application (case study)

• Calculating trajectory of a particle

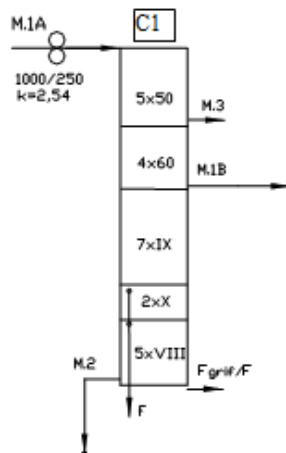


Fig. 3 Diagram of first reduction roll compartment of 100 t / 24 h mill

Given the importance of knowing radius of the circle on which it is moving the particle and the velocity of particles on the sieve surface, We determined these parameters for the five sifting surfaces in the first plansifter compartment in reduction phase of a milling plant with capacity of 100 t/ 24 h.

As can be seen, radius of the circle on which it is moving the particle (ec. 6) as well as the particle velocity (ec. 13) depends on the radius r_1 of the circle on which it is moving the equipment, so we have the following consultative table from which this radius (r_1) is taken:

Table 1 [1, 2, 3, 4]:

n, [rot/min]	180	200	225	275	300
r_1 , [mm]	50	45	40	35	30

In fig. 3 is presented the diagram of first reduction phase.

At the same time we used the average values of the experimental data for the static coefficient of friction (table 2) determined by the method of inclined plane.

The analyzed mill is on type SPP 624 and has revolution of $n = 225 \text{ rot/min}$. From table 1 results that radius $r_1 = 40 \text{ mm}$. Thus, angular speed of the sieve will be:

$$\omega = \frac{\pi \cdot n}{30} = \frac{\pi \cdot 225}{30} = 23,562 \text{ rad / s}$$

Table 2. The average values of the coefficient of static friction and of mean diameter.

Grist fractions	Mean diameter, d_m (mm)	Coefficient of static friction, μ		
		Steel sheet	Cotton canvas	Fiber glass
C1 Intrare	0.30	0.694	1.750	1.232
C1 M3	0.60	0.582	1.760	0.756
C1 M1B	0.34	0.567	1.506	0.791
C1 M2	0.25	0.747	1.760	0.891
C1 F	0.10	0.956	1.760	1.226
C1 Fgrif	0.17	0.849	1.739	1.118

The first package of the compartment is for sifting of refusals, thus it is considered that frames surfaces from package are metal tape (no. 50), choosing, from table 2, for fractions C1 Intrare and C1 M3, value for static friction coefficient on steel sheet. Sifting surfaces used in package 2 of compartment (no. 60) are made of plastic, thereby taking into account the coefficient of static friction obtained for glass fiber. And sieves from packages 3, 4 and 5 are sieves for sifting of flour (no. VIII, IX și X) being produced from cotton, for this choosing the coefficient for static friction values determined on cotton cloth.

In table 3 are given values used for the coefficient of static friction (from table 2), values of $\cos \alpha$ (relation 10), values of radius of the circle on which it is moving a particle (relation 11) and values of velocity of a particle on the sifting surface (relation 13).

Table 3 Values of $\cos \alpha$ (relation 10), of r_p (relation 11) and of v_p (relation 13)

Grist fractions	Coefficient of static friction, μ	$\cos \alpha$	r_p , (mm)	v_p , (mm/s)
C1 Intrare	0.694	0.307	38.074	897.092
C1 M3	0.582	0.257	38.655	910.795
C1 M1B	0.791	0.349	37.478	883.065
C1 M2	1.760	0.778	25.155	592.710
C1 F	1.760	0.778	25.155	592.710
C1 Fgrif	1.739	0.768	25.607	603.360

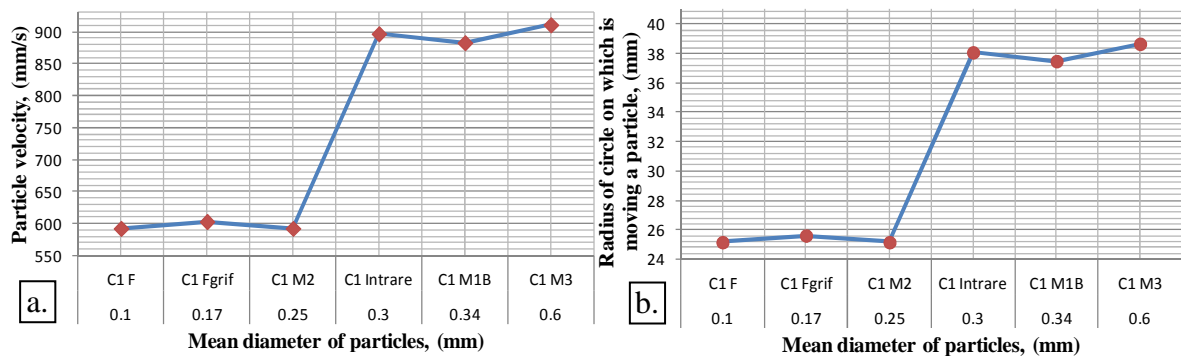


Fig. 4 The variation of a particle on the sifting surface (a) and the radius of circle on which is moving the particle (b) with mean diameter of grist fractions at plansifter compartment C1 of analyzed mill.

In fig. 4 is presented the variation of a particle on the sifting surface (a) and the radius of circle on which is moving the particle (b) with mean diameter of grist fractions at plansifter compartment C1 of analyzed mill in reduction phase. The values of mean diameter were determined by particle size analysis and are presented in table 2.

It is observed (table 3) that radius of the circle on which moves a grist particle is dependent on the coefficient of static friction of respective the particle. It is noted that having an higher value of coefficient of friction values radius of the circle on which it is moving a particle and thus values of the speed at which the particle moves on the surface of sifting will be lower, and vice versa. It also can be seen (fig. 4) that the particles with small diameter (see

fraction C1 F) will move at a low speed (592.71 mm/s for C1 F and C1 M2) on a circle with a smaller radius also (25.155 mm for C1 F and C1 M2), when large-diameter particles (see fraction C1 M3) will move at a speed high enough (910.795 mm/s for C1 M3) on a circle of radius also high (38.655 mm for C1 M3), close to radius of actuating mechanism eccentric.

- **Estimation of speed limit of displacement of the particles on sifting surface**

Analysis for estimation of speed limit of displacement of the particles on sifting surface was made to the same compartment. From the analysis of fig. 3 is observed that the first compartment is made of 4 packages with 5 different types of fabric whose characteristics (correlated with that in fig. 2) are given in table 4.

Distance between two wires was calculated with the relationship:

$$l = \sqrt{\frac{S_e \cdot D^2}{100}} \quad (39)$$

Using relations 14, 16 and 19 were calculated distance z, space crossed of particle S and speed limit of the particle and using relation 15 was calculated time of falling t. Values are presented in table 5.

Table 4 The characteristics of the sieving surface from fig. 3

No. of manufacturing of sieve	D, (mm)	No. of wire on cm	Free surface, S_e (%)	l, (mm)	d, (mm)
50	0.526	19	50	0.372	0.154
60	0.282	23	41	0.181	0.101
IX	0.176	38.5	45	0.118	0.058
X	0.146	43	39	0.091	0.055
VIII	0.197	34	45	0.132	0.065

Table 5 Values of z (rel. 14), t (rel. 15), S (rel. 16) and v_{plim} (rel. 19).

Grist fractions	z, (mm)	t, (s)	S, (mm)	v_{plim} , (mm/s)
C1 intrare	0.227	0.007	6.103	53.302
C1 M3	0.377	0.009	7.985	41.361
C1 M1B	0.221	0.007	5.924	39.582
C1 M2	0.154	0.006	3.321	37.440
C1 F	0.077	0.004	2.355	48.091
C1 Fgrif	0.117	0.005	2.952	45.357

It is noted that actual speed of the particle calculated and extracted in table 3 is greater than of limit speed calculated of particles. From here we deduce that revolution is well chosen, because all particles, regardless of their size, will have time to be sifted. Figure 5 shows the variation speed limit of the particle with the mean diameter.

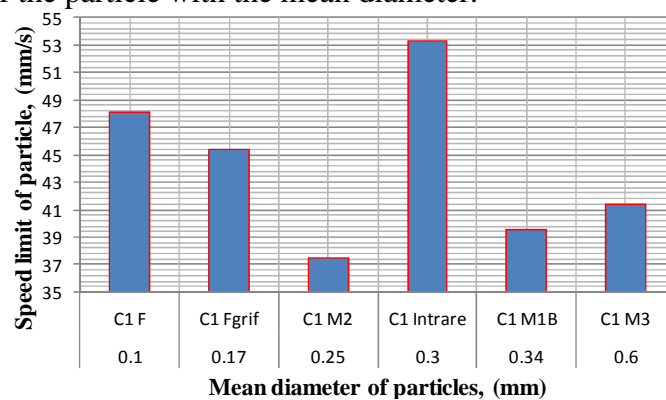


Fig. 5 Variation of speed limit of particle on sifting surface with mean diameter of grist fractions at plansifter compartment C1 of analyzed milling plant in reduction phase.

Fraction C1 Intrare is a mixture from all 5 fractions sorted at compartment C1. This fraction feeds this compartment, so that the first frame of package 1 will appear a stratification

large enough of material. From fig. 5 it is noted that the speed limit value of the particles is quite high compared with other fractions, precisely because of this. Also, fraction C1 F is separated on surfaces of sifting made from cotton. Due to the two types of friction (particle-particle, particle-sieve) appear the phenomenon of static electricity, pflour particles forming aggregates and separating harder through sieve aperture, thus that the speed limit will be higher.

3. CONCLUSIONS

From those presented above we drawn the following conclusions:

- a. The processing capacity of a sieve depends on the amount of material which is separated through apertures per unit of time. It increases with increasing of displacement sieve and with thickness of the material;
- b. Reduction of the length of the sieve and increase of displacement sieve has a negative influence on the extraction coefficient, which impose the find of their optimal values in order to obtain high processing capacities and an effect of separating good;
- c. Material layer thickness on sieve must be chosen such as to allow a proper stratification of it without being disturbed in its movement;
- d. A high feed rate and a more rapid movement of material on sieve increases the processing capacity but decreases the separation efficiency of sifting, sifting operation must be repeated to not lose sifting remained in refusal, unnecessarily uploading the next technological stages;

In order to ensure the sifting is necessary to choose the movement speed of particles on the sieve, thus as to permit sifting of their. And refusal not to remain stuck in apertures.

When the suspended main shaft revolution, exceeds the value calculated, the particles are no longer moves along with sieve surface, but on this surface there is a displacement after own trajectories.

For the sifting can be carried out must be met the following conditions:

- Sifting particle to reach over the aperture of sieve;
- Upon reaching over the aperture the particle must have time to fall through it in the high $z=(d+a)/2$, otherwise it will not be engaged in passing through the aperture.

Also refusal particles tend to plug the sieve apertures. For the sieving process can continue and refusal to be evacuated from the sieve, the inertial forces acting on the refusal particle must be large enough to cause its removal from apertures.

AKNOWLEDGEMENTS

The work has been funded by the Sectoral Operational Programme Human Resources Development 2007-2013 of the Romanian Ministry of Labour, Family and Social Protection through the Financial Agreement POSDRU/107/1.5/S.76903.

References

- [1] Moraru C., *Tehnologia și utilajul industriei morăritului și crupelor*, Litografiere, Univ. din Galați, 1988.
- [2] Panțuru D., Bârsan I.G, *Calculul și construcția utilajelor din industria morăritului* – Editura Tehnică, București, 1997;
- [3] Voicu Gh., T. Cășândroiu, Biriș S.S., David M.F., Tudose E.M., Constantin G.A., *Cercetări teoretice și experimentale privind procesele de lucru dintr-o unitate de morărit pentru cereale în vederea modernizării și creșterii performanțelor acestora*, Research Report, Proiect Program IDEI-PCE, contract nr.753 / 15.01.2009, cod ID_1726
- [4] Voicu Gh., Cășândroiu T., *Utilaje pentru morărit și panificație, curs, vol.I - Procese și utilaje pentru morărit*, Litografia U.P.B., 1995;

RESEARCH ON IMPROVEMENT OF INJECTION DEVICES COMPONENTS OF FERTIGATION EQUIPMENT

Gabriela MATACHE¹, Gheorhge ȘOVĂIALA¹, Ștefan ALEXANDRESCU¹,
Sava ANGHEL¹, Ilie BIOLAN²

ABSTRACT

Fertigation has several advantages arising from the following considerations:- it replaces the traditional system of chemical fertilizers management; - it facilitates quick access of fertilizing substances to the root system of plants, at the appropriate moment, and their higher capitalization; - it significantly reduces losses of active ingredients by evaporation, gravitational leakage or drainage beneath the roots of plants, under the influence of unfavorable climatic factors (high temperatures associated with strong winds, showery rainfalls), of chemical fertilizers stationary for a long time on the soil surface; - it allows very precise dosing of fertilizing solution components, depending on the nutritional requirements of plants, determined by chemical analysis of the soil; - it facilitates management of fertilizers in the final stages of plant growth and development, when the access of fertilization equipment in the crop field is virtually impossible; not applying the norms of fertilizers for these stages of vegetation usually leads to decreased quality of seeds.

Key words: fertigation equipment, membranes, multiplier

1. FIELD OF APPLICATION

The technical solution adopted to achieve the equipment for injection of fertilizing substance into the irrigation water, type positive displacement double pump with membranes, ensures proportionality of injected flow rate and irrigation facility flow rate. The driving fluid which actuates the shaft of pump, which is mounted in parallel with the main circuit of irrigation facility, is represented by water taken from its supply pipe. Overpressure necessary to inject nutrients in the same pipeline is achieved by adopting the principle of difference between surfaces of drive chamber and injection chamber.

Linking the technical elements of irrigation to the technical elements of fertigation allows, at the end of watering, once there is reached the depth of water penetration in the area of predominant developing of the root system of plants, to be injected all the fertilizing solution necessary to plants, determined according to the stage of crop growth.

2. DESCRIPTION OF THE HYDRAULIC FERTIGATION FACILITY

The injection equipment is characterized by the fact that in the irrigation facility pipe there are inserted in pulses equal doses of fertilizing solution. Pulsation frequency is adjustable by changing the water flow entering the drive chambers of double displacement pump with membranes (hydraulic injection amplifier).

Generally, a fertigation facility has the structure shown in Figure 1:

¹ INOE 2000 – IHP Bucharest, 14, Cutitul de Argint Street, district 4, Bucharest – ROMANIA, +4021-336.39.91, fluidas@fluidas.ro

² INCDF-ISPFI, 35 – 37 Oltenitei Ave., Bucharest 4 – ROMANIA, +4021.332.29.20

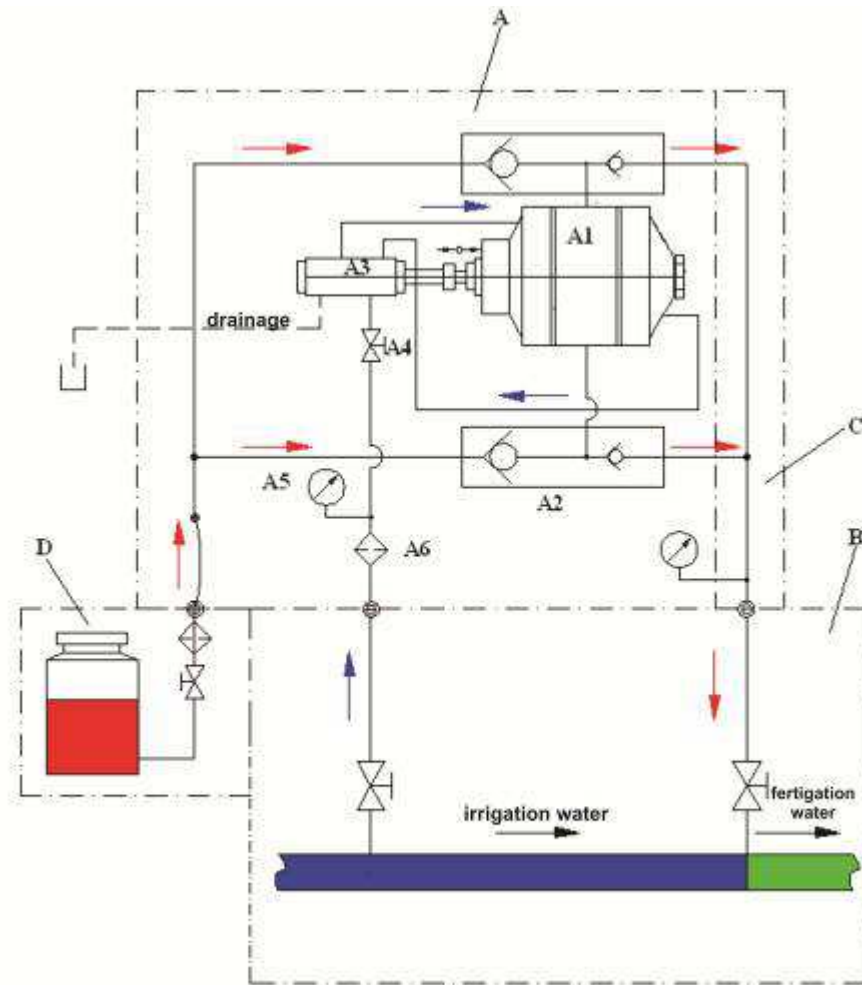


Figure1. A- fertilizing solution injection equipment; B- irrigation pipe section, C- system for monitoring the hydraulic parameters of fertilizing solution; D- fertilizer container with related accessories.

The injection equipment (A) is coupled to the special section of the irrigation facility (B), respectively to the container of liquid fertilizer (D). Tap valves on these circuits shall be opened so that the fluid under pressure, after opening the tap valve A4, will come, along one of the ways of the A3 directional control valve, into the hydraulic injection amplifier chambers – figure 2.

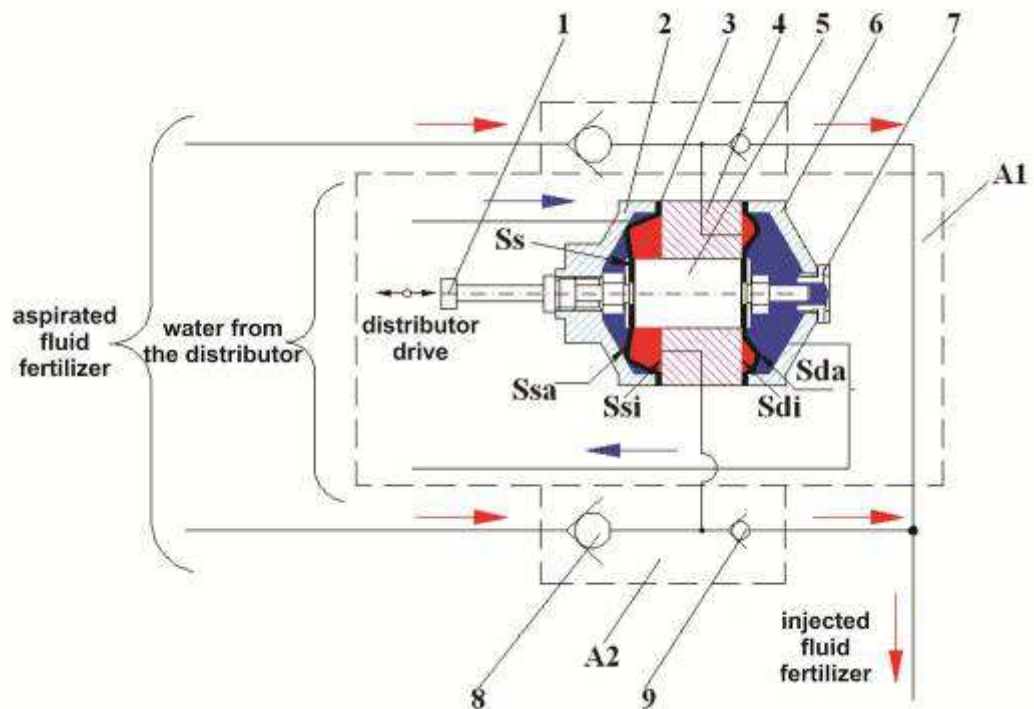


Figure 2. Hydraulic schematic diagram of the multiplier: 1- axial drive rod, 2- left lid, 3 -membrane, 4- case, 5- piston, 6- right lid, 7- plug, 8- intake valve, 9- discharge valve.

- Ssa, Sda – circular surfaces, left and right, on which water acts;
- Ssi, Sdi – circular surfaces, left and right, on which fluid fertilizer acts;
- Ss – piston circular surface

If the pressurized water enters the chamber on the right, the subassembly made up of the two membranes, rod and piston will move to the left, there will be achieved injection of fertilizer through the injection valve located at the top of Figure, as the effect of water pressure on surface Sda. At the same time, the fertilizer is drawn from the container through the check valve 8; rod 1 will act on the directional control valve A3 (Fig. 1), changing its position, and the injection operation is repeated identically on the left side of the hydraulic injection amplifier.

As one can see, the hydraulic amplifier injector does not need another source of energy, using the pressurized water itself passing through the irrigation equipment.

3. ALTERNATIVE ACTUATION OF THE MULTIPLIER

As regards the hydraulic directional control valve controlling the reciprocating motion of hydraulic injection amplifier, there are several constructive versions. In Figures 3 and 4 there is presented a directional control valve with front closure with elastomeric sealing.

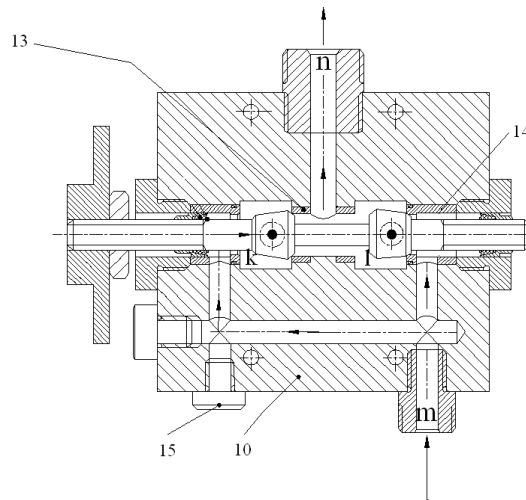


Figure 3. Cross section in horizontal plane through the hydraulic directional control valve: 10 - body, 13- central seats, 14- side seats, 15 - plug, m- connecting pipe for pressurized water supply, n- discharge connecting pipe.

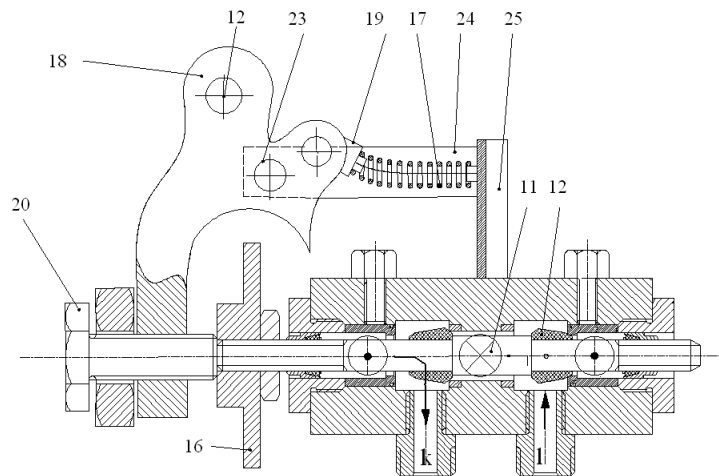


Figure 4. Cross section in vertical plane through the hydraulic directional control valve: 11-shaft; 12- fixed valves, 16- bushing by which the shaft is driven through mechanical control, 17- swinging spring, 18-fork, 19- rotation coupling, 20- adjustable screw, 23-shaft, 24- fork carriage, 25- mechanical control support profile, m- connecting pipe for pressurized water supply, n- discharge connecting pipe, k,l- consumers of directional control valve actuating the multiplier.

Upon completion of the amplifier stroke, rod 1 drives, through a system of levers, the fork 18, this swings over the spring 17, changing the position of the distributor slide valve, and thus the drive direction of pressure in the chambers of membranes. The disadvantage of this drive is that during operation mechanical system goes out of order and to a point swinging is no longer performed.

Adjustment of the hydraulic amplifier injection frequency is made by adjusting the supply flow rate of hydraulic directional control valve. Decreasing the flow rate by closing the tap valve creates pressure drop, there being a risk that at certain amount of pressure in the drive chambers the amplifier to stop working.

4. INNOVATIVE PRODUCT AS A RESULT OF RESEARCH

Analyzing the shortcomings of currently existing injection equipment, researchers at IHP-Bucharest have developed a new product - Figure 5, with the following characteristics:

- simple construction based on attachable parts;
- long life span;
- application field at low pressure within irrigation facilities, approximately 1 bar;
- predictive maintenance at low cost;
- low overall dimensions and weight;
- chemical resistance of materials the equipment is made of to all chemical fertilizers used in agriculture.

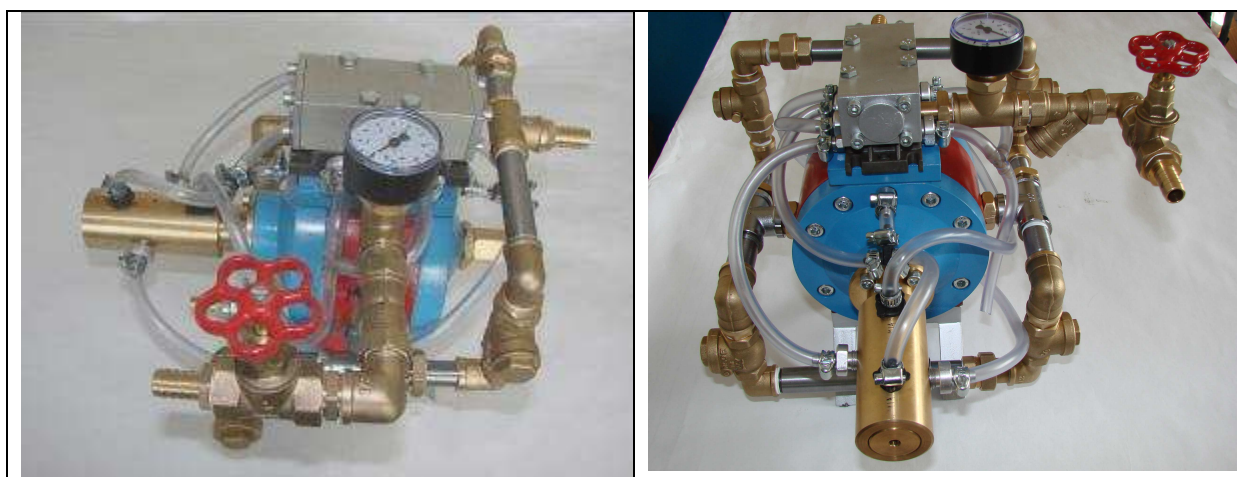


Figure 5. The injection device within the structure of fertirrigation equipment – innovative product

Echipamentul de injectie se poate utiliza si in alte domenii, de exemplu in transvazarea lichidelor corozive.

Hydraulic schematic diagram of the multiplier is shown in Figure 6, where it can be seen that the multiplier rod drives directly axially the slide valve of the tracking distributor A3.2, which in return drives hydraulically the actuation distributor A3.1. This construction eliminates the complicated method of drive through leverages and spring which requires additionally a series of mechanical adjustments.

Another advantage is that the injection frequency adjustment is done via miniaturized tap valves A4.1, A4.2, mounted on the control circuits, modifying low flows along the circuits, throttle effect being thus diminished.

This injection equipment can be used in other areas as well, e.g. for pouring corrosive fluids.

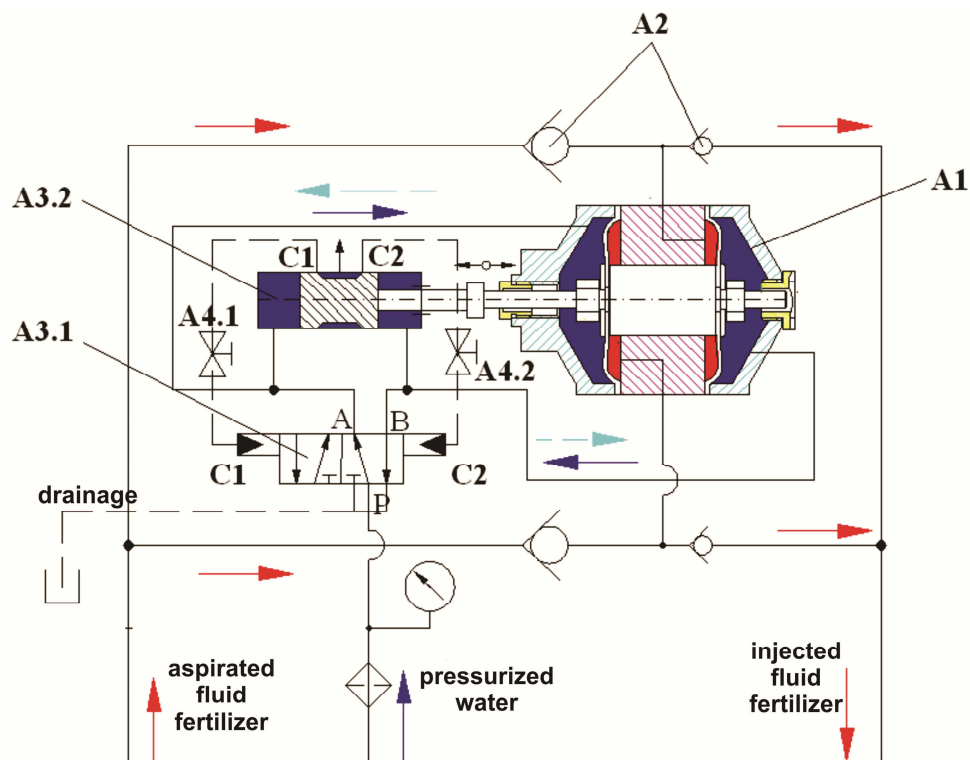


Figure 6. Hydraulic schematic diagram in its innovative version: A1-multiplier, A2- check valves unit, A3.1- directional control valve for actuation, A3.2- directional control valve for tracking, A4.1;A4.2- miniaturized tap valves, C1,C2 drive (pilot) chambers of directional control valve for actuation.

General Specifications:

- Maximum working pressure.....	P = 6 bar;
- Flow of injected liquid fertilizer	Q = 2...4 l / min;
- Total injection stroke	c = 18 mm;
- Working surface area	S = 61 cm ² ;
- Motor capacity / pump capacity ratio	I = 2 / 1;
- Pressure loss in the supply circuit	$\Delta p = 0.02$ bar;
- Overall dimensions	336 x 350 x 282 mm;
- Weight	11 Kg.

References

- [1]. Radcenco, V. 1985 –*Calculul si proiectarea elementelor si schemele pneumatice de automizare (Calculus and design of pneumatic automation elements and schematic diagrams)* Bucharest, Technical Publishing House.
- [2]. Deacu, L, et al. 1989 *Tehnica hidraulicii proportionale (Technique of Proportional Hydraulics)* Cluj-Napoca , Dacia Publishing House.
- [3]. Biolan, I. et al.– *Dosing pump, Romanian Patent* no. 102887/1993;
- [4]. Biolan, I. et al. – *Fertigation installation, Romanian Patent* no. 121612/2007;
- [5]. Fertigation – key to higher yields, healthy crops, pg 19-21, Haifa Chemical Ltd., Israel
- [6]. TMB Fertilizers pump LTD. – “WP-10” – Fertilizer pump, USA prospect;
- [7]. Biolan I. – The hydraulic propulsion of irrigation installation on hydraulic bellow engine, Agricultural Mechanization no.12/1999, Romania

USING THE GAS GENERATOR TO SUPPLY THE IRRIGATION MOTOR PUMPS

PhD. Eng. Adrian MIREA¹⁾, Dipl. Eng. Sava ANGHEL²⁾,
PhD. Eng. Gabriela MATAACHE²⁾, PhD. St. Eng. Adrian PANTIRU²⁾

¹⁾S.C. ROMFLUID S.A.

²⁾INOE 2000 - IHP

1. PURPOSE OF THE WORK AND APPROACH

Irrigation works performed in the rural area (area with reduced financial and technical support) require as necessary to minimize production costs given that sustainable development is planned.

Energy expenditures is a sensitive chapter in agriculture, thus reuse of local waste materials that can not be recycled in a superior manner but have usable energy potential is the only way to improve the costs within this field.

The gas powered motor has displacement of $287 \text{ cm}^3/\text{rev}$, rated rotational speed of 3000 rev/min and torque of 716.2 daNm. Its rated power is 4.6 hp or 3.38 kW, and the efficiency is 5.5%.

For sprinkler irrigation of crops in small areas, one can use the horizontal multistage pump SADU, in the following sizes (which represent the diameter of the suction head): 50; 65; 80 and 100 mm. Rated diameter of the discharge side is 40; 50; 65 and 80 mm.

2. SCIENTIFIC INNOVATION AND RELEVANCE

The schematic diagram of the experimental installation made by INOE 2000 - IHP in collaboration with CCSB within UPB is shown in Figure 1.

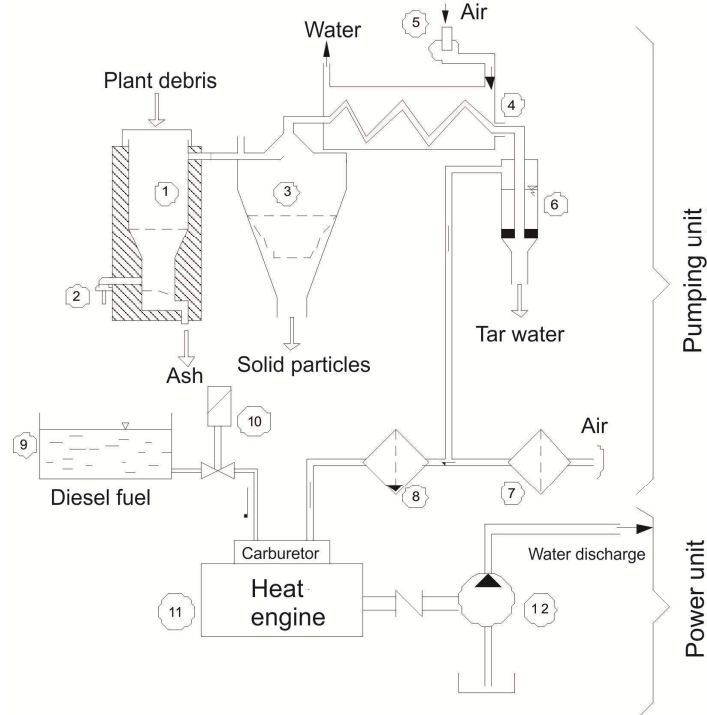


Figure 1 Experimental installation

Gas generation element (1) consists of a metal tank lined with refractory material in which plant debris are inserted through the top side, and they burn in the presence of air pumped by an air blower (2) through the intermediate side. Ash is discharged through the bottom of the generator.

Result of generation passes through the cyclone (3) where it is washed from insoluble solid particles, which are removed through the bottom of the cyclone.

3. THE EFFICIENCY OF FUEL COMBUSTION PRODUCT INSTALLATION

3.1 Standard gas composition

Considering the standard gas mixture of gas produced by gasification of beech wood shavings, the resulting composition is shown in Table 1.

Table1

TIP GAZ	CO H ₂	CH ₄ C _m H _m	CO ₂	O ₂	N ₂
%	29 14	3 0,4	0,5	0,2	46,9
CLASIFICARE	Combustibil	Neglijabile	Inerte		

Significance notations from the table:

CO carbon monoxide

H₂ hydrogen

CH₄ metan

C_mH_m other hydrocarbons

CO₂ dioxid de carbon

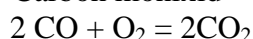
O₂ oxygen

N₂ azot

Classification of the components is done in three categories: gas; negligible quantity inert.

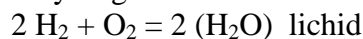
3.2 Burning of combustible gases

- Carbon monoxid



$$1 \text{ Kg (CO)} + \frac{4}{7} \text{ Kg (O}_2) = \frac{11}{7} \text{ Kg (CO}_2) + 2420 \text{ Kcal}$$

- Hydrogen



$$1 \text{ Kg (H}_2) + 8 \text{ Kg (O}_2) = 9 \text{ Kg (H}_2\text{O)} + 33910 \text{ Kcal}$$

3.3 Energy balance

It consists of determination of oxygen for burning combustible gas mass of 1 kg and heat energy released. Balance is shown in Table 2.

Tabelul 2

GAS	Weight		Required O ₂ la 1 Kg composition	Required O ₂ la 1 Kg gaz gazogen	ENERGIA (Kcal)
	%	Kg			
CO	29	0,29	0,57	0,165	702
H ₂	14	0,14	8	1,120	4747
INERT	57	0,57	-	-	-
MASA COMBUSTIBILĂ		0,43	-	1,285	5450

3.4 The amount of air (with 21% oxygen) needed to burn a gas-producing gas Kg

$$M_{aer} = \frac{1,285 (O_2)}{0,21} = 6,112 \text{ Kg (aer)}$$

3.5 The ratio of the amount of gas-producing gas and the amount of air necessary for combustion (3.4)

$$r = \frac{M_{gaz}}{M_{aer}} \cong \frac{1}{6} \frac{[Kg \text{ gas - producing}]}{[Kg \text{ aer}]}$$

4. EXPECTED EFFECTIVENESS OF THE USE OF GAS-PRODUCING ENGINE FOR FOOD GRAIN AL 75-B METROM BV

4.1 Engine parameters:

Displacement $V_g = 287 \text{ cm}^3 / \text{rot}$; the degree of filling $\varepsilon = 0,85$ la $T = +25^\circ \text{ C}$; turația nominală

$$n = 3000 \frac{\text{rot}}{\text{min}}$$

rated $N = 4,6 \text{ CP}$ (expected power $N_p = 3,36 \text{ CP}$)

- Fuel mixture flow required to operate

$$Q = \varepsilon \cdot V_g \cdot n_{nom} = 0,85 \cdot 0,287 \cdot 300 = 732 \frac{\text{dm}^3}{\text{min}} \left(0,012 \frac{\text{m}^3}{\text{s}} \right)$$

- Rated torque

$$M = 716,2 \frac{N}{n} = 716,2 \frac{4,6}{3000} = 1,11 \text{ daN m}$$

4.2 The density of the fuel gas

In Table 3 are given relative density (ρ_{rel}), absolute density (ρ_i) and proportions of components (P_i) of gas in Table 3.

Tabelul 3

GAS SIZES	CO AER	H ₂	CH ₄	N ₂	CO ₂	O ₂
ρ_{rel}	0,97 1	0,07	0,554	0,96	1,529	1,105
$\rho_i \left(\frac{Kg}{m^3} \right)$	1,2 1,24	0,087	0,686	1,19	1,895	1,37
P_i (%)	29 -	14	3	46,9	6,5	0,2

Doing weighted average

$$\rho_{gaz} = \frac{1}{100} \sum_i \rho_i P_i = 1,336 \frac{Kg}{m^3}$$

4.3 Specific power is the ratio of the amount of power produced by the engine and the mass of fuel consumed per hour (C_M)

$$C_M = \frac{C}{m} = \frac{860 N_p}{\rho_{gaz} rQ \cdot t} = \frac{860 \cdot 3,36}{1,336 \cdot \frac{1}{6} 0,012 \cdot 3600} = 302 \frac{Kcal}{Kg}$$

5 RESULTS

Estimated efficiency of the engine is considered to be the ratio of specific power (4.3) and the amount of energy released by combustible gaseous components shown in table 2.

$$\eta = \frac{C_M}{C_{CO} + C_{H_2}} = \frac{302}{702 + 4747} \cong 5.5\%$$

When estimating efficiency there was not considered the energy absorbed by the incombustible gases which is considered to have an "insulating" behavior.

5.CONCLUSION

The cost for 1 Kg of gas produced by a gas generator is estimated to be equal to 1/8 of the cost of collecting timber to be turned into gas, and it has a value of 0.28 RON, producing 5400 Kcal / Kg, compared to 1 kg of diesel that produces 10000 Kcal / Kg, but now is over 10 times more expensive.

Fuel used is expected to consist of 10% diesel fuel and 90% gas, case in which the price of motor pump supply is

$$S = 0.1 \cdot 10000 + 0.9 \cdot 2400 = 3160 \text{ lei/Kg}$$

thus reduced by more than 3 times compared to classical supply.

References

HÜTLE – *Manualul inginerului (Engineer Handbook)*, Technical Publishing House 1994 and Technical Publishing House 1999

Prof.Dr. C HERA ș.a. – *Cercetarea științifică în agricultură (Scientific research in agriculture)*, AGRIS 2000 Publishing House

Dr.ing. C. NICOLESCU – *Creșterea eficienței irigațiilor prin echiparea cu microhidroagregat (Increasing irrigation efficiency by equipping with micro hydropower units)*, Bulletin AGIR III 2000

xxx – *Gasification and pyrolysis* Technology Environment Economy 2002

xxx – *Waste products* Technology Environment Economy 2002

EXPERIMENTAL VERIFICATION IN STATIC REGIME OF PNEUMATIC ACTUATORS OF MEDIUM AND HIGH PRESSURE

Eng. Nita Ionel, PhD Eng. Matache Gabriela , Eng. Marinescu Alexandru,
PhD. Student Eng. Pantiru Adrian, Eng. Popescu Alina

1. INTRODUCTION

In order to achieve operational functions for which it was created any pneumatic technological equipment must contain in its structure three distinct functional blocks: the source of energy, transmission devices of this energy and devices to transform this energy into mechanical work. Functional link between these blocks is done to control devices.

System of components that compete in a pneumatic technologic equipment to achieve operational functions is called *drive system*. In Figure 1. its block diagram is shown.

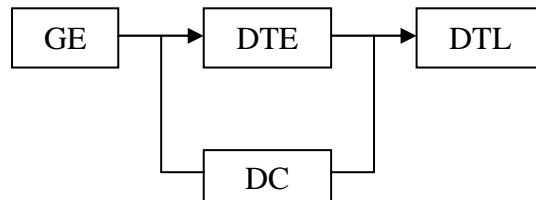


Fig. 1. Block diagram of a pneumatic drive system:

GE- energy generator; DTE - energy conversion device; DTL - work energy conversion device; DC- command transfer device

- a. Depending on how it is structured DC- command transfer device, the system can be:
 - Classic Drive System (DC uses standard pneumatic elements of control-command)
 - Servo-analog or digital System (DC uses proportional pneumatic elements of control-order). Pneumatic actuators enter in this category.
- b. Depending on how DC- command transfer device works, the system can operate:
 - In static regime (DC's transfer function, $\lambda = \text{ct.}$)
 - In dynamic regime (transfer function of DC, $\lambda = \text{variable}$)

Pneumatic servo systems and their constituent parts are working pneumatic equipment in automatic mode, they can be analyzed in two aspects:

- a) **Static** - when is modified a parameter in their function, others being either constant or negligible. In experimental pneumatic, use of perfect gases law is specific analysis of this type of operation.
- b) **Dynamic** - when is modified (at least) an external parameter in their function, being achieved control of the system in real time;

2. STRUCTURE OF PNEUMATIC SYSTEMS WITH ACTUATORS FOR MEDIUM AND HIGH PRESSURE

Pneumatic systems with actuators are systems of complex processes, which mainly, consist of the following parts:

- The execution part of pneumatic (linear or rotary motor);
- The control part that provide regulation and control of the output parameters of the mechanical system or servo systems;
- Monitoring system of translation or rotation (with the help of transducers and sensors);
- Electronic control system of movements (control unit).

a) For the execution part – represented by the pneumatic actuator itself

classical variant-specific to medium pressure (10-16 bars):

In this variant execution element can be a linear motor (pneumatic cylinder) or a rotary motor (swing motor), they are most commonly found in classical pneumatic applications.

Modernized version – specific to high pressure (16-40 bars):

This construction differs from the standard version:

- It has two work pneumatic chambers: one of low pressure (below 10 bars) and one of high pressure (which can generate up to 40 bars);
- Pneumatic controls are analog thereof;
- The amplification process can multiply the pressure (force, moment), or flow (linear or rotational speed) to power on;
- Floor amplification can be achieved in many variants (Piston or membrane amplification).

b) For controls elements (regulation and control) or servo control (ERC)

Pneumatic components designed to work at low or high pressure or are: standard or proportional distributor, check valves, chokes, standard or proportional pressure control valves.

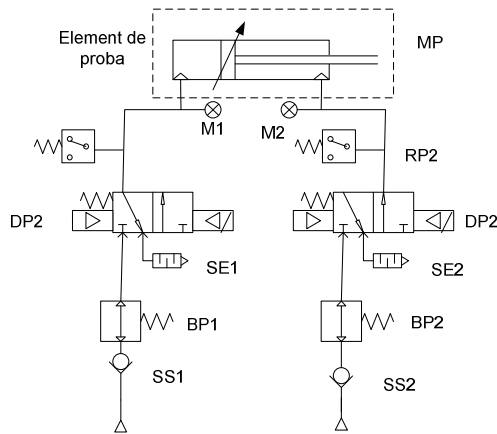


Fig. 2 - Representative simplified scheme of a pneumatic drive system with linear actuator, for high pressure (without amplification floor)

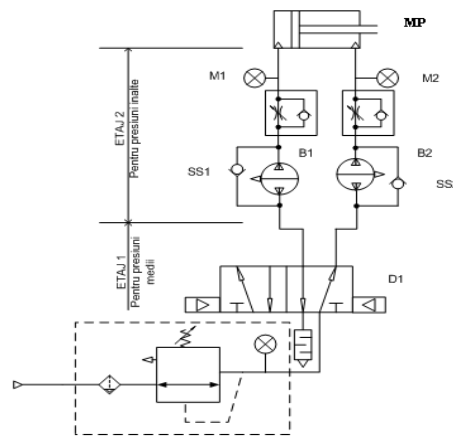


Fig.3 Representative scheme of a pneumatic drive system with linear actuator for high pressure (with amplifier block)

The structure of this scheme is the following: the actuator itself, M1 and M2 - input-output gauge test equipment, DC1 and DC2 - chokes track, B1 and B2 - 4:1 pressure amplifiers, DP-pneumatic proportional distributor, D - mass flow meter; GPA - air training Group, SS1 and SS2, check valve.

The scheme works on the 1st floor (medium pressure) with pressure network, and on the 2nd floor (high pressure) with air pressure maximum amplified 4:1 (up to 40 bars);

- Components of 1st floor are standard building; Components of the 2nd floor are special and lasts up to 40 bars.

- The compressor is standard construction. The structure of this scheme is as follows: MP-actuator itself, M1 and M2 - input-output gauge test equipment, RP1 and RP2 - pressure relays, DP1 and DP2- pneumatic distributor 3/2 with pneumatic command, SE1 and SE2 - quick exhaust valves, SP1 and SP2, pressure regulators, SS1 and SS2 - check valves;

- All the components are of special construction and can last up to 50 bars;
- Do not use high pressure servo components;
- Servo components order distributors of 50 bars (low pressure or medium)
- The compressor must generate high pressure (special design)
- The scheme works with a single-stage pressure (high);
- Orders are working at low pressure.

3. EXPERIMENTAL ANALYSIS OF PNEUMATIC SYSTEMS

3.1 Types of systems operated actuators (open circuit, closed circuit)

a) Process block diagram of control system of position / force and its structural scheme

It can work in two ways:

- Dynamic, closed circuit, as represented;
- Static, in open or closed-circuit without PID controller.

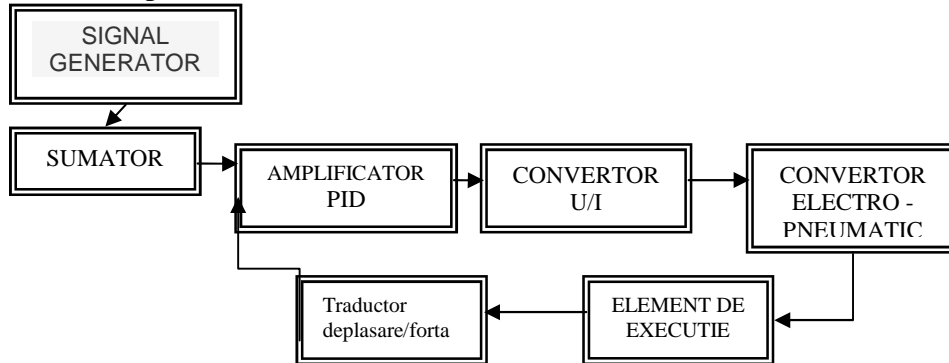


Fig. 4 Simplified process diagram

b) Verification pneumatic scheme for static behavior of a pneumatic servo echipament with actuators (test stand)

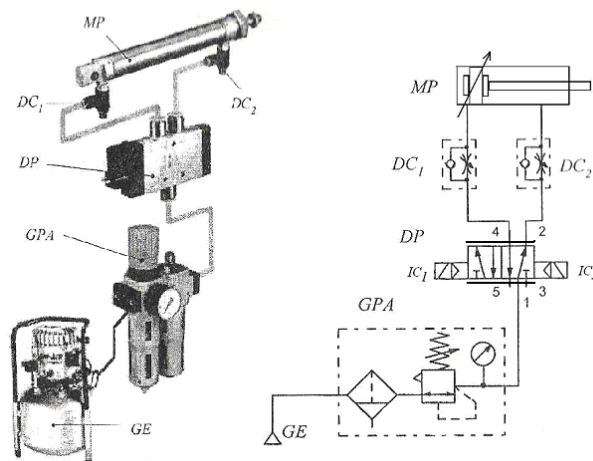


Fig. 5 Tests stand

The structure of this scheme is as follows: MP-actuator itself, M1 and M2 - input-output gauge test equipment, RP1 and RP2 - pressure relays, DP1 and DP2- pneumatic distributors 3/2 with pneumatic command, SE1 and SE2 - quick exhaust valves, SP1 and SP2, pressure regulators, SS1 and SS2 - check valves.

3.2. Determinations in static regime

At this stage, check the functionality of a pneumatic servo can cause:

The characteristics of the servo control

- $I = f(v)$

In this case the flow rate Q is adjusted at nominal sampling flow value, at pressures of the work environment and with mass flow Q_m (to eliminate the influence of temperature on the physical state of the work agent). At higher air pressures can work with volumetric flow rate Q_v . Record the kinematic parameters (displacement and actuator velocity v) for each value of the control signal applied (between $0 \dots I_{max}$).

- $I = f(F)$

In this case the pressure is adjusted to the maximum value for testing $p = p_{\max}$. Record the force F for each control signal applied (between 0 ... I_{\max}). Adjustment feature, ideally, should be a linear curve with an increasing trend from 0 to the maximum value. In reality, this feature is a deviation of hysteresis depending on the evolution piston. Hysteresis is more pronounced when the servo is working on medium and low pressure than at high pressure (typically shrinks after $p > 30$ bars).

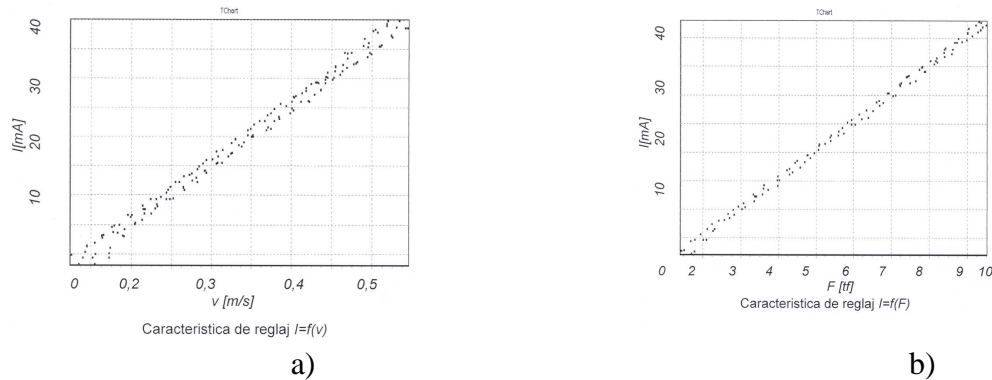


Fig.6 Adjustment feature

To establish control characteristics is varying the control current in the range 0 ... I_{\max} variation with a variation frequency of 0.025 Hz, drawing the characteristics of v or F (depending on adjustment feature). Through testing programme, a data acquisition system can be automatically drawn and recorded these features.

4. CONCLUSIONS

The main conclusions obtained from experimenting with pneumatic actuators systems are the following:

- It is found that at the pressure below 16 bars (low pressure and medium), servo actuators functioning depends on the variation of the load F and of the work temperature T , the work agent being compressible;
- It is found that at pressures above 16 bars (30 bars - high pressure), the operation of servo actuators depends only on the load variation F , and the influence of the operating temperature T , being negligible, and the work agent being practically incompressible.
- It is found that the parameters that influence the dynamics of the actuator are: Size and geometry of drive system; Type of seals and the mobile assembly, which can grow very large forces; Servo valve sizing; Length of the supply system with pressure (of pipes and connection elements); The value that has to be developed by the actuator (force, precision positioning and velocity); Pressures supply field (medium or high); Mentioned parameters have a non - linear influence that may affect system performances.

b) References

1. Avram M.: "Actionari hidraulice si pneumatice-Echipamente si sisteme clasice si mecatronice", Publishing House: Universitara – Bucharest, 2005;
2. G. Belforte, Bertetto, Mazza: "Pneumatico-curso completo", Publishing House: Tecniche nuove, Milano, 2004;
5. Pneumatische Division Kaeser Universitat: "High pressure And Free-oi Pneumatische Technologies", Verlag gmbH .Munich , 2005

MODERN METHODS OF PERFORMANCE OPTIMIZING FOR CONVECTIVE DRYERS WITH BIOMASS

Eng. Pantiriu A., Ph.D.Eng. Matache G., Eng. Anghel S.
INOE 2000 – IHP Bucharest

Tel: 021 336 39 91.; E-mail: fluidas@fluidas.ro

Abstract: *The paper aims to develop an overview of existing models of dryers at the moment.*

Is presented the options for use of the local energy sources, biomass. Currently for the full use of the energy produced by burning wood gas-producing biomass are used several types of cogeneration equipment. The difference between them is the working pressure and the price

Keywords: *convective dryers, biomass, vegetable product*

1. CURRENT STATUS IN MINI AND MICRO DRYING INSTALLATION FOR VEGETABLE PRODUCT

Drying fruits and vegetables is the process which removes a certain amount of water, after which the state actually provides a physical-chemical proper maintenance of their nutritional value and other terms of quality (taste, odor, flavor), leading to their consumer acceptance.

The development in the food drying area has led especially by improving technology, equipment, automated management of the drying process, etc.

In the past ten years, the dehydration of fruits and vegetables has been affected by the energy crisis which has led to the increasing of price and decreasing of the supply, the emergence of new energy consumers, regulations becoming more restrictive on pollution and development level of scientific and technical knowledge. The main global concern in dehydrated vegetables and fruits in the last ten years have focused on the drying process and ways to control it. Developing techniques for computer-aided two and three-dimensional design (CAD) allowed improving the design and manufacture of drying equipment. Development of knowledge about the degree of drying processes, resulting in models and simulation programs have enabled the development of evolved algorithms for conducting automated processes. Such optimal management programs have been developed increasingly more complex with data acquisition possibilities and the state estimation process in real time. This led to the improvement and modernization of process control for drying equipment. Measuring equipment mounted on the dryers measures in real time the main quantities (temperature, pressure, flow, speed of drying agent, humidity, energy consumption, etc.) which defines the process which are extracted by a process computer that, with a specialized management program estimates the state parameters of the process and draws the necessary management control process sizes. Dryers products now have advanced automatic control systems which twenty years ago were only in laboratories and were at prohibitive price ten years ago. The most significant effects of the automatic management of the drying process which translates into reducing the specific costs of production are:

- reducing the number of processors and associated costs;
- reducing specific energy consumption;
- changes in fans speed control and other elements for optimal management of the drying process

A second direction in which is has acted in the last 20 years in the fruit and vegetables dehydration is the use of unconventional energy sources. Drying facilities were made which use solar energy, geothermal heat water, biogas installations, combustible waste incineration, biomass gasification chemothermal, etc... Compared to the world in the field, in our country, due to the structural changes in agriculture and industry on one hand and and on the other hand, the low fitting with measuring equipment and automatic driving, the technological obsolescence, the domain of drying fruit and vegetables remained at the level of 1980. reviving tis sector is necessary and possible due to Romania's agricultural potential amd rising demand in international trade with dry products.

Simultaneously we can also use local energy sources. Therefore were designed and produced convective dryers with power and production capacity according to the market demands. In Figure 1 we have shown electrically powered dryers. In Figure 2 we have presented biomass supplied driers.



Fig. 1 Electrically powered dryers

a- Harvest Saver, b- R-12, c- domestic dyer Ezidri FD 1000



Fig. 2 Biomass supplied driers/ *Deshidratoare alimentate cu biomasa*

a- FD-50 dryer powered by a crossdraft generator
b- FD-200 dryer powered by a chopped biomass burner

In convective drying process with biomass also need a eberg source to power the electric fan, the transducers, control panel, which limits the use areas of the drying facility tio a power source. Thus appeared the idea of creating an energy independent dryer as well as mobile, a instalation which is easy to transport in mountain areas and not in need of an outlet. In materialization of this idea was created several types of dryers, some using solar panels to obtain the required electrical energy.

Currently for the nearly integral use of energy produced by the complete burning of wood biomass thee can be use several types of cogeneration facilities, depending on the thermal energy produced and the electricity needed, we can choose linear motors or steam turbines. The difference between the two, the linear motors and the steam turbines, is given by the work

pressure and the installation cost. Turbines require a high pressure steam in the facility, requiring a greater investment in isolation, being more expensive, but the energy produced is greater than that produced by a steam engine.

In figure 3 is presented the block diagram of convective dryers which is under study to achieve energy independence.

2. ENERGY INDEPENDENT DRYER WITH ELECTRICALLY DRIVEN FAN.

To achieve energy independence, we used a steam heating system with low pressure steam, lower than 6bar, that consists of a steam boiler that burns cross draft gazgen produced by a generator. Steam is the heat that enters a steam-powered electric generators.

Currently they have made and sold electric generating free piston steam engines, which are relatively simple but requires a constructive power conversion unit. The generator consists of a linear motor in which there is a free piston on to which are mounted permanent magnets, and it varies within a wrapped stator there by generating electricity.

The advantage of using this method would be that after this c besides the dryer independence energy we have the advantage of having two outlets, a 240 V AC and a DC 24 V, which can be used during and after the operation of the installation.

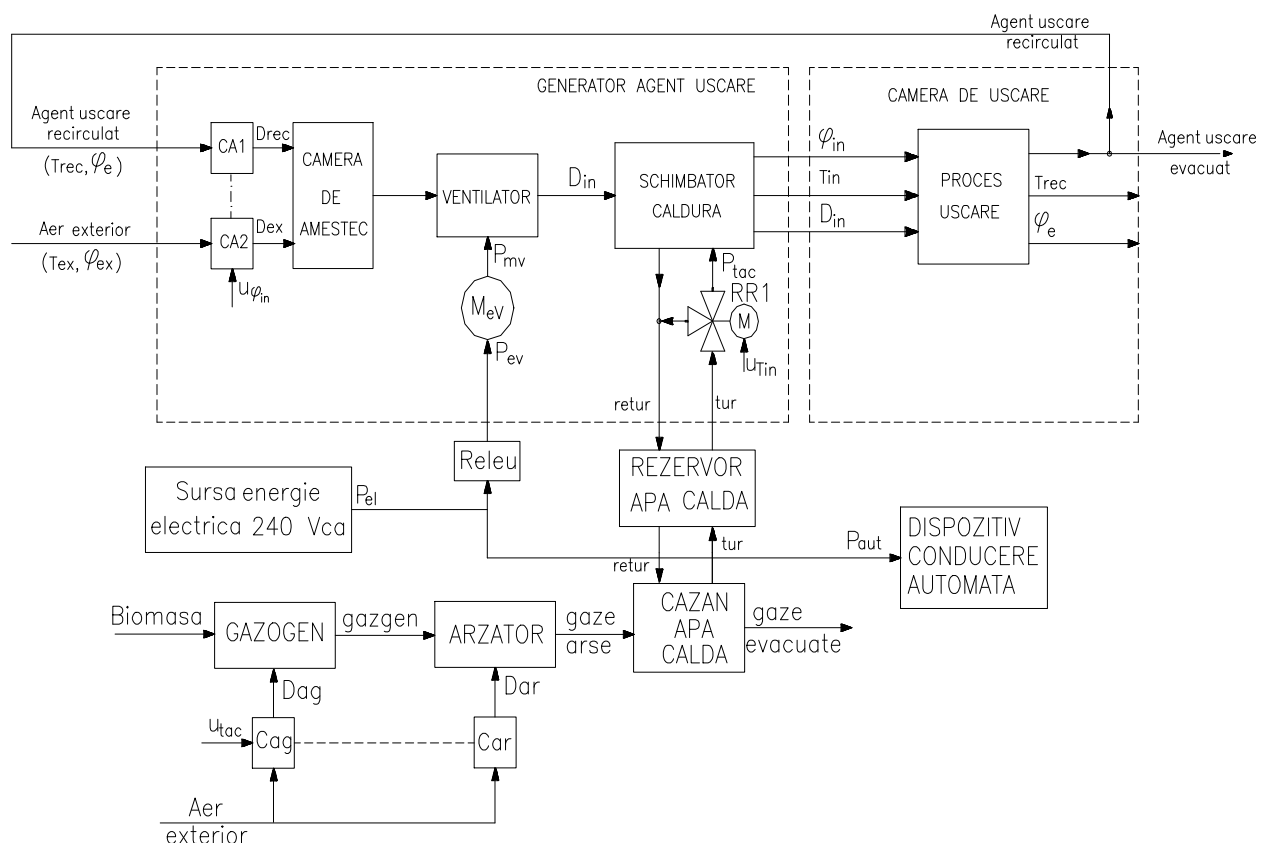


Fig.3. Block diagram of convective dryers with generator and heat exchanger hot-water/air

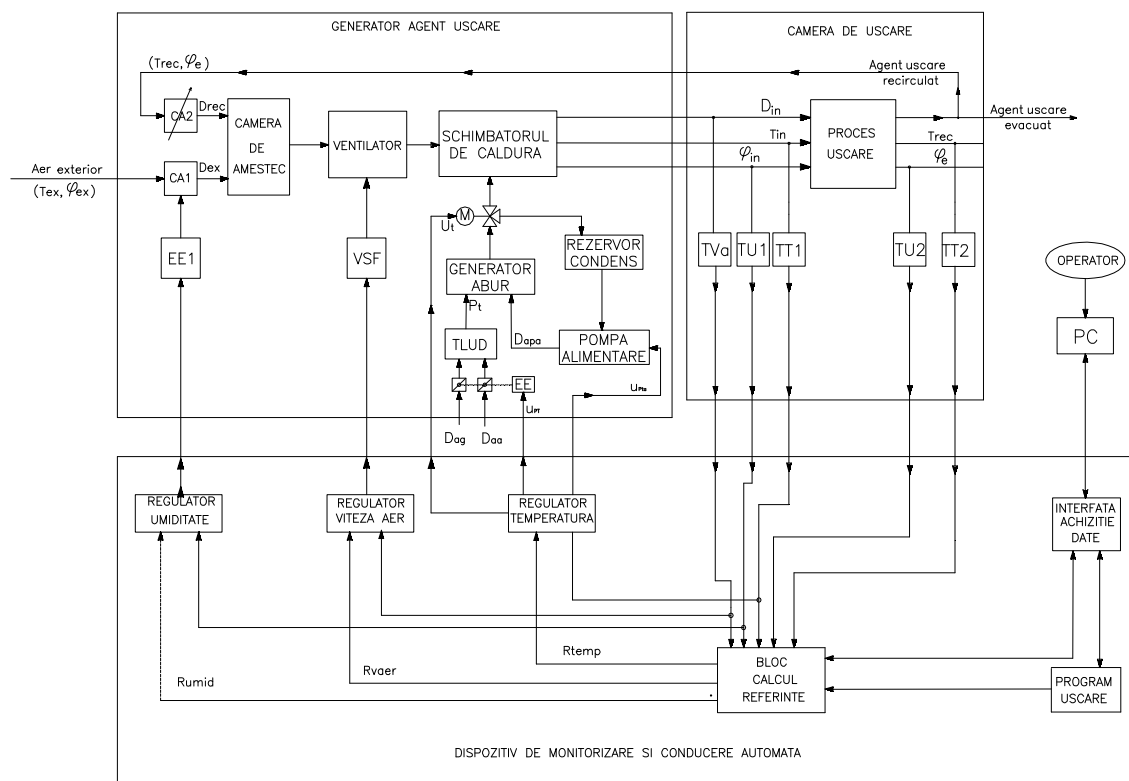


Fig. 4. Block diagram of the drying installation with cogeneration equipment

3. INTRODUCING THE DRYING FACILITY AND THE OPERATING MODE.

In Fig. 5. we have the functional scheme of the drying facility with cogeneration equipment.

The installation is composed of several parts: drying chamber, air drying generation unit, cogeneration facility, steam generation unit.

Drying chamber (6) is composed of rack on to which the drying cassettes (5) are positioned, cassettes which are distributed to a distance of 25 mm from one another to ensure a high uniformity of final moisture of the dried product.

Drying agent generating facility consists of fan (1) heat exchanger (2) recirculated air agent flap control (3). The air is pushed by the fan to the heat exchanger, where it reaches the drying chamber, where it takes of a part of the dried products moisture, then moves towards the discharge outlet (4), which stands outside. To adjust the humidity of the drying agent before entering the drying chamber, outside air is mixed with one part of the recirculated air, whose moisture is higher. Drying agent mixture is carried out by the outdoor air fan and recirculated agent, which enters the fan's chamber through the recirculation flap (4).

Steam generation plant consists of a biomass burner TLUD (12) Flach type steam generator (11), water boiler (17).

TLUD biomass burner is supplied with pressurized air, air that is preheated inside chamber (18) and routed through the pipe (15) to the burner, powered by an axial fan driven by an electric motor, usually continuous current. Biomass is introduced into the reactor and rests on a grill through which passes, from the bottom up, primary air for maintenance of the flame front for pyrolysis and partial gasification of coal produced in the pyrolysis process. Pyrolysis process takes place in front consuming biomass pyrolysis reactor. The resulting

pyrolysis tar passing through partly gasified coal layer, which is partly due to the heat radiated by the pyrolysis front and the higher flame.

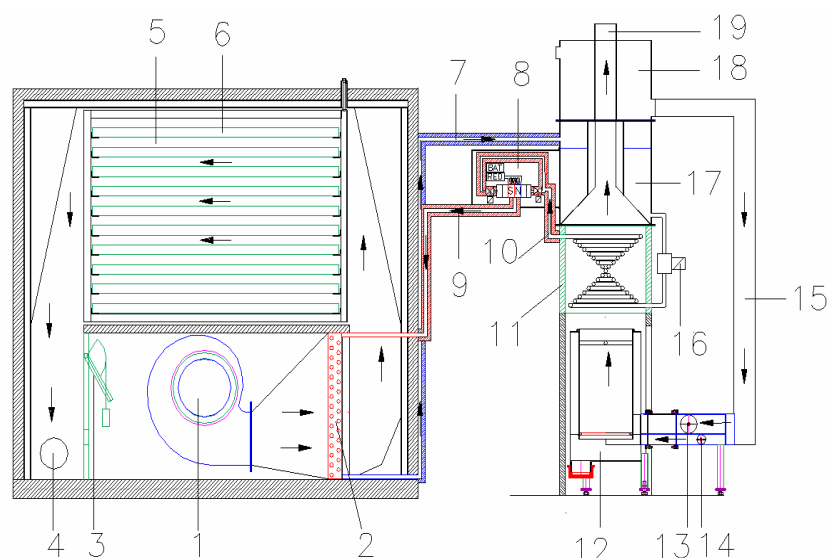


Fig. 5. *Convectiv dryer scheme with cogeneration equipment/ Schema uscatorului convectiv cu echipament de cogenerare*

Resulting gases are mixed with the secondary combustion air which is introduced through holes arranged at the top of the reactor and burn with a high flame at the mouth of the reactor, which also serves as the burner. Primary and secondary air flows are controlled with two valves, valve (13) and secondary air valve (14) for combustion air. This adjustment can be done mechanically, or by varying the fan speed to change in thermal power produced by the system. This type of procedure do not totally consumes the carbon in biomass, the end result cast ash and about 20% uncapped coal.

Flach type steam generator (11) is positioned above the burner, consisting of a well insulated body and two wound as guide pyramid for better heat emitted by the burner. You can also use a spiral, depending on thermal power necessary, for a whirl and we have 3 kW thermal power and for 2 we have 6 kW thermal heat. In steam generator gets 4g of water using a pump (16) from the water tank. As for the generator air, and water is preheated, the tank being placed on the side of the exhaust chimney (19) of the combustion fumes from the TLUD burner. It requires less energy to vaporize water at 25 ° C than at 13 ° C water.

Cogeneration plant represents the linear generator which is linked, in terms of power to a rectifier and is connected to a battery, the battery that powers the fans of the generator and the dryer, transducers and cogeneration equipment

4. CONCLUSIONS

Following kilowatt price rising more and more developers are moving towards buying dryers supplied with heat through burning biomass, but this does not solve the problem of electric power supply, needed in the drying process surveillance and controlling. Equipping the dryer with a cogeneration facility, it allows a high mobility factor, it can be transported to the place of harvest of the dry material and a lower production cost.

5. Bibliography

1. Drumea P., Murad E., Anghel S., Bratu M., *Motor-pump for irrigation, supplied on gas produced by the gasification of vegetal waste*, Conferința Internațională MEDIU – ENERGIE CIEM 2003, UPB , Bucuresti , nov. **2003**
2. Murad E., Prisăcaru T., Lica C., *Instalație de producere a energiei termice și electrice prin gazeificarea termică a biomasei - Structura și parametrii principali*. Raport cercetare, Etapa I-a 2004, Contract Mener 252/**2004** - Instalație de producere a energiei termice și electrice prin gazeificarea termică a biomasei, București, decembrie **2004**.
3. Quirijns. E.J., L.G. van Willigengurg, A.J.B. van Boxtel, *New perspectives for optimal control of drying processes*, *Adchem200*: International symposium on Advanced Control of Chemical Processes, Pisa, Italy, **2000**

TESTING OF DYNAMIC RESPONSE OF PROPORTIONAL ELECTROHYDRAULIC VALVES USING FFT SPECTRUM ANALYZER TECHNOLOGY

R. I. Rădoi¹⁾, I. C. Duțu¹⁾

¹⁾ Servotechnics and Electronics Department, Hydraulics & Pneumatics Research Institute (INOE 2000 - IHP), Bucharest, Romania

ABSTRACT

The paper presents the possibilities of using an FFT spectrum analyzer to determine the dynamic response of proportional electro-hydraulic valves. Measurement method is simple and fast because it does not require a data acquisition system and complex data processing software. The laboratory tests were conducted using a proportional directional valve with integrated electronics which can be operated with unified voltage signals, having an output signal which is proportional with the input command signal. Thus it is simple to connect with the analyzer which was configured to determine dynamic characteristics of amplitude and phase depending on the frequency, using a logarithmic scale. The results are comparable to those given in the manufacturer's datasheet of electro-hydraulic proportional directional valve. For equipments without embedded electronics can be used a device equipped with a dynamic cylinder for measurement of proportional valve flow using an electronic module and a LVDT. The resulted signal is send to the FFT analyzer.

Keywords: Dynamic, Proportional, Electro-hydraulic, FFT analysis, Transfer function.

1. INTRODUCTION

Dynamic testing of hydraulic proportional equipments is generally done on specialized stands equipped with data acquisition systems and complex software that must be configured separately for each equipment.

The paper presents experiments performed to determine the dynamic characteristics of electro-hydraulic proportional equipment using a FFT spectrum analyzer. Hydraulic equipment used was a size 10 proportional directional valve (type 4WREE) produced by Bosch Rexroth (Fig. 1). The spectrum analyzer is a SR 780 type produced by Stanford Research Systems. The analyzer's input signal is digitized at a high sampling rate. The Nyquist theorem says that as long the sampling rate is greater than twice the highest component of the signal, and then the sampled data will accurately represent the input signal in frequency domain. In the SR780, sampling occurs at 262 kHz. To make sure that the Nyquist theorem is satisfied the input signal passes through an analog anti-aliasing filter that removes all frequency components above 102.4 kHz. The resulting digital time record is then mathematically transformed into a frequency spectrum using an algorithm known as the Fast Fourier Transform (FFT). The resulting spectrum shows the frequency components of the input signal [1].

2. FEATURES OF TESTED PRODUCT

The tested product was a direct operated proportional directional control valve type 4WREE produced by Bosch Rexroth [2].

Features of 4WREE proportional valve:

- Nominal size: 10
- Maximum working pressure: 315 bar
- Maximum flow: 50 l/min
- Spring centered spool
- Electric feedback
- On board electronics
- Supply voltage: 24 Vcc
- A1 Interface (± 10 V)
- Coil resistance: $2 \div 3 \Omega$
- Power consumption: 1,8 A (3A peak)

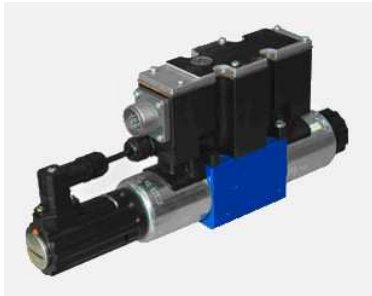
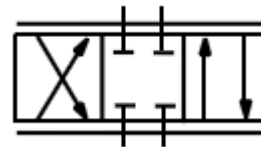


Fig.1 Proportional directional valve type 4WREE
produced by Bosch Rexroth

Spool symbol



3. CONFIGURATION OF THE TEST BENCH

Test bench is composed by hydraulic pumping unit, test device (figure 3) on which is mounted the proportional directional valve, network signal analyzer (figure 4) and a 24 V DC power source for to supply electronic amplifier of directional valve. Test device is formed by a hydraulic block which has inside a cylindrical chamber that together with a piston of low mass and friction form a dynamic response cylinder.

In figure 3 can be seen the scheme of test bench, used for experimentation in order to obtain frequency response of the proportional directional valve.

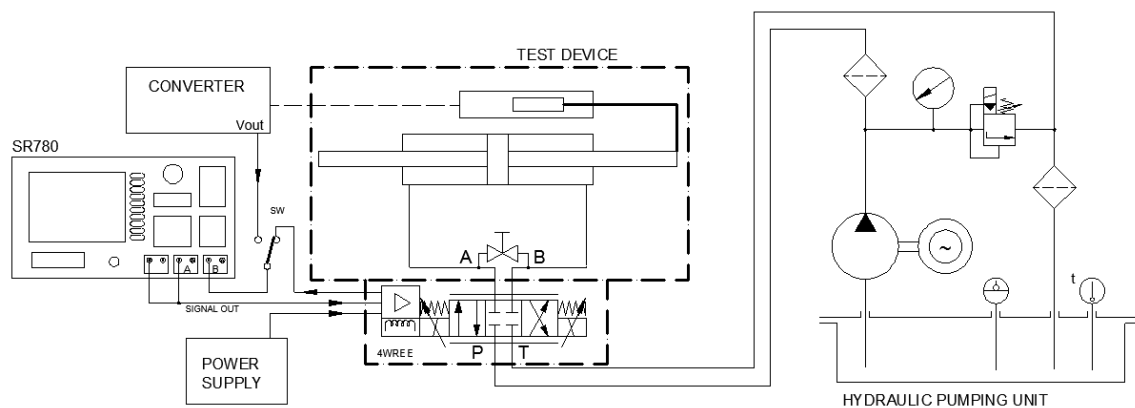


Figure 2 Configuration of the test bench

On piston rod is placed an LVDT transducer for measuring flow of proportional directional valve without embedded electronics. Signal proportional to flow rate that is captured by the LVDT is converted into a voltage signal to be inserted into the analyzer.

If case of directional proportional valve with OBE output signal is taken from the "actual value" pinout which is the signal from stroke transducer of the valve spool.

In this case no need to measure the flow with hydraulic cylinder and opens the tap from scheme, achieving a bypass between ports A and B of proportional directional valve.

Through testing device are connected the ports of the proportional valve to the tank and pressure ports of test bench and hydraulic cylinder chambers have provided special ports to connect the bypass tap.

In the scheme can be seen a switch used to direct taking the signal from the proportional valve or through flow-voltage converter from the test device.

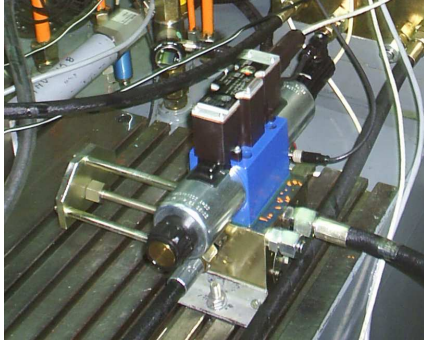


Figure 3 Proportional directional valve used during tests and dynamic cylinder for non OBE equipments

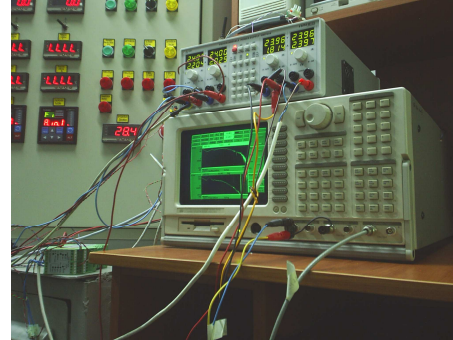


Figure 4 Cables connected to the analyzer during testing with FFT Signal Analyzer type SR780

To obtain charts, the signal generated by the internal source of the analyzer is applied to a voltage controlled input of the proportional directional valve and also to one input channel of the analyzer. Response signal from the position transducer of the valve's spool (actual value output signal) was applied to the other input channel of the analyzer.

The chart frequency - attenuation is given by:

$$A \text{ (dB)} = 20 \lg \frac{Ch2}{Ch1}$$

It is calculated as the ratio of the amplitude of the output signal from the equipment under test measured by channel 2 and the amplitude of the reference signal which is introduced into the equipment and measured by the channel 1 and is expressed in decibels.

The chart frequency - phase shift is given by:

$$\phi[^\circ] = \frac{\Delta t}{T} \times 360^\circ$$

where:

Δt - time difference between the intersection with time axis of control signal and intersection with the time axis of response signal on a half-period.

T - source signal period.

Set up of the analyzer to obtain dynamic response characteristics is achieved through a series of steps as follows:

- Reset the unit to default settings
- Set the source to chirp output
- Set the FFT frequency span to 200 Hz
- Set the amplitude of the chirp
- Set the percentage of the chirp to 100 % for continuous output
- Set ch1 and ch2 to auto range
- Set the active display A for transfer function measurement, set the units to dB and auto scale
- Set display option for display A to log x axis
- Set the active display B for phase response and set auto scale

- Set display option for display B to log x axis
In Figure 5 are presented the plots captured from analyzer screen

Magnitude chart [dB] ⇒

Phase shift chart [deg] ⇒

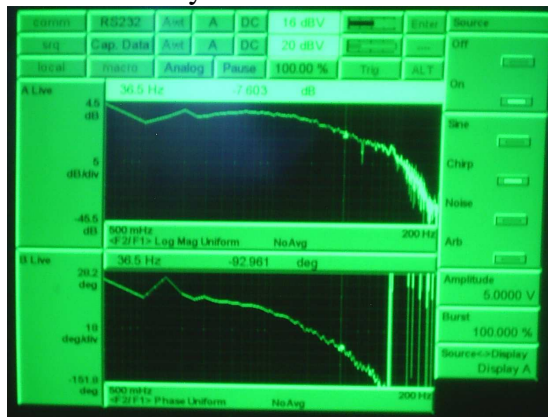


Figure 5 Response to a sinusoidal input signal up to 200 Hz, amplitude of 5 V

The charts frequency-attenuation and phase shift-frequency (Bode plots) of proportional directional valve transposed from analyzer screen looks like in figure 6.

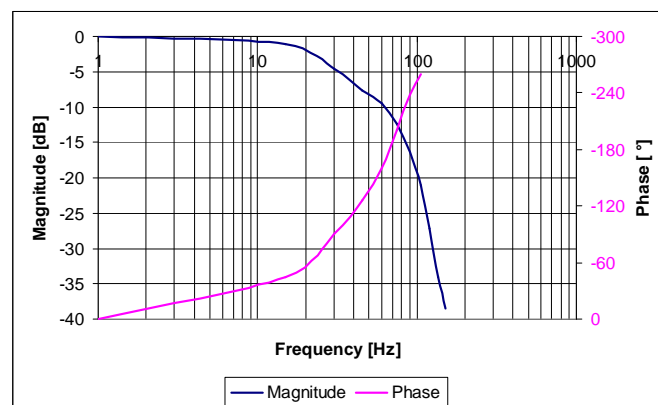


Fig. 6 Charts attenuation – frequency and phase shift – frequency

4. CONCLUSIONS

With test bench and a test device can be determined very simply the dynamic performances of proportional directional valve. Test bench can be used for equipments without on board electronics and stroke transducer of the spool and for those with integrated electronics and electrical reaction.

References

- [1] <http://www.thinksrs.com/downloads/PDFs/ApplicationNotes/AboutFFTs.pdf>;
- [2] http://www.boschrexroth.com/country_units/america/united_states/sub_websites/brus_brh_i/en/products_ss/08_proportional_servo_valves/a_downloads/re29061_2005-10.pdf;
- [3] Blejan M., Ilie I., Comes M., Lupu B., *Signal conditioner for LVDT displacement sensors*, – Proceedings of International Conference “Advanced Topics in Optoelectronics, Microelectronics and Nanotechnologies” ATOM-N 2008, 28 – 31 august, Constanta, Romania.

A NEW TECHNOLOGY TO OBTAIN BRIQUETTES FROM MAIZE STALKS

Eng. Anghel SAVA¹, Ph.D.Eng. Catalin DUMITRESCU¹, Ph.D.Eng. Gh. SOVAIALA¹,
Ph.D.Eng. Iulian Dutu, Ph.D.Eng. Gabriela MATACHE

¹ – HYDRAULICS & PNEUMATICS RESEARCH INSTITUTE INOE 2000-IHP Bucharest, Romania

Abstract: *One of the modalities of finding new ecological energetic resources is the use of vegetal waste as fuel. From the agricultural activities result various secondary products like: straw, maize stalks, sunflower stalks, grape cords. These vegetal waste is usually burnt in the fields in order to clear space for allowing performing the further agricultural activities.*

This paper presents some results obtained after briquetting the maize stalks at various degrees of humidity, for using it as fuel. The means utilised were hydraulic power manual presses provided with force and displacement transducers for determining the optimum kind of pressing

The final tests were performed by means of a hydraulic press used for obtaining sawdust. Were found the new drive patterns depending on humidity and the changes required to be done for using it at pressing the maize stalks.

1. INTRODUCTION

One of the main concerns of the Romanian research nowadays is to find a solution for using efficiently in economy the vegetal wastes, which are commonly burnt or spread on the land.

A lot of land cultivated with maize remain uncleared of the corn stalks every year, being necessary extra consumption of energy for fulfilling this action and preparing land for a new agricultural cycle.

The making of maize briquettes to be used as fuel may become of interest if it is proven its economic efficiency. Taking into account the fact that by burning these vegetal wastes are saved huge wooden surfaces it may be taken into consideration the granting of subsidies for supporting this activity. It is more profitable to use as fuel vegetal wastes for impeding the huge deforestations, than to invest more money in replanting woods.

The paper presents the experimental tests performed in order to get maize briquettes by using pressing machines projected and made initially for sawdust. It was aimed to reach the pressing parameters depending on the various degrees of humidity of the maize stalks. The presses are provided with force and displacement transducers for determining the optimum pressing modality.

The hydraulic press, see fig.1 is composed of an actuator including a servo valve and a displacement transducer which is fixed on the downside part of a layer. The layer, two guys and an upper support form a close framework. In this framework supported by the rod of the actuator it is introduced a cylinder provided with a piston. On the rod of the actuator is mounted a force transducer.

The check up method at pressing

The cylinder is filled with chipped stalks, it is introduced the piston with the force transducer and the assembly is set on the rod of the actuator. The actuator is set into action until when the transducer is propped by the upper support. It is continued the action, performing the pressing. Are measured the pressing force, displacement and it is found the displacement speed depending on time. It is made the diagram of force depending on displacement and pressing speed depending on displacement.

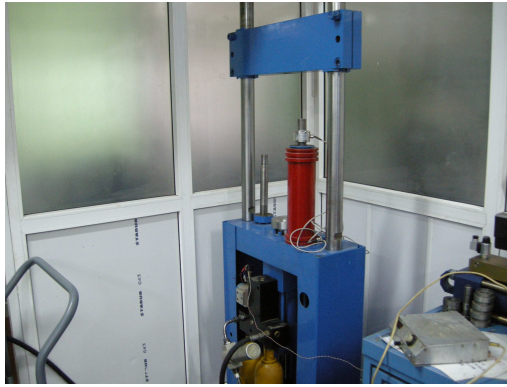


Fig.1 Hydraulic press for determining the pressing drive of the briquettes



Fig.2 Briquette in the pressing cylinder it is shown how the material is felting

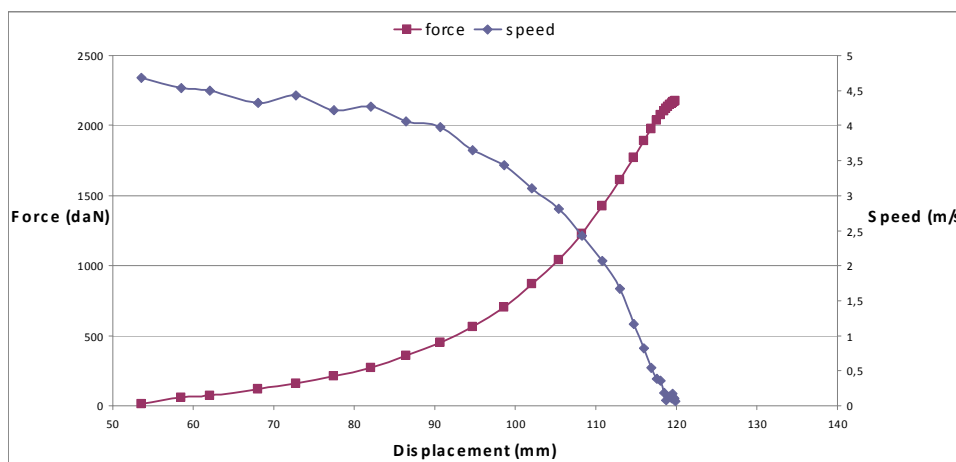


Fig.3 Diagram showing the pressing of the briquettes which is represented by the pressing force and the piston speed

In the diagram from fig.3 it is shown the graphic of the pressing force which depends on the piston displacement. The force from the axis y gets higher when the displacement from the axis x reaches that (this presenting the briquette pressing). It is also presented the graphic of the piston speed depending on the pressing degree (displacement).

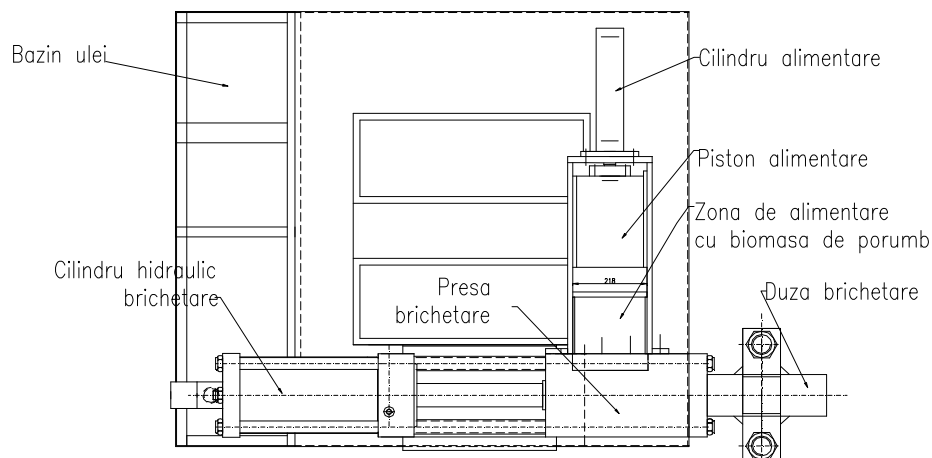


Fig.4 Graphic representation of the press for obtaining maize stalks briquettes

The press for briquetting see fig.4 is composed of a hydraulic cylinder for briquetting driven by a hydraulic installation which presses the material through a **choke**. The material is introduced in the press by a cylinder by means of a charging piston which takes over the maize bio mass from the charging zone and pushes it in the briquetting press. The briquetting **choke** releases the briquette after it is performed the pressing stroke by the piston of the hydraulic cylinder.



Fig.5 Maize stalks briquettes obtained on the sawdust presses by changing the operational drive

Were performed tests on a hydraulic press (see fig. 4) used for sawdust briquettes. The new operational drives were found depending on the humidity and the changes required for working at pressing maize stalks.

The studies pursued to put into evidence the following aspects:

- To obtain briquettes with a good caloric power for being used in stoves for heating
- The briquettes should not lose their shape in time

Were used only maize stalks without any binders. The technology consists of the following steps:

- Collect maize stalks from the fields
- Dry the stalks until the leaves become fragile
- Chip stalks using a hammer chipper
- Press the raw stalks

The heating power of these briquettes is given below in comparison with the sawdust:

N o	Material	Determinations		
		Caloric Power [Mj/kg]	Ash [g/kg]	Humidity [%]
1	Sawdust pellets	17,993	15,24	6,78
2	Maize stalks briquettes	16,036	55,95	8,40

In what regards the energetic consumption must be taken into account the following aspects:

- the collecting of the stalks it is necessary no matter if these are used for producing briquettes or for other purposes – feeding animals, clearing fields

- the drying is made where are stored these stalks using sun heat
- the chipping requires energy supply. Were performed tests with various screens, being obtained various chipping degrees at different productivities. It was more used the chipper without screens or with 8 mm screen. At chipping without screens were obtained long maize stripes and a high productivity. At the 8 mm screen were obtained a lower productivity and a softly chipped product.

- Pressing was performed on a press used for sawdust briquettes

During pressing were found the following:

- a) Pressing of the chipped product with a 8 mm screen must be performed at high power for obtaining a compact product. The felting is lower. The loading compartment is easily filling, the power to be used is higher than for sawdust. The piston of the press gets stucked cause of the high friction.

- b) Pressing the product in stripes is made with a lower energetic consumption. It appears felting which leads to the acquirement of briquettes at lower pressing power. The filling of the loading compartment is made harder cause the maize stalks require bigger space. The material used is smaller. Cause of the felting the length of a briquette is given by the maize mass which enters in the loading compartment at one pressing.

CONCLUSIONS

It is possible to obtain briquettes from maize stalks using common presses used for sawdust, without being necessary any binders, by changing the pressing drive pressure by using an adequate technology of collecting storing drying chipping and pressing.

For being efficient it is recommended to use a technological line in flux.

Due to the big benefits given by the use of vegetal waste as fuel instead of wood it seems necessary to find financial support from governmental and European subsidies for producing vegetal waste briquettes.

References:

- [1] Prospects of companies.
- [2] Marin V.:Hydraulic systems Tehnica Publishing House 1981.
- [3] Oprean A., Marin V.: Hydrostatic systems of the tool machines and presses Tehnica Publishing House Bucharest 1965.
- [4] Drăghici I.: Guide for projection in machine constructions Tehnica Publishing house 1092.

DIGITAL HYDRAULICS REDUCES ENERGY CONSUMPTION IN FLUID POWER DRIVES

Petrin DRUMEA¹, Marius-Alexandru STOILĂ¹, Ștefan SIMIONESCU¹

¹INOE 2000– IHP Bucharest, e-mail:fluidas@fluidas.ro

ABSTRACT

This paper presents an older concept of hydraulics, recently rediscovered – *digital hydraulics* – as an alternative for traditional control with servo or proportional equipments. Important advantages of digital technology are robustness, repeatability, optimizing of energy consumption and fault tolerance.

The article analyzes the characteristics of various digital systems with components such as motors, 2 ways on/off valves and pumps, all digital type, these themselves having a number of key characteristics of efficiency and control and a number of benefits. There are discussed the functionality, controllability and losses, and the conclusion is that the digital technology provides an optimal energy management.

Key words: digital hydraulics, switching hydraulics, alternating flow.

1. BRIEF HISTORY OF DIGITAL HYDRAULICS

The idea to develop switching systems for developing a sort of hydraulic transformers is an old idea, as the hydraulic ram of Montgolfier from 1796 and Pollard's work on pulsating hydraulic power transmission (1964) show. The major motivation for the current attempts to realize hydraulic switching control is the success of switching control in modern electric drive technology [1].

The parallel connection principle is very old. An example is the London Hydraulic Power Company, which started the setup of water hydraulic power distribution network in 1883. The typical pumping station consisted of six steam engines and the output power was adjusted both by the speed of engines and the number of running engines. The control principle was simple: when the weight of the weight-loaded accumulator dropped low enough, the operator started the next engine. The system was the largest hydraulic system ever built and had 296 km of 5.5 MPa pressure line and 7.5 billion liters of annual output in the 1930s.

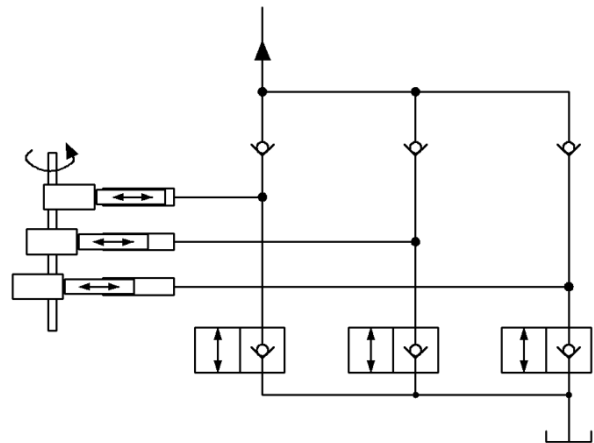


Fig. 1. Digital piston pump

An on/off switchable piston pump has been presented in the Aldric's patent in 1920. The pump can be enabled and disabled by the mechanism, which either allows the normal operation of the suction valves or keeps them open all the time. This is close to the digital pump shown in **Figure 1**, with the exception that pistons cannot be enabled or disabled independently [3].

1999 will be remembered as the year in which the researcher Matti Linjama from the University of Tampere, Finland presents for the first time his idea of digital hydraulics. Linjama's innovation led to a collaboration between universities and industry, which provides employment opportunities for students and graduates. As it often happens with innovations, Linjama's idea about the digital hydraulics didn't have an immediate success. This was taken into consideration a few years later, when his supervisor, professor Matti Vilenius was in search of new research topics. Today, the technology is used by companies in the area of mechanical engineering.

After consulting several Finnish companies working in the field of mechanical engineering since 1970, professor Vilenius immediately promoted the idea, convinced that it will have a big impact. However, he knew that after the fundamental theoretical research, they had to gain the trust of the scientific and business communities, which do not catch up new concepts without tangible demonstrations. "It was a long and difficult work. Luckily, I were able to unite our forces and gradually take the idea further. I had the necessary contacts and took a reserved position at the meetings when we started to talk publicly about the new technology", says Vilenius.

In 2009, the affiliated technology transfer company TUT Tamlink Ltd. signed a research contract with Bosch Rexroth AG for the development of the digital hydraulics. This German company is one of the world's leading experts in the field of industrial and mobile hydraulics. This is the result of the research for which Linjama and Vilenius worked [4].

Another notable technique discovery, dated 2001, was that made by the researcher Elton Bishop, who invented the Digital Hydraulic Transformer (DHT). Using a unique and simple linear reciprocating mechanism, the DHT is a paradigm shift from conventional rotary hydraulic transformer designs to convert hydraulic power from one flow and pressure to another flow and pressure. Simply said, the DHT allows cyclic use and re-use of hydraulic, potential and kinetic energies [2].

In October 2010, the third workshop on digital fluid power gathered 115 persons from seven countries, which is clear sign of growing interest on digital fluid power technology. As the technology is new, its characteristics, benefits, challenges, and scope are not widely recognized. This paper gives an overview of the technology [3].

2. INTRODUCTION

The term "*Digital Fluid Power*" is broad and not fully defined. A definition could be as follows: "*Digital Fluid Power means hydraulic and pneumatic systems having discrete valued components actively controlling the system output*" [3].

A system may be called digital if it was built using at least one digital component – pump, valve or motor.

The "classic" hydraulic system comprises three main groups: the pumping group consisting of fixed or variable flow hydraulic machinery; the distribution group and the group of working hydraulic motors, linear or rotary, also including fixed or adjustable rate machines. In operation, the hydraulic system produces an excess energy which can be used and converted into heat, which is necessary for removal of the cooling system. Dimensions of the components of the classical system are in most cases much greater than that of a digital hydraulic drive system.

In the case of a "digital" hydraulic drive system, the hydraulic power output is controlled by the components operating with discrete values, which are strictly related to the energy requirements of each technological operation.

The main advantages of digital hydraulics, compared to classical hydraulics, are listed:

- energy savings of up to 40-50%;
- reduction/elimination of required cooling energy;
- the use of simple on/off valves as components, instead of more complex servo or proportional valves;
- better performance because of faster valves, for generating very rapid movement to move heavy loads;
- easier control: better repeatability, low hysteresis;
- higher efficiency in the distribution of hydraulic energy – the same pump can serve several hydraulic work motors, with their necessary flow and pressure;

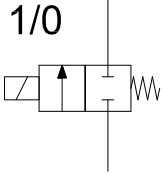
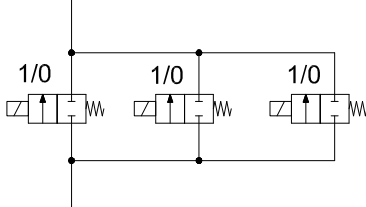
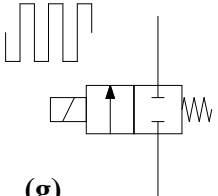
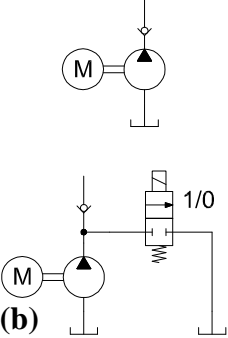
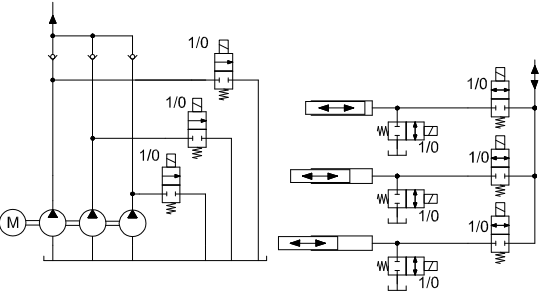
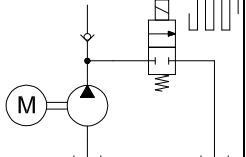
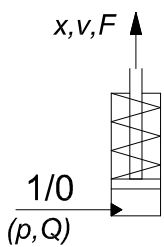
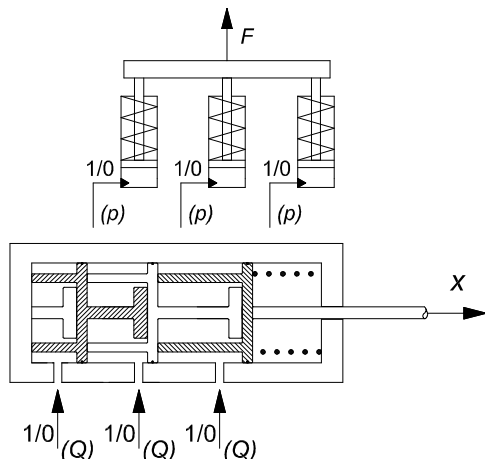
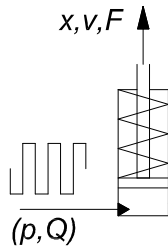
- possibility of recovery, storage and restoring to the process, at the necessary time, of potential and kinetic energy produced by the served process units;
 - superior control and flexibility of the distribution, which can dynamically allocate the required flow to the pump or motor, as needed during the technological phase;
 - significant reduction in the size of the hydraulic motors;
 - productivity growth for the served technological facilities;
 - higher degree of flexibility and programmability, through the system controller;
 - higher efficiency, low maintenance and operating costs;
 - less pollution, by reducing losses,
- so medium and long term benefits are considerable, especially for the industrial field.

Of course, systems based on digital hydraulics must also face some challenges:

- pressure and noise pulsations;
- durability and lifetime with switching technology;
- physical size and price for parallel-connection technology;
- complicated and unconventional control.[3]

3. CLASSIFICATION OF DIGITAL PRINCIPLES IN HYDRAULICS

Digital hydraulics can be divided into three major classes as shown in **Table 1**.

Compo- nents	On/Off Technologies	Digital Hydraulics	Switching Technologies
Valves	 <p>(a)</p>	 <p>(d)</p>	 <p>(g)</p>
Pumps	 <p>(b)</p>	 <p>(e)</p>	 <p>(h)</p>
Cylin- ders	 <p>(c)</p>	 <p>(f)</p>	 <p>(i)</p>

The simplest technology is the traditional on/off technology, in which the output of the system has only two discrete values, such as motor/pump turned on/off, cylinder driven or stopped, high or low pressure.

The hydraulic cylinder controlled at one or another end can also be included in this class. The second class refers to the use of parallel-connected components (**d,e,f**). The systems are truly digital because the output has only discrete values. Output level is defined as a sum of outputs of ON components.

The essential difference compared to switching techniques is that no switching is needed to maintain any of discrete output values. The third major class is switching technique (**g,h,i**), which mimics the principles of electric switching systems. The most popular variant is pulse width modulated (PWM) on/off valve.

4. DIGITAL HYDRAULIC PUMPS

In **Figure 2** there is presented the symbolization of adjustable hydraulic pumps and is highlighted the difference between continuous classic adjusting and adjusting with "discrete steps" achievable through digital hydraulics.

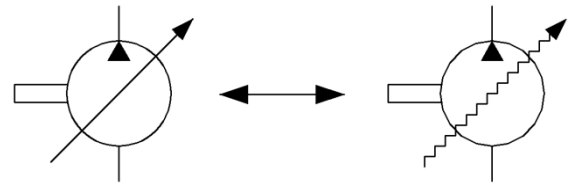


Fig. 2. Adjustable pump symbols

Another way to implement a digital pump is to control each piston of a piston pump independently by active on/off valves. An example of circuit is depicted in **Figure 3**. The version (**a**) is a pure pump and each piston can pump into the system or run in the idle mode. The average flow rate is controlled by the ratio of pumping and idling pistons. Partial pumping strokes are also possible. The version (**b**) is a pump-motor and each piston can run in pump, idle or motor mode. The motor mode requires continuous switching of the control valves.

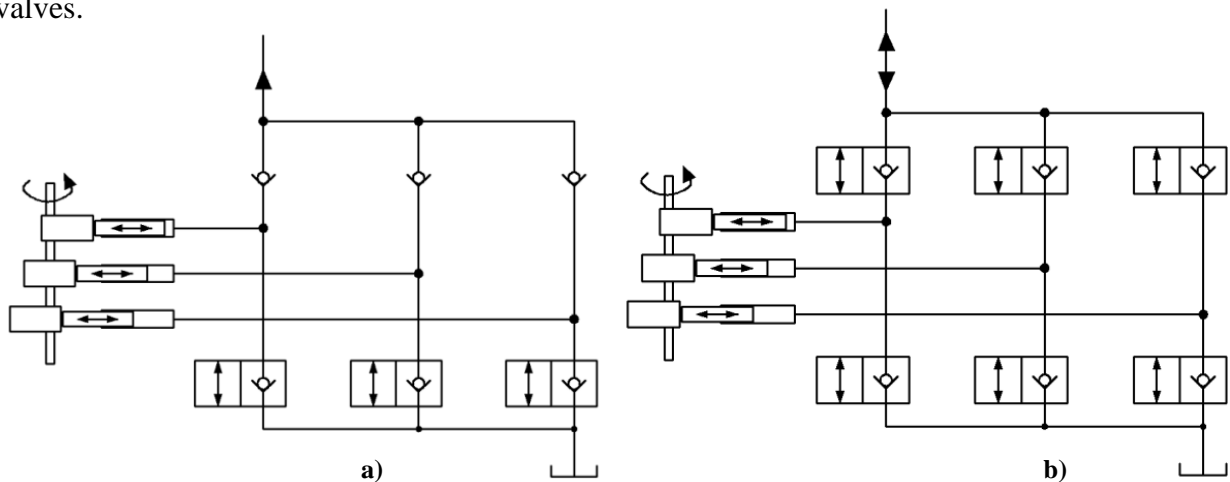


Fig. 3. Piston type digital pump (a) and pump-motor (b)

5. DIGITAL HYDRAULIC VALVES

Figure 4 shows how to implement the digital hydraulic four-way valve. The approach is the same as in analogue distributed valve systems. However, the implementation of fast, leak free and bi-directional valves is easier in the digital technique.

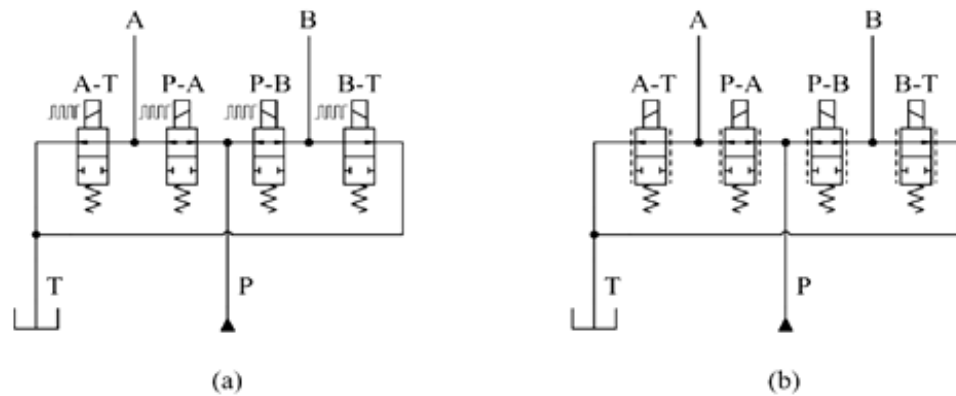


Fig. 4. Constructive solution with 4 on/off valves (a) and 4 DFCUs (b)

6. DIGITAL HYDRAULIC ACTUATORS

The hydraulic actuator is a device that converts pressure force into torque or force. **Figure 5** shows the implementation of digital motors, which are the inverse of digital pumps. Continuous switching version switches between maximum and minimum torque, while the version of connection in parallel has several independent motors on the same axle or shaft, and the amount of useful flow can be selected according to system requirements.

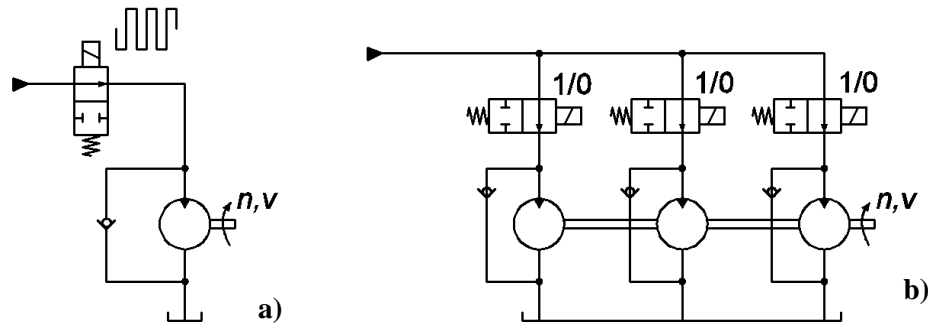


Fig. 5. Hydraulic switching motor (a) and motors connected in parallel (b)

7. DIGITAL HYDRAULIC TRANSFORMER

Digital hydraulics offers some interesting alternatives to traditional hydraulic transformers made of variable flow pump and motor. Linear transformer connected in parallel uses a multi-chamber differential cylinder, an example being shown in **Figure 6 (right)**.

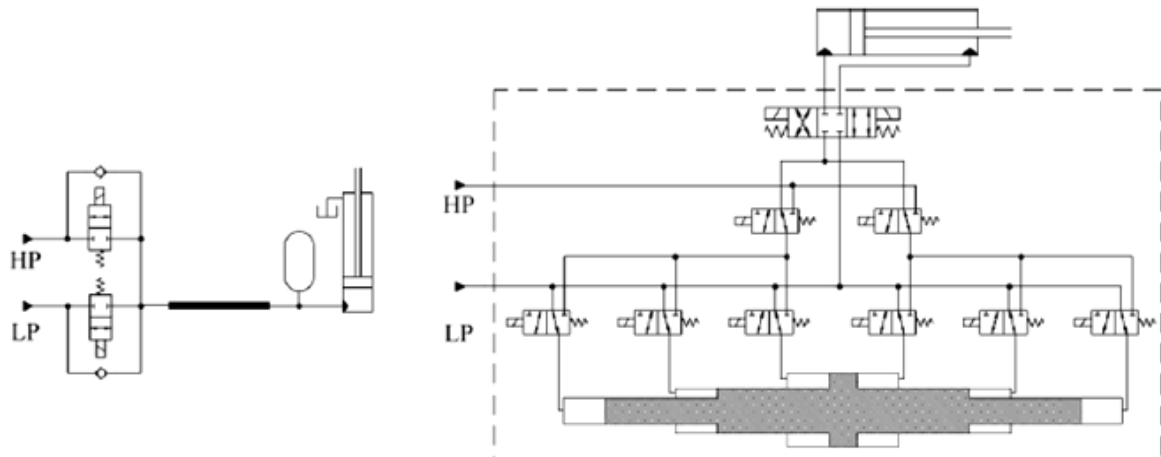


Fig. 6. Switching converter (left) and linear converter based on parallel connection (right)

8. PARALLEL CONNECTION TECHNOLOGY

A fundamental characteristic of systems with elements connected in parallel is that the output flow can be quantified. If the system is made of n parallel components, each one with two positions - closed-open - the total number of combinations of positions is 2^n . Each of these combinations can give a different output flow and thus the maximum number of output values equals the number of combinations of positions.

The system of parallel connection of digital pumps (**Fig. 7**) has a number of fixed displacement pumps with different capacities placed on the same axle, and each of them can be independently connected to the system or the tank.

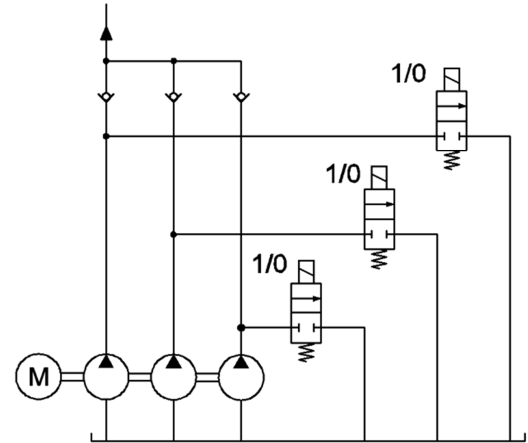


Fig. 7. Parallel mounted digital pumps

The actual number of output values depends on the of the encoding method and the relative size of the components. The smallest number of output values is done using k pumps of the same size, and the number of output values is $k + 1$. This method is known as The modulation of the number of pulses (PNM encoding). At the other extreme are binary and ternary encoding, in which each combination of positions gives different output values.

In the case of binary encoding is required k number of positive displacement pumps with different capacities, driven by a single electric motor. By switching them for load or idle operation, there can be achieved a number of discrete flow rates 2^k . For example, using three pumps there will be achieved eight different flow rates (**Fig. 8, a**).

For ternary encoding, if there is used also a number of k pumps of different capacities, which can however operate as hydraulic motors as well, there can be obtained a number of flow rates equal to $(3^k + 1)/2$. For example, with 3 pumps there will be obtained 14 different discrete flow rates (**Fig. 8, b**).[9]

Binary encoding (**Fig. 8, a**)

- number of possible flow rates: 2^k
- reversibility pump-motor is not required
- k - number of pumps with constant flow

1	2	4	Q
			0
+			1
	+		2
+	+		3
		+	4
+		+	5
	+	+	6
+	+	+	7

Ternary encoding (**Fig. 8, b**)

- number of possible flow rates: $(3^k + 1)/2$
- reversibility pump-motor is required
- k - number of reversible constant flow units

1	3	9	Q
			0
+			1
--	+		2
	+		3
+	+		4
--	--	+	5
	--	+	6
+	--	+	7
--		+	8
		+	9
+		+	10
--	+	+	11
	+	+	12
+	+	+	13

Figure 9, a shows how the parallel connection of 2/2 type valves is made. The name DFCU (digital flow control unit) is used for such a valves block, and the simplified symbol is shown in **Figure 9, b**. The flow section of DFCU is the sum of the flow areas of open valves.

Two factors determine the characteristics of the equilibrium state: the number of n valves connected in parallel and the relative flow rates of the valves.

The binary encoding system is the most commonly used, and the flow is in 1:2:4:8 etc. ratios. Other encoding systems include the Fibonacci system (1:1:2:3:5 etc.) and modulation of the number of pulses (1:1:1:1 etc.).

Regardless the encoding, the DFCU has 2^n drive combinations, which are called the positions of DFCU. In the case of binary encoding, each position has a different flow section, while in the other encoding methods there are various levels of redundancy.

The essential advantage at switching valves is that a DFCU does not require any switching to maintain any of the possible discrete values. Switches are required only when position is changed.

The version of parallel connection of digital hydraulic motors has several implementation options. The simplest option is to connect in parallel a number of cylinders (**Fig.10, a**), but a more compact construction can be achieved by designing a multi-chamber differential cylinder (**Fig.10, b, c**). Four integrated chambers mean a maximum from a practical point of view, resulting in 16 possible discrete values of the force depending on the combination of the positions of valves. The continuous increase of force values can be obtained by increasing the number of supply pressures or increasing the supply pressure. The number of force values is N^M , where N is the number of supply pressures and M the number of chambers.

Similar to other systems for connecting in parallel, different characteristics can be obtained by changing the encoding scheme, in this case the relative area of the piston.

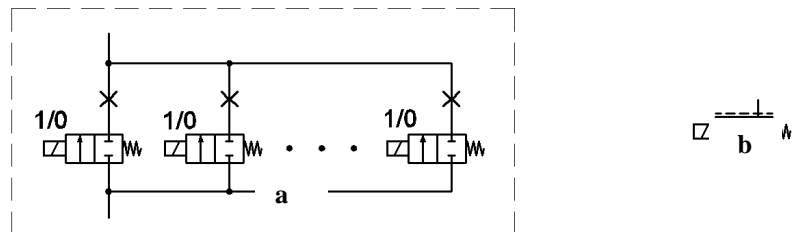


Fig. 9. Parallel connected valves: digital flow control unit – DFCU (a); simplified symbol (b)

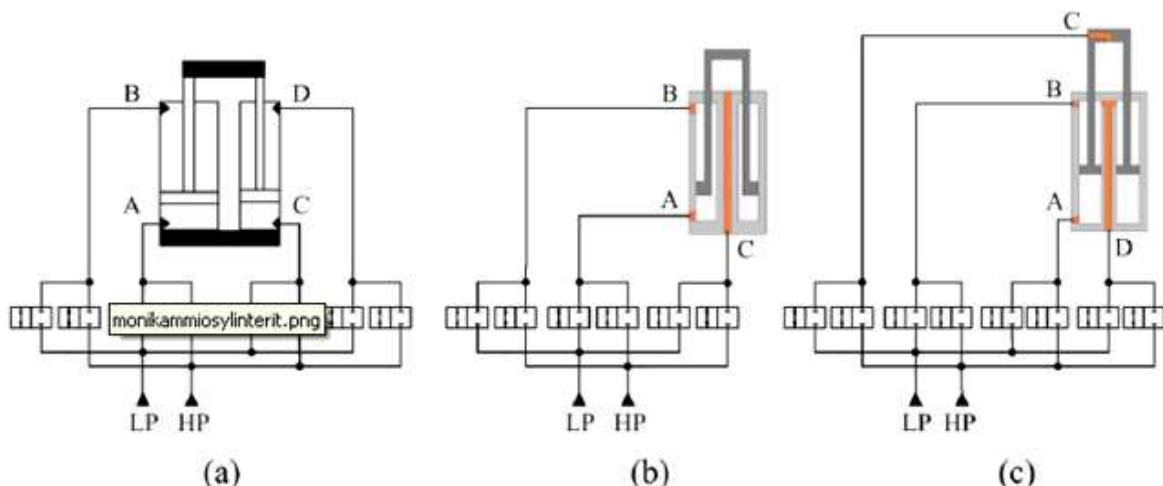


Fig. 10. Different implementations of multi-chamber cylinders. LP=low pressure line; HP=high pressure line.

An important feature of the parallel connected systems is that no switching is needed in order to maintain any of the discrete output values.

Once the state combination is selected and the control valves have achieved their positions, the output remains constant without any further actions. Some valve switchings are needed only when the state combination changes.

The digital flow control unit is the most famous example of the parallel connected system. Each valve has two states and the output is the total flow area of the valves. Under constant pressure difference over the DFCU, the flow rate and actuator velocity are directly related to the flow area.[3]

9. SWITCHING VALVES

Switching control operates through switching of On/Off valves through means of an electronic controller. The input parameters are the delay characteristics of valves which can be individual pulse duration and frequency of switching.

The basic motivations for switching control are:

- the use as components of simple switching valves, instead of more complex servo or proportional valves, to achieve one or several of the following goals: lower costs, higher robustness, better standardization;
- easier control: better repeatability, less hysteresis;
- better energy efficiency by the application of energy saving converter principles;
- generating very rapid movement to move heavy loads.

In the case of digital pumps, switching version has a fixed displacement pump, and the flow is switched continuously between the system and tank (fig. 11).

Figure 12 shows the symbolization of a 2/2 switching control valve. It controls the average flow section through high modulation frequency (HMF) and pulse width modulation (PWM), this being the most common method. Theoretically, the average flow section can have any value between the maximum and minimum, but dynamic functioning limits the maximum and minimum opening.

The controllability depends also on the switching frequency. A low frequency improves controllability of the average flow area, but increases the pressure pulsation. A basic hydraulic switching control system (**Fig. 13**) uses a fixed capacity pump and two 2/2 valves that switch the flow continuously between the system and the tank [3].

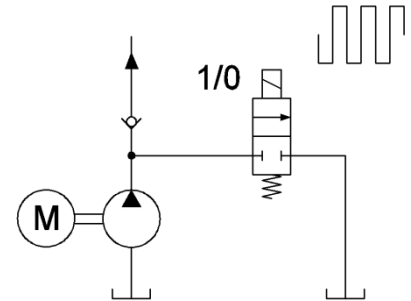


Fig. 11. Digital switching pump

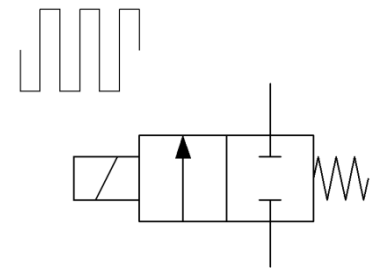


Fig. 12. 2/2 on/off valve with switching control

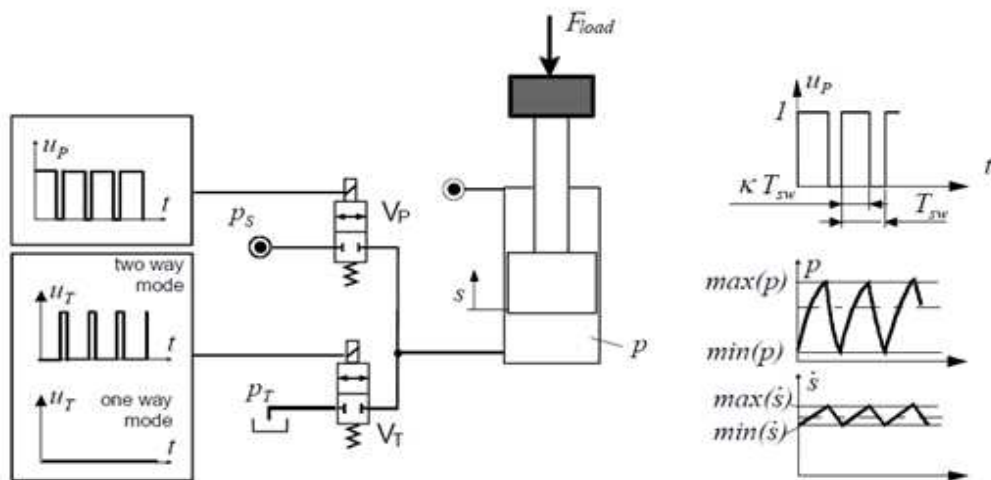


Fig. 13. Diagram for a basic switching control system (left); electrical output signals (right)

Other components, such as pulse attenuation elements or long pipes and fittings between the manifold and cylinder are not present, because they lead to a more difficult to verify dynamic behavior.

The switching frequency is the main parameter for achieving of high performances with such a system, and it is known that high frequencies attenuate pressure and speed pulsations [1].

10. CONCLUSIONS

This paper shows that digital fluid power is a broad research field, with future development opportunities. The technology offers several new ways to implement highly efficient hydraulic systems. An interesting feature is that systems are not complicated; they may have several components but they all are the same type. Digital fluid power means big harmonization of hydraulics because all functions can be implemented by simple on/off valves and fixed displacement pumping units. The side effect is that control code becomes complicated because it implements all the functionality.

The biggest obstacle of the application of digital fluid power is the lack of commercial valves. There is an urgent need for good valves, valve packages and control electronics, all integrated in a package.

REFERENCES

- [1] Hydraulic switching control – objectives, concepts, challenges and potential applications - **Rudolf Scheidl**, HERVEX 2012
- [2] <http://digitalhydraulic.com> – **Elton Bishop**
- [3] *DIGITAL FLUID POWER – STATE OF THE ART* – **Matti Linjama**
- [4] <http://www.tut.fi/en/about-tut/departments/intelligent-hydraulics-and-automation/research/digital-hydraulics/index.htm>
- [5] *Digital Hydraulics – Towards perfect Valve Technology* – **Matti Linjama, Matti Vilenius** (article, journal Digitalna Hidravlika - Slovenia)
- [6] **A.Oprean, V.Marin, A.Dorin.** – *Hydraulic drives*-Technical Press House, Bucharest,1976;
- [7] **Andrei-Mugur Georgescu, Sanda-Carmen Georgescu** - *Pipeline hydraulics and hydraulic machines*, Printech Press House, Bucharest, 2007
- [8] Digital hydraulics – Towards perfect valve technology – **Matti Linjama, Matti Vilenius**
- [9], **PhD.Eng. Heinrich THEISSEN** - *Fluid Power For Sustainability*- Proceeding of 2011 International Salon of Hydraulics and Pneumatics – HERVEX.

ISSN 1843 - 3359